Orbital electron capture by the nucleus*

W. Bambynek

Bureau Central de Mesures Nucléaires, EURATOM, B—2440 Geel, Belgium

H. Behrens

Zentralstelle für Atomkernenergie-Dokumentation, Kernforschungszentrum Karlsruhe, 7514 Eggenstein-Leopoldshafen 2, Germany

M. H. Chen and B. Crasemann

Department of Physics, University of Oregon, Eugene, Oregon 97403, U.S.A.

M. L. Fitzpatrick and K. W. D. Ledingham

Department of Natural Philosophy, University of Glasgow, Kelvin Laboratory, N.E.L., East Kilbride, Lanarkshire, Scotland

H. Genz and M. Mutterer

Institut für Kernphysik, Technische Hochschule Darmstadt, 61 Darmstadt, Germany

R. L. Intemann

Department of Physics, Temple University, Philadelphia, Pennsylvania 19122, U.S.A.

The theory of nuclear electron capture is reviewed in the light of current understanding of weak interactions. Experimental methods and results regarding capture probabilities, capture ratios, and EC/β^+ ratios are summarized. Radiative electron capture is discussed, including both theory and experiment. Atomic wavefunction overlap and electron exchange effects are covered, as are atomic transitions that accompany nuclear electron capture. Tables are provided to assist the reader in determining quantities of interest for specific cases.

CONTENTS

*This work was supported in part by Gerbundforschung at Ruhr-Universität Bochum, Germany, by the U. S. Army Research Office and by the National Aeronautics and Space Administration.

I. INTRODUCTION

A. History

In β decay, a nucleus can capture an electron (or a positron) instead of emitting one. This possibility, inherent in the Fermi (1934) theory of β emission, was first suggested by Yukawa and Sakata (1935, 1936, 1937). The density of atomic bound electrons at the nucleus makes orbital electron capture significant, particularly for s electrons in heavy atoms. Detection of the emitted neutrino is a major experimental undertaking that has not yet met with success (Davis *et al.*, 1968; see also *Physics Today* **25**, August 1972, p. 17; Bahcall, 1972). Even the nuclear recoil from neutrino emission is very difficult to detect (Crane, 1948), unless extraordinary ingenuity is brought to bear (Goldhaber *et al.*, 1958). X rays and Auger electrons emitted in the de-excitation of the ionized daughter provide more readily detectable, al-

beit indirect, signals of the capture process.

Alvarez (1937) first gained experimental evidence for the existence of nuclear electron capture by detecting Ti K x rays emitted in the decay of ^{48}V. A Geiger counter was employed; positrons were bent away by a magnetic field, and the x-ray energy was established approximately from an Al absorption curve. Gamma-ray internal conversion could not be excluded as a possible origin of the Ti K x rays. A completely conclusive demonstration was brought about the following year, when Alvarez (1938a, b) used differential absorption to identify Zn K x rays from the decay of ^{67}Ga. Related cloud-chamber experiments were performed by Oldenburg (1938) and by Williams and Pickup (1938), after an unsuccessful attempt by Jacobsen (1937). The capture of L electrons was first observed by Kirkwood *et al.* (1948) and Pontecorvo *et al.* (1949), who mixed radioactive ^{37}Ar with the gas in a proportional counter and found a peak due to Cl L x rays in the spectrum. Dougan (1961) first measured M electron capture in ^{71}Ge.

Following the work of Fermi (1934) and Yukawa and Sakata (1935, 1936, 1937), the theory of allowed electron capture was developed by Bethe and Bacher (1936) and Møller (1937a, b). Generalizations including forbidden transitions were carried out by Marshak (1942), Bouchez *et al.* (1950; Bouchez, 1952), Brysk and Rose (1958), Hubbard (1965), Robinson (1965), Zweifel (1954, 1957, 1958), Konopinski (1966), and Behrens and Jänecke (1969), among others. The subject has been reviewed by Robinson and Fink (1955, 1960), Bouchez and Depommier (1960), and Berényi (1963a, 1968a). Introductions to the theory are contained in the books by Schopper (1966), Wu and Moszkowski (1966), and Morita (1973).

B. Energetics

We denote by W_0+1 the energy (mass) difference between parent and daughter neutral atoms

$$W_0 = \Delta W_{\rm nucl} - \Delta\left|\Sigma E_x\right| , \tag{1.1}$$

in units such that $\hbar = m_e = c = 1$. Here, $\Delta W_{\rm nucl}$ is the energy difference between the parent nucleus (A, Z) and the daughter nucleus $(A, Z-1)$. The quantity $\Delta\left|\Sigma E_x\right|$ is the *total* change in electron binding energy between parent and daughter atoms, which arises because all electron energy levels move up in the potential well as the nuclear charge decreases by one unit (the electron cloud "expands"). The binding-energy charge $\Delta\left|\Sigma E_x\right|$ is not negligible; it amounts to ~20 keV for $Z=85$, for example.

Let E'_x be the binding energy of the captured electron in the daughter atom. We neglect the energy of atomic recoil from neutrino emission; its largest value, in ^{7}Be decay, is only 57 eV. Because of imperfect atomic wavefunction overlap, the daughter atom's electronic excitation energy will exceed $\left|E'_x\right|$ by an amount that we denote by E_R. The average of this *rearrangement energy* E_R, taken over many atoms, is small (of the order of a few eV), but in those individual transitions in which substantial shakeup or shakeoff (internal ionization) occurs, E_R can be quite significant (Sec. V). The neutrino energy is

$$q = W_0 + 1 - \left|E'_x\right| - E_R \tag{1.2}$$

or

$$q = \Delta W_{\rm nucl} - \Delta\left|\Sigma E_x\right| + 1 - \left|E'_x\right| - E_R . \tag{1.3}$$

The atomic excitation energy $\left|E'_x\right| + E_R$ is released after the capture event in a cascade of Auger and radiative transitions, except for energy carried into the continuum in shakeoff. The energy threshold for electron capture from orbital x is

$$\Delta W_{\rm nucl} \geq -1 + \Delta\left|\Sigma E_x\right| + \left|E'_x\right| + E_R . \tag{1.4}$$

Positron emission is energetically possible, and competes with orbital electron capture (Secs. III.D, III.E) if $W_0 \geq 1$, or

$$\Delta W_{\rm nucl} \geq 1 + \Delta\left|\Sigma E_x\right| + E_R . \tag{1.5}$$

C. Atomic effects

Nuclear electron capture by its very nature stands at the interface between nuclear and atomic physics. Only in the crudest of approximations can the atomic electron cloud be treated as merely the donor of the electron that is captured. Nevertheless, the importance of treating β decay in general, and electron capture in particular, as transformations of the whole atom was not quantitatively taken into account until Benoist-Gueutal (1950, 1953a, b) wrote her thesis. The idea of including atomic variables in the description of initial and final states was pursued by Odiot and Daudel (1956), and formulated elegantly by Bahcall (1962a, 1963a, b).

The fact that the entire atom is transformed in electron-capture decay is reflected in the energetics (Sec. I.B) and in the effect of imperfect atomic wavefunction overlap on the transition rate (Sec. II.E). Furthermore, atomic transitions such as shakeup and shakeoff (internal ionization) can take place as an integral part of the radioactive decay (Sec. V), quite distinct from the Auger and x-ray cascade through which the daughter atom is subsequently de-excited. Atomic effects in nuclear decay have recently been reviewed by Emery (1972), Crasemann (1973), Freedman (1974), and Walen and Briançon (1975).

D. Radiative electron capture

The existence of a low-intensity continuous photon spectrum accompanying $\beta^{\pm}$ decay was first observed by Aston (1927) and Bramson (1930). The basic theory of radiative β decay was developed independently by Knipp and Uhlenbeck (1936), who were seeking an explanation for the observed photon continuum, and by Bloch (1936), who was unaware of the experimental work and was motivated by purely theoretical considerations based on Fermi's theory of β decay and Dirac's theory of the positron. Møller (1937a, b) and Morrison and Schiff (1940) pointed out that internal bremsstrahlung (IB) should be emitted in the course of nuclear electron capture as well as in β decay, and independently worked out the theory. Møller (1937a, b), in particular, was interested in differentiating between the Fermi and Konopinski–Uhlenbeck couplings. Internal bremsstrahlung from electron capture was first detected by Bradt *et al.* (1946). A

number of reports followed, describing the observation of IB at high energies; all of these data were consistent with the Morrison–Schiff theory. A study of the ^{55}Fe IB spectrum by Madansky and Rasetti (1954), however, showed an unexpected steep rise of the IB intensity at low photon energies. These data were only explained after Glauber and Martin (1956; Martin and Glauber, 1958) developed an elaborate and much more accurate theory of IB in electron capture, in which Coulomb and screening effects are taken into account and capture from L and M shells is included. Although originally restricted to allowed transitions, this theory was later generalized to electron-capture transitions of arbitrary degree of forbiddenness by Zon and Rapoport (1968; Zon, 1971).

E. Significance

Research on electron-capture probabilities and ratios is being pursued as a facet of basic science and because of the importance of applications. Electron capture plays a part in the decay schemes of some 500 radionuclides, ~60 of which are commercially available. Nuclear decay by electron capture is not only relevant to nuclear science but also to geochemistry, cosmology and astrophysics (Trimble and Reines, 1973), nuclear medicine (Dillman, 1968, 1970), and technology. The measurement of K/β^+ ratios is one of the more sensitive ways of determining an upper limit on the Fierz interference term (Schopper, 1968). Ratios of allowed electron capture from various shells are independent of nuclear factors and reflect purely atomic properties; these ratios are sensitive to bound-electron wavefunctions at the nuclear surface and to electron exchange and imperfect atomic wavefunction overlap (Bahcall, 1962a, 1963a, b).

F. Scope of review

In Sec. II of this article, we discuss the theory of allowed and forbidden nuclear electron capture. Formulae and tables are provided that enable the reader to calculate transition rates and ratios of interest. Special attention is paid, in Sec. II.E, to electron-exchange and atomic wavefunction overlap effects on the transition probability. Experimental methods for the measurement of electron-capture probabilities and ratios and of EC/β^+ ratios are described and compared in Sec. III. Published data are listed, critically evaluated, and compared with theory. In Sec. IV, the theory of radiative electron capture and experimental work on internal bremsstrahlung are thoroughly reviewed and tables for the calculation of IB spectra are provided. Section V is devoted to a discussion of atomic transitions that accompany nuclear electron capture.

We have made an effort at completeness in covering the subject. Some information has been included that is now of merely historical interest, but we have attempted to be adequately critical in the final evaluation and comparison of results. Meson capture, though interesting and closely related to our subject, has not been included.

We hope that this article may prove useful for both theoretical and experimental researchers in need of a complete survey of what is known about nuclear electron capture, and that it will be of help to nuclear physicists and chemists and to workers in radionuclide metrology, nuclear medicine, and in related areas.

II. ELECTRON-CAPTURE THEORY

A. The β-decay and electron-capture Hamiltonian and transition rates

It is usually assumed that all the weak interaction processes can be described by a universal fundamental Hamiltonian density (current-current interaction) (Marshak *et al.*, 1969; Schopper, 1966; Blin-Stoyle, 1973). A general discussion of such phenomenological interaction currents in nuclear systems is given by Lock *et al.* (1974). For the special case of nuclear β decay, this Hamiltonian density has the form[1]

$$H_\beta(x) = -G_\beta 2^{-1/2}[J_\mu(x)L_\mu^\dagger(x) + \text{h.c.}], \tag{2.1}$$

where J_μ and L_μ denote the hadron and the lepton current, respectively. The β-decay coupling constant G_β is related to the universal weak coupling constant G by

$$G_\beta = G\cos\theta, \tag{2.2}$$

where θ is the Cabbibo angle.

Although Eq. (2.1) well describes such processes as β and μ decay, it represents an incomplete theory because it is not renormalizable. Thus higher-order corrections cannot be calculated. In the last few years, however, renormalizable models (first proposed by Weinberg, 1967, and Salam, 1968) have been developed. These models are based on gauge theories unifying the weak and electromagnetic interactions (Abers and Lee, 1973; Lee, 1973; Bernstein, 1974; Weinberg, 1974; Beg and Sirlin, 1974). These gauge theories imply that the weak interaction operates through a neutral current in addition to the previously known charged current. Phenomena induced by neutral currents occur mostly in high-energy physics, but they can be found in nuclear and atomic physics as well (Bouchiat and Bouchiat, 1974). Nevertheless, for the purposes of the present paper, the Hamiltonian of Eq. (2.1) is sufficient and we shall deal only with this form of the weak-interaction theory.

In nuclear β decay, we must consider the three processes

$$(Z,A) \to (Z+1,A) + e^- + \bar{\nu}_e \quad (\beta^- \text{ decay}),$$

$$(Z,A) \to (Z-1,A) + e^+ + \nu_e \quad (\beta^+ \text{ decay}),$$

$$(Z,A) + e^- \to (Z-1,A) + \nu_e \quad (\text{electron capture}).$$

Here, (Z,A) signifies an atomic nucleus of mass number A and atomic number Z, e^- denotes an electron, e^+ denotes a positron, ν_e is the neutrino, and $\bar{\nu}_e$ is the antineutrino.

In order to discuss the general features of these weak-interaction processes and their interrelations, we first consider the decay of a single neutron or proton, assum-

[1] We have $A^\dagger = \{A_1^\dagger, A_2^\dagger, A_3^\dagger, -A_4^\dagger\}$. In the following we assume pure $V-A$ interaction to be valid, where V stands for vector, and A, for axial vector. An extensive discussion of this point is given by Schopper (1966).

ing that the individual nucleons in the nucleus are independent of one another and behave like free particles.

In the case of nuclear β decay, we need only the electron part of the lepton current, which can be expressed as

$$L_\mu(x) = i\bar{\psi}_{\nu_e}(x)\gamma_\mu(1+\gamma_5)\psi_e(x)\,, \tag{2.3}$$

where ψ_{ν_e} and ψ_e are the field operators,[2] and γ_λ the Dirac matrices.[3]

The nucleons, unlike the leptons, interact strongly as well. This leads to complications, and consequently it is not possible to express the hadron current so simply in terms of field operators (Marshak *et al.*, 1969; Blin-Stoyle, 1973). If, however, we approximately treat the nucleons as point particles, neglecting the influence of the strong interaction, then the hadron current is

$$J_\mu(x) = i\bar{\psi}_p\gamma_\mu(1+\lambda\gamma_5)\psi_n\,, \tag{2.4}$$

where $\lambda = -C_A/C_V = 1.251 \pm 0.009$ (Kropf and Paul, 1974). The Hamiltonian density then has the form

$$H_\beta(x) = G_\beta 2^{-1/2}\{\bar{\psi}_p(x)\gamma_\mu(1+\lambda\gamma_5)\psi_n(x)\bar{\psi}_e(x)\gamma_\mu(1+\gamma_5)\psi_{\nu_e}(x) + \text{h.c.}\}\,. \tag{2.5}$$

The corresponding transition matrix elements for the three basic processes in nuclear β decay are

$$n \to p + e^- + \bar{\nu}_e \qquad M_{\beta^-} = \langle pe^-\bar{\nu}_e \left| \int H_\beta(x)\, d^4x \right| n\rangle\,, \tag{2.6a}$$

$$p \to n + e^+ + \nu_e \qquad M_{\beta^+} = \langle ne^+\nu_e \left| \int H_\beta(x)\, d^4x \right| p\rangle \tag{2.6b}$$

$$p + e^- \to n + \nu_e \qquad M_{\mathrm{EC}} = \langle n\nu_e \left| \int H_\beta(x)\, d^4x \right| pe^-\rangle\,. \tag{2.6c}$$

With $H_\beta(x)$ according to Eq. (2.5), the transition matrix elements become

$$M_{\beta^-} = G_\beta 2^{-1/2}(2\pi)^4\delta(q_p + q_{e^-} + q_{\bar{\nu}_e} - q_n) \times [\bar{u}_p\gamma_\mu(1+\lambda\gamma_5)u_n][\bar{u}_e\gamma_\mu(1+\gamma_5)v_\nu]\,, \tag{2.7a}$$

$$M_{\beta^+} = G_\beta 2^{-1/2}(2\pi)^4\delta(q_n + q_{e^+} + q_{\nu_e} - q_p) \times [\bar{u}_n\gamma_\mu(1+\lambda\gamma_5)u_p][\bar{u}_\nu\gamma_\mu(1+\gamma_5)v_e]\,, \tag{2.7b}$$

$$M_{\mathrm{EC}} = G_\beta 2^{-1/2}(2\pi)^4\delta(q_n + q_{\nu_e} - q_p - q_e) \times [\bar{u}_n\gamma_\mu(1+\lambda\gamma_5)u_p][\bar{u}_\nu\gamma_\mu(1+\gamma_5)u_e]\,. \tag{2.7c}$$

The q's are the four-momenta of the particles indicated by the subscripts, and $\delta(q)$ is the Dirac delta function.

Equations (2.7) have been derived for the decay of a single, pointlike nucleon. To consider the decay of a nucleon in a complex nucleus, we transform the wave-function used in Eqs. (2.7) from momentum space to configuration space. For this purpose, the three-dimensional momentum-dependent part of the delta function is replaced by

$$\delta(\mathbf{p}) = (2\pi)^{-3}\int e^{-i\mathbf{p}\cdot\mathbf{r}}\, d^3r \tag{2.8}$$

(Blin-Stoyle, 1973). We introduce the plane-wave solutions of the Dirac equation for the particles,

$$\phi_a(\mathbf{p}_a, \mathbf{r}) = u_a e^{i\mathbf{p}_a\cdot\mathbf{r}}\,, \tag{2.9a}$$

and for the antiparticles

$$\phi_b(-\mathbf{p}_b, \mathbf{r}) = C\phi_a(\mathbf{p}_a, \mathbf{r}) = -\gamma_2\phi_a^*(\mathbf{p}_a, \mathbf{r}) = v_b e^{-i\mathbf{p}_b\cdot\mathbf{r}}\,. \tag{2.9b}$$

Here, a and b denote particles and antiparticles, respectively, and C is the charge conjugation operator. We find

$$M_{\beta^-} = G_\beta 2^{-1/2}2\pi\delta(E_p + E_{e^-} + E_{\bar{\nu}_e} - E_n) \times \int \bar{\phi}_p(\mathbf{p}_p, \mathbf{r})\gamma_\mu(1+\lambda\gamma_5) \times \phi_n(\mathbf{p}_n, \mathbf{r})\bar{\phi}_{e^-}(\mathbf{p}_e, \mathbf{r})\gamma_\mu(1+\gamma_5)\phi_{\bar{\nu}_e}(-p_{\bar{\nu}_e}, \mathbf{r})\,; \tag{2.10a}$$

$$M_{\beta^+} = G_\beta 2^{-1/2}2\pi\delta(E_n + E_{e^+} + E_{\nu_e} - E_p) \times \int \bar{\phi}_n(\mathbf{p}_n, \mathbf{r})\gamma_\mu(1+\lambda\gamma_5) \times \phi_p(\mathbf{p}_p, \mathbf{r})\bar{\phi}_{\nu_e}(\mathbf{p}_{\nu_e}, \mathbf{r})\gamma_\mu(1+\gamma_5)\phi_{e^+}(-\mathbf{p}_{e^+}, \mathbf{r})\, d^3r\,; \tag{2.10b}$$

$$M_{\mathrm{EC}} = G_\beta 2^{-1/2}2\pi\delta(E_n + E_{\nu_e} - E_p - E_{e^-}) \times \int \bar{\phi}_n(\mathbf{p}_n, \mathbf{r})\gamma_\mu(1+\lambda\gamma_5) \times \phi_p(\mathbf{p}_p, \mathbf{r})\bar{\phi}_{\nu_e}(\mathbf{p}_{\nu_e}, \mathbf{r})\gamma_\mu(1+\gamma_5)\phi_{e^-}(\mathbf{p}_e, \mathbf{r})\, d^3r\,. \tag{2.10c}$$

Inside the nucleus, we replace the nucleon plane waves by bound spinor wave functions, and represent electrons or positrons by wave functions which are solutions of the Dirac equation for an extended charged nucleus surrounded by atomic electrons.[4] Furthermore, it is convenient to split off the delta function and the factor 2π by writing $M_\beta = 2\pi\delta(E_i - E_f)\langle f|H_\beta|i\rangle$.

The hadron parts of Eqs. (2.10a)–(2.10c) can now be expanded into multipoles (Schopper, 1966; Konopinski, 1966; Bouchez and Depommier, 1960; Weidenmüller, 1961):

$$[\bar{\phi}_f\gamma_\mu(1+\lambda\gamma_5)\phi_i]\gamma_4\gamma_\mu = \sum_{KLsM}(-1)^{K+M}a^M_{KLs}(r)T^{-M}_{KLs}(\hat{r})\,. \tag{2.11}$$

Here, i and f denote initial and final states, and

$$T_{LL0} = i^L Y^M_L \tag{2.12a}$$

and

$$T_{KL1} = (-1)^{L-K+1}i^L \mathbf{Y}^M_{KL}\cdot\boldsymbol{\alpha} \tag{2.12b}$$

are the multipole operators.[5]

---

[2] The field operators are given by

$$\psi(x) = V^{-1/2}\sum_q\sum_r\{e^{iqx}a_r(q)u_r(q) + b_r^\dagger(q)v_r(q)e^{-iqx}\}\,,$$

$$\bar{\psi}(x) = V^{-1/2}\sum_q\sum_r\{e^{-iqx}a_r^\dagger(q)\bar{u}_r(q) + b_r(q)\bar{v}_r(q)e^{iqx}\}\,;$$

$r = 1, 2$.

The $a_r(q)$ and $a_r^\dagger(q)$ are the annihilation and creation operators for a fermion of momentum q and spin r, respectively, $b_r(q)$ and $b_r^\dagger(q)$ are the corresponding operators for the antiparticles. The $u_r(q)$ and $v_r(q)$ are both the free-particle Dirac spinors. We have $\bar{u}_r(q) = u_r^\dagger(q)\gamma_4$ and $\bar{v}_r(q) = v_r^\dagger(q)\gamma_4$.

[3] We use the Dirac equation $(-\boldsymbol{\alpha}\mathbf{p} - \beta m - W)\psi = 0$ and the notation $\gamma_\mu = -i\beta\alpha_\mu$, $\gamma_4 = -\beta$, $\gamma_5 = \gamma_1\gamma_2\gamma_3\gamma_4$, $\sigma = \alpha\gamma_5$, $\boldsymbol{\alpha} = \sigma\gamma_5$, and $\sigma_{\mu\nu} = -\frac{1}{2}i(\gamma_\mu\gamma_\nu - \gamma_\nu\gamma_\mu)$.

[4] In the following, we use natural units $\hbar = m_e = c = 1$.

[5] We have $\hat{r} = \mathbf{r}/r$, and $d\Omega$ is the solid angle.

The expansion coefficients $a^M_{KLs}(r)$ can be derived from the relation

$$a^M_{KLs}(r) = \int \phi_f^\dagger (1+\lambda\gamma_5) T^M_{KLs} \phi_i \, d\Omega_{\text{nucl}} . \tag{2.13}$$

Inserting Eqs. (2.11) and (2.13) in Eqs. (2.10a)–(2.10c), we find for the matrix elements

$$\langle f|H_{\beta^-}|i\rangle = G_\beta 2^{-1/2} \sum_{KLsM} (-1)^{K+M} \times \int\left[\int \phi_p^\dagger (1+\lambda\gamma_5) T^M_{KLs} \phi_n \, d\Omega_{\text{nucl}}\right] \times \left[\int \phi_e^\dagger(Z)(1+\gamma_5) T^{-M}_{KLs} \phi_{\bar\nu_e}(-\mathbf{q}) \, d\Omega_{\text{lept}}\right] r^2 \, dr ; \tag{2.14a}$$

$$\langle f|H_{\beta^+}|i\rangle = G_\beta 2^{-1/2} \sum_{KLsM} (-1)^{K+M} \times \int\left[\int \phi_n^\dagger (1+\lambda\gamma_5) T^M_{KLs} \phi_p \, d\Omega_{\text{nucl}}\right] \times \left[\int \phi_{\nu_e}^\dagger(q)(1+\gamma_5) T^{-M}_{KLs} \phi_{e^+}(-Z) \, d\Omega_{\text{lept}}\right] r^2 \, dr ; \tag{2.14b}$$

$$\langle f|H_{\text{EC}}|i\rangle = G_\beta 2^{-1/2} \sum_{KLsM} (-1)^{K+M} \times \int\left[\int \phi_n^\dagger (1+\lambda\gamma_5) T^M_{KLs} \phi_p \, d\Omega_{\text{nucl}}\right] \times \left[\int \phi_{\nu_e}^\dagger(q)(1+\gamma_5) T^{-M}_{KLs} \phi_{e^-}(Z) d\Omega_{\text{lept}}\right] r^2 \, dr . \tag{2.14c}$$

Here, $\mathbf{q}$ denotes the momentum for neutrino or antineutrino, and $\phi_e\pm(\mp Z)$ is the electron or positron wavefunction in the Coulomb field of a nucleus of atomic number Z.

We expand the electron (positron) and neutrino (antineutrino) continuum wave functions in partial spherical waves ϕ^μ_κ (Konopinski, 1966; Schülke, 1964; Weidenmüller, 1961):

$$\phi_{e^-}(Z) = \sum_{\kappa_e\mu_e} a_{\kappa_e\mu_e} \phi^{\mu_e}_{\kappa_e}(Z) , \tag{2.15a}$$

$$\phi_{\nu_e}(q) = \sum_{\kappa_\nu\mu_\nu} b_{\kappa_\nu\mu_\nu} \phi^{\mu_\nu}_{\kappa_\nu}(q) , \tag{2.15b}$$

$$\phi_{e^+}(-Z) = -\gamma_2 \phi^*_{e^-}(Z) = \sum_{\kappa_e\mu_e} (-1)^{j(\kappa_e)+\mu_e} a^*_{\kappa_e\mu_e} \phi^{-\mu_e}_{\kappa_e}(-Z) , \tag{2.15c}$$

$$\phi_{\bar\nu_e}(-q) = -\gamma_2 \phi^*_{\nu_e}(q) = \sum_{\kappa_\nu\mu_\nu} (-1)^{j(\kappa_\nu)+\mu_\nu} b^*_{\kappa_\nu\mu_\nu} \phi^{-\mu_\nu}_{\kappa_\nu}(-q) . \tag{2.15d}$$

The spherical waves ϕ^μ_κ here have the form

$$\phi^\mu_\kappa(Z) = \begin{pmatrix} (\text{sign}\kappa) f_\kappa(Z,r) \chi^\mu_{-\kappa} \\ g_\kappa(Z,r)\chi^\mu_\kappa \end{pmatrix}, \tag{2.16}$$

where we have

$$\chi^\mu_\kappa = i^l \sum_m C(l\tfrac{1}{2}j;\, \mu - m\, m)\, Y^{\mu-m}_l \chi^m , \tag{2.17}$$

the χ^m ($m = \pm\frac{1}{2}$) are two-component Pauli spinors, the $C(l\frac{1}{2}j;\, \mu - m\, m)$ are Clebsch–Gordan coefficients, and the Y^μ_l are spherical harmonics. The index κ is

$$\kappa = \begin{cases} l, & j = l - \frac{1}{2} \\ -(l+1), & j = l + \frac{1}{2} \end{cases}, \tag{2.18}$$

and $g_\kappa(Z,r)$ and $f_\kappa(Z,r)$ are the large and small radial wavefunctions, respectively.

The antiparticle (positron) wavefunction is (Rose, 1961)

$$\bar\phi^\mu_\kappa(-Z) = \begin{pmatrix} g_\kappa(-Z,r)\chi^{-\mu}_\kappa \\ (-\text{sign}\kappa) f_\kappa(-Z,r)\chi^{-\mu}_{-\kappa} \end{pmatrix}. \tag{2.19}$$

The neutrino radial wavefunctions can be written explicitly:

$$\phi^\mu_\kappa(q) = \begin{pmatrix} j_{\bar l}(qr)\chi^\mu_{-\kappa} \\ j_l(qr)\chi^\mu_\kappa \end{pmatrix}, \tag{2.20}$$

where $l - \bar l = \text{sign}\kappa$, and $j_l(qr)$ is the spherical Bessel function. For the antineutrino we have

$$\bar\phi^\mu_\kappa(-q) = \begin{pmatrix} j_l(qr)\chi^{-\mu}_\kappa \\ -j_{\bar l}(qr)\chi^{-\mu}_{-\kappa} \end{pmatrix}. \tag{2.21}$$

The expansion coefficients $a_{\kappa\mu}$ and $b_{\kappa\mu}$ in Eqs. (2.15) are determined by the condition that the continuum wavefunctions $\phi_{e^-}(Z)$ and $\phi_{\nu_e}(q)$ become asymptotically equal to a plane wave plus incoming (or outgoing) spherical waves (Schülke, 1964; Weidenmüller, 1961):

$$a_{\kappa_e\mu_e}(\mathbf{p}, s_e) = 4\pi p^{-1} C(l_e\tfrac{1}{2}j_e;\, \mu_e - s_e s_e) \times Y^{*\mu_e - s_e}_{l}(\hat p) e^{-i[\Delta_{\kappa_e} + (\pi/2)(l_e+1)]} , \tag{2.22}$$

$$b_{\kappa_\nu\mu_\nu}(\mathbf{q}, s_\nu) = 4\pi C(l_\nu\tfrac{1}{2}j_\nu;\, \mu_\nu - s_\nu s_\nu) Y^{*\mu_\nu - s_\nu}_{l}(\hat q) . \tag{2.23}$$

Here, Δ_κ is the Coulomb phase (Bühring, 1965, 1967).

It is useful, furthermore, to introduce reduced hadron and lepton matrix elements by applying the Wigner–Eckart theorem. From Eqs. (2.14a)–(2.14c) and (2.15a)–(2.15c) we find

$$\langle f|H_{\beta^-}|i\rangle = G_\beta 2^{-1/2} \sum_{KLsM} \sum_{\substack{\kappa_e\mu_e \\ \kappa_\nu\mu_\nu}} (-1)^{J_f - M_f + j_e - \mu_e} (-1)^{K+M+j_\nu+\mu_\nu} \begin{pmatrix} J_f & K & J_i \\ -M_f & M & M_i \end{pmatrix} \begin{pmatrix} j_e & K & j_\nu \\ -\mu_e & -M & -\mu_\nu \end{pmatrix} \times a^*_{\kappa_e\mu_e} b^*_{\kappa_\nu\mu_\nu} \int \langle \phi_p \| (1+\lambda\gamma_5) T_{KLs} \| \phi_n \rangle \langle \phi_{\kappa_e}(Z) \| (1+\gamma_5) T_{KLs} \| \phi_{\kappa_\nu}(-q) \rangle r^2 \, dr ; \tag{2.24a}$$

$$\langle f|H_{\beta^+}|i\rangle = G_\beta 2^{-1/2} \sum_{KLsM} \sum_{\substack{\kappa_e\mu_e \\ \kappa_\nu\mu_\nu}} (-1)^{J_f-M_f+j_\nu-\mu_\nu}(-1)^{K+M+j_e+\mu_e} \begin{pmatrix} J_f & K & J_i \\ -M_f & M & M_i \end{pmatrix} \begin{pmatrix} j_\nu & K & j_e \\ -\mu_\nu & -M & -\mu_e \end{pmatrix}$$

$$\times a^*_{\kappa_e\mu_e} b^*_{\kappa_\nu\mu_\nu} \int \langle \phi_n||(1+\lambda\gamma_5)T_{KLs}||\phi_p\rangle \langle \phi_{\kappa_\nu}(q)||(1+\gamma_5)T_{KLs}||\phi_{\kappa_e}(-Z)\rangle r^2\, dr\,; \tag{2.24b}$$

$$\langle f|H_{\mathrm{EC}}|i\rangle = G_\beta 2^{-1/2} \sum_{KLsM} \sum_{\kappa_\nu\mu_\nu} (-1)^{J_f-M_f+j_\nu-\mu_\nu}(-1)^{K+M} \begin{pmatrix} J_f & K & J_i \\ -M_f & M & M_i \end{pmatrix} \begin{pmatrix} j_\nu & K & j_x \\ -\mu_\nu & -M & \mu_x \end{pmatrix} b^*_{\kappa_\nu\mu_\nu}$$

$$\times \int \langle \phi_n||(1+\lambda\gamma_5)T_{KLs}||\phi_p\rangle \langle \phi_{\kappa_\nu}(q)||(1+\gamma_5)T_{KLs}||\phi_{\kappa_x}(Z)\rangle r^2\, dr\,. \tag{2.24c}$$

Here, x ($=K, L_1, L_2, L_3, M_1, \ldots$) denotes the different shells and subshells of the atomic cloud from which the electron can be captured. The states of the initial neutron or proton are specified by $|J_iM_i\rangle$, and those of the final nucleon by $|J_fM_f\rangle$.

The similarity of Eqs. (2.24a), (2.24b), and (2.24c) suggests that we need to derive the final formulae of the observables for only one type of decay (β^-, β^+, or EC) and can hence obtain results for the other decay modes. For this purpose, we transform Eqs. (2.24b) and (2.24c) into a form that is similar to that of Eq. (2.24a), by interchanging initial and final states in the reduced lepton matrix elements. Taking into account the relation (Weidenmüller, 1961)

$$\langle f||(1+\gamma_5)T_{KLs}||i\rangle^* = (-1)^{K-s+j_i-j_f}\langle i||(1+\gamma_5)T_{KLs}||f\rangle \tag{2.25}$$

and the fact that here the reduced matrix elements are defined as real quantities, we obtain

$$\langle f|H_{\beta^+}|i\rangle = G_\beta 2^{-1/2} \sum_{KLsM} \sum_{\substack{\kappa_e\mu_e \\ \kappa_\nu\mu_\nu}} (-1)^{J_f-M_f+j_e-\mu_e}(-1)^{K-s+M+j_\nu+\mu_\nu+1} \begin{pmatrix} J_f & K & J_i \\ -M_f & M & M_i \end{pmatrix} \begin{pmatrix} j_e & K & j_\nu \\ -\mu_e & -M & -\mu_\nu \end{pmatrix}$$

$$\times a^*_{\kappa_e\mu_e} b^*_{\kappa_\nu\mu_\nu} \int \langle \phi_n||(1+\lambda\gamma_5)T_{KLs}||\phi_p\rangle \langle \phi_{\kappa_e}(-Z)||(1+\gamma_5)T_{KLs}||\phi_{\kappa_\nu}(q)\rangle r^2\, dr\,; \tag{2.26a}$$

$$\langle f|H_{\mathrm{EC}}|i\rangle = G_\beta 2^{-1/2} \sum_{KLsM} \sum_{\kappa_\nu\mu_\nu} (-1)^{J_f-M_f+j_x-\mu_x}(-1)^{K-s+M+j_\nu+\mu_\nu+1} \begin{pmatrix} J_f & K & J_i \\ -M_f & M & M_i \end{pmatrix} \begin{pmatrix} j_x & K & j_\nu \\ \mu_x & -M & -\mu_\nu \end{pmatrix}$$

$$\times b^*_{\kappa_\nu\mu_\nu}(-1)^{j_x+\mu_x} \int \langle \phi_n||(1+\lambda\gamma_5)T_{KLs}||\phi_p\rangle \langle \phi_{\kappa_x}(Z)||(1+\gamma_5)T_{KLs}||\phi_{\kappa_\nu}(q)\rangle r^2\, dr\,. \tag{2.26b}$$

The transition probability per unit time can now be found from standard quantum-mechanical formulae. By applying first-order time-dependent perturbation theory (the "Golden Rule"), the decay constant λ and the half-life t are given by

$$\lambda_{\beta^\pm} = (\ln 2)(t_{\beta^\pm})^{-1} = 2\pi(2J_i+1)^{-1} \sum_{M_i,M_f} \sum_{s_e,s_\nu} \int\int\int |\langle f|H_{\beta^\pm}|i\rangle|^2 p^2 q^2\, dp\, d\Omega_e\, d\Omega_\nu (2\pi)^{-6} \tag{2.27}$$

for $\beta^\pm$ decay, and by

$$\lambda_x = (\ln 2)(t_x)^{-1} = 2\pi(2J_i+1)^{-1} \sum_{M_i,M_f} \sum_{\mu_x,s_\nu} \int |\langle f|H_{\mathrm{EC}}|i\rangle|^2 q_x^2\, d\Omega_\nu (2\pi)^{-3} \tag{2.28}$$

for electron capture from the atomic x shell. By inserting the matrix element given by Eq. (2.24a) in Eq. (2.27) and making use of the orthogonality relations for Clebsch–Gordan coefficients and $3j$ symbols, we find

$$\lambda_{\beta^-} = G_\beta^2 (2\pi)^{-3}(2J_i+1)^{-1} \int \frac{1}{2} \sum_K \sum_{\kappa_e\kappa_\nu} \left\{ \sum_{Ls} \int (2K+1)^{-1/2}(4\pi)^{1/2} \langle \phi_p||(1+\lambda\gamma_5)T_{KLs}||\phi_n\rangle \right.$$

$$\left. \times (4\pi)^{1/2} \langle \phi_{\kappa_e}(Z)||(1+\gamma_5)T_{KLs}||\phi_{\kappa_\nu}(-q)\rangle r^2\, dr \right\}^2 q^2\, dp\,. \tag{2.29}$$

Similarly, by combining Eqs. (2.26a) and (2.27), we have

$$\lambda_{\beta^+} = G_\beta^2 (2\pi)^{-3}(2J_i+1)^{-1} \int \frac{1}{2} \sum_K \sum_{\kappa_e\kappa_\nu} \left\{ \sum_{Ls} (-1)^s \int (2K+1)^{-1/2}(4\pi)^{1/2} \langle \phi_n||(1+\lambda\gamma_5)T_{KLs}||\phi_p\rangle \right.$$

$$\left. \times (4\pi)^{1/2} \langle \phi_{\kappa_e}(-Z)||(1+\gamma_5)T_{KLs}||\phi_{\kappa_\nu}(q)\rangle r^2\, dr \right\}^2 q^2\, dp\,. \tag{2.30}$$

The electron-capture decay constant is found by inserting Eq. (2.26b) in Eq. (2.28)

$$\lambda_x = G_\beta^2 (2\pi)^{-3}(2J_i+1)(1/2) \sum_K \sum_{\kappa_\nu} \left\{ \sum_{Ls} \int (-1)^s (2K+1)^{-1/2}(4\pi)^{1/2} \langle \phi_n||(1+\lambda\gamma_5)T_{KLs}||\phi_p\rangle \right.$$

$$\left. \times (4\pi)^{1/2} \langle \phi_{\kappa_x}(Z)||(1+\gamma_5)T_{KLs}||\phi_{\kappa_\nu}(q)\rangle r^2\, dr \right\}^2 q_x^2\,. \tag{2.31}$$

The neutrino momentum q_x is given by

$$q_x = W_0 + W'_x , \tag{2.32}$$

where W_0 is the total transition energy between initial and final states (the difference between the atomic masses, minus m_0c^2, see Sec. I.B), and W'_x denotes the energy of the bound electron (in the daughter atom). This is $W'_x = 1 - |E'_x|$, where E'_x is the binding energy of the electron. Because the electron and neutrino wavefunctions are well known [Eqs. (2.16)–(2.21)], we can evaluate the reduced lepton matrix elements explicitly (Schülke, 1964; Weidenmüller, 1961). For the three kinds of reduced lepton matrix elements appearing in Eqs. (2.29), (2.30), and (2.31), we have the following:

$$\begin{aligned}(4\pi)^{1/2}&\langle\phi_{\kappa_e}(Z)||(1+\gamma_5)T_{KLs}||\phi_{\kappa_\nu}(q)\rangle \\ &= g_{\kappa_e}(Z)[j_{l_\nu}G_{KLs}(\kappa_e,\kappa_\nu) + j_{\bar{l}_\nu}G_{KLs}(\kappa_e,-\kappa_\nu)] \\ &\quad + (\mathrm{sign}\kappa_e) f_{\kappa_e}(Z)[j_{l_\nu}G_{KLs}(-\kappa_e,\kappa_\nu) + j_{\bar{l}_\nu}G_{KLs}(-\kappa_e,-\kappa_\nu)]\end{aligned} \tag{2.33}$$

for the electron-neutrino matrix element;

$$\begin{aligned}(4\pi)^{1/2}&\langle\phi_{\kappa_e}(Z)||(1+\gamma_5)T_{KLs}||\phi_{\kappa_\nu}(-q)\rangle \\ &= g_{\kappa_e}(Z)[j_{l_\nu}G_{KLs}(\kappa_e,\kappa_\nu) - j_{\bar{l}_\nu}G_{KLs}(\kappa_e,-\kappa_\nu)] \\ &\quad + (\mathrm{sign}\kappa_e) f_{\kappa_e}(Z)[j_{l_\nu}G_{KLs}(-\kappa_e,\kappa_\nu) - j_{\bar{l}_\nu}G_{KLs}(-\kappa_e,-\kappa_\nu)]\end{aligned} \tag{2.34}$$

for the electron-antineutrino matrix element; and

$$\begin{aligned}(4\pi)^{1/2}&\langle\phi_{\kappa_e}(-Z)||(1+\gamma_5)T_{KLs}||\phi_{\kappa_\nu}(q)\rangle \\ &= g_{\kappa_e}(-Z)[j_{l_\nu}G_{KLs}(\kappa_e,\kappa_\nu) + j_{\bar{l}_\nu}G_{KLs}(\kappa_e,-\kappa_\nu)] \\ &\quad - (\mathrm{sign}\kappa_e) f_{\kappa_e}(-Z)[j_{l_\nu}G_{KLs}(-\kappa_e,\kappa_\nu) + j_{\bar{l}_\nu}G_{KLs}(-\kappa_e,-\kappa_\nu)]\end{aligned} \tag{2.35}$$

for the positron-neutrino matrix element. The quantity $G_{KLs}(n_f, n_i)$, introduced by Weidenmüller (1961), represents the spin-angular part of these reduced lepton matrix elements

$$\begin{aligned}&G_{KLs}(n_f,n_i) \\ &= \{(2s+1)(2K+1)[2l_f(n_f)+1][2l(n_i)+1](2j_f+1)(2j_i+1)\}^{1/2} \\ &\quad \times i^{l(n_i)+l(n_f)+L}(-1)^{j_i-j_f}\, C(l(n_f)l(n_i)L;00)\begin{Bmatrix} K & s & L \\ j_f & \frac{1}{2} & l(n_f) \\ j_i & \frac{1}{2} & l(n_i)\end{Bmatrix}.\end{aligned} \tag{2.36}$$

Here, we have $l(n) = n$ if $n > 0$ and $l(n) = |n| - 1$ if $n < 0$, where n stands for $+\kappa$ and $-\kappa$; C is a Clebsch–Gordan coefficient, and the braces denote a Wigner $9j$ symbol.

We now consider the relation between β^- and β^+ decay. It is easily shown that the following relations hold

$$\begin{aligned}(-1)^{1-s}&(4\pi)^{1/2}\langle\phi_{\kappa_e}(Z)||(1-\gamma_5)T_{KLs}||\phi_{\kappa_\nu}(-q)\rangle \\ &= g_{\kappa_e}(Z)[j_{l_\nu}G_{KLs}(\kappa_e,\kappa_\nu) + j_{\bar{l}_\nu}G_{KLs}(\kappa_e,-\kappa_\nu)] \\ &\quad - (\mathrm{sign}\kappa_e) f_{\kappa_e}(Z)[j_{l_\nu}G_{KLs}(-\kappa_e,\kappa_\nu) + j_{\bar{l}_\nu}G_{KLs}(-\kappa_e,-\kappa_\nu)].\end{aligned} \tag{2.37}$$

Thus we see from Eq. (2.35) that the product of the two reduced matrix elements in Eq. (2.30) can be replaced as follows

$$\begin{aligned}&\langle||(1+\lambda\gamma_5)T_{KLs}||\rangle\langle||(1-\gamma_5)T_{KLs}||\rangle \\ &\quad = \langle||T_{KLs}||\rangle\langle||(1-\gamma_5)T_{KLs}||\rangle \\ &\quad\quad - \langle||\lambda\gamma_5 T_{KLs}||\rangle\langle||\gamma_5(1-\gamma_5)T_{KLs}||\rangle .\end{aligned} \tag{2.38}$$

Consequently we can derive the formulae for β^+ decay from those for β^- decay by making the following substitutions

β^- decay		β^+ decay
λ	→	$-\lambda$
Z	→	$-Z$
G	→	$-G$.

(2.39)

Here, G represents the terms which are due to parity nonconservation (e.g., electron polarization or β–γ circular polarization correlation). The relation between β^+ decay and electron capture is established by the substitutions [cf., Eqs. (2.30), (2.31), (2.33), (2.35)]

β^+ decay		electron capture
$f_{\kappa_e}(-Z)$	→	$-f_{\kappa_e}(Z)$
$g_{\kappa_e}(-Z)$	→	$g_{\kappa_e}(Z)$,

(2.40)

where $g_{\kappa_e}(Z)$ and $f_{\kappa_e}(Z)$ are the large and small components of the bound-state electron radial wavefunctions, respectively. Alternatively, we can start from β^- decay [cf., Eqs. (2.29) and (2.34) vs. Eqs. (2.31) and (2.33)]

β^- decay		electron capture
$j_{l_\nu}(qr)$	→	$j_{l_\nu}(qr)$
$j_{\bar{l}_\nu}(qr)$	→	$-j_{\bar{l}_\nu}(qr)$
$\langle f\|\|(1+\lambda\gamma_5)T_{KLs}\|\|i\rangle$	→	$(-1)^s\langle f\|\|(1+\lambda\gamma_5)T_{KLs}\|\|i\rangle$
continuum-electron wavefunction	→	bound-electron wavefunction .

(2.41a)

For the decay probabilities as given in Eqs. (2.29) and (2.31), this prescription can be replaced by one mentioned by Behrens and Jänecke (1969):

β^- decay		electron capture
q	→	$-q$

$$\langle f||(1+\lambda\gamma_5)T_{KLs}||i\rangle \to (-1)^{K-s}\langle f||(1+\lambda\gamma_5)T_{KLs}||i\rangle . \tag{2.41b}$$

In this description of the electron-capture and β-decay processes, three important points have not been considered:

(1) The hadron current in the form of Eq. (2.4) is an approximation which is only valid for bare nucleons. The exact form of this current is discussed under the heading *Induced Interactions* in Sec. II.B.3.

(2) The Hamiltonian and transition matrix elements used here refer to a single-particle process. The description must be generalized for the case of many nucleons in the initial and final states. This point is discussed in Sec. II.B.3.

(3) A complete description of the initial and final states must include the electrons of the atomic cloud. Since the nuclear charge and the number of electrons are different in the initial and final states, the atomic-electron wave-

functions of these two states are not orthogonal, and the overlap between them is not perfect. This leads to some modifications of the transition rate (exchange and overlap corrections) and to higher-order processes (e.g., autoionization). These points are discussed in Secs. II.E and V.

B. Electron-capture transition rates

1. General relations for the transition probabilities

In discussing transition matrix elements and transition rates for the three weak nuclear decay modes, we have pointed out how these decay types are related. From here on, we consider electron capture only. We simplify Eq. (2.31), discuss the electron and neutrino radial wavefunctions in the lepton part, and generalize the hadron part through methods of elementary-particle physics.

We first note that Eq. (2.33) is invariant under the substitution $\kappa_\nu \to -\kappa_\nu$ and set $k_\nu = |\kappa_\nu|$. We also introduce the abbreviation (Bühring, 1963a, 1963b; Behrens and Bühring, 1971)

$$\beta_x[M_K(k_x,k_\nu)+(\kappa_x/k_x)m_K(k_x,k_\nu)] = \sum_{Ls}(4\pi)^{1/2}[(2J_i+1)(2K+1)]^{-1/2}(-1)^s \int \langle\phi_n||(1+\lambda\gamma_5)T_{KLs}||\phi_p\rangle$$
$$\times\{g_{\kappa_x}(Z)[j_{l_\nu}G_{KLs}(\kappa_x,k_\nu)+j_{\bar{l}_\nu}G_{KLs}(\kappa_x,-k_\nu)]$$
$$+(\mathrm{sign}\kappa_x)f_{\kappa_x}(Z)[j_{l_\nu}G_{KLs}(-\kappa_x,k_\nu)+j_{\bar{l}_\nu}G_{KLs}(-\kappa_x,-k_\nu)]\}r^2\,dr\,, \tag{2.42}$$

where $k_x = |\kappa_x|$, and β_x is the *Coulomb amplitude* (Behrens and Jänecke, 1969) of the bound-state electron radial wavefunction (ERWF), discussed in Sec. II.B.2. For $\kappa_x = -1$ we have $\beta_x = g_{-1}(0)$ equal to the value of the wavefunction $g_{-1}(r)$ at $r = 0$.

For the total capture probability from all atomic shells we then have

$$\lambda_c = (\ln 2)(t_c)^{-1} = G_\beta^2(2\pi^3)^{-1}\sum_x n_x C_x f_x \tag{2.43}$$

(Behrens and Jänecke, 1969; Bouchez and Depommier, 1960; Brysk and Rose, 1958). The sum in Eq. (2.43) extends over all atomic subshells from which an electron can be captured. For closed shells, n_x equals 1. For partially filled shells, n_x is equal to the relative occupation number of electrons in the shell. The quantity C_x corresponds to the shape factor of β decay. Taking into account only the lowest-order terms in the summation over κ and k_ν, C_x has the form

$$\begin{aligned} C_x = {} & [M_L(k_x,k_\nu^{(1)})+(\kappa_x/k_x)m_L(k_x,k_\nu^{(1)})]^2 \\ & + [M_L(k_x,k_\nu^{(2)})+(\kappa_x/k_x)m_L(k_x,k_\nu^{(2)})]^2 \\ & + [M_{L+1}(k_x,k_\nu^{(2)})+(\kappa_x/k_x)m_{L+1}(k_x,k_\nu^{(2)})]^2 \\ & + \delta_{\Delta J,0}[M_0(1,1)+(\kappa_x/k_x)m_0(1,1)]^2\,. \end{aligned} \tag{2.44}$$

The classification of allowed and forbidden electron-capture transitions is similar to that in β decay (Schopper, 1966; Konopinski, 1966; Behrens and Jänecke, 1969)

$$\begin{aligned} &\Delta J = 0,1 \quad \pi_i\pi_f = +1 \quad \text{allowed}\,, \\ &\Delta J = 0,1 \quad \pi_i\pi_f = -1 \quad \text{first nonunique forbidden}\,, \\ &\Delta J = n > 1 \quad \pi_i\pi_f = (-1)^n \quad n\text{th nonunique forbidden}\,, \\ &\Delta J = n > 1 \quad \pi_i\pi_f = (-1)^{n-1} \quad (n-1)\text{th unique forbidden}\,. \end{aligned} \tag{2.45}$$

Here, (J_i,π_i) and (J_f,π_f) denote spins and parities of the initial and final nuclear states, and we have $\Delta J = |J_i - J_f|$. Hence, we can write in Eq. (2.44)

$$\begin{aligned} &L = \Delta J \quad \text{for } \Delta J > 0 \\ &L = 1 \quad \text{for } \Delta J = 0 \\ &k_\nu^{(1)} = L - k_x + 1 \\ &k_\nu^{(2)} = L - k_x + 2\,. \end{aligned} \tag{2.46}$$

The quantities κ_x and k_x are related by Eq. (2.18) to the total angular momentum j_x and the orbital angular momentum l_x of the bound electron. Similarly, κ_ν and k_ν determine j_ν and l_ν of the continuum wavefunction of the emitted neutrino.

The values of κ_x for bound electrons are as follows

$K\,(1s)$ $\kappa_x = -1$	$M_1\,(3s)$ $\kappa_x = -1$
$L_1\,(2s)$ $\kappa_x = -1$	$M_2\,(3p_{1/2})$ $\kappa_x = +1$
$L_2\,(2p_{1/2})$ $\kappa_x = +1$	$M_3\,(3p_{3/2})$ $\kappa_x = -2$
$L_3\,(2p_{3/2})$ $\kappa_x = -2$	$M_4\,(3d_{3/2})$ $\kappa_x = +2$
	$M_5\,(3d_{5/2})$ $\kappa_x = -3\,.$

(2.47)

The function f_x in Eq. (2.43), which corresponds to the integrated Fermi function of β decay, has the form

$$f_x = (\pi/2)q_x^2\beta_x^2 B_x\,. \tag{2.48}$$

The factor B_x takes account of the effects of electron exchange and overlap; it is discussed in Sec. II.E.

2. Bound-state electron radial wavefunctions

The electron radial wavefunctions $f_\kappa(r)$ and $g_\kappa(r)$ are a solution of the Dirac radial differential equation or of the equivalent integral equation (Rose, 1961; Behrens and Bühring, 1971). It is convenient to consider instead the functions $H_k(r)$, $h_k(r)$, $D_k(r)$, and $d_k(r)$ introduced by Bühring (1963a)

$$\left.\begin{aligned} f_{k_x}(r) &= \beta_x (p_x r)^{k_x-1}[(2k_x-1)!!]^{-1} \\ &\quad \times [H_{k_x}(r) + h_{k_x}(r)] \end{aligned}\right\} \kappa_x > 0 , \tag{2.49a}$$

$$\left.\begin{aligned} g_{k_x}(r) &= \beta_x (p_x r)^{k_x-1}[(2k_x-1)!!]^{-1} \\ &\quad \times (r/R)[D_{k_x}(r) + d_{k_x}(r)] \end{aligned}\right\} \kappa_x > 0 , \tag{2.49b}$$

$$\left.\begin{aligned} f_{-k_x}(r) &= -\beta_x (p_x r)^{k_x-1}[(2k_x-1)!!]^{-1} \\ &\quad \times (r/R)[D_{k_x}(r) - d_{k_x}(r)] \end{aligned}\right\} \kappa_x < 0 . \tag{2.49c}$$

$$\left.\begin{aligned} g_{-k_x}(r) &= \beta_x (p_x r)^{k_x-1}[(2k_x-1)!!]^{-1} \\ &\quad \times [H_{k_x}(r) - h_{k_x}(r)] \end{aligned}\right\} \kappa_x < 0 . \tag{2.49d}$$

Here, R is the nuclear radius, or equivalent radius of a uniformly charged nucleus.

The first of two aspects of the electron radial wavefunctions that require more detailed consideration is the behavior of these functions inside the nucleus: the dependence of the electron and neutrino radial wavefunctions on the distance r from the center of the nucleus must be subsumed into the nuclear matrix elements [cf. Eq. (2.42)]. The r-dependence of the electron radial wavefunctions inside the nucleus depends essentially on the form of the nuclear charge distribution.

Secondly, the Coulomb amplitudes β_x must be considered; they can only be calculated numerically by solving the Dirac equation for an extended nucleus and for a self-consistent atomic potential. The value of β_x is essentially determined by the shape of the charge distribution of the surrounding atomic electrons.

In many of the earlier papers on β decay and electron capture, the expansion of the functions $H_k(r)$, $D_k(r)$, $h_k(r)$, and $d_k(r)$ in powers of r is carried out (Behrens and Bühring, 1970)

$$H_k(r) = \sum_{n=0}^{\infty} H_n(k)(r/R)^n ; \tag{2.50}$$

the different powers of r are then incorporated into the definition of the nuclear matrix elements (Behrens and Jänecke, 1969; Bühring, 1963a, b). The nuclear charge distribution has been approximated throughout by a uniformly charged sphere of radius R, equal to the nuclear radius. Because this charge distribution is discontinuous at R, the power-series expansion of the electron radial wavefunctions is only valid inside the nucleus. Usable β-decay and electron-capture formulae have been derived by truncating this series and extrapolating the resulting polynomials outside the nuclear radius (Behrens and Jänecke, 1969; Bühring, 1963a). However, this approach is unsatisfactory: contrary to general belief, a significant contribution (or even the main contribution) to the nuclear matrix elements originates from the region $r > R$, particularly if the initial and final nucleons are in different shells (Behrens and Bühring, 1971; de Raedt, 1968).

It might be expected that this difficulty could be avoided by using a more realistic, smooth nuclear charge distribution, such as a modified Gaussian or a Fermi distribution. However, for such distributions the β-decay and electron-capture formulae do not converge at all (Behrens and Bühring, 1970, 1971), because the nuclear matrix elements are introduced by integrating a power series term by term, a dubious procedure if the upper limit of the integral is infinity. Only if the potential $V(r)$ vanishes identically, as for the neutrino, is this procedure justified. Thus the neutrino radial wavefunctions (spherical Bessel functions) can be expanded in powers of r. The electron radial wavefunctions, on the other hand, can be expanded in powers of the mass and energy parameters of the electron and the nuclear charge. The coefficients in this expansion still are functions of r and depend on the shape of the charge distribution. We find (Behrens and Bühring, 1971)

$$H_{k_x}(r) = \sum_{\mu=0}^{\infty} \sum_{\nu=0}^{\mu} \sum_{\rho=0}^{2\nu} \frac{(2k_x-1)!!}{(2\mu)!!(2\mu+2k_x-1)!!} (-1)^{\nu} \binom{\mu}{\nu} \binom{2\nu}{\rho} \left(\frac{r}{R}\right)^{2\mu} I(k_x, 2\mu, 2\nu, \rho; r)(m_e R)^{2\mu-2\nu}(W_x R)^{2\nu-\rho}(\alpha Z)^{\rho} , \tag{2.51a}$$

$$h_{k_x}(r) = \sum_{\mu=1}^{\infty} \sum_{\nu=1}^{\mu} \sum_{\rho=1}^{2\nu-1} \frac{(2k_x-1)!!}{(2\mu)!!(2\mu+2k_x-1)!!} (-1)^{\nu} \binom{\mu}{\nu} \binom{2\nu-1}{\rho} \left(\frac{r}{R}\right)^{2\mu} I(k_x, 2\mu, 2\nu-1, \rho; r)(m_e R)^{2\mu-2\nu+1}(W_x R)^{2\nu-1-\rho}(\alpha Z)^{\rho} , \tag{2.51b}$$

$$D_{k_x}(r) = \sum_{\mu=0}^{\infty} \sum_{\nu=0}^{\mu} \sum_{\rho=0}^{2\nu+1} \frac{(2k_x-1)!!}{(2\mu)!!(2\mu+2k_x+1)!!} (-1)^{\nu} \binom{\mu}{\nu} \binom{2\nu+1}{\rho} \left(\frac{r}{R}\right)^{2\mu} I(k_x, 2\mu+1, 2\nu+1, \rho; r)(m_e R)^{2\mu-2\nu}(W_x R)^{2\nu+1-\rho}(\alpha Z)^{\rho} , \tag{2.51c}$$

$$d_{k_x}(r) = \sum_{\mu=0}^{\infty} \sum_{\nu=0}^{\mu} \sum_{\rho=0}^{2\nu} \frac{(2k_x-1)!!}{(2\mu)!!(2\mu+2k_x+1)!!} (-1)^{\nu} \binom{\mu}{\nu} \binom{2\nu}{\rho} \left(\frac{r}{R}\right)^{2\mu} I(k_x, 2\mu+1, 2\nu, \rho; r)(m_e R)^{2\mu+1-2\nu}(W_x R)^{2\nu-\rho}(\alpha Z)^{\rho} . \tag{2.51d}$$

The symbol m_e has been retained in these equations, even though we use natural units $\hbar = c = m_e = 1$, because m_e will be used as an expansion parameter. The expansion coefficients $I(k_x, m, n, \rho; r)$ depend on the form of the nuclear charge distribution and on the parameters k_x, m, n, and ρ. The order m is the sum of the exponents of $(m_e R)$, (WR), and αZ; the number n is the sum of the exponents of (WR) and (αZ). The functions I with $\rho = 0$ are trivial

$$I(k_x, m, n, 0; r) \equiv 1 . \tag{2.52}$$

The functions I with $\rho > 0$, up to order $m = 3$, are listed

in Appendix 2 (Behrens and Bühring, 1971). For $\alpha Z = 0$, Eqs. (2.51) reduce to the usual expansion in powers of r (Bühring, 1963a).

Up to and including terms of order $\mu = 0$, the functions $H_{k_x}(r)$, $h_{k_x}(r)$, $D_{k_x}(r)$, and $d_{k_x}(r)$ are

$$H_{k_x}(r) = 1 + \cdots , \tag{2.53a}$$

$$h_{k_x}(r) = 0 + \cdots , \tag{2.53b}$$

$$D_{k_x}(r) = \frac{W_x R}{2k_x + 1} + \frac{\alpha Z}{2k_x + 1} I(k_x, 1, 1, 1; r) + \cdots , \tag{2.53c}$$

$$d_{k_x}(r) = \frac{m_e R}{2k_x + 1} + \cdots . \tag{2.53d}$$

As usual, α is the fine-structure constant, and Z is the atomic number of the parent nucleus.

The important function $I(k_x, 1, 1, 1; r)$, which gives the large Coulomb terms in nonunique forbidden transitions, takes the following form for the three most widely used charge distributions (Behrens and Bühring, 1970, 1971):

(i) For a uniform charge distribution

$$\rho(r) = \begin{cases} -3\alpha Z/R, & 0 \le r \le R \\ 0, & R < r \le \infty \end{cases} \tag{2.54}$$

we have (Behrens and Bühring, 1971)

$$I(k_x, 1, 1, 1; r) = \begin{cases} \dfrac{3}{2} - \dfrac{2k_x + 1}{2(2k_x + 3)} \left(\dfrac{r}{R}\right)^2, & 0 \le r \le R \\ \dfrac{2k_x + 1}{2k_x} \dfrac{R}{r} - \dfrac{3}{2k_x(2k_x + 3)} \left(\dfrac{R}{r}\right)^{2k_x + 1}, & R \le r . \end{cases} \tag{2.55}$$

(ii) In a shell-model or modified Gaussian distribution (Behrens and Bühring, 1970)

$$\rho(r) = N\{1 + A(r/a)^2\} e^{-(r/a)^2} , \tag{2.56a}$$

where

$$N = -8\alpha Z/(2 + 3A) a^3 \sqrt{\pi} , \tag{2.56b}$$

the equivalent uniform radius R is related to the parameters a and A as

$$R = a[5(2 + 5A)/2(2 + 3A)]^{1/2} ; \tag{2.57}$$

for this distribution, we have

$$I(k_x, 1, 1, 1; r) = \frac{2k_x + 1}{2k_x} \frac{R}{r} \left\{ \operatorname{erf}(y) - \left(1 + \frac{2k_x A}{2 + 3A}\right) \frac{(2k_x - 1)!!}{2k_{x_y} 2k_x} \times \left[\operatorname{erf}(y) - \frac{2}{\sqrt{\pi}} e^{-y^2} \sum_{m=0}^{k_x - 1} \frac{2^m y^{2m+1}}{(2m+1)!!} \right] \right\} , \tag{2.58}$$

where $\operatorname{erf}(y)$ is the error function,

$$\operatorname{erf}(y) = 2\pi^{-1/2} \int_0^y e^{-t^2} dt, \quad y = \beta r/R$$

and

$$\beta = [5(2 + 5A)/2(2 + 3A)]^{1/2} .$$

(iii) For a Fermi distribution (Behrens and Bühring, 1970)

$$\rho(r) = -3\alpha Z c^{-3} N [1 + e^{(r-c)/b}]^{-1} , \tag{2.59}$$

with

$$N = [1 + \pi^2 (b/c)^2 - 6 w_3(b, c; 0)]^{-1} ,$$

the equivalent uniform radius R is

$$R = c \left[\frac{3c^5 + 10\pi^2 c^3 b^2 + 7\pi^4 c b^4 - 360 b^5 w_5(b, c; 0)}{3c^5 + 3\pi^2 c^3 b^2 - 18 c^2 b^3 w_3(b, c; 0)} \right]^{1/2} . \tag{2.60}$$

The function $I(k_x, 1, 1, 1; r)$ takes the form

$$I(k_x, 1, 1, 1; r) = \frac{3}{2} \frac{R}{c} N \left\{ 1 + \frac{1}{3}\pi^2 \left(\frac{b}{c}\right)^2 - \frac{1}{3} \frac{2k_x + 1}{2k_x + 3} \left(\frac{r}{c}\right)^2 - 2(2k_x + 1) \frac{c}{r} \left[w_3(b, c; r) - \frac{1}{k_x} w_3(b, c; 0) \right] + 2(2k_x + 1)(2k_x + 2) \left(\frac{c}{r}\right)^2 \sum_{m=0}^{2k_x - 1} (-1)^m \frac{(2k_x - 1)!}{(2k_x - 1 - m)!} \left(\frac{c}{r}\right)^m w_{4+m}(b, c; r) \right\} , \tag{2.61}$$

where the functions w_n are defined as

$$w_n(b, c; r) = \begin{cases} \left(\dfrac{b}{c}\right)^n \displaystyle\sum_{m=1}^{\infty} (-1)^m m^{-n} (e^{(r-c)/b})^m , & r \le c \\ \left(\dfrac{b}{c}\right)^n \displaystyle\sum_{m=0}^{[n/2]} a_m^{(n)} \left(\dfrac{r - c}{b}\right)^{n-2m} + (-1)^{n-1} \displaystyle\sum_{m=1}^{\infty} (-1)^m m^{-n} (e^{-(r-c)/b})^m , & r \ge c \end{cases} \tag{2.62}$$

(Schucan, 1965). Here, $a_m^{(n)}$ stands for

$$a_m^{(n)} = (-1)^m \frac{(2^{2m} - 2)}{(2m)!(n - 2m)!} B_{2m} ,$$

where the B_{2m} are Bernoulli numbers

$$B_0 = 1, \quad B_2 = \tfrac{1}{6}, \quad B_4 = -\tfrac{1}{30}, \quad B_6 = \tfrac{1}{42}, \ldots .$$

At $r = c$, w_n is given by

$$w_n(b, c; c) = \left(\frac{b}{c}\right)^n \sum_{m=1}^{\infty} (-1)^m m^{-n} = \left(\frac{b}{c}\right)^n (2^{1-n} - 1)\zeta(n) , \tag{2.63}$$

where $\zeta(n)$ is the Rieman zeta function.

The functions $I(k_x, 1, 1, 1)$ [Eqs. (2.55), (2.58), and (2.61)] have been derived neglecting the small influence of the atomic electron cloud on the r dependence of the electron radial wavefunctions inside the nucleus. These functions are illustrated in Fig. 1.

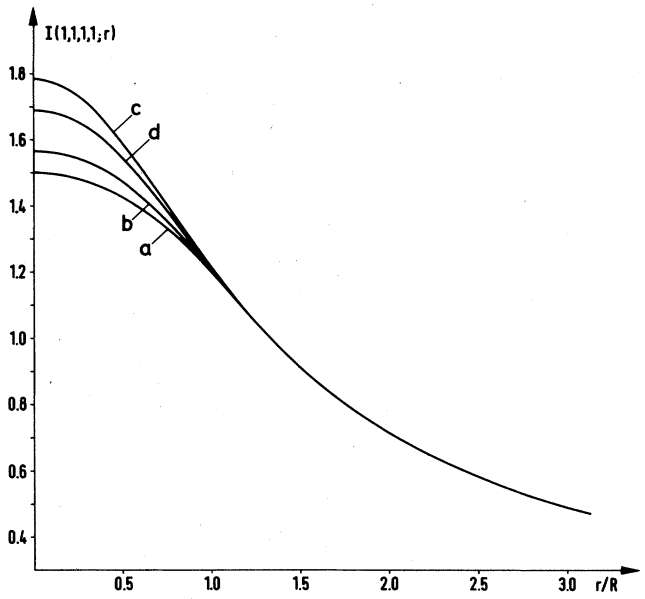

FIG. 1. The function $I(1,1,1;r)$ vs distance r from the origin (in multiples of the nuclear radius R) for various nuclear charge distributions: (a) uniform charge distribution [Eq. (2.55)]; (b) Fermi distribution, with $t=0.4R$ [Eq. (2.61)]; (c) Gaussian distribution, with $A=0$ [Eq. (2.58)]; (d) modified Gaussian distribution, with $A=1$.

We consider next the Coulomb amplitudes β_x of the bound atomic electrons. These quantities can be calculated by integrating the Dirac equation in the potential of the nuclear and atomic charge distributions.[6] The value of β_x is essentially determined by the potential outside the nucleus, i.e., by the electronic screening of the nuclear electrostatic field. The finite nuclear size and the shape of the nuclear charge distribution have less influence on β_x. The potential produced by the nuclear charge and the atomic electron cloud can be derived approximately from statistical models (Gombas, 1956, 1967), by solving the Thomas–Fermi or the Thomas–Fermi–Dirac equations. A more exact form of the potential can be derived through self-consistent Hartree–Fock methods (Hartree, 1957; Slater, 1960; Mayers, 1972; Burke and Grant, 1967; Grant, 1970; Lindgren and Rosén, 1974).

Both methods of finding the extranuclear potential can only be carried out numerically and have been pursued by many investigators. The Thomas–Fermi and Thomas–Fermi–Dirac equations have been solved for potentials and eigenvalues, for example, by Gombas (1956), Thomas (1954), Latter (1955), Shalitin (1965, 1967), and Yonei (1966, 1967). The self-consistent field methods offer the best possibility for obtaining good atomic electron wavefunctions, but require extensive numerical calculations (Hartree, 1957; Slater, 1960; Mayers, 1972; Burke and Grant, 1967; Grant, 1970; Lindgren and Rosén, 1974). In a simplification first introduced by Slater (1960, Vol. 2), the exact exchange potential is approximated by the exchange potential of an electron gas with local electron density $\rho(r)$, i.e.,

$$V_{ex}(r)=\frac{3}{2}\alpha\,\frac{3\rho(r)^{1/3}}{\pi}\,. \tag{2.64}$$

This Slater exchange potential tends to zero as the radius becomes large, while the exact potential tends to α/r. To correct this discrepancy, Latter (1955) has suggested replacing the Slater term in the region of large radius by α/r. Statistical exchange potentials have been discussed extensively by Gombas (1967).

Herman and Skillman (1963) have tabulated nonrelativistic Hartree–Fock–Slater potentials and wavefunctions for elements with $Z=2$–103, including the Latter tail correction. Extensive nonrelativistic calculations with the exact Hartree–Fock form of the exchange potential have been performed by Froese-Fischer (1972b) and Mann (1967, 1968). Approximate analytic nonrelativistic Hartree–Fock wavefunctions have been derived by Watson and Freeman (1961a,b), Malli (1966), and Roetti and Clementi (1974).

Because relativistic effects in atomic structure are remarkably important, even for light elements, a number of relativistic self-consistent-field calculations (mostly Hartree–Fock–Slater) have been carried out (Liberman *et al.*, 1965; Nestor *et al.*, 1966; Tucker *et al.*, 1969). Most comprehensive is the work of Lu *et al.* (1971), who have published tables of energies and of expectation values of r, r^{-1}, r^{-3}, r^2, and r^4 for each orbital, of the total energy, and of the potential function. They have included the effect of finite nuclear size, using a Fermi charge distribution.

The possibility of making better approximations than Slater's for the exchange potential has been discussed by Kohn and Sham (1965), Rosén and Lindgren (1968), and Lindgren and Schwarz (1971).

The most sophisticated method of calculating atomic wavefunctions involves the use of relativistic Hartree–Fock codes; here the exchange term is included without approximation (see, e.g., Mann and Waber, 1973; Desclaux, 1973).

Unfortunately, in most published atomic-structure calculations, no explicit values are given for the Coulomb amplitudes or electron wavefunctions at the nuclear radius. For applications to electron capture, special calculations have therefore been carried out; these are listed in Table I. For comparison among the various calculations, the most important electron radial wavefunction ratios are listed in Tables II–VIII. For s electrons, the nonrelativistic ratios for a point nucleus are included in the comparison. For $p_{1/2}$ electrons, on the other hand, it is meaningless to compare nonrelativistic wavefunctions in the field of a point nucleus (proportional to ar at small r) with relativistic electron wavefunctions in the field of a finite nucleus [proportional to $b(1+cr^2+\cdots)$]. We also do not compare absolute values of electron wavefunctions, nor do we list other ratios than those contained in Tables II–VIII, because the magnitudes of the nuclear radius R chosen by different authors are not the same, and moreover, some authors report $g_\kappa(R)$ and $f_\kappa(R)$, while others instead report the amplitudes β_x.

We can draw the following conclusions from Tables

[6]The electron radial wave functions can also be calculated approximately as hydrogenic wavefunctions for a point nucleus of charge reduced by the appropriate Slater screening constants (Slater, 1930).

TABLE I. List of calculations of electron radial wavefunctions inside or near the nucleus.

References	R/NR[a]	Atomic potential[b]	Nuclear charge distribution	Z	Shells	Remarks
Brysk and Rose (1955)	R	TFD	Uniform	10–100	K,L	Results presented graphically
Band *et al.* (1956, 1958)	R	TFD	Uniform	18–98	K,L	
Brewer *et al.* (1961)	R	TFD	Uniform	55–90	M	Every fifth atomic number is listed
Watson and Freeman (1961)	NR	HF	Point	3–42	All	Analytical wave functions are used
Herman and Skillman (1963)	NR	HFS	Point	2–100	All	
Winter (1968)	NR[c]	HF	Point	3–42	K,L	L_1/K ratios only
Behrens and Jänecke (1969)	R	HF ($Z<36$) TFD ($Z\geq 36$)	Uniform	1–102	K,L,M	
Suslov (1969, 1970b)	R	NR HFS ($Z<72$) R HFS ($Z\geq 72$)	Uniform	2–98	K,L,M N_1,N_2	
Martin and Blichert-Toft (1970)	R	HFS[d]	Fermi	5–98	K,L	
Froese-Fischer (1972b)	NR	HF	Point	2–86	All	
Mann and Waber (1973)	R	HF	Fermi	1–102	All	

[a] NR = nonrelativistic; R = relativistic.
[b] TFD = Thomas–Fermi–Dirac; HF = Hartree–Fock; HFS = Hartree–Fock–Slater.
[c] Supplementary relativistic corrections are applied to results from NR analytic wavefunctions of Watson and Freeman (1961) and Malli (1966).
[d] Nestor *et al.* (1966); Tucker *et al.* (1969); Lu *et al.* (1971).

II–VIII:

(1) For the s-electron ratios (Tables II-V), there is excellent agreement between the nonrelativistic Hartree–Fock calculations of Froese-Fischer (1972b) and Winter (1968) and the relativistic Hartree–Fock calculations of Mann and Waber (1973). An exception is the $g^2_{O_1}/g^2_{N_1}$ ratio. However, here relativistic effects might play some role because of the high atomic numbers ($Z \geq 70$).

(2) Relativistic effects become notable in $g^2_{L_1}/g^2_K$ for $Z > 15$, in $g^2_{M_1}/g^2_{L_1}$ for $Z > 30$, and in $g^2_{N_1}/g^2_{M_1}$ and $g^2_{O_1}/g^2_{N_1}$ for $Z > 60$. For $g^2_{L_1}/g^2_K$, relativistic and nonrelativistic ratios differ by ~50% for very heavy nuclei. For all other ratios, relativistic effects are small (less than 2% for the $g^2_{M_1}/g^2_{L_1}$ and $g^2_{N_1}/g^2_{M_1}$, less than 8% for the $g^2_{O_1}/g^2_{N_1}$).

(3) The electron radial wavefunction ratios from Hartree–Fock calculations lie systematically below those from Hartree–Fock–Slater and Thomas–Fermi–Dirac calculations, especially for low atomic numbers.

(4) For the K, L, and M ratios, the Hartree–Fock–Slater calculations agree with the Thomas–Fermi–Dirac calculations to within 2.5% for $Z > 40$.

(5) The $g^2_{L_1}/g^2_K$ ratios of Brysk and Rose (1958) deviate systematically from all other calculations in the range $20 < Z < 80$ (Table II). Therefore, these values should be discarded.

Of the various methods discussed above, the self-consistent relativistic Dirac–Hartree–Fock calculations of atomic structure are based on the soundest theoretical grounds (Mayers, 1972; Burke and Grant, 1967). It might consequently be expected that the wavefunctions of Mann and Waber (1973) would be most accurate, and should preferably be used for analyzing electron-capture experiments.[7] Table IX contains a compilation of electron radial wavefunction amplitudes according to Mann and Waber (1973). For practical reason, we have listed the products $\beta_\varkappa p_\varkappa^{k_\varkappa - 1}$ instead of

[7] However, for the inner shells and for medium and high atomic numbers, there is only a negligible difference between the wavefunctions of Mann and Waber (1973) and those from Hartree–Fock–Slater calculations (Suslov, 1969 and 1970b; Dzhelepov *et al.*, 1972; Martin and Blichert-Toft, 1970) or Thomas–Fermi–Dirac calculations (Behrens and Jänecke, 1969; Band *et al.*, 1956, 1958).

TABLE II. Calculated electron radial wavefunction ratios $g_{L_1}^2/g_K^2$.

	Nonrelativistic					Relativistic						HF	
	HFS	HF		Brysk and	TFD			HFS	Calculated[a] with the				
Z	Herman and Skillman (1963)	Froese-Fischer (1972b)	Winter (1968)	Rose (1958)	Band *et al.* (1956, 1958)	Behrens and Jänecke (1969)	Suslov (1969, 1970)	Martin and Blichert-Toft (1970)	codes of Fricke *et al.* (1971)	Winter (1968) corrected[b]	Mann and Waber (1973)
5	0.049	0.041	0.041				0.049	0.041	0.049	0.041	0.041
10	0.058	0.055	0.055	0.075			0.059	0.058	0.059	0.055	0.055
15	0.075	0.074	0.074	0.079		0.077	0.076	0.076	0.076	0.074	0.074
20	0.085	0.084	0.084	0.083	0.085	0.086	0.086	0.086	0.086	0.086	0.086
30	0.095	0.095	0.095	0.093	0.099	0.100	0.100	0.100	0.100	0.099	0.099
40	0.101	0.101		0.103	0.109	0.109	0.109	0.109	0.109	0.108	0.109
50	0.104	0.105		0.113	0.118	0.118	0.119	0.118	0.118		0.118
60	0.107	0.107		0.125	0.128	0.128	0.128	0.128	0.128		0.127
70	0.109	0.109		0.137	0.139	0.140	0.140	0.139	0.139		0.138
80	0.110	0.111		0.151	0.153	0.154	0.152	0.152	0.152		0.151
90	0.111			0.166	0.169	0.170	0.167	0.167	0.168		0.167
100	0.112			0.184		0.190			0.187		0.186

[a] The parameters in the Slater exchange term [Eq. (6) of Fricke *et al.* (1971)] are $C=1$, $n=1$, and $m=1$.
[b] Nonrelativistic results multiplied by a correction factor for relativistic effects.

the amplitudes β_x. It is always this product which appears in the formulae for the decay constant [Eq. (2.49)].

Because the electron-capture rate is essentially proportional to the electron density at the nucleus, different chemical environments or other macroscopic perturbations (pressure, temperature, etc.) can affect the decay constant. Such effects are most noticeable in capture from outer electron shells (Emery 1972; Crasemann, 1973).

3. Nuclear form factors and nuclear matrix elements

a. Form factors and form-factor coefficients

The electron-capture transition matrix elements [Eq. (2.7c)] were formulated in Sec. II.A under the assumption that the vector and axial vector interactions govern the process. However, the hadron part of this transition matrix element is only an approximation. In the most general case, we must make the substitution

$$\langle i\bar{u}_n\gamma_\mu(1+\lambda\gamma_5)u_p\rangle \to \langle f|\,V_\mu - A_\mu\,|i\rangle \tag{2.65}$$

in Eq. (2.7c), where f and i represent the final and initial nuclear states, respectively. The vector and axial vector hadron weak current are denoted by V_μ and A_μ. According to Stech and Schülke (1964) and Schülke (1964), we decompose this $V-A$ nuclear current into form factors depending on the square of the momentum transfer (Armstrong and Kim, 1972; Bottino and Ciochetti, 1973; Donnelly and Walecka, 1972, 1973; Holstein, 1974). We use a covariant decomposition, which is strictly valid in the Breit system. A transformation in the frame in which the initial nucleus is at rest is easily performed because the decay energies are low compared with the nuclear rest masses. The correction due to this transformation is of the order $|\mathbf{k}|/M$, where $\mathbf{k}$ is the momentum of the nucleus and M is its mass. In this approximation, the hadron matrix element depends only on the momentum transfer $\mathbf{q}=\mathbf{k}_f-\mathbf{k}_i$. It can be expanded as

$$\begin{aligned}\langle f|\,V_\mu - A_\mu\,|i\rangle\gamma_4\gamma_\mu &= \sum_{KLsM}(-1)^{J_f-M_f+M}(-1)^L(4\pi)^{1/2}(2J_i+1)^{1/2}\\ &\times\begin{pmatrix} J_f & K & J_i\\ -M_f & M & M_i\end{pmatrix} T^{-M}_{KLs}(\hat{q})\,\frac{(qR)^L}{(2L+1)!!}F_{KLs}(q^2).\end{aligned} \tag{2.66}$$

Here, T_{KLs} is the irreducible tensor defined by Eqs. (2.12); J_i, J_f and M_i, M_f denote the spins and magnetic quantum numbers of the initial and final nuclear states, respectively, and R is the nuclear radius.

This treatment of the nuclear current, similar to methods used in elementary-particle physics, has the advantage of being completely independent of any assumption about the detailed form of the β-decay operators. All information about the nuclear current and all effects due to the strong interaction (induced terms, exchange currents, relativistic nucleon motion inside the nucleus, etc.) are contained in the form factors $F_{KLs}(q^2)$; they determine the outcome of β decay and electron-capture experiments, and are the only quantities, as far as nuclear structure is concerned, that can

TABLE III. Calculated electron radial wavefunction ratios $g^2_{M_1}/g^2_{L_1}$.

	Nonrelativistic					Relativistic		
	HFS	HF		TFD		HFS		HF
Z	Herman and Skillman (1963)	Watson and Freeman (1961)	Froese–Fischer (1972b)	Brewer *et al.*[a] (1961)	Behrens and Jänecke (1969)	Suslov (1969, 1970)	Calculated with the codes of Fricke *et al.* (1971)	Mann and Waber (1973)
15	0.095	0.075	0.076			0.095	0.095	0.076
20	0.132	0.118	0.119			0.133	0.133	0.119
25	0.144	0.134	0.136			0.145	0.145	0.136
30	0.148	0.144	0.143		0.162	0.150	0.150	0.144
40	0.174		0.172		0.184	0.176	0.176	0.174
50	0.194		0.193		0.201	0.197	0.196	0.195
60	0.208		0.208	0.216	0.214	0.212	0.211	0.210
70	0.218		0.218	0.228	0.224	0.224	0.222	0.222
80	0.225		0.225	0.237	0.233	0.231	0.231	0.230
90	0.231			0.242	0.240	0.237	0.238	0.237
100	0.235				0.245		0.243	0.242

[a]Here, $g^2_{L_1}$ has been taken from the tables of Behrens and Jänecke (1969).

be extracted from experimental data.

We neglect, for the moment, the initial electromagnetic interaction between electron and nucleus, i.e., the fact that there is a bound electron in the initial state. Then the form factors $F_{KLs}(q^2)$ can be expanded in powers of q^2 [in analogy with the expansion of spherical Bessel functions (Stech and Schülke, 1964)]

$$F_{KLs}(q^2)=F^0_{KLs}-\frac{(qR)^2}{2(2L+3)}F^1_{KLs}+\cdots. \tag{2.67}$$

The form-factor coefficients are then

$$F^N_{KLs}=\frac{(-1)^N(2N+2L+1)!!(2N)!!}{R^{2N}(2L+1)!!N!}\left(\frac{d}{dq^2}\right)^N F_{KLs}(q^2)\Big|_{q^2=0}. \tag{2.68}$$

These form-factor coefficients contain all the information about the initial and final nuclear states and the $V-A$ operator. Since q equals W_0 if the initial nucleus is at rest, we have $qR<0.1$, whence the form factors are slowly varying functions of q^2. Therefore, only the first one or two terms will be significant.

In reality, however, we must take into account the fact that there is a bound-state electron wavefunction in the initial state. Hence the momentum transfer $\mathbf{q}_N$ to the nucleus is $\mathbf{q}_N=\mathbf{p}_e-\mathbf{q}_x$ if the center of mass of the initial nucleus and electron is at rest. The Fourier transform[8] of the lepton part of Eq. (2.10c) is

$$L(\mathbf{q}_N)=\int e^{-i\mathbf{q}_N\cdot\mathbf{r}}\bar{u}_\nu\gamma_\mu(1+\gamma_5)\phi_{e^-}(r)\,d^3r \tag{2.69}$$

or

$$L(\mathbf{q}_N)=\bar{u}_\nu\gamma_\mu(1+\gamma_5)\phi_{e^-}(\mathbf{q}_N+\mathbf{q}_x) \tag{2.70}$$

TABLE IV. Calculated electron radial wavefunction ratios $g^2_{N_1}/g^2_{M_1}$.

	Nonrelativistic			Relativistic		
	HFS	HF		HFS		HF
Z	Herman and Skillman (1963)	Watson and Freeman (1961)	Froese–Fischer (1972b)	Suslov (1969, 1970); Dzhelepov *et al.* (1972)	Calculated with the codes of Fricke *et al.* (1971)	Mann and Waber (1973)
35	0.116	0.094	0.094		0.116	0.094
40	0.162		0.143	0.163	0.162	0.143
45	0.184		0.168	0.186	0.185	0.167
50	0.203		0.188	0.206	0.204	0.189
60	0.233		0.224	0.236	0.235	0.225
70	0.237		0.232	0.245	0.243	0.236
80	0.251		0.248	0.257	0.257	0.251
90	0.266			0.271	0.271	0.267
100	0.279				0.283	0.279

[8]The Fourier transform of the electron wavefunction $\phi_{e^-}(r)$ is

$$\phi_{e^-}(\mathbf{p}_e)=\int e^{-i\mathbf{p}_e\cdot\mathbf{r}}\phi_{e^-}(\mathbf{r})\,dr^3.$$

TABLE V. Calculated electron radial wavefunction ratios $g^2_{O_1}/g^2_{N_1}$.

	Nonrelativistic		Relativistic	
	HFS	HF	HFS	HF
Z	Herman and Skillman (1963)	Froese–Fischer (1972b)	Calculated with the codes of Fricke *et al.* (1971)	Mann and Waber (1973)
70	0.155	0.135	0.161	0.146
75	0.182	0.163	0.186	0.171
80	0.203	0.183	0.208	0.192
85	0.229	0.211	0.232	0.216
90	0.252		0.252	0.239
95	0.263		0.266	0.254
100	0.272		0.278	0.279

(Schopper, 1966; Stech and Schülke, 1964). Hence Eq. (2.7c) becomes

$$M_{\mathrm{EC}} \approx \int \langle f | V_\mu - A_\mu | i' \rangle \bar{u}_\nu \gamma_\mu (1+\gamma_5) \phi_{e^-}(\mathbf{q}'_N + \mathbf{q}_x)\, d\mathbf{q}'_N. \tag{2.71}$$

The hadron matrix element corresponds to a transition from the initial state i' to the final state f, whereas the Fourier transform $\phi_{e^-}(\mathbf{q}'_N + \mathbf{q}_x)$ induces an electromagnetic transition from i to i'. The integral over q'_N corresponds to an integration over all momenta of the intermediate initial states, because we have $\mathbf{q}'_N = -\mathbf{k}'_i - \mathbf{q}_x$. The Coulomb interaction in the initial state therefore entails that terms of the form

$$\int_0^\infty I(q'_N) F_{KLs}(q'^2_N) q'^2_N\, dq'_N \tag{2.72}$$

appear in electron-capture formulae (Schülke, 1964), where $I(q'_N)$ has four different possible forms [Eq. (2.42)]

$$I(q'_N) = \frac{(q'_N R)^L}{(2L+1)!!} \begin{cases} \int g_\kappa(r) j_L(q_x r) j_L(q'_N r) r^2\, dr \\ \int g_\kappa(r) j_{\bar{L}}(q_x r) j_L(q'_N r) r^2\, dr \\ \int f_\kappa(r) j_L(q_x r) j_L(q'_N r) r^2\, dr \\ \int f_\kappa(r) j_{\bar{L}}(q_x r) j_L(q'_N r) r^2\, dr. \end{cases} \tag{2.73}$$

By expanding the spherical Bessel functions in powers of r and the electron radial wavefunctions $g_\kappa(r)$ and $f_\kappa(r)$ as discussed in Sec. II.B.2 [Eqs. (2.49) and (2.51)], we obtain new form-factor coefficients (Behrens and Bühring, 1971)

TABLE VI. Calculated relativistic electron radial wavefunction ratios $f^2_{L_2}/g^2_{L_1}$.

	TFD			HFS		HF
Z	Brysk and Rose (1955)	Band *et al.* (1956, 1958)	Behrens and Jänecke (1969)	Suslov (1969, 1970b); Dzhelepov *et al.* (1972)	Martin and Blichert-Toft (1970)	Calculated with the codes of Fricke *et al.* (1971)	Mann and Waber (1973)
10	0.001			0.000 52	0.000 53	0.000 52	0.000 46
15	0.002		0.001 60	0.001 55	0.001 55	0.001 55	0.001 43
20	0.003	0.002 35	0.003 18	0.003 08	0.003 06	0.003 06	0.002 90
25	0.005	0.004 92	0.005 25	0.005 15	0.005 12	0.005 12	0.004 89
30	0.007	0.007 51	0.007 86	0.007 78	0.007 74	0.007 74	0.007 46
40	0.013	0.0145	0.0149	0.0148	0.0147	0.0147	0.0143
50	0.022	0.0241	0.0247	0.0246	0.0244	0.0244	0.0238
60	0.034	0.0368	0.0377	0.0376	0.0371	0.0371	0.0364
70	0.052	0.0538	0.0548	0.0546	0.0538	0.0538	0.0527
80	0.077	0.0757	0.0771	0.0755	0.0755	0.0754	0.0741
90	0.111	0.1056	0.1068	0.1043	0.1042	0.1041	0.1023
100	0.154		0.1474			0.1432	0.1407

TABLE VII. Calculated relativistic electron radial wavefunction ratios $f^2_{M_2}/g^2_{M_1}$.

	TFD		HFS		
Z	Brewer *et al.* (1961)	Behrens and Jänecke (1969)	Suslov (1969, 1970b) Dzhelepov *et al.* (1972)	Calculated with the codes of Fricke *et al.* (1971)	Mann and Waber (1973)
15			0.001 12	0.001 11	0.001 02
20			0.002 82	0.002 81	0.002 59
25			0.004 95	0.004 92	0.004 70
30		0.0079	0.007 66	0.007 61	0.007 30
40		0.0158	0.0156	0.0155	0.0150
50		0.0268	0.0267	0.0264	0.0258
60	0.0409	0.0416	0.0415	0.0409	0.0400
70	0.0601	0.0610	0.0609	0.0599	0.0588
80	0.0834	0.0865	0.0848	0.0847	0.0831
90	0.1179	0.1201	0.1176	0.1173	0.1153
100		0.1661		0.1616	0.1589

$$F^N_{KLs}(k,m,n,\rho) = \int_0^\infty J(q) F_{KLs}(q^2) q^2\, dq\,, \tag{2.74}$$

where

$$J(q) = \frac{2}{\pi} \frac{(qR)^L}{(2L+1)!!} \int_0^\infty \left(\frac{r}{R}\right)^{L+2N} I(k,m,n,\rho;r) j_L(qr) r^2\, dr\,. \tag{2.75}$$

Terms in which these new form factors occur always contain powers of αZ. Terms that are independent of αZ contain the simpler form-factor coefficients F^N_{KLs} [Eqs. (2.67) and (2.68)].

b. Relation between form-factor coefficients and nuclear matrix elements

The form factors or form-factor coefficients can only be expressed in terms of nuclear matrix elements, in general, if some approximations are made. First, it is assumed that the nucleons inside the nucleus interact with leptons in the same way as free nucleons do (impulse-approximation treatment). Meson exchange (Blin-Stoyle, 1973; Lock *et al.*, 1974) and other many-body effects are hence neglected.

The β-decay Hamiltonian must be used with various many-body nuclear wavefunctions that can only be calculated in the framework of specific nuclear models. Thus the uncertainties of nuclear-structure theory are carried over into the nuclear matrix elements or form-factor coefficients.

Finally, the axial-vector constant λ for nucleons embedded in a complex nucleus is renormalized in a different way from that for free nucleons, because the mesonic currents behave differently for free and bound nucleons, and new mesonic currents appear that are absent for free nucleons. Thus λ is in principle not a constant over the whole range of nuclei. For light nuclei, a deviation of λ from the free-nucleon value by ~7% has been found (Wilkinson, 1973a, 1973b, 1974a; Szybisz, 1975; Ericson *et al.*, 1973; Ohta and Wakamatsu, 1974).

Under these assumptions, we develop the relation between form-factor coefficients and nuclear matrix elements for a pure $V-A$ nucleon current of the form given in Eq. (2.4). Induced terms will be discussed later. We have (Stech and Schülke, 1964; Behrens and Bühring, 1971)[9]

TABLE VIII. Calculated relativistic electron radial wavefunction ratios $f^2_{N_2}/g^2_{N_1}$.

	HFS		HF
Z	Suslov (1969, 1970b) Dzhelepov *et al.* (1972)	Calculated with the codes of Fricke *et al.* (1971)	Mann and Waber (1973)
35		0.0078	0.0076
40	0.0134	0.0133	0.0126
45	0.0185	0.0182	0.0176
50	0.0247	0.0244	0.0237
60	0.0400	0.0394	0.0385
70	0.0594	0.0583	0.0572
80	0.0836	0.0836	0.0821
90	0.117	0.117	0.115
100		0.162	0.160

[9] In the formulae for β^- and β^+ decay, the axial-vector coupling constant λ has the opposite sign [Sec. II.A, Eq. (2.39)]. For electron capture, there are hence two ways of defining the axial-vector form-factor coefficients in terms of matrix elements and coupling constants, i.e., by using the same sign definition for λ as in the β^--decay formulae or the same as in the β^+-decay formulae. In the present work, the definition of the form-factor coefficients corresponds, as in Behrens and Jänecke (1969), to those in β^- decay. Consequently, in addition to the substitution indicated in Eq. (2.40), we must replace ${}^A F_{KLs}$ by $-{}^A F_{KLs}$ when going from β^+ decay to electron capture.

TABLE IX. Amplitudes $\beta_x p_x^{k_x-1}$ of the bound electron radial wavefunctions. (After Mann and Waber, 1973 and private communication.) Columns are headed by atomic numbers Z. (Outermost electrons have been omitted.)

	1	2	3	4	5	6	7	8
K	0.124 70E-02	0.296 58E-02	0.578 43E-02	0.917 67E-02	0.130 59E-01	0.173 86E-01	0.221 25E-01	0.272 56E-01
LI	0.0	0.0	0.903 18E-03	0.167 27E-02	0.263 79E-02	0.372 20E-02	0.490 69E-02	0.619 94E-02
LII	0.0	0.0	0.0	0.0	0.0	0.0	0.671 40E-04	0.100 80E-03

	9	10	11	12	13	14	15	16
K	0.327 62E-01	0.386 34E-01	0.448 67E-01	0.514 61E-01	0.584 05E-01	0.657 06E-01	0.733 54E-01	0.813 64E-01
LI	0.759 54E-02	0.909 22E-02	0.109 84E-01	0.130 42E-01	0.152 35E-01	0.175 60E-01	0.200 13E-01	0.225 96E-01
LII	0.143 02E-03	0.194 56E-03	0.272 59E-03	0.366 44E-03	0.478 22E-03	0.609 05E-03	0.758 40E-03	0.928 53E-03
LIII	0.0	0.0	0.536 74E-03	0.719 72E-03	0.935 26E-03	0.118 50E-02	0.147 21E-02	0.179 78E-02
MI	0.0	0.0	0.0	0.0	0.351 74E-02	0.451 17E-02	0.551 93E-02	0.656 60E-02
MII	0.0	0.0	0.0	0.0	0.0	0.0	0.176 36E-03	0.233 45E-03

	17	18	19	20	21	22	23	24
K	0.897 21E-01	0.934 31E-01	0.107 54E 00	0.117 02E 00	0.126 84E 00	0.137 07E 00	0.147 70E 00	0.158 75E 00
LI	0.253 04E-01	0.231 40E-01	0.311 29E-01	0.342 59E-01	0.375 22E-01	0.409 30E-01	0.444 81E-01	0.481 89E-01
LII	0.112 05E-02	0.133 57E-02	0.157 73E-02	0.184 55E-02	0.214 16E-02	0.246 73E-02	0.282 41E-02	0.321 61E-02
LIII	0.216 40E-02	0.257 29E-02	0.302 68E-02	0.352 72E-02	0.407 80E-02	0.468 02E-02	0.533 56E-02	0.604 69E-02
MI	0.765 70E-02	0.879 64E-02	0.102 59E-01	0.118 12E-01	0.132 21E-01	0.146 48E-01	0.161 13E-01	0.174 94E-01
MII	0.298 83E-03	0.373 10E-03	0.480 51E-03	0.600 71E-03	0.719 56E-03	0.849 55E-03	0.992 08E-03	0.113 44E-02
MIII	0.0	0.0	0.0	0.0	0.136 90E-02	0.160 56E-02	0.186 10E-02	0.211 92E-02
MIV	0.0	0.0	0.0	0.0	0.0	0.0	0.0	0.240 81E-04

	25	26	27	28	29	30	31	32
K	0.170 20E 00	0.182 10E 00	0.194 41E 00	0.207 24E 00	0.220 43E 00	0.234 16E 00	0.248 31E 00	0.263 01E 00
LI	0.520 39E-01	0.560 57E-01	0.602 26E-01	0.645 83E-01	0.690 83E-01	0.737 78E-01	0.786 36E-01	0.837 01E-01
LII	0.364 06E-02	0.410 48E-02	0.460 73E-02	0.515 25E-02	0.574 10E-02	0.637 26E-02	0.705 09E-02	0.778 09E-02
LIII	0.681 32E-02	0.763 95E-02	0.852 69E-02	0.947 97E-02	0.104 97E-01	0.115 84E-01	0.127 41E-01	0.139 74E-01
MI	0.191 93E-01	0.208 21E-01	0.225 05E-01	0.242 60E-01	0.259 29E-01	0.279 57E-01	0.300 96E-01	0.323 69E-01
MII	0.131 61E-02	0.149 84E-02	0.169 56E-02	0.190 95E-02	0.212 31E-02	0.238 86E-02	0.268 24E-02	0.300 65E-02
MIII	0.243 95E-02	0.276 66E-02	0.311 89E-02	0.349 85E-02	0.387 99E-02	0.434 10E-02	0.484 54E-02	0.539 45E-02
MIV	0.325 69E-04	0.400 24E-04	0.485 29E-04	0.581 94E-04	0.660 18E-04	0.813 68E-04	0.988 43E-04	0.118 62E-03
MV	0.0	0.0	0.0	0.0	0.0	0.0	0.189 83E-03	0.227 60E-03

	33	34	35	36	37	38	39	40
K	0.279 25E 00	0.293 97E 00	0.310 35E 00	0.327 21E 00	0.344 74E 00	0.362 89E 00	0.381 72E 00	0.401 17E 00
LI	0.889 70E-01	0.944 30E-01	0.100 14E 00	0.106 04E 00	0.112 21E 00	0.118 62E 00	0.125 29E 00	0.132 22E 00
LII	0.856 45E-02	0.940 28E-02	0.103 04E-01	0.112 64E-01	0.122 94E-01	0.133 91E-01	0.145 67E-01	0.158 18E-01
LIII	0.152 84E-01	0.166 74E-01	0.181 49E-01	0.197 09E-01	0.213 60E-01	0.231 04E-01	0.249 47E-01	0.268 89E-01
MI	0.347 67E-01	0.372 81E-01	0.399 30E-01	0.426 88E-01	0.455 90E-01	0.486 24E-01	0.517 88E-01	0.550 79E-01
MII	0.335 81E-02	0.373 89E-02	0.415 21E-02	0.459 65E-02	0.507 83E-02	0.559 57E-02	0.615 34E-02	0.675 09E-02
MIII	0.599 06E-02	0.663 20E-02	0.732 20E-02	0.806 08E-02	0.884 73E-02	0.968 52E-02	0.105 76E-01	0.115 20E-01
MIV	0.141 02E-03	0.166 12E-03	0.194 17E-03	0.225 32E-03	0.260 01E-03	0.298 38E-03	0.341 00E-03	0.387 94E-03
MV	0.269 80E-03	0.316 92E-03	0.369 41E-03	0.427 58E-03	0.492 16E-03	0.563 45E-03	0.641 84E-03	0.727 63E-03
NI	0.965 08E-02	0.109 47E-01	0.122 73E-01	0.136 30E-01	0.154 19E-01	0.172 94E-01	0.190 62E-01	0.208 27E-01
NII	0.0	0.0	0.0	0.0	0.151 85E-02	0.179 70E-02	0.206 24E-02	0.233 81E-02
NIII	0.0	0.0	0.0	0.0	0.0	0.0	0.355 34E-02	0.401 41E-02

	41	42	43	44	45	46	47	48
K	0.421 35E 00	0.442 16E 00	0.463 70E 00	0.486 09E 00	0.509 29E 00	0.533 19E 00	0.558 11E 00	0.583 64E 00
LI	0.139 43E 00	0.146 91E 00	0.154 69E 00	0.162 79E 00	0.171 23E 00	0.179 84E 00	0.189 11E 00	0.198 53E 00
LII	0.171 54E-01	0.185 72E-01	0.200 84E-01	0.216 97E-01	0.234 13E-01	0.252 30E-01	0.271 70E-01	0.292 19E-01
LIII	0.289 36E-01	0.310 88E-01	0.333 51E-01	0.357 31E-01	0.382 33E-01	0.408 53E-01	0.436 09E-01	0.464 86E-01
MI	0.585 04E-01	0.620 71E-01	0.657 96E-01	0.696 64E-01	0.737 07E-01	0.778 93E-01	0.822 90E-01	0.868 34E-01
MII	0.739 15E-02	0.807 38E-02	0.880 53E-02	0.958 58E-02	0.104 20E-01	0.113 07E-01	0.122 57E-01	0.132 65E-01
MIII	0.125 20E-01	0.135 79E-01	0.146 98E-01	0.158 80E-01	0.171 27E-01	0.184 40E-01	0.198 25E-01	0.212 79E-01

TABLE IX. (*Continued*)

	41	42	43	44	45	46	47	48
MIV	0.439 77E-03	0.495 83E-03	0.557 30E-03	0.623 84E-03	0.696 41E-03	0.774 78E-03	0.860 27E-03	0.952 64E-03
MV	0.821 27E-03	0.923 67E-03	0.103 47E-02	0.115 60E-02	0.128 71E-02	0.142 95E-02	0.158 22E-02	0.174 63E-02
NI	0.224 68E-01	0.242 97E-01	0.263 41E-01	0.231 21E-01	0.301 32E-01	0.320 82E-01	0.343 66E-01	0.367 88E-01
NII	0.260 15E-02	0.291 98E-02	0.328 05E-02	0.361 88E-02	0.400 27E-02	0.439 08E-02	0.484 62E-02	0.533 99E-02
NIII	0.445 83E-02	0.494 74E-02	0.550 75E-02	0.600 36E-02	0.657 51E-02	0.713 45E-02	0.781 25E-02	0.854 17E-02
NIV	0.0	0.128 77E-03	0.161 11E-03	0.180 17E-03	0.209 28E-03	0.231 74E-03	0.275 40E-03	0.322 76E-03
	49	50	51	52	53	54	55	56
K	0.610 29E 00	0.637 74E 00	0.666 27E 00	0.695 48E 00	0.726 57E 00	0.758 13E 00	0.791 23E 00	0.825 11E 00
LI	0.208 40E 00	0.218 61E 00	0.229 27E 00	0.240 25E 00	0.251 97E 00	0.263 93E 00	0.276 52E 00	0.289 49E 00
LII	0.314 04E-01	0.337 17E-01	0.361 75E-01	0.387 66E-01	0.415 59E-01	0.444 85E-01	0.476 11E-01	0.509 02E-01
LIII	0.495 09E-01	0.526 68E-01	0.559 79E-01	0.594 29E-01	0.630 71E-01	0.668 51E-01	0.708 18E-01	0.749 43E-01
MI	0.915 96E-01	0.965 36E-01	0.101 70E 00	0.107 03E 00	0.112 71E 00	0.118 54E 00	0.124 68E 00	0.131 01E 00
MII	0.143 44E-01	0.154 91E-01	0.167 13E-01	0.180 06E-01	0.194 01E-01	0.208 69E-01	0.224 42E-01	0.241 02E-01
MIII	0.228 12E-01	0.244 22E-01	0.261 17E-01	0.278 92E-01	0.297 72E-01	0.317 31E-01	0.337 95E-01	0.359 49E-01
MIV	0.105 26E-02	0.116 04E-02	0.127 67E-02	0.140 16E-02	0.153 67E-02	0.168 12E-02	0.183 67E-02	0.200 30E-02
MV	0.192 31E-02	0.211 29E-02	0.231 66E-02	0.253 45E-02	0.276 85E-02	0.301 79E-02	0.328 47E-02	0.356 88E-02
NI	0.393 31E-01	0.420 01E-01	0.448 09E-01	0.477 29E-01	0.508 43E-01	0.540 54E-01	0.574 49E-01	0.609 73E-01
NII	0.588 11E-02	0.646 74E-02	0.709 32E-02	0.776 06E-02	0.848 38E-02	0.924 99E-02	0.100 76E-01	0.109 54E-01
NIII	0.932 66E-02	0.101 63E-01	0.110 57E-01	0.120 04E-01	0.130 12E-01	0.140 77E-01	0.151 96E-01	0.163 72E-01
NIV	0.374 49E-03	0.430 54E-03	0.492 17E-03	0.558 86E-03	0.631 35E-03	0.709 54E-03	0.794 51E-03	0.886 33E-03
NV	0.681 49E-03	0.783 00E-03	0.891 68E-03	0.100 87E-02	0.113 52E-02	0.127 11E-02	0.141 86E-02	0.157 73E-02
NVI	0.0	0.0	0.113 89E-04	0.127 00E-04	0.140 44E-04	0.154 06E-04	0.172 55E-04	0.191 79E-04
NVII	0.0	0.0	0.0	0.0	0.0	0.0	0.139 33E-06	0.161 36E-06
	57	58	59	60	61	62	63	64
K	0.860 70E 00	0.897 69E 00	0.936 16E 00	0.975 57E 00	0.101 66E 01	0.105 90E 01	0.110 34E 01	0.114 85E 01
LI	0.303 17E 00	0.317 46E 00	0.332 42E 00	0.347 81E 00	0.363 90E 00	0.380 63E 00	0.398 23E 00	0.416 23E 00
LII	0.544 19E-01	0.581 58E-01	0.621 34E-01	0.663 15E-01	0.707 55E-01	0.754 54E-01	0.804 64E-01	0.857 06E-01
LIII	0.792 71E-01	0.838 01E-01	0.885 41E-01	0.934 59E-01	0.985 95E-01	0.103 95E 00	0.109 54E 00	0.115 33E 00
MI	0.137 69E 00	0.144 68E 00	0.152 01E 00	0.159 55E 00	0.167 45E 00	0.175 66E 00	0.184 29E 00	0.193 14E 00
MII	0.258 80E-01	0.277 74E-01	0.297 93E-01	0.319 20E-01	0.341 83E-01	0.365 81E-01	0.391 47E-01	0.418 31E-01
MIII	0.382 16E-01	0.406 01E-01	0.431 07E-01	0.457 12E-01	0.484 39E-01	0.512 88E-01	0.542 73E-01	0.573 66E-01
MIV	0.218 17E-02	0.237 35E-02	0.257 90E-02	0.279 75E-02	0.303 08E-02	0.327 94E-02	0.354 62E-02	0.382 72E-02
MV	0.387 20E-02	0.419 75E-02	0.454 63E-02	0.491 37E-02	0.530 40E-02	0.571 78E-02	0.615 53E-02	0.661 61E-02
NI	0.646 75E-01	0.682 71E-01	0.717 98E-01	0.756 35E-01	0.796 32E-01	0.837 77E-01	0.881 46E-01	0.927 98E-01
NII	0.118 98E-01	0.128 41E-01	0.137 89E-01	0.148 41E-01	0.159 58E-01	0.171 42E-01	0.184 09E-01	0.197 88E-01
NIII	0.176 14E-01	0.188 15E-01	0.199 84E-01	0.212 81E-01	0.226 34E-01	0.240 43E-01	0.255 27E-01	0.271 37E-01
NIV	0.986 40E-03	0.108 38E-02	0.117 89E-02	0.128 95E-02	0.140 77E-02	0.153 37E-02	0.166 83E-02	0.182 12E-02
NV	0.174 83E-02	0.191 25E-02	0.207 14E-02	0.225 47E-02	0.244 88E-02	0.265 42E-02	0.287 46E-02	0.312 07E-02
NVI	0.209 71E-04	0.228 09E-04	0.248 39E-04	0.288 25E-04	0.331 51E-04	0.378 57E-04	0.430 37E-04	0.505 27E-04
NVII	0.181 47E-06	0.112 85E-05	0.115 32E-05	0.121 15E-05	0.127 14E-05	0.133 31E-05	0.777 73E-04	0.920 61E-04
	65	66	67	68	69	70	71	72
K	0.119 64E 01	0.124 55E 01	0.129 68E 01	0.135 01E 01	0.140 58E 01	0.146 27E 01	0.152 27E 01	0.158 43E 01
LI	0.435 39E 00	0.455 16E 00	0.475 92E 00	0.497 61E 00	0.520 34E 00	0.543 76E 00	0.568 50E 00	0.594 11E 00
LII	0.913 39E-01	0.972 68E-01	0.103 58E 00	0.110 28E 00	0.117 39E 00	0.124 88E 00	0.132 87E 00	0.141 30E 00
LIII	0.121 41E 00	0.127 72E 00	0.134 31E 00	0.141 17E 00	0.148 33E 00	0.155 74E 00	0.163 49E 00	0.171 52E 00
MI	0.202 56E 00	0.212 30E 00	0.222 52E 00	0.233 20E 00	0.244 41E 00	0.255 97E 00	0.268 17E 00	0.280 82E 00
MII	0.447 32E-01	0.477 85E-01	0.510 40E-01	0.544 97E-01	0.581 79E-01	0.620 55E-01	0.661 95E-01	0.705 64E-01
MIII	0.606 28E-01	0.640 19E-01	0.675 68E-01	0.712 75E-01	0.751 49E-01	0.791 72E-01	0.833 85E-01	0.877 65E-01
MIV	0.413 18E-02	0.445 29E-02	0.479 50E-02	0.515 86E-02	0.554 52E-02	0.595 40E-02	0.638 70E-02	0.684 49E-02
MV	0.710 68E-02	0.762 38E-02	0.817 05E-02	0.874 78E-02	0.935 75E-02	0.999 86E-02	0.106 75E-01	0.113 85E-01
NI	0.973 62E-01	0.102 26E 00	0.107 41E 00	0.112 78E 00	0.118 41E 00	0.124 22E 00	0.130 51E 00	0.137 09E 00
NII	0.211 63E-01	0.226 68E-01	0.242 72E-01	0.259 76E-01	0.277 91E-01	0.297 02E-01	0.317 99E-01	0.340 30E-01
NIII	0.286 83E-01	0.303 66E-01	0.321 26E-01	0.339 64E-01	0.358 87E-01	0.378 83E-01	0.400 48E-01	0.423 21E-01
NIV	0.196 33E-02	0.212 50E-02	0.229 72E-02	0.248 04E-02	0.267 52E-02	0.288 15E-02	0.311 20E-02	0.335 95E-02
NV	0.335 50E-02	0.361 66E-02	0.389 38E-02	0.418 70E-02	0.449 72E-02	0.482 40E-02	0.518 51E-02	0.557 03E-02
NVI	0.547 63E-04	0.613 89E-04	0.685 82E-04	0.763 77E-04	0.848 20E-04	0.939 36E-04	0.106 46E-03	0.120 07E-03
NVII	0.989 50E-04	0.110 86E-03	0.123 74E-03	0.137 65E-03	0.152 68E-03	0.168 86E-03	0.191 71E-03	0.216 28E-03
OI	0.0	0.0	0.413 30E-01	0.432 81E-01	0.453 23E-01	0.474 27E-01	0.507 22E-01	0.541 79E-01
OII	0.0	0.0	0.0	0.0	0.0	0.0	0.111 89E-01	0.122 14E-01

TABLE IX. (*Continued*)

	73	74	75	76	77	78	79	80
K	0.164 89E 01	0.171 58E 01	0.178 56E 01	0.185 73E 01	0.193 30E 01	0.201 12E 01	0.209 32E 01	0.217 75E 01
LI	0.621 03E 00	0.649 10E 00	0.678 53E 00	0.708 99E 00	0.741 23E 00	0.774 77E 00	0.810 10E 00	0.846 65E 00
LII	0.150 28E 00	0.159 78E 00	0.169 89E 00	0.180 54E 00	0.191 95E 00	0.204 01E 00	0.216 87E 00	0.230 43E 00
LIII	0.179 90E 00	0.188 61E 00	0.197 68E 00	0.207 07E 00	0.216 89E 00	0.227 08E 00	0.237 70E 00	0.248 69E 00
MI	0.294 12E 00	0.307 98E 00	0.322 56E 00	0.337 64E 00	0.353 62E 00	0.370 25E 00	0.387 78E 00	0.405 94E 00
MII	0.752 24E-01	0.801 65E-01	0.854 26E-01	0.909 77E-01	0.969 25E-01	0.103 22E 00	0.109 95E 00	0.117 04E 00
MIII	0.923 43E-01	0.971 14E-01	0.102 10E 00	0.107 27E 00	0.112 69E 00	0.118 33E 00	0.124 22E 00	0.130 34E 00
MIV	0.733 08E-02	0.784 53E-02	0.839 00E-02	0.896 48E-02	0.957 50E-02	0.102 19E-01	0.109 02E-01	0.116 21E-01
MV	0.121 34E-01	0.129 22E-01	0.137 51E-01	0.146 21E-01	0.155 38E-01	0.165 00E-01	0.175 12E-01	0.185 70E-01
NI	0.144 04E 00	0.151 34E 00	0.159 02E 00	0.167 01E 00	0.175 50E 00	0.184 35E 00	0.193 71E 00	0.203 46E 00
NII	0.364 24E-01	0.389 78E-01	0.417 05E-01	0.445 96E-01	0.477 04E-01	0.510 04E-01	0.545 41E-01	0.582 87E-01
NIII	0.447 18E-01	0.472 34E-01	0.498 79E-01	0.526 44E-01	0.555 56E-01	0.586 05E-01	0.618 00E-01	0.651 27E-01
NIV	0.362 54E-02	0.391 02E-02	0.421 28E-02	0.453 44E-02	0.487 81E-02	0.524 30E-02	0.563 20E-02	0.604 44E-02
NV	0.598 10E-02	0.641 71E-02	0.688 17E-02	0.737 35E-02	0.789 56E-02	0.845 00E-02	0.903 62E-02	0.965 01E-02
NVI	0.134 88E-03	0.150 95E-03	0.168 57E-03	0.187 62E-03	0.208 24E-03	0.230 52E-03	0.254 54E-03	0.280 39E-03
NVII	0.242 79E-03	0.271 39E-03	0.302 05E-03	0.335 10E-03	0.370 77E-03	0.409 00E-03	0.450 29E-03	0.494 77E-03
OI	0.578 35E-01	0.616 66E-01	0.657 28E-01	0.699 52E-01	0.744 15E-01	0.799 83E-01	0.836 25E-01	0.890 77E-01
OII	0.133 14E-01	0.144 88E-01	0.158 28E-01	0.172 52E-01	0.187 82E-01	0.203 46E-01	0.220 85E-01	0.240 04E-01
OIII	0.0	0.0	0.186 81E-01	0.200 49E-01	0.214 85E-01	0.228 40E-01	0.244 04E-01	0.261 92E-01

	81	82	83	84	85	86	87	88
K	0.226 51E 01	0.235 69E 01	0.245 32E 01	0.255 42E 01	0.226 04E 01	0.276 06E 01	0.287 46E 01	0.299 17E 01
LI	0.884 86E 00	0.925 11E 00	0.967 56E 00	0.101 23E 01	0.105 95E 01	0.110 49E 01	0.115 63E 01	0.120 94E 01
LII	0.244 81E 00	0.260 16E 00	0.276 54E 00	0.294 04E 00	0.312 75E 00	0.331 46E 00	0.352 47E 00	0.374 62E 00
LIII	0.260 11E 00	0.272 06E 00	0.284 41E 00	0.297 34E 00	0.310 82E 00	0.324 30E 00	0.338 80E 00	0.353 77E 00
MI	0.424 94E 00	0.444 97E 00	0.466 10E 00	0.488 38E 00	0.511 93E 00	0.534 61E 00	0.560 27E 00	0.586 83E 00
MII	0.124 58E 00	0.132 63E 00	0.141 24E 00	0.150 44E 00	0.160 28E 00	0.170 15E 00	0.181 23E 00	0.192 91E 00
MIII	0.136 71E 00	0.143 36E 00	0.150 32E 00	0.157 59E 00	0.165 19E 00	0.172 82E 00	0.181 04E 00	0.189 55E 00
MIV	0.123 80E-01	0.131 84E-01	0.140 35E-01	0.149 35E-01	0.158 88E-01	0.168 65E-01	0.179 22E-01	0.190 32E-01
MV	0.196 80E-01	0.208 46E-01	0.220 71E-01	0.233 56E-01	0.247 06E-01	0.260 91E-01	0.275 67E-01	0.291 08E-01
NI	0.213 68E 00	0.224 46E 00	0.235 86E 00	0.247 90E 00	0.260 65E 00	0.273 00E 00	0.286 95E 00	0.301 42E 00
NII	0.622 83E-01	0.665 63E-01	0.711 46E-01	0.760 55E-01	0.813 20E-01	0.866 27E-01	0.925 81E-01	0.988 79E-01
NIII	0.686 07E-01	0.722 55E-01	0.760 85E-01	0.801 01E-01	0.843 13E-01	0.885 71E-01	0.931 53E-01	0.979 15E-01
NIV	0.648 24E-02	0.694 82E-02	0.744 38E-02	0.797 06E-02	0.853 07E-02	0.910 96E-02	0.973 68E-02	0.103 99E-01
NV	0.102 98E-01	0.109 83E-01	0.117 05E-01	0.124 67E-01	0.132 71E-01	0.141 02E-01	0.149 91E-01	0.159 23E-01
NVI	0.308 24E-03	0.338 28E-03	0.370 63E-03	0.405 46E-03	0.442 92E-03	0.482 62E-03	0.525 67E-03	0.571 71E-03
NVII	0.542 53E-03	0.593 83E-03	0.648 88E-03	0.707 88E-03	0.771 10E-03	0.838 01E-03	0.910 14E-03	0.987 02E-03
OI	0.947 51E-01	0.100 79E 00	0.107 19E 00	0.113 99E 00	0.121 19E 00	0.128 30E 00	0.136 26E 00	0.144 58E 00
OII	0.260 97E-01	0.283 76E-01	0.308 08E-01	0.334 26E-01	0.362 46E-01	0.391 29E-01	0.423 55E-01	0.457 86E-01
OIII	0.281 10E-01	0.301 45E-01	0.323 13E-01	0.346 03E-01	0.370 22E-01	0.395 11E-01	0.421 52E-01	0.449 09E-01
OIV	0.214 80E-02	0.239 68E-02	0.266 99E-02	0.295 93E-02	0.326 64E-02	0.358 61E-02	0.393 17E-02	0.429 88E-02
OV	0.0	0.0	0.415 15E-02	0.457 97E-02	0.502 97E-02	0.549 68E-02	0.600 11E-02	0.653 30E-02
OVI	0.0	0.0	0.0	0.0	0.0	0.0	0.440 33E-04	0.486 52E-04

	89	90	91	92	93	94	95	96
K	0.311 89E 01	0.324 08E 01	0.337 81E 01	0.351 18E 01	0.366 13E 01	0.381 36E 01	0.396 97E 01	0.413 26E 01
LI	0.126 73E 01	0.132 36E 01	0.138 69E 01	0.144 93E 01	0.151 91E 01	0.159 07E 01	0.166 48E 01	0.174 25E 01
LII	0.398 82E 00	0.423 27E 00	0.450 59E 00	0.478 46E 00	0.509 49E 00	0.542 08E 00	0.576 44E 00	0.613 08E 00
LIII	0.369 59E 00	0.385 47E 00	0.402 51E 00	0.419 71E 00	0.438 09E 00	0.457 00E 00	0.476 48E 00	0.496 72E 00
MI	0.615 74E 00	0.643 95E 00	0.675 61E 00	0.706 91E 00	0.741 85E 00	0.777 77E 00	0.814 94E 00	0.853 98E 00
MII	0.205 69E 00	0.218 62E 00	0.233 06E 00	0.247 82E 00	0.264 25E 00	0.281 52E 00	0.299 74E 00	0.319 18E 00
MIII	0.198 56E 00	0.207 64E 00	0.217 39E 00	0.227 28E 00	0.237 85E 00	0.248 76E 00	0.260 04E 00	0.271 78E 00
MIV	0.202 17E-01	0.214 37E-01	0.227 52E-01	0.241 10E-01	0.255 70E-01	0.270 97E-01	0.286 98E-01	0.303 83E-01
MV	0.307 35E-01	0.324 07E-01	0.341 89E-01	0.360 23E-01	0.379 69E-01	0.399 94E-01	0.420 99E-01	0.442 97E-01
NI	0.317 15E 00	0.332 59E 00	0.349 81E 00	0.366 92E 00	0.385 98E 00	0.405 60E 00	0.425 95E 00	0.447 35E 00
NII	0.105 77E 00	0.112 78E 00	0.120 58E 00	0.128 59E 00	0.137 50E 00	0.146 88E 00	0.156 79E 00	0.167 39E 00
NIII	0.102 96E 00	0.108 08E 00	0.113 56E 00	0.119 14E 00	0.125 11E 00	0.131 28E 00	0.137 69E 00	0.144 37E 00
NIV	0.111 08E-01	0.113 42E-01	0.126 34E-01	0.134 56E-01	0.143 42E-01	0.152 70E-01	0.162 47E-01	0.172 79E-01
NV	0.169 10E-01	0.178 32E-01	0.190 19E-01	0.201 44E-01	0.213 41E-01	0.225 89E-01	0.238 95E-01	0.252 62E-01
NVI	0.621 30E-03	0.673 74E-03	0.730 77E-03	0.790 91E-03	0.855 73E-03	0.925 12E-03	0.998 03E-03	0.107 58E-02
NVII	0.106 94E-02	0.115 64E-02	0.124 94E-02	0.134 77E-02	0.145 28E-02	0.156 40E-02	0.168 23E-02	0.180 73E-02
OI	0.153 55E 00	0.162 46E 00	0.172 00E 00	0.181 65E 00	0.192 30E 00	0.203 13E 00	0.214 52E 00	0.226 62E 00
OII	0.495 41E-01	0.533 99E-01	0.574 71E-01	0.617 51E-01	0.664 87E-01	0.713 83E-01	0.767 22E-01	0.824 71E-01

TABLE IX. (*Continued*)

	89	90	91	92	93	94	95	96
OIII	0.478 36E-01	0.508 29E-01	0.538 07E-01	0.569 27E-01	0.602 38E-01	0.635 60E-01	0.670 82E-01	0.708 57E-01
OIV	0.469 60E-02	0.511 17E-02	0.548 69E-02	0.590 91E-02	0.636 11E-02	0.680 18E-02	0.731 36E-02	0.787 49E-02
OV	0.709 90E-02	0.768 78E-02	0.823 81E-02	0.883 76E-02	0.946 95E-02	0.100 94E-01	0.107 71E-01	0.115 19E-01
OVI	0.532 03E-04	0.576 51E-04	0.210 69E-03	0.240 24E-03	0.270 99E-03	0.291 48E-03	0.325 87E-03	0.372 15E-03
OVII	0.811 85E-06	0.897 32E-06	0.309 26E-05	0.328 07E-05	0.348 45E-05	0.364 21E-05	0.531 52E-03	0.616 03E-03
OVIII	0.0	0.0	0.964 13E-06	0.104 38E-05	0.113 08E-05	0.120 65E-05	0.385 82E-05	0.413 39E-05
OIX	0.0	0.0	0.0	0.0	0.0	0.0	0.0	0.930 45E-07

	97	98	99	100	101	102
K	0.430 58E 01	0.448 68E 01	0.467 41E 01	0.487 76E 01	0.508 26E 01	0.530 13E 01
LI	0.182 56E 01	0.191 29E 01	0.200 40E 01	0.210 31E 01	0.220 40E 01	0.231 21E 01
LII	0.652 63E 00	0.694 88E 00	0.739 76E 00	0.788 90E 00	0.840 26E 00	0.895 89E 00
LIII	0.517 90E 00	0.539 89E 00	0.562 65E 00	0.586 67E 00	0.611 24E 00	0.636 96E 00
MI	0.895 67E 00	0.939 53E 00	0.985 30E 00	0.103 51E 01	0.108 58E 01	0.114 02E 01
MII	0.340 18E 00	0.362 62E 00	0.386 46E 00	0.412 57E 00	0.439 86E 00	0.469 43E 00
MIII	0.284 10E 00	0.296 92E 00	0.310 22E 00	0.324 28E 00	0.338 71E 00	0.353 86E 00
MIV	0.321 69E-01	0.340 49E-01	0.360 22E-01	0.381 23E-01	0.403 10E-01	0.426 26E-01
MV	0.466 03E-01	0.490 10E-01	0.515 18E-01	0.541 58E-01	0.568 91E-01	0.597 54E-01
NI	0.470 17E 00	0.494 21E 00	0.519 32E 00	0.546 61E 00	0.574 49E 00	0.604 33E 00
NII	0.178 82E 00	0.191 06E 00	0.204 08E 00	0.218 33E 00	0.233 27E 00	0.249 45E 00
NIII	0.151 38E 00	0.158 70E 00	0.166 30E 00	0.174 35E 00	0.182 63E 00	0.191 32E 00
NIV	0.183 72E-01	0.195 27E-01	0.207 42E-01	0.220 40E-01	0.233 94E-01	0.248 31E-01
NV	0.266 99E-01	0.282 05E-01	0.297 78E-01	0.314 38E-01	0.331 62E-01	0.349 72E-01
NVI	0.115 84E-02	0.124 63E-02	0.133 97E-02	0.143 95E-02	0.154 48E-02	0.165 69E-02
NVII	0.194 11E-02	0.208 23E-02	0.223 16E-02	0.239 05E-02	0.255 77E-02	0.273 57E-02
OI	0.239 25E 00	0.252 67E 00	0.266 71E 00	0.281 93E 00	0.297 52E 00	0.314 20E 00
OII	0.886 01E-01	0.952 09E-01	0.102 25E 00	0.109 97E 00	0.118 07E 00	0.126 86E 00
OIII	0.745 87E-01	0.785 88E-01	0.827 45E-01	0.871 35E-01	0.916 56E-01	0.964 01E-01
OIV	0.842 60E-02	0.903 04E-02	0.966 71E-02	0.103 46E-01	0.110 56E-01	0.118 10E-01
OV	0.122 21E-01	0.129 99E-01	0.138 13E-01	0.146 71E-01	0.155 64E-01	0.165 03E-01
OVI	0.400 21E-03	0.440 73E-03	0.483 70E-03	0.529 57E-03	0.578 11E-03	0.629 86E-03
OVII	0.653 59E-03	0.719 10E-03	0.787 83E-03	0.860 69E-03	0.937 11E-03	0.101 63E-02
OVIII	0.432 18E-05	0.457 21E-05	0.483 31E-05	0.511 59E-05	0.540 55E-05	0.571 55E-05

$$
\begin{aligned}
{}^{V}F^{N}_{KLs}(k_x,m,n,\rho) &= (-1)^{K-L}\,{}^{V}\mathfrak{M}^{N}_{KLs}(k_x,m,n,\rho),\\
{}^{A}F^{N}_{KLs}(k_x,m,n,\rho) &= (-1)^{K-L}\lambda\,{}^{A}\mathfrak{M}_{KLs}(k_x,m,n,\rho),
\end{aligned}
\tag{2.76}
$$

where the nuclear matrix elements are denoted by ${}^{V}\mathfrak{M}^{N}_{KLs}(k_x,m,n,\rho)$ and ${}^{A}\mathfrak{M}^{N}_{KLs}(k_x,m,n,\rho)$. The meaning of the indices has been explained in connection with the form-factor coefficients.

The nuclear matrix elements are [Eq. (2.42)]

$$
\begin{aligned}
(-1)^{J_f-M_f}&\begin{pmatrix} J_f & K & J_i \\ -M_f & M & M_i \end{pmatrix}\{{}^{V}\mathfrak{M}^{N}_{KLs}(k_x,m,n,\rho)+\lambda\,{}^{A}\mathfrak{M}^{N}_{KLs}(k_x,m,n,\rho)\}\\
&=[4\pi/(2J_i+1)]^{1/2}\int\int\cdots\int\psi^{\dagger}_{f}(1,2,\ldots A;J_fM_f\pi_f)\\
&\times\sum_{j=1}^{A}\left\{\left(\frac{r}{R}\right)^{L+2N}I(k_x,m,n,\rho;r)(1+\lambda\gamma_5)T^{M}_{KLs}t^{+}\right\}_j\psi_i(1,2,\ldots A;J_iM_i\pi_i)\,d\tau_1\,d\tau_2\cdots d\tau_A.
\end{aligned}
\tag{2.77}
$$

Here, ψ_f and ψ_i are the nuclear many-particle wavefunctions of the final and initial state, respectively, which depend on all the coordinates of the A nucleons. The sum over j runs over the A nucleons, and all the operators are single-particle operators operating on the jth nucleon only. The t^{+} is the isospin operator changing a proton into a neutron. The term with 1 gives the V matrix element, while the term with $\lambda\gamma_5$ leads to the A matrix element. The multipole operators T^{M}_{KLs} have been defined in Eqs. (2.45).

The nuclear matrix elements of Eq. (2.77) must be calculated on the basis of appropriate nuclear models. This is a complicated problem which requires special considerations for each particular β transition. One-body operators O^{M}_{K} must be used in Eq. (2.77), which can be expanded (Bohr and Mottelson, 1969) as

$$O=\sum_{\alpha,\beta}\langle\alpha|O|\beta\rangle a_\beta c_\alpha^\dagger, \tag{2.78}$$

where a_β is the annihilation operator for a proton in the single-particle state β and $c_\alpha^\dagger$ is the creation operator for a neutron in the single-particle state α. Here, α and β represent a complete set of single-particle quantum numbers. We can, therefore, write

$$^i\mathfrak{M}^N_{KLs}(k_x,m,n,\rho)=\sum_{\alpha,\beta}(-1)^{j_\alpha+j_\beta-K}(2K+1)^{-1/2}\langle\alpha||\,{}^iO^M_K\,||\beta\rangle C_{\alpha\beta}, \tag{2.79}$$

with $i=V,A$ and

$$^VO^M_K=\left(\frac{r}{R}\right)^{L+2N}I(k_x,m,n,\rho;r)T_{KLs},$$
$$^AO^M_K=\left(\frac{r}{R}\right)^{L+2N}I(k_x,m,n,\rho;r)\gamma_5 T_{KLs}. \tag{2.80}$$

The expansion coefficients $C_{\alpha\beta}$ are

$$C_{\alpha\beta}=\langle\psi_f^{J_f}|[\{\bar a_\beta c_\alpha^\dagger\}^K_M\psi_i^{J_i}]^{J_f}\rangle, \tag{2.81}$$

where

$$\bar a_{jm}=(-1)^{j+m}a_{j-m}.$$

It follows that, however complicated the nuclear states may be, the exact nuclear matrix elements between many-body states can be expanded in a linear combination of single-particle matrix elements (Donnelly and Walecka, 1972, 1973). For example, methods of calculating the coefficients $C_{\alpha\beta}$ in the framework of the shell model are discussed by de Shalit and Talmi (1963). Formulae for nuclear matrix elements within the isospin formalism are also given by de Shalit and Talmi (1963).

Once the set of numerical coefficients $C_{\alpha\beta}$ has been determined, the nuclear matrix elements can be computed if we are able to deduce reliable values for the single-particle matrix elements. In Eqs. (2.84), we therefore list the single-particle expressions for all the nuclear matrix elements in terms of radial-integral and angular-momentum quantum numbers (Brysk, 1952; Talmi, 1953; Rose and Osborn, 1954; Berthier and Lipnik, 1966; Lipnik and Sunier, 1966; Delabaye and Lipnik, 1966; Strubbe and Callebaut, 1970). The compact form of Eqs. (2.84) is that given by Behrens and Bühring (1971). The orbits of the nucleons are assumed to have definite angular momentum, as in the jj-coupling shell model. In the same notation as used for the electron wavefunctions [Eqs. (2.16) and (2.17)], the nuclear wavefunctions can be written

$$\phi^\mu_\kappa(r)=\begin{cases}(\text{sign }\kappa)f_\kappa(r)\chi^\mu_{-\kappa}\\ g_\kappa(r)\chi^\mu_\kappa.\end{cases} \tag{2.82}$$

The orbit of a nucleon is identified by the number κ, defined as for leptons

$$|\kappa|=j+\tfrac12;\begin{cases}\kappa>0 & \text{if } l=j+\frac12\\ \kappa<0 & \text{if } l=j-\frac12.\end{cases} \tag{2.83}$$

The large component of the nuclear radial wavefunctions is denoted by g_κ and the small component, by f_κ. The single-particle values of the nuclear matrix elements then are

$$^V\mathfrak{M}^N_{KK0}(k_x,m,n,\rho)=\sqrt2(2J_i+1)^{-1/2}\Big\{G_{KK0}(\kappa_f,\kappa_i)\int_0^\infty g_f(r,\kappa_f)\left(\frac{r}{R}\right)^{K+2N}I(k_x,m,n,\rho;r)g_i(r,\kappa_i)r^2\,dr$$
$$+\,\text{sign}(\kappa_f)\text{sign}(\kappa_i)G_{KK0}(-\kappa_f,-\kappa_i)\int_0^\infty f_f(r,\kappa_f)\left(\frac{r}{R}\right)^{K+2N}I(k_x,m,n,\rho;r)f_i(r,\kappa_i)r^2\,dr\Big\}, \tag{2.84a}$$

$$^A\mathfrak{M}^N_{KL1}(k_x,m,n,\rho)=\sqrt2(2J_i+1)^{-1/2}\Big\{G_{KL1}(\kappa_f,\kappa_i)\int_0^\infty g_f(r,\kappa_f)\left(\frac{r}{R}\right)^{L+2N}I(k_x,m,n,\rho;r)g_i(r,\kappa_i)r^2\,dr$$
$$+\,\text{sign}(\kappa_f)\text{sign}(\kappa_i)G_{KL1}(-\kappa_f,-\kappa_i)\int_0^\infty f_f(r,\kappa_f)\left(\frac{r}{R}\right)^{L+2N}I(k_x,m,n,\rho;r)f_i(r,\kappa_i)r^2\,dr\Big\}, \tag{2.84b}$$

$$^A\mathfrak{M}^N_{KK0}(k_x,m,n,\rho)=\sqrt2(2J_i+1)^{-1/2}\Big\{\text{sign}(\kappa_i)G_{KK0}(\kappa_f,-\kappa_i)\int_0^\infty g_f(r,\kappa_f)\left(\frac{r}{R}\right)^{K+2N}I(k_x,m,n,\rho;r)f_i(r,\kappa_i)r^2\,dr$$
$$+\,\text{sign}(\kappa_f)G_{KK0}(-\kappa_f,\kappa_i)\int_0^\infty f_f(r,\kappa_f)\left(\frac{r}{R}\right)^{K+2N}I(k_x,m,n,\rho;r)g_i(r,\kappa_i)r^2\,dr\Big\}, \tag{2.84c}$$

$$^V\mathfrak{M}^N_{KL1}(k_x,m,n,\rho)=\sqrt2(2J_i+1)^{-1/2}\Big\{\text{sign}(\kappa_i)G_{KL1}(\kappa_f,-\kappa_i)\int_0^\infty g_f(r,\kappa_f)\left(\frac{r}{R}\right)^{L+2N}I(k_x,m,n,\rho;r)f_i(r,\kappa_i)r^2\,dr$$
$$+\,\text{sign}(\kappa_f)G_{KL1}(-\kappa_f,\kappa_i)\int_0^\infty f_f(r,\kappa_f)\left(\frac{r}{R}\right)^{L+2N}I(k_x,m,n,\rho;r)g_i(r,\kappa_i)r^2\,dr\Big\}. \tag{2.84d}$$

The indices i and f refer to the initial and final states of the nucleon undergoing decay. The radial quantum numbers of the orbits are not explicitly indicated. The quantity $G_{KLs}(n_f,n_i)$ is defined through Eq. (2.36).

If relativistic nuclear wavefunctions are used (Miller and Green, 1972; Miller, 1972; Krutov and Savashkin, 1973; Krutov *et al.*, 1974), the nuclear radial wavefunctions must be normalized to satisfy the condition

$$\int_0^\infty g^2(r,\kappa)r^2\,dr+\int_0^\infty f^2(r,\kappa)r^2\,dr=1. \tag{2.85}$$

In most cases, relativistic nuclear wavefunctions are not known, whence actual calculations must be performed in the context of nonrelativistic nuclear models. It is then necessary to find the small components $f(r,\kappa)$ of the nuclear radial wavefunctions.[10] It is possible to express $f(r,\kappa)$ in terms of $g(r,\kappa)$ by using the Dirac equation in the nonrelativistic limit, if the spin angular and the radial parts of the wavefunctions are considered separately (Behrens and Bühring, 1971). In the nonrelativistic limit one then finds

$$f(r,\kappa)=\frac{1}{2M}\left[\frac{d}{dr}+\frac{\kappa+1}{r}\right]g(r,\kappa), \tag{2.86}$$

where M is the nucleon mass, and $g(r,\kappa)$ is the solution of the single-particle Schrödinger equation. In this case, the radial wavefunctions $g(r,\kappa)$ must be normalized according to

$$\int_0^\infty g^2(r,\kappa)r^2\,dr=1. \tag{2.87}$$

The matrix elements of Eqs. (2.84a) and (2.84b) are usually called nonrelativistic because their radial parts depend only on the radial functions $g(r,\kappa)$. The terms containing both $f_f(r,\kappa_f)$ and $f_i(r,\kappa_i)$ constitute small relativistic corrections that can usually be omitted. On the other hand, the matrix elements of Eqs. (2.84c) and (2.84d), which contain $f(r,\kappa)$, are called relativistic matrix elements.

The radial momentum operator p_r is

$$p_r=\frac{1}{i}\left(\frac{d}{dr}+\frac{1}{r}\right); \tag{2.88}$$

hence we have

$$f(r,\kappa)=\frac{1}{2M}\left\{ip_r+\frac{\kappa}{r}\right\}g(r,\kappa). \tag{2.89}$$

For a bound nucleon state in a spherical potential, on the other hand, the relation

$$+\frac{1}{2M}\left(p_r^2+\frac{\kappa(\kappa+1)}{r^2}\right)g(r,\kappa)=E_{\rm kin}g(r,\kappa) \tag{2.90}$$

holds, where $E_{\rm kin}$ is the kinetic energy of the nucleon. The ratio of relativistic to nonrelativistic single-particle matrix elements can, therefore, be estimated as

$$M_{\rm R}/M_{\rm NR}\approx(E_{\rm kin}/2M)^{1/2}\approx 0.1. \tag{2.91}$$

It has been shown that some approximations must be made in going from relativistic nuclear wavefunctions to the nonrelativistic limit. Some of the relativistic form-factor coefficients, however, can be related to nonrelativistic coefficients on the basis of CVC theory (Stech and Schülke, 1964; Fujita, 1962; Eichler, 1963; Damgaard and Winther, 1965; Schopper, 1966; Blin-Stoyle and Nair, 1966; Blin-Stoyle, 1973). The most important such relations are (Behrens and Bühring, 1971)

$$\begin{aligned}-{}^VF^{N-1}_{011}(k_x,m,n,\rho)&=(W_0+2.5)\left\{\int\int_0^r\left(\frac{x}{R}\right)^{2N-1}I(k_x,m,n,\rho;x)\,dx\,T_{000}j_0^V\right\}\\&\quad-\frac{\alpha Z}{R}\left\{\int\int_0^r\left(\frac{x}{R}\right)^{2N-1}I(k_x,m,n,\rho;x,\,dx\,U(r)T_{000}j_0^V\right\}\end{aligned} \tag{2.92}$$

and

$$\begin{aligned}&-(2K+1+2N)[K/(2K+1)]^{1/2}\,{}^VF^N_{KK-11}\\&\quad-2N[(K+1)/(2K+1)]^{1/2}\,{}^VF^{N-1}_{KK+11}\\&\qquad=(W_0+2.5)R\,{}^VF^N_{KK0}-\alpha Z\left[\int\left(\frac{r}{R}\right)^{K+2N}U(r)T_{KK0}j_0^V\right].\end{aligned} \tag{2.93}$$

Additional relations are given by Behrens and Bühring (1971).

Because the old Cartesian notation for nuclear matrix elements is used in many papers, the connection between form-factor coefficients and nuclear matrix elements is listed in Cartesian notation in Table X.

c. *Induced interactions*

As indicated in Sec. II.A, the hadron current is influenced by the presence of the strong interactions. It can be shown (Delorme and Rho, 1971), that hence the simple nuclear current of Eq. (2.4) must be replaced by the most general current

$$\begin{aligned}J_\mu=i\bar\psi_n(p')\sum_{i=V,\,S,M,\,A,P,\,T}&[g_iO^i_\mu+F_i(i\gamma\mathbf{p}'+M)O^i_\mu\\&+G_iO^i_\mu(i\gamma\mathbf{p}+M)\\&+H_i(i\gamma\mathbf{p}'+M)O^i_\mu(i\gamma\mathbf{p}+M)]\psi_p(p),\end{aligned} \tag{2.94}$$

where we have

$$O^V_\mu=\gamma_\mu,\quad O^S_\mu=iq_\mu,\quad O^M_\mu=\sigma_{\mu\lambda}q_\mu,\quad O^A_\mu=\gamma_\mu\gamma_5,\quad O^P_\mu=iq_\mu\gamma_5$$

and

$$O^T_\mu=\sigma_{\mu\lambda}q_\lambda\gamma_5.$$

Because the binding energy B of the nucleons inside the nucleus is always small compared with their mass M, the off-mass-shell effects are expected to be negligible (of order B/M). In the standard impulse-approximation treatment, the nucleons are therefore taken on their mass shell, i.e., $(i\gamma\mathbf{p}+M)u(p)=0$ is assumed. Then the terms associated with the coupling constants, F_i, G_i, and H_i vanish. On replacing q_μ by the corresponding differential operator (Behrens and Bühring, 1971; 1974), we obtain

$$\begin{aligned}J_\mu=i\bar\psi_p\Big[&\gamma_\mu+if_M\sigma_{\mu\nu}\left(\frac{\partial}{\partial x_\nu}+ieA_\nu\right)+f_S\left(\frac{\partial}{\partial x_\mu}+ieA_\mu\right)\\&+\lambda\gamma_\mu\gamma_5+if_T\sigma_{\mu\nu}\gamma_5\left(\frac{\partial}{\partial x_\nu}+ieA_\nu\right)+f_P\gamma_5\left(\frac{\partial}{\partial x_\mu}+ieA_\mu\right)\Big]\psi_N\end{aligned} \tag{2.95}$$

[10] There is another possibility of going to the nonrelativistic limit. By applying the Foldy–Wouthuysen transformation on the total (nuclear plus β-decay) Hamiltonian, one can construct an effective V–A transition operator that can be used with nonrelativistic single-particle wavefunctions (Rose and Osborn, 1954; Blin-Stoyle, 1973; Konopinski, 1966). The operators α and γ_5 which appear in the relativistic matrix elements are replaced in the nuclear space by

$$\alpha\to-\frac{\mathbf{p}}{M};\quad\gamma_5\to\frac{\sigma\cdot\mathbf{p}}{M}.$$

This treatment of the relativistic nuclear single-particle matrix elements is fully equivalent to that described in the text.

TABLE X. Relations between form-factor coefficients and nuclear matrix elements in Cartesian notation. (After Behrens and Jänecke, 1969; Bühring, 1963b; Bühring and Schülke, 1965).

Type of transition	Form-factor coefficient	Matrix element in Cartesian notation
Allowed	${}^{V}F^{(0)}_{000}$	$\int 1$
	${}^{A}F^{(0)}_{101}$	$-\lambda \int \sigma$
First-forbidden non-unique	${}^{A}F^{(0)}_{000}$	$\lambda \int \gamma_5$
	${}^{A}F^{(0)}_{011}$	$\lambda \quad i\frac{\boldsymbol{\sigma}\cdot\mathbf{r}}{R}$
	${}^{A}F^{(0)}_{011}(1,1,1,1)$	$\lambda \int i\frac{\boldsymbol{\sigma}\cdot\mathbf{r}}{R} I(1,1,1,1;r)$
	${}^{V}F^{(0)}_{101}$	$\int \boldsymbol{\alpha}$
	${}^{V}F^{(0)}_{110}$	$\sqrt{3} \int i\frac{\mathbf{r}}{R}$
	${}^{V}F^{(0)}_{110}(1,1,1,1)$	$\sqrt{3} \int i\frac{\mathbf{r}}{R} I(1,1,1,1;r)$
	${}^{A}F^{(0)}_{111}$	$-\lambda(\frac{3}{2})^{1/2} \int \frac{\boldsymbol{\sigma}\cdot\mathbf{r}}{R}$
	${}^{A}F^{(0)}_{111}(1,1,1,1)$	$-\lambda(\frac{3}{2})^{1/2} \int \frac{\boldsymbol{\sigma}\cdot\mathbf{r}}{R} I(1,1,1,1;r)$
	${}^{A}F^{(0)}_{211}$	$-\lambda\frac{\sqrt{3}}{2} \int \frac{iB_{ij}}{R}$
Lth forbidden non-unique	${}^{V}F^{(0)}_{LL0}$	$\left(\frac{(2L+1)!!}{L!}\right)^{1/2} \int \frac{i^L R_{i_1\cdots i_L}}{R^L}$
	${}^{V}F^{(0)}_{LL0}(k,1,1,1)$	$\left(\frac{(2L+1)!!}{L!}\right)^{1/2} \int \frac{i^L R_{i_1\cdots i_L}}{R^L} I(k,1,1,1;r)$
	${}^{V}F^{(0)}_{L,L-1,1}$	$\frac{1}{L!}\left(\frac{(2L-1)!!}{(L-1)!}\right)^{1/2} \int \frac{i^{L-1} A_{i_1\cdots i_L}}{R^{L-1}}$
	${}^{A}F^{(0)}_{LL1}$	$\lambda\frac{1}{L!}\left(\frac{(2L+1)!!}{L!}\frac{L}{L+1}\right)^{1/2} \int \frac{i^{L+1} T_{i_1\cdots i_L}}{R^L}$
	${}^{A}F^{(0)}_{LL1}(k,1,1,1)$	$\lambda\frac{1}{L!}\left(\frac{(2L+1)!!}{L!}\frac{L}{L+1}\right)^{1/2} \int \frac{i^{L+1} T_{i_1\cdots i_L}}{R^L} I(k,1,1,1;r)$
	${}^{A}F^{(0)}_{L+1,L,1}$	$-\lambda\frac{1}{(L+1)!}\left(\frac{(2L+1)!!}{L!}\right)^{1/2} \int \frac{i^L B_{i_1\cdots i_{L+1}}}{R^L}$
First-forbidden unique	${}^{A}F^{(0)}_{211}$	$-\lambda\frac{\sqrt{3}}{2} \int i\frac{B_{ij}}{R}$
$(L-1)$st forbidden unique	${}^{A}F^{(0)}_{L,L-1,1}$	$-\lambda\frac{1}{L!}\left(\frac{(2L-1)!!}{(L-1)!}\right)^{1/2} \int \frac{i^{L-1} B_{i_1\cdots i_L}}{R^{L-1}}$

for the case of β^- decay. In β^+ decay and electron capture, the Hermitian conjugate current is

$$J_\mu^\dagger = i\bar{\psi}_n\Big[\gamma_\mu + if_M\sigma_{\mu\nu}\Big(\frac{\partial}{\partial x_\nu} - ieA_\nu\Big) - f_S\Big(\frac{\partial}{\partial x_\mu} - ieA_\mu\Big) + \lambda\gamma_\mu\gamma_5 - if_T\sigma_{\mu\nu}\gamma_5\Big(\frac{\partial}{\partial x_\nu} - ieA_\nu\Big) + f_P\gamma_5\Big(\frac{\partial}{\partial x_\mu} - ieA_\mu\Big)\Big]\psi_p. \tag{2.96}$$

By comparing Eqs. (2.95) and (2.96), the formal substitutions can be determined that must be made for the induced coupling constants in going from β^- to β^+ decay, from β^+ decay to electron capture, or from β^- decay to electron capture (Behrens and Bühring, 1974).

Between β^- and β^+ decay, the following correspondences hold [in addition to those indicated in Eq. (2.39)]

β^- decay		β^+ decay
f_M	→	f_M
f_S	→	$-f_S$
f_T/λ	→	$-f_T/\lambda$
f_P/λ	→	f_P/λ
ieA_μ	→	$-ieA_\mu$.

(2.97)

For β^+ decay and electron capture, the hadron current (and therefore also the hadron part of the transition matrix element) has the same form. Thus, beyond the substitutions indicated in Eq. (2.40), it is only necessary to replace W_0 by $W_0 + W_x$ to go from β^+ decay to electron capture.

Starting from β^- decay, on the other hand, the following substitutions apply [in addition to those indicated in Eqs. (2.41) and (2.42)]

β^- decay		electron capture
f_M	→	f_M
f_S	→	$-f_S$
f_T/λ	→	$-f_T/\lambda$
f_P/λ	→	f_P/λ
ieA_μ	→	$-ieA_\mu$.

(2.98)

The quantities f_M, f_S, f_T and f_P are the coupling constants for the weak magnetic, induced scalar, induced tensor, and induced pseudoscalar interactions, respectively (Marshak *et al.*, 1969; Schopper, 1966; Blin-Stoyle, 1973; Blin-Stoyle and Nair, 1966; Kim, 1974).

The conserved-vector-current theory predicts the values (Blin-Stoyle and Nair, 1966)

$$f_M = (\mu_p - \mu_n)/2M \approx 0.0010, \qquad f_S = 0, \tag{2.99}$$

for f_M and f_S; here, μ_p and μ_n are the anomalous magnetic moments of the proton and neutron, and M is the nucleon mass.

The quantity $A_\mu = (A, i\phi)$ in Eq. (2.98) is the potential of the external electromagnetic field, which in this case is the static electric field of the nuclear charge, for which we have $A = 0$, $-e\phi = V(r) = (\alpha Z/R)U(r)$. The terms containing A_μ must be included to assure gauge invariance of the Hamiltonian.

By applying the Dirac equation, the operator $\partial/\partial x_4$ in Eq. (2.96) can be replaced by the transition energy $W_0' = W_0 + W_x$.

Like the simple current of Eq. (2.4), the general current given by Eq. (2.96) consists of two parts, one of which Lorentz transforms like a four-vector, the other like an axial vector. We make use of this property. In the nuclear matrix elements without induced interactions [Eq. (2.77)], the spherical tensor operators T_{KLs} and $\gamma_5 T_{KLs}$ occur

$$\begin{aligned} &1 \cdot T^M_{LL0} = 1 \cdot i^L Y^M_L, \\ &\lambda\gamma_5 \cdot T^M_{LL0} = \lambda\gamma_5 \cdot i^L Y^M_L, \\ &1 \cdot T^M_{KL1} = \boldsymbol{\alpha} \cdot (-1)^{L-K+1} i^L \mathbf{Y}^M_{KL}, \\ &\lambda\gamma_5 \cdot T^M_{KL1} = \lambda\boldsymbol{\sigma} \cdot (-1)^{L-K+1} i^L \mathbf{Y}^M_{KL}. \end{aligned} \tag{2.100}$$

The nuclear operators 1, $\lambda\gamma_5$, $\boldsymbol{\alpha}$ and $\lambda\boldsymbol{\sigma}$ behave under rotation like scalars, pseudoscalars, vectors, and axial vectors, respectively. Introduction of the general current of Eq. (2.96) makes it necessary to replace these operators by more complicated operators which have the same transformation properties (Behrens and Bühring, 1971)

$$\begin{aligned} &1 \to j_0^V = 1 - if_M\beta\boldsymbol{\alpha} \cdot \nabla + f_S\beta[W_0' - (\alpha Z/R)U(r)], \\ &\lambda\gamma_5 \to j_0^A = \lambda\gamma_5 + if_T\beta\boldsymbol{\sigma} \cdot \nabla - f_P\beta\gamma_5[W_0' - (\alpha Z/R)U(r)], \\ &\boldsymbol{\alpha} \to -\mathbf{j}^V = \boldsymbol{\alpha} + f_M\beta[\boldsymbol{\sigma}\times\nabla] \\ &\qquad + f_M\beta\boldsymbol{\alpha}[W_0' - (\alpha Z/R)U(r)] - if_S\beta\nabla, \\ &\lambda\boldsymbol{\sigma} \to -\mathbf{j}^A = \lambda\boldsymbol{\sigma} - f_T\beta[\boldsymbol{\alpha}\times\nabla] \\ &\qquad - f_T\beta\boldsymbol{\sigma}[W_0' - (\alpha Z/R)U(r)] + if_P\beta\gamma_5\nabla. \end{aligned} \tag{2.101}$$

These substitutions, in Eq. (2.76) via Eq. (2.77), lead to the form-factor coefficients that correspond to the general nuclear current. The expressions for the observables in terms of form-factor coefficients remain unchanged (Sec. II.B.3; Stech and Schülke, 1964; Bühring and Schülke, 1965). Only the definition of the form-factor coefficients in terms of nuclear matrix elements and coupling constants is changed.

The form-factor coefficients in terms of nuclear matrix elements appropriate for electron capture are as follows:

$$\begin{aligned} {}^V F^N_{KK0}(k,m,n,\rho) = {}^V\mathfrak{M}^N_{KK0}(k,m,n,\rho) &+ f_M R^{-1}\Big\{[K/(2K+1)]^{1/2}\Big(\int (r/R)^{K+2N-1}[(2K+1+2N)I(r) + rI'(r)]\beta\, T_{KK-11}\Big) \\ &+ [(K+1)/(2K+1)]^{1/2}\Big(\int (r/R)^{K+2N-1}[2NI(r) + rI'(r)]\beta T_{KK+11}\Big)\Big\} \\ &+ f_S R^{-1}\Big(\int (r/R)^{K+2N} I(r)[W_0' R - \alpha Z\, U(r)]\beta T_{KK0}\Big), \end{aligned} \tag{2.102a}$$

$$
{}^{A}F^{N}_{KK0}(k,m,n,\rho)=\lambda^{A}\mathfrak{M}^{N}_{KK0}(k,m,n,\rho)-f_T R^{-1}\Big\{[K/(2K+1)]^{1/2}\Big(\int (r/R)^{K+2N-1}[(2K+1+2N)I(r)+rI'(r)]\beta\gamma_5 T_{KK-11}\Big)
$$
$$
+[(K+1)/(2K+1)]^{1/2}\Big(\int (r/R)^{K+2N-1}[2NI(r)+rI'(r)]\beta\gamma_5 T_{KK+11}\Big)\Big\}
$$
$$
-f_P R^{-1}\Big(\int (r/R)^{K+2N} I(r)[W_0'R-\alpha Z\,U(r)]\beta\gamma_5 T_{KK0}\Big), \tag{2.102b}
$$

$$
{}^{V}F^{N}_{KK1}(k,m,n,\rho)={}^{V}\mathfrak{M}^{N}_{KK1}(k,m,n,\rho)+f_M R^{-1}\Big\{[(K+1)/(2K+1)]^{1/2}\Big(\int (r/R)^{K+2N-1}[(2K+1+2N)I(r)+rI'(r)]\beta\gamma_5 T_{KK-11}\Big)
$$
$$
-[K/(2K+1)]^{1/2}\Big(\int (r/R)^{K+2N-1}[2NI(r)+rI'(r)]\beta\gamma_5 T_{KK+11}\Big)
$$
$$
+\Big(\int (r/R)^{K+2N} I(r)[W_0'R-\alpha Z\,U(r)]\beta T_{KK1}\Big)\Big\}, \tag{2.102c}
$$

$$
{}^{A}F^{N}_{KK1}(k,m,n,\rho)=\lambda^{A}\mathfrak{M}^{N}_{KK1}(k,m,n,\rho)-f_T R^{-1}\Big\{[(K+1)/(2K+1)]^{1/2}\Big(\int (r/R)^{K+2N-1}[(2K+1+2N)I(r)+rI'(r)]\beta T_{KK-11}\Big)
$$
$$
-[K/(2K+1)]^{1/2}\Big(\int (r/R)^{K+2N-1}[2NI(r)+rI'(r)]\beta T_{KK+11}\Big)
$$
$$
+\Big(\int (r/R)^{K+2N} I(r)[W_0'R-\alpha Z\,U(r)]\beta\gamma_5 T_{KK1}\Big)\Big\}, \tag{2.102d}
$$

$$
-{}^{V}F^{N}_{KK-11}(k,m,n,\rho)={}^{V}\mathfrak{M}^{N}_{KK-11}(k,m,n,\rho)+f_M R^{-1}\Big\{-[(K+1)/(2K+1)]^{1/2}\Big(\int (r/R)^{K+2N-2}[2NI(r)+rI'(r)]\beta\gamma_5 T_{KK1}\Big)
$$
$$
+\Big(\int (r/R)^{K+2N-1} I(r)[W_0'R-\alpha Z\,U(r)]\beta T_{KK-11}\Big)\Big\}
$$
$$
-f_S R^{-1}[K/(2K+1)]^{1/2}\Big(\int (r/R)^{K+2N-2}[2NI(r)+rI'(r)]\beta T_{KK0}\Big), \tag{2.102e}
$$

$$
-{}^{A}F^{N}_{KK-11}(k,m,n,\rho)=\lambda^{A}\mathfrak{M}^{N}_{KK-11}(k,m,n,\rho)-f_T R^{-1}\Big\{-[(K+1)/(2K+1)]^{1/2}\Big(\int (r/R)^{K+2N-2}[2NI(r)+rI'(r)]\beta T_{KK1}\Big)
$$
$$
+\Big(\int (r/R)^{K+2N-1} I(r)[W_0'R-\alpha Z\,U(r)]\beta\gamma_5 T_{KK-11}\Big)\Big\}
$$
$$
+f_P R^{-1}[K/(2K+1)]^{1/2}\Big(\int (r/R)^{K+2N-2}[2NI(r)+rI'(r)]\beta\gamma_5 T_{KK0}\Big), \tag{2.102f}
$$

$$
-{}^{V}F^{N}_{KK+11}(k,m,n,\rho)={}^{V}\mathfrak{M}^{N}_{KK+11}(k,m,n,\rho)+f_M R^{-1}\Big\{[K/(2K+1)]^{1/2}\Big(\int (r/R)^{K+2N}[(2K+3+2N)I(r)+rI'(r)]\beta\gamma_5 T_{KK1}\Big)
$$
$$
+\Big(\int (r/R)^{K+1+2N} I(r)[W_0'R-\alpha Z\,U(r)]\beta T_{KK+11}\Big)\Big\}
$$
$$
-f_S R^{-1}[(K+1)/(2K+1)]^{1/2}\Big(\int (r/R)^{K+2N}[(2K+3+2N)I(r)+rI'(r)]\beta T_{KK0}\Big), \tag{2.102g}
$$

$$
-{}^{A}F^{N}_{KK+11}(k,m,n,\rho)=\lambda^{A}\mathfrak{M}^{N}_{KK+11}(k,m,n,\rho)-f_T R^{-1}\Big\{[K/(2K+1)]^{1/2}\Big(\int (r/R)^{K+2N}[(2K+3+2N)I(r)+rI'(r)]\beta T_{KK1}\Big)
$$
$$
+\Big(\int (r/R)^{K+1+2N} I(r)[W_0'R-\alpha Z\,U(r)]\beta\gamma_5 T_{KK+11}\Big)\Big\}
$$
$$
+f_P R^{-1}[(K+1)/(2K+1)]^{1/2}\Big(\int (r/R)^{K+2N}[(2K+3+2N)I(r)+rI'(r)]\beta\gamma_5 T_{KK0}\Big). \tag{2.102h}
$$

For brevity, we have written $I(r)$ instead of $I(k_x,m,n,\rho;r)$; we have $I'(r)\equiv dI/dr$. In addition to the single-particle matrix elements of Eqs. (2.84), the following are required:

$$
\Big(\int (r/R)^{K+2N}\phi(r)\beta T_{KK0}\Big)=[2/(2J_i+1)]^{1/2}\Big\{-G_{KK0}(\kappa_f,\kappa_i)\int_0^\infty g_f(r,\kappa_f)(r/R)^{K+2N}\phi(r)g_i(r,\kappa_i)r^2\,dr
$$
$$
+\mathrm{sign}(\kappa_f)\mathrm{sign}(\kappa_i)G_{KK0}(-\kappa_f,-\kappa_i)\int_0^\infty f_f(r,\kappa_f)(r/R)^{K+2N}\phi(r)f_i(r,\kappa_i)r^2\,dr\Big\}, \tag{2.103a}
$$

$$\left(\int (r/R)^{L+2N}\phi(r)\beta\gamma_5 T_{KL1}\right) = [2/(2J_i+1)]^{1/2}\left\{-G_{KL1}(\kappa_f,\kappa_i)\int_0^\infty g_f(r,\kappa_f)(r/R)^{L+2N}\phi(r)g_i(r,\kappa_i)r^2\,dr\right.$$
$$\left. + \text{sign}(\kappa_f)\text{sign}(\kappa_i)G_{KL1}(-\kappa_f,-\kappa_i)\int_0^\infty f_f(r,\kappa_f)(r/R)^{L+2N}\phi(r)f_i(r,\kappa_i)r^2\,dr\right\}, \tag{2.103b}$$

$$\left(\int (r/R)^{K+2N}\phi(r)\beta\gamma_5 T_{KK0}\right) = [2/(2J_i+1)]^{1/2}\left\{-\text{sign}(\kappa_i)G_{KK0}(\kappa_f,-\kappa_i)\int_0^\infty g_f(r,\kappa_f)(r/R)^{K+2N}\phi(r)f_i(r,\kappa_i)r^2\,dr\right.$$
$$\left. + \text{sign}(\kappa_f)G_{KK0}(-\kappa_f,\kappa_i)\int_0^\infty f_f(r,\kappa_f)(r/R)^{K+2N}\phi(r)g_i(r,\kappa_i)r^2\,dr\right\}, \tag{2.103c}$$

$$\left(\int (r/R)^{L+2N}\phi(r)\beta\, T_{KL1}\right) = [2/(2J_i+1)]^{1/2}\left\{-\text{sign}(\kappa_i)G_{KL1}(\kappa_f,-\kappa_i)\int_0^\infty g_f(r,\kappa_f)(r/R)^{L+2N}\phi(r)f_i(r,\kappa_i)r^2\,dr\right.$$
$$\left. + \text{sign}(\kappa_f)G_{KL1}(-\kappa_f,\kappa_i)\int_0^\infty f_f(r,\kappa_f)(r/R)^{L+2N}\phi(r)g_i(r,\kappa_i)r^2\,dr\right\}. \tag{2.103d}$$

Here, $\phi(r)$ stands for $I(k_x,m,n,\rho;r)$ or $rI'(k_x,m,n,\rho;r)$ or a linear combination of these integrals. The question whether a finite coupling constant f_T exists for the induced tensor interaction has aroused great interest of late. Second-class currents (Weinberg, 1958) manifest themselves in principle only through the coupling constants f_S and f_T, and f_S vanishes in accord with the conserved vector current theory. Hence, the determination of f_T is connected with the very question of the existence of second-class currents in β decay and electron capture.[11] Although this problem has been discussed extensively in the literature (Wilkinson, 1970a, 1971, 1972a, 1971/72, 1974b; Alburger and Wilkinson, 1970; Kim, 1971; Holstein and Treiman, 1971; Vatai, 1971, 1972b; Wilkinson and Alburger, 1971; Blomquist, 1971; Wolfenstein and Henley, 1971; Lipkin, 1970, 1971; Kim and Fulton, 1971; Blin-Stoyle *et al.*, 1971; Laverne and Dang, 1971; Alburger, 1972; Tribble and Garvey, 1974; Towner, 1973; Greenland, 1975) an unambiguous answer concerning the existence of second-class currents has not yet been obtained. An excellent review of this matter has been written by Wilkinson (1971/72).

In view of the uncertainty about second-class currents, Kubodera *et al.* (1973) have recently pointed out that one cannot neglect the nucleon binding effects, i.e., off-mass-shell phenomena and exchange currents. Thus, at least as far as the axial-vector part is concerned, one should start with the most general current [Eq. (2.94)]. But then the large number of coupling constants complicates the problem to such an extent that it can be dealt with only under some simplifying assumptions, i.e., minimal coupling. Furthermore, special models for the meson exchange current must be used. Following this line of attack, Kubodera *et al.* (1973) were able to calculate explicitly off-mass-shell and meson-exchange effects for some special cases, and to demonstrate their importance (Eman *et al.*, 1973).

[11] First- and second-class currents are defined on the basis of their behavior under a G operation. If we split the hadron current into first- and second-class terms (Weinberg, 1958; Kim and Primakoff, 1969),

$$J_\mu = J_\mu^{\mathrm{I}} + J_\mu^{\mathrm{II}},$$

we have

$$2J_\mu^{\mathrm{I}} = J_\mu + GJ_\mu G^{-1},$$
$$2J_\mu^{\mathrm{II}} = J_\mu - GJ_\mu G^{-1},$$

and hence,

$$GJ_\mu^{\mathrm{I}}G^{-1} = +J_\mu^{\mathrm{I}},$$
$$GJ_\mu^{\mathrm{II}}G^{-1} = -J_\mu^{\mathrm{I}}.$$

Here, J_μ^{I} is a first-class element of the hadron current, and J_μ^{II} is a second-class element. The G operator is defined as

$$G = Ce^{i\pi T_2},$$

where C is the charge-conjugation operator, and T_2 is the second isospin component.

4. Explicit expressions for the quantities $M_K(k_x,k_\nu)$ and $m_K(k_x,k_\nu)$

By expanding electron and neutrino radial wavefunctions as outlined in Sec. II.B.2 and introducing the form-factor coefficients defined in Sec. II.B.3, we can derive from Eq. (2.42) explicit expansions of the quantities $M_K(k_x,k_\nu)$ and $m_K(k_x,k_\nu)$. If we take into account only dominant terms (of lowest order in the expansion of electron and neutrino radial wavefunctions), we arrive at the following simple forms for $M_K(k_x,k_\nu)$ and $m_K(k_x,k_\nu)$ (Behrens and Jänecke, 1969; Behrens and Bühring, 1971):

For allowed transitions,

$$\begin{aligned} M_0(1,1) &= {}^{V}F^0_{000}, \\ M_1(1,1) &= -{}^{A}F^0_{101}; \end{aligned} \tag{2.104}$$

for first-forbidden transitions,

$$\begin{aligned} M_0(1,1) &= {}^{A}F^0_{000} + \tfrac{1}{3}\alpha Z\,{}^{A}F_{011}(1,1,1,1) - \tfrac{1}{3}W_0R\,{}^{A}F^0_{011}, \\ m_0(1,1) &= \tfrac{1}{3}R\,{}^{A}F^0_{011}, \\ M_1(1,1) &= -{}^{V}F^0_{101} + \tfrac{1}{3}\alpha Z(1/3)^{1/2}\,{}^{V}F^0_{110}(1,1,1,1) \\ &\quad - \tfrac{1}{3}W_0R(1/3)^{1/2}\,{}^{V}F^0_{110} \\ &\quad - \tfrac{1}{3}\alpha Z(2/3)^{1/2}\,{}^{A}F^0_{111}(1,1,1,1) \\ &\quad - \tfrac{1}{3}(W_x+q_x)R(2/3)^{1/2}\,{}^{A}F^0_{111}, \\ m_1(1,1) &= \tfrac{1}{3}R[(1/3)^{1/2}\,{}^{V}F^0_{110} - (2/3)^{1/2}\,{}^{A}F^0_{111}], \\ M_1(1,2) &= -\tfrac{1}{3}q_xR[(2/3)^{1/2}\,{}^{V}F^0_{110} - (1/3)^{1/2}\,{}^{A}F^0_{111}], \\ M_1(2,1) &= -\tfrac{1}{3}p_xR[(2/3)^{1/2}\,{}^{V}F^0_{110} + (1/3)^{1/2}\,{}^{A}F^0_{111}], \\ M_2(1,2) &= -\tfrac{1}{3}q_xR\,{}^{A}F^0_{211}, \\ M_2(2,1) &= -\tfrac{1}{3}p_xR\,{}^{A}F^0_{211}. \end{aligned} \tag{2.105}$$

For higher forbidden transitions, we have

$$M_L(k_x,k_\nu^{(1)})=K_L(p_xR)^{k_x-1}(q_xR)^{k_\nu^{(1)}-1}\{-[(2L+1)/L]^{1/2}\,{}^VF^0_{LL-11}+(2k_x+1)^{-1/2}\alpha Z\,{}^VF^0_{LL0}(k_x,1,1,1)$$
$$+[(2k_x+1)^{-1}(2k_\nu^{(1)}+1)^{-1}q_xR]\,{}^VF^0_{LL0}-(2k_x+1)^{-1}\alpha Z[(L+1)/L]^{1/2}\,{}^AF^0_{LL1}(k_x,1,1,1)$$
$$-[(2k_x+1)^{-1}W_xR+(2k_\nu^{(1)}+1)^{-1}q_xR][(L+1)/L]^{1/2}\,{}^AF^0_{LL1}\},\tag{2.106a}$$

$$m_L(k_x,k_\nu^{(1)})=K_L(p_xR)^{k_x-1}(q_xR)^{k_\nu^{(1)}-1}(2k_x+1)^{-1}R\{{}^VF^0_{LL0}-[(L+1)/L]^{1/2}\,{}^AF^0_{LL1}\},\tag{2.106b}$$

$$M_L(k_x,k_\nu^{(2)})=-\tilde K_L(p_xR)^{k_x-1}(q_xR)^{k_\nu^{(2)}-1}(L+1)^{1/2}[(2k_x-1)(2k_\nu^{(2)}-1)]^{-1/2}\{{}^VF^0_{LL0}+(k_x-k_\nu^{(2)})(L+1)^{-1}[(L+1)/L]^{1/2}\,{}^AF^0_{LL1}\},\tag{2.106c}$$

$$M_{L+1}(k_x,k_\nu^{(2)})=-\tilde K_L(p_xR)^{k_x-1}(q_xR)^{k_\nu^{(2)}-1}\,{}^AF^0_{(L+1)L1}.\tag{2.106d}$$

Here we have introduced the abbreviations

$$K_L=(1/2)^{1/2}[(2L)!!/(2L+1)!!]^{1/2}\times[(2k_x-1)!(2k_\nu^{(1)}-1)!]^{-1/2};\tag{2.107a}$$

$$\tilde K_L=[(2L)!!/(2L+1)!!]^{1/2}[(2k_x-1)!(2k_\nu^{(2)}-1)!]^{-1/2}.\tag{2.107b}$$

The two quantities K_L and $\tilde K_L$ are related by

$$\tilde K_{L-1}=[(2L+1)/L]^{1/2}K_L.\tag{2.108}$$

The energy of the bound electron in the parent atom is defined as $W_x=1-|E_x|$, where E_x is the binding energy in the parent atom. The electron momentum p_x is given by

$$p_x=(1-W_x^2)^{1/2}.\tag{2.109}$$

The form-factor coefficients are ${}^VF^N_{KLs}$, ${}^AF^N_{KLs}$, ${}^VF^N_{KLs}(k_x,m,n,\rho)$ and ${}^AF^N_{KLs}(k_x,m,n,\rho)$; they are related to the nuclear matrix elements as indicated previously. The symbols V and A refer to *vector* and *axial vector*; K specifies the rank, L the multipolarity, and s the spin of the spherical tensor operators that are involved. The radial dependence of this operator is r^{L+2N} or $r^{L+2N}I(k_x,m,n,\rho;r)$. These form-factor coefficients occur in accordance with the expansion of the electron radial wavefunctions discussed in Sec. II.B.2.

In Eqs. (2.47) through (2.49) we have only presented the dominant terms of the multipole expansion and the expansion of the electron radial wavefunctions for linear combinations of form-factor coefficients. Complete expressions are listed in Appendix 1 (Behrens and Bühring, 1971). Unless there are strong cancellations between different terms connected with the form-factor coefficients, the higher-order terms can be neglected.

C. Formulae for allowed and forbidden transitions

1. Allowed transitions

In allowed transitions, electrons can only be captured from orbits with $\kappa_x=\pm1$, i.e., from the $K,L_1,L_2,M_1,M_2,\ldots$ shells [cf., Eqs. (2.44)–(2.47)]. This result is based on the approximate neglect of contributions from higher-order (so-called second-forbidden) terms (see Appendix 2). Capture from orbits with $\kappa=\pm2$, for example, would be governed by matrix-element combinations $M_1(2,1)$, $M_2(2,1)$, etc., which are smaller than $M_0(1,1)$ and $M_1(1,1)$ by at least a factor $p_xR\lesssim0.02$. Consequently, we have

$$C_x(\kappa=\pm2)\lesssim4\times10^{-4}C_x(\kappa=\pm1)$$

[Eq. (2.44)], and capture from orbits with $\kappa=\pm2$ can be expected to be difficult to observe. However, capture from such states in principle offers a possibility of determining the higher-forbidden contributions separately from the leading terms.

For the quantity C_x we find

$$C_x=({}^VF^0_{000})^2+({}^AF^0_{101})^2\tag{2.110}$$

[Eqs. (2.44) and (2.104)]. Inserting this result in Eq. (2.43) leads to

$$\lambda_c=(g^2/4\pi^2)\{({}^VF^0_{000})^2+({}^AF^0_{101})^2\}\times|n_Kq_K^2\beta_K^2B_K+n_{L_1}q_{L_1}^2\beta_{L_1}^2B_{L_1}+n_{L_2}q_{L_2}^2\beta_{L_2}^2B_{L_2}+\cdots|\tag{2.111}$$

for the decay constant. Hence it is easy to derive the ratios of the capture probabilities from different subshells. The L_1/K ratio, for example, is

$$\lambda_{L_1}/\lambda_K=(n_{L_1}q_{L_1}^2\beta_{L_1}^2B_{L_1})/(n_Kq_K^2\beta_K^2B_K).\tag{2.112}$$

2. First-forbidden nonunique transitions

Considering, as before, only the dominant terms in nonunique, first-forbidden transitions, we find that electrons with the quantum numbers $\kappa_x=\pm1,\pm2$ are captured. For $K,L_1,L_2,M_1,M_2,\ldots$ capture, we have

$$C_x=[M_0(1,1)\mp m_0(1,1)]^2+[M_1(1,1)\mp m_1(1,1)]^2+M_1^2(1,2)+M_2^2(1,2)\tag{2.113}$$

[Eqs. (2.44)–(2.46)]. The upper sign holds for $K,L_1,M_1,\ldots$ capture and the lower for $L_2,M_2,\ldots$ capture. The quantities $M_L(k_x,k_\nu)$ in Eq. (2.113) are defined through Eqs. (2.105). If there is no cancellation between the different terms in Eqs. (2.105), we can simplify Eq. (2.113). Because we have $W_x=1-|E_K|$, with $|E_K|\lesssim0.2$ and $R=0.0031A^{1/3}<0.02$, we can usually neglect terms multiplied by R and W_xR. Then we find (Vatai, 1973)

$$C_x=[{}^AF^0_{000}+\tfrac{1}{3}\alpha Z\,{}^AF^0_{011}(1,1,1,1)-\tfrac{1}{3}W_0R\,{}^AF^0_{011}]^2+[{}^VF^0_{101}-(\alpha Z/3)(1/\sqrt3)\times\{{}^VF^0_{110}(1,1,1,1)-\sqrt2\,{}^AF^0_{111}(1,1,1,1)\}+(W_0R/3)(1/\sqrt3)\{{}^VF^0_{110}+\sqrt2\,{}^AF^0_{111}\}]^2+(W_0R)^2/9[\{(2/3)^{1/2}\,{}^VF^0_{110}-(1/\sqrt3)\,{}^AF^0_{111}\}^2+\{{}^AF^0_{211}\}^2].\tag{2.114}$$

This result shows that, even in the case of first-forbidden nonunique transitions, the quantity C_x to a very good approximation does not depend on the particular subshell from which the electron is captured. As for allowed electron capture, the ratios of the capture probabilities from different subshells are therefore independent of the form-factor coefficients. Thus these ratios have the same form as given in Eq. (2.81).

In many cases, especially for the heavier nuclei, we have $\alpha Z \gg W_0 R$. Then Eq. (2.114) can be simplified further:

$$C_x = [{}^A F^0_{000} + \tfrac{1}{3}\alpha Z\, {}^A F^0_{011}(1,1,1,1)]^2 + [{}^V F^0_{101} - (\alpha Z/3)(1/\sqrt{3}) \times \{{}^V F^0_{110}(1,1,1,1) - \sqrt{2}\, {}^A F^0_{111}(1,1,1,1)\}]^2. \quad (2.115)$$

For capture from $\kappa = \pm 2$ $(L_3, M_3, M_4, \ldots)$ states, we have

$$C_x = \{M_1(2,1)\}^2 + \{M_2(2,1)\}^2, \quad (2.116)$$

or explicitly [cf. Eqs. (2.105)]

$$C_x = [(p_x R)^2/9][\{(2/3)^{1/2}\, {}^V F^0_{110} + (1/\sqrt{3})\, {}^A F^0_{111}\}^2 + \{{}^A F_{211}\}^2]. \quad (2.117)$$

Comparison of Eq. (2.117) with Eq. (2.114) suggests that $\kappa = \pm 2$ capture is negligibly small as against capture from $\kappa = \pm 1$ orbits.

3. First-forbidden unique transitions

Considering dominant terms in Eqs. (2.105) for unique first-forbidden transitions, we find that subshells with $\kappa = \pm 1, \pm 2$ can contribute (Behrens and Jänecke, 1969). For capture from $\kappa_x = \pm 1$ $(K, L_1, L_2, M_1, M_2, \ldots)$ states, we have

$$C_x = ({}^A F^0_{211})^2 (R^2/9) q_x^2, \quad (2.118)$$

and for capture from $\kappa_x = \pm 2$ $(L_3, M_3, M_4, \ldots)$ orbits, we find

$$C_x = ({}^A F^0_{211})^2 (R^2/9) p_x^2. \quad (2.119)$$

It follows from Eqs. (2.43) and (2.118) that the L_1/K capture ratio is

$$\lambda_{L_1}/\lambda_K = (n_{L_1} q_{L_1}^4 \beta_{L_1}^2 B_{L_1})/(n_K q_K^4 \beta_K^2 B_K). \quad (2.120)$$

Expressions for the L_2/K, M_1/K, L_2/L_1, and M_1/L_1 capture ratios are entirely analogous. For the L_3/L_1 ratio, on the other hand, we have

$$\lambda_{L_3}/\lambda_{L_1} = (n_{L_3} p_{L_3}^2 q_{L_3}^2 \beta_{L_3}^2 B_{L_3})/(n_{L_1} q_{L_1}^4 \beta_{L_1}^2 B_{L_1}). \quad (2.121)$$

Other $k_x = 2$ to $k_x = 1$ capture ratios are analogous to Eq. (2.121).

4. $(L-1)$-forbidden unique transitions

Taking only dominant terms in Eq. (2.106d) into account, we have for $L \geq k_x$

$$C_x = \frac{(2L-2)!!}{(2L-1)!!} ({}^A F^0_{LL-11})^2 R^{2(L-1)} \frac{p_x^{2(k_x-1)} q_x^{2(L-k_x)}}{(2k_x-1)!\{2(L-k_x)+1\}!}. \quad (2.123)$$

For $K, L_1, L_2, M_1, M_2, \ldots$ capture, for example, we obtain

$$C_x = ({}^A F^0_{LL-11})^2 \{(2L-1)!!\}^{-2} (q_x R)^{2(L-1)}. \quad (2.124)$$

5. Some general remarks on higher-forbidden nonunique transitions

Special formulae for the higher-forbidden nonunique capture rates can easily be derived from Eqs. (2.106) in analogy with the first-forbidden nonunique transition rate [Eqs. (2.113) to (2.115)]. The following general statements can be made regarding such higher-forbidden capture transitions:

(i) As for $\Delta J = 1$ first-forbidden nonunique transitions, these capture rates depend only on six different form-factor coefficients, viz., ${}^V F^{(0)}_{LL-11}$, ${}^V F^{(0)}_{LL0}$, ${}^V F^{(0)}_{LL0}(k_x, 1, 1, 1)$, ${}^A F^{(0)}_{LL1}$, ${}^A F_{LL1}(k_x, 1, 1, 1)$, ${}^A F^{(0)}_{L+1,L,1}$. Expressions for these rates are therefore no more complicated than those for first-forbidden transitions.

(ii) If we neglect terms multiplied by R and $W_x R$, as in Eq. (2.114), the capture ratios from shells with the same k_x value do not depend on the nuclear form-factor coefficients. Form-factor coefficients can therefore be determined by investigating capture ratios only if ratios of capture from states with different k_x are measured (e.g., L_3/K, M_3/K) (Vatai, 1973).

(iii) Nonunique Lth-forbidden capture rates are always proportional to a factor

$$\{(2L+1)!!\}^{-4} (q_x R)^{2L} (p_x/q_x)^{2k_x}$$

[Eqs. (2.106)]. Consequently, such capture probabilities decrease very rapidly with increasing degree of forbiddenness.

D. Electron-capture to positron-decay ratios

1. General expressions

For allowed as well as forbidden transitions, the following general result for EC/β^+ ratios holds [Eqs. (2.2), (2.7), (2.10)]:

$$\lambda_{EC}/\lambda_{\beta^+} = \Big(\sum_x n_x C_x f_x\Big) \Big/ \Big(f_{\beta^+} \overline{C(W)}\Big). \quad (2.125)$$

Here, f_{β^+} is the integrated Fermi function (Behrens and Jänecke, 1969)

$$f_{\beta^+} = \int_0^{p_0} p^2 (W_0 - W)^2 F(Z', W)\, dp, \quad (2.126)$$

where p is the positron momentum (in units of $m_0 c$), the maximum momentum is $p_0 = (W_0^2 - 1)^{1/2}$, W is the positron energy (in units of $m_0 c^2$), Z' is the atomic number of the daughter nucleus, $F(Z, W)$ is the Fermi function, and $\overline{C(W)}$ is the spectrum shape factor, averaged over the β^+ spectrum. The form of the shape factor for different types of β^+ decay has been discussed, for example, by Schopper (1966), Behrens and Jänecke (1969), and Behrens and Bühring (1971).

To calculate the integrated Fermi function f we need the continuum-electron radial wavefunctions $g_{-1}(r)$ and $f_{+1}(r)$. Conventionally, these functions (and hence the Fermi function) are evaluated at the nuclear radius ($r = R$). However, recent discussions indicate that a less ambiguous result is achieved if the Fermi function is evaluated at the center of the nucleus ($r = 0$) (Schopper,

1966; Behrens and Bühring, 1968, 1972; Blin-Stoyle, 1969). This latter definition of the Fermi function is appropriate for the electron-capture formalism in the present paper (Sec. II.B.2). A number of detailed calculations and tabulations of the Fermi function $F(Z,W)$ and of the integrated Fermi function $f(Z,W_0)$ exist. However, in many instances finite nuclear size and screening by orbital electrons has not been taken fully into account. The Fermi function for a point nucleus without screening is listed in the National Bureau of Standards Tables (1952) and in a paper by Rose and Perry (1953). Dzhelepov and Zyryanova (1956) have calculated the Fermi function and the integrated Fermi function (at $r=R$) by adding corrections for screening and finite size to the functions for a point nucleus. Several authors (Matese and Johnson, 1966; Durand, 1964; Brown, 1964), however, have noted that the screening corrections of Reitz (1950) used by Dzhelepov and Zyryanova are incorrect for higher electron momenta.

Fermi functions evaluated numerically (at $r=R$) from an exact solution of the Dirac equation for a nucleus with finite size, but without screening, have been tabulated by Bhalla and Rose (1960, 1961, 1962, 1964). It was later shown, however, that these tables are not entirely correct for positrons of higher momenta (Bühring, 1967; Huffacker and Laird, 1967; Behrens and Bühring, 1968; Blin-Stoyle, 1973, p. 38; Asai and Ogata, 1974). For a few elements, Bühring (1965) has carried out an exact numerical integration of the Dirac equation, taking into consideration finite nuclear size and screening. By employing a method similar to that of Bühring, extensive tables of the Fermi function (at $r=0$) and graphs of the integrated Fermi function have been published by Behrens and Jänecke (1969); this calculation takes exact account of both finite nuclear size and electron screening. Numerical integration of the Dirac equation, including finite size and screening, has also been carried out by Suslov (1966, 1967, 1968a). Theoretical K/β^+ ratios have also been listed by Suslov (1970b). The extensive tabulations of the Fermi function (at $r=R$) and of the integrated Fermi function by Dzhelepov, Zyryanova, and Suslov (1972) are based on these calculations. Suslov, however, included in the electrostatic potential caused by the atomic electrons a Slater exchange term.[12] While the exchange term is applicable to the bound orbital electrons, it is not appropriate for the continuum states; this is self-evident for positrons and has also been shown for emitted β^- particles (Matese and Johnson, 1966; Behrens and Jänecke, 1969, p. 25). It may be for this reason that Suslov's calculations do not agree at low β^+ energies with his Thomas–Fermi–Dirac calculations and with results of other authors (Behrens and Jänecke, 1969; Bhalla and Rose, 1960, 1961, 1962, 1964).

An extensive tabulation of $\log f$ (at $r=R$) and of capture-to-positron ratios, with an accuracy of two to three digits, has been compiled by Gove and Martin (1971). These values were obtained by correcting point-nucleus continuum radial wavefunctions for finite nuclear size and screening.

In all calculations discussed so far, the finite size of the nucleus was represented by the simplest model, viz., a uniformly charged sphere of radius R, equal to the nuclear radius. A more realistic charge distribution has been employed by Behrens and Bühring (1970), who have shown that the influence of the shape of the charge distribution on the Fermi function can be neglected in most cases (see also Asai and Ogata, 1974). An analytical parametrization of the Fermi function and of the integrated Fermi function (for a pointlike nucleus), of the screening corrections, the finite nuclear-size effects, and of the dependence of allowed β decay on the nuclear radius has been derived by Wilkinson (1970b, 1970c, 1970d, 1970e, 1972b, 1973c; Wilkinson and Macefield, 1974).

2. Allowed transitions

For allowed transitions, for which we have $C(W)=C_x=({}^V F^0_{000})^2+({}^A F^0_{101})^2$, the EC/$\beta^+$ ratio has a very simple form

$$\lambda_K/\lambda_{\beta^+}=f_K/f_{\beta^+}. \tag{2.127}$$

This ratio consequently does not depend on the form-factor coefficients, just like the capture ratios. However, for the EC/β^+ ratio there are two effects that can lead to small deviations from the result predicted by Eq. (2.127):

(i) If higher-order terms (Appendix 1) contribute significantly, the differences between C_x and $C(W)$ must be taken into account [Sec. II.A; Eq. (2.40)]. For allowed transitions, the correction factor of Eq. (2.127) can be given explicitly. Neglecting terms in $F^{(N)}_{121}(1,m,n,\rho)$ and form-factor coefficients of rank two, we find (Appendix 1; Behrens and Bühring, 1971)[13]

[12] Suslov used the nonrelativistic self-consistent Hartree–Fock–Slater potential of Herman and Skillman (1963).

[13] (a) Note that $q_x-\bar{q}=W_x+\overline{W}$. A correction formula given by Firestone *et al.* (1975b) might contain an error of sign and therefore should not be used. (b) Form-factor coefficients not included in Table X are related as follows to the nuclear matrix elements (without induced terms):

$${}^V F^{(1)}_{000}=\int\left(\frac{r}{R}\right)^2,\quad {}^V F^{(0)}_{011}=\int i\,\frac{\boldsymbol{\alpha}\mathbf{r}}{R},$$

$${}^V F^{(N)}_{000}(k,m,n,\rho)=\int\left(\frac{r}{R}\right)^{2N} I(k,m,n,\rho;r),$$

$${}^V F^{(0)}_{111}=-\left(\frac{3}{2}\right)^{1/2}\int\frac{\boldsymbol{\alpha}\times\mathbf{r}}{R},\quad {}^A F^{(0)}_{110}=\lambda\sqrt{3}\int\sqrt{5}\,\frac{i\mathbf{r}}{R},$$

$${}^A F^{(1)}_{101}=-\lambda\int\sigma\left(\frac{r}{R}\right)^2,$$

$${}^A F^{(N)}_{101}(k,m,n,\rho)=-\lambda\int\sigma\left(\frac{r}{R}\right)^{2N} I(k,m,n,\rho;r).$$

(c) In the case of a mixture between V,A interaction and S,T interaction (where S stands for scalar, and T, for tensor), the EC/β^+ ratio depends on the so-called Fierz interference term b (Fierz, 1937). For allowed transitions and K capture we have, for example,

$$\frac{\lambda_K}{\lambda_{\beta^+}}=\frac{f_K}{f_{\beta^+}}\,\frac{1+b/W_K}{1-b/W}.$$

The term b is proportional to an interference between S and V or T and A interactions (see, e.g., Schopper, 1966). For the pure V–A interaction, however, which is discussed here, we have $b=0$.

$$\lambda_K/\lambda_{\beta^+} = (f_K/f_{\beta^+})[1 + (A_1 + y^2 A_2)/(1+y^2)], \tag{2.128}$$

where

$$\begin{aligned} A_1 = {} & (2/3)^{3/2}\{2(W_K + \overline{W}) - [1 + (\overline{\mu}_1\gamma_1)/\overline{W}]\} R({}^V F^{(0)}_{111}/{}^A F^{(0)}_{101}) \\ & + 2(3)^{-3/2}[1 + (\overline{\mu}_1\gamma_1)/\overline{W}] R({}^A F^{(0)}_{110}/{}^A F^{(0)}_{101}) \\ & - \tfrac{2}{3}(W_K + \overline{W}) R\alpha Z[\tfrac{1}{9}({}^A F^{(1)}_{101}(1,1,1,1)/{}^A F^{(0)}_{101}) \\ & \qquad + ({}^A F^{(1)}_{101}(1,2,2,1)/{}^A F^{(0)}_{101})] \\ & - \tfrac{1}{27} W_0 R^2\{20(W_K + \overline{W}) - 2[1 + (2\overline{\mu}_1\gamma_1)/\overline{W}]\}({}^A F^{(1)}_{101}/{}^A F^{(0)}_{101}), \end{aligned} \tag{2.129}$$

$$\begin{aligned} A_2 = {} & -\tfrac{2}{3}[1 + (\overline{\mu}_1\gamma_1)/\overline{W}] R({}^V F^{(0)}_{011}/{}^V F^{(0)}_{000}) \\ & - \tfrac{2}{3}(W_K + \overline{W}) R\alpha Z[({}^V F^{(1)}_{000}(1,2,2,1)/{}^V F^{(0)}_{000}) \\ & \qquad - ({}^V F^{(1)}_{000}(1,1,1,1)/3\,{}^V F^{(0)}_{000})] \\ & + \tfrac{2}{9} W_0 R^2\{2(W_K + \overline{W}) - [1 + (\overline{\mu}_1\gamma_1)/\overline{W}]\}({}^V F^{(1)}_{000}/{}^V F^{(0)}_{000}), \end{aligned} \tag{2.130}$$

and $y = {}^V F^{(0)}_{000}/{}^A F^{(0)}_{101}$. Here, the energy $\overline{W}$ and the Coulomb function $\overline{\mu}_1$ are averaged over the β^+ spectrum (Behrens and Jänecke, 1969); γ_1 stands for $[1-(\alpha Z)^2]^{1/2}$.

Equations (2.128) to (2.130) also apply to other allowed EC/β^+ ratios ($L_1/\beta^+, L_2/\beta^+, M_1/\beta^+, \ldots$). In most mixed allowed transitions, the form-factor coefficient ${}^V F^{(0)}_{000}$ is isospin-forbidden, and hence very small. Thus we generally have $y \ll 1$ (Blin-Stoyle, 1973; Bertsch and Mekjian, 1972). Hence A_1 is the important correction term. The form-factor coefficient ratio ${}^V F^{(0)}_{111}/{}^A F^{(0)}_{101}$, relativistic over nonrelativistic, depends sensitively on the nuclear structure and is difficult to calculate. This ratio is of the order ~0.1. The ratios ${}^A F^{(1)}_{101}(1,1,1,1)/{}^A F^{(0)}_{101}$, ${}^A F^{(1)}_{101}(1,2,2,1)/{}^A F^{(0)}_{101}$, and ${}^A F^{(1)}_{101}$ can, however, be estimated more easily. They generally lie in the range 0.5–2.0. Taking into account only the latter form-factor coefficient ratios leads to the estimate $A_1 \approx -0.03$ for $Z = 80$.

(ii) A second cause for deviations of the EC/β^+ ratio from the prediction of Eq. (2.127) lies in electromagnetic radiative corrections to the electron-capture and β^+ decay rates, for example for the emission of internal bremsstrahlung. Radiative corrections for allowed β transitions, especially for the superallowed $0^+ \to 0^+$ transitions, have been discussed extensively (Marshak *et al.*, 1969; Sirlin, 1967; Källen, 1967; Dicus and Norton, 1970; Beg *et al.*, 1972; Jaus and Rasche, 1970; Jaus, 1972; Sirlin, 1974; Roos, 1974; Suzuki and Yokoo, 1975).

For allowed β transitions, the effect of radiative corrections can be described, first, by a renormalization of the vector and axial-vector coupling constants

$$C_V \to C_V(1 + \alpha C/4\pi), \tag{2.131}$$

$$C_A \to C_A(1 + \alpha D/4\pi), \tag{2.132}$$

(Blin-Stoyle, 1973), and second, by a known modification of the β spectrum. This second point affects the integrated Fermi function

$$f_{\beta^+} \to f_{\beta^+}\{1 + \delta_R(W, Z)\}. \tag{2.133}$$

In Eqs. (2.131) and (2.132), C and D are the so-called model-dependent radiative corrections; they depend on details of the weak and strong interaction theories (Sirlin, 1967; Källen, 1967; Dicus and Norton, 1970; Beg *et al.*, 1972; Sirlin, 1974; Roos, 1974; Wilkinson, 1975). These model-dependent radiative corrections cannot as yet be calculated without ambiguity, but they cancel in EC/β^+ ratios. The model-independent radiative correction factor $[1 + \delta_R(W, Z)]$ is well-known to order α (Sirlin, 1967; Källen, 1967; Dicus and Norton, 1970). This correction factor can be found, for example, in the work of Wilkinson and Macefield (1970), where semianalytical formulae and nomograms are given. The terms of order $Z\alpha^2$ and $Z^2\alpha^3$ have also been calculated (Jaus and Rasche, 1970; Jaus, 1972). For electron capture this model-independent part of the radiative correction differs, however, from that discussed for β^+ decay. Unfortunately, no explicit calculation has been carried out as yet.

Some contrary statements notwithstanding (Vatai, 1971, 1972b; Eman *et al.*, 1973), Behrens and Bühring (1974) have pointed out that the existence of second-class currents, i.e., of a finite value of f_T, does not significantly affect EC/β^+ ratios. This fact follows in principle from the equality[14] of the hadron parts, or of the form-factor coefficients, for electron capture and β^+ decay (Sec. II.B.3).

3. Nonunique forbidden transitions

The EC/β^+ ratios for nonunique forbidden transitions are proportional to an additional factor $C_x/\overline{C(W)}$. The quantity C_x is given by Eqs. (2.44), (2.105), and (2.106). The corresponding formulae for the shape factor $C(W)$ can, for example, be found in the papers by Behrens and Jänecke (1969) and in Behrens and Bühring (1971). These formulae show that the EC/β^+ ratios for nonunique forbidden transitions generally depend on the relative values of the nuclear form-factor coefficients, i.e., on the details of the nuclear structure.

There is one exception from this rule, however, in the case of nonunique first-forbidden transitions. When the ξ approximation [Eq. (2.115)] is applicable, the EC/β^+ ratios from $k_x = 1$ states are independent of the nuclear matrix elements, and have the same values as for allowed transitions. The applicability of the ξ approximation can be tested experimentally by investigating the shape factor of the β^+ spectrum.

4. Unique forbidden transitions

For the $(L-1)$st unique forbidden transitions, explicit expressions for the ratios $C_x/\overline{C(W)}$ can be given. The formulae for C_x can be taken from Eq. (2.123), and for

[14] There is only a small difference between the form-factor coefficients for electron capture and β^+ decay, because of the different decay energies. In the former case, the decay energy is $W_0' = W_0 + W_x$, while in the latter case it is W_0. This energy difference leads to the following correction factor (Behrens and Bühring, 1974):

$$\frac{\lambda_K}{\lambda_{\beta^+}} = \frac{f_K}{f_{\beta^+}}\left\{1 + 2\frac{f_T}{\lambda}\left[W_K - \frac{1}{3}\left(1 + \frac{\overline{\mu}_1\gamma_1}{W}\right)\right]\right\}.$$

Because we can assume $|f_T/\lambda| < 3\times10^{-3}$ (Blin-Stoyle, 1973; Wilkinson, 1970a; Alburger and Wilkinson, 1970; Wilkinson and Alburger, 1971; Eman *et al.*, 1973), we obtain a correction

$$\left|\frac{f_T}{\lambda}\right|\left\{W_K - \frac{1}{3}\left(1 + \frac{\overline{\mu}_1\gamma_1}{\overline{W}}\right)\right\} \leq 2\times10^{-3}.$$

This value is smaller than the contributions from higher-order terms [Eqs. (2.128)–(2.131)] and from the radiative corrections.

$C(W)$, for example, from the work of Behrens and Jänecke (1969). We find

$$C_x/\overline{C(W)} = \{(2k_x-1)!\,[2(L-k_x)+1]!\}^{-1}[p_x^{2(k_x-1)}q_x^{2(L-k_x)}] \times\left\{\sum_{n=1}^{L}\overline{[\lambda_n p^{2(n-1)}q^{2(L-n)}]}\{(2n-1)!\,[2(L-n)+1]!\}^{-1}\right\}^{-1}. \quad (2.134)$$

Here, λ_n is a special Coulomb function defined, for example, by Behrens and Jänecke (1969). As before, barred symbols denote quantities averaged over the β^+ spectrum.

For $K, L_1, L_2, M_1, M_2, \ldots$ capture, Eq. (2.134) takes the simpler form

$$C_x/\overline{C(W)} = [(2L-1)!]^{-1}q_x^{2(L-1)} \times\left\{\sum_{n=1}^{L}\overline{[\lambda_n p^{2(n-1)}q^{2(L-n)}]}\{(2n-1)!\,[2(L-n)+1]!\}^{-1}\right\}^{-1}. \quad (2.135)$$

E. Atomic matrix elements: Exchange and overlap corrections

1. Introduction

According to the usual theory of allowed orbital electron capture (Sec. II.C). the probability that a K electron is captured by the nucleus is

$$\lambda_K \propto G^2q^2\xi\,|\psi_K(0)|^2, \quad (2.136)$$

where G is the β-decay coupling constant, q is the energy of the neutrino that is emitted, ξ is the appropriate combination of nuclear matrix elements, and $|\psi_K(0)|^2$ is the square of the parent atom's $1s$ electron wavefunction at the nucleus. In Eq. (2.136), no atomic matrix elements are included.

Benoist-Gueutal (1950, 1953b) first suggested that atomic electrons must be included in a complete description of the nuclear electron-capture process. She estimated the effect of imperfect atomic overlap on the total electron-capture rate of ^{7}Be by calculating the electron-capture probability for various final atomic states. Due to the lack of accurately known wavefunctions for excited Li atoms, Benoist-Gueutal only concluded that the decrease in the total decay rate was less than 30%. Odiot and Daudel (1956) made a quantitative calculation of the ^{37}Ar L-to-K capture ratio, using wavefunctions for the entire atom. Odiot and Daudel's prediction of 0.10 for the ^{37}Ar L-to-K capture ratio has subsequently been verified by experiment.

The discrepancy between the traditional theory of electron capture (Brysk and Rose, 1958) and experiments on L-to-K electron-capture ratios indicated that a critical examination of the theory was needed. Bahcall (1962a, 1963a, b, 1965a) made a comprehensive study of the role of atomic electrons in the nuclear electron-capture process, emphasizing the importance of the indistinguishability of electrons and of the change in nuclear charge by one unit from initial to final atomic states, aspects which were neglected in the usual theory. In Bahcall's work, ground-state wavefunctions were used for the initial and final atoms. The importance of the presence of an inner-shell hole in the daughter atom was pointed out by Vatai (1968b).

In this section, we consider the effect of atomic overlap and exchange corrections on the total electron-capture rate and on various subshell capture ratios. We also discuss the calculation of atomic matrix elements. This subject has recently been reviewed by Genz (1973a) and Vatai (1973c). The calculations of electron density at the nuclear surface are discussed in Sec. II.B.

2. Effect of atomic overlap and exchange on total capture rates

Bahcall (1963a, b) used second quantization to formulate the nuclear electron-capture process. For allowed transitions, the probability per unit time that a nucleus will capture any of its atomic electrons and leave the daughter atom in the final state $|A'\rangle$ is

$$\lambda(A') = G^2\xi(2\pi)^{-1}q^2(A')M^\dagger(A')(1+\gamma_5)M(A'), \quad (2.137)$$

where

$$M(A') \equiv \langle A'|\phi_e(0)|G\rangle \quad (2.138)$$

and

$$q(A') = W_0 + 1 + [E(G) - E(A') - 1]. \quad (2.139)$$

Here, W_0 is the difference between initial and final nuclear masses; $E(G)$ and $E(A')$ are the total energies of the initial and final atomic electrons, including their rest masses.

If one uses a single-particle representation of $|G\rangle$, the total electron-capture rate can be written

$$\lambda \cong \lambda^0[1 + \lambda'/\lambda^0 + \Delta\lambda/\lambda^0], \quad (2.140)$$

where

$$\lambda_0 \equiv G^2\xi(2\pi)^{-1}\textstyle\sum_b q^2(b')\,|\phi_b(0)|^2 \quad (2.141)$$

is the usual total electron-capture rate. We have

$$\lambda' \equiv G^2\xi\pi^{-1}q(1s')\textstyle\sum_b|\phi_b(0)|^2[-\epsilon(1s') + \epsilon(b') + \sum_{A'}\Delta q(A')\langle G|a_b^\dagger|A'\rangle\langle A'|a_b|G\rangle], \quad (2.142)$$

and

$$\Delta\lambda = q(1s')G^2\xi\pi^{-1}\sum_{b_1,b_2,A}{}' \phi_{b_1}^\dagger(0)\phi_{b_2}(0)\Delta q(A') \times\langle G|a_{b_1}^\dagger|A'\rangle\langle A'|a_{b_2}|G\rangle, \quad (2.143)$$

and

$$q(1s') \equiv W_0 + E(G) - E(G') - \epsilon(1s'), \quad (2.144)$$

and

$$\Delta q(A') = E(G') - E(A') + \epsilon(1s'), \quad (2.145)$$

where $\epsilon(1s')$ is the K binding energy in the final atom.

The second and third terms in Eq. (2.140) are the contributions due to imperfect atomic overlap and exchange capture, respectively. By applying closure to sum the electron-capture probability over all possible final atom-

ic states, Bahcall found

$$\frac{\lambda'}{\lambda^0} \cong \frac{1}{q(1s')} \frac{\partial^2 E(G)}{\partial Z^2} \tag{2.146}$$

and

$$\frac{\Delta\lambda}{\lambda} \cong \frac{4}{q(1s')} \frac{R_{2s}(0)}{R_{1s}(0)} \left[\left(\frac{1}{r} \right)_{2s,1s} + \sum_{b'} \langle b'2s \left| \frac{1}{r_{12}} \right| b'1s \rangle \right] . \tag{2.147}$$

The contributions of overlap and exchange are of the opposite sign. They partially cancel each other in the total capture rate. The net effect on the total capture probability does not exceed a few percent if $q(1s')$ is greater than, or of the order of, 50 keV.

3. Overlap and exchange corrections on capture ratios

The electron-capture rate, including the atomic matrix element in the theory, can be written

$$\lambda_i = \lambda_i^0 B_i , \quad i = K, L, M, N, \ldots , \tag{2.148}$$

where λ_i^0 is the transition rate from the usual theory and B_i is the exchange-correction factor introduced by Bahcall to take account of the exchange and overlap contribution.

For allowed transitions, the L/K capture ratio can then be written

$$\frac{\lambda_L}{\lambda_K} = \left(\frac{\lambda_{L_1}}{\lambda_K} \right)^0 \frac{B_{L_1}}{B_K} \left[1 + \left(\frac{\lambda_{L_2}}{\lambda_{L_1}} \right)^0 \frac{B_{L_2}}{B_{L_1}} \right] . \tag{2.149}$$

For unique forbidden transitions, the L/K ratio becomes

$$\frac{\lambda_L}{\lambda_K} = \left(\frac{\lambda_{L_1}}{\lambda_K} \right)^0_{\Delta J} \frac{B_{L_1}}{B_K} \left[1 + \left(\frac{\lambda_{L_2}}{\lambda_{L_1}} \right)^0 \frac{B_{L_2}}{B_{L_1}} + \frac{3(\Delta J - 1)(2\Delta J - 1)}{(q_{L_1} R_0)^2} \frac{g_{L_3}^2}{g_{L_1}^2} \frac{B_{L_3}}{B_{L_1}} \right] , \tag{2.150}$$

where

$$\left(\frac{\lambda_i}{\lambda_j} \right)^0 = \frac{g_i^2 q_i^2}{g_j^2 q_j^2} , \tag{2.151}$$

$$\left(\frac{\lambda_{L_1}}{\lambda_K} \right)^0_{\Delta J} = \frac{g_{L_1}^2}{g_K^2} \left(\frac{q_{L_1}^2}{q_K^2} \right)^{\Delta J} . \tag{2.152}$$

The q's are neutrino energies and the g's, charge densities at the nuclear surface.

In Eqs. (2.149) and (2.150), the difference in binding energy among the L subshells has been neglected.

A similar expression applies for M/L capture ratios

$$\frac{\lambda_M}{\lambda_L} = \left(\frac{\lambda_{M_1}}{\lambda_{L_1}} \right)^0 \frac{B_{M_1}}{B_{L_1}} \left[1 + \left(\frac{\lambda_{M_2}}{\lambda_{M_1}} \right)^0 \frac{B_{M_2}}{B_{M_1}} - \left(\frac{\lambda_{L_2}}{\lambda_{L_1}} \right)^0 \frac{B_{L_2}}{B_{L_1}} \right] . \tag{2.153}$$

Most theoretical and experimental work has been done on K, L, and M capture for allowed transitions. Little research has been performed on N capture. We proceed to review various theoretical calculations dealing with the overlap and exchange corrections.

a. Bahcall's approach

In order to overcome the difficulty of calculating and summing an infinite number of separate contributions from the final atomic states. Bahcall (1962a, 1963a, b, 1965a) used the following approximations: (1) The innermost electrons are almost inert. (2) The outer-electron states (outside the 3*s* shell) form a practically complete set. (3) The energy available for a given nuclear transition is nearly independent of the particular states occupied by the outer electrons in the final atom.

Bahcall separated the atomic state vectors into two independent parts

$$|\text{atomic}\rangle = |\text{inner}\rangle \times |\text{outer}\rangle . \tag{2.154}$$

He then invoked closure to perform the sum over the infinite number of final atomic states, obtaining

$$\lambda_i = \lambda_i^0 B_i , \tag{2.155}$$

where λ_i^0 is the usual electron-capture rate, and we have

$$B_i = \left| \frac{f_i}{\psi_i(0)} \right|^2 . \tag{2.156}$$

The capture amplitudes are

$$f(3s') = \langle 1s' | 1s \rangle \langle 2s' | 2s \rangle \psi_{3s}(0) - \langle 1s' | 3s \rangle \langle 2s' | 2s \rangle \psi_{1s}(0) - \langle 2s' | 3s \rangle \langle 1s' | 1s \rangle \psi_{2s}(0) ; \tag{2.157}$$

$$f(2s') = \langle 1s' | 1s \rangle \langle 3s' | 3s \rangle \psi_{2s}(0) - \langle 1s' | 2s \rangle \langle 3s' | 3s \rangle \psi_{1s}(0) - \langle 3s' | 2s \rangle \langle 1s' | 1s \rangle \psi_{3s}(0) ; \tag{2.158}$$

$$f(1s') = \langle 2s' | 2s \rangle \langle 3s' | 3s \rangle \psi_{1s}(0) - \langle 2s' | 1s \rangle \langle 3s' | 3s \rangle \psi_{2s}(0) - \langle 3s' | 1s \rangle \langle 2s' | 2s \rangle \psi_{3s}(0) . \tag{2.159}$$

The primed orbitals pertain to the daughter atom. The L_1-to-K and M_1-to-L_1 capture ratios can be written

$$\frac{\lambda_{L_1}}{\lambda_K} = \left(\frac{\lambda_{L_1}}{\lambda_K} \right)^0 \frac{B_{L_1}}{B_K} = \left(\frac{\lambda_{L_1}}{\lambda_K} \right)^0 X^{L_1/K} \tag{2.160}$$

and

$$\frac{\lambda_{M_1}}{\lambda_{L_1}} = \left(\frac{\lambda_{M_1}}{\lambda_{L_1}} \right)^0 \frac{B_{M_1}}{B_{L_1}} = \left(\frac{\lambda_{M_1}}{\lambda_{L_1}} \right)^0 X^{M_1/L_1} , \tag{2.161}$$

where the exchange correction factors are

$$X^{L_1/K} = \frac{B_{L_1}}{B_K} = \left| \frac{f(2s')\psi_{1s}(0)}{f(1s')\psi_{2s}(0)} \right|^2 , \tag{2.162}$$

$$X^{M_1/L_1} = \frac{B_{M_1}}{B_{L_1}} = \left| \frac{f(3s')\psi_{2s}(0)}{f(2s')\psi_{3s}(0)} \right|^2 . \tag{2.163}$$

To compare these calculated capture ratios with measurements, correction must be made for capture from $p_{1/2}$ states.

To calculate the atomic matrix elements $\langle ns' | ns \rangle$, Bahcall used nonrelativistic Hartree-Fock ground-state wavefunctions for parent and daughter atoms (Watson, 1960; Watson and Freeman, 1961b).

The following comments can be made on Bahcall's theory:

(1) The assumption that the neutrino energy is independent of final states of the atom, and the use of the closure approximation without correction for occupied states, tend to lead toward underestimation of the overlap correction.

(2) The overlap correction is small for K and L_1 capture, but is much larger for M_1 capture. Therefore, Bahcall's approach will overestimate the M_1-to-L_1 capture ratio correction factor X^{M_1/L_1}.

(3) Multiple exchange processes and the exchange between inner and outer electrons are neglected.

(4) The effect of the inner-shell vacancy in the daughter atom is neglected.

b. Vatai's ansatz

Vatai (1968b, 1970a, 1973b) calculated the capture transition to the most prominent state $|A\rangle$ of the final atom. In state $|A\rangle$, except for the captured electron, all the other electrons retain their quantum numbers. Vatai obtained the exchange and overlap correction coefficients as

$$B_i = \left| \frac{f_i}{\psi_i(0)} \right|^2 \tag{2.164}$$

and

$$\begin{aligned} f_K = {} & \psi_{1s}(0)\langle 2s' | 2s\rangle\langle 2p' | 2p\rangle\langle 3s' | 3s\rangle \cdots \\ & - \psi_{2s}(0)\langle 2s' | 1s\rangle\langle 2p' | 2p\rangle\langle 3s' | 3s\rangle \cdots \\ & - \psi_{3s}(0)\langle 3s' | 1s\rangle\langle 2s' | 2s\rangle\langle 2p' | 2p\rangle \cdots \\ & - \cdots . \end{aligned} \tag{2.165}$$

Similar expressions for f_L and f_M are obtained by exchange of $1s$ with $2s$ and $1s$ with $3s$, respectively, in the f_K expression. If overlap corrections for p and d electrons are neglected, one obtains the same f_i expressions as those of Bahcall [Eqs. (2.157) to (2.159)].

In Vatai's calculation, the effect of the inner hole in the daughter atom on the exchange integral is estimated by perturbation theory.

Vatai used the analytic Hartree–Fock wavefunctions of Watson and Freeman (1961b) for the initial state and as unperturbed wavefunctions for the final-state calculation. He estimated the overlap correction for the inner p and d electrons including the multiplicity by calculating the overlap integral with the wavefunctions of Watson and Freeman for both parent and daughter atoms. The overlap integrals of outer electrons are set equal to 1 in Vatai's calculation.

With regard to Vatai's approach, we note the following points:

(1) Some contributions due to processes involving shakeup or shakeoff are neglected.

(2) The use of perturbation theory to calculate the exchange integrals introduces a discrepancy of 10–40% in the value of these integrals compared with Froese's HF calculations (Faessler *et al.*, 1970).

(3) The overlap corrections are only rough estimates.

(4) Vatai, like Bahcall, neglects multiple exchange processes.

c. Faessler's calculation

Faessler *et al.* (1970) recalculated the Bahcall exchange corrections, taking into account the inner-shell vacancy that after electron capture exists in the daughter atom. Faessler *et al.* used the Herman–Skillman (1963) Hartree–Fock–Slater and Froese–Fischer (1965, 1969) Hartree–Fock programs to calculate hole–state wavefunctions and exchange and overlap integrals. Although some of the exchange integrals calculated with the two programs differ by as much as 50%, the exchange correction factors agree to within 3%. This indicates that the exchange correction, being a ratio, is insensitive to the model wavefunctions, due to cancellation of errors. Faessler *et al.* concluded that the influence of rearrangement effects on the L/K and M/L capture ratios is far too small to account for the discrepancy between theory and experiment, although it does affect the theoretical capture ratios in the right direction.

d. Relativistic calculations

Suslov (1970a) followed Bahcall's approach and used relativistic Hartree–Fock–Slater wavefunctions to calculate the exchange and overlap corrections for $14 \leq Z \leq 98$. The wavefunctions were obtained by numerical integration of Dirac's equation, using a nonrelativistic potential (Herman and Skillman, 1963) for $14 \leq Z \leq 73$, and an analogous relativistic potential (Liberman *et al.*, 1965) for $Z \geq 74$. Finite nuclear size was included through the uniformly-charged-sphere model. For $15 \leq Z \leq 37$, the new relativistic values of B_K, B_{L_1}, B_{M_1}, $X^{L/K}$, and X^{M_1/L_1} are quite close to Bahcall's (1963a, b) results; the differences do not exceed 5%. For $Z \geq 38$, the exchange correction decreases as Z increases, and for large Z it is nearly constant. The relativistic exchange-corrected capture ratios do not narrow the gap between theory and experiment.

Martin and Blichert-Toft (1970) performed another relativistic calculation of electron-capture ratios for $6 \leq Z \leq 98$ using the same approach as Vatai's. The required wavefunctions and electron radial densities were calculated with a relativistic Hartree–Slater program with finite nuclear size. The K and L_1 electron radial density at the nuclear surface, calculated by Martin and Blichert-Toft (1970), agrees with other calculations (Zyryanova and Suslov, 1968; Behrens and Jänecke, 1969; Winter, 1968; Suslov, 1970a) within 1%, and the exchange-overlap corrections to the capture ratios agree very well with the present results based on Vatai's approach.

4. Evaluation of atomic matrix elements

Atomic matrix elements $\langle ms' | ns\rangle$ are required not only for the calculation of exchange and overlap corrections, but also for determining autoionization rates in β-decay and electron-capture transitions, and for shakeup calculations (Sec. V). The degree of orthogonality of the wavefunctions is the important point in the evaluation of the overlap integrals $\langle ms' | ns\rangle$. Overlap integrals that involve ground-state wavefunctions from parent to daughter atoms are not very sensitive to the choice of the atomic potential, because the inner shells are closed shells. Overlap integrals calculated with the analytic Hartree–Fock wavefunctions of Watson and Freeman, with Herman–Skillman Hartree–Fock–Slater wavefunctions, or with Froese–Fischer Hartree–Fock wavefunctions, all agree to better than 5% (Faessler *et al.*, 1970). However, for calculations of inner-shell vacancy states (e.g., $1s$ and $2s$ hole states), the atomic model is important, as the hole–state wavefunctions are sensitive to the potential. In the Herman and Skillman (1963) code, single electronic configurations having open shells are treated on the same basis as configurations having only

closed shells. Consequently the wavefunction of an electron in an open shell is not necessarily orthogonal to a single-electron wavefunction that describes an electron of the same symmetry species and in the same configuration, but from a closed shell. For example, the 1*s* electron wavefunction for an atom with a *K* vacancy may not be orthogonal to the 2*s* wavefunction of the atom, if it has a full L_1 subshell. The overlap integrals between open-shell and closed-shell single-electron wavefunctions, involving the ground state of the parent atom and a deep hole state of the daughter, can therefore contain a sizable error if it is computed with Herman–Skillman wavefunctions (Faessler *et al.*, 1970).

In Froese–Fischer's (1965, 1969) and Bagus' (1964, 1965) approaches, the orthogonality between self-consistent field orbital wavefunctions with the same symmetry is taken into account by introducing off-diagonal Lagrangian multipliers into the Hartree–Fock equations. For closed shells, a unitary transformation can be found between the occupied orbitals, such that the Lagrangian multipliers are in diagonal form. The additional requirement that the off-diagonal Lagrangian multipliers be zero serves as a unique definition of the self-consistent field orbitals. For open-shell systems, it is not possible to reduce the Lagrangian multipliers that couple open and closed shells of the same symmetry to zero (Roothaan, 1960; Roothaan and Bagus, 1963).

The Ne-like and Ar-like *ns* hole states have been calculated by Bagus (1964, 1965). The off-diagonal Lagrangian multipliers between open and closed shells $\theta_{ns,ms'}$ are large for 1*s* hole states and become smaller for 3*s* hole states. The effect of including the off-diagonal Lagrangian multipliers for Ar-like ions is that the 1*s* orbitals of the 1*s*-hole states have a node; an extended tail appears in the 1*s* wavefunctions (Bagus, 1964). For large r, $P_{1s}(r)$ becomes

$$P_{1s}(r) \cong -\frac{\theta_{2s,1s}}{\epsilon_{1s}} P_{2s}(r) - \frac{\theta_{3s,1s}}{\epsilon_{1s}} P_{3s}(r) . \qquad (2.166)$$

The features introduced by the off-diagonal Lagrangian multipliers in the Froese–Fischer Hartree–Fock hole-state wavefunctions explain the differences between overlap integrals obtained by using Herman–Skillman and Froese–Fischer wavefunctions in the work of Faessler *et al.* (1970).

To resolve the discrepancy between the overlap matrix elements $\langle n'l|nl\rangle$ of Faessler *et al.* and of Vatai, we have recalculated these matrix elements for Ar *K*, *L*, and *M* capture with Bagus' accurate analytic Hartree–Fock Ar ground-state and Cl^- *ns* hole-state wavefunctions (Bagus, 1964). Our results from Bagus' wavefunctions agree with the overlap matrix elements calculated by Faessler *et al.* (1970) with the Hartree–Fock program of Froese–Fischer to better than 1%.

5. Comparison among theoretical exchange corrections to capture ratios

In Sec. II.E.4, we have described evidence that the Hartree–Fock program of Froese–Fischer is best suited for the evaluation of the exchange and overlap integrals. We have therefore recalculated the exchange correction factors using the Froese–Fischer program (Froese–Fischer, 1972a). Two sets of values were computed, one based on Bahcall's approach, the other following Vatai's *ansatz* that includes the overlap correction for both inner and outer electrons (Table XI). In both sets of values, the effect of the hole in the daughter atom has been included. Corrections to capture ratios computed previously according to Bahcall's approach (Faessler *et al.*, 1970; Suslov, 1970a; Bahcall, 1963a, b, 1965a) agree well (within 5%) with our recalculated "Bahcall" corrections (Table XII). The exchange correction factors $X^{L_1/K}$ and X^{M_1/L_1} of Martin and Blichert-Toft (1970) coincide with our present calculations based on Vatai's approach. In Figs. 2 and 3, the exchange correction factors $X^{L_1/K}$ and X^{M_1/L_1} are shown, as recalculated by us with the Froese–Fischer (1972a) code. For comparison, the results from the two relativistic calculations (Suslov, 1970a; Martin and Blichert-Toft, 1970) are also included. In general, the results from Vatai's approach are smaller than those following Bahcall's theory.

6. Correlation effects in electron-capture ratios

All theoretical work reviewed in Sec. II.E.3 contains the independent-particle approximation. Effects due to electron correlations are neglected.

Goverse and Blok (1974c) have observed that the experimental L/K capture ratios seem to oscillate about the theoretical curve, and suggested that correlation effects between the orbital electrons might cause this discrepancy. This assertion remains to be proven.

7. Conclusion

The exchange and overlap correction factors are not very sensitive to the choice of the atomic potential, due to compensation between the electron density at the nucleus and the atomic matrix element $\langle ns|ms'\rangle$. The importance of including an appropriate inner-shell hole in the daughter atom after electron capture, stressed by Vatai (1968b, 1970a), is not borne out by the work of Faessler *et al.* (1970) nor by our present calculations, if Bahcall's approach is followed. On the other hand, the presence of the inner hole has a significant effect on these correction factors if they are calculated with Vatai's formulae.

The effect of exchange on electron-capture ratios has been treated in a similar way in the two existing theories, those of Bahcall (1963a, b, 1965a) and Vatai (1970), while the overlap corrections are treated differently. In Bahcall's approach, the closure relation is invoked to perform the sum over the infinite number of final atomic states; this leads to an overestimate of the contribution due to processes that involve shakeup or shakeoff. On the other hand, contributions involving shakeup or shakeoff are simply neglected in Vatai's approach. Because the overlap corrections are important for low-Z elements, the difference in exchange and overlap correction factors between Bahcall's and Vatai's approaches shows up clearly in light atoms.

Our recalculated correction factors permit a direct comparison of results based on Bahcall's and Vatai's approaches. Vatai's formulation causes an underestimation of L/K capture ratios at low Z, but leads to M/L

TABLE XI. Exchange and overlap correction factors B_i for i-electron capture and $X^{i/j}$ for i/j capture ratios, recalculated with the Hartree–Fock code of Froese–Fischer. Columns labeled "V" are computed according to the approach of Vatai; columns labeled "B" are calculated with Bahcall's formulas. In both approaches, the effect of the hole in the daughter atom has been included. Asterisks indicate elements for which the calculations were performed *ab initio*; the remaining factors were determined by a 4-point Lagrangian interpolation procedure. (M. H. Chen, private communication).

	B(K)		B(L1)		B(M1)		B(N1)		X(L1/K)		X(M1/L1)		X(N1/M1)	
Z	V	B	V	B	V	B	V	B	V	B	V	B	V	B
4*	0.816	0.900	2.222	3.045					2.723	3.383				
5	0.866	0.924	1.875	2.432					2.164	2.633				
6	0.903	0.941	1.636	2.009					1.811	2.134				
7*	0.928	0.954	1.482	1.738					1.597	1.822				
8	0.944	0.962	1.391	1.580					1.474	1.642				
9	0.953	0.967	1.341	1.496					1.408	1.547				
10*	0.957	0.970	1.309	1.449					1.368	1.494				
11	0.959	0.971	1.272	1.399					1.327	1.441				
12*	0.961	0.972	1.209	1.309	1.651	2.134			1.258	1.347	1.366	1.630		
13	0.964	0.973	1.185	1.272	1.541	1.960			1.230	1.307	1.300	1.541		
14	0.966	0.974	1.167	1.242	1.463	1.829			1.208	1.275	1.255	1.473		
15*	0.968	0.975	1.152	1.219	1.411	1.733			1.190	1.250	1.225	1.422		
16	0.970	0.976	1.140	1.200	1.375	1.661			1.176	1.230	1.206	1.383		
17	0.972	0.977	1.130	1.185	1.348	1.603			1.163	1.213	1.193	1.353		
18*	0.973	0.978	1.121	1.171	1.322	1.549			1.152	1.197	1.179	1.323		
19	0.974	0.979	1.111	1.157	1.288	1.489			1.140	1.182	1.160	1.287		
20*	0.975	0.980	1.099	1.141	1.239	1.414	1.593	2.130	1.127	1.164	1.127	1.239	1.286	1.506
21	0.976	0.981	1.090	1.133	1.235	1.390			1.117	1.155	1.133	1.227		
22	0.977	0.981	1.084	1.125	1.230	1.369			1.109	1.147	1.135	1.217		
23*	0.978	0.982	1.079	1.119	1.225	1.350	1.339	1.800	1.103	1.140	1.135	1.206	1.093	1.333
24	0.979	0.983	1.076	1.113	1.220	1.333	1.329	1.748	1.099	1.133	1.134	1.197	1.090	1.312
25	0.979	0.983	1.074	1.108	1.214	1.317	1.318	1.700	1.096	1.127	1.131	1.189	1.086	1.291
26*	0.980	0.984	1.072	1.103	1.208	1.303	1.308	1.658	1.094	1.121	1.127	1.181	1.083	1.272
27	0.981	0.985	1.071	1.098	1.202	1.290	1.297	1.621	1.092	1.116	1.123	1.175	1.079	1.256
28	0.981	0.985	1.069	1.094	1.197	1.279	1.287	1.588	1.090	1.110	1.119	1.169	1.076	1.242
29	0.982	0.986	1.067	1.090	1.191	1.268	1.276	1.561	1.087	1.105	1.116	1.164	1.071	1.231
30*	0.983	0.986	1.064	1.085	1.186	1.258	1.265	1.538	1.082	1.100	1.115	1.159	1.067	1.223
31	0.984	0.987	1.063	1.083	1.174	1.243	1.258	1.519	1.080	1.098	1.105	1.147	1.071	1.222
32*	0.985	0.987	1.061	1.081	1.164	1.230	1.252	1.499	1.077	1.095	1.097	1.138	1.076	1.219
33	0.986	0.987	1.059	1.078	1.155	1.219	1.247	1.479	1.075	1.092	1.091	1.130	1.079	1.213
34	0.986	0.988	1.057	1.075	1.147	1.209	1.242	1.459	1.072	1.089	1.085	1.124	1.083	1.207
35	0.986	0.988	1.055	1.072	1.140	1.200	1.238	1.439	1.070	1.085	1.081	1.119	1.086	1.199
36*	0.986	0.988	1.053	1.069	1.134	1.192	1.234	1.420	1.068	1.082	1.077	1.115	1.088	1.191
37	0.986	0.988	1.051	1.066	1.128	1.185	1.230	1.402	1.066	1.079	1.074	1.111	1.090	1.184
38	0.986	0.988	1.049	1.064	1.123	1.177	1.226	1.386	1.063	1.076	1.071	1.107	1.092	1.177
39	0.986	0.989	1.047	1.061	1.117	1.170	1.221	1.371	1.061	1.074	1.067	1.102	1.093	1.172
40*	0.987	0.989	1.045	1.060	1.112	1.162	1.216	1.359	1.059	1.072	1.064	1.096	1.094	1.170
41	0.987	0.989	1.043	1.058	1.108	1.157	1.211	1.347	1.057	1.069	1.062	1.093	1.093	1.164
42	0.988	0.989	1.042	1.056	1.105	1.152	1.206	1.335	1.055	1.067	1.060	1.091	1.091	1.159
43	0.988	0.990	1.041	1.054	1.102	1.147	1.201	1.324	1.054	1.065	1.058	1.088	1.090	1.154
44*	0.988	0.990	1.040	1.053	1.099	1.143	1.196	1.314	1.053	1.064	1.057	1.085	1.088	1.150
45	0.988	0.990	1.039	1.052	1.097	1.139	1.191	1.304	1.052	1.062	1.055	1.083	1.086	1.145
46	0.988	0.991	1.038	1.050	1.094	1.135	1.187	1.295	1.051	1.060	1.054	1.081	1.085	1.141
47	0.989	0.991	1.038	1.049	1.092	1.132	1.182	1.287	1.050	1.059	1.052	1.078	1.083	1.137
48*	0.989	0.991	1.037	1.048	1.090	1.128	1.178	1.279	1.049	1.058	1.051	1.076	1.081	1.134
49	0.989	0.991	1.036	1.047	1.088	1.125	1.174	1.271	1.047	1.056	1.050	1.074	1.079	1.130
50	0.990	0.991	1.035	1.045	1.086	1.121	1.169	1.264	1.046	1.055	1.049	1.073	1.077	1.127
51*	0.990	0.991	1.034	1.044	1.083	1.118	1.165	1.257	1.044	1.053	1.047	1.071	1.076	1.124
52	0.990	0.991	1.033	1.042	1.080	1.115	1.161	1.250	1.043	1.052	1.046	1.069	1.074	1.122
53	0.990	0.991	1.031	1.041	1.077	1.111	1.156	1.244	1.042	1.050	1.044	1.067	1.073	1.119
54*	0.990	0.991	1.030	1.039	1.074	1.107	1.151	1.237	1.040	1.048	1.043	1.065	1.072	1.117

TABLE XII A. Comparison of published exchange and overlap corrections B_K, B_L, B_M, and B_N for selected values of Z.

		Exchange and overlap corrections B_K					
						Recalculated in this work as described in Sec. II.E after:	
Z	Elements	Bahcall (1963)	Vatai (1970)	Martin and Blichert-Toft (1970)	Suslov (1970)	Bahcall [a]	Vatai
4	Be					0.900	0.816
5	B					0.924	0.866
6	C			0.938		0.941	0.903
7	N			0.948		0.954	0.928
8	O			0.958		0.962	0.944
9	F			0.964		0.967	0.953
10	Ne			0.969		0.970	0.957
11	Na			0.973		0.971	0.959
12	Mg			0.974		0.972	0.961
13	Al		0.987	0.975		0.973	0.964
14	Si	0.924	0.988	0.976	0.9231	0.974	0.966
15	P	0.939	0.988	0.977	0.9391	0.975	0.968
16	S	0.947	0.988	0.978	0.9479	0.976	0.970
17	Cl	0.954	0.988	0.979	0.9542	0.977	0.972
18	Ar	0.959	0.988	0.980	0.9589	0.978	0.973
19	K	0.963	0.988	0.981	0.9600	0.979	0.974
20	Ca	0.966	0.989	0.982	0.9650	0.980	0.975
25	Mn	0.976	0.990	0.985	0.9731	0.983	0.979
30	Zn	0.981	0.991	0.987	0.9794	0.986	0.983
35	Br	0.983	0.992	0.989	0.9822	0.988	0.986
40	Zr			0.990	0.9844	0.989	0.987
50	Sn			0.991	0.9878	0.991	0.990
60	Nd			0.992	0.9888		
70	Yb			0.992	0.9896		
80	Hg			0.992	0.9898		
90	Th			0.992	0.9899		

		Exchange and overlap corrections				B_{L_1}		B_{L_2}, B_{L_3}
						Recalculated in this work as described in Sec. II.E after:		
Z	Elements	Bahcall (1963)	Vatai (1970)	Martin and Blichert-Toft (1970)	Suslov (1970)	Bahcall [a]	Vatai	Martin and Blichert-Toft (1970)
4	Be					3.045	2.222	
5	B					2.432	1.875	
6	C					2.009	1.636	
7	N			1.475		1.738	1.482	
8	O			1.405		1.580	1.391	
9	F			1.360		1.496	1.341	
10	Ne			1.309		1.449	1.309	
11	Na			1.283		1.399	1.272	
12	Mg			1.248		1.309	1.209	
13	Al		1.250	1.212		1.272	1.185	
14	Si	1.199	1.229	1.186	1.205	1.242	1.167	0.921
15	P	1.193	1.211	1.169	1.189	1.219	1.152	0.929
16	S	1.181	1.196	1.154	1.179	1.200	1.140	0.935
17	Cl	1.172	1.183	1.143	1.168	1.185	1.130	0.940
18	Ar	1.162	1.170	1.132	1.159	1.171	1.121	0.944
19	K	1.153	1.158	1.120	1.150	1.157	1.111	0.946
20	Ca	1.145	1.149	1.113	1.140	1.141	1.099	0.948
25	Mn	1.112	1.116	1.085	1.108	1.108	1.074	0.958
30	Zn	1.090	1.095	1.070	1.090	1.085	1.067	0.967
35	Br	1.075	1.077	1.060	1.075	1.072	1.055	0.971
40	Zr			1.050	1.064	1.060	1.045	0.974
50	Sn			1.037	1.050	1.045	1.035	0.978
60	Nd			1.029	1.040			0.980
70	Yb			1.025	1.035			0.981
80	Hg			1.022	1.031			0.982
90	Th			1.021	1.028			0.982

TABLE XII A. *(Continued)*

		Exchange and overlap corrections B_{M_1}						B_N		
						Recalculated in this work as described in Sec. II.E after:			Recalculated in this work as described in Sec. II.E after:	
Z	Elements	Bahcall (1963)	Vatai (1970)	Martin and Blichert-Toft (1970)	Suslov (1970)	Bahcall [a]	Vatai	Vatai (1970)	Bahcall [a]	Vatai
4	Be									
5	B									
6	C									
7	N									
8	O									
9	F									
10	Ne									
11	Na									
12	Mg					2.134	1.651			
13	Al		1.432	1.628		1.960	1.541			
14	Si	1.804	1.408	1.510	1.769	1.829	1.463			
15	P	1.711	1.385	1.434	1.686	1.733	1.411			
16	S	1.639	1.369	1.388	1.621	1.661	1.375			
17	Cl	1.579	1.346	1.358	1.567	1.603	1.348			
18	Ar	1.530	1.327	1.328	1.522	1.549	1.322			
19	K	1.489	1.315	1.285	1.486	1.489	1.288			
20	Ca	1.454	1.299	1.255	1.453	1.414	1.239		2.139	1.593
25	Mn	1.335	1.241	1.226	1.339	1.317	1.214	1.283	1.700	1.318
30	Zn	1.266	1.202	1.190	1.273	1.258	1.186	1.236	1.538	1.265
35	Br	1.222	1.170	1.150		1.200	1.140	1.215	1.459	1.238
40	Zr			1.121		1.162	1.112		1.359	1.216
50	Sn			1.093		1.121	1.086		1.264	1.169
60	Nd			1.070						
70	Yb			1.062						
80	Hg			1.056						
90	Th			1.051						

[a] Including the effect of the ns hole in the daughter atom.

TABLE XII B. Comparison of exchange and overlap corrections for L/K, M/L, and N/M ratios.

		Exchange and overlap corrections $X^{L/K}$							
								Recalculated in this work as described in Sec. II.E after:	
Z	Elements	Bahcall (1963)	Vatai (1970)	Martin and Blichert-Toft (1970)	Suslov (1970)	Faessler *et al.* (1970)	Faessler *et al.* (1970) [a]	Bahcall [a]	Vatai
4	Be					3.504	2.947	3.383	2.723
5	B							2.633	2.164
6	C							2.134	1.811
7	N			1.556				1.822	1.597
8	O			1.467				1.642	1.474
9	F			1.411				1.547	1.408
10	Ne			1.351				1.494	1.368
11	Na			1.319				1.441	1.327
12	Mg			1.281				1.347	1.258
13	Al		1.266	1.243				1.307	1.230
14	Si	1.298	1.244	1.215	1.293			1.275	1.208
15	P	1.271	1.226	1.197	1.266			1.250	1.190
16	S	1.248	1.210	1.180	1.243			1.230	1.176
17	Cl	1.228	1.197	1.168	1.224			1.213	1.163
18	Ar	1.212	1.184	1.155	1.208	1.207	1.195	1.197	1.152
19	K	1.197	1.171	1.142	1.194			1.182	1.140
20	Ca	1.184	1.162	1.133	1.181			1.164	1.127
25	Mn	1.139	1.127	1.102	1.139	1.135	1.127	1.127	1.096
30	Zn	1.112	1.104	1.084	1.113	1.110	1.103	1.100	1.082
35	Br	1.093	1.085	1.072	1.094			1.085	1.070
40	Zr			1.061	1.081			1.072	1.059
50	Sn			1.046	1.063			1.055	1.046
60	Nd			1.037	1.052				
70	Yb			1.033	1.046				
80	Hg			1.030	1.042				
90	Th			1.029	1.038				

TABLE XII B. *(Continued)*

		Exchange and overlap corrections $X^{M/L}$							
								Recalculated in this work as described in Sec. II.E after:	
Z	Elements	Bahcall (1963)	Vatai (1970)	Martin and Blichert–Toft (1970)	Suslov (1970)	Faessler *et al.* (1970)	Faessler *et al.* (1970) [a]	Bahcall [a]	Vatai
10	Ne								
11	Na								
12	Mg							1.630	1.366
13	Al	1.584	1.146	1.343				1.541	1.300
14	Si	1.505	1.146	1.273	1.482			1.473	1.255
15	P	1.433	1.144	1.227	1.419			1.422	1.225
16	S	1.387	1.140	1.203	1.375			1.383	1.206
17	Cl	1.347	1.138	1.188	1.341			1.353	1.193
18	Ar	1.316	1.134	1.173	1.314	1.311	1.289	1.323	1.179
19	K	1.291	1.137	1.147	1.292			1.287	1.160
20	Ca	1.270	1.123	1.128	1.275			1.239	1.127
25	Mn	1.201	1.112	1.130	1.209	1.190	1.178	1.189	1.131
30	Zn	1.161	1.098	1.112	1.168	1.153	1.147	1.159	1.115
35	Br	1.137	1.086	1.085	1.143			1.119	1.081
40	Zr			1.068	1.126			1.094	1.061
50	Sn			1.054	1.101			1.073	1.049
60	Nd			1.040	1.086				
70	Yb			1.036	1.076				
80	Hg			1.033	1.070				
90	Th			1.029	1.066				

	Exchange and overlap corrections $X^{N/M}$			
			Recalculated in this work as described in Sec. II.E after:	
Z	Elements	Vatai (1970)	Bahcall [a]	Vatai
18	Ar			
19	K			
20	Ca		1.506	1.286
25	Mn	1.034	1.291	1.086
30	Zn	1.028	1.223	1.067
35	Br	1.038	1.199	1.086
40	Zr		1.170	1.094
50	Sn		1.127	1.077
60	Nd			
70	Yb			
80	Hg			
90	Th			

[a] Including the effect of the ns hole in the daughter atom.

capture ratios in fair agreement with experiment. On the other hand, Bahcall's approach yields better agreement to L/K ratios with experiment, but overestimates the M/L capture ratios.

To solve this problem, a new calculation is needed in which overlap corrections are treated more carefully. Electron correlation must be included, at least by means of configuration interactions. More accurate experimental capture ratios in the low-Z region are needed to provide a better test of theory.

III. EXPERIMENTAL METHODS AND RESULTS

The experimental determination of nuclear electron-capture ratios from various atomic shells and of K-capture to positron-emission (K/β^+) ratios has been the subject of considerable effort because of the importance of these quantities in various contexts. Aspects of orbital electron capture have been reviewed by Robinson and Fink (1955, 1960), Bouchez and Depommier (1960, 1965), Depommier (1968), Fink (1965, 1966, 1968, 1969), Berényi (1963a, 1965a, 1968a), Genz (1971b, 1973a), and Fitzpatrick (1973). In recent years, several new measurements of L/K, M/L, and K/β^+ ratios have been performed and much effort has been devoted to reducing experimental uncertainties, so that comparisons can be made with different theoretical calculations of atomic wavefunctions and of electron exchange and imperfect atomic wavefunction overlap effects.

In this section we classify the methods employed to determine capture ratios and compare their potential reliability. From the vast body of experimental data reported in the literature, we select a limited list of capture and K/β^+ ratios that can be considered highly reliable and use these values for comparison with theory.

Relative transition probabilities are commonly used in experimental work; these are related as follows to the transition probabilities per unit time as defined in Eqs. (2.27), (2.28), and (2.43):

$$P_{\mathrm{EC}}=\frac{\lambda_c}{\lambda_{\mathrm{tot}}}\,,\quad P_{\beta^+}=\frac{\lambda_{\beta^+}}{\lambda_{\mathrm{tot}}}\,,\quad P_{\beta^-}=\frac{\lambda_{\beta^-}}{\lambda_{\mathrm{tot}}}\,, \tag{3.1}$$

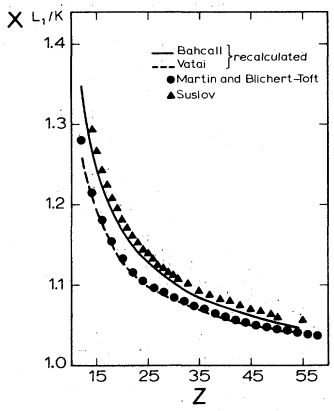

FIG. 2. L_1/K exchange and overlap correction factors. The solid and broken curves were recalculated according to the approaches of Bahcall (1963a, b; 1965a) and Vatai (1968, 1970), respectively, with wavefunctions from the Hartree–Fock program of Froese–Fischer (1972a). Results of the relativistic calculation of Suslov (1970a), following Bahcall's theory, are indicated by triangles, and those of the calculation of Martin and Blichert-Toft (1970), based on the same approach as Vatai's, are indicated by solid dots.

where

$$P_{EC}+P_{\beta^+}+P_{\beta^-}=1\,, \tag{3.2}$$

and

$$P_K=\frac{\lambda_K}{\lambda_c}\,,\quad P_L=\frac{\lambda_L}{\lambda_c}\,,\quad P_M=\frac{\lambda_M}{\lambda_c}\,,\ldots \tag{3.3}$$

where

$$P_K+P_L+P_M+\cdots=1\,. \tag{3.4}$$

Corresponding relations hold for capture from subshells.

The probability of orbital electron capture from the K shell or from any of the L or M subshells depends upon the nature and energy of the transition. The capture process cannot be detected directly because of the extremely low interaction probability of the emitted neutrino. The capture rate can therefore only be determined from the intensity of subsequently emitted radiation, such as x rays or Auger electrons given off during reorganization of the electronic cloud after capture and γ rays or conversion electrons from the daughter nucleus. In principle, the recoil of the final nucleus can also be measured, but the recoil kinetic energy is always very small. The largest recoil (57 eV) occurs in the transition $^7\mathrm{Be}\rightarrow{}^7\mathrm{Li}$.

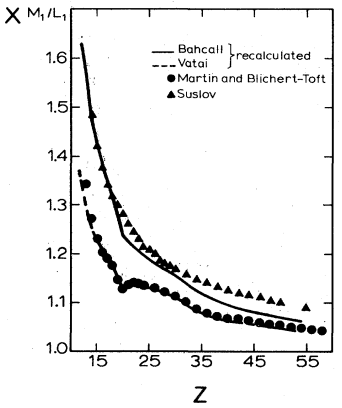

FIG. 3. M_1/L_1 exchange and overlap correction factors. See caption of Fig. 2 for details.

Methods for measuring capture probabilities vary according to the decay scheme of the radionuclide, the energy and relative intensity of the emitted radiation, available detectors, and requirements for necessary corrections. The methods can be classified according to the information they provide.

One group of methods yields ratios of capture probabilities from different shells,

$$\frac{P_L}{P_K}=\frac{\lambda_L}{\lambda_K}\,,\quad \frac{P_M}{P_L}=\frac{\lambda_M}{\lambda_L}\,. \tag{3.5}$$

From these ratios, a consistent set of capture probabilities can be deduced with the aid of Eq. (3.4):

$$P_K=\left\{1+\frac{P_L}{P_K}\left[1+\frac{P_M}{P_L}\left(1+\frac{P_N}{P_M}\right)\right]\right\}^{-1}\,,$$

$$P_L=P_K(P_L/P_K)\,, \tag{3.6}$$

$$P_M=P_L(P_M/P_L)\,.$$

Equations (3.6) can also be used with reliable theoretical capture ratios.

Some methods pertain to situations in which the L and M x-ray or Auger-electron peaks cannot be resolved. Such methods lead to the determination of a capture ratio $P_{LM\ldots}/P_K$, from which the relative K-capture probability can be obtained directly

$$\frac{P_{LM\ldots}}{P_K}=\frac{1}{P_K}-1\,. \tag{3.7}$$

In several other methods, $P_K\omega_K$ is determined, where ω_K is the K-shell fluorescence yield. With the appropriate value for ω_K (Bambynek *et al.*, 1972), the relative K-capture probability can be calculated.

If the transition energy exceeds twice the electron rest energy ($2mc^2$), then positron emission is possible as an alternative nuclear decay process. In such cases, it is of interest to measure ratios of K-capture to positron-emission probability or of the total electron-capture to positron-emission rate,

$$\frac{P_K}{P_{\beta^+}}=\frac{\lambda_K}{\lambda_{\beta^+}}\,,\quad \frac{P_{EC}}{P_{\beta^+}}=\frac{\lambda_c}{\lambda_{\beta^+}}\,. \tag{3.8}$$

Table XIII contains a compilation of methods reported in the literature; these are discussed in Secs. III.A, III.B, and III.D. The usual corrections for background, dead time, detector efficiency, etc., are taken for granted.

A. Determination of capture ratios

Capture ratios have been determined both with external and internal sources. In general, it is difficult to measure capture ratios with external sources, because large corrections are required for source self-absorption, air scattering, window absorption, and fluorescence yields. During the last few years, capture ratios have therefore more frequently been measured by internal-source

TABLE XIII. Methods that have been used for the determination of electron-capture probabilities.

No.	Method	Source	Detectors [a]	Measured	Deduced	Estimated accuracy of the method (%)
1	Spectroscopy of K, L, and M events without x-ray escape	Internal Gaseous	mw NaI(Tl)	I_L/I_K, I_M/I_L $I_{L-\gamma}/I_{K-\gamma}$	P_L/P_K P_M/P_L	1
2	Spectroscopy of K and L events with complete K x-ray escape	Internal Gaseous	pc	I_L/I_K	P_L/P_K	5
3	Spectroscopy of K, L, and M events	Internal Gaseous	pc	I_L/I_K I_M/I_L	P_L/P_K P_M/P_L	1
4	Cloud chamber technique	Internal Gaseous	cc	I_L/I_K	P_L/P_K	20
5	Spectroscopy of K, L, and M events	Internal Solid	NaI(Tl) CsI(Tl) CsI(Na) Ge(Li) $Cs_2Pt(CN)_4H_2O$	I_L/I_K I_M/I_L, $I_{L-\gamma}/I_{K-\gamma}$	P_L/P_K P_M/P_L	1
6	Spectroscopy of K and L x-rays	External Solid	pc NaI(Tl)	I_{LX}/I_{KX} $I_{LX-\gamma}/I_{KX-\gamma}$	P_L/P_K	10
7	Measurement of (K x-ray)–(L x-ray) coincidences	External Solid	pc NaI(Tl)	I_{KX-LX}, I_{LX}, I_{KX}	P_L/P_K	8
8	Spectroscopy of K x rays and γ rays	External Solid	pc,NaI(Tl) Ge(Li)	I_{KX}/I_γ	P_K	8
9	Spectroscopy of K x-rays or K Auger electrons and K conversion electrons	External Solid	sd NaI(Tl)	I_{KX}/I_{eK} I_{KA}/I_{eK}	$P_K\omega_K$ P_K	15
10	Determination of K x-ray emission rate and disintegration rate	External Solid	pc NaI(Tl)	I_{KX}, I_0	$P_K\omega_K$	1
11	Measurement of (K x-ray)–(γ-ray) coincidences	External Solid	pc,NaI(Tl) Ge(Li) Si(Li)	$I_{KX-\gamma}/I_\gamma$ $I_{KX-\gamma_1-\gamma_2}/I_{\gamma_1-\gamma_2}$	$P_K\omega_K$	5
12	Measurement of (K x-ray)–(γ-ray) coincidences at different levels	External Solid	NaI(Tl) Ge(Li) Si(Li)	$I_{KX-\gamma_1}/I_{\gamma_1}$ $I_{KX-\gamma_2}/I_{\gamma_2}$	P_{K1}/P_{K2}	5
13	Measurement of (K-event)–(γ-ray) coincidences	External Solid	pc,NaI(Tl) CsI(Tl)	$I_{K-\gamma}/I_\gamma$	P_K	3
14	Measurement of (K x-ray)–(γ-ray) sum coincidences	External Solid	NaI(Tl) CsI(Tl) Ge(Li)	$I_{KX+\gamma}/I_\gamma$ $I_{KX+\gamma_1+\gamma_2}/I_{\gamma_1+\gamma_2}$	$P_K\omega_K$	8
15	Measurement of (K x-ray)–(γ-ray) and (K x-ray)–(K x-ray) or (K x-ray)–(K conversion electron) coincidences	External Solid	NaI(Tl) Si(Li) sd	$I_{KX-\gamma}/I_\gamma$ I_{KX-KX}/I_{KX} I_{KX-eK}/I_{eK}	P_K	3
16	Measurement of (K x-ray)–(K conversion electron) and (K x-ray)–(L conversion electron) coincidences	External Solid	NaI(Tl) sd	I_{KX-eK}/I_{eK} I_{KX-eL}/I_{eL}	P_K	3
17	Measurement of (K Auger electron)–(K conversion electron) and (K Auger electron)–(L conversion electron) coincidences	External Solid	sd,sl	I_{KA-eK}/I_{eK} I_{KA-eL}/I_{eL}	P_K	3
18	Measurement of (K x-ray)–(K conversion electron) coincidences	External Solid	pc,sc NaI(Tl) Ge(Li)	I_{KX-eK}/I_{eK} I_{KX-eK}/I_{KX} I_{eK}, I_{KX}	$P_K\omega_K$ P_K	5 7
19	Measurement of (K x-ray)–(γ-ray)–(K or L conversion electron) coincidences	External Solid	NaI(Tl) Ge(Li) sd	$I_{KX-\gamma-e_L}/I_{\gamma-e_L}$ $I_{KX-\gamma-e_K}/I_{\gamma-e_K}$	$P_K\omega_K$ P_K	5
20	Spectroscopy of K events and positrons (no K x-ray escape)	Internal Gaseous	pc	I_K/I_{β^+}	P_K/P_{β^+}	6
21	Spectroscopy of K events and positrons (no K x-ray escape)	Internal Gaseous	apc	I_K/I_{β^+}	P_K/P_{β^+}	3
22	Spectroscopy of K events and positrons	Internal Solid	NaI(Tl)	I_K/I_{β^+}	P_K/P_{β^+}	2
23	Spectroscopy of K Auger electrons and positrons	External Solid	gm, pc	I_{KA}/I_{β^+}	P_K/P_{β^+}	9
24	Spectroscopy of K x rays and positrons	External Solid	NaI(Tl), Si(Li), pc	I_{KX}/I_{β^+}	P_K/P_{β^+}	1
25	Spectroscopy of K x rays and β^+ annihilation photons	External Solid	NaI(Tl), Si(Li), pc,Ge(Li)	I_{KX}/I_{511}	P_K/P_{β^+}	1.5
26	Spectroscopy of nuclear and β^+ annihilation photons	External Solid	NaI(Tl), Ge(Li)	I_γ/I_{511}	P_{EC}/P_{β^+}	3
27	Measurement of (positron)–(γ ray) coincidences	External Solid	pc,pl NaI(Tl), Ge(Li)	I_γ, $I_{\beta-\gamma}$	P_{EC}/P_{β^+}	2.5

TABLE XIII. *(Continued)*

No.	Method	Source	Detectors [a]	Measured	Deduced	Estimated accuracy of the method (%)
28	Measurement of (positron)−(γ ray) N and (positron)−(γ ray) S coincidences	External Solid	pc,NaI(Tl)	$I_{\beta^+}, I_{\gamma N}, I_{\gamma S}, I_{\beta-\gamma N}, I_{\beta-\gamma S}$	$P_{EC}/P_{\beta+}$	0.3
29	Measurement of (γ ray)−(511 keV γ)−(511 keV γ) triple coincidences	External Solid	NaI(Tl), Ge(Li)	$I_\gamma, I_{\text{triple}}$	$P_{EC}/P_{\beta+}$	2
30	Measurement of (γ ray)−(511 keV) β^+ annihilation photon coincidences	External Solid	NaI(Tl), Ge(Li)	$I_\gamma, I_{\gamma-511}$	$P_{EC}/P_{\beta+}$	3
31	Miscellaneous	–	–	–	–	–

[a] The following abbreviations are used: apc, anticoincidence proportional counter; cc, cloud chamber; gm, Geiger–Müller counter; pc, proportional counter; pl, plastic scintillator; mw, multi-wire proportional counter; sc, semiconductor; sd, double-focussing spectrometer; se, lens spectrometer.

techniques in which these difficulties are avoided, provided the radioactive atoms can be dispersed throughout the sensitive volume of the counter. Internal-source methods fall into two major classes: at low atomic numbers, gaseous compounds are mixed with the counting gas of a proportional counter, while at high Z crystal scintillators are preferred that have the radioactive atoms built into the lattice, thus minimizing distortions due to escape of x rays from the sensitive counter volume.

1. Spectrometry with internal gas sources

A radioactive gas or the vapor of a radioactive metal-organic compound is added to the counting gas of a proportional counter. The prompt cascade of x rays and Auger electrons, which follows the capture event, is integrated by the detector to produce a single K peak at the K-electron binding energy of the daughter atom. Similarly, $L, M, \ldots$ peaks are produced by events from higher shells. It is usually assumed that all L and M x rays and Auger electrons are completely absorbed inside the counter. However, as Vatai (1968d, 1970b) has pointed out, the escape of L x rays is not always negligible *a priori*, and becomes especially important if the L x-ray energy lies just below the K-shell binding energy of the counter gas. The L peak contains a contribution from K-capture events which arises from K x rays that escape from the sensitive volume of the counter.

Typical K, L, and M peaks from an internal ^{71}Ge source are shown in Fig. 4. From the measured intensities I_K, I_L, I_M of these peaks, the ratio of capture probabilities can be deduced:

$$\frac{P_L}{P_K} = \frac{I_L}{I_K}\left[1 - \omega_K(k_\alpha P_{K\alpha} + k_{\beta'} P_{K\beta'})\right] - \omega_K k_\alpha P_{K\alpha}\,, \tag{3.9}$$

$$\frac{P_M}{P_L} = \frac{I_M}{I_L}\left[1 + \frac{P_K}{P_L}\,\omega_K P_{K\alpha} k_\alpha\right] - \frac{P_K}{P_L}\,\omega_K P_{K\beta} k_{\beta'} - P_{L\alpha}\omega_L l_\alpha\left[1 + \frac{P_K}{P_L}\,\omega_K P_{K\alpha} k_\alpha\right]. \tag{3.10}$$

Here, ω_K and ω_L are the K- and L-shell fluorescence yields of the daughter atom, and k_α, $k_{\beta''}$, and l_α the fractions of $K\alpha$, $K\beta'$, and $L\alpha$ x rays in the K and L series. The K and L x-ray escape probabilities from the detector sensitive volume are denoted by $P_{K\alpha}P_{K\beta}$ and $P_{L\alpha}$.

There are two limiting cases. The first of these is Method 1 of Table XIII, in which escape of x rays from the counter volume is avoided. Then Eqs. (3.9) and (3.10) have the simple form

$$\frac{P_L}{P_K} = \frac{I_L}{I_K}\,; \quad \frac{P_M}{P_L} = \frac{I_M}{I_L}\,. \tag{3.11}$$

Absence of x-ray escape can be realized approximately

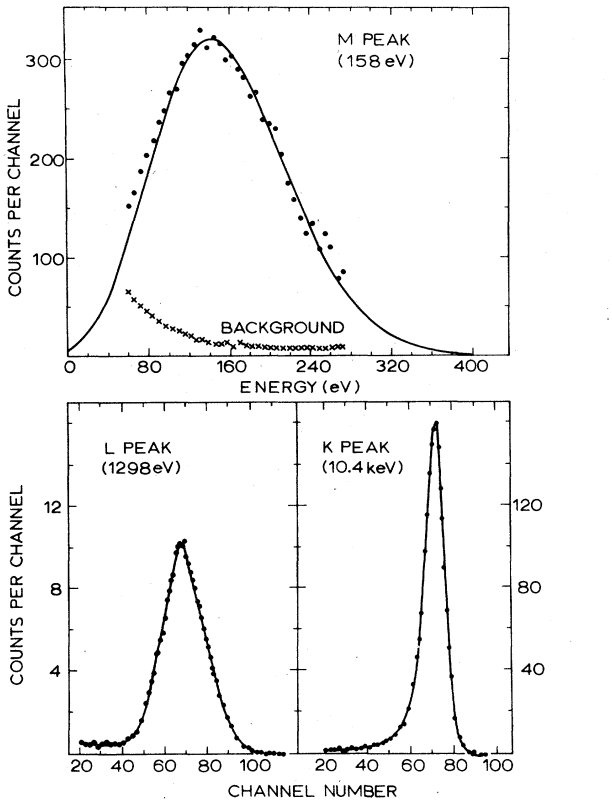

FIG. 4. Typical K, L, and M spectra from the decay of ^{71}Ge measured with a multiwire counter system. In the M spectrum, background and degradation tails were subtracted and a Poisson distribution fitted to the data (after Genz, 1971a).

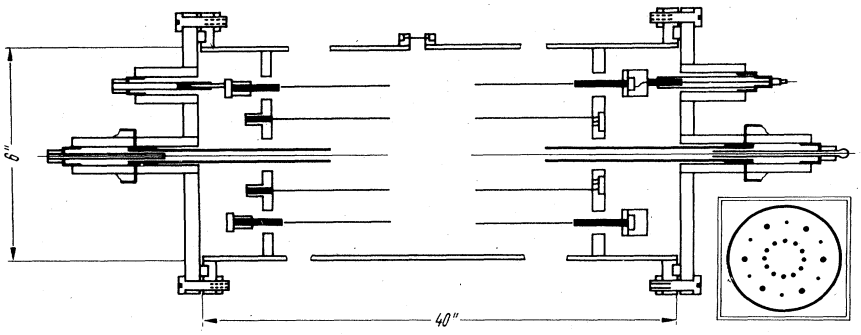

FIG. 5. Multiwire proportional counter (after Scobie *et al.*, 1959).

when the counter is operated at high pressure. Gas fillings of argon-propane and argon-methane mixtures at up to 22 atm have been used. Since the development of the wall-less multiwire proportional counter (Drever *et al.*, 1957a, 1957b), this type of detector has been employed successfully by various groups. The principal advantage of such a multiwire counter is that escape can be made very small. A central counter is surrounded by a ring of additional counters (Fig. 5). An inner circle of wires serves as the cathode for the central counter. Alternate wires in an outer circle serve as anodes and cathodes of a set of ring counters. The sensitive volume of the detector is then separated into two parts. The main central counter and the ring counters are operated in anticoincidence.

A block diagram of electronics for the operation of a multiwire proportional counter is shown in Fig. 6. Negative high voltage is often applied to the outer case of the counter and to the field tubes. This approach is superior to grounding the cathode and using positive high voltage on the center wire, with a large potential difference across the coupling capacitor between center wire and the first preamplifier stage, leading to problems of leakage and spurious discharge.

For the determination of L/K ratios at $Z<20$ and M/L ratios at $Z<40$ it is necessary to detect Auger electrons and soft x rays below 500 eV, down to a few eV. Most recent advances in low-energy proportional-counter technique are related to the electronic system (Dougan *et al.*, 1962; Renier *et al.*, 1968; Genz *et al.*, 1971a). Proportional-counter spectrometry of radiation below ~500 eV is affected by certain problems that are less important or negligible at higher energies:

(1) Afterpulses from primary ionizing events can occur (Dougan *et al.*, 1962a; Renier *et al.*, 1968; Genz *et al.*, 1971a; Campion, 1968, 1973);

(2) degradation tails from peaks of higher energy can appear (Renier *et al.*, 1968; Genz *et al.*, 1971a; Heuer, 1966; Vaninbroukx and Spernol, 1965; Spernol, 1967);

(3) small pulses can be mutually induced between ring and center counters in multiwire detectors (Genz *et al.*, 1971a; Drever *et al.*, 1957);

(4) the anticoincidence gate may cause front- and back-edge clipping of large pulses, producing smaller pulses (Dougan *et al.*, 1962a; Renier *et al.*, 1968; Genz *et al.*, 1971a);

(5) large dead time may arise when radiation of higher energy is present in high intensity (Dougan *et al.*, 1962a; Renier *et al.*, 1968; Genz *et al.*, 1971a). The electronic system shown in Fig. 6 is designed to overcome these problems, except for long dead time and degradation tails.

The shape of the spectrum produced by events between a few and 500 eV depends on the initial number of ion pairs. The energy required to produce an ion pair in an argon-propane mixture is ~27 eV. Peaks produced by

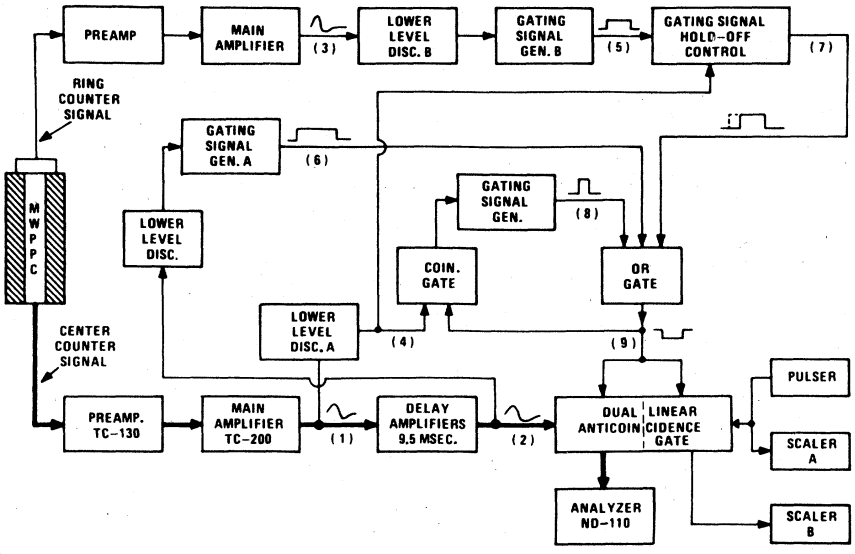

FIG. 6. Block diagram of multiwire-proportional-counter electronic system (after Genz *et al.*, 1971a).

several ion pairs can be satisfactorily fitted with a Poisson distribution (Campbell and Ledingham, 1966), while the spectrum due to single-electron events cannot be represented accurately by an exponential or quasi-exponential function, as it varies with gas multiplication (Gold and Bennet, 1966; Genz, 1968, 1973b).

Corrections for several effects must be applied:

(1) Escape probabilities $P_{K\alpha}$ and $P_{K\beta}$ of $K\alpha$ and $K\beta$ x rays from the sensitive volume of the counter must be accounted for. These escape probabilities can be separated into the additive probabilities P_1, that a K x ray escapes from the central counter through the ends, P_2, that a K x ray escapes from the central counter and hits a cathode wire, and P_3, that an x ray escapes from the central counter and passes through a ring counter without being detected. All these corrections can be kept below 1%. A careful study of the escape probability in multiwire counters has been made by Vatai (1970b).

(2) An important correction must be made for degraded L and K events in the energy region below the peaks. The total contribution from such events can be determined by extrapolation parallel to the energy axis to low energy, as has been demonstrated down to 80 eV (Genz *et al.*, 1971a). The degradation correction can amount to several percent but has not been taken into account in many investigations. This leads to appreciable differences in results (Heuer, 1966; Totzek and Hoffmann, 1967; Genz *et al.*, 1971a; Pengra *et al.*, 1972).

(3) Condensation of radioactive metal-organic vapor on the counter wall can lead to an increase in background.

(4) Values of the fluorescence yield ω_K and of the $K\alpha/K\beta'$ x-ray intensity ratios can usually be taken from literature. The largest source of error in this method arises from the uncertainty in the I_L/I_K or I_M/I_L intensity ratio. In the determination of M/L capture ratios, errors in P_L/P_K largely cancel [see Eq. (3.10)]. Uncertainties in k_α and k_β have been greatly reduced since the new calculations of Scofield (1974) became available, which agree very well with experiment (Scofield, 1975).

If transitions take place to several levels in the daughter nucleus, then only mean capture ratios are measured. Several of the most reliable mean ratios have been measured by internal gas-source spectrometry. In the use of nuclides that decay by electron capture to a level that is de-excited by a γ transition, coincidences can be measured between K and L events detected in a multiwire counter and γ rays detected with NaI(Tl) scintillators surrounding the proportional counter. The capture ratio for transitions to the excited state can be deduced from the measured intensities $I_{L\text{-}\gamma}$ and $I_{K\text{-}\gamma}$ of L and K events gated by the γ rays. Equation (3.9) applies, with I_L and I_K replaced by $I_{L\text{-}\gamma}$ and $I_{K\text{-}\gamma}$. An analogous procedure can be employed in M/L-ratio measurements. In addition to the corrections already mentioned, accidental and sum coincidences must be taken into account.

In the second limiting case of internal gas spectrometry (Method 2 of Table XIII), all K x rays are allowed to escape from the sensitive volume of the counter. Then we have $P_{K\alpha}=1$ and $P_{K\beta}=1$, Eq. (3.9) yields

$$\frac{P_L}{P_K}=\frac{I_L}{I_K}(1-\omega_K)-\omega_K k_\alpha\,, \tag{3.12}$$

and Eq. (3.10) becomes

$$\frac{P_M}{P_L}=\frac{I_M}{I_L}\left[1+\frac{P_K}{P_L}\omega_K k_\alpha\right]-\frac{P_K}{P_L}\omega_K k_{\beta''}\,. \tag{3.13}$$

Here, L x-ray escape is considered negligible. Experimentally, total K x-ray escape has been approximated with single-wire proportional counters filled with a low-Z gas at low pressure (Pontecorvo *et al.*, 1949; Langevin, 1954b, 1955, 1956; Langevin and Radvanyi, 1954a, 1955; Radvanyi, 1955a; Scobie, 1957a; Kiser and Johnston, 1959). Corrections are needed to account for: (1) nonescape of K x rays, (2) escape of L x rays, (3) wall and end effects, (4) the fluorescence yield ω_K, and (5) the fraction k_α of $K\alpha$ x rays in the total x-ray group. Additional uncertainties may arise from separation of the K and L peaks and from their degradation tails.

With single-wire proportional counters containing a gaseous radioactive source mixed with the counter gas, reliable measurements are no longer limited to events with energies above ~200 eV. Recent advances in single-wire proportional-counter techniques (No. 3 in Table XIII) have extended the sensitivity of precision measurements to make possible the detection of single- and few-electron events down to essentially zero energy, even in the presence of intense more energetic radiation (Fink, 1968; Genz, 1968, 1973a). These improvements were attained with more sophisticated low-noise electronics and through an understanding of the degradation spectrum (Genz *et al.*, 1971a) and of after-pulses (Genz *et al.*, 1968). Single- and few-electron peaks have been resolved on the basis of their spectral shape (Renier *et al.*, 1968) or by fitting a Poisson distribution (Genz *et al.*, 1971a, 1972; Pengra *et al.*, 1972). The techniques of single-electron spectrometry have been applied by Renier *et al.* (1968) in a precision measurement of the M/L capture ratio of ^{37}Ar. In this case, the peak due to capture of L-shell electrons has a mean energy of 280 eV, and the M spectrum is a single-electron peak because the energy released in a capture event (~5 eV) is lower than that required to produce an ion pair (~26.5 eV in argon–propane). The spectrum due to single electrons was determined experimentally by introducing ultraviolet photons into the counter to produce photoelectrons of only a few eV. This experimentally determined single-electron spectrum was fitted in the M region (Fig. 7) of the composite M and L spectrum (Fig. 8) and extrapolated to zero energy. The small afterpulses which may follow a primary event in the counter gas were kept from entering the analyzer by introducing an electronic paralysis time of up to 3.8 msec following each primary pulse. A block diagram of the electronic circuit is shown in Fig. 9.

The principal errors in this method arise from fitting the single-electron spectrum to the M-peak shape and from establishing the zero-energy calibration of the analyzer. The spectrum must be corrected for background and degradation tails. The ratio P_M/P_L is a very sensitive function of k_α, but it is rather insensitive to ω_K [Eq. (3.13)].

Internal gas spectrometry for the precision determination of electron-capture ratios is limited to sources with atomic numbers below ~50, because with heavier atoms too many x rays escape from the sensitive counter vol-

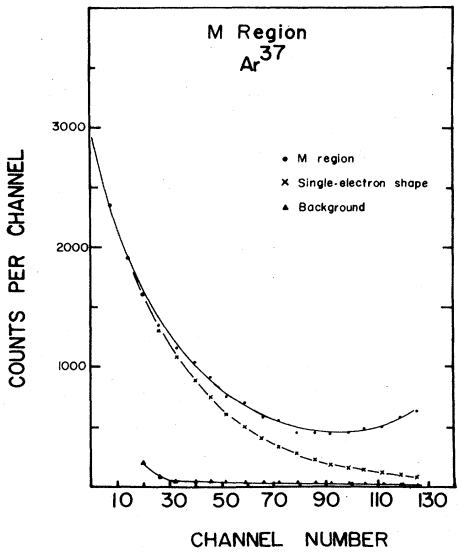

FIG. 7. The M region of the ^{37}Ar spectrum, with the single-electron spectrum produced by introducing ultraviolet photons from an external source, normalized to the M spectrum (after Renier *et al.*, 1968).

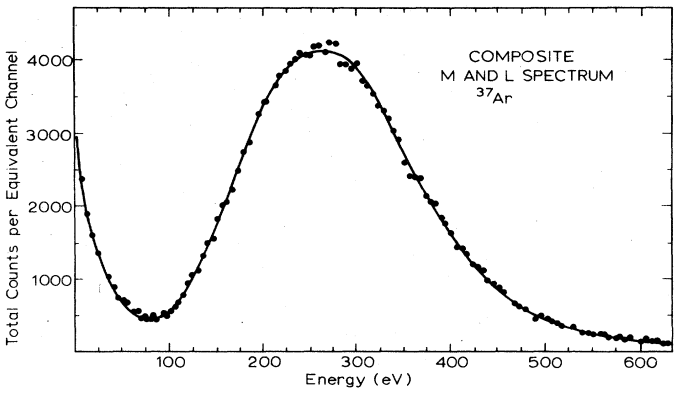

FIG. 8. The normalized M and L spectra from ^{37}Ar decay, corrected for dead time and background (after Renier *et al.*, 1968).

ume, even at high counting-gas pressures. Although this escape probability can be calculated in principle, the accuracy of the measurements is severely affected.

In earlier days, some L/K capture ratios were determined by measuring trajectories produced in a cloud chamber by K and L events from a radioactive gas (Radvanyi, 1952a, 1955a). This approach is included in Table XIII for historical reasons as Method 4.

2. Spectrometry with internal solid sources

The internal gas spectrometry technique fails at high Z because too many K x rays escape. To circumvent the problem, the proportional counter can be replaced by scintillation crystals if the radioactive atoms can be built into the crystal lattice (der Mateosian, 1953). From the measured intensities of K, L, and M events the capture ratios can then be deduced. The advantage of the method (No. 5 in Table XIII) is that self-absorption of the emitted radiation can be neglected. It is required, however, that the scintillation behavior not be disturbed by addition of the source material. Clustering must be avoided.

The source crystal can be placed directly on the photocathode of the multiplier tube. Groups at Heidelberg have used NaI(Tl) and CsI(Na) crystals doped with appropriate isotopes for the determination of electron-capture ratios by the internal-source technique. Leutz *et al.* (1966) grew NaI(Tl) crystals containing ^{202}Tl and ^{204}Tl as a constituent of the crystal lattice, and Schulz (1967a) doped the scintillator with ^{83}Rb and ^{185}Os. Furthermore, ^{131}Cs has been built into the lattice of CsI(Na) scintillation crystals. To use doped crystals for spectrometry it is necessary that the radioactive nuclei be uniformly distributed in the scintillator. To avoid absorption effects caused by possible surface concentration and precipitation of activity at grain boundaries, Ravn and Bøgeholt (1971) used $Cs_2Pt(CN)_4 \cdot H_2O$ doped with ^{193}Pt for the determination of the M/L capture ratio in the decay of ^{193}Pt. This scintillator material has several advantages.

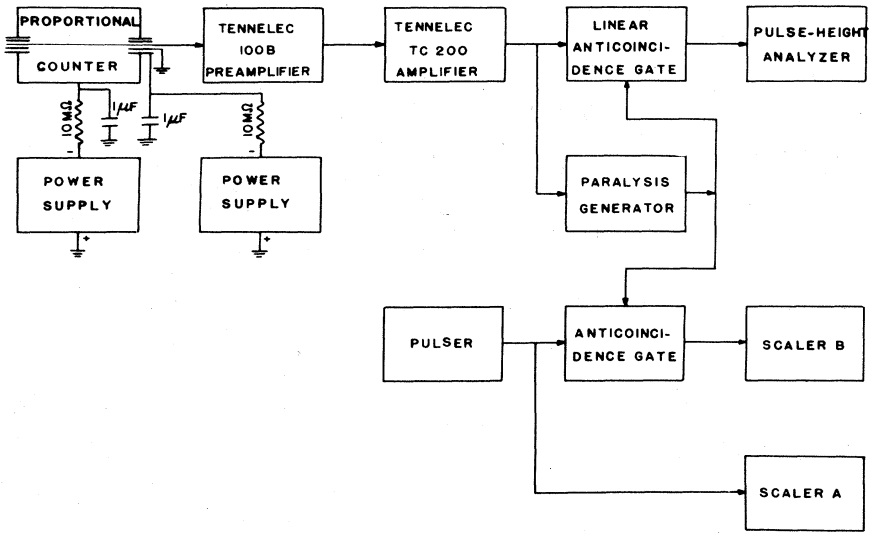

FIG. 9. Block diagram of single-wire proportional-counter electronic system (after Genz *et al.*, 1972).

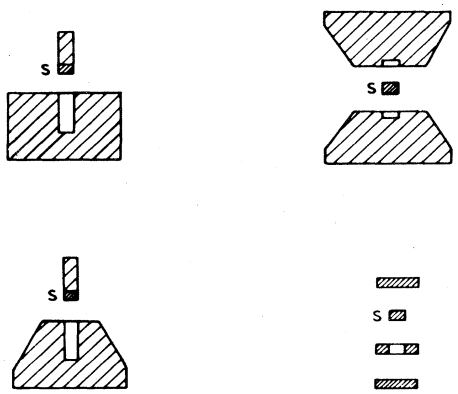

FIG. 10. Assemblies of source and enveloping crystals (after Goedbloed *et al.*, 1970a).

Platinum being one of the main constituents of the crystal, ^{193}Pt is for chemical reasons ensured a completely uniform distribution. The crystal exhibits light yields and relaxation times comparable to those of NaI(Tl).

Two principal sources of error must be overcome in this method. The radioactive source must form a true solution; if the radioactivity lodges nonuniformly at dislocations or grain boundaries, absorption effects occur. Schultz (1967b) has investigated the problem and has developed a chemical and a physical criterion to decide which radioactive isotopes form true mixed crystals with NaI(Tl). She finds that Rb, Cs, Ba, Os, Tl, and Pb do form such mixed crystals, whereas P, Ca, Mn, Zn, As, Y, Sn, Ce, and Bi do not. Joshi *et al.* (1963) have studied the effects of nonuniformity of mixing and the phenomena of overactivation and poisoning. The second main source of error arises from K x-ray escape from regions near the surface, which results in the recording of K-capture events as L- or M-capture events.

To correct for x-ray escape, basically two methods have been used. A well-type NaI(Tl) hollow crystal can be employed to surround the NaI(Tl) crystal that contains the internal radioactive source (Fig. 10). Escaping K x rays from electron capture and iodine K x rays associated with the detection process are absorbed in the outer crystal and are recorded as simultaneous events, so that no x-ray escape corrections are required. The method has been used by Joshi and Lewis (1960), Joshi (1961), Smith and Lewis (1966), Goedbloed (1970a), and by Goedbloed *et al.* (1968, 1970b) who have discussed it in detail.

An alternative approach to correct for x-ray escape involves measurement of the ratios of the areas A, B, and C of the K, L, and M peaks for several source crystals of different sizes (Figs. 11 and 12). Leutz *et al.* (1966) have shown that correction for escape can be most accurately performed by plotting the ratios $A/(A+B)$ and C/B against the surface-to-volume ratio of the doped crystal and extrapolating linearly to a surface-to-volume ratio of zero. Thus, values of $P_K/(P_K+P_L)$ and P_M/P_L are found that correspond to a measurement with an infinitely large crystal.

Corrections must be applied for (1) sum effects, (2) self-absorption, if clustering occurs, (3) possible influence of internal conversion or β^- background (as in the case of ^{204}Tl). K x-ray escape is accounted for if one of the above-described techniques is used. The method of internal solid source spectrometry can be made very accurate.

A reduction in the noise level was attained by Ravn and Bøgeholt (1971) by means of a coincidence system in which two low-noise photomultiplier tubes were coupled to a ^{193}Pt-doped crystal. Crystal and photomultiplier assembly were cooled to −35°C to reduce dark current (Fig. 13).

In the case of nuclides that undergo electron capture to an excited state, internal solid-source spectrometry with coincident γ rays is possible. The intensities of L and K events are measured in the source crystal in coincidence with ensuing γ rays (Fig. 14). Accidental coincidences must be taken into account. In favorable cases this method can be made quite accurate.

3. Spectrometry of K and L x rays with external sources

This method (No. 6 in Table XIII) is based on the determination of the intensities I_{LX} of L x rays and I_{KX} of K x rays from singles spectra as measured with proportional counters or NaI(Tl) detectors. The sources, placed outside the sensitive volume of the detector, are usually prepared by drop deposition, but metal grains (Johns *et al.*, 1957), sources prepared by painting (Fujiwara *et al.*, 1964), and vacuum-evaporated sources (Venugopala Rao and Crasemann, 1965) have been used. The L/K ratio is deduced from the relation

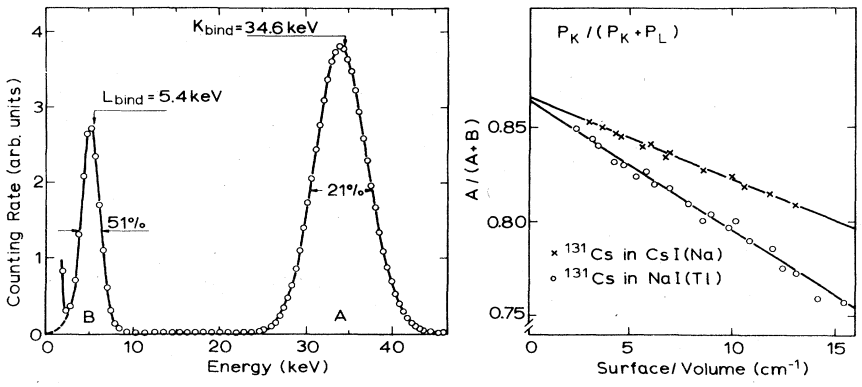

FIG. 11. Spectrum of ^{131}Cs measured with a doped NaI(Tl) crystal. Elimination of escape effects by extrapolating to a zero surface-to-volume ratio (after Schulz, 1967a).

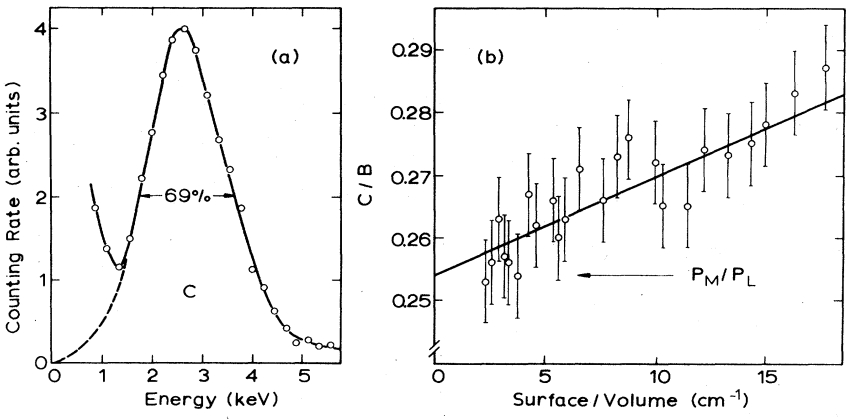

FIG. 12. M-electron capture decay to the 646-keV level of ^{185}Re. (a) Spectrum of M events. (b) Extrapolation to correct for escape effects (after Schulz, 1967a).

$$\frac{P_L}{P_K}=\frac{I_{LX}}{I_{KX}}\frac{\omega_K}{\omega_{LL}}-\frac{\omega_{LK}}{\omega_{LL}}n_{KL}\,, \tag{3.14}$$

where ω_K is the K-shell fluorescence yield, ω_{LL} is the partial L-shell fluorescence yield following L capture, ω_{LK} is the partial L fluorescence yield following $K\alpha$ x-ray emission, and n_{KL} is the number of L-shell vacancies produced on the average when a K-shell vacancy is filled.

Corrections must be made to account for (1) self-absorption, (2) absorption between source and detector, (3) solid angle, if different detectors are used for the measurement of L and K x rays, (4) efficiency of the detectors, (5) interfering effects due to γ rays and internal-conversion electrons. There is some uncertainty in n_{KL} and in the fluorescence yields ω_K, ω_{LK}, and ω_{LL}, which can usually be found in the literature (Bambynek *et al.*, 1972). An additional uncertainty can arise from degraded L x rays at the low-energy side of the L peak.

Capture ratios can be determined by this method in the case of nuclides that decay from ground state to ground state or to an excited metastable state. For nuclei that decay by a prominent transition, among others, to the ground state of the daughter, mean L/K ratios can be obtained. Though often used, the method is not very accurate, because P_L/P_K is a small difference between two large quantities, and the partial L-shell fluorescence yield greatly affects the result.

Venugopala Rao and Crasemann (1965), and Venugopala Rao *et al.* (1966a) have measured the L and K x-ray intensities relative to the K x-ray intensity of a ^{109}Cd reference source and thus deduced P_L/P_K of ^{181}W and ^{204}Tl. Kramer *et al.* (1956) have determined P_L/P_K of ^{202}Tl by comparing the intensity ratio I_{LX}/I_{KX} with that of a ^{203}Hg reference source. In addition to the need for corrections indicated earlier, the quantities n_{KL}, ω_{LL}, ω_{LK} and the internal conversion coefficients α_L and α_K of the reference source must be known. With an appropriately chosen reference nuclide these corrections can partly cancel.

For nuclides decaying to an excited state that is followed by γ-ray emission, coincidences can be determined between K x rays and γ rays and between L x rays and γ rays. From the measured coincidence counting rates $I_{KX\text{-}\gamma}$ and $I_{LX\text{-}\gamma}$ and from the singles rate I_γ, the L/K-capture ratio can be found:

$$\frac{P_L}{P_K}=\left(\frac{I_{LX\text{-}\gamma}/I_\gamma}{I_{KX\text{-}\gamma}/I_\gamma}\right)\frac{\omega_K}{\omega_{LL}}-n_{KL}\left(\frac{\omega_{KL}}{\omega_{LL}}\right). \tag{3.15}$$

The L x rays have usually been measured with proportional counters, and the K x rays and γ rays, with

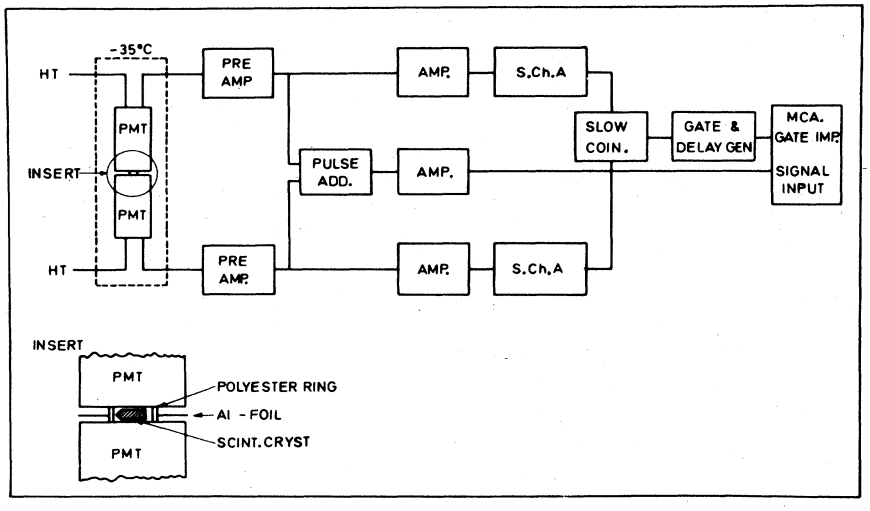

FIG. 13. Block diagram of coincidence apparatus to measure ^{193}Pt M- and L-capture peaks (after Ravn and Bøgeholt, 1971).

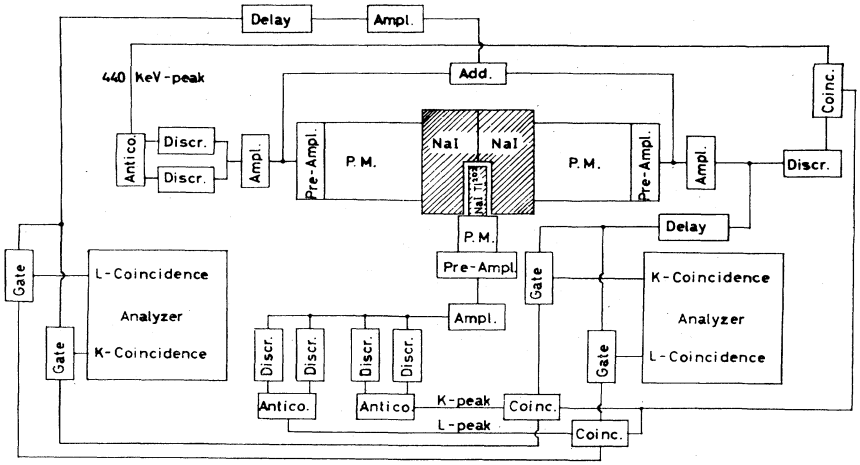

FIG. 14. Block diagram for coincidence measurements with internal solid sources (after Leutz *et al.*, 1966).

NaI(Tl) detectors. This method is an extension of that based on Eq. (3.14). It requires the same principal corrections and suffers from the same uncertainties; accidental and sum coincidences must also be taken into account.

A special technique was employed by McCann and Smith (1968) in their work on ^{133}Ba. These authors used a NaI(Tl) detector to measure the L and K x-ray spectra gated by the sum coincidence peak of the 356-keV and 81-keV γ rays, which were absorbed in another NaI(Tl) detector.

Measurement of (L-event)–(K-x-ray) Coincidences. This method (No. 7 in Table XIII) has been employed by Christmas (1964) to determine the L/K-capture ratio of ^{204}Tl. Coincidences between L x rays and K x rays were measured by means of two NaI(Tl) detectors, and P_L/P_K was deduced. In a similar approach, Konstantinov and Perepelkin (1961) used a 4π proportional counter filled with a Xe–CH_4 mixture. Coincidences between L events (L x rays and L Auger electrons) in the top part and K x rays in the bottom part of the counter were detected. A sufficiently thick backing material permitted only K x rays to penetrate to the bottom counter.

The method requires corrections for (1) self-absorption of L x rays and Auger electrons, (2) absorption of K x rays in the backing foil, (3) escape of K x rays from the detectors, (4) detector efficiencies, including solid angle, (5) accidental and sum coincidences, and (6) influence of possible γ rays. Values of n_{KL} and K-shell and L-shell fluorescence yields can usually be found in the literature (Bambynek *et al.*, 1972); they contribute to the overall uncertainty. The method yields mean P_L/P_K values if the nuclide decays by more than one electron-capture branch.

B. Determination of the relative K-capture probability P_K

In addition to the determination of capture ratios, there are various other methods from which the relative capture probability P_K can be deduced. Some of these constitute a direct measurement of P_K. In various others the product $P_K\omega_K$ is determined. All measurements described in this section employ external sources, placed outside the sensitive volume of the detector.

1. Measurement of K x rays or Auger electrons and γ rays or conversion electrons

a. Spectrometry of K x rays and γ rays

The principle of this method (No. 8 in Table XIII) is to measure the intensities I_{KX} of the emitted K x rays and I_γ of the γ rays and hence to deduce the K-capture probability

$$I_{KX}/I_\gamma = \alpha_K\omega_K[1 + P_K(1+\alpha)/\alpha_K]\,. \tag{3.16}$$

Here, ω_K is the K-shell fluorescence yield, while α_K and α are the K-shell and total conversion coefficients. Sources have been prepared by simple drop deposition. Proportional counters as well as NaI(Tl) and Ge(Li) detectors have been used.

Principal corrections are required for (1) self-absorption of the K x rays, (2) absorption between source and sensitive volume of the detectors, (3) efficiencies of the detectors for K x rays and γ rays, and (4) solid angles. Values for the fluorescence yield ω_K and the conversion coefficients are required. If internal conversion can be neglected, Eq. (3.16) becomes simply $I_{KX}/I_\gamma = P_K\omega_K$.

Bayer *et al.* (1972) used this method to measure the K x-ray intensities in the ^{140}Nd → ^{140}Pr → ^{140}Ce decay chain and to deduce P_K of ^{140}Nd. Wapstra *et al.* (1954, 1957) and Friedlander and Orr (1951b) employed two nuclides that decay to the same excited level in the daughter nucleus, one by electron capture and the other by β^- emission. The intensity ratio of the K x rays and γ rays from the two nuclides was determined and hence the K-capture probability

$$(I_{KX}/I_\gamma)_{EC}(I_{KX}/I_\gamma)_\beta^{-1} = 1 + P_K(1+\alpha)/\alpha_K\,. \tag{3.17}$$

Corrections are required mainly for (1) sum effects, and (2) contributions of radiation from higher levels. K-shell and total conversion coefficients are usually taken from the literature.

b. Spectrometry of K x rays or Auger electrons and K conversion electrons

The principle of this method (No. 9) is to measure the intensity I_{KX} of K x rays and I_{eK} of K conversion electrons (Avignon *et al.*, 1955). The K-capture probability

is found from the equation

$$I_{KX}/I_{eK} = \omega_K[1 + P_K(1+\alpha)/\alpha_K] . \quad (3.18)$$

Moussa and Juillard (1956) have measured the intensities I_{KA} of K Auger electrons and I_{eK} of K conversion electrons and used a relation similar to Eq. (3.18) with I_{KX} and ω_K replaced by I_{KA} and $(1-\omega_K)$, respectively. Magnetic β^- spectrometers were used to detect the electrons and a NaI(Tl) scintillation counter for the x rays.

Corrections must be made for (1) self-absorption of the K x rays or Auger electrons, (2) absorption between source and detector; (3) efficiencies of the detectors including solid angles; and (4) radiation from higher levels, if present. Fluorescence yields and internal conversion coefficients are usually taken from the literature.

c. Determination of K x-ray emission rate and disintegration rate

This method (No. 10) requires determination of the K x-ray emission rate I_{KX}, preferably with a large proportional counter filled to a sufficient pressure to absorb all K x rays. In addition, the disintegration rate I_0 must be determined, preferably by means of a coincidence technique as used in absolute standardization of radioactive sources. The value $P_K\omega_K$ is found from the relationship

$$P_K\omega_K = I_{KX}/I_0 , \quad (3.19)$$

where ω_K is the K-shell fluorescence yield.

The method is described in detail by Taylor and Merritt (1965). To check the K x-ray emission rate, a second fairly independent approach can be used (Bambynek, 1967a) utilizing a medium-solid-angle arrangement with a proportional counter or a thin NaI(Tl) crystal as detector (Bambynek *et al.*, 1966; Bambynek, 1967b). The detection system for determining the disintegration rate has been described by Campion (1959). It consists of a 4π flow-type pillbox proportional counter placed between two NaI(Tl) detectors. A calibrated γ spectrometer (Vaninbroukx and Grosse, 1966) has also been used to determine the disintegration rate.

Radioactive sources have been prepared for experiments of this type by drop deposition, electrodeposition, and evaporation in vacuum. Sources have been mounted on thin metallized plastic foils for the determination of the disintegration rates, then they were sandwiched between absorber foils to stop all Auger electrons, so that K x-ray emission rates could be measured in a high-pressure proportional counter.

The principal corrections that must be applied in the K x-ray measurements are for (1) self-absorption, (2) foil absorption, (3) x-ray counter efficiency (normally near unity), and (4) the effect of γ rays and β^+ particles, if present. The corrections in the determination of the disintegration rate by the coincidence method are small and well-understood, and involve only parameters that can be determined experimentally as an integral part of the measurement. The fluorescence yield ω_K is usually taken from the literature (Bambynek *et al.*, 1972).

This method has been applied in laboratories specializing in the standardization of radionuclides, and has yielded several of the most reliable $P_K\omega_K$ values.

2. Coincidence measurements

With nuclides that decay by electron capture to an excited level in the daughter nucleus, coincidences can be measured between x rays or Auger electrons (from the capture process) and γ rays or conversion electrons (from the deexcitation of the daughter state). Such measurements can serve to determine capture probabilities or their ratios.

a. Measurement of K x-ray and γ-ray coincidences

In this method (No. 11), coincidences are measured between K x rays in one detector and γ rays in another detector. One finds

$$P_K\omega_K = I_{KX\text{-}\gamma}/I_\gamma , \quad (3.20)$$

where $I_{KX\text{-}\gamma}$ is the (K x-ray)–(γ-ray) coincidence counting rate, I_γ is the singles γ rate, and ω_K is the K-shell fluorescence yield of the daughter atom. Sources for such experiments have mostly been prepared by drop evaporation; however, plated (Grotheer *et al.*, 1969), electroplated (Thomas *et al.*, 1963), gaseous external sources (Bresesti *et al.*, 1964; Winter *et al.*, 1965b), and metal powders (Perrin, 1960; Millar *et al.*, 1959) have also been used.

Different combinations of detectors have been employed; in most cases proportional counters served for the K x rays and NaI(Tl) detectors for the γ rays or for both radiations. Solid state detectors have also been used recently: NaI(Tl)–Ge(Li) (Raeside *et al.*, 1969; Mysĺek *et al.*, 1971); Ge(Li)–Ge(Li) (Schmidt-Ott and Fink, 1972), and Si(Li)–Ge(Li) (Genz *et al.*, 1973c).

Corrections must be applied principally for the following effects: (1) self-absorption and absorption of K x rays between source and sensitive volume of the detector, (2) efficiency of the K x-ray detector, including solid angle, (3) detection of γ rays or conversion electrons in the x-ray detector, (4) contributions from positrons, if present, and (5) sum and accidental coincidences. Values of the fluorescence yield ω_K can usually be taken from the literature. In order to avoid uncertainties due to the insufficiently known fluorescence yields, De Wit and Wapstra (1965) in their measurements on ^{195}Au and ^{197}Hg compared the intensity ratios $I_{KX\text{-}\gamma}/I_\gamma$ with that of a ^{202}Hg reference source. With an appropriately chosen reference nuclide, the fluorescence yields practically cancel. On the other hand, knowledge of P_K of the reference nuclide is required.

With nuclides decaying to an excited level that is followed by a γ-γ cascade to the ground state, triple coincidences have been measured. The K-capture probability can then be found from the relation

$$P_K\omega_K = I_{KX\text{-}\gamma1\text{-}\gamma2}/I_{\gamma1\text{-}\gamma2} , \quad (3.21)$$

where $I_{KX\text{-}\gamma1\text{-}\gamma2}$ is the rate of the (K x-ray)–(γ_1)–(γ_2) triple coincidences, and $I_{\gamma1\text{-}\gamma2}$ is the (γ_1)–(γ_2) coincidence rate. In addition to the corrections mentioned previously, directional correlations must be taken into account.

The coincidence method permits determination of the K-capture probability for transitions to an excited level in the daughter nucleus. By appropriate choice of γ-ray

window settings one can select a particular electron-capture transition among several in the same decay. This technique (No. 12) has been employed to determine the ratio of K-capture probabilities to different levels (denoted here by 1 and 2)

$$\frac{P_{K1}}{P_{K2}} = \left(\frac{I_{KX-\gamma 1}}{I_{\gamma 1}}\right) \Big/ \left(\frac{I_{KX-\gamma 2}}{I_{\gamma 2}}\right) . \tag{3.22}$$

The result does not depend upon the fluorescence yield and the efficiency of the K x-ray detector. In most cases, NaI(Tl) detectors have been used for the K x rays and γ rays (Lewin *et al.*, 1965), but NaI(Tl)–Ge(Li) (Schmidt-Ott *et al.*, 1968; Schmidt-Ott, 1970; Cook and Johns, 1969; Lourens *et al.*, 1970) and Si(Li)–Ge(Li) combinations (Lourens, *et al.*, 1970) have also been employed. The method has been used mostly to determine the energies of electron capture transitions.

b. Measurement of (K x-ray and Auger-electron)–(γ-ray) coincidences

If coincidences between K x rays or Auger electrons and γ rays are measured (Method 13), the K-capture probability P_K can be directly deduced

$$P_K = I_{K-\gamma}/I_\gamma . \tag{3.23}$$

Very thin (e.g., vacuum-evaporated) sources of large area are required to keep self-absorption down. Kramer *et al.* (1962a) employed this method with a double proportional counter operated at sufficiently high pressure to detect all K x rays and Auger electrons. The source was placed so as to attain a ~4π solid angle. Gamma rays were detected with a NaI(Tl) scintillation counter. Vatai and Hohmuth (1968) employed a 4π CsI(Tl) detector system to register K events and a CsI(Tl) detector for the γ rays.

Corrections are required for (1) self-absorption of K x rays and Auger electrons, (2) absorption of x rays and electrons in the backing foil of the source, (3) incomplete realization of the 4π solid angle, (4) accidental coincidences, (5) detection of γ rays in the K-event detector, and (6) influence of positrons, if present.

C. Measurement of (K x-ray)–(γ-ray) sum coincidences

In this method (No. 14), which was first used by Gupta and Iha (1956), the pulse-height spectrum of K x rays and γ rays is measured in one single detector. The spectrum (Fig. 15) contains a K x-ray peak, a γ-ray peak, and a sum peak arising from (K x-ray)–(γ-ray) coincidences in the detector. From the measured areas A_γ and $A_{X\gamma}$ of these peaks, the capture probability can be deduced:

$$P_K\omega_K = \frac{I_{KX-\gamma}}{I_\gamma} = \frac{A_{X\gamma}}{A_\gamma + A_{X\gamma}} . \tag{3.24}$$

In most cases, a NaI(Tl) detector has been employed for measurements of this type. Das Mahapatra and Mukherjee (1974) used a Ge(Li) detector, and Campbell and NcNelles (1972) employed a sandwich detector consisting of two CsI(Tl) crystals with the source in between.

Corrections must be made for (1) self-absorption and absorption of K x rays between source and sensitive volume of the detector, (2) efficiency of the K x-ray counter, including solid angle, (3) accidental coincidences, and (4) separation of overlapping parts of the γ-ray and sum peaks.

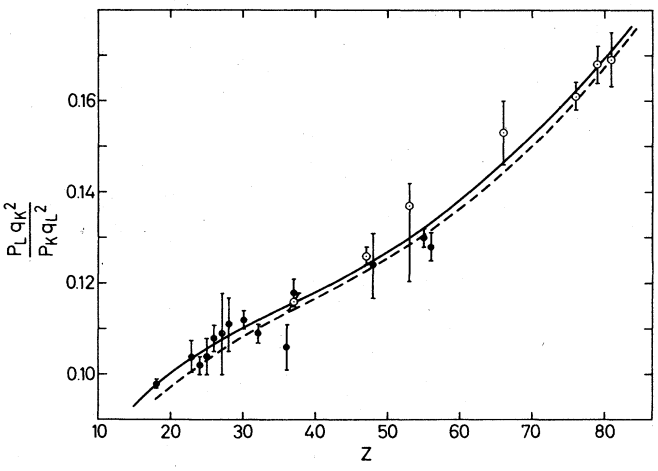

FIG. 15. Comparison of experimentally determined L/K capture ratios for allowed transitions (solid circles) and first-forbidden nonunique transitions (open circles) with theoretical predictions based on wavefunctions of Mann and Waber (1973) and exchange and overlap corrections $X^{L/K}$ according to Bahcall (1963, 1965) (solid curve) and Vatai (1970a) and Martin and Blichert-Toft (1970) (broken curve).

Gupta (1958) has used this method with triple sum coincidences. He observed the pulse-height spectrum in a single NaI(Tl) detector and determined the areas A_{X12} and A_{12} of $Kx-\gamma_1-\gamma_2$ and $\gamma_1-\gamma_2$ sum coincidence peaks. The K-capture probability is

$$P_K\omega_K = \frac{I_{KX+\gamma 1+\gamma 2}}{I_{\gamma 1+\gamma 2}} = \frac{A_{X12}}{A_{12}+A_{X12}} . \tag{3.25}$$

Instead of employing a single detector, it is possible to measure coincidences between K x rays in one NaI(Tl) detector and sum coincidences of γ_1 and γ_2 in a second NaI(Tl) detector. The K x rays are then gated by the $\gamma_1+\gamma_2$ sum coincidences. The ratio of the corresponding intensities is equal to $P_K\omega_K$. In a few cases, in which K capture is forbidden due to energetics, the L-capture fraction can be measured directly (Wapstra *et al.*, 1962; de Beer *et al.*, 1964; Pengra, 1976).

d. Measurement of (K x-ray)–(γ-ray) and (K x-ray)–(K x-ray) or (K x-ray)–(K conversion electron) coincidences

This method (No. 15) can be applied to nuclides that decay to an excited level in the daughter nucleus that is deexcited by a converted γ transition. The approach was developed by Pruett and Wilkinson (1954); it is based on measuring coincidences between K x rays from the electron-capture process and γ rays from the daughter nucleus, and additionally, coincidences between K x rays from the electron-capture process and K x rays from internal conversion. The K-capture probability can be deduced from the relation

$$2(I_{KX-\gamma}/I_\gamma)/(I_{KX-KX}/I_{KX}) = 1 + P_K(1+\alpha)/\alpha_K , \tag{3.26}$$

where $I_{KX-\gamma}$ and I_{KX-KX} are the coincidence counting rates, and I_γ and I_{KX} the corresponding singles rates.

Drop-deposited sources and NaI(Tl) detectors were used in these experiments. Results are independent of the fluorescence yields, but the K-shell and total conversion coefficients must be known. Corrections for accidental and sum coincidences must be applied.

Hansen (1975) has determined P_K of ^{139}Ce by measuring coincidences between K x rays and γ rays and K x rays and K conversion electrons. The photons were measured by Si(Li) and NaI(Tl) detectors, and the electrons, by means of a magnetic β spectrometer. P_K can be deduced from the relation

$$\frac{1+P_K}{P_K}=\left(\frac{I_{KX\text{-}eK}}{I_{eK}}\right)\Big/\left(\frac{I_{KX\text{-}\gamma}}{I_\gamma}\right). \tag{3.27}$$

In addition to the usual corrections, sum and accidental coincidences must be considered. Fluorescence yield and conversion coefficients need not be known. The method is only applicable to nuclides with a simple decay scheme lacking a γ cascade in the daughter.

e. Measurements of coincidences between K x rays or Auger electrons and conversion electrons

Coincidence measurements of this type (Method 16) for the determination of P_K were first made by Brosi *et al.* (1959), who observed the K x-ray spectrum gated by K- and L-conversion electrons (Fig. 16) and determined coincidence and singles intensities. The K-capture probability can be deduced from the relation

$$\frac{1+P_K}{P_K}=\left(\frac{I_{KX\text{-}eK}}{I_{eK}}\right)\Big/\left(\frac{I_{KX\text{-}eL}}{I_{eL}}\right), \tag{3.28}$$

where $I_{KX\text{-}eK}$ and $I_{KX\text{-}eL}$ are the (K x-ray)–(K-conversion electron) and (K x-ray)–(L-conversion electron) intensities, respectively, and I_{eK} and I_{eL} are the corresponding singles rates. The K x rays have been measured with NaI(Tl) detectors, and the conversion electrons, with magnetic β spectrometers. Knowledge of the K-shell fluorescence yield and the x-ray and electron detector efficiencies is not required. Corrections must be made to account for (1) accidental coincidences, (2) sum effects due to K x rays from electron capture and internal conversion, (3) possible effects of other converted γ transitions in cascade, and (4) possible effects of electron capture to higher levels.

Instead of utilizing coincidences between x rays and conversion electrons, it is possible to determine P_K from coincidences between K Auger electrons and K or L conversion electrons. From the measured intensities, P_K is found

$$\frac{1+P_K}{P_K}=\left(\frac{I_{KA\text{-}eK}}{I_{eK}}\right)\Big/\left(\frac{I_{KA\text{-}eL}}{I_{eL}}\right). \tag{3.29}$$

Here, $I_{KA\text{-}eK}$ and $I_{KA\text{-}eL}$ are the coincidence rates between K Auger electrons and K and L conversion electrons, respectively. This method (No. 17) has been used by Marelius *et al.* (1967), who employed two magnetic spectrometers. The necessary corrections are essentially the same as those in Method 16.

A slight variation of this approach has been used by Sparrman *et al.* (1966), who measured the K Auger-electron spectrum in coincidence with K and L conversion electrons by means of two long-lens spectrometers. The

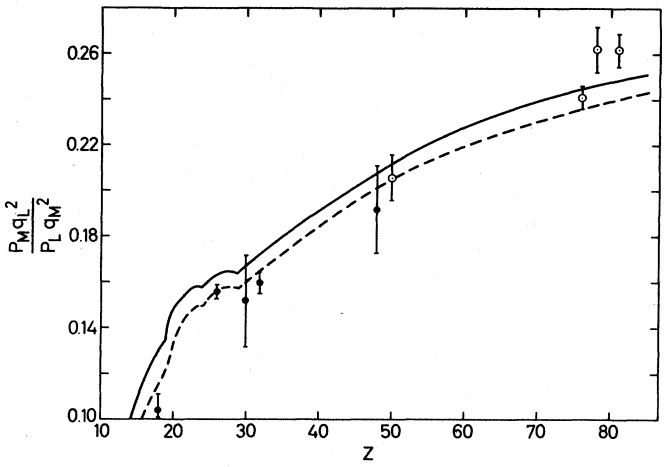

FIG. 16. Comparison of experimentally determined M/L capture ratios for allowed transitions (solid circles) and first-forbidden nonunique transitions (open circles) with theoretical predictions based on wavefunctions of Mann and Waber and exchange and overlap corrections $X^{M/L}$ according to Bahcall (1963, 1965) (solid curve) and Vatai (1970a), and Martin and Blichert-Toft (1970) (broken curve).

value for P_K was found from

$$\frac{1+P_K}{P_K}=\left(\frac{I_{KA\text{-}eK}}{I_{KA\text{-}eL}}\right)\frac{\alpha_L}{\alpha_K}. \tag{3.30}$$

The K and L conversion coefficients must be known. In addition to the corrections mentioned above, efficiencies for detecting K and L conversion electrons and the absorption of these electrons between source and detector must be taken into account.

Plch *et al.* (1971) measured the K x-ray spectrum in a Ge(Li) detector gated by K conversion electrons which were detected in a proportional counter. By this method (No. 18), they determined P_K from the ratio of the (K x-ray)–(K-conversion electron) coincidence rate $I_{KX\text{-}eK}$ and the K conversion-electron singles intensity I_{eK}

$$(1+P_K)\omega_K=I_{KX\text{-}eK}/I_{eK}. \tag{3.31}$$

Corrections are needed for (1) accidental and sum coincidences, (2) self-absorption and absorption of K x rays between source and detector, and (3) efficiency of the K x-ray detector.

With nuclides decaying to a metastable level of the daughter, Durosinmi-Etti *et al.* (1966) have measured K x rays by means of a NaI(Tl) detector in coincidence with K conversion electrons detected with a surface barrier detector. The K-capture probability was deduced from the equation

$$P_K=\frac{I_{KX}I_{eK}}{I_\gamma I_{KX\text{-}eK}}\frac{1}{1+\alpha}-\frac{\alpha_K}{1+\alpha}. \tag{3.32}$$

Here, I_{KX}, I_{eK}, and I_γ are the measured intensities of K x rays, K conversion electrons, and γ rays, respectively; $I_{KX\text{-}eK}$ is the (K x-ray)–(K-conversion electron) coincidence rate, α_K is the K conversion coefficient, and α, the total conversion coefficient. These conversion coefficients must be known. Corrections are needed for (1) X and γ detector efficiencies, including solid

angle; (2) absorption between source and detectors, and (3) overlap of spectrum peaks.

f. Measurement of triple coincidences between K x rays, γ rays, and internal-conversion electrons

This method (No. 19) was used by Thun *et al.* (1966), who determined the triple coincidence rate $I_{KX\text{-}\gamma\text{-}eL}$, measuring K x rays with a NaI(Tl) crystal, γ rays with a Ge(Li) detector, and L conversion electrons with a magnetic spectrometer; the coincidence rate $I_{\gamma\text{-}eL}$ between γ rays and L conversion electrons was simultaneously determined. Then we have

$$P_K\omega_K=\frac{I_{KX\text{-}\gamma\text{-}eL}}{I_{\gamma\text{-}eL}}\,. \tag{3.33}$$

A different approach was taken by Törnkvist and Ström (1968) in their measurements on ^{133}Ba decay. These workers determined P_K directly from triple coincidences between K x rays, γ rays, and K or L conversion electrons detected with a lens spectrometer. The K-capture probability was deduced from

$$\frac{1+P_K}{P_K}=\left(\frac{I_{KX\text{-}\gamma\text{-}eK}}{I_{\gamma\text{-}eK}}\right)\Big/\left(\frac{I_{KX\text{-}\gamma\text{-}eL}}{I_{\gamma\text{-}eL}}\right). \tag{3.34}$$

Sources were prepared by evaporation in vacuum. Corrections must account for (1) accidental and sum coincidences, (2) directional correlations (which can be minimized by proper choice of the angle between detectors), and (3) escape of iodine K x rays from the NaI(Tl) detector.

C. Experimental capture probabilities P_K, P_L, and P_M; comparison with theory

1. Experimental results

All experimentally determined, published values of P_L/P_K, P_M/P_L, $P_{LM_{\circ\circ}}/P_K$, $P_K\omega_K$, and P_K are listed in Table XIV. In the many cases in which authors quote P_K while they actually have measured $P_K\omega_K$, we list the latter product, recalculated from the authors' P_K and ω_K. In some cases, authors do not specify the value of ω_K which they used; these are indicated by "+." Some entries in Table XIV have been revised from the original publication. For example, the $P_{LM_{\circ\circ}}/P_K$ ratio for ^{109}Cd (Moler and Fink, 1965) was revised by the authors, who communicated this to Durosinmi-Etti (1966). Vatai (1968b, 1970b) has noted that the ^{109}Cd P_M/P_L value of Moler and Fink (1965) was not corrected for escape of Ag L x rays. Applying a corresponding correction and making use of newly reported values for k_α and k_β, (Salem *et al.*, 1974) and ω_K (Bambynek *et al.*, 1972) and a theoretical P_L/P_K ratio yields $P_M/P_L=0.205\pm0.020$. Similar corrections have been made to the ^{113}Sn P_M/P_L ratio of Manduchi *et al.* (1964b).

From among the entries in Table XIV, we have selected those results that can with certainty be judged as reliable, because they were derived from measurements with pure, carefully prepared sources, all necessary corrections being determined and clearly described. (The importance of pure sources has been emphasized, for example, by Raman *et al.* (1973), who suggest that discrepancies in measured P_L/P_K ratios of ^{113}Sn may be due to variable amounts of 250d ^{119}Sn present in the 115d ^{113}Sn.) We have omitted results published without indication of error limits, or with errors in excess of 15%. The information provided in most publications is unfortunately less than complete. It is therefore probable that we have omitted some "good" results from the list of selected values. The selected P_L/P_K measurements are listed in Table XV, the P_M/P_L ratios in Table XVI, and selected values of $P_{LM_{\circ\circ}}/P_K$, $P_K\omega_K$, and P_K in Table XVII. The K-shell fluorescence yields used to deduce the capture ratios P_K in Table XVII were calculated from the equation

$$[\omega_K/(1-\omega_K)]^{1/4}=A+BZ+CZ^3\,. \tag{3.35}$$

The constants A, B, C were determined by fitting this expression to the selected "most reliable" experimental fluorescence yields listed by Bambynek *et al.* (1972), with exception of those deduced from $P_K\omega_K$ measurements. The fluorescence yields calculated in this manner are practically the same as those recommended by Bambynek *et al.* (1972); slight changes in the last digit are within the stated error limits.

We use the transition energies $Q_{\rm EC}$ evaluated by Wapstra and Gove (1971), except in cases where these were deduced from measurements of electron capture ratios. In those cases, we have used $Q_{\rm EC}$ determined from measurements of internal-bremsstrahlung spectra or (p,n) reaction thresholds. For a few transitions, no independent $Q_{\rm EC}$ energies were available; these are indicated by an asterisk in Tables XV and XVII.

2. Theoretical predictions

The last three columns of Tables XV and XVII contain theoretical L/K and M/L ratios. These were calculated (see Sec. II) from the relations

$$\frac{P_L/P_K}{(q_{L_1}/q_K)^2}=\left(\frac{g_{L_1}}{g_K}\right)^2\left[1+\left(\frac{f_{L_2}}{g_{L_1}}\right)^2\right]X^{L/K} \tag{3.36}$$

and

$$\frac{P_M/P_L}{(q_{M_1}/q_{L_1})^2}=\left(\frac{g_{M_1}}{g_{L_1}}\right)^2\left[\frac{1+(f_{M_2}/g_{M_1})^2}{1+(f_{L_2}/g_{L_1})^2}\right]X^{M/L} \tag{3.37}$$

for allowed transitions, and

$$\frac{P_L/P_K}{(q_{L_1}/q_K)^4}=\left(\frac{g_{L_1}}{g_K}\right)^2\left[1+\left(\frac{f_{L_2}}{g_{L_1}}\right)^2+\left(\frac{p_{L_3}g_{L_3}}{g_{L_3}g_{L_1}}\right)^2\right]X^{L/K} \tag{3.38}$$

for unique first-forbidden transitions. The electron radial wavefunction amplitudes $g_K, g_{L_1}, f_{L_2}, g_{M_1}, f_{M_2}$, as well as $p_{L_3}g_{L_3}$ were taken from the relativistic Hartree–Fock calculations of Mann and Waber (1973) as listed in Table IX. The exchange and overlap correction factors $X^{L_1/K}=B_{L_1}/B_K$ and $X^{M_1/L_1}=B_{M_1}/B_{L_1}$ were recalculated in the present work according to the *ansatz* of Bahcall (1963a, c, 1965a) and that of Vatai (1968b, 1970a) as described in Sec. II.E. For $Z>32$, the correction factors of Suslov (1970) are used in continuation of the Bahcall factors, and those of Martin and Blichert-Toft (1970) in extension of the recalculated Vatai factors. Assumptions and approximations underlying the calculation of these correction factors are discussed in Sec. II.E. Equations (3.36)–(3.38) contain the simplifications

$$(q_{L_2}/q_{L_1})^2=(q_{L_3}/q_{L_1})^2=(q_{M_2}/q_{M_1})^2=1 \tag{3.39}$$

and

$$X^{L_2/L_1} = X^{L_3/L_1} = X^{M_2/M_1} = 1 . \quad (3.40)$$

These approximations affect the capture ratios by less than 0.04% for $Z = 20$, and less than 0.3% for $Z = 75$.

The theoretical K-capture probabilities P_K listed in the last column of Table XVII were calculated from theoretical capture ratios $P_L/P_K, P_M/P_L, P_N/P_M$ for $Z > 3$ and also P_O/P_N for $Z > 67$, according to Eq. (3.6). Exchange and overlap corrections $X^{L/K}$ and $X^{M/L}$ were applied as discussed above, using our recalculated factors for $Z \leq 32$ and those of Suslov or Martin and Blichert-Toft for heavier atoms. For the outer shells no exchange correction was made, none being available.

The theoretical capture ratios and probabilities listed in Tables XV–XVII for first-forbidden nonunique transitions are calculated for allowed transitions. This approximation is justified because for such transitions the ratios of capture probabilities from the $ns_{1/2}$ and $np_{1/2}$ subshells are independent of the form-factor coefficients (Sec. II.C.2).

3. Comparison of experimental and theoretical electron-capture ratios

For comparison with theory, the selected experimental L/K and M/L ratios for allowed and nonunique first-forbidden transitions (Tables XV and XVI) were divided by the energy-dependent factors

$$\left(\frac{q_{L_1}}{q_K}\right)^2 = \left(\frac{E_{EC} - E_{L_1}}{E_{EC} - E_K}\right)^2 \quad (3.41)$$

and

$$\left(\frac{q_{M_1}}{q_{L_1}}\right)^2 = \left(\frac{E_{EC} - E_{M_1}}{E_{EC} - E_{L_1}}\right)^2 \quad (3.42)$$

respectively, where the capture transition energy is

$$E_{EC} = Q_{EC} - E_\gamma \quad (3.43)$$

and E_K, E_{L_1} and E_{M_1} are electron binding energies taken from Bearden and Burr (1967). In the case of measurements pertaining to transitions to several levels, we divided the measured mean L/K capture ratios by the factor

$$\overline{\left(\frac{q_{L_1}}{q_K}\right)^2} = \sum_v a_v \left(\frac{q_{L_1}}{q_K}\right)_v^2 . \quad (3.44)$$

The index v labels the final-state levels; the a_v are branching ratios subject to $\sum a_v = 1$. A corresponding procedure was used for mean M/L ratios. The branching ratios were taken from the *Nuclear Data Sheets* edited by the Nuclear Data Group, Oak Ridge National Laboratory.

The reduced experimental capture ratios $(P_L/P_K)/(q_{L_1}/q_K)^2$ and $(P_M/P_L)/(q_{M_1}/q_{L_1})^2$ are compared with theoretical ratios (Tables XV and XVI) in Figs. 15 and 16. For clarity, we have combined results for each atomic number and plotted weighted mean values and their uncertainties.

P_L/P_K capture ratios. Figure 15 shows that agreement between experimentally determined L/K capture ratios and exchange-corrected theoretical predictions is fairly good for all atomic numbers, both for allowed and for nonunique first-forbidden transitions. The difference between theoretical ratios, due to different exchange and overlap corrections, is largest for light atoms (Sec. II.E).

In cases in which the electron-capture transition energy is not much larger than the K-shell binding energy, the $(q_{L_1}/q_K)^2$ ratio is very sensitive to Q_{EC}. Errors in Q_{EC} can then lead to erroneous conclusions in the comparison with theory. Such is the case for ^{206}Bi, and probably also for ^{109}Cd, ^{133}Ba, ^{159}Dy, ^{195}Au, and ^{202}Tl. More accurate measurements on ^{79}Kr and ^{159}Dy should be performed. For ^{126}I a mean L/K ratio has been measured, due to 60% nonunique and 40% unique first-forbidden transitions. The experimental result agrees well with predictions for either type of transition. The few available measurements pertaining to pure unique first-forbidden transition also agree well with theory. Table XV includes the four measured L/K ratios for nonunique second-forbidden transitions, but these are not compared with theoretical ratios.

Vatai (1973a, 1974) has suggested that the ratio of nonrelativistic to relativistic nuclear matrix elements could be estimated from L_3/K ratios, and attempted to do this by evaluating the L_3/K fraction of the measured L/K ratios of ^{93}Mo (Hohmuth *et al.*, 1964) and ^{97}Tc (Katcoff, 1958), and the $LM.../K$ ratio of ^{138}La (Turchinetz and Pringle, 1956). The fact that the $(L_1 + L_2)/K$ ratio is independent of nuclear matrix elements made the separation possible. The experimental ratios unfortunately are not very accurate; improved measurements on these cases and on additional second and higher forbidden nonunique transitions would be useful. Vatai (1973a, 1974) has further pointed out that in the presence of K capture determinations of M/K ratios would be more useful than of M/L ratios, because the former are more sensitive to nuclear matrix elements. Chew *et al.* (1974a) have followed Vatai's suggestion and calculated the ratio of nuclear matrix elements $R = ({}^V F^0_{220} - \sqrt{3/2} \cdot {}^A F^0_{221})/{}^V F^0_{221}$ in the decay of ^{59}Ni from L_3/K deduced from the total measured L/K ratio. Daniel (1968) has noticed that for allowed transitions the reduced capture ratios $(P_L/P_K)/(q_L/q_K)^2$ are in surprisingly good agreement with the ratios of the $M1$ internal conversion coefficients α_L/α_K.

P_M/P_L capture ratios. From Fig. 16 it is seen that experimental M/L capture ratios agree fairly well with exchange-corrected theoretical calculations for all Z. Precision measurements of additional M/L ratios of light atoms would be most useful to test exchange and overlap corrections.

A new more precise measurement on ^{65}Zn is needed. Further experimental evidence is also required in the medium-Z region; the M/L capture ratios in the decay of ^{81}Kr, ^{109}Cd and ^{127}Xe should be determined.

P_N/P_M capture ratios. The only measurement of an N/M capture ratio performed to date is that of Pengra (1976) on ^{205}Pb. With a gaseous source of ^{205}Pb tetramethyl, Pengra determined $P_M/P_L = 0.524 \pm 0.010$ and $P_N/P_M = 0.286 \pm 0.020$. Comparison with theory is impeded by lack of reliable information on the transition energy. An indirect determination of the $(N+...)/M$ ratio of ^{202}Tl has been made from measurements of $(M+N+...)/L$ and M/L ratios (Leutz *et al.*, 1966), but the accuracy of this result is insufficient for meaningful comparison with theory.

TABLE XIV. Experimental electron-capture values

Z	Elements	A	Q_{EC} [a] (keV)	Final state (keV)	$J_i^\pi \to J_f^\pi$	P_L/P_K	P_M/P_L	$P_{LM..}/P_K$	$P_K\omega_K$ [b]	P_K	Method [c]	References
17	Cl	36	1144	0	$2^+ - 0^+$	0.112 ±0.008					1	Dougan (1962b)
18	Ar	37	814	0	$\frac{3}{2}^+ - \frac{3}{2}^+$	$0.092^{+0.010}_{-0.005}$					2	Langevin (1955c)
						0.102 ±0.008					2	Kiser (1959)
						0.103 ±0.003					1	Santos Ocampo (1960)
						0.0971 ±0.0005					1	Manduchi (1961)
						0.102 ±0.004					1	Dougan (1962a)
						0.102 ±0.003					1	Winter (1964)
						0.097 ±0.003					1	Heuer (1966)
						0.098 ±0.003					1	Totzek (1967)
							$0.104^{+0.007}_{-0.003}$				3	Renier (1968)
						0.098 ±0.002					1	Krahn (1972)
19	K	40	1505	1460;0	$4^- - 2^+;0^+$			1.34 ±0.35			8	Heintze (1954)
								0.34 ±0.08			5	McCann (1967)
								0.44 ±0.09			8	Ažman (1968)
23	V	48	4015	Several		0.104 ±0.004					1	Bertmann (1972)
				2297	$4^+ - 4^+$	0.115 ±0.015					1	Bertmann (1972)
				Several					0.2005 ±0.0030		11	Albrecht (1975)
23	V	49	601	0	$\frac{7}{2}^- - \frac{7}{2}^-$	0.106 ±0.004					1	Krahn (1972)
24	Cr	51	751	320;0	$\frac{7}{2}^- - \frac{5}{2}^-;\frac{7}{2}^-$	0.10 ±0.02					7	Konstantinov (1961)
						0.1026 ±0.0004					1	Fasioli (1962)
				320	$\frac{7}{2}^- - \frac{5}{2}^-$				0.227 ±0.003		10	Taylor (1963)
				320		0.1044 ±0.0021					1	Heuer (1966)
				320;0		0.1033 ±0.0031					1	Heuer (1966)
				320					0.196 ±0.016		11	Mukerji (1967b)
25	Mn	54	1374	835.5	$3^+ - 2^+$					0.901 ±0.006	13	Kramer (1962a)
						0.098 ±0.006					1	Moler (1963)
									0.257 ±0.004		10	Taylor (1963)
						0.106 ±0.003					1	Manduchi (1963)
									0.243 ±0.012		10	Leistner (1965)
									0.2514 ±0.0017		10	Bambynek (1967a)
									0.250 ±0.005		10	Petel (1967)
									0.2492 ±0.0017		11	Hammer (1968)
										0.900 ±0.014	10	Dobrilović (1972)
									0.247 ±0.009		11	Mukerji (1973)
26	Fe	55	232	0	$\frac{3}{2}^- - \frac{5}{2}^-$	0.108 ±0.006					1	Scobie (1959)
						0.106 ±0.003					1	Manduchi (1962a)
						0.106 ±0.005					1	Moler (1963)
						0.117 ±0.001	0.157 ±0.003				1	Pengra (1972)

TABLE XIV. *(Continued)*

Z	Elements	A	Q_{EC} [a] (keV)	Final state (keV)	$J_i^\pi \to J_f^\pi$	P_L/P_K	P_M/P_L	$P_{LM..}/P_K$	$P_K\omega_K$ [b]	P_K	Method [c]	References
27	Co	57	837	136	$\frac{7}{2}^- - \frac{5}{2}^-$			0.20 ±0.13			9	Moussa (1956)
				136					0.254 ±0.011		11	Kramer (1962a)
				136;706	$\frac{7}{2}^- - \frac{5}{2}^-;\frac{5}{2}^-$	0.099 ±0.011					1	Moler (1963)
				136					0.262 ±0.008		11	Thomas (1963)
				136					0.3044±0.0043		11	Rubinson (1968)
				136				0.15 ±0.02		0.87 ±0.02[+]	11	Bosch (1969)
				706	$\frac{7}{2}^- - \frac{5}{2}^-$			0.088 ±0.040		0.92 ±0.03[+]	11	Bosch (1969)
				136					0.317 ±0.006		11	Mukerji (1973)
27	Co	58	2308	1675;810	$2^+ - 2^+;2^+$	0.107 ±0.004					1	Moler (1963)
				1675;810					0.3050±0.0022		10	Bambynek (1968b)
28	Ni	56	2133	1720	$0^+ - 1^+$	0.115 ±0.006					1	Winter (1967)
28	Ni	57	3243	Several		0.100 ±0.006					1	Winter (1967)
28	Ni	59	1073	0	$\frac{3}{2}^- - \frac{7}{2}^-$	0.121 ±0.002					1	Chew (1974a)
30	Zn	65	1350	1115	$\frac{5}{2}^- - \frac{5}{2}^-$				0.369 ±0.023		11	Perrin (1960)
				1115;0	$\frac{5}{2}^- - \frac{5}{2}^-;\frac{3}{2}^-$	0.13 ±0.002					7	Konstantinov (1961)
				1115;0		0.119 ±0.007					1	Santos Ocampo (1962)
				1115						0.878±0.006	13	Kramer (1962a)
				1115;0					0.400 ±0.006		10	Taylor (1963)
				1115;0		0.111 ±0.006					1	Totzek (1967)
				1115		0.117 ±0.007					5	McCann (1968)
				1115					0.3927±0.0026		11	Hammer (1968)
				1115;0					0.3894±0.0016		10	Bambynek (1968a)
				1115;0		0.118 ±0.003					1	Krafft (1970)
				1115		0.120 ±0.003	0.153±0.020				1	Krafft (1970)
				1115					0.386 ±0.010		11	Mukerji (1973)
32	Ge	71	235	0	$\frac{1}{2}^- - \frac{3}{2}^-$	0.30 ±0.02					2	Langevin (1956)
						0.116 ±0.005					1	Drever (1959)
						0.13 ±0.02					7	Konstantinov (1961)
						0.1187±0.0008	0.142±0.010				1	Manduchi (1962)
						0.117 ±0.001	0.162±0.003				1	Genz (1971a)
33	As	73	340	67	$\frac{3}{2}^- - \frac{1}{2}^-$					0.85 ±0.05	16	Kyles (1970)
33	As	74	2564	Several		0.085 ±0.020					2	Scobie (1957)
34	Se	75	865	401	$\frac{5}{2}^+ - \frac{5}{2}^+$				0.457		11	Perrin (1960)
									0.460 ±0.004		11	Rao (1966b)
									0.462 ±0.012		11	Raeside (1969)
									0.516 ±0.021		11	Chew (1973)
36	Kr	79	1631	Several		0.27 ±0.09					4	Radvanyi (1955a)
						0.26 ±0.03					2	Langevin (1955a)
						0.108 ±0.005					1	Drever (1959)
36	Kr	81	290	0	$\frac{7}{2}^+ - \frac{3}{2}^-$	0.146 ±0.005					1	Chew (1974b)

TABLE XIV. *(Continued)*

Z	Elements	A	Q_{EC} [a] (keV)	Final state (keV)	$J_i^\pi \rightarrow J_f^\pi$	P_L/P_K	P_M/P_L	$P_{LM..}/P_K$	$P_K\omega_K$ [b]	P_K	Method [c]	References
37	Rb	83	1038	571;562	$\frac{5}{2}^- - \frac{3}{2}^-;\frac{3}{2}^-$	0.121 ±0.002					5	Schulz (1967a)
				571		0.128 ±0.002					5	Goedbloed (1970b)
				562		0.132 ±0.002		0.164 ±0.002			5	Goedbloed (1970b)
37	Rb	84	2680	880	$2^- - 2^+$				0.580 ±0.025		11	Welker (1955)
						0.116 ±0.002					5	Schulz (1967a)
						0.119 ±0.002					5	Goedbloed (1970b)
38	Sr	85	1064	514	$\frac{9}{2}^+ - \frac{9}{2}^+$					0.88 ±0.04 [+]	11	Bisi (1956a)
									0.5959 ± 0.0035		11	Grootheer (1969)
									0.586 ±0.003		10	Bambynek (1970)
39	Y	88	3619	2734	$4^- - 3^-$				0.6290 ± 0.0032		11	Grootheer (1969)
				2734;1836	$4^- - 3^-;2^+$				0.613 ±0.004		10	Bambynek (1973)
42	Mo	93	398	30;0	$\frac{5}{2}^+ - \frac{1}{2}^-;\frac{9}{2}^+$	0.36 ±0.04					6	Hohmuth (1964)
43	Tc	97	347	0	$\frac{9}{2}^+ - \frac{5}{2}^+$	$0.21^{+0.14}_{-0.10}$					6	Katcoff (1958)
45	Rh	101	554	325;127	$\frac{1}{2}^- - \frac{1}{2}^-;\frac{3}{2}^+$					0.65	11	Perrin (1960)
46	Pd	103	553	Several						0.56 ±7	8	Avignon (1953)
										0.95	9	Avignon (1955)
47	Ag	105	1341 [d]	344	$\frac{1}{2}^- - \frac{1}{2}^+$	0.128 ±0.003					5	Schulz (1967d)
				1088	$\frac{1}{2}^- - \frac{3}{2}^-$	0.152 ±0.002					5	Schulz (1967d)
48	Cd	109	182	87.7	$\frac{5}{2}^+ - \frac{7}{2}^+$			0.28 ±0.03			5	Der Mateosian (1953)
						0.32 ±0.04					6	Bertolini (1954)
										0.805 ± 0.027	8	Wapstra (1957)
						0.195 ±0.005		0.228 ±0.003			5	Leutz (1965)
						0.237 ±0.015	0.223 ± 0.020 [e]	0.267 ±0.015 [f]			2	Moler (1965)
								0.26 ±0.03			18	Durosinmi-Etti (1966)
						0.193 ±0.003		0.226 ±0.003			5	Goedbloed (1970a)
49	In	111	826	419	$\frac{9}{2}^+ - \frac{7}{2}^+$					0.867 ± 0.007	17	Sparrman (1966)
49	In	114 [m]	1623	1283	$5^+ - 4^-$					0.75	11	Perrin (1960)
50	Sn	113	1025	648	$\frac{1}{2}^+ - \frac{3}{2}^-$				$0.26^{+0.09}_{-0.07}$		11	Bhatki (1957)
				648						1.01 ±0.17 [+]	11	Greenwood (1961)
				648;393	$\frac{1}{2}^+ - \frac{3}{2}^-;\frac{1}{2}^-$	0.44 ±0.04	0.223 ± 0.020 [g]				1	Manduchi (1964)
				393	$\frac{1}{2}^+ - \frac{1}{2}^-$	0.16 ±0.02					18	Durosinmi-Etti (1966)
				648	$\frac{1}{2}^+ - \frac{3}{2}^-$					0.75 ±0.10 [+]	11	Bosch (1967)
53	I	125	177 [q]	35.5	$\frac{5}{2}^+ - \frac{3}{2}^+$					0.77 ±0.08	8	Friedlander (1951b)
								0.23 ±0.03			5	Der Mateosian (1953)
								0.2543 ± 0.0027			5	Leutz (1964)
								0.253 ±0.005			5	Smith (1966)
									0.685 ±0.018		11	Karttunen (1969)
									0.699 ±0.030		11	Tolea (1974)
									0.685 ±0.012		11	Plch (1974a)

TABLE XIV. *(Continued)*

Z	Elements	A	Q_{EC} [a] (keV)	Final state (keV)	$J_i^\pi \to J_f^\pi$	P_L/P_K	P_M/P_L	$P_{LM..}/P_K$	$P_K\omega_K$ [b]	P_K	Method [c]	References
53	I	126	2151	Several		$0.142^{+0.005}_{-0.018}$					5	Scobie (1958)
54	Xe	127	664	375	$\frac{1}{2}^+ - \frac{1}{2}^+$				0.705 ±0.004		11	Bresesti (1964)
				203	$\frac{1}{2}^+ - \frac{3}{2}^+$				0.750 ±0.016		11	Bresesti (1964)
				375	$\frac{1}{2}^+ - \frac{1}{2}^+$				0.53 ±0.05		11	Winter (1965b)
				375;203;0	$\frac{1}{2}^+ - \frac{1}{2}^+;\frac{3}{2}^+;\frac{5}{2}^+$		0.183 ±0.025				1	Winter (1965b)
55	Cs	131	355	0	$\frac{5}{2}^+ - \frac{3}{2}^+$	0.153 ±0.008					5	Joshi (1960)
						0.155 ±0.002					5	Schulz (1967a)
									0.734 ±0.006		11	Plch (1974b)
55	Cs	132	2099	Several		0.136 ±0.001					5	Goverse (1974a)
56	Ba	128	700	273	$0^+ - 1^+$					0.71 ±0.05 [+]	11	Gopych (1974)
56	Ba	131	1340	696;620		0.135 ±0.009					5	Smith (1963)
56	Ba	133	516 [h]	137	$\frac{1}{2}^+ - \frac{1}{2}^+$		0.282				11	Koički (1958)
										$0.46^{+0.05}_{-0.04}$ [+]	11	Gupta (1958b)
									0.419 ±0.015		11	Ramaswamy (1960)
									0.319 ±0.013		19	Thun (1966)
						0.371 ±0.007					5	Schulz (1967c)
				384	$\frac{1}{2}^+ - \frac{3}{2}^+$	0.221 ±0.005					5	Schulz (1967c)
56	Ba	133	516 [h]	437		0.67 ±0.15					6	McDonnel (1968)
				437				0.45 ±0.04			19	Törnkvist (1968)
				437					0.576 ±0.038		14	Narang (1968)
				437						0.47 ±0.02 [+]	6	Bosch (1969)
				437					0.644 ±0.034		11	Schmidt-Ott (1972)
				384					0.72 ±0.06		11	Schmidt-Ott (1972)
				437						0.76 ±0.06 [+]	14	Das Mahapatra (1974)
				384						0.87 ±0.014 [+]	14	Das Mahapatra (1974)
				437;384						0.79 ±0.07 [+]	14	Das Mahapatra (1974)
				437					0.676 ±0.087		14	Nicaise (1975)
57	La	138	1794	1426	$5^- - 2^+$			1.4 ±0.25			8	Turchinetz (1956)
58	Ce	134	500	0	$0^+ - 1^+$					0.72 ±0.08	8	Aleksandrov (1972)
								0.21			15	Pruett (1954)
58	Ce	139	275	165	$\frac{3}{2}^+ - \frac{5}{2}^+$			0.37 ±0.02			15	Ketelle (1956)
				165						0.83 ±0.04 [+]	11	Stanford (1960)
				165						0.68 ±0.02	17	Marelius (1967)
				165						0.750 ±0.010	16	Adamowicz (1968)
				165						0.69 ±0.02	13	Vatai (1968)
				165					0.707 ±0.018		11	Schmidt-Ott (1972)
				165					0.649 ±0.017	0.725 ±0.02	14	Campbell (1972)
				165						0.68 ±0.03	8	Bayer (1974)
				165					0.639 ±0.006		11	Plch (1975)
				165						0.726 ±0.010	15	Hansen (1975)
				165					0.66 ±0.06	0.73 ±0.07	14	Dasmahapatra (1975b)

TABLE XIV. *(Continued)*

Z	Elements	A	Q_{EC} [a] (keV)	Final state (keV)	$J_i^\pi \to J_f^\pi$	P_L/P_K	P_M/P_L	$P_{LM..}/P_K$	$P_K\omega_K$ [b]	P_K	Method [c]	References
60	Nd	140	470	0	$0^+ - 1^+$	$0.8^{+1.6}_{-0.7}$					6	Vitman (1960)
										0.745 ± 0.048	8	Bayer (1972)
61	Pm	145	170*	Several		1.8					6	Carey (1958)
				67	$\frac{5}{2}^+ - \frac{3}{2}^-$			0.85 ± 0.03			16	Brosi (1959)
				67					0.558 ± 0.022		11	Tolea (1974)
				72	$\frac{5}{2}^+ - \frac{5}{2}^-$				0.509 ± 0.022		11	Tolea (1974)
62	Sm	145	647 [i]	Several		2.0					6	Carey (1958)
				492	$\frac{7}{2}^- - \frac{3}{2}^+$			0.61 ± 0.10			15	Brosi (1959)
				61	$\frac{7}{2}^- - \frac{5}{2}^+$			0.20 ± 0.02			16	Brosi (1959)
				Several		$0.6^{+3.0}_{-0.6}$					6	Vitman (1960)
				492						0.27 ± 0.03 [+]	11	Mysłek (1971)
63	Eu	152	1886	1529	$3^- - 2^-$					0.78	11	Perrin (1960)
				1529						0.79 ± 0.02		Lu (1962)
				1529					0.71 ± 0.08		14	Dasmahapatra (1975a)
				1234	$3^- - 3^+$				0.82 ± 0.10		14	Dasmahapatra (1975a)
				Several				0.55 ± 0.02			8	Dasmahapatra (1972)
63	Eu	152 [m]	1935	950	$0^- - 1^-$					0.82	11	Perrin (1960)
64	Gd	151	484 [r]	350	$\frac{7}{2}^- - \frac{9}{2}^-$				0.664 ± 0.009		11	Genz (1973c)
				307	$\frac{7}{2}^- - \frac{3}{2}^+$				0.754 ± 0.014		11	Genz (1973c)
64	Gd	153	490 [j]	103	$\frac{3}{2}^+ - \frac{3}{2}^+$				0.679 ± 0.020		14	Gupta (1956)
				103				0.42			15	Bhattacherjee (1956)
				103					0.543 ± 0.006		14	Bisi (1956b)
				97;103	$\frac{3}{2}^+ - \frac{5}{2}^-; \frac{3}{2}^+$			0.34 ± 0.02			5	Leutz (1960)
				173	$\frac{3}{2}^+ - \frac{5}{2}^+$			0.85 ± 0.30			5	Leutz (1960)
64	Gd	153	490 [j]	173					0.375 ± 0.022		11	Blok (1962)
				103					0.66 ± 0.07		11	Blok (1962)
				97					0.67 ± 0.05		11	Blok (1962)
				173					0.35 ± 0.03		11	Cretzu (1964)
65	Tb	157	64* [k]	0	$\frac{3}{2}^+ - \frac{3}{2}^-$	2.64					6	Bhat (1962)
						2.18					6	Fujiwara (1964)
						2.65 ± 0.20					6	Naumann (1967)
66	Dy	159	365	0;58	$\frac{3}{2}^- - \frac{3}{2}^+; \frac{5}{2}^+$	1.0 ± 0.3					6	Grigorev (1958b)
				0;58		$0.3^{+0.7}_{-0.3}$					6	Vitman (1960)
				58	$\frac{3}{2}^- - \frac{5}{2}^+$					0.85 ± 0.11 [+]	11	Greenwood (1960)
				0	$\frac{3}{2}^- - \frac{5}{2}^+$	0.198 ± 0.009					5	Leiper (1971)
				58	$\frac{3}{2}^- - \frac{5}{2}^+$				0.752 ± 0.024		11	Genz (1973c)
67	Ho	160	2920	Several		$1.2^{+3.8}_{-1.1}$					6	Vitman (1960)
68	Er	160	800	60	$0^+ - 2^+$					0.795 ± 0.020	8	Aleksandrov (1972)
68	Er	165	371	0	$\frac{5}{2}^- - \frac{7}{2}^-$	1.2 ± 0.4					6	Grigorev (1958b)
70	Yb	166	260*	82	$2^+ - 2^+$				$0.68^{+0.06}_{-0.02}$		14	Jasinski (1963a)
72	Hf	175	607*	433	$\frac{5}{2}^+ - \frac{7}{2}^+$				0.64 ± 0.04		11	Funke (1965)
				433						0.712 ± 0.008	16	Jasinski (1968)
				343	$\frac{5}{2}^+ - \frac{5}{2}^+$					$0.767^{+0.030}_{-0.016}$	16	Jasinski (1968)

TABLE XIV. *(Continued)*

Z	Elements	A	Q_{EC} [a] (keV)	Final state (keV)	$J_i^\pi \to J_f^\pi$	P_L/P_K	P_M/P_L	$P_{LM..}/P_K$	$P_K\omega_K$ [b]	P_K	Method [c]	References
73	Ta	177	1158	1058	$\frac{7}{2}^+ - \frac{7}{2}^-$					0.42 ±0.07+	16	West (1961)
73	Ta	179	119*	0	$\frac{7}{2}^+ - \frac{9}{2}^+$	1.4 ±0.4					6	Bisi (1956c)
						0.63 ±0.06					6	Jopson (1961)
74	W	178	89	0	$0^+ - 1^+$					0.29 ±0.02	8	Nielsen (1967)
74	W	181	193 [l]	0;6	$\frac{9}{2}^+ - \frac{7}{2}^-;\frac{9}{2}^-$	1.54					6	Bisi (1955c)
						0.23 ±0.05					6	Jopson (1961)
						0.358 ±0.070					6	Muir (1961)
						0.27 ±0.05					6	Rao (1966a)
75	Re	183	558*	453	$\frac{5}{2}^+ - \frac{3}{2}^-$				0.38 ±0.07		11	Kuhlmann (1969)
76	Os	185	1015	Several		0.35 ±0.15					6	Miller (1951)
				Several		0.38 ±0.07					6	Johns (1957)
				875	$\frac{1}{2}^- - \frac{3}{2}^+$				0.457 ±0.008		11	Bisi (1957)
				873;878	$\frac{1}{2}^- - \frac{3}{2}^+;\frac{1}{2}^+$	0.600 ±0.006					5	Schulz (1967a)
				646	$\frac{1}{2}^- - \frac{1}{2}^+$	0.228 ±0.004	0.254 ±0.005				5	Schulz (1967a)
77	Ir	192	1050	691	$4^- - 3^+$				0.67 ±0.06		14	Dasmahapatra (1975)
78	Pt	188	540*	195	$0^+ - 1^-$					0.744 ±0.020	16	Hanson (1968)
				187	$0^+ - 1^-$					0.766 ±0.023	16	Hanson (1968)
78	Pt	193	61	0	$\frac{1}{2}^- - \frac{3}{2}^+$		0.386 ±0.014				5	Ravn (1971)
79	Au	195	229*	130	$\frac{3}{2}^+ - \frac{5}{2}^-$				0.143 ±0.019		11	Bisi (1959, 1954)
				130					0.146 ±0.010		11	Goedbloed (1964)
				130					0.188 ±0.005		11	De Wit (1965)
				130					0.123 ±0.009		11	Harris (1965)
				99	$\frac{3}{2}^+ - \frac{3}{2}^-$				0.38 ±0.09		11	Harris (1965)
				99						0.458 ±0.012	16	Jasinski (1968)
				99		0.873 ±0.044	0.478 ±0.020 [p]	1.28 ±0.06		0.438 ±0.011	5	Goverse (1973)
				130		3.055 ±0.086	0.697 ±0.078 [p]	5.25 ±0.66		0.160 ±0.017	5	Goverse (1973)
				0	$\frac{3}{2}^+ - \frac{1}{2}^-$	0.337 ±0.007					5	Goverse (1973)
79	Au	196	1482	689	$2^- - 2^+$		0.31 ±0.05				14	Gupta (1958a)
80	Hg	197	684 [m]	268	$\frac{1}{2}^- - \frac{3}{2}^+$				0.52 ±0.06		11	De Wit (1965)
				268;77	$\frac{1}{2}^- - \frac{3}{2}^+;\frac{1}{2}^+$				0.741 ±0.012		18	Plch (1971)
81	Tl	201	484 [n]	167	$\frac{1}{2}^+ - \frac{1}{2}^+$				0.67 ±0.04		11	Gupta (1960)
81	Tl	202	1372 [o]	Several						0.7	6	Huizenga (1954)
				Several		0.90 ±0.27					6	Kramer (1956)
				440	$2^- - 2^+$				$0.613^{+0.014}_{-0.013}$		14	Gupta (1957)
				440		0.638 ±0.030			0.523 ±0.011		6;11	Hamers (1957)
				440		0.23 ±0.05			0.76 ±0.05		8;11	Hagedoorn (1958)
				440					$0.761^{+0.015}_{-0.008}$		14	Jha (1959)
				440					0.751 ±0.014		14	Blok (1959)
				440					0.75 ±0.03		11	Gupta (1960)
				965	$2^- - 2^+$				0.50 ±0.05		11	Gupta (1960)
				440		0.196 ±0.002	0.269 ±0.007	0.265 ±0.010			5	Leutz (1966)
				440			0.35 ±0.04 [p]				5	Leutz (1966)
				965		0.305 ±0.020					5	Leutz (1966)
				0	$2^- - 0^+$	$0.22^{+0.02}_{-0.015}$					5	Leutz (1966)

TABLE XIV. *(Continued)*

Z	Elements	A	Q_{EC} [a] (keV)	Final state (keV)	$J_i^\pi \to J_f^\pi$	P_L/P_K	P_M/P_L	$P_{LM..}/P_K$	$P_K\omega_K$ [b]	P_K	Method [c]	References
81	Tl	204	345	0	$2^- - 0^+$	0.33					6	Jaffe (1954)
				0		0.42 ±0.05					5	Joshi (1961)
				0		0.41 ±0.03					5	Leutz (1962)
				0		0.60 ±0.055					7	Christmas (1964)
				0		0.48 ±0.04						Robinson (1963)
				0		0.43 ±0.16					6	Rao (1965)
				0		0.52 ±0.02					5	Klein (1966)
82	Pb	203	982	279	$\frac{5}{2}^- - \frac{3}{2}^+$				0.82 ±0.05		11	Prescott (1954)
				680	$\frac{5}{2}^- - \frac{5}{2}^+$				0.70 ±0.05		11	Prescott (1954)
				279						0.74 ±0.05	8	Wapstra (1954)
				680		0.36 ±0.07			0.66 ±0.04		6;11	Hagedoorn (1958)
				279		0.208 ±0.005			0.755 ±0.014		6;11	Hagedoorn (1958)
82	Pb	205	≈43	0			0.524 ±0.010				1	Pengra (1976)
				279					0.750 ±0.019		11	Persson (1961)
83	Bi	205	2704	2566	$\frac{9}{2}^- - \frac{9}{2}^+$	1.17 ±0.16					6	Bonacalza (1962)
83	Bi	206	3652	3279	$6^+ - 5^-$	0.264 ±0.010	0.228 ±0.007				5	Goverse (1974b)
				3403	$6^+ - 5^-$	0.281 ±0.009	0.276 ±0.008				5	Goverse (1974b)
				3563	$6^+ - 5^-$	0.509 ±0.015	0.282 ±0.010				5	Goverse (1974b)
83	Bi	208	2868	2615	$5^+ - 3^-$				0.230 ±0.008		11	Millar (1959)
85	At	210	3875	3726	$5^+ - 6^+$					0.45 ±0.09	8	Schima (1963)
85	At	211	793	0	$\frac{9}{2}^- - \frac{9}{2}^+$	0.143					6	Hoff (1953)
93	Np	235	123	0	$\frac{5}{2}^- - \frac{7}{2}^-$	30 ±2					6	Hoffman (1956)
				0		36.7	0.46				6	Gindler (1958)
93	Np	236	977	Several		2.0 ±0.4					6	Orth (1951)
94	Pu	237	233	Several		1.2						Kalkstein (1957)
				60	$\frac{7}{2}^- - \frac{5}{2}^-$	2.8 ±0.8					6	Hoffman (1958)
97	Bk	245	819	250	$\frac{3}{2}^- - \frac{5}{2}^+$				0.74 ±0.03		11	Magnusson (1956)

[a] Q_{EC} values are taken from Wapstra and Gove (1971). There are some values that originate from electron-capture measurements. They are replaced by values obtained from other methods, except for a few cases, indicated by an asterisk, where no recent other result is available.

[b] If P_K is given, the fluorescence yield used by the authors was used to calculate the measured value $P_K\omega_K$. There are some cases in which ω_K is not quoted. They are indicated by the sign "+".

[c] Methods are identified by numbers explained in Table XIII.

[d] Q_{EC} value from Bertrand (1974).

[e] Revised value using k_β/k_α=0.212 (Salem *et al.*, 1974) and ω_K=0.832 (see Table XVII).

[f] Value revised by the author, private communication to Durosinmi-Etti (1966).

[g] Revised value using k_β/k_α=0.217 (Salem *et al.*, 1974) and ω_K=0.852 (see Table XVII).

[h] Q_{EC} value from Henry (1974).

[i] Q_{EC} value from Berényi (1970).

[j] Q_{EC} value from Kroger (1973).

[k] Q_{EC} very uncertain.

[l] Q_{EC} value from Ellis (1973).

[m] Q_{EC} value from Jasinski (1963b).

[n] Q_{EC} value from Auble (1971a).

[o] Q_{EC} value from Auble (1971b).

[p] $P_{MN..}/P_L$ value.

[q] Q_{EC} value from Gopinathan (1968).

[r] Q_{EC} value from Ford (1970).

TABLE XV. Experimental and theoretical P_L/P_K ratios

						Experimental values					Theor. values $\frac{P_L/P_K}{(q_{L_1}/q_K)^2}$ [c]	
Z	Elements	A	Q_{EC} [a] (keV)	Final state (keV)	$J_i^\pi - J_f^\pi$	P_L/P_K	$(q_{L_1}/q_K)^2$	$\frac{P_L/P_K}{(q_{L_1}/q_K)^2}$	Method [b]	Reference	Bahcall	Vatai
					A. Allowed transitions $\Delta J=0,1;\ \pi_i\pi_f=+1$							
18	Ar	37	814.1 ± 0.6	0	$\frac{3}{2}^+ - \frac{3}{2}^+$	0.102 ± 0.008	1.006	0.101 ± 0.008	2	Kiser (1959)	0.098	0.095
						0.103 ± 0.003		0.102 ± 0.003	1	Santos Ocampo (1960)		
						0.0971 ± 0.0005		0.0965 ± 0.0005	1	Manduchi (1961)		
						0.102 ± 0.004		0.101 ± 0.004	1	Dougan (1962a)		
						0.102 ± 0.003		0.101 ± 0.003	1	Winter (1964)		
						0.097 ± 0.003		0.096 ± 0.003	1	Heuer (1966)		
						0.098 ± 0.003		0.097 ± 0.003	1	Totzek (1967)		
						0.098 ± 0.002		0.097 ± 0.002	1	Krahn (1972)		
23	V	48	4015.4 ± 2.8	Several		0.104 ± 0.004	1.007	0.103 ± 0.004	1	Bertmann (1972)	0.104	0.101
				2297	$4^+ - 4^+$	0.115 ± 0.015	1.005	0.114 ± 0.015	1	Bertmann (1972)		
23	V	49	601.2 ± 1.0	0	$\frac{7}{2}^- - \frac{7}{2}^-$	0.106 ± 0.004	1.015	0.104 ± 0.004	1	Krahn (1972)	0.104	0.101
24	Cr	51	751.4 ± 0.9	320;0	$\frac{7}{2}^- - \frac{5}{2}^-;\frac{7}{2}^-$	0.1026 ± 0.0004	1.014	0.1012 ± 0.0004	1	Fasioli (1962)	0.105	0.102
24	Cr	51	751.4 ± 0.9	320	$\frac{7}{2}^- - \frac{5}{2}^-$	0.1044 ± 0.0021	1.023	0.1021 ± 0.0021	1	Heuer (1966)		
				320;0	$\frac{7}{2}^- - \frac{5}{2}^-;\frac{7}{2}^-$	0.1033 ± 0.0031	1.022	0.1011 ± 0.0031	1	Heuer (1966)		
25	Mn	54	1374.9 ± 3.6	835	$3^+ - 2^+$	0.106 ± 0.003	1.020	0.104 ± 0.003	1	Manduchi (1963)	0.106	0.103
26	Fe	55	231.7 ± 0.7	0	$\frac{3}{2}^- - \frac{5}{2}^-$	0.108 ± 0.006	1.052	0.103 ± 0.006	1	Scobie (1959)	0.107	0.104
						0.106 ± 0.003		0.103 ± 0.003	1	Manduchi (1962a)		
						0.106 ± 0.005		0.103 ± 0.005	1	Moler (1963)		
						0.117 ± 0.001		0.111 ± 0.001	1	Pengra (1972)		
28	Ni	56	2133 ± 11	1720	$0^+ - 1^+$	0.115 ± 0.006	1.034	0.111 ± 0.006	1	Winter (1967)	0.109	0.107
28	Ni	57	3243 ± 7	Several		0.100 ± 0.006	1.008	0.099 ± 0.006	1	Winter (1967)	0.109	0.107
27	Co	58	2308.0 ± 2.5	1675;811	$2^+ - 2^+;2^+$	0.110 ± 0.008 [f]	1.009	0.109 ± 0.009	1	Moler (1963)	0.108	0.106
30	Zn	65	1350.7 ± 1.1	1115;0	$\frac{5}{2}^- - \frac{5}{2}^-;\frac{3}{2}^-$	0.119 ± 0.007	1.043	0.114 ± 0.007	1	Santos Ocampo (1962)	0.110	0.108
				1115;0		0.111 ± 0.006		0.106 ± 0.006	1	Totzek (1967)		
				1115		0.117 ± 0.007	1.071	0.109 ± 0.007	5	McCann (1968)		
				1115;0		0.118 ± 0.003	1.043	0.113 ± 0.003	1	Krafft (1970)		
				1115		0.120 ± 0.003	1.071	0.112 ± 0.003	1	Krafft (1970)		
32	Ge	71	235.1 ± 1.7	0	$\frac{1}{2}^- - \frac{3}{2}^-$	0.116 ± 0.005	1.082	0.107 ± 0.005	1	Drever (1959)	0.112	0.110
						0.1187 ± 0.0008		0.1097 ± 0.0007	1	Manduchi (1962a)		
						0.117 ± 0.001		0.108 ± 0.001	1	Genz (1971a)		
36	Kr	79	1631 ± 9	Several		0.108 ± 0.005	1.017	0.106 ± 0.005	1	Drever (1959)	0.115	0.113
37	Rb	83	1038 ± 32	571;562	$\frac{5}{2}^- - \frac{3}{2}^-;\frac{3}{2}^-$	0.121 ± 0.002	1.056	0.115 ± 0.002	5	Schulz (1967a)	0.116	0.115
				571		0.128 ± 0.002	1.056	0.121 ± 0.002	5	Goedbloed (1970b)		
				562		0.132 ± 0.002	1.056	0.125 ± 0.002	5	Goedbloed (1970b)		
48	Cd	109	182.0 ± 3.0	88	$\frac{5}{2}^+ - \frac{7}{2}^+$	0.195 ± 0.005	1.735 ± 0.018	0.112 ± 0.028	5	Leutz (1965)	0.125	0.124
						0.237 ± 0.005		0.137 ± 0.024	2	Moler (1965)		
						0.193 ± 0.003		0.117 ± 0.028	5	Goedbloed (1970a)		
55	Cs	131	355 ± 6	0	$\frac{5}{2}^+ - \frac{3}{2}^+$	0.153 ± 0.008	1.190	0.129 ± 0.007	5	Joshi (1960)	0.133	0.131
						0.155 ± 0.002		0.130 ± 0.002	5	Schulz (1967a)		

TABLE XV. *(Continued)*

						Experimental values					Theor. values $\frac{P_L/P_K}{(q_{L_1}/q_K)^2}$ [c]	
Z	Elements	A	Q_{EC} [a] (keV)	Final state (keV)	$J_i^\pi - J_f^\pi$	P_L/P_K	$(q_{L_1}/q_K)^2$	$\frac{P_L/P_K}{(q_{L_1}/q_K)^2}$	Method [b]	Reference	Bahcall	Vatai
56	Ba	131	1340 ±19	696;620	$\frac{1}{2}^+ - \frac{1}{2}^+;\frac{3}{2}^+$	0.135 ±0.009	1.091	0.124 ±0.008	5	Smith (1963)	0.134	0.132
56	Ba	133	515.8 ±3.0 [d]	437	$\frac{1}{2}^+ - \frac{1}{2}^+$	0.371 ±0.007	2.914 ±0.085	0.127 ±0.004	5	Schulz (1967c)	0.134	0.132
				384	$\frac{1}{2}^+ - \frac{3}{2}^+$	0.221 ±0.005	1.732 ±0.013	0.128 ±0.003	5	Schulz (1967c)		
					B. First nonunique forbidden transitions $\Delta J = 0,1;\ \pi_i \pi_f = -1$							
37	Rb	84	2679.8 ±2.9	880	$2^- - 2^+$	0.116 ±0.002	1.014	0.114 ±0.002	5	Schulz (1967a)	0.116	0.115
						0.119 ±0.002		0.117 ±0.002	5	Goedbloed (1970b)		
47	Ag	105	1341 ±9 [e]	344	$\frac{1}{2}^- - \frac{1}{2}^+$	0.128 ±0.003	1.043	0.123 ±0.003	5	Schulz (1967d)	0.124	0.123
				1088	$\frac{1}{2}^- - \frac{3}{2}^-$	0.152 ±0.002	1.190	0.127 ±0.002	5	Schulz (1967d)		
53	I	126	2151 ±5	Several		$0.142^{+0.005}_{-0.018}$	1.035 ±0.015	$0.137^{+0.005}_{-0.017}$	5	Scobie (1958)	0.130	0.129
55	Cs	132	2099 ±23	Several		0.136 ±0.001	1.048 ±0.012	0.130 ±0.002	5	Goverse (1974a)	0.133	0.131
66	Dy	159	365.4 ±1.0	0	$\frac{3}{2}^- - \frac{3}{2}^+$	0.198 ±0.009	1.295	0.153 ±0.007	5	Leiper (1971)	0.146	0.146
76	Os	185	1015.0 ±0.7	874;880	$\frac{1}{2}^- - \frac{3}{2}^+;\frac{1}{2}^+$	0.600 ±0.006	3.62 ±0.14	0.166 ±0.007	5	Schulz (1967a)	0.162	0.160
				646	$\frac{1}{2}^- - \frac{1}{2}^+$	0.228 ±0.004	1.438	0.160 ±0.003	5	Schulz (1967a)		
79	Au	195	229.0 ±1.0*	99	$\frac{3}{2}^+ - \frac{3}{2}^-$	0.873 ±0.044	5.047 ±0.055	0.173 ±0.009	5	Goverse (1973)	0.168	0.165
				130	$\frac{3}{2}^+ - \frac{5}{2}^-$	3.055 ±0.086	16.74 ±0.61	0.183 ±0.008	5	Goverse (1973)		
				0	$\frac{3}{2}^+ - \frac{1}{2}^-$	0.337 ±0.007	2.040	0.165 ±0.003	5	Goverse (1973)		
81	Tl	202	1372 ±22 [g]	440	$2^- - 2^+$	0.196 ±0.002	1.167 ±0.002	0.168 ±0.002	5	Leutz (1966)	0.171	0.169
				960	$2^- - 2^+$	0.305 ±0.020	1.458 ±0.017	0.209 ±0.014	5	Leutz (1966)		
83	Bi	206	3652 ±25 [h]	3279	$6^+ - 5^-$	0.264 ±0.010			5	Goverse (1974b)	0.175	0.173
				3403	$6^+ - 5^-$	0.281 ±0.009			5	Goverse (1974b)		
				3563	$6^+ - 5^-$	0.509 ±0.015			5	Goverse (1974b)		
					C. Second nonunique forbidden transitions $\Delta J = 2;\ \pi_i \pi_f = +1$							
17	Cl	36	1144.1 ±1.7	0	$2^+ - 0^+$	0.112 ±0.008			1	Dougan (1962b)		
28	Ni	59	1073.1 ±1.1	0	$\frac{3}{2}^- - \frac{7}{2}^-$	0.121 ±0.002			1	Chew (1974a)		
42	Mo	93	398 ±4	30;0	$\frac{5}{2}^+ - \frac{1}{2}^-;\frac{9}{2}^+$	0.36 ±0.04			6	Hohmuth (1964)		
43	Tc	97	347 ±9	0	$\frac{9}{2}^+ - \frac{5}{2}^+$	$0.21^{+0.14}_{-0.10}$			6	Katcoff (1958)		

TABLE XV. *(Continued)*

Z	Elements	A	Q_{EC} [a] (keV)	Final state (keV)	$J_i^\pi - J_f^\pi$	Experimental values P_L/P_K	$(q_{L_1}/q_K)^4$	$\frac{P_L/P_K}{(q_{L_1}/q_K)^4}$	Method [b]	Reference	Theor. values $\frac{P_L/P_K}{(q_{L_1}/q_K)^4}$ [c] Bahcall	Vatai
						D. First unique forbidden transitions [i] $\Delta J=2;\ \pi_i\,\pi_f=-1$						
36	Kr	81	290 ±100	0	$\frac{7}{2}^+ - \frac{3}{2}^-$	0.146 ±0.005	1.179	0.124 ±0.006	1	Chew (1974b)	0.127	0.126
53	I	126	1251 ±5	Several		$0.142^{+0.005}_{-0.018}$	1.071 ±0.016	$0.133^{+0.005}_{-0.018}$	5	Scobie (1958)	0.131	0.130
81	Tl	202	1372 ±22 [g]	0	$2^- - 0^+$	$0.22^{+0.02}_{-0.015}$	1.230 ±0.004	$0.179^{+0.016}_{-0.012}$	5	Leutz (1966)	0.173	0.171
81	Tl	204	345 ±4	0	$2^- - 0^+$	0.42 ±0.05	2.256 ±0.016	0.17 ±0.02	5	Joshi (1961)	0.204	0.201
				0		0.41 ±0.03		0.16 ±0.01	5	Leutz (1962)		
				0		0.60 ±0.055		0.24 ±0.02	7	Christmas (1964)		
				0		0.48 ±0.04		0.19 ±0.02		Robinson (1963)		
				0		0.43 ±0.16		0.17 ±0.06	6	Rao (1965)		
				0		0.52 ±0.02		0.20 ±0.01	5	Klein (1966)		

[a] Q_{EC} values are taken from Wapstra and Gove (1971). There are some values that originate from electron-capture measurements. They are replaced by values obtained from other methods, except for a few cases, indicated by an asterisk where no recent other result is available.

[b] Methods are identified by numbers explained in Table XIII.

[c] The theoretical L/K ratios are derived from wavefunctions of Mann and Waber (1973) and exchange and overlap corrections $X^{L/K}$ as described in Sec. II.E. For $Z>54$ the correction factors of Suslov (1970) are used in continuation of the Bahcall factors and those of Martin and Blichert-Toft (1970) in extension of the recalculated Vatai factors.

[d] Q_{EC} value from Henry (1974).

[e] Q_{EC} value from Bertrand (1974).

[f] Revised value; see Grinberg *et al.* (1973).

[g] Q_{EC} value from Auble (1971b).

[h] The Q_{EC} value is obviously too low. No reliable comparison with theoretical values can be given.

[i] First unique forbidden transitions; the factor $(q_{L_1}/q_K)^2$ has been squared and in the theoretical values the contribution of the L_3 shell has been allowed for.

TABLE XVI. Experimental and theoretical P_M/P_L ratios.

Z	Elements	A	Q_{EC}[a] (keV)	Final state (keV)	$J_i^\pi - J_f^\pi$	Experimental values P_M/P_L	$(q_{M_1}/q_{L_1})^2$	Experimental values $\frac{P_M/P_L}{(q_{M_1}/q_{L_1})^2}$	Method[b]	References	Theor. values $\frac{P_M/P_L}{(q_{M_1}/q_{L_1})^2}$[c] Bahcall	Vatai
					A. Allowed transitions $\Delta J=0,1$; $\pi_i\pi_f=+1$							
18	Ar	37	814.1±0.6	0	$\frac{3}{2}^+ - \frac{3}{2}^+$	$0.104^{+0.007}_{-0.003}$	1.000	$0.104^{+0.007}_{-0.003}$	3	Renier (1968)	0.130	0.116
26	Fe	55	231.7±0.7	0	$\frac{3}{2}^- - \frac{5}{2}^-$	0.157±0.003	1.006	0.156±0.003	1	Pengra (1972)	0.163	0.156
30	Zn	65	1350.7±1.1	1115	$\frac{5}{2}^- - \frac{5}{2}^-$	0.153±0.020	1.008	0.152±0.020	1	Krafft (1970)	0.167	0.160
32	Ge	71	235.1±1.7	0	$\frac{1}{2}^- - \frac{3}{2}^-$	0.142±0.010	1.010	0.141±0.010	1	Manduchi (1962b)	0.170	0.164
						0.162±0.003		0.160±0.003	1	Genz (1971a)		
48	Cd	109	182.0±3.0	88	$\frac{5}{2}^+ - \frac{7}{2}^+$	0.205±0.020[d]	1.070	0.192±0.019	2	Moler (1965)	0.206	0.202
					B. First nonunique forbidden transitions $\Delta J=0,1$; $\pi_i\pi_f=-1$							
50	Sn	113	1025 ±15	648; 393	$\frac{1}{2}^+ - \frac{3}{2}^-; \frac{1}{2}^-$	0.220±0.010[e]	1.011	0.218±0.010	1	Manduchi (1964b)	0.209	0.205
76	Os	185	1015.0±0.7	646	$\frac{1}{2}^- - \frac{1}{2}^+$	0.254±0.005	1.055	0.241±0.005	5	Schulz (1967a)	0.245	0.236
78	Pt	193	61.2±3.0	0	$\frac{1}{2}^- - \frac{3}{2}^+$	0.386±0.014	1.475	0.262±0.010	5	Ravn (1971)	0.247	0.239
81	Tl	202	1372 ±22[f]	440	$2^- - 2^+$	0.269±0.007	1.025	0.262±0.007	5	Leutz (1966)	0.249	0.240
83	Bi	206	3652 ±25[g]	3279	$6^+ - 5^-$	0.228±0.007			5	Goverse (1974b)	0.250	0.242
				3403	$6^+ - 5^-$	0.276±0.008			5	Goverse (1974b)		
				3563	$6^+ - 5^-$	0.282±0.010			5	Goverse (1974b)		

[a] Q_{EC} values are taken from Wapstra and Gove (1971).

[b] Methods are identified by numbers explained in Table XIII.

[c] The theoretical M/L ratios are determined from wavefunctions of Mann and Waber (1973) and exchange and overlap corrections $X^{M/L}$ as described in Sec. II.E. For $Z>54$ the correction factors of Suslov (1970) are used in continuation of the Bahcall factors and those of Martin and Blichert-Toft (1970) in extension of the recalculated Vatai factors.

[d] Revised value using $k_\beta/k_\alpha=0.212$ (Salam *et al.* 1974) and $\omega_K=0.832$ (see Table XVII).

[e] Revised value using $k_\beta/k_\alpha=0.217$ (Salam *et al.* 1974) and $\omega_K=0.852$ (see Table XVII).

[f] Q_{EC} value from Auble (1971b).

[g] The Q_{EC} value is obviously too low. No reliable comparison with theoretical values can be given.

TABLE XVII. Experimental and theoretical P_K values.

						Experimental values					Theor. P_K values[c]	
Z	Elements	A	Q_{EC}[a] (keV)	Final state (keV)	$J_i^\pi - J_f^\pi$	$P_{LM..}/P_K$	$P_K\omega_K$	ω_K[b]	P_K	Method[d]	References	Bahcall	Vatai
					A. Allowed transitions $\Delta J = 0, 1;\ \pi_i \pi_f = +1$								
23	V	48	4015.4 ± 2.8	Several			0.2005 ± 0.0030	0.225 ± 0.009	0.891 ± 0.036	11	Albrecht (1975)	0.892	0.896
24	Cr	51	751.4 ± 0.9	320	$\frac{7}{2}^- - \frac{5}{2}^-$		0.227 ± 0.003	0.256 ± 0.007	0.887 ± 0.008	10	Taylor (1965)	0.890	0.893
25	Mn	54	1374.9 ± 3.6	835	$3^+ - 2^+$		0.257 ± 0.004	0.283 ± 0.007	0.908 ± 0.008	10	Taylor (1965)	0.889	0.891
							0.243 ± 0.012		0.859 ± 0.014	10	Leistner (1965)		
							0.2514 ± 0.0017		0.888 ± 0.007	10	Bambynek (1967a)		
							0.250 ± 0.005		0.883 ± 0.009	10	Petel (1967)		
							0.2492 ± 0.0017		0.881 ± 0.009	11	Hammer (1968)		
									0.900 ± 0.014	10	Dobrilovic (1972)		
							0.247 ± 0.009		0.873 ± 0.011	11	Mukerji (1973)		
27	Co	57	836.9 ± 0.7	136	$\frac{7}{2}^- - \frac{5}{2}^-$		0.3044 ± 0.0043	0.344 ± 0.008	0.885 ± 0.009	11	Rubinson (1968)	0.887	0.890
						0.15 ± 0.02			0.87 ± 0.02	11	Bosch (1969)		
							0.317 ± 0.006		0.922 ± 0.010	11	Mukerji (1973)		
				706	$\frac{7}{2}^- - \frac{5}{2}^-$	0.088 ± 0.040			0.92 ± 0.03	11	Bosch (1969)	0.878	0.881
27	Co	58	2308.0 ± 2.5	1675;810	$2^+ - 2^+;2^+$		0.3050 ± 0.0022	0.344 ± 0.008	0.887 ± 0.008	10	Bambynek (1968b)	0.887	0.890
30	Zn	65	1350.7 ± 1.1	1115	$\frac{5}{2}^- - \frac{5}{2}^-$			0.441 ± 0.009	0.878 ± 0.006	13	Kramer (1962a)	0.882	0.884
							0.3927 ± 0.0026		0.890 ± 0.009	11	Hammer (1968)		
							0.386 ± 0.010		0.875 ± 0.013	11	Mukerji (1973)		
				1115;0	$\frac{5}{2}^- - \frac{5}{2}^-;\frac{3}{2}^-$		0.400 ± 0.006		0.907 ± 0.011	10	Taylor (1965)	0.882	0.884
							0.3894 ± 0.0016		0.883 ± 0.009	10	Bambynek (1968a)		
33	As	73	340 ± 15	67	$\frac{3}{2}^- - \frac{1}{2}^-$				0.85 ± 0.05	16	Kyles (1970)	0.874	0.875
34	Se	75	864.7 ± 1.0	401	$\frac{5}{2}^+ - \frac{5}{2}^+$		0.460 ± 0.004	0.576 ± 0.031	0.799 ± 0.031	11	Rao (1966a)	0.876	0.878
							0.462 ± 0.012		0.802 ± 0.033	11	Raeside (1969)		
							0.516 ± 0.021		0.896 ± 0.037	11	Chew (1973)		
37	Rb	83	1038 ± 32	562	$\frac{5}{2}^- - \frac{3}{2}^-$	0.164 ± 0.002			0.859 ± 0.002	5	Goedbloed (1970b)	0.872	0.874
38	Sr	85	1064 ± 7	514	$\frac{9}{2}^+ - \frac{9}{2}^+$				0.88 ± 0.04	11	Bisi (1956a)	0.871	0.873
							0.5959 ± 0.0035	0.676 ± 0.008	0.882 ± 0.009	11	Grotheer (1969)		
							0.586 ± 0.003		0.867 ± 0.009	10	Bambynek (1970)		
39	Y	88	3619 ± 4	2734	$4^- - 3^-$		0.6290 ± 0.0032	0.700 ± 0.009	0.898 ± 0.009	11	Grotheer (1969)	0.871	0.874
				2734;1836	$4^- - 3^-;2^+$		0.613 ± 0.004		0.876 ± 0.010	10	Bambynek (1973)	0.871	0.874
48	Cd	109	182.0 ± 3.0	88	$\frac{5}{2}^+ - \frac{7}{2}^+$	0.28 ± 0.03			0.871 ± 0.018	5	Der Mateosian (1953)	0.785	0.787
									0.805 ± 0.027	8	Wapstra (1957)		
						0.228 ± 0.003			0.814 ± 0.002	5	Leutz (1965)		
						0.26 ± 0.03			0.794 ± 0.025	18	Durosinmi-Etti (1966)		
						0.226 ± 0.003			0.816 ± 0.002	5	Goedbloed (1970a)		
49	In	111	826 ± 29	419	$\frac{9}{2}^+ - \frac{7}{2}^+$				0.867 ± 0.007	17	Sparrmann (1966)	0.848	0.850
53	I	125	177.0[e] ± 1.2	35.5	$\frac{5}{2}^+ - \frac{3}{2}^+$	0.23 ± 0.03			0.813 ± 0.020	5	Der Mateosian (1953)	0.796	0.798
						0.2543 ± 0.0027			0.7972 ± 0.0017	5	Leutz (1964)		
						0.253 ± 0.005			0.789 ± 0.003	5	Smith (1966)		
							0.685 ± 0.018	0.876 ± 0.028	0.782 ± 0.033	11	Karttunen (1969)		
							0.699 ± 0.030		0.798 ± 0.041	11	Tolea (1974)		
							0.685 ± 0.012		0.782 ± 0.029	11	Plch (1974a)		

TABLE XVII. *(Continued)*

Z	Elements	A	Q_{EC} [a] (keV)	Final state (keV)	$J_i^\pi - J_f^\pi$	$P_{LM..}/P_K$	Experimental values $P_K\omega_K$	ω_K [b]	P_K	Method [d]	References	Theor. P_K values [c] Bahcall	Vatai
54	Xe	127	664 ±4	375	$\frac{1}{2}^+ - \frac{1}{2}^+$		0.705 ±0.004	0.883 ±0.028	0.798 ±0.028	11	Bresesti (1964)	0.830	0.832
				203	$\frac{1}{2}^+ - \frac{3}{2}^+$		0.750 ±0.016		0.849 ±0.032	11	Bresesti (1964)	0.842	0.843
55	Cs	131	355 +6	0	$\frac{5}{2}^+ - \frac{3}{2}^+$		0.734 ±0.006	0.889 ±0.020	0.826 ±0.020	11	Plch (1974b)	0.831	0.835
56	Ba	133	515.8 [f] ±3.0	437	$\frac{1}{2}^+ - \frac{1}{2}^+$	0.45 ±0.04			0.69 ±0.02	19	Törnkvist (1968)	0.662 ±0.010	0.667 ±0.010
							0.676 ±0.087		0.755 ±0.097	14	Nicaise (1975)		
							0.576 ±0.038	0.895 ±0.012	0.652 ±0.040	14	Narang (1968)		
							0.644 ±0.034		0.72 ±0.04	11	Schmidt-Ott (1972)		
				384	$\frac{1}{2}^+ - \frac{3}{2}^+$		0.72 ±0.06		0.80 ±0.07	11	Schmidt-Ott (1972)	0.769	0.773
58	Ce	139	275 ±15	165	$\frac{5}{2}^+ - \frac{5}{2}^+$	0.37 ±0.02			0.73 ±0.01	15	Ketelle (1956)	0.724 ±0.014	0.729 ±0.014
									0.68 ±0.02	17	Marelius (1967)		
									0.750 ±0.010	16	Adamowicz (1968)		
									0.69 ±0.02	13	Vatai (1968a)		
							0.707 ±0.018	0.906 ±0.026	0.78 ±0.03	11	Schmidt-Ott (1972)		
							0.649 ±0.017		0.725 ±0.02	14	Campbell (1972)		
							0.639 ±0.006		0.705 ±0.030	11	Plch (1975)		
									0.726 ±0.010	15	Hansen (1975)		
64	Gd	151	484 [g] ±30	352	$\frac{7}{2}^- - \frac{9}{2}^-$		0.664 ±0.009	0.930 ±0.015	0.714 ±0.017	11	Genz (1973c)	0.704 ±0.015	0.709 ±0.015
70	Yb	166	260 ±20*	82	$2^+ - 2^+$		$0.68^{+0.06}_{-0.02}$	0.946 ±0.020	$0.72^{+0.06}_{-0.03}$	14	Jasinski (1963a)	0.711 ±0.011	0.715 ±0.011
81	Tl	201	484 ±17 [h]	167	$\frac{1}{2}^+ - \frac{1}{2}^+$		0.67 ±0.04	0.964 ±0.017	0.70 ±0.04	11	Gupta (1960)	0.722 ±0.014	0.726 ±0.014
					B. First nonunique forbidden transitions $\Delta J = 0, 1;\ \pi_i \pi_f = -1$								
37	Rb	84	2679.8 ±2.9	880	$2^- - 2^+$		0.580 ±0.025	0.653 ±0.030	0.888 ±0.039	11	Welker (1955)	0.876	0.878
61	Pm	145	170 ±7*	67	$\frac{5}{2}^+ - \frac{3}{2}^-$		0.558 ±0.022	0.919 ±0.024	0.607 ±0.033	11	Tolea (1974)	0.676 ±0.011	0.681 ±0.011
				72	$\frac{5}{2}^+ - \frac{5}{2}^-$		0.509 ±0.022		0.554 ±0.033	11	Tolea (1974)	0.660 ±0.011	0.665 ±0.011
62	Sm	145	647 ±14 [k]	61	$\frac{7}{2}^- - \frac{5}{2}^+$	0.20 ±0.02			0.833 ±0.014	16	Brosi (1959)	0.830	0.833
64	Gd	151	484 ±30 [g]	307	$\frac{7}{2}^- - (\frac{3}{2}, \frac{7}{2})^+$		0.754 ±0.014	0.930 ±0.015	0.811 ±0.021	11	Genz (1973c)	0.754 ±0.009	0.759 ±0.009
66	Dy	159	365.4 ±1.0	58	$\frac{5}{2}^- - \frac{5}{2}^+$		0.752 ±0.024	0.936 ±0.022	0.803 ±0.033	11	Genz (1973c)	0.793	0.797
72	Hf	175	607 ±8*	433	$\frac{5}{2}^- - \frac{7}{2}^+$		0.64 ±0.04	0.950 ±0.020	0.67 ±0.04	11	Funke (1965)	0.689 ±0.005	0.693 ±0.005
									0.712 ±0.008	16	Jasinski (1968)		
				343	$\frac{5}{2}^- - \frac{5}{2}^+$				$0.767^{+0.030}_{-0.016}$	16	Jasinski (1968)	0.753 ±0.002	0.757 ±0.002
78	Pt	188	540 ±10*	195	$0^+ - 1^-$				0.744 ±0.020	16	Hanson (1968)	0.748	0.752
				187	$0^+ - 1^-$				0.766 ±0.023	16	Hanson (1968)	0.750	0.754

TABLE XVII. *(Continued)*

						Experimental values						Theor. P_K values[c]	
Z	Elements	A	Q_{EC}[a] (keV)	Final state (keV)	$J_i^\pi - J_f^\pi$	$P_{LM..}/P_K$	$P_K\omega_K$	ω_K[b]	P_K	Method[d]	References	Bahcall	Vatai
79	Au	195	229.0 ± 1.0*	130	$\frac{3}{2}^+ - \frac{5}{2}^-$		0.188 ± 0.005	0.961 ± 0.018	0.196 ± 0.019	11	De Wit (1965)	0.202 ±0.006	0.206 ±0.006
						5.25 ± 0.66			0.160 ± 0.017	5	Goverse (1973)		
				99	$\frac{3}{2}^+ - \frac{3}{2}^-$				0.458 ± 0.012	16	Jasinski (1968)	0.461 ±0.003	0.466 ±0.003
						1.28 ± 0.06			0.438 ± 0.011	5	Goverse (1973)		
80	Hg	197	684 ± 40[i]	268;77	$\frac{1}{2}^- - \frac{3}{2}^+;\frac{1}{2}^+$		0.741 ± 0.012	0.963 ± 0.017	0.769 ± 0.021	18	Plch (1971)	0.754 ±0.002	0.758 ±0.002
81	Tl	202	1372 ± 22[j]	440	$2^- - 2^+$		0.76 ± 0.05	0.964 ± 0.017	0.79 ± 0.05	11	Hagedoorn (1958)	0.790	0.793
							$0.761^{+0.015}_{-0.008}$		$0.789^{+0.022}_{-0.019}$	14	Jha (1959)		
							0.751 ± 0.014		0.779 ± 0.022	14	Blok (1959)		
							0.75 ± 0.03		0.778 ± 0.034	11	Gupta (1960)		
						0.265 ± 0.010			0.791 ± 0.006	5	Leutz (1966)		
82	Pb	203	982 ± 12	680	$\frac{5}{2}^- - \frac{5}{2}^+$		0.66 ± 0.04		0.69 ± 0.04	11	Hagedoorn (1958)	0.709 ±0.003	0.713 ±0.003
				279	$\frac{5}{2}^- - \frac{3}{2}^+$		0.755 ± 0.014		0.783 ± 0.022	11	Hagedoorn (1958)	0.777	0.780
							0.750 ± 0.019		0.776 ± 0.025	11	Persson (1961)		
					C. First unique forbidden transitions $\Delta J = 2;\ \pi_i \pi_f = -1$								
19	K	40	1505.1 ± 0.7	1460;0	$4^- - 2^+;0^+$	0.34 ± 0.08			0.75 ± 0.05	5	McCann (1967)	0.741[l]	0.749[l]
						0.44 ± 0.09			0.69 ± 0.04	8	Ažman (1968)		

[a] Q_{EC} values are taken from Wapstra and Gove (1971). There are some values that originate from electron-capture measurements. They are replaced by values obtained from other methods, except for a few cases, indicated by an asterisk, where no recent other result is available.

[b] Fluorescence yields were calculated from the equation $[\omega_K/(1-\omega_K)]^{1/4} = A + BZ + CZ^3$. The constants A, B, C were determined by fitting the selected "most reliable" experimental values of Bambynek *et al.* (1972) to this equation. We have omitted from the list of the "most reliable" values those that were deduced from $P_K\omega_K$ measurements.

[c] The theoretical P_K values were derived from wavefunctions of Mann and Waber (1973) and exchange and overlap corrections as described in Sec. II.E. For $Z > 54$ the correction factors of Suslov (1970) are used in continuation of the Bahcall factors and those of Martin and Blichert-Toft (1970) in extension of the recalculated Vatai factors. Uncertainties are quoted only in those cases where they are significant. They originate from the uncertainties of the Q_{EC} value.

[d] Methods are identified by numbers explained in Table XIII.

[e] Q_{EC} value from Gopinathan (1968).

[f] Q_{EC} value from Henry (1974).

[g] Q_{EC} value from Ford (1970).

[h] Q_{EC} value from Auble (1971a).

[i] Q_{EC} value from Jasinski (1963b).

[j] Q_{EC} value from Auble (1971b).

[k] Q_{EC} value from Berényi (1970).

[l] Theoretical value for a unique first-forbidden transition.

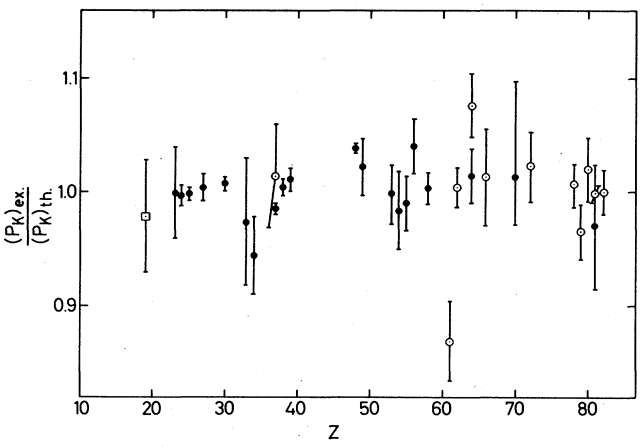

FIG. 17. Comparison of experimentally determined P_K values for allowed transitions (solid circles), first-forbidden nonunique transitions (open circles), and first-forbidden unique transitions (squares) with theoretical predictions based on wave functions of Mann and Waber (1973) and exchange and overlap corrections according to Bahcall (1963, 1965).

Capture probability P_K. Selected K-capture probabilities for allowed and first-forbidden transitions are compared in Table XVII with theoretical predictions for allowed transitions. Two selected measurements on ^{40}K are compared with theoretical capture probabilities for unique first-forbidden transitions. The K-capture probability, unlike the reduced capture ratio, depends on the transition energy as well as on the atomic number. In Fig. 17 we have plotted the ratio of experimental to theoretical P_K vs Z. The recalculated exchange and overlap corrections according to Bahcall (1963a, c, 1965a) (Sec. II.E) were used in the theoretical calculations. For several nuclides (e.g., ^{133}Ba, ^{145}Pm, ^{151}Gd, ^{195}Au), the energy Q_{EC} is not known with sufficient accuracy. New, more accurate measurements for P_K are desirable for some nuclides, e.g., for ^{73}As, ^{75}Se, ^{83}Rb, ^{84}Rb, ^{166}Yb, and ^{195}Au. The spin of the 307-keV level of ^{151}Eu is not exactly known; it is quoted as $(3/2)^+$ or $(7/2)^+$. The transition from the $(7/2)^-$ ^{151}Gd ground state to this level can therefore be nonunique or unique first forbidden. Comparison of the measured $P_K = 0.811 + 0.021$ with the theoretical $P_K = 0.740$ for a nonunique and $P_K = 0.428$ for a unique transition supports the $(7/2)^+$ assignment.

Experimental and theoretical K-capture ratios are seen from Fig. 17 to agree within ~5%; there is no systematic difference between allowed and first-forbidden nonunique transitions.

4. Conclusions and recommendations

From Tables XV–XVII and from Figs. 15, 16, and 17 we find that experimental and theoretical electron-capture data agree rather well, viz., on the average to ~3% in the case of L/K ratios, ~9% for M/L ratios, and 5% for P_K values. The experimental accuracy is insufficient to distinguish between the theoretical correction factors for exchange and overlap effects. These effects are expected to be largest in the decay of ^{7}Be (Odiot and Daudel, 1956; Bahcall, 1963). Experiments to measure the P_L/P_K ratio of ^{7}Be have been unsuccessful due to experimental limitations (Renier *et al.*, 1968).

New, more accurate measurements of capture ratios and P_K should be performed. More accurate results for second- and higher-order forbidden transitions would be useful to deduce nuclear matrix elements. Furthermore, more accurate Q_{EC} energies are very much needed.

D. Determination of K/β^+ and EC/β^+ ratios

In Secs. III.D and III.E we list all available experimental K/β^+ and EC/β^+ ratios and describe the experimental techniques involved in these measurements. We compare experimental ratios for allowed, unique first-forbidden and nonunique first-forbidden transitions with the appropriate theoretical values.

Source preparation is an important aspect of these measurements. Allowed β^+ emitters are generally short-lived, many of them having half-lives of the order of seconds, minutes, or hours (Fig. 18). In order to study β^+ emitters with comparative ease a continuous supply of the source is therefore often necessary. Positron emitting nuclei are normally deficient in neutrons, hence one cannot prepare them by slow-neutron bombardment of stable isotopes in reactors. Instead, the stable isotopes are usually converted to radioactive isotopes by such reactions as (γ, n), using machines like synchrotrons or electron linear accelerators, or by $(n, 2n)$ reactions with fast neutrons from such devices as Cockroft–Walton generators or high-current electrostatic accelerators. Cyclotron irradiation with protons, deuterons or alpha particles to produce proton-rich (neutron-deficient) nuclei is another useful method of preparing positron emitters.

The radioactive source must be transported to the detector in a time that is short compared with the half-life. This problem has been solved, for example, by fast pneumatic transfer systems in which solid sources can be conveyed from the irradiation site to the detector in a fraction of a second. Continuous gas flow systems (Fig. 19) have also been used extensively (Ledingham *et al.*,

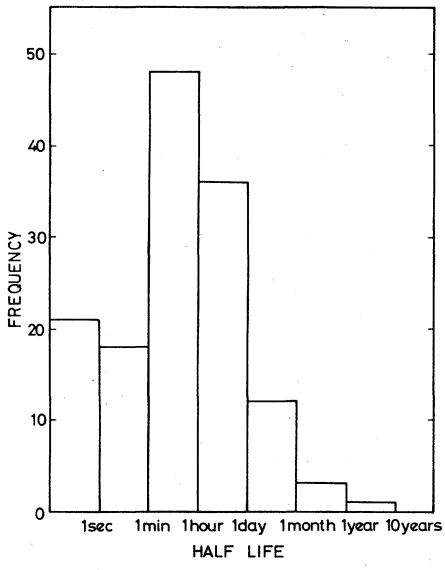

FIG. 18. Number of allowed positron emitters, as a function of half-life.

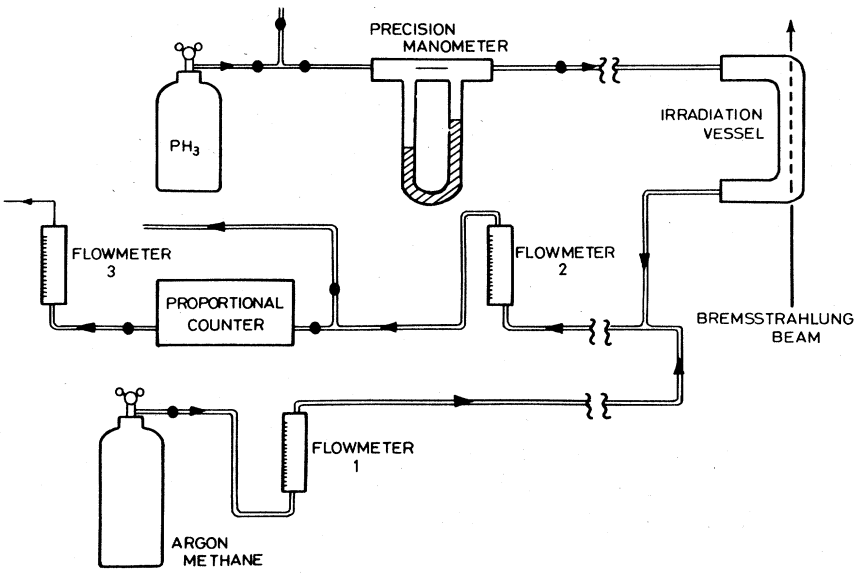

FIG. 19. Continuous gas-flow system used for K/β^+ measurements with short-lived low-Z isotopes.

1965); if narrow-bore tubing is used in conjunction with a gas pressure of several atmospheres, the radioactive source (in gaseous form) can be conveyed to the detector in a very short time. Where the sources cannot be obtained in suitable solid or gaseous forms, the problem can often be solved by using liquids under pressure with the radioactive source dissolved in the medium or in suspension.

The main types of measurement used to determine K/β^+ and EC/β^+ ratios are summarized in Table XIII. These various techniques and the sources of error involved in them are described in Secs. III.D.1–III.D.3.

1. Measurements of K/β^+ ratios with internal sources

a. Internal-source proportional counter

In this method (No. 20), the radioactive source in gaseous form is mixed with the normal proportional-counter gas. If the half-life of the source is sufficiently long, the gases may be static, but for short-lived nuclei continuous production of the source and gas flow through the counter is employed. The electron-capture events are detected as discrete peaks superimposed on the positron continuum. A major part of the error in these measurements comes from the procedure adopted in separating the K-capture peak from the continuum.

Measurements of K/β^+ ratios by this technique have generally been made under conditions where K x-ray escape from the counter is very small. For high-Z nuclei, the proportional counter must therefore be operated at high pressure. For low-Z nuclei, counters can be operated at normal pressure, but for such nuclei the K/β^+ ratio is usually extremely small, whence it is often difficult to resolve the K peak from the positron spectrum.

We assume that the radioactive source can be produced with negligible competing activities, a situation which is usually attainable in practice. The positrons and K-capture events are detected with practically 100% efficiency. Then we have

$$P_K/P_{\beta^+} = I_K/I_{\beta^+}, \tag{3.45}$$

where I_K and I_{β^+} are the measured intensities of the K peak and the β^+ spectrum, respectively. Corrections have to be applied to I_{β^+} to account for the number of positrons which, unlike the K x rays and Auger electrons, may enter the sensitive volume from the ends of the proportional counter. This correction was calculated to be 4.6% in the case of ^{18}F (Drever *et al.*, 1956).

Solid internal sources may also be employed (e.g., Avignon, 1956) but corrections for the absorption of the x rays, Auger electrons, and positrons in the source itself must then be taken into account.

In cases where the decay leads to an excited state of the daughter nucleus it is sometimes possible to measure coincidences between the spectrum in the proportional counter and the de-excitation γ ray, thus reducing the background. This technique was applied by Kramer *et al.* (1962b) to the decay of ^{58}Co.

b. Internal-source proportional counter with anticoincidence

This technique (No. 21) is similar to Method 20 and is particularly suitable for K/β^+ measurements on light nuclei where the K-capture events are generally very much less intense than the positrons. In order to resolve weak K-capture peaks from the positron continuum, an anticoincidence counter is employed. One such counter with a plastic scintillator as anticoincidence detector is shown in Fig. 20. Both the positron and electron-capture events are detected in the central proportional counter; only the positrons can reach the surrounding counter. Thus, if signals from the central counter are taken in anticoincidence with those from the surrounding plastic scintillator, a well-resolved K peak is obtained. Figure 21 shows a typical K peak from ^{30}P, measured with the counter shown in Fig. 20.

From the total spectrum in the central counter and the K peak in the anticoincidence spectrum, I_K and I_{β^+} are

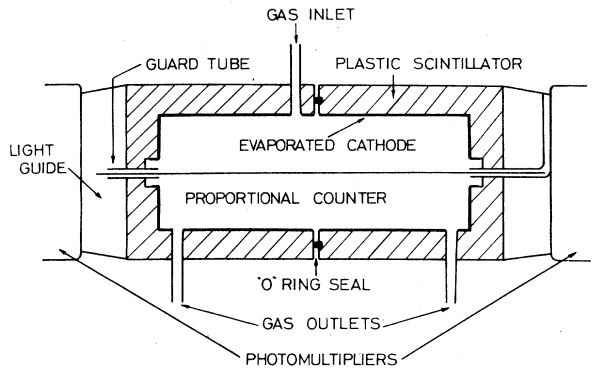

FIG. 20. Diagram of counter used to determine K/β^+ ratios of ^{11}C, ^{13}N, ^{15}O, ^{19}Ne and ^{30}P. K-capture events and positrons are detected in the central counter; only positrons have sufficient energy to be detected in the plastic scintillator.

obtained and Eq. (3.45) applies as in Method 20.

Unless high-pressure counters are employed, this method becomes complicated for nuclei with $Z \gtrsim 18$ because corrections for x-ray escape must be made. The method then becomes intrinsically less accurate, and hence has so far been employed only in the low-Z region.

c. *Internal-source scintillation counter*

In this technique (Method 22), the radioactive source is distributed in a scintillating crystal (usually NaI) by introducing it into the melt from which the crystal is grown. The capture and positron events are detected in the scintillator, with the K x rays and K Auger electrons producing a well-defined peak so that the K/β^+ ratio can be determined. The interpolation of the continuum under the peak is a major source of error. Examples of this technique are the measurements of the K/β^+ ratios for ^{22}Na with an error of 9% (McCann and Smith, 1969) and for ^{58}Co with an error of 2% (Joshi and Lewis, 1961). In both of these isotopes the decay leads to an excited state of the daughter nucleus which then de-excites by γ-ray emission. To reduce background, the positron and electron-capture events were measured in coincidence with the de-excitation gamma rays, detected in a second scintillation counter.

Corrections must be applied for the escape of positrons from the source crystal before they have deposited sufficient energy to be detected. If coincidences are taken with a de-excitation gamma ray, allowance should furthermore be made for the loss of positron counts due to the summing of the gamma ray with a 511-keV positron-annihilation photon. A K peak from ^{22}Na (McCann and Smith, 1969) is shown in Fig. 22. The difficulty of obtaining peaks at these very low energies with a scintillation counter is considerable. Specially selected low-noise photomultiplier tubes must be used in conjunction with an electronic system that is capable of eliminating afterpulses from long-lived phosphorescence associated with large energy deposition by positrons in the radioactive scintillator.

Because the positrons and the K-capture events are detected with approximately 100% efficiency, Eq. (3.45) again applies, allowing for the corrections described above.

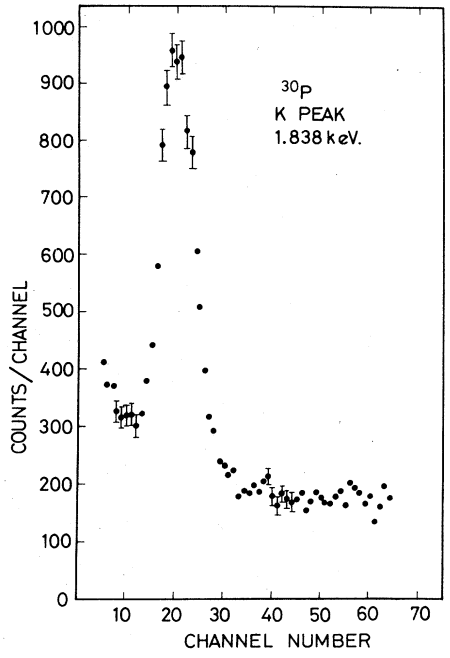

FIG. 21. Typical pluse-height spectrum from the central proportional counter in Fig. 20, in anticoincidence with the plastic scintillator. The counter gas, introduced in flow mode, was 90% Ar and 10% CH_4. Radioactive phosphine (PH_3) was introduced in trace amounts (<1% of Ar/CH_4) from an irradiation vessel to the main flow line carrying the counting mixture.

2. Measurements of K/β^+ ratios with external sources

a. *Spectroscopy of positrons and K Auger electrons*

In this type of measurement (No. 23), the areas under the Auger lines and the positron spectrum are measured. Since the Auger electrons and the positrons are oppositely charged, a magnetic spectrometer with a Geiger, proportional, or scintillation counter is often used to analyze the radiations. The difficulty of subtracting a β^+ spectrum from a K peak is thus avoided.

In order to determine a K/β^+ ratio from such measure-

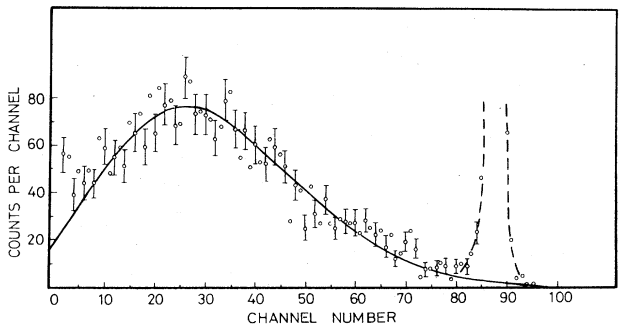

FIG. 22. The 870-eV K-capture peak of ^{22}Na, measured with an internal-source scintillation counter in coincidence with another NaI detector, closely located to register the 1.274-MeV de-excitation γ rays of ^{22}Ne.

ments, the value of the K-shell fluorescence yield ω_K must be known. There were often fairly large errors in the values of ω_K employed in the early experiments. However, Bambynek *et al.* (1972) have selected reliable measurements of ω_K and carried out a semiempirical fit to these values. Thus, for many cases, uncertainty in ω_K need no longer seriously limit the accuracy of this method.

The relation

$$P_K/P_{\beta^+}=I_{KA}/(1-\omega_K)I_{\beta^+} \tag{3.46}$$

applies, where I_{KA} is the total intensity of the K Auger lines. Corrections for absorption of low-energy Auger electrons and β^+ in the source are very important and contribute significantly to the errors involved in this technique.

b. Spectroscopy of K x rays and positrons

In this method (No. 24), a solid source is placed outside of semiconductor or scintillation counters. The K x rays and positron continuum are detected either in the same or separate counters, the Auger electrons generally being absorbed before reaching the detectors. A major uncertainty again arises from the subtracting of the β^+ spectrum from the K x-ray peak. As with Method 23, this technique requires knowledge of the fluorescence yield. Assuming that there are no competing activities, and correcting for absorption, the equation applicable to this method is

$$P_K/P_{\beta^+}=I_{KX}/I_{\beta^+}\omega_K . \tag{3.47}$$

Account must be taken of any differences in solid angle for the detection of K x rays and positrons. Self-absorption of x rays in the source is an important factor in this technique and makes the use of thin sources desirable.

Figure 23 shows how clearly the K x rays may be separated from the continuum in the decay of ^{91}Mo (Fitzpatrick *et al.*, 1975). This spectrum was obtained from a 5-mg/cm^2 thick, activated molybdenum foil placed 2 cm from a Si(Li) detector (area 30 mm^2, thickness 5 mm). The $K\alpha$ and $K\beta$ x rays of Nb are well resolved and the fluorescent K x rays of Mo caused by positron excitation of the foil can also be seen. Although the intensity of the K-capture branch in the decay of ^{91}Mo is small (~5%), the error in estimating the areas of the K x-ray peaks can easily be kept as low as 1%. There is, however, a difficulty in ensuring that the solid angles for the x rays and the positrons are the same, even when a single detector is employed. This difficulty can be reduced by using a detector with a large surface area. The K x-ray spectrum of ^{91}Mo measured with a 5.1-cm $\times$ 0.63-cm NaI(Tl) detector is shown in Fig. 24. The fine structure in the spectrum of Fig. 23 is unfortunately lost due to the intrinsically inferior resolution of NaI(Tl). Corrections are required for absorption of the K x rays and positrons and for the scattering of positrons out of the detector before they have deposited sufficient energy to be detected.

An interesting development of this technique is shown in Fig. 25 (Campbell *et al.*, 1975). Here, the radioactive sample is placed between two CaF_2(Eu) scintillators in a 4π arrangement. This arrangement overcomes the problem caused by positrons being scattered

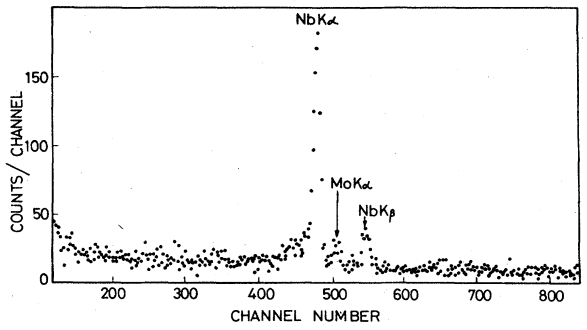

FIG. 23. Niobium K x rays from the decay of ^{91}Mo, measured with a Si(Li) detector with a resolution of 185 eV at 5.9 keV. The Nb $K\alpha$ and $K\beta$ peaks are well-resolved, even in the presence of a β^+ spectrum twenty times as intense as the K-capture branch. The Mo $K\alpha$ peak is caused by $\beta^\pm$ induced fluorescence in the source.

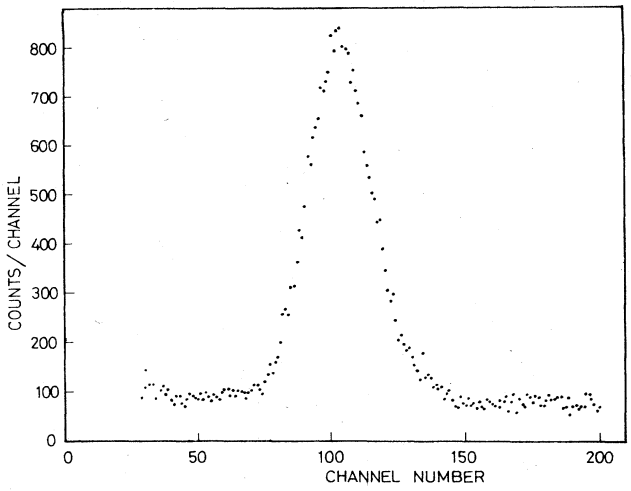

FIG. 24. Molybdenum-91 K x-ray spectrum measured with a 5.7 $\times$ 0.63 cm NaI(Tl) counter of 28% resolution at 22 keV. The fine structure evident in Fig. 23 is no longer visible.

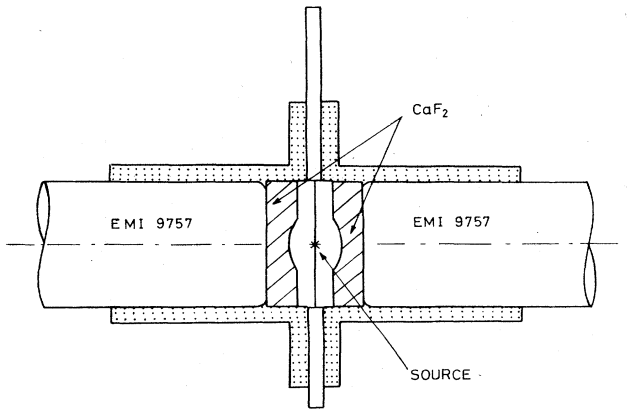

FIG. 25. Thin, self-supporting evaporated sources are placed between two CaF_2(Eu) crystals. Although CaF_2 has inherently a lower light output than NaI(Tl), the crystals are nonhygroscopic and can be used without windows between source and crystal.

out of the detector before depositing sufficient energy to be detected, or being scattered into the detector from surrounding material.

Many of the early K/β^+ measurements in this category (Method 24) employed absorption techniques, typically with a Geiger counter and different absorbers to determine the relative intensities of the K x rays and the positrons. The accuracy of these measurements is very poor.

c. Spectroscopy of K x rays and β^+ annihilation photons

This technique (No. 25) is similar to the previous method, but instead of detecting the β^+ continuum, the positrons are stopped in an absorber and the 511-keV annihilation photons are detected. The source must be surrounded by sufficient material to ensure that all positrons are stopped at a well-defined position, as close to the source as possible. The K x rays and the annihilation photons may be counted simultaneously, with corrections applied to both intensities to allow for the presence of the β^+ absorber. Alternatively, when the half-life of the source is sufficiently long, spectra taken with and without the absorber may be used to determine I_{511} and I_{KX}, respectively.

The K/β^+ ratio is deduced from the relation

$$P_K/P_{\beta^+} = 2I_{KX}/\omega_K I_{511}\,. \tag{3.48}$$

A correction must be applied to I_{511} for the loss of 511-keV γ rays due to the summing of two such γ rays; the size of this correction depends on details of geometry and the type of detector. The effect on I_{511} of β^+ annihilation in flight (e.g., Kantele and Valkonen, 1973) must also be considered, although in many cases this has been assumed to be negligibly small.

3. Measurement of EC/β^+ ratios

EC/β^+ ratios are determined by measuring the number of positrons emitted by the parent leading to an excited state of the daughter nucleus, and the number of γ rays or conversion electrons from that level in a given time interval. Since the total number of γ rays plus conversion electrons is equal to the total number of positrons and electron-capture events—corrected with reference to the decay scheme where necessary—the ratio EC/β^+ of total electron capture to β^+ emission can be determined. Errors in these measurements can be kept very small, especially if the decay scheme is well-known. For example, the EC/β^+ ratios for ^{22}Na and ^{58}Co have been determined to ~0.3% and ~0.7%, respectively. Errors in the decay scheme can, however, be large, and have led to large systematic errors in many of these measurements.

a. Spectroscopy of γ rays or conversion electrons and β^+ annihilation photons

One of the simplest forms of EC/β^+ measurements consists of a comparison of the relative photopeak intensities of the de-excitation γ rays and the β^+ annihilation photons in, for example, a scintillation or semiconductor detector (Method 26). As for Method 25, the source must be surrounded by sufficient material to annihilate the positrons near the source to ensure that the solid angle is the same for both the nuclear and the annihilation photons. Corrections are required for absorption in the source and detector window, for decays to other levels in the daughter nucleus, for summing, and for annihilation of positrons in flight. In cases where the energy of the de-excitation γ rays is high it may be necessary to correct for a contribution to the annihilation photons due to internal and external pair production (e.g., Rupnik, 1972).

The total capture to β^+ emission ratio is given by

$$\frac{P_{\mathrm{EC}}}{P_{\beta^+}} = \frac{2I_\gamma(1+\alpha)}{I_{511}} - 1, \tag{3.49}$$

where I_γ and I_{511} are the photopeak areas of the de-excitation γ ray and β^+ annihilation photons, respectively, and α is the internal conversion coefficient.

A variation of this technique which has often been employed, particularly in the early measurements, is the comparison of the photopeak areas of the 511-keV and de-excitation γ rays for the source being investigated with similar areas for a source with a known EC/β^+ ratio. Thus, if the subscripts a and b refer to the source with known and unknown EC/β^+ ratio, respectively, we have

$$\left(\frac{P_{\mathrm{EC}}}{P_{\beta^+}}\right)_b = \left(\frac{I_\gamma}{I_{511}}\right)_q \left(\frac{I_{511}}{I_\gamma}\right)_a \frac{\epsilon_{\gamma a}}{\epsilon_{\gamma b}}\left[\left(\frac{P_{\mathrm{EC}}}{P_{\beta^+}}\right)_a + 1\right]\left(\frac{1+\alpha_b}{1+\alpha_a}\right) - 1. \tag{3.50}$$

This method is suitable when the de-excitation γ rays for the two sources are of similar energy, since the ratio of efficiencies $\epsilon_{\gamma a}/\epsilon_{\gamma b}$ is then approximately unity. Hence the EC/β^+ ratio is then independent of detector efficiency. The accuracy of this method is obviously limited by the error in the EC/β^+ ratio of the standard source. Often ^{22}Na was used for this comparison but the range of reported EC/β^+ values for this isotope is large (Table XVIII). Some authors did not even state which comparison value they employed.

A less common variation of this technique consists of measuring the intensities of the β^+ annihilation photons and the conversion electrons, rather than the de-excitation γ rays. This method is only feasible in special cases where the internal conversion coefficient is high.

Several measurements have been carried out employing a similar technique in which the positron activity was determined from the area under the β^+ spectrum rather than from the intensity of the annihilation photons. As above, comparison with an isotope with a well-known EC/β^+ ratio was often employed. The results reported from this technique, however, have very large errors (> 20%).

b. Measurement of β^+-γ-ray coincidences

The principle of this method (No. 27) is to determine the number of γ rays, I_γ, and of positron-γ-ray coincidences, $I_{\beta^+\text{-}\gamma}$. Various combinations of detectors may be employed. Typically, scintillation or semiconductor detectors have been used for the γ rays while the positrons were detected in proportional or scintillation counters. A 4π proportional counter or an internal-source scintillation counter (Leutz and Wenninger, 1967) have also been employed to detect the positrons.

TABLE XVIII. Experimental K/β^+ and EC/β^+ ratio.

Z	Elements	A	Q_{EC}[a] (keV)	Final state (keV)	$J_i^\pi - J_f^\pi$	P_K/P_{β^+}	P_{EC}/P_{β^+}	Method[b]	References
6	C	11	1982.2 ± 1.0	0	$\frac{3}{2}^- \rightarrow \frac{3}{2}^-$	$(1.9 \pm 0.3) \times 10^{-3}$		20	Scobie (1957b)
						$(2.30^{+0.14}_{-0.11}) \times 10^{-3}$		21	Campbell (1967)
7	N	13	2220.5 ± 0.9	0	$\frac{1}{2}^- \rightarrow \frac{1}{2}^-$	$(1.68 \pm 0.12) \times 10^{-3}$		21	Ledingham (1965)
8	O	15	2759.2 ± 0.9	0	$\frac{1}{2}^- \rightarrow \frac{1}{2}^-$	$(1.07 \pm 0.06) \times 10^{-3}$		21	Leiper (1972)
9	F	18	1655.3 ± 0.9	0	$1^+ \rightarrow 0^+$	$(3.00 \pm 0.18) \times 10^{-2}$		20	Drever (1956)
10	Ne	19	3238.2 ± 0.9	0	$\frac{1}{2}^+ \rightarrow \frac{1}{2}^+$	$(9.6 \pm 0.3) \times 10^{-4}$		21	Leiper (1972)
11	Na	22	2842.3 ± 0.5	1274.6	$3^+ \rightarrow 2^+$	0.105 ± 0.009		22	McCann (1969)
							0.10 ± 0.05	26	Bouchez (1952)
							0.110 ± 0.006	27	Sherr (1954)
							0.124 ± 0.010	26	Kreger (1954)
							0.09 ± 0.06	27	Sehr (1954)
							0.122 ± 0.010	31	Allen (1955)
							0.065 ± 0.009	23	Charpak (1955)
							0.124 ± 0.012	27	Hagedoorn (1957)
							0.109 ± 0.008	27	Konijn (1958/59)
							0.112 ± 0.004	27	Ramaswamy (1959a)
							0.1041 ± 0.0010	28	Williams (1964, 1968)
							0.1048 ± 0.0007	27	Leutz (1967)
							0.103 ± 0.018	31	Steyn (1966)
							0.1042 ± 0.0010	27	Vatai (1968c)
							0.1077 ± 0.0003	27	MacMahon (1970)
13	Al	26	4004.7 ± 0.5	1810	$5^+ \rightarrow 2^+$		0.135 ± 0.023	26	Rightmire (1959)
							0.12	31	Jastram (1961)
15	P	30	4227.4 ± 2.6	0	$1^+ \rightarrow 0^+$	$(1.24 \pm 0.04) \times 10^{-3}$		21	Ledingham (1971)
17	Cl	36	1144.1 ± 1.7	0	$2^+ \rightarrow 0^+$	$(1.4^{+0.2}_{-0.6}) \times 10^3$		Combination of 21 and 31	Dougan (1962b)
						$(7.5 \pm 3.0) \times 10^2$		31	Berényi (1962) and (1963b)
21	Sc	44	3649 ± 6	Several	$2^+ \rightarrow$ several		0 ± 0.1	26	Langevin (1954c)
							0.05 ± 0.15	26	Langevin (1954c)
							0.11 ± 0.05	26	Blue (1955)
							0.073 ± 0.017	27	Blue (1955)
							0.023 ± 0.019	27	Konijn (1958/59)
							0.049	26	Dillman (1963)
23	V	48	4015.4 ± 2.8	Several	$4^+ \rightarrow$ several		0.72 ± 0.11	31	Good (1946)
							0.46 ± 0.09	26	Sterk (1953)
				2295	$4^+ \rightarrow 4^+$		1.04 ± 0.17	26	Casson (1953)
							0.75 ± 0.09	31	Bock (1955)
							0.74 ± 0.07	...	van Nooijen (1957) revised by Konijn (1967b)
							0.74 ± 0.02	27	Hagedoorn (1957)
							0.43 ± 0.03	26	Ristinen (1963)

TABLE XVIII. (*Continued*)

Z	Elements	A	Q_{EC} [a] (keV)	Final state (keV)	$J_i^\pi - J_f^\pi$	P_K/P_{β^+}	P_{EC}/P_{β^+}	Method [b]	References
23	V	48					0.77±0.04	29	Biryukov (1966)
							0.77±0.06	27	Konijn (1967a)
							0.83±0.06	27	Konijn (1967b)
							0.76±0.035	29	Konijn (1967b)
							0.69±0.03	27	Albrecht (1975)
25	Mn	52	4709.8±3.5	3112	$6^+ \rightarrow 6^+$		1.86±0.17	31	Good (1946)
							2.01±0.24	27	Sehr (1954)
							1.95±0.19	...	Konijn (1958c) revised by Konijn (1967b)
							1.84±0.20	30	Wilson (1962)
							2.04±0.24	26	Freedman (1966)
							1.80±0.13	27	Konijn (1967b)
							2.12±0.17	29	Konijn (1967b)
26	Fe	52	2372±12	548	$0^+ \rightarrow (1)^+$		0.77±0.18	31	Arbman (1955)
							0.82	31	Juliano (1959)
							1.6±0.4	24	Friedlander (1951a)
27	Co	56	4568.2±1.9	Several	$4^+ \rightarrow$ several		4.3±0.2	26	Cook (1956)
				3120	$4^+ \rightarrow (5)^+$		12	26	Sakai (1954)
				2085	$4^+ \rightarrow 4^+$		0.35±0.07	26	Sakai (1954)
							0.014±0.152	27	Berényi (1965c)
							0.23±0.22	26	Berényi (1965c)
							0.117±0.089	27	Vatai (1966)
27	Co	58	2308.0±2.5	810.5	$2^+ \rightarrow 2^+$	4.92±0.09		22	Joshi (1961)
						4.83±0.10		20	Kramer (1962b)
						5.05±0.09		24 & 31	Bambynek (1968b)
				Several	$2^+ \rightarrow$ several		5.9±0.2	31	Good (1946)
							5.9±0.2	26	Cook (1956)
				810.5	$2^+ \rightarrow 2^+$		5.67±0.14	27	Konijn (1958a)
							5.49±0.18	30	Ramaswamy (1961)
							5.48±0.09	29	Biryukov (1966)
							5.76±0.13	28	Williams (1970) and Goodier (1971)
28	Ni	57	3243±7	Several	$\frac{3}{2}^- \rightarrow$ several	1.0±0.1		24	Friedlander (1950)
							1.0±0.1	26	Konijn (1956)
							1.13±0.01	26	Konijn (1958a)
							1.15±0.04	27	Konijn (1958b)
							1.68±0.2	30	Chilosi (1962)
							1.14±0.1	26	Bakhru (1967)
				1890	$\frac{3}{2}^- \rightarrow (\frac{5}{2}^-)$		18±6	27	Konijn (1958b)
							27±3	30	Chilosi (1962)
							22	27	Bakhru (1967)
				1750	$\frac{3}{2}^- \rightarrow (\frac{3}{2}^-)$		6±1	30	Chilosi (1962)

TABLE XVIII. (*Continued*)

Z	Elements	A	Q_{EC}[a] (keV)	Final state (keV)	$J_i^\pi \to J_f^\pi$	P_K/P_{β^+}	P_{EC}/P_{β^+}	Method[b]	References
28	Ni	57					~7	27	Bakhru (1967)
				1490	$\frac{3}{2}^- \to \frac{1}{2}^-$		1.438 ± 0.059	27	Konijn (1958b)
							2 ± 0.4	30	Chilosi (1962)
							1.5 ± 0.08	27	Bakhru (1967)
				1370	$\frac{3}{2}^- \to \frac{3}{2}^-$		0.805 ± 0.040	27	Konijn (1958b)
							1 ± 0.2	30	Chilosi (1962)
							1 ± 0.1	27	Bakhru (1967)
				1590	$\frac{3}{2}^- \to$?		~4	30	Chilosi (1962)
							~5	27	Bakhru (1967)
				1460	$\frac{3}{2}^- \to$?		2.5 ± 1	27	Bakhru (1967)
29	Cu	61	2245.2 ± 2.3	Several	$\frac{3}{2}^- \to$ several	0.55 ± 0.06		25	Bouchez (1949)
						0.32 ± 0.03		31	Huber (1949)
29	Cu	64	1677.5 ± 1.8	1340; 0	$1^+ \to 2^+; 0^+$	3.5 ± 1		23	Cook (1948)
						2.65 ± 0.4		25	Bouchez (1949)
						1.75 ± 0.2		25	Huber (1949)
						2.18 ± 0.20		23	Plassmann (1951)
							2.32 ± 0.28	31	Reynolds (1950)
30	Zn	62	1690 ± 8	Several	$0^+ \to$ several		0.1	31	Hayward (1950)
				0	$0^+ \to 1^+$	4.4 ± 0.9		31	Hoffman (1969)
30	Zn	65	1350.7 ± 1.1	0	$\frac{5}{2}^- \to \frac{3}{2}^-$	27		24	Watase (1940)
						18.8		27	Zumwalt (1947)
						25 ± 10		31	Major (1952)
						21.3 ± 1.4		31	Major (1952)
						21.8 ± 2.7		23	Yuasa (1952)
						28.0 ± 3.2		23	Perkins (1953)
						26 ± 3		20	Avignon (1955)
						25 ± 2		31	Gleason (1959)
						27.7 ± 1.5		31	Hammer (1968)
							24	31	Good (1946)
							24.9 ± 1.5	27	Sehr (1954)
							29.6 ± 0.5	31	Steyn (1966)
31	Ga	66	5175.0 ± 3.0	Several	$0^{(+)} \to$ several	0.52		23	Langer (1950)
31	Ga	68	2919.4 ± 3.9	1078	$1^+ \to 2^+$	1.28 ± 0.12		31	Ramaswamy (1959b)
				0	$1^+ \to 0^+$	0.1 ± 0.02		31	Ramaswamy (1959b)
32	Ge	66	2102 ± 13	Several	$0^+ \to$ several		1.45 ± 0.2	31	Ricci (1960)
32	Ge	69	2225.5 ± 2.4	Unknown	Unknown	2		31	McCown (1948a)
33	As	71	2009 ± 7	Several	$\frac{5}{2}^- \to$ several	2.1 ± 1		23	Thulin (1954a)
						~2		31	McCown (1948b)
33	As	74	2563.7 ± 2.9	Several	$2^- \to$ several	1.42		20	Scobie (1957a)
				596	$2^- \to 2^+$	1.5		26	Johansson (1951)

TABLE XVIII. (*Continued*)

Z	Elements	A	Q_{EC} [a] (keV)	Final state (keV)	$J_i^\pi - J_f^\pi$	P_K/P_{β^+}	P_{EC}/P_{β^+}	Method [b]	References
33	As	74				1.49		20	Scobie (1957a)
							1.32 ± 0.14	31	Grigor'ev (1958a)
							1.47 ± 0.35	26	Horen (1959)
							1.288 ± 0.018	27	Vatai (1968c)
				1200	$2^- \rightarrow 2^+$		>3.2	31	Horen (1959)
34	Se	73	2740 ± 10	Several	$(\frac{9}{2}^+) \rightarrow$ several	0.59		23	Scott (1951)
				425	$(\frac{9}{2}^+) \rightarrow \frac{9}{2}^+$	0.45		26	Scott (1951)
35	Br	75	3010 ± 20	Unknown	Unknown	~0.1		26	Baskova (1961)
35	Br	76	5100 SYST	Several	$1 \rightarrow$ several	0.5 ± 0.2		24	Girgis (1959b)
35	Br	77	1364.5 ± 2.8	Several	$\frac{3}{2}^- \rightarrow$ several	20		24	Woodward (1948b)
							39.8 ± 6.2	27	Sehr (1954)
36	Kr	77	3000 ± 30	Several	$(\frac{5}{2}^-) \rightarrow$ several	2.6		31	Woodward (1948a)
						0.21 ± 0.1		23	Thulin (1955)
36	Kr	79	1631 ± 9	Several	$\frac{1}{2}^- \rightarrow$ several	50		31	Woodward (1948a)
						~10		23	Bergström (1951)
						8 ± 4		23	Bergström (1952)
						14.1 ± 4.0		23	Radvanyi (1952b)
						9.3 ± 2		23	Thulin (1954b)
						$14.1^{+4.9}_{-3.2}$		23	Radvanyi (1955b)
				261.3	$\frac{1}{2}^- \rightarrow \frac{3}{2}^-$	57 ± 10		29	Langhoff (1966)
				398	$\frac{1}{2}^- \rightarrow ?$	430 ± 100		29	Langhoff (1966)
37	Rb	84	2679.8 ± 2.9	Several	$2^- \rightarrow$ several	0.07		24	Karraker (1950)
				0	$2^- \rightarrow 0^+$	2.06 ± 0.36		31	Welker (1955)
						1.12 ± 0.25		31	Konijn (1958/59)
				880	$2^- \rightarrow 2^+$	5.15 ± 0.38		31	Welker (1955)
						3.96 ± 0.16		22	Goedbloed (1970c)
							5.72 ± 0.12	27	Konijn (1958a)
39	Y	87	1882 ± 7	388	$\frac{1}{2}^- \rightarrow \frac{1}{2}^-$		46	26	Zoller (1969)
40	Zr	89	2834.1 ± 3.0	Several	$\frac{9}{2}^+ \rightarrow$ several		~3	26	Goldhaber (1951)
							4 ± 1	26	Shore (1953)
				910	$\frac{9}{2}^+ \rightarrow \frac{9}{2}^+$		3.48 ± 0.15	...	Monaro (1961) revised by van Patter (1964)
							3.43 ± 0.10	26	van Patter (1964)
							3.47 ± 0.21	26	Hinrichsen (1968)
40	Zr	89*m*	3422.1 ± 3.0	1510	$\frac{1}{2}^- \rightarrow \frac{3}{2}^-$		$4.7^{+2.3}_{-1.8}$	...	Derived by van Patter (1964) from results of Shore (1953)
							3.76 ± 0.19	31	van Patter (1964)
42	Mo	90	2487 ± 4	Several	$0^+ \rightarrow$ several		3.0 ± 0.5	26	Cooper (1965)

TABLE XVIII. (*Continued*)

Z	Elements	A	Q_{EC} [a] (keV)	Final state (keV)	$J_i^{\pi} - J_f^{\pi}$	P_K/P_{β^+}	P_{EC}/P_{β^+}	Method [b]	References
42	Mo	91	4443 ± 28	0	$\frac{9}{2}^+ \rightarrow \frac{9}{2}^+$	$(5.05 \pm 0.34) \times 10^{-2}$		24	Fitzpatrick (1975)
43	Tc	93	3186 ± 13	Several	$(\frac{9}{2}^+) \rightarrow$ several		7.20 ± 0.67	27	Sehr (1954)
				1350; 1500	$(\frac{9}{2}^+) \rightarrow$?	6.7 ± 2.2		26 & 31	Levi (1954)
43	Tc	94	4260 ± 6	Several	$(6^+, 7^+) \rightarrow$ several		6.1	26	Monaro (1962)
							14.9 ± 0.7	31	Matuszek (1963)
				2422	$(6^+, 7^+) \rightarrow 6^+$		7.5 ± 1.8	26	Hamilton (1964)
43	Tc	95*m*	1740 ± 11	Several	$(\frac{1}{2}^-) \rightarrow$ several		2.5×10^2	31	Medicus (1950)
							3.8×10^2	31	Levi (1957)
							$(2.5 \pm 1) \times 10^2$	31	Unik (1959)
							$(2.3 \pm 0.2) \times 10^2$	31	Cretzu (1965)
				204.2	$(\frac{1}{2}^-) \rightarrow \frac{3}{2}^+$	78		31	Levi (1959)
							62	31	Cretzu (1965)
				0	$(\frac{1}{2}^-) \rightarrow \frac{5}{2}^+$	28		31	Levi (1959)
45	Rh	100	3630 ± 20	Several	$1, 2^- \rightarrow$ several		~19	24	Lindner (1948)
46	Pd	101	1990 ± 15	Several	$(\frac{5}{2}^+) \rightarrow$ several		~9	24	Lindner (1948)
							~24	24	Katcoff (1956)
47	Ag	108	1921 ± 8	0	$1^+ \rightarrow 0^+$	9.6		25	Perlman (1953)
						5.6 ± 1		25	Frevert (1965)
							9.3	31	Wahlgren (1960)
48	Cd	107	1417 ± 4	Several	$\frac{5}{2}^+ \rightarrow$ several	320 ± 20		26	Bradt (1945)
49	In	114	1431 ± 7	Several	$1^+ \rightarrow$ several	5.4 ± 10^2		31	Grodzins (1956)
50	Sn	111	2508 ± 26	Several	$\frac{7}{2}^+ \rightarrow$ several	2.50 ± 0.25		26	McGinnis (1951)
							2.7 ± 0.2	25	Snyder (1965)
				0	$\frac{7}{2}^+ \rightarrow \frac{9}{2}^+$		2.20 ± 0.15	31	Rivier (1971)
51	Sb	113	3898 ± 32	Several	$\frac{5}{2}^+ \rightarrow$ several	0.25 ± 0.04		26	Kiselev (1969)
51	Sb	115	3030 ± 20	Several	$\frac{5}{2}^+ \rightarrow$ several		1.99	26	Vartanov (1963)
						1.22 ± 0.06		26	Kiselev (1969)
51	Sb	116	4500 ± 40	Several	$(3, 2^+) \rightarrow$ several		3.5	26	Fink (1961)
51	Sb	116*m*	5000 ± 40	2900	$(8^-) \rightarrow 7^-$		4.22 ± 0.20	29	Bolotin (1964)
51	Sb	117	1753 ± 40	158	$\frac{5}{2}^+ \rightarrow \frac{3}{2}^+$		38.5 ± 7.4	30	McGinnis (1955)
						0.977		26	Baskova (1964)
51	Sb	118*m*	3885 ± 6	2572	$(8^-) \rightarrow 7^-$		620 ± 40	29	Bolotin (1961)
51	Sb	120	2680 ± 7	0	$1^+ \rightarrow 0^+$	1.057 ± 0.035		24	Campbell (1975)
51	Sb	122	1610.1 ± 3.3	0	$2^- \rightarrow 0^+$	300 ± 130		31	Glaubman (1955)
						300 ± 50		31	Perlman (1958)

TABLE XVIII. (*Continued*)

Z	Elements	A	Q_{EC}[a] (keV)	Final state (keV)	$J_i^\pi - J_f^\pi$	P_K/P_{β^+}	P_{EC}/P_{β^+}	Method[b]	References
52	Te	117	3490 ± 30	Several	$\frac{1}{2}^+ \rightarrow$ several		2.3	31	Fink (1961)
53	I	118	6100 SYST	Unknown	Unknown	0.76 ± 0.16		24	Andersson (1965)
53	I	119	3200 ± 400	Unknown	Unknown	0.86 ± 0.10		24	Andersson (1965)
53	I	120	5300 SYST	Unknown	Unknown	1.04 ± 0.09		24	Andersson (1965)
53	I	121	2370 SYST	Several	$(\frac{5}{2}^+) \rightarrow$ several	9 ± 1		24	Andersson (1965)
53	I	124	3160 ± 10	Several	$2^- \rightarrow$ several		~2.3	31	Marquez (1950)
						2.7 ± 0.4		25	Girgis (1959a)
						2.2		25	Mitchell (1959)
53	I	126	2151 ± 5	0	$2^- \rightarrow 0^+$	12.5^{+7}_{-3}		31	Marty (1953)
						21 ± 8		31	Perlman (1954)
						20.2 ± 2.0		31	Koerts (1955)
				667	$2^- \rightarrow 2^+$	>75		31	Marty (1953)
						95 ± 10		31	Koerts (1955)
						200		31	Singh (1970)
							165 ± 5	29	Harmer (1959)
53	I	128	1254 ± 4	0	$1^+ \rightarrow 0^+$	1800 ± 400		31	Langhoff (1961)
55	Cs	125	3070 ± 20	Unknown	Unknown		1.03 ± 0.07	25	Friedlander (1962)
55	Cs	127	2090 ± 20	Several	$\frac{1}{2}^+ \rightarrow$ several		27.7 ± 1.7	25	Friedlander (1962)
55	Cs	132	2099 ± 23	667.8	$2^- \rightarrow 2^+$	78 ± 26		31	Jha (1961)
						53.5 ± 8.7		22	Goverse (1974a)
							$(1.6 \pm 0.6) \times 10^2$	26	Robinson (1962)
							$(3.3 \pm 1.7) \times 10^2$	29	Taylor (1963)
							1.7×10^2	30	Taylor (1963)
57	La	131	2960 ± 40	Several	$\frac{1}{2}^+ \rightarrow$ several	2.31 ± 0.31		25	Creager (1959/60)
57	La	134	3710 ± 25	Several	$1^+ \rightarrow$ several		1.3	24	Stover (1951)
				0	$1^+ \rightarrow 0^+$	0.40 ± 0.04		25	Biryukov (1965)
57	La	136	2870 ± 70	Several	$1^+ \rightarrow$ several		2	24	Naumann (1950)
58	Ce	131	4300 SYST	Unknown	Unknown		~8	26	Norris (1966)
59	Pr	136	5200 SYST	Several	$(2, 3^+) \rightarrow$ several	1.8 ± 0.4		25	Danby (1958)
						0.65 ± 0.01		25	Ketelle (1971)
59	Pr	137	2750 ± 40	Several	$(\frac{5}{2}^+) \rightarrow$ several	2.05 ± 0.3		25	Danby (1958)
						2.5 ± 0.2		25	van Hise (1967)
59	Pr	138	4437 ± 10	Several	$(6, 7, 8) \rightarrow$ several		7.7	24	Stover (1951)
							3.35 ± 1.13	26	Fujioka (1964)
						4.5 ± 1.2		25	Danby (1958)

TABLE XVIII. (*Continued*)

Z	Elements	A	Q_{EC}[a] (keV)	Final state (keV)	$J_i^\pi - J_f^\pi$	P_K/P_{β^+}	P_{EC}/P_{β^+}	Method[b]	References
59	Pr	139	2112 ± 20	Several	$(\frac{5}{2}^+) \rightarrow$ several		16	24	Stover (1951)
						11.3 ± 1.0		25	Danby (1958)
				0	$(\frac{5}{2}^+) \rightarrow \frac{3}{2}^+$	7.1		25	Biryukov (1963b)
59	Pr	140	3388 ± 6	Several	$(1^+) \rightarrow$ several		2	24	Wilkinson (1949)
							0.85	···	Rasmussen (1957)
						1.0 ± 0.1		25	Browne (1952)
						0.897		23	Brabec (1960)
						0.90 ± 0.08		25	Evans (1972)
				0	$(1^+) \rightarrow 0^+$	0.76		25	Biryukov (1960)
						0.74 ± 0.03		25	Biryukov (1962) and (1970)
60	Nd	141	1805 ± 15	Several	$\frac{3}{2}^+ \rightarrow$ several	~60		24	Wilkinson (1949)
						48 ± 9		25	Polak (1958)
							35.6 ± 3.6	25	Grisson (1966)
							21.9	25	Beery (1968)
						30.4 ± 2.3		25	Evans (1972)
				0	$\frac{3}{2}^+ \rightarrow \frac{5}{2}^+$	21.1 ± 1.0		25	Biryukov (1963a)
						28 ± 1		25	Biryukov (1970)
61	Pm	141	3730 ± 40	Unknown	Unknown	~0.67		25	Gratot (1959)
61	Pm	142	4820 ± 100	Unknown	Unknown	~0.05		24	Gratot (1959)
						0.30 ± 0.04		25	Penev (1974)
62	Sm	143	3479 ± 28	Several	$\frac{3}{2}^+ \rightarrow$ several	~1.7		24	Gratot (1959)
						0.98 ± 0.09		25	Belyanin (1966)
						1.27 ± 0.11		25	Evans (1972)
				0	$\frac{3}{2}^+ \rightarrow \frac{5}{2}^+$	0.92 ± 0.09		25	Biryukov (1970)
				1173.1	$\frac{3}{2}^+ \rightarrow \frac{1}{2}^+$		63 ± 10[c]	31	Firestone (1974)
				1403.1	$\frac{3}{2}^+ \rightarrow$ unknown		35 ± 5[c]	31	
				1515.0	$\frac{3}{2}^+ \rightarrow$ unknown		30 ± 7[c]	31	

TABLE XVIII. (*Continued*)

Z	Elements	A	Q_{EC} [a] (keV)	Final state (keV)	$J_i^\pi - J_f^\pi$	P_K/P_{β^+}	P_{EC}/P_{β^+}	Method [b]	References
63	Eu	143	5000 ± 200	1536.7	$\frac{5}{2}^+ \rightarrow \frac{5}{2}^+$		0.62 ± 0.06 [d]	31	Firestone (1974)
				1565.9	$\frac{5}{2}^+ \rightarrow (\frac{3}{2}^+ \frac{5}{2}^+)$		0.69 ± 0.15 [d]	31	
				1715.1	$\frac{5}{2}^+ \rightarrow (\frac{5}{2}^+)$		0.75 ± 0.17 [d]	31	
				1912.6	$\frac{5}{2}^+ \rightarrow (\frac{3}{2}^+ \frac{5}{2}^+)$		1.07 ± 0.11 [d]	31	
63	Eu	145	2720 ± 15	0	$\frac{5}{2}^+ \rightarrow \frac{7}{2}^-$	<5		31	Avotina (1965a)
						3.4		31	Zhelev (1967)
						3.0 ± 0.5		31	Muziol' (1966)
				894	$\frac{5}{2}^+ \rightarrow \frac{3}{2}^-$	100 ± 20		31	Avotina (1965a)
						120		31	Zhelev (1967)
						70 ± 9		31	Muziol' (1966)
						80		31	Adam (1967b)
63	Eu	146	3872 ± 9	Several	$(4^-) \rightarrow$ several		21	25	Takekoshi (1964)
				1384	$(4^-) \rightarrow$?	7.9 ± 1.2		25	Funk (1962)
				2051	$(4^-) \rightarrow$?	19 ± 8		25	Funk (1962)
63	Eu	147	1762 ± 9	198.1	$\frac{5}{2}^+ \rightarrow \frac{3}{2}^-$	160 ± 30		31	Avotina (1966; 1965b)
						155 ± 50		31	Muziol' (1966)
						302 ± 150		31	Adam (1967a)
				121.8	$\frac{5}{2}^+ \rightarrow \frac{5}{2}^-$	170 ± 30		31	Avotina (1966; 1965b)
						165 ± 35		31	Muziol' (1966)
						257 ± 100		31	Adam (1967a)
				0	$\frac{5}{2}^+ \rightarrow \frac{7}{2}^-$	87 ± 45		31	Muziol' (1966)
						258 ± 100		31	Adam (1967a)
66	Dy	155	2099 ± 6	227.0	$(\frac{3}{2}^-) \rightarrow \frac{5}{2}^-$	44 ± 5		31	Persson (1963)
68	Er	161	2050 ± 40	211.1	$\frac{3}{2}^- \rightarrow \frac{1}{2}^+$	400 ± 200		31	Gromov (1965)
69	Tm	162	4700 ± 100	Several	$1^- \rightarrow$ several	12		25	Chu (1971)
69	Tm	166	3035 ± 12	?	$2^+ \rightarrow 4^+$	9		31	Wilson (1960)

TABLE XVIII. (*Continued*)

Z	Elements	A	Q_{EC}[a] (keV)	Final state (keV)	$J_i^\pi - J_f^\pi$	P_K/P_{β^+}	P_{EC}/P_{β^+}	Method[b]	References
64	Gd	145	5311 ± 120	808.5	$\frac{1}{2}^+ \rightarrow \frac{1}{2}^+$		18 ± 8	31	Firestone (1974; 1975)
				1041.9	$\frac{1}{2}^+ \rightarrow (\frac{3}{2}^+)$		1.0 ± 0.1	31	
				1567.3	$\frac{1}{2}^+ \rightarrow (\frac{1}{2}^+\frac{3}{2}^+\frac{5}{2}^+)$		37 ± 18	31	
				1599.9	$\frac{1}{2}^+ \rightarrow (\frac{1}{2}^+\frac{3}{2}^+\frac{5}{2}^+)$		13 ± 6	31	
				1757.8	$\frac{1}{2}^+ \rightarrow \frac{3}{2}^+$		1.87 ± 0.09	31	
				1761.9	$\frac{1}{2}^+ \rightarrow$ unknown		2.6 ± 0.8	31	
				1845.4	$\frac{1}{2}^+ \rightarrow (\frac{3}{2}^+\frac{5}{2}^+)$		43 ± 21	31	
				1880.6	$\frac{1}{2}^+ \rightarrow (\frac{1}{2}^+\frac{3}{2}^+)$		2.15 ± 0.12	31	
				2048.9	$\frac{1}{2}^+ \rightarrow$ unknown		4.2 ± 1.0	31	
				2113.9	$\frac{1}{2}^+ \rightarrow (\frac{3}{2}^+\frac{5}{2}^+)$		10 ± 4	31	
				2494.8	$\frac{1}{2}^+ \rightarrow (\frac{1}{2})$		4.8 ± 0.5	31	
				2642.2	$\frac{1}{2}^+ \rightarrow$ unknown		8.1 ± 0.9	31	
70	Yb	162	2300 SYST		$0^+ \rightarrow 1^+$	36		31	Abdurazakov (1974)
71	Lu	168	4360 ± 80	Several	$(1^-) \rightarrow$ several		8	31	Merz (1961)
72	Hf	171	2600 SYST	662.0	$\frac{7}{2}^+ - \frac{7}{2}^-$	144 ± 3	4	25	Wilson (1969)
								26	Gnatovich (1974)
73	Ta	178	1910 ± 100	0	$1^+ \rightarrow 0^+$	110 ± 70		25	Gallagher (1961)
77	Ir	186	3831 ± 20	868.7	Unknown $\rightarrow 6^+$	6.5 ± 3		26	Emery (1963)
				1453.1	Unknown $\rightarrow (8^+)$	17		26	Emery (1963)
79	Au	190	4400 SYST	Several	$1^- \rightarrow$ several	50		25	Jastrzebski (1961)
81	Tl	200	2454 ± 5	367.97	$2^- \rightarrow 2^+$	110 ± 10		31	Konijn (1960)
						102 ± 9		27	van Nooijen (1962)
83	Bi	207	2405 ± 8	569.6	$\frac{9}{2}^- \rightarrow \frac{5}{2}^-$		$(6 \pm 1) \times 10^2$	26	Rupnik (1972)

[a] Q_{EC} values are taken from Wapstra and Gove (1971).
[b] Methods are identified by numbers explained in Table XIII.
[c] Relative measurements, normalized to the transition to the 1056.6 keV state of ^{143}Pm.
[d] Relative measurements, normalized to the transition to the 1107.2 keV state of ^{143}Sm.

The EC/β^+ ratio is given by

$$P_{EC}/P_{\beta^+} = (I_\gamma/I_{\beta^+-\gamma}) - 1. \quad (3.51)$$

Comparison of I_γ and $I_{\beta^+-\gamma}$ with measurements for a source of known EC/β^+ ratio has often been employed.

c. Sum-coincidence technique

In this more sophisticated coincidence technique (No. 28), the quantities measured are the positron intensity I_{β^+}, the γ-ray intensities $I_{\gamma N}$ and $I_{\gamma S}$, and the positron–γ-ray coincidence intensities $I_{\beta^+-\gamma N}$ and $I_{\beta^+-\gamma S}$, where γ_N refers to the normal de-excitation γ ray, and γ_S is the sum of a β^+ annihilation photon and γ_N. It can be shown (Williams, 1964) that the relation

$$I_{\beta^+} I_{\gamma N} / I_{\beta^+-\gamma N} = I_0 \quad (3.52)$$

holds, where I_0 represents the total number of disintegrations. Furthermore, we have

$$I_{\beta^+} I_{\gamma S} / I_{\beta^+-\gamma S} = I_0 P_{\beta^+}, \quad (3.53)$$

whence

$$\frac{P_{EC}}{P_{\beta^+}} = (I_{\beta^+-\gamma S} I_{\gamma N} / I_{\beta^+-\gamma N} I_{\gamma S}) - 1. \quad (3.54)$$

In a measurement of the EC/β^+ ratio for ^{22}Na (Williams, 1964), the β^+ activity was determined with a 4π proportional counter. For the detection of γ_S, two large NaI(Tl) crystals were used to obtain a high efficiency for the summation events. For γ_N, one smaller NaI(Tl) crystal was used to minimize the efficiency to summation events. The simplifying assumptions involved in Eq. (3.54) and the corrections which must be applied are discussed in detail by Williams (1964).

d. Measurement of triple coincidences

The EC/β^+ ratio can be obtained by taking the γ-ray spectrum in triple coincidence with two β^+ annihilation photons (Method No. 29). The two counters for annihilation photons are placed opposite each other with analyzer channels set to record the 511-keV photopeaks only. Due to the nature of the annihilation process, the efficiency for the detection of coincidences of two 511-keV γ rays at 180° is sufficiently increased over other coincidences that even very weak positron emission can be detected . A typical electronic arrangement for this type of measurement is shown in Fig. 26. The γ-ray singles intensity I_γ and the triple coincidence intensity I_C are measured. If similar measurements are made for a source a whose EC/β^+ ratio is known, then the unknown EC/β^+ ratio for source b is

$$\left(\frac{P_{EC}}{P_{\beta^+}}\right)_b = \left(\frac{I_\gamma}{I_C}\right)_b \left(\frac{I_C}{I_\gamma}\right)_a \left[\left(\frac{P_{EC}}{P_{\beta^+}}\right)_a + 1\right] \left(\frac{1+\alpha_b}{1+\alpha_a}\right) - 1. \quad (3.55)$$

Corrections are required for such effects as summing, β^+ annihilation in flight, differences in the detection of annihilation radiation for the two sources due to possible differences in solid angle and in summing of the γ rays and the annihilation radiation, and the possibility of coincidences due to Compton events from high-energy γ rays being registered in the analyzer window of the annihilation detectors.

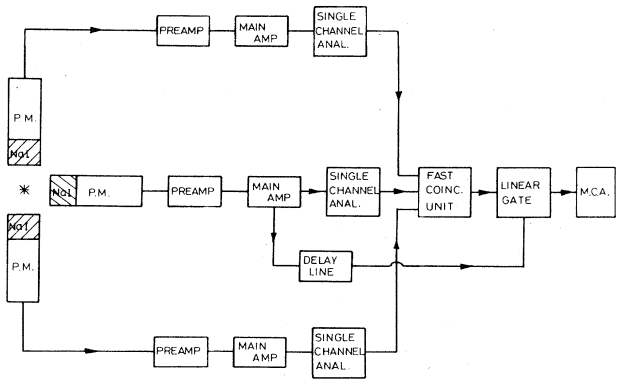

FIG. 26. Typical electronic arrangement for triple-coincidence measurements.

e. Measurement of (γ-ray)–(β^+-annihilation-photon) coincidences

The various coincidence techniques are very similar in principle and this method (No. 30) is essentially a variation of Method 27. The quantities measured are the number of nuclear γ rays I_γ and the number of coincidences of nuclear and β^+ annihilation photons $I_{511-\gamma}$. The usual corrections for absorption, summing, and β^+ annihilation in flight are required. The EC/β^+ ratio is given by

$$\frac{P_{EC}}{P_{\beta^+}} = (2I_\gamma/I_{511-\gamma}) - 1. \quad (3.56)$$

f. Miscellaneous

The experiments in this group (No. 31) do not fall readily into any of the other categories. Many of the experiments were carried out by employing various combinations of Methods 20–30. No loss of accuracy need be implied. This category also includes methods which have been employed in only very few, exceptional cases and because of their limited application do not warrant description as a separate technique. Also included in the miscellaneous category are a few experimental results whose methods are in doubt due to incomplete details provided in the published papers.

One different approach to EC/β^+ measurements is the technique employed by Allen *et al.* (1955) for the determination of the EC/β^+ ratio for ^{22}Na. This involves a comparison of the number of positrons emitted from the source with the number of daughter atoms produced (Alvarez, 1937). The positron activity was determined using a 4π Geiger counter and the rate of evolution of the daughter (Ne) was determined by gas analysis.

Another interesting technique has been applied by Gleason (1959) to ^{65}Zn which decays by electron capture and β^+ emission to the ground state and by electron capture to the first excited state of ^{65}Cu. Using a measured value for the efficiency of detection of the de-excitation γ ray, the total electron capture decay rate and the electron capture branching ratio were determined from measurements of the K x-ray counting rate, the γ-ray singles rate, and the (K-x-ray)–(γ-ray) coincidence counting rate. The assumption was made that the ratio of K-electron capture to total electron capture was the

same for both branches. The β^+ emission rate was determined by counting coincidences of annihilation photons in two detectors at 180° and thus the EC/β^+ ratio for the ground state transition was found. The important feature of this technique is that although K x rays were used to indicate the occurrence of electron capture, the deduced value of the EC/β^+ ratio is independent of the fluorescence yield.

E. Experimental results and comparison with theory for K/β^+ and EC/β^+ ratios

1. Results

All published experimental K/β^+ and EC/β^+ ratios are listed in Table XVIII. Table XIX contains selected experimental K/β^+ and EC/β^+ ratios for allowed transitions. Only ratios for transitions to a single final state in the daughter nucleus are included. Unfortunately, information provided on some measurements was not complete and these results had to be rejected. Where the ω_K values were stated, results were recalculated using the latest reliable fluorescence yields, derived with the aid of Eq. (3.35). The remaining K/β^+ and EC/β^+ ratios were found to lie in two distinct groups, one with errors ranging up to 12.5% and the other, consisting mainly of the earlier measurements, with considerably larger errors. Since the two groups are well separated only the results from the former are considered further.

Tables XX and XXI contain selected results for first-forbidden unique and first-forbidden nonunique transitions. Results with errors greater than 25% or without quoted errors were excluded.

2. Theoretical predictions

a. Allowed transitions

The theoretical K/β^+ ratios for allowed transitions in Table XIX have been calculated according to the relation

$$\frac{P_K}{P_{\beta^+}} = \frac{\pi\beta_K^2(W_0+W_K)^2B_K}{2\int_0^{p_0}p^2(W_0-W)^2F(Z',W)\,dp} \tag{3.57}$$

[See Eqs. (2.111), (2.125), and (2.126)]. Small corrections [Eq. (2.128)] were neglected. The values of β_K were taken from Mann and Waber (1973) (Sec. II.B.2) and the intensity of the β^+ spectrum was computed with the tables of Fermi functions of Behrens and Jänecke (1969). The energies W_0 were taken from the atomic mass tables of Wapstra and Gove (1971). Errors in the theoretical K/β^+ ratios in Table XIX reflect only the uncertainty in W_0 obtained from Wapstra and Gove. The value of B_K used in these calculations is discussed in Sec. III.E.3.

The theoretical EC/β^+ ratio for allowed transitions is

$$\frac{P_{\rm EC}}{P_{\beta^+}} = \frac{P_K}{P_{\beta^+}}\frac{P_{\rm EC}}{P_K} = \frac{P_K}{P_{\beta^+}}\frac{\Sigma q_x^2\beta_x^2B_x}{q_K^2\beta_K^2B_K}, \tag{3.58}$$

where x stands for K, L_1, L_2, M_1, or M_2, and P_K/P_{β^+} is the theoretical K/β^+ ratio for an allowed transition [Eq. (3.58)].

b. Unique forbidden transitions

In general, the K/β^+ ratio for forbidden transitions is

$$\frac{P_K}{P_{\beta^+}} = \frac{\pi\beta_K^2(W_0+W_K)^2C_KB_K}{2\int_0^{p_0}p^2(W_0-W)^2F(Z',W)\overline{C(W)}\,dp}, \tag{3.59}$$

where C_K and $C(W)$ are shape factors and the bar represents averaging over the β^+ spectrum [Eq. (2.134)]. The shape factors contain matrix elements and are functions of W and W_0. For unique forbidden transitions it is possible to separate the matrix element and the energy dependence of C_K and $C(W)$ to give explicit expressions for the ratio $C_K/\overline{C(W)}$ (Sec. II.D.4).

For first-forbidden unique transitions Eq. (2.135) is simplified to

$$\frac{C_K}{\overline{C(W)}} = \frac{(W_0+W_K)^2}{\overline{q^2+\lambda_2p^2}}, \tag{3.60}$$

where q is the neutrino momentum, p is the positron momentum, and the bar represents averaging over the β^+ spectrum. The theoretical first-forbidden unique K/β^+ ratios shown in Table XX have been calculated using these expressions, with values of λ_2 from the tables of Behrens and Jänecke (1969). For comparison of theory and experiments, one can use the approximations $W_K\approx 1$ and $q^2+\lambda_2p^2\approx\frac{1}{2}(W_0^2-1)$, whence

$$\frac{C_K}{\overline{C(W)}} \approx \frac{2(W_0+1)}{W_0-1}. \tag{3.61}$$

Equation (3.61) has an accuracy of a few percent.

c. Nonunique forbidden transitions

For nonunique forbidden transitions, K/β^+ ratios cannot, in general, be calculated explicitly (Sec. II.D.3). For the special case of nonunique first-forbidden transitions, however, which exhibit a β^+ spectrum with an allowed shape, the K/β^+ ratio is expected to be the same as for allowed transitions. Information about the shapes of some β spectra is given by Paul (1966) and Daniel (1968). For many of the nonunique first-forbidden decays listed in Table XXI, however, details of the spectrum shape are not available. Nevertheless, to provide a general comparison, allowed theoretical K/β^+ and EC/β^+ ratios are indicated for all cases.

3. Comparison of experiment and theory

a. Allowed transitions

Theoretical and selected experimental values for K/β^+ and EC/β^+ ratios are listed in Table XIX. Exchange and overlap corrections have been neglected in the theoretical EC/β^+ ratios; they affect the total capture probability and β^+ emission rate only slightly (Bahcall, 1963a). The EC probability for ^{7}Be, e.g., is affected by $<0.1\%$, and that of ^{37}Ar, by $<0.3\%$ through exchange and overlap; the ^{65}Zn β^+ decay rate is affected by $\sim 0.1\%$, and that of ^{14}O, by $<0.1\%$. The theoretical K/β^+ ratios in Table XIX include a correction factor according to Bahcall (Table XI); from $Z>32$, the factors of Suslov (1970) were used. At present, EC/β^+-ratio measurements (Table XIX) are not nearly accurate enough to help decide between the two sets of exchange and overlap correction factors listed in Table XI.

TABLE XIX. Allowed transitions—comparison of selected results with theory

Z	Elements	A	Q_{EC} [a] (keV)	Final state (keV)	$J_i^\pi - J_f^\pi$	Experimental values P_K/P_{β^+}	Method [b]	References	Theoretical values P_K/P_{β^+}
					A. Results for K/β^+ ratios.				
6	C	11	1982.2 ± 1.0	0	$\frac{3}{2}^- - \frac{3}{2}^-$	$(2.30^{+0.14}_{-0.11})10^{-3}$	21	Campbell (1967)	$(2.11 \pm 0.01)10^{-3}$
7	N	13	2220.5 ± 0.9	0	$\frac{1}{2}^- - \frac{1}{2}^-$	$(1.68 \pm 0.12)10^{-3}$	21	Ledingham (1965)	$(1.800 \pm 0.006)10^{-3}$
8	O	15	2759.2 ± 0.9	0	$\frac{1}{2}^- - \frac{1}{2}^-$	$(1.07 \pm 0.06)10^{-3}$	21	Leiper (1972)	$(0.911 \pm 0.002)10^{-3}$
9	F	18	1655.3 ± 0.9	0	$1^+ - 0^+$	$(3.00 \pm 0.18)10^{-2}$	20	Drever (1956)	$(3.14 \pm 0.02)10^{-2}$
10	Ne	19	3238.2 ± 0.9	0	$\frac{1}{2}^+ - \frac{1}{2}^+$	$(9.6 \pm 0.3)10^{-4}$	21	Leiper (1972)	$(9.28 \pm 0.02)10^{-4}$
11	Na	22	2842.3 ± 0.5	1274.6	$3^+ - 2^+$	0.105 ± 0.009	22	McCann (1969)	0.1023 ± 0.0004
15	P	30	4227.4 ± 2.6	0	$1^+ - 0^+$	$(1.24 \pm 0.04)10^{-3}$	21	Ledingham (1971)	$(1.233 \pm 0.005)10^{-3}$
27	Co	58	2308.0 ± 2.5	810.5	$2^+ - 2^+$	4.92 ± 0.09	22	Joshi (1961)	4.97 ± 0.11
						4.83 ± 0.10	20	Kramer (1962b)	
						5.05 ± 0.09	Combination of 24 and 31	Bambynek (1968b)	
30	Zn	65	1350.7 ± 1.1	0	$\frac{5}{2}^- - \frac{3}{2}^-$	28.0 ± 3.2	23	Perkins (1953)	30.5 ± 0.4
						25 ± 2	31	Gleason (1959)	
						27.7 ± 1.5	31	Hammer (1968)	
31	Ga	68	2919.4 ± 3.9	1078	$1^+ - 2^+$	1.28 ± 0.12	31	Ramaswamy (1959b)	1.36 ± 0.03
42	Mo	91	4443 ± 28	0	$\frac{9}{2}^+ - \frac{9}{2}^+$	$(5.05 \pm 0.34)10^{-2}$	24	Fitzpatrick (1975)	$(5.50 \pm 0.22)10^{-2}$
51	Sb	120	2680 ± 7	0	$1^+ - 0^+$	1.057 ± 0.035	24	Campbell (1975)	1.24 ± 0.02
57	La	134	3710 ± 25	0	$1^+ - 0^+$	0.40 ± 0.04	25	Biryukov (1965)	0.48 ± 0.02
59	Pr	140	3388 ± 6	0	$(1^+) - 0^+$	0.74 ± 0.03	25	Biryukov (1962, 1970)	0.85 ± 0.01
60	Nd	141	1805 ± 15	0	$\frac{3}{2}^+ - \frac{5}{2}^+$	28 ± 1	25	Biryukov (1970)	35.3 ± 3.2
62	Sm	143	3479 ± 28	0	$\frac{3}{2}^+ - \frac{5}{2}^+$	0.92 ± 0.09	25	Biryukov (1970)	0.98 ± 0.05
66	Dy	155	2099 ± 6	227.0	$(\frac{3}{2}^-) - \frac{5}{2}^-$	44 ± 5	31	Persson (1963)	44.0 ± 1.5
					B. Results for EC/β^+ ratios.				
11	Na	22	2842.3 ± 0.5	1274.6	$3^+ - 2^+$	0.1041 ± 0.0010	28	Williams (1964, 1968)	0.1117 ± 0.0004
						0.1048 ± 0.0007	27	Leutz (1967)	
						0.1042 ± 0.0010	27	Vatai (1968c)	
						0.1077 ± 0.0003	27	MacMahon (1970)	
23	V	48	4015.4 ± 2.8	2295	$4^+ - 4^+$	0.77 ± 0.04	29	Biryukov (1966)	0.78 ± 0.01
						0.83 ± 0.06	29	Konijn (1967b)	
						0.76 ± 0.035	27	Konijn (1967b)	
25	Mn	52	4709.8 ± 3.5	3112	$6^+ - 6^+$	1.86 ± 0.17	31	Good (1946)	2.09 ± 0.06
						2.01 ± 0.24	27	Sehr (1954)	
						1.84 ± 0.20	30	Wilson (1962)	
						2.04 ± 0.24	26	Freedman (1966)	
						1.80 ± 0.13	27	Konijn (1967b)	
						2.12 ± 0.17	29	Konijn (1967b)	
27	Co	58	2308.0 ± 2.5	810.5	$2^+ - 2^+$	5.67 ± 0.14	27	Konijn (1958a)	5.62 ± 0.12
						5.49 ± 0.18	30	Ramaswamy (1961)	
						5.48 ± 0.09	29	Biryukov (1966)	
						5.76 ± 0.13	28	Williams (1970) and Goodier (1971)	
28	Ni	57	3243 ± 7	1490	$\frac{3}{2}^- - \frac{1}{2}^-$	1.438 ± 0.059	27	Konijn (1958b)	1.48 ± 0.07
						1.5 ± 0.08	27	Bakhru (1967)	
				1370	$\frac{3}{2}^- - \frac{3}{2}^-$	0.805 ± 0.040	27	Konijn (1958b)	0.888 ± 0.032
						1.0 ± 0.1	27	Bakhru (1967)	
30	Zn	65	1350.7 ± 1.1	0	$\frac{5}{2}^- - \frac{3}{2}^-$	24.9 ± 1.5	27	Sehr (1954)	34.5 ± 0.4
40	Zr	89	2834.1 ± 3.0	910	$\frac{9}{2}^+ - \frac{9}{2}^+$	3.48 ± 0.15	···	Monaro (1961) revised by van Patter (1964)	3.40 ± 0.05
						3.43 ± 0.10	26	van Patter (1964)	
						3.47 ± 0.21	26	Hinrichsen (1968)	
40	Zr	89*m*	3422.1 ± 3.0	1510	$\frac{1}{2}^- - \frac{3}{2}^-$	3.76 ± 0.19	31	van Patter (1964)	3.55 ± 0.06
50	Sn	111	2508 ± 26	0	$\frac{7}{2}^+ - \frac{9}{2}^+$	2.20 ± 0.15	31	Rivier (1971)	1.87 ± 0.16
51	Sb	116*m*	5000 ± 40	2900	$(8^-) - 7^-$	4.22 ± 0.20	29	Bolotin (1964)	5.9 ± 1.1
51	Sb	118*m*	3885 ± 6	2572	$(8^-) - 7^-$	620 ± 40	29	Bolotin (1961)	830 ± 80

[a] Q_{EC} values are taken from Wapstra and Gove (1971).
[b] Methods are identified by numbers explained in Table XIII.

TABLE XX. First-forbidden unique transitions.

Z	Elements	A	Q_{EC} [a] (keV)	Final state (keV)	Experimental values $J_i^\pi - J_f^\pi$	P_K/P_{β^+}	Method [b]	References	Theoretical 1st unique forbidden values P_K/P_{β^+}
37	Rb	84	2679.8 ± 2.9	0	$2^- - 0^+$	1.12 ± 0.25	31	Konijn (1958/59)	0.94 ± 0.01
51	Sb	122	1610.1 ± 3.3	0	$2^- - 0^+$	300 ± 50	31	Perlman (1958) and Glaubman (1955)	254 ± 11
53	I	126	2151 ± 5	0	$2^- - 0^+$	20.2 ± 2.0	31	Koerts (1955)	21.1 ± 0.7

[a] Q_{EC} values are taken from Wapstra and Gove (1971).
[b] Methods are identified by numbers explained in Table XIII.

Figure 27 shows the ratio of experimental to theoretical values for all the results in Table XIX. The interesting and very accurate point for ^{22}Na is plotted in the inset. For most of the decays, the experiment/theory ratio is less than unity; exceptions are ^{11}C, ^{15}O, ^{19}Ne, ^{89}Zr, ^{89m}Zr, and ^{111}Sn. The disagreement between experiment and theory apparently increases with Z.

In the theory of allowed transitions, only s-wave leptons are considered and the EC/β^+ and K/β^+ ratios are independent of nuclear matrix elements. In the general case, leptons do not leave the nucleus only radially, and small contributions from p and d waves must be considered. This gives rise to higher-order matrix elements that do not cancel in the ratios (Sec. II.D.2). A correction factor has been determined [Eq. (2.128)] that slightly reduces the theoretical ratios, by as much as 3% at $Z = 80$.

The possible existence of second-class currents does not significantly affect electron-capture to positron-emission ratios (Behrens and Bühring, 1974).

b. *First-forbidden unique transitions*

For these transitions the experimental K/β^+ ratios are compared in Table XX with first-forbidden unique theoretical ratios. There is agreement within the errors between experiment and theory, but the experimental accuracy is fairly poor.

c. *First-forbidden nonunique transitions*

The experimental K/β^+ and EC/β^+ ratios for these transitions are compared in Table XXI with the corresponding theoretical ratios for allowed transitions. The comparison is made for interest only; a complete theoretical treatment requires knowledge of the nuclear matrix elements which for these transitions do not cancel.

4. Conclusions and recommendations

It can be seen from Fig. 27 that theoretical allowed K/β^+ and EC/β^+ ratios are systematically larger than experimental ratios; the discrepancy apparently increases with Z. Higher-order effects, such as second-class currents, corrections of the type described by Eq. (2.128), and radiative corrections are insufficient to resolve the difficulty. The question of radiative corrections is still unsettled; it has been shown (Sec. II.D.2) that these corrections partially cancel out. There

TABLE XXI. First-forbidden nonunique transitions.

Z	Elements	A	Q_{EC} [a] (keV)	Final state (keV)	Experimental values $J_i^\pi - J_f^\pi$	P_K/P_{β^+}	Method [b]	References	Theoretical (allowed) P_K/P_{β^+}
					A. K/β^+ Ratios				
37	Rb	84	2679.8 ± 2.9	880	$2^- - 2^+$	5.15 ± 0.38	31	Welker (1955)	3.51 ± 0.06
						3.96 ± 0.16	22	Goedbloed (1970c)	
53	I	126	2151 ± 5	667	$2^- - 2^+$	95 ± 10	31	Koerts (1955)	138 ± 7
63	Eu	145	2720 ± 15	0	$\frac{5}{2}^+ - \frac{7}{2}^-$	3.0 ± 0.5	31	Muziol' (1966)	3.39 ± 0.14
				894	$\frac{5}{2}^+ - \frac{3}{2}^-$	100 ± 20	31	Avotina (1965a)	43.9 ± 4.2
						70 ± 9	31	Muziol' (1966)	
63	Eu	147	1762 ± 9	198.1	$\frac{5}{2}^+ - \frac{3}{2}^-$	160 ± 30	31	Avotina (1966)	197 ± 16
				121.8	$\frac{5}{2}^+ - \frac{5}{2}^-$	170 ± 30	31	Avotina (1966)	
						165 ± 35	31	Muziol' (1966)	119 ± 8
55	Cs	132	2099 ± 23	667.8	$2^- - 2^+$	53.5 ± 8.9	22	Goverse (1974)	264 ± 71
81	Tl	200	2454 ± 5	367.97	$2^- - 2^+$	110 ± 10	31	Konijn (1960)	65.7 ± 1.4
						102 ± 9	27	van Nooijen (1962)	
					B. EC/β^+ Ratios				
33	As	74	2563.7 ± 2.9	596	$2^- - 2^+$	1.32 ± 0.14	31	Grigor'ev (1958a)	1.24 ± 0.01
						1.288 ± 0.018	27	Vatai (1968c)	
37	Rb	84	2679.8 ± 2.9	880	$2^- - 2^+$	5.72 ± 0.12	27	Konijn (1958a)	3.97 ± 0.07
53	I	126	2151 ± 5	667	$2^- - 2^+$	165 ± 5	29	Harmer (1959)	159 ± 8

[a] Q_{EC} values are taken from Wapstra and Gove (1971).
[b] Methods are identified by numbers explained in Table XIII.

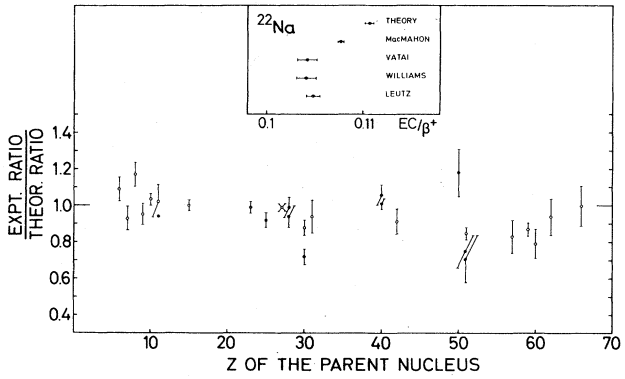

FIG. 27. Ratio of experimental to theoretical allowed K/β^+ and EC/β^+ ratios.

remains a model-independent part of the radiative corrections, however, which differs in the case of electron capture from that in positron emission. This model-independent correction includes the well-known emission of real photons (internal bremsstrahlung). Calculations for β^+ emission have been carried out to order α, e.g., by Wilkinson and Macefield (1970); an increase in the probability of β^+ emission is found which thus reduces the theoretical capture-to-positron ratios. The correction factor increases as W_0 decreases and as Z increases and amounts to 1.5% for ^{58}Co (Williams, 1970) if it is assumed that the correction is multiplicative and not additive. Radiative corrections for electron capture have not yet been calculated.

It would be of interest to establish with greater accuracy the Z dependence of the trend shown in Fig. 27, if indeed such a simple functional dependence on Z exists. Remeasurements, preferably using different techniques, for any of the decays in Table XIX would be useful. The decays of ^{65}Zn, ^{111}Sn, and any high-Z isotope are possibly the most interesting for study. The question of whether there is real agreement between theory and experiment in the case of first-forbidden unique transitions is still open; measurements on ^{84}Rb, ^{122}Sb, and ^{126}I should be repeated with greater accuracy.

The theory of atomic exchange and imperfect wave-function overlap effects needs to be refined and calculations must be extended to low Z. Critical experiments on capture/β^+ ratios which would differentiate between theoretical approaches have yet to be carried out. The problem of establishing the overlap and exchange correction for the K shell cannot be resolved by measuring K/β^+ ratios alone. The most sensitive isotope for study is ^{7}Be, which decays solely by electron capture; a measurement of P_K for this isotope is very desirable (Sec. III.C.4).

Some new and interesting EC/β^+ ratios have recently been reported by Firestone *et al.* (1974, 1975a). Anomalously high ratios are found for hindered allowed transitions in ^{145}Gd and ^{143}Sm; these are attributed to the interference of higher-order nuclear matrix elements. It would be of great value to verify this experimental finding.

Theoretical K/β^+ ratios for allowed transitions are plotted in Figs. 28 and 29 as functions of Z and of the β^+ end-point kinetic energy. These ratios were calcu-

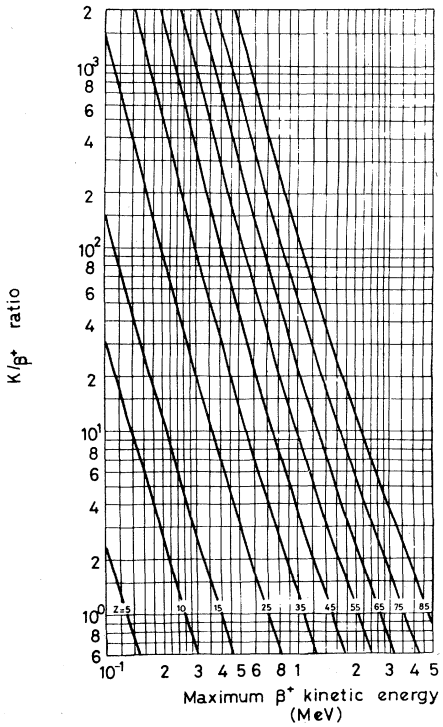

FIG. 28. Theoretical K-capture to positron-emission ratios for allowed transitions.

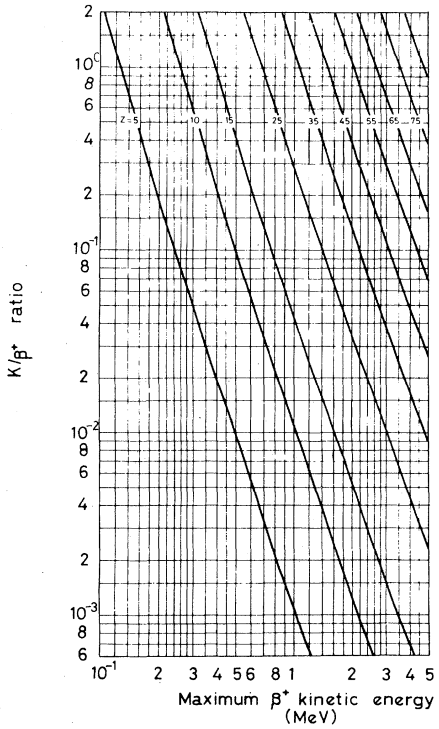

FIG. 29. Theoretical K/β^+ ratios.

lated according to Eq. (3.58) with $B_K = 1$; the graphs may be used where an accuracy of ~ 10% is sufficient.

IV. RADIATIVE ELECTRON CAPTURE

A. Theory

Radiative electron capture consists of processes which lead to the production of a continuous spectrum of electromagnetic radiation during electron-capture decays. Such processes involve the emission of one or more photons during a single electron-capture event. The energy released in the decay is shared statistically among these photons and the neutrino, thus accounting for the continuous nature of the resulting spectra. The most probable radiative electron-capture events are those in which a single photon accompanies the neutrino. The radiation emitted even in this mode is quite weak, the total probability for the emission of a single photon being of the order of 10^{-4} per electron-capture event. Radiative electron-capture processes in which more than one photon is emitted occur with far smaller probabilities.[15] Their contributions to the radiation spectra are completely insignificant and will not be considered further.

From the point of view of perturbation theory, radiative electron capture is a second-order process involving both beta and electromagnetic radiative transitions. The two transitions connect the initial and final states of the system through a set of virtual intermediate states. In general, there are two fundamentally different types of intermediate states through which the process can proceed. They are represented pictorially by the Feynman diagrams shown in Fig. 30. The first type [Fig. 30(a)] involves only excited electron states, and the radiation is produced by the sudden acceleration of charge and magnetic moment associated with the orbital electron's capture. This radiation is commonly referred to as internal bremsstrahlung (IB). The second type [Figs. 30(b) and (c)] involves excited nuclear states and the radiation arises from a nuclear transition which may either precede or follow the virtual electron-capture decay. These two decay modes are variously denoted as electronic beta-gamma and nuclear beta-gamma transitions or, more simply, direct and detour transitions. In allowed decays, detour transitions are expected to occur at a ~ 10^6 times smaller rate than direct transitions. In forbidden decays, this difference can be less pronounced (Longmire, 1949; Horowitz, 1952).

Extensive calculations on detour transitions were carried out by Rose *et al.* (1962) and Lassila (1963) for the especially interesting situation in which the initial and intermediate nuclear states, connected by a virtual electron-capture transition, are almost degenerate. It was shown that the spectrum of the radiation arising from detour transitions is sharply peaked near the end point under these circumstances, in contrast to the usual IB spectrum. It was hoped that this deviation of the photon spectrum from its IB form might be observable,

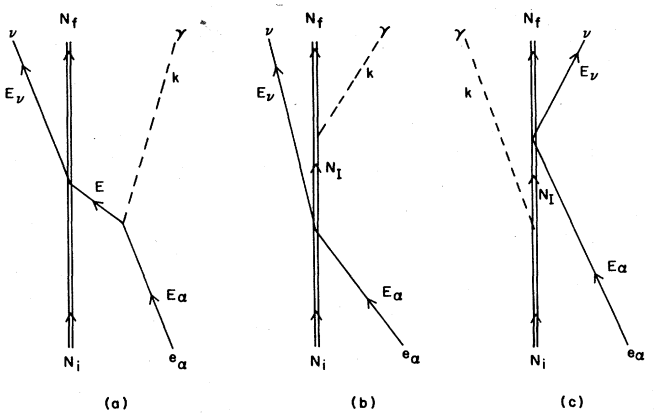

FIG. 30. Feynman diagrams for electronic and nuclear mode contributions to radiative electron capture.

revealing the presence of detour transitions, even though their contribution was still expected to be quite small. An experiment designed to test these ideas was reported shortly thereafter by Schmorak (1963), who studied ^{59}Ni, a nucleus possessing a decay scheme with the required characteristics, and found that the observed spectrum did indeed show a very small distortion from the predicted IB form near the end point. Attributing this distortion to the presence of detour transitions, Schmorak (1963) concluded that such transitions account for no more than ~ 0.6% of the total radiative K-capture transition rate.

While the contribution of detour transitions is of great interest for the study of nuclear structure, such transitions usually do not significantly affect the shape or intensity of radiative electron-capture spectra.[16] For this reason, and because available theoretical results on detour transitions are very limited, such transitions will be disregarded here and all calculations will be confined to the determination of the direct-transition amplitude shown diagrammatically in Fig. 30(a). Clearly, a highly accurate theory of the direct-transition process will be necessary to permit the identification of any detour-transition contributions in observed spectra.

1. Matrix elements and transition rates

Radiative electron capture is expected to occur with significant probability only for the innermost electrons of the atom. Since the available energy is usually greater than the K-shell binding energy, the K electrons, which spend the most time in the neighborhood of the nucleus, are expected to provide the dominant contribution to the IB spectra (except at very low photon energies where $2p$-state capture provides the dominant contribution). In all but the very lightest atoms, the potential in which the innermost electrons move is primarily the Coulomb potential of the nucleus. For this reason, all electron–electron interactions and the screening and correlation effects for which they are responsible are neglected in current theories, and it is assumed that each orbital electron is initially moving under the influence of only the nuclear Coulomb field.

[15] The total integrated intensity of a two-photon spectrum, for example, is expected to be no greater than ~10^{-4} times that of the corresponding one-photon spectrum. Two-photon IB and the directional correlation between the photons have been studied by Menhardt (1957).

[16] The adequacy of this procedure has been questioned by Koonin and Persson (1972), but it underlies all theoretical work reported so far.

Accordingly, the unperturbed electron-field operator $\Psi_e(x)$ is chosen to satisfy a Dirac equation containing the nuclear Coulomb field

$$(\gamma_\mu \partial_\mu + 1 + \gamma_4 Z\alpha/r)\Psi_e(x) = 0 . \tag{4.1}$$

In this representation, the interaction Hamiltonian density is

$$H_I(x) = H_\gamma(x) + H_{\rm EC}(x) , \tag{4.2}$$

where H_γ represents the interaction of the electron field with the Maxwell field, and $H_{\rm EC}$ represents the electron-capture interaction, assumed to be of the standard $V - \lambda A$ form. The matrix element associated with diagram (a) of Fig. 30 is derivable by standard quantum-field theoretic methods. As Glauber and Martin (1956) have shown, it can be written

$$M_\alpha = ieC_v\left(\frac{2\pi}{k}\right)^{1/2}\int d\mathbf{r}_N\, j_\mu^N(\mathbf{r}_N)\bar{\Phi}^\nu(\mathbf{r}_N)\Gamma_\mu \int d\mathbf{r}\, G_E(\mathbf{r}_N, \mathbf{r}) \times \boldsymbol{\gamma}\cdot\mathbf{e}^* e^{-i\mathbf{k}\cdot\mathbf{r}}\Phi_\alpha(\mathbf{r}) , \tag{4.3}$$

with the matrix element of the nuclear electron-capture current density defined by

$$j_\mu^N(\mathbf{r}_N) = \langle N_f |\bar{\Psi}_n(\mathbf{r}_N, 0)\Lambda_\mu \Psi_p(\mathbf{r}_N, 0)| N_i\rangle . \tag{4.4}$$

In these equations, C_v is the weak-interaction vector coupling constant, and we have $\lambda = |C_A/C_V|$, $\Lambda_\mu = \gamma_\mu(1+\lambda\gamma_5)$, and $\Gamma_\mu = \gamma_\mu(1+\gamma_5)$. The Ψ_n and Ψ_p are the nucleon field operators, and Φ^ν and Φ_α are the Dirac spinor wavefunctions for a neutrino of momentum $\mathbf{P}_\nu$ and an initial electron in state α, respectively. The one-photon state, characterized by momentum $\mathbf{k}$ and polarization $\mathbf{e}$, has been normalized to a unit volume. The intermediate-state sum which appears in Eq. (4.3) has been identified as the eigenfunction expansion for the Dirac–Coulomb Green's function,

$$G_E(\mathbf{r}_N, \mathbf{r}) = \sum_\beta \frac{\Phi_\beta(\mathbf{r}_N)\bar{\Phi}_\beta(\mathbf{r})}{(E_\beta - E)} , \tag{4.5}$$

with $E = E_\alpha - k$, where E_α is the relativistic energy of the orbital electron undergoing capture.

Two comments on the structure of the matrix element are in order. First, it should be noted that the role played by positrons in the radiative capture process is included implicitly in the structure of M_α. One type of path through which the radiative capture process can proceed is the emission of a virtual positron by the nucleus followed by its single-quantum annihilation with an orbital electron. Such paths are accounted for by the presence of the various negative-energy eigenstates in the expansion of the Green's function. Thus the structure of the Green's function is such that complete account is taken of the role of positrons in the radiative capture process.

Since the theory developed so far assumes the presence of any number of orbital electrons moving independently in the Coulomb field of the nucleus, the Pauli exclusion principle forbids virtual radiative transitions to intermediate states which are already occupied. Presumably such occupied intermediate states should then be excluded from the eigenfunction expansion. However, as was first pointed out quite generally by Feynman (1949) and emphasized by Glauber and Martin (1956) in reference to radiative electron capture, the presence of an obstructing electron makes another path possible for the radiative capture process, which is not otherwise available. This path consists of virtual electron capture of the obstructing electron followed by a radiative transition. Feynman has shown that, for a noninteracting system, the total amplitude for such a new path exactly compensates for that of the forbidden intermediate states; thus one may perform the calculation as if all the other states were unoccupied.

Feynman's result is easily generalized to include the presence of a static external field, such as the field of the nucleus, and consequently it has been assumed valid in all theoretical studies on radiative electron capture. However, as pointed out by Persson and Koonin (1972), radiation before capture takes place in the Coulomb field of element Z, while radiation following capture takes place in the field of element $Z-1$. Consequently, those terms in the eigenfunction expansion for the Green's function which correspond to occupied atomic states should really be represented by Coulomb eigenfunctions for element $Z-1$ rather than element Z. Undoubtedly, for $Z \gg 1$, the corrections resulting from such a modification of the eigenfunction expansion are entirely negligible. However, for very low-Z elements, especially at the lower photon energies ($k \lesssim Z\alpha$) where the poles corresponding to the bound states contribute strongly to the transition amplitude, such a modification of the Green's function may prove to be of importance.

The Green's function introduced in Eq. (4.3) and defined by the eigenfunction expansion [Eq. (4.5)] is seen to satisfy the inhomogeneous differential equation

$$G_E(\mathbf{r}_N, \mathbf{r})\gamma_4[H_c(\mathbf{r}) - E] = \delta(\mathbf{r}_N - \mathbf{r}) , \tag{4.6}$$

where H_c is the Dirac–Coulomb Hamiltonian. As Glauber and Martin (1956) have shown, the evaluation of M_α is facilitated by the introduction of the second-order Dirac–Coulomb Green's function $g_E(\mathbf{r}_N, \mathbf{r})$, defined by

$$G_E(\mathbf{r}_N, \mathbf{r}) = g_E(\mathbf{r}_N, \mathbf{r})[\boldsymbol{\gamma}\cdot\nabla + \gamma_4(E + Z\alpha/r) + 1] \tag{4.7}$$

and satisfying the inhomogeneous second-order equation

$$g_E(\mathbf{r}_N, \mathbf{r})[\nabla^2 + (E + Z\alpha/r)^2 - 1 - iZ\alpha\,\boldsymbol{\alpha}\cdot(\nabla 1/r)] = -\delta(\mathbf{r}_N - \mathbf{r}) . \tag{4.8}$$

With the introduction of Eq. (4.7), the matrix element of Eq. (4.3) lends itself to considerable simplification and can be written

$$M_\alpha = ieC_v\left(\frac{2\pi}{k}\right)^{1/2}\int d\mathbf{r}_N\, j_\mu^N(\mathbf{r}_N)\bar{\Phi}^\nu(\mathbf{r}_N)\Gamma_\mu \int d\mathbf{r}\, g_E(\mathbf{r}_N, \mathbf{r})e^{-i\mathbf{k}\cdot\mathbf{r}} \times[-2\mathbf{e}^*\cdot\nabla + \mathbf{e}^*_\lambda \Sigma_{\lambda\delta} k_\delta]\Phi_\alpha(\mathbf{r}) . \tag{4.9}$$

In the Secs. IV.A.2–IV.A.4, the evaluation of M_α and related quantities is described and final results are presented for allowed and first-forbidden transitions. We note that the differential transition rate is determined by the usual formula of time-dependent perturbation theory (Fermi's "Golden Rule No. 2") and is given by

$$dw_\alpha = (2\pi)^{-5}|M_\alpha|^2\delta(E_\nu + k - q_\alpha)\, d\mathbf{P}_\nu\, d\mathbf{k} , \tag{4.10}$$

where $q_\alpha = Q_{\rm EC} - B_\alpha$ has been introduced to represent the total available energy, shared between the photon and the neutrino.

2. IB spectra from allowed transitions

For allowed transitions, the lepton functions of $\mathbf{r}_N$ are usually replaced by their values at $\mathbf{r}_N = 0$. However, one must exercise some caution in doing this since the Coulomb Green's function $g_E(\mathbf{r}_N, \mathbf{r})$ is known to be weakly singular at $\mathbf{r}_N = 0$. To get around this difficulty it is necessary to take account of the fact that the electron-capture interaction actually takes place over a finite nuclear volume, by averaging the Green's function over this volume.[17] This averaged Green's function will be denoted by $\langle g_E(\mathbf{r}_N, \mathbf{r})\rangle_\Omega$. Thus for allowed transitions the matrix element of Eq. (4.9) is simplified to

$$M_\alpha = ieC_v\left(\frac{2\pi}{k}\right)^{1/2} J_\mu^N \bar{\Phi}^\nu(0)\Gamma_\mu \int d\mathbf{r}\,\langle g_E(\mathbf{r}_N, \mathbf{r})\rangle_\Omega\, e^{-i\mathbf{k}\cdot\mathbf{r}} \times[-2\mathbf{e}^*\cdot\nabla + e^*_\lambda \Sigma_{\lambda\delta} k_\delta]\Phi_\alpha(\mathbf{r}), \tag{4.11}$$

where the nuclear electron-capture transition current has been introduced, defined by $J_\mu^N = \int d\mathbf{r}_N\, j_\mu^N(\mathbf{r}_N)$. A nonrelativistic approximation for the nuclear motion leads to $J_\mu^N = (i\lambda\langle\sigma\rangle, \langle 1\rangle)$, where $\langle 1\rangle$ and $\langle\sigma\rangle$ are the familiar matrix elements associated with Fermi and Gamow–Teller transitions.

a. Coulomb-free theory

The earliest theory of IB spectra in allowed transitions was developed independently by Møller (1937a) and by Morrison and Schiff (1940).[18] This theory is presently of interest because of its simplicity and because it yields IB spectra that are accurate at high photon energies. The more sophisticated theory developed later by Glauber and Martin (1956) may be viewed as providing correction factors for the basic results.

Morrison and Schiff (1940) simplified the problem by neglecting the momentum (and binding energy) of the initial electron and by neglecting the influence of the Coulomb field on the intermediate electron states. The first of these assumptions is only valid when the recoil momentum of the electron after photon emission greatly exceeds its initial momentum (of average value $Z\alpha$). The second approximation consists of assuming a Born-approximation treatment of the intermediate states. For its validity, this approximation requires that $Z\alpha/v \ll 1$, where v is the velocity of the electron after photon emission. It is evident that both approximations restrict the results to photons in the high-energy region where k is much larger than $Z\alpha$.

Ignoring the Coulomb field in the intermediate states amounts to using the free-particle relativistic Green's function found by solving Eq. (4.8) with $Z = 0$. The initial momentum of the electron is neglected by approximating its wavefunction by a constant, equal to the value of the wavefunction at the origin. Under these approximations, the calculation of the matrix element of Eq. (4.11) is greatly simplified and leads to the result

$$M_{ns} = ieC_v(\pi/2k^3)^{1/2} J_\mu^N \bar{\Phi}^\nu(0)\Gamma_\mu e^*_\lambda \Sigma_{\lambda\delta} k_\delta \Phi_{ns}(0). \tag{4.12}$$

It is important to note that as a consequence of neglecting the momentum of the initial electron, radiative electron capture from an initial electron state of nonvanishing angular momentum is forbidden. Both the electric and magnetic contributions to the IB radiation vanish under these circumstances; this is immediately evident from the structure of the matrix element of Eq. (4.12).

When Eq. (4.12) is substituted into Eq. (4.10) and the appropriate momentum and spin summations are completed, the IB spectra associated with ns-state capture are found to be

$$dw_{ns} = \frac{2\alpha}{\pi^2} C_v^2 J^N \circ J^{N*} |\Phi_{ns}(0)|^2 k(q_{ns} - k)^2\, dk. \tag{4.13}$$

The ratio of the radiative capture rate to that for ordinary K capture is

$$\frac{dw_{ns}}{w_K} = \frac{\alpha}{\pi}\,\frac{|\Phi_{ns}(0)|^2}{|\Phi_{1s}(0)|^2}\,\frac{k(q_{ns}-k)^2}{q_{1s}^2}\,dk. \tag{4.14}$$

Hence the total radiative capture rate per K-capture event is

$$\frac{w_{ns}}{w_K} = \frac{1}{w_K}\int_0^{q_{ns}} \frac{dw_{ns}}{dk}\,dk = \frac{\alpha}{\pi}\,\frac{q_{ns}^2}{12}\,\frac{|\Phi_{ns}(0)|^2}{|\Phi_{1s}(0)|^2}\left(\frac{q_{ns}}{q_{1s}}\right)^2. \tag{4.15}$$

More generally, if only photons with $k \geq k_0$ are detected, the integrated radiative capture rate per K-capture event is given by

$$\frac{w_{ns}(k_0)}{w_K} = \frac{1}{w_K}\int_{k_0}^{q_{ns}} \frac{dw_{ns}}{dk}\,dk = \frac{w_{ns}}{w_K}\left[4(1-k_0/q_{ns})^3 - 3(1-k_0/q_{ns})^4\right]. \tag{4.16}$$

For radiative K capture in particular, these formulas are simplified. The IB spectrum then is

$$\frac{dw_{1s}}{w_K} = \frac{\alpha}{\pi}\, q_{1s}^2\,\epsilon(1-\epsilon)^2 d\epsilon, \tag{4.17}$$

where we have $\epsilon = k/q_{1s}$. The total radiative K-capture rate is

$$\frac{w_{1s}}{w_K} = \frac{\alpha}{\pi}\,\frac{q_{1s}^2}{12}. \tag{4.18}$$

Equations (4.17) and (4.18) were first derived by Møller (1937a) and by Morrison and Schiff (1940).[19] The more general results for arbitrary s-state capture [Eqs. (4.14) and (4.15)] were first reported by Glauber and Martin (1956).

b. Theory of Glauber and Martin

The results of the Coulomb-free theory of Møller (1937a) and Morrison and Schiff (1940) are expected to

[17] For a possible exception to this statement, see Smirnov and Batkin (1974).

[18] Unfortunately, Møller's work is much less well-known than that of Morrison and Schiff. Thus the theory has come to be known by the names of the latter authors. Yet it was Møller who first envisaged IB as arising from the emission of a virtual positron, followed by its single-quantum annihilation with one of the K electrons.

[19] Winter (1957) has shown how to construct a simple classical model for radiative K capture which correctly predicts the low-energy portion of the IB spectrum [Eq. (4.17)] and, to within a factor of ln2, the total radiative capture rate [Eq. (4.18)]. Neither the high-energy portion of the IB spectrum, however, nor the IB angular distribution are correctly given by the model.

hold only for large k and small Z; otherwise it is essential to include Coulomb effects in the evaluation of the matrix element M_α. Such calculations, in which account is taken of both relativistic and Coulomb effects, have been reported by Glauber and Martin in two well-known papers.

In their first paper on the subject, Glauber and Martin (1956) developed the general formalism for allowed transitions (Sec. IV.A.1) and evaluated M_α to a relative accuracy of order $Z\alpha$ for both s- and p-state capture. Certain relativistic corrections that are important for s-state capture at low energies were also calculated. In their second paper, Martin and Glauber (1958) developed more elaborate methods which make detailed calculations possible in which relativistic and Coulomb effects are included to all orders in $Z\alpha$. These results lead to certain integrals which cannot be evaluated exactly in closed form or tabulated easily. To obtain numerical results, Martin and Glauber developed $Z\alpha$ expansions for these integrals and carried out their evaluation to a relative accuracy of order $(Z\alpha)^2$. This limitation on their otherwise exact results for radiative K capture has been removed recently, however, by Intemann (1971), who has shown how to evaluate the integrals exactly using partly numerical methods. We briefly outline this theory and summarize its final results.

Nonrelativistic calculations. For moderately light nuclei it is expected that the initial electronic states can be described adequately by nonrelativistic Coulomb wave functions, especially for capture from the higher shells. In view of the greater complexity attendant to the use of Dirac–Coulomb wavefunctions, it is natural that nonrelativistic calculations be considered first. In general, these are expected to yield results with a relative accuracy of order $Z\alpha$. In order to preserve this level of accuracy at all photon energies, however, it is necessary to employ somewhat more accurate wavefunctions, correcting for certain relativistic effects which have a pronounced influence on the low-energy portions of the s-state spectra (Glauber and Martin, 1956).

A particular advantage of introducing the second-order Green's function is that, consistent with the use of nonrelativistic wavefunctions, an approximate Green's function $g'_E(\mathbf{r}_N, \mathbf{r})$ can be employed,[20] which has a particularly simple structure. This Green's function, obtained by neglecting the $(Z\alpha/r)^2$ and $Z\alpha\boldsymbol{\alpha}\cdot(\nabla 1/r)$ terms in Eq. (4.8) and solving the resulting equation, has been studied in considerable detail by Glauber and Martin (1956). In particular, $g'_E(0,r)$ has been shown to possess the integral representation[21]

$$g'_E(0,r) = (\mu/2\pi)e^{-\mu r}\int_0^\infty ds\, s^{-\eta}(1+s)^{\eta}e^{-2\mu r s}, \qquad (4.19)$$

where $\mu = (1-E^2)^{1/2}$ and $\eta = Z\alpha E/\mu$.

(i) *s-state radiative capture.* For radiative capture from an s state, the contribution to M_α from the $\mathbf{e}^*\cdot\nabla$ term vanishes from symmetry considerations; when terms of order $Z\alpha$ are neglected, the remaining contribution can be evaluated using only very general properties of the Green's function.[22] Final results for the transition rates are identical with those of the Coulomb-free theory [Eq. (4.14) *et seq.*]. The calculations of Glauber and Martin (1956) reveal, however, that the range of validity of the Coulomb-free theory is much greater than could have been anticipated on the basis of the calculations of Møller (1937a) or Morrison and Schiff (1940). Indeed, it was established by Glauber and Martin (1956) that the Coulomb-free theory yields results for the IB spectra associated with s-state capture which are formally correct to order $Z\alpha$ for all photon energies. It is also true, however, that for the low-energy portion of s-state spectra, the factor of $Z\alpha$ is partially compensated by an increased probability of radiation. Consequently, in order to obtain results for which the actual error is not greater than order $Z\alpha$, it is necessary to carry the calculations to the next order in $Z\alpha$ and omit only those terms which are actually of order $Z\alpha$ or less. Glauber and Martin (1956) accomplished this by means of a Foldy–Wouthysen transformation applied to the Dirac–Coulomb wavefunctions and Green's function. The result, valid for $\eta<2$ and $k\lesssim Z\alpha$, is

$$M_{ns} = ieC_v(\pi/2k^3)^{1/2}J^N_\mu\,\bar{\Phi}^\nu(0) \times\Gamma_\mu[\Sigma\cdot\mathbf{e}^*\times\mathbf{k} + ik\boldsymbol{\alpha}\cdot\mathbf{e}^* B_{ns}]\Phi_{ns}(0). \qquad (4.20)$$

The function $B_{ns}(k)$ is defined by

$$B_{ns}(k) = 1 + \frac{2}{3\Phi_{ns}(0)}\int d\mathbf{r}\, g_E^{(1)}(0,r) r\frac{d}{dr}\Phi_{ns}(r), \qquad (4.21)$$

where $g_E^{(1)}(0,r)$ is the p-wave contribution to the partial-wave expansion of the approximate Green's function $g'_E(\mathbf{r}_N,\mathbf{r})$, $g'_E(\mathbf{r}_N,\mathbf{r}) = g'_E(0,r) + g_E^{(1)}(0,r)\mathbf{r}_N\cdot\mathbf{r} + \cdots$. The transition rate is calculated as before, with the result

$$\frac{dw_{ns}}{w_K} = \left(\frac{dw_{ns}}{w_K}\right)_{\mathrm{CF}} R_{ns} = \frac{\alpha}{\pi}\frac{|\Phi_{ns}(0)|^2}{|\Phi_{1s}(0)|^2}\frac{k(q_{ns}-k)^2}{q_{1s}^2}R_{ns}\,dk. \qquad (4.22)$$

The correction factor $R_{ns}(k)$, which describes the modification of the Coulomb-free result brought about by inclusion of the most important relativistic and Coulomb effects, is defined by

$$R_{ns}(k) = \tfrac{1}{2}(1+B_{ns}^2). \qquad (4.23)$$

The evaluation of the functions $B_{ns}(k)$ has been described in great detail by Glauber and Martin (1956). Here we quote only the final results,

$$B_{1s}(k) = 1 - \frac{4}{3}\frac{\eta_1}{(1+\eta_1)}\left\{1 + \frac{\eta_1}{(1-\eta_1)}[2K(\lambda_1)-1]\right\}, \qquad (4.24)$$

with $\lambda_1 = (1-\eta_1)/(1+\eta_1)$, and

[20] Because $g'_E(\mathbf{r}_N,\mathbf{r})$ is well behaved as $\mathbf{r}_N\to 0$, it is unnecessary to average it over the nuclear volume.

[21] Of greatest interest are those electron-capture transitions for which competing positron emission is energetically impossible. Then we have $k\lesssim 2-B_\alpha$ and $|E|<1$. In this case, the Green's function cannot represent a freely propagating wave. Rather, it decreases rapidly with distance from the nucleus and has a range which depends on k.

[22] In this approximation, Glauber and Martin neglect the retardation factor $e^{i\mathbf{k}\cdot\mathbf{r}}$ for photon energies $k\lesssim Z\alpha$. This approximation is discussed further and a calculation of the 1s-state capture spectrum of ^{37}Ar in which this approximation is not made is given by Paquette (1962).

$$B_{2s}(k) = 1 - \frac{\eta_2}{(1-\eta_2^2/4)}\left(\frac{4}{3}+\frac{5}{6}\eta_2\right) - \frac{\eta_2^2}{(1-\eta_2^2/4)^2}\left[\frac{8}{3}(1-\eta_2^2)K(\lambda_2) - 3 - \eta_2 + \frac{5}{4}\eta_2^2\right], \tag{4.25}$$

with $\lambda_2 = (2-\eta_2)/(2+\eta_2)$. The function $K(\lambda)$ is

$$K(\lambda) = \lambda \int_0^1 \frac{dX X^{-\eta}}{(1+\lambda X)}. \tag{4.26}$$

For the purpose of evaluation, $K(\lambda)$ can be represented conveniently by the rapidly converging series expansion

$$K(\lambda) = \ln(1+\lambda) - \eta \sum_{j=1}^{\infty} \frac{(-\lambda)^j}{j(j-\eta)}. \tag{4.27}$$

In arriving at these final results, advantage has been taken of the fact that E may be set equal to one in the correction term, so that $\eta = Z\alpha/\mu$. Consequently the two parameters Z and k, upon which the functions B_{ns} depend, enter only in the single combination η which, in the present approximation, is given by $\eta_1 = (1+k/B_{1s})^{-1/2}$ for $1s$-state capture and by $\eta_2 = (\frac{1}{4}+k/B_{1s})^{-1/2}$ for $2s$-state capture. Here, B_{1s} is the $1s$-state binding energy. This simplification greatly facilitates tabulation of final results.

With the aid of Eq. (4.27), we have evaluated Eq. (4.24) and Eq. (4.25) numerically (Tables XXII and XXIII). Although for energies not greatly exceeding the binding energy, $B_{1s}(k)$ increases quite rapidly from its value of zero at $k=0$, the function approaches its asymptotic value of unity quite slowly. The correction factor $R_{1s}(k)$ therefore remains substantially less than unity, even at energies very much larger than the binding energy. Like $R_{1s}(k)$, $R_{2s}(k)$ also slowly approaches unity for large k. Unlike $B_{1s}(k)$, however, $B_{2s}(k)$ does not go to zero as k approaches zero; rather, as may be shown analytically, $B_{2s}(0) = -\frac{3}{2}$.

The functions $B_{ns}(k)$ for $n \geq 3$ can be evaluated similarly. However, the contributions to radiative electron capture from ns states with $n \geq 3$ can usually be neglected entirely, compared with contributions from $1s$ and $2s$ states. For example, according to the above results the $3s$-state intensity is only ~4% of the $1s$-state intensity; when screening effects are taken into account, its contribution is reduced even more.

(ii) *p-state radiative capture.* From the calculations of Morrison and Schiff (1940) it can be concluded that the p-state capture contribution to the IB spectrum is negligibly small for $k \gg Z\alpha$. As the calculations of Glauber and Martin (1956) bear out, however, the p-state intensity becomes quite appreciable for $k \lesssim Z\alpha$ and indeed exceeds the s-state spectrum over a large part of this range. Discussion of p-state radiative capture can therefore be restricted to photon energies $k \lesssim Z\alpha$. In this energy region, the transition matrix element can be reduced to

$$M_{np} = -2ieC_v\left(\frac{2\pi}{k}\right)^{1/2} J_\mu^N \bar{\Phi}^\nu(0)\Gamma_\mu \int d\mathbf{r}\, g'_E(0,r)\mathbf{e}^* \cdot \nabla\Phi_{np}(\mathbf{r}) \tag{4.28}$$

when terms of order $Z\alpha$ are neglected. It is clear that the IB radiation associated with p-state capture is distributed isotropically.

Since the three np-state wavefunctions transform like the components of a vector under rotations, one of them can conveniently be chosen to be the component in the direction of $\mathbf{e}$. The remaining two component states then do not contribute to the matrix element, and a single calculation takes into account the contributions from all three magnetic substates. On this basis, the matrix element can be written

$$M_{np} = -2ieC_v(Z\alpha/k)^{1/2} J_\mu^N \bar{\Phi}^\nu(0)\Gamma_\mu \chi_{np} Q_{np}, \tag{4.29}$$

where χ_{np} is the spin part of the np-state wavefunction, and the integral $Q_{np}(k)$ is

$$Q_{np}(k) = \left(\frac{2\pi}{Z\alpha}\right)^{1/2} \int d\mathbf{r}\, g'_E(0,r)\mathbf{e}^* \cdot \nabla\Phi_{np}(\mathbf{r}). \tag{4.30}$$

The transition rate is calculated as before, with the result

$$\frac{dw_{np}}{w_K} = \frac{4}{\pi Z^2\alpha}[Q_{np}(k)]^2 \frac{k(q_{np}-k)^2}{q_{1s}^2} dk. \tag{4.31}$$

Evaluation of the integrals $Q_{np}(k)$ is similar to that of $B_{ns}(k)$ and has also been described in detail by Glauber and Martin (1956). The final results are

$$Q_{2p}(k) = \frac{\eta_2^2}{4(1-\eta_2^2/4)^2}[1 + \tfrac{2}{3}\eta_2 - \tfrac{7}{12}\eta_2^2 + \tfrac{4}{3}\eta_2^2 K(\lambda_2)] \tag{4.32}$$

and

$$Q_{3p}(k) = \frac{4}{27}\frac{\eta_3^2}{(1-\eta_3^2/9)^3}\{(1-\eta_3/3)[1+\eta_3 - 2(\eta_3/3)^2 - 8(\eta_3/3)^3] + \tfrac{4}{3}\eta_3^2(1-\eta_3^2/3)K(\lambda_3)\}, \tag{4.33}$$

where $\eta_3 = (1/9 + k/B_{1s})^{-1/2}$, all other quantities having been defined previously. Evaluation of Eqs. (4.32) and (4.33) yields the results shown in Table XXIV.

(iii) *Results.* To illustrate the results of the theory of Glauber and Martin (1956), the predicted spectra associated with $1s$-, $2s$-, $2p$-, and $3p$-state radiative capture in ^{55}Fe have been plotted in Fig. 31. As stated, terms of order $Z\alpha$ were neglected, introducing an error of ~20% for ^{55}Fe. It is evident from Fig. 31 that the s-state spectra do not differ greatly in form from the simple $k(q_{ns}-k)^2$ shape predicted by the Coulomb-free theory. Figure 31 also shows the existence of very intense p-state spectra at low photon energies. Indeed, p-state contributions to the IB spectrum become more dominant with increasing charge and decreasing available energy.

For states of still higher orbital angular momentum, the radiative capture probability is expected to be much smaller than for capture from s or p states, because the probability of finding the electron in the neighborhood of the nucleus is smaller and the radiation is of a higher multipole order than the predominantly $M1$ and $E1$ radiation associated with s- and p-state radiative capture, respectively. Indeed, within the framework defined by the approximations used in treating p-state capture, the transition amplitude for radiative capture from a state of orbital angular momentum >1 vanishes.

Relativistic calculations. The preceding calculations were intended to provide results with a relative accuracy of order $Z\alpha$. To achieve even this level of accuracy

TABLE XXII. The function $B_{1s}(k)$ given by Eq. (4.24), and the associated relativistic correction factor $R_{1s}(k)$, for various values of the photon energy k, measured in units of the K-shell binding energy $B_K = (Z\alpha)^2/2$.

k	$B_{1s}(k)$	$R_{1s}(k)$	k	$B_{1s}(k)$	$R_{1s}(k)$
1.0	0.2745	0.5377	9.5	0.6466	0.7090
1.1	0.2898	0.5420	10.0	0.6537	0.7137
1.2	0.3042	0.5463	11.0	0.6668	0.7223
1.3	0.3175	0.5504	12.0	0.6784	0.7301
1.4	0.3300	0.5545	13.0	0.6888	0.7372
1.5	0.3418	0.5584	14.0	0.6982	0.7438
1.6	0.3529	0.5623	16.0	0.7146	0.7554
1.7	0.3634	0.5660	18.0	0.7285	0.7654
1.8	0.3733	0.5697	20.0	0.7405	0.7742
1.9	0.3828	0.5733	22.0	0.7510	0.7820
2.0	0.3917	0.5767	24.0	0.7602	0.7890
2.1	0.4003	0.5801	26.0	0.7685	0.7953
2.2	0.4084	0.5834	28.0	0.7759	0.8010
2.3	0.4162	0.5866	30.0	0.7826	0.8063
2.4	0.4237	0.5897	35.0	0.7970	0.8176
2.5	0.4308	0.5928	40.0	0.8089	0.8271
2.6	0.4377	0.5958	45.0	0.8188	0.8352
2.7	0.4443	0.5987	50.0	0.8272	0.8422
2.8	0.4506	0.6015	60.0	0.8411	0.8537
2.9	0.4567	0.6043	70.0	0.8520	0.8629
3.0	0.4626	0.6070	80.0	0.8609	0.8706
3.2	0.4738	0.6122	90.0	0.8683	0.8770
3.4	0.4842	0.6172	100.0	0.8747	0.8825
3.6	0.4940	0.6220	120.0	0.8850	0.8916
3.8	0.5032	0.6266	140.0	0.8930	0.8988
4.0	0.5118	0.6310	160.0	0.8996	0.9046
4.2	0.5200	0.6352	180.0	0.9051	0.9096
4.4	0.5278	0.6393	200.0	0.9097	0.9138
4.6	0.5351	0.6432	220.0	0.9138	0.9175
4.8	0.5421	0.6470	240.0	0.9173	0.9207
5.0	0.5488	0.6506	260.0	0.9204	0.9236
5.5	0.5642	0.6592	280.0	0.9232	0.9261
6.0	0.5780	0.6670	300.0	0.9257	0.9285
6.5	0.5905	0.6743	350.0	0.9310	0.9334
7.0	0.6018	0.6811	400.0	0.9354	0.9374
7.5	0.6122	0.6874	450.0	0.9389	0.9408
8.0	0.6218	0.6933	500.0	0.9420	0.9437
8.5	0.6307	0.6989	700.0	0.9508	0.9520
9.0	0.6389	0.7041	1000.0	0.9586	0.9595

requires that some consideration be given to relativistic effects when treating radiative capture from s states. The importance of relativistic effects in s-state capture, even for moderately light nuclei, is primarily due to the fact that such transitions involve a spin flip, a process which results in large photon energies, and hence in a relativistic recoil by the electron. Furthermore, a nonrelativistic calculation does not take account of paths that involve virtual positron emission and neglects electron capture through intermediate p states, a path made possible by spin-orbit coupling.

The results described above are usually adequate to determine the IB spectra of moderately light nuclei for photon energies that are small compared with the electron rest energy. For heavy nuclei or large photon energies, these results are wholly inadequate. Martin and Glauber (1958) therefore developed a more general theory, taking full account of relativistic and Coulomb effects. The nonrelativistic results indicate that relativistic and Coulomb effects to all orders in $Z\alpha$ are most important in radiative capture from 1s states, hence Martin and Glauber (1958) applied their full theory to this specific calculation.

It should be noted that Yukawa (1956) has also attempted a fully relativistic calculation of the K-capture IB spectrum. Yukawa found it necessary, however, to introduce an approximation in constructing a usable form for the relativistic Coulomb Green's function; it is not entirely clear how reliable this approximation is. The results of Yukawa (1956) are at least as complicated as those of Martin and Glauber (1958) and have the serious drawback of being inapplicable to heavy nuclei. For these reasons, we do not discuss Yukawa's calculations further.

(i) 1s-*state radiative capture*. The starting point for the fully relativistic calculations of Martin and Glauber (1958) is the general expression (4.11) for the allowed-transition matrix element. To evaluate this matrix element exactly within the one-electron Coulomb approximation, appropriate forms for Φ_{1s} and $g_E(\mathbf{r}_N, \mathbf{r})$ must first be introduced. For Φ_{1s}, the usual ground-state solution of the Dirac equation for an electron moving in

TABLE XXIII. The functions $B_{2s}(k)$ given by Eq. (4.25), and the associated relativistic correction factor $R_{2s}(k)$, for various values of the photon energy k, measured in units of the K-shell binding energy $B_K=(Z\alpha)^2/2$.

k	$B_{2s}(k)$	$R_{2s}(k)$	k	$B_{2s}(k)$	$R_{2s}(k)$
1.0	−.0439	0.5010	9.5	0.6000	0.6800
1.1	−.0069	0.5000	10.0	0.6093	0.6856
1.2	0.0262	0.5003	11.0	0.6262	0.6960
1.3	0.0561	0.5016	12.0	0.6410	0.7054
1.4	0.0832	0.5035	13.0	0.6541	0.7139
1.5	0.1080	0.5058	14.0	0.6659	0.7217
1.6	0.1308	0.5085	16.0	0.6861	0.7354
1.7	0.1518	0.5115	18.0	0.7031	0.7471
1.8	0.1713	0.5147	20.0	0.7175	0.7574
1.9	0.1894	0.5179	22.0	0.7299	0.7664
2.0	0.2063	0.5213	24.0	0.7409	0.7744
2.1	0.2222	0.5247	26.0	0.7505	0.7817
2.2	0.2371	0.5281	28.0	0.7592	0.7882
2.3	0.2511	0.5315	30.0	0.7670	0.7942
2.4	0.2644	0.5349	35.0	0.7836	0.8070
2.5	0.2769	0.5383	40.0	0.7970	0.8176
2.6	0.2888	0.5417	45.0	0.8082	0.8266
2.7	0.3001	0.5450	50.0	0.8177	0.8343
2.8	0.3109	0.5483	60.0	0.8331	0.8470
2.9	0.3211	0.5516	70.0	0.8451	0.8571
3.0	0.3309	0.5547	80.0	0.8549	0.8654
3.2	0.3492	0.5610	90.0	0.8630	0.8723
3.4	0.3661	0.5670	100.0	0.8698	0.8783
3.6	0.3816	0.5728	120.0	0.8809	0.8880
3.8	0.3960	0.5784	140.0	0.8896	0.8957
4.0	0.4094	0.5838	160.0	0.8966	0.9019
4.2	0.4220	0.5890	180.0	0.9024	0.9071
4.4	0.4337	0.5940	200.0	0.9073	0.9116
4.6	0.4447	0.5989	220.0	0.9115	0.9155
4.8	0.4551	0.6036	240.0	0.9153	0.9188
5.0	0.4649	0.6081	260.0	0.9185	0.9218
5.5	0.4872	0.6187	280.0	0.9214	0.9245
6.0	0.5068	0.6284	300.0	0.9241	0.9270
6.5	0.5243	0.6375	350.0	0.9296	0.9321
7.0	0.5400	0.6458	400.0	0.9341	0.9363
7.5	0.5542	0.6536	450.0	0.9379	0.9398
8.0	0.5672	0.6608	500.0	0.9410	0.9427
8.5	0.5790	0.6676	700.0	0.9501	0.9513
9.0	0.5899	0.6740	1000.0	0.9582	0.9590

the Coulomb field of a nuclear charge Ze is chosen. For the exact second-order Green's function $g_E(\mathbf{r}_N, \mathbf{r})$, Martin and Glauber (1958) constructed an eigenfunction expansion from the solutions of Eq. (4.8). The smallness of the nuclear radius ($2\mu r_N \lesssim 10^{-3}$) allows some simplification. The region occupied by the nucleus may be safely neglected in integrating over $\mathbf{r}$, and those functions in the Green's-function expansion which depend on $\mathbf{r}_N$ can be replaced by the first term in their power-series expansion. The errors associated with the use of this simplified form of the exact Green's function are expected to be no greater than $\sim 10^{-3}$.

Using the above representations, Martin and Glauber (1958) calculated the transition matrix element for allowed radiative K capture without further approximations

$$M_{1s}=\frac{ieC_\nu}{k}\left(\frac{\pi}{k}\right)^{1/2} J^{N}_{\lambda}\langle\Phi_{1s}\rangle_\Omega \bar{\Phi}^{\nu}(0) \times \Gamma_\lambda[A_{1s}\Sigma\cdot\mathbf{e}^*\times\mathbf{k}+ikB_{1s}\boldsymbol{\alpha}\cdot\mathbf{e}^*]\chi^\mu_+. \tag{4.34}$$

The particular angular-momentum substate of the initial K electron is represented through the spin function $\chi^\mu_+ = \binom{\chi^\mu}{0}$, where χ^μ are the usual two-component Pauli spinors, and the integrals $A_{1s}(k)$ and $B_{1s}(k)$ are defined by

$$A_{1s}(k)=\frac{(\lambda_1+1)k}{\Gamma(2\lambda_1+1)\mu}\int_0^\infty dr\int_0^\infty ds\left\{j_0(kr)\left[1+\frac{a^2}{3(\lambda_1+1)^2}\right]-\frac{j_1(kr)2a^2}{kr(\lambda_1+1)^2}-\frac{j_2(kr)2a^2}{3(\lambda_1+1)^2}\right\}s^{-\eta+\lambda_1-1}(1+s)^{\eta+\lambda_1-1}(2\mu r)^{2\lambda_1}e^{-(2s+1)\mu r}e^{-ar},$$

$$B_{1s}(k)=\frac{(\lambda_1+1)k}{\Gamma(2\lambda_1+1)\mu}\int_0^\infty dr\int_0^\infty ds\left\{j_0(kr)\left[1-\frac{4a}{3(\lambda_1+1)}\left(\frac{\lambda_1}{kr}-\frac{a}{k}\right)+\frac{a^2}{3(\lambda_1+1)^2}\right]\right. \tag{4.35a}$$

$$\left.+\,j_2(kr)\left[\frac{4a}{3(\lambda_1+1)}\left(\frac{a}{k}+\frac{(3-2\lambda_1)}{2kr}\right)-\frac{2a^2}{3(\lambda_1+1)^2}\right]\right\}s^{-\eta+\lambda_1-1}(1+s)^{\eta+\lambda_1-1}(2\mu r)^{2\lambda_1}e^{-(2s+1)\mu r}e^{-ar}. \tag{4.35b}$$

TABLE XXIV. The functions $Q_{2p}(k)$, given by Eq. (4.32), and $Q_{3p}(k)$, given by Eq. (4.33), for various values of the photon energy k, measured in units of the K-shell binding energy $B_K=(Z\alpha)^2/2$.

k	$Q_{2p}(k)$	$Q_{3p}(k)$	k	$Q_{2p}(k)$	$Q_{3p}(k)$
1.0	1.5215	1.7104	6.4	0.0548	0.0326
1.1	1.0737	0.9070	6.6	0.0528	0.0314
1.2	0.8259	0.6183	6.8	0.0510	0.0303
1.3	0.6690	0.4691	7.0	0.0492	0.0292
1.4	0.5608	0.3778	7.2	0.0476	0.0283
1.5	0.4819	0.3161	7.4	0.0460	0.0273
1.6	0.4219	0.2715	7.6	0.0446	0.0265
1.7	0.3747	0.2379	7.8	0.0432	0.0257
1.8	0.3367	0.2115	8.0	0.0419	0.0249
1.9	0.3055	0.1903	8.2	0.0407	0.0242
2.0	0.2793	0.1729	8.4	0.0396	0.0235
2.1	0.2572	0.1584	8.6	0.0385	0.0229
2.2	0.2382	0.1460	8.8	0.0375	0.0223
2.3	0.2217	0.1354	9.0	0.0365	0.0217
2.4	0.2072	0.1262	9.5	0.0343	0.0204
2.5	0.1945	0.1181	10.0	0.0323	0.0192
2.6	0.1832	0.1110	10.5	0.0305	0.0181
2.7	0.1731	0.1047	11.0	0.0289	0.0172
2.8	0.1640	0.0990	11.5	0.0275	0.0163
2.9	0.1557	0.0939	12.0	0.0262	0.0155
3.0	0.1483	0.0893	12.5	0.0250	0.0148
3.2	0.1352	0.0813	13.0	0.0239	0.0142
3.4	0.1242	0.0745	13.5	0.0229	0.0136
3.6	0.1148	0.0688	14.0	0.0220	0.0131
3.8	0.1067	0.0639	14.5	0.0212	0.0126
4.0	0.0996	0.0596	15.0	0.0204	0.0121
4.2	0.0934	0.0558	15.5	0.0196	0.0117
4.4	0.0879	0.0525	16.0	0.0190	0.0112
4.6	0.0830	0.0495	16.5	0.0183	0.0109
4.8	0.0785	0.0468	17.0	0.0177	0.0105
5.0	0.0746	0.0444	17.5	0.0172	0.0102
5.2	0.0709	0.0423	18.0	0.0166	0.0099
5.4	0.0677	0.0403	18.5	0.0161	0.0096
5.6	0.0647	0.0385	19.0	0.0157	0.0093
5.8	0.0619	0.0368	19.5	0.0152	0.0090
6.0	0.0594	0.0353	20.0	0.0148	0.0088
6.2	0.0570	0.0339			

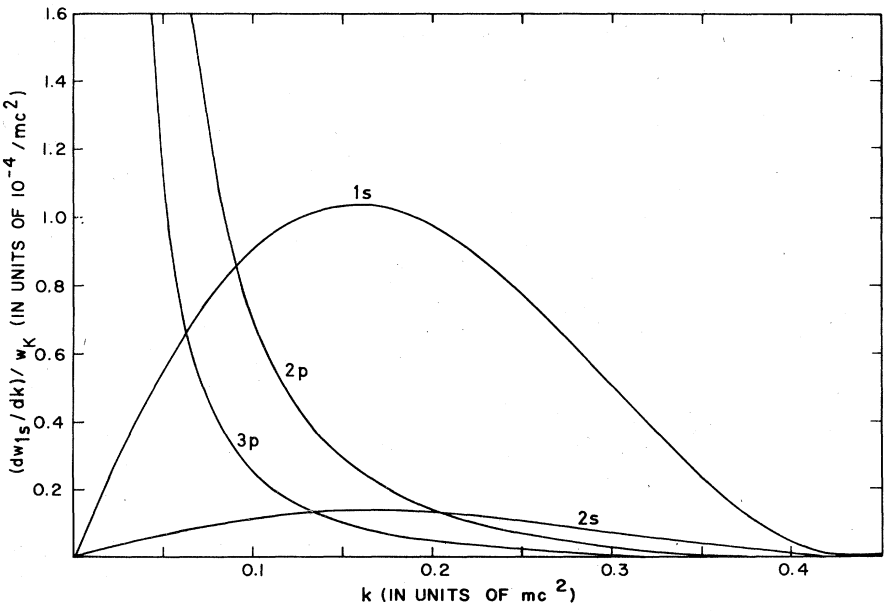

FIG. 31. IB spectra for radiative capture from various atomic shells of ^{55}Fe, according to the theory of Glauber and Martin (1956).

In Eqs. (4.35), the previous definitions of μ and η have been retained, and we have $a = Z\alpha$ and $\lambda_1 = (1-a^2)^{1/2} = E_{1s}$.

The energy spectrum of the IB, calculated as before, is

$$\frac{dw_{1s}}{w_K} = \frac{\alpha}{\pi}\frac{k(q_{1s}-k)^2}{q_{1s}^2}R_{1s}\,dk. \tag{4.36}$$

This expression is the same as Eq. (4.22) for 1s capture, except that $R_{1s}(k)$ is defined by

$$R_{1s}(k) = \tfrac{1}{2}(A_{1s}^2 + B_{1s}^2), \tag{4.37}$$

with $A_{1s}(k)$ and $B_{1s}(k)$ given by Eqs. (4.35). Unfortunately, the integrals appearing in Eqs. (4.35) cannot be evaluated exactly analytically in closed form and depend separately on Z and k, rather than on the single combined parameter $k/(Z\alpha)^2$ as do the integrals B_{ns} and $Q_{n\rho}$ discussed earlier.

A number of limited and, in most cases, approximate analytic results for A_{1s} and B_{1s} are reported by Martin and Glauber (1958). For example, Eqs. (4.35) can be simplified, transformed, and expanded if one neglects terms of order $(Z\alpha)^2$ or smaller and the remaining contribution to $B_{1s}(k)$ from the $j_2(kr)$ term. The results are

$$A_{1s}(k) = \mathrm{Im}[2/(\mu + a - ik) + (\eta\mu/k)(\lambda_1 + ia)\zeta], \tag{4.38a}$$

$$B_{1s}(k) = A_{1s}(k)(1 + \tfrac{2}{3}a^2/k) - \tfrac{2}{3}(a/k)\,\mathrm{Im}\,\zeta, \tag{4.38b}$$

where

$$\zeta = 2\left[\ln\left(\frac{\mu + a + ik}{2\mu}\right) + \eta\sum_{n=1}^{\infty}\frac{1}{n(n-\eta)}\left(\frac{a+ik-\mu}{a+ik+\mu}\right)^n\right]. \tag{4.39}$$

Because of the underlying approximations, these expressions are expected to hold well only at low photon energies and for elements which are not too heavy.

For $k \gtrsim 1$, it is feasible to expand the Green's function and the initial-state wavefunction in powers of $Z\alpha$. Carried to first order in $Z\alpha$, such expansions yield

$$A_{1s}(k) = 1 - Z\alpha\left\{\frac{\mu}{k} + 2\left(1 - \frac{1}{k}\right)\tan^{-1}\left(\frac{k}{\mu}\right)\right\}, \tag{4.40a}$$

$$B_{1s}(k) = 1 - Z\alpha\left\{\frac{\mu}{k}\left(1 + \frac{1}{k}\right) + 2\left(1 - \frac{1}{k^2}\right)\tan^{-1}\left(\frac{k}{\mu}\right)\right\}. \tag{4.40b}$$

For three particular photon energies, more accurate results can easily be obtained because of special circumstances which simplify the calculation in each case. In the neighborhood of $k = 0$, A_{1s} and B_{1s} are given, exact to all orders in $Z\alpha$, by

$$A_{1s}(k) = [(2\lambda_1 + 1)/3](1 - k), \tag{4.41a}$$

$$B_{1s}(k) = 0 + \mathcal{O}(k/Z\alpha). \tag{4.41b}$$

The integrals can be evaluated conveniently to second order in $Z\alpha$ for $k = \lambda_1$ $(\eta = 0)$,

$$A_{1s}(k) = 1 - Z\alpha + \pi(Z\alpha)^2/4, \tag{4.42a}$$

$$B_{1s}(k) = 1 - 2Z\alpha + (4 - \pi/2)(Z\alpha)^2, \tag{4.42b}$$

and for $k = 1 + \lambda_1$ $(\mu = 0)$,

$$A_{1s}(k) = 1 - \pi Z\alpha/2 + 2(Z\alpha)^2, \tag{4.43a}$$

$$B_{1s}(k) = 1 - 3\pi Z\alpha/4 + 9(Z\alpha)^2/2. \tag{4.43b}$$

These approximate results are expected to be fairly reliable for the lighter elements. In general, however, it is necessary to resort to numerical procedures. The above results are still of interest, though, since they provide a valuable check on the accuracy of numerical computations.

A relatively simple procedure for obtaining exact numerical results for A_{1s} and B_{1s} for arbitrary k and Z has been reported by Intemann (1971). The integration over r in Eqs. (4.35) is performed first, then the change of variable $x = s/(1+s)$ is made in the remaining integrals. After algebraic reduction, one finds

$$A_{1s}(k) = C\int_0^1 dx\, x^{-\eta+\lambda_1-1} f_A(x), \tag{4.44a}$$

$$B_{1s}(k) = \frac{C}{2k(1-\lambda_1)}\int_0^1 dx\, x^{-\eta+\lambda_1-1} f_B(x), \tag{4.44b}$$

where $C = -(2\mu)^{2\lambda_1-1}/[\lambda_1(2\lambda_1 - 1)k^2]$. To define f_A and f_B, it is convenient to introduce the definitions

$$\Sigma = k^2 + (\mu + a)^2, \quad s = \Sigma + \epsilon x + \delta x^2,$$

$$\epsilon = 2(\mu^2 - a^2 - k^2), \quad \sigma = a + \mu(1+x)/(1-x),$$

$$\delta = k^2 + (\mu - a)^2, \quad \theta = \tan^{-1}(k/\sigma),$$

whence f_A and f_B can be written

$$f_A(x) = [2k\lambda_1\sigma\cos(2\lambda_1\theta) - \sigma^2\sin(2\lambda_1\theta)]/s^{\lambda_1}, \tag{4.45a}$$

$$f_B(x) = 2k\lambda_1\sigma[a\sigma - 2a^2 + (1-\lambda_1)k]\cos(2\lambda_1\theta) + \{k^2(2\lambda_1 - 1)[k(\lambda_1 - 1) - 2a^2 + a\sigma] + \sigma^2[2a^2 - k(1-\lambda_1) - a\sigma]\}\sin(2\lambda_1\theta)/s^{\lambda_1}. \tag{4.45b}$$

Now f_A and f_B are very slowly varying functions of x over the entire range of integration, for all physical values of k and Z of interest. After an integration by parts to remove the weak singularity in each of the integrands at $x = 0$, the remaining integrals which appear in A_{1s} and B_{1s} thus can easily be evaluated numerically. The correction factors $R_{1s}(k)$, evaluated exactly in this manner for several nuclides of interest, are displayed in Fig. 32.

It is considerably easier to evaluate A_{1s} and B_{1s} by means of the low-k approximation [Eqs. (4.38) and (4.39)] or the high-k approximation [Eqs. (4.40)], than to employ the exact results [Eqs. (4.44)]. Therefore it is of interest to compare the functions $R_{1s}(k)$ obtained in these three ways, in order to assess the circumstances under which either of the approximate results can be employed without significant error. We have evaluated $R_{1s}(k)$ exactly and in the high- and low-k approximations for three very different values of Z. The results, shown in Fig. 33, are indistinguishable for very small Z over almost the entire energy range. For intermediate Z, the low-k approximation fits the exact curve quite well, even in the high-energy region where it does better than the high-k approximation. For large Z, neither approximation fits the exact result very well, and both approximations are totally wrong in their description of the low-energy behavior of $R_{1s}(k)$.

To compare the various calculations and indicate the importance of relativistic and Coulomb effects, we have plotted in Fig. 34 the 1s-state radiative capture spectra

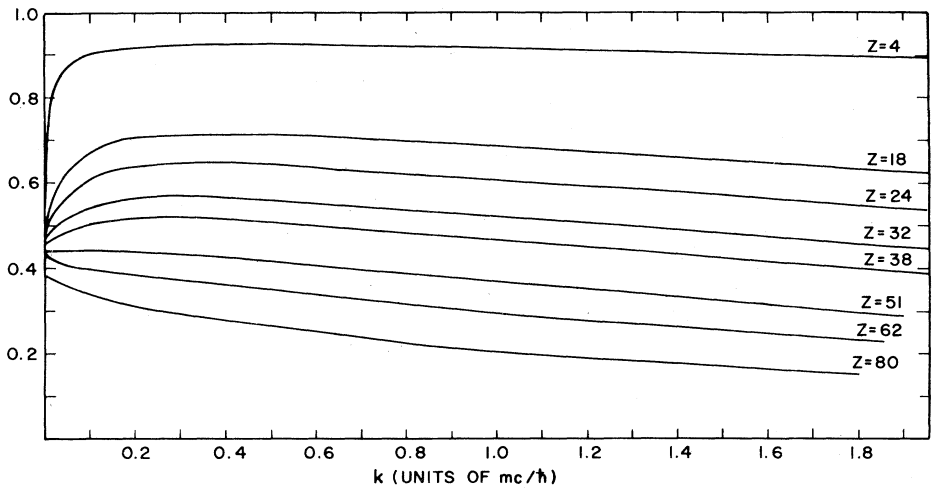

FIG. 32. Relativistic correction factor $R_{1s}(k)$, according to the exact results of Martin and Glauber (1958) and Intemann (1971).

predicted for the moderately light nucleus ^{55}Fe. It is evident from Fig. 34 that the shape of the 1*s* spectrum is not substantially altered by the inclusion of relativistic and Coulomb effects, but that the overall intensity experiences a very significant reduction. As is to be expected for a moderately light nucleus, the results of the exact calculation (MG) and that in which terms of order $Z\alpha$ are neglected (GM) agree fairly well. There will be no such agreement for heavy nuclei or for photon energies $k \gtrsim 1$.

(ii) *L*- and *M*-*shell radiative capture*. Although Martin and Glauber (1958) limited their fully relativistic calculations to 1*s*-state capture, their relativistic theory provides an equally valid basis for describing radiative capture from an arbitrary atomic shell. The general results of such a calculation are given by Zon (1971). The complexity of the expressions has precluded the derivation of analytical results; not even approximate results have been derived in which only terms through first order in $Z\alpha$ are retained. Zon (1971) does, however, report the construction of a computer program which permits numerical evaluation of the amplitude for radiative capture from the *L* and *M* shells, although few details are given and the only spectra reported in Zon's paper are those for ^{165}Er (Fig. 35).

Two general features of the ^{165}Er spectra are worth noting since they undoubtedly will be exhibited by the radiative capture spectra of other nuclei as well. A resonance in the 2*s*-state capture spectrum appears which is associated with a forbidden 2*s*-1*s* atomic transition. This resonance is quite sharp and therefore modifies the result of Glauber and Martin (1956) only in the binding-energy region. Elsewhere, the results of Zon (1971) and of Glauber and Martin (1956) are indistinguishable. Also to be noted are the modifications of the *p*-state spectra brought about by the inclusion of all relativistic and Coulomb effects. While these modifications appear to be only slight for capture from 3*p* states, they are quite important for the 2*p*-state spectrum (at least for heavy nuclei). In the case of ^{165}Er, they cause a reduction by a factor of ~2 in the overall intensity of the 2*p*-state spectrum. There is, however, no appreciable change in the form of the *p*-state capture energy distributions.

Some years ago it was suggested by Koh *et al.* (1962),

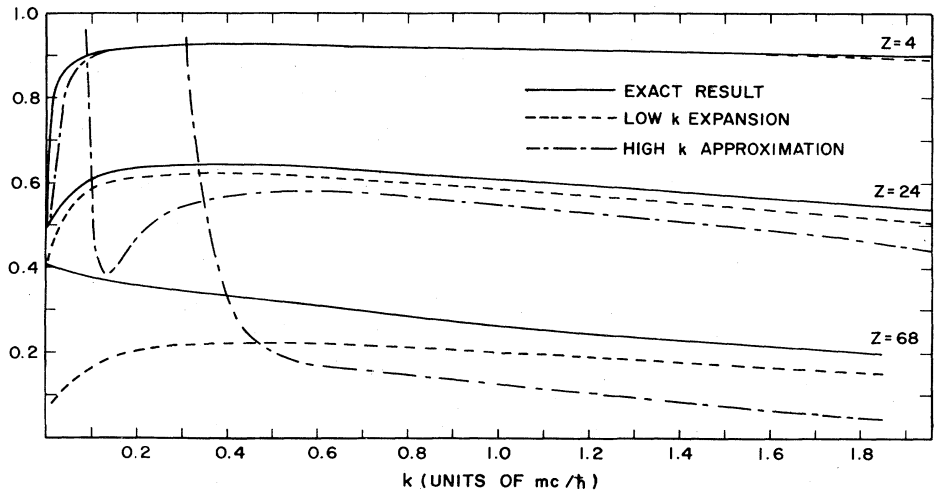

FIG. 33. Comparison of several theoretical results for the relativistic correction factor $R_{1s}(k)$. The exact result is deduced from Eqs. (4.44) and (4.45), the low-k expansion, from Eqs. (4.38) and (4.39), and the high-k approximation, from Eq. (4.40).

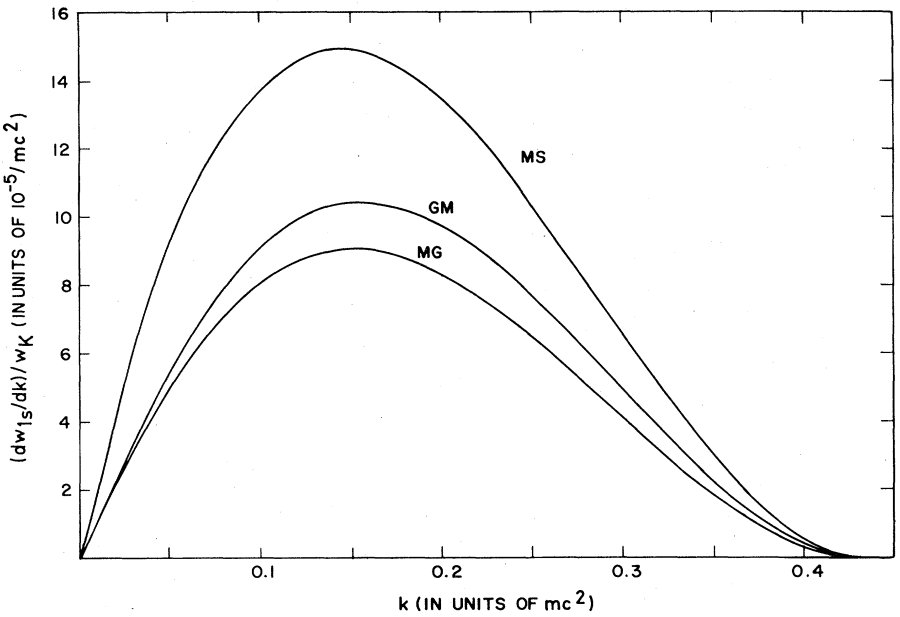

FIG. 34. K-capture IB spectrum for ^{55}Fe according to the theories of Morrison and Schiff (1940) (MS) [Eq. (4.14)], Glauber and Martin (1956) (GM) [Eq. (4.22)], and Martin and Glauber (1958) (MG) [Eq. (4.36)]. GM includes relativistic effects to lowest order in $Z\alpha$, while MG is fully relativistic.

and again by Koh (1965), that the IB spectrum possesses a cusp-shaped irregularity in the neighborhood of the positron threshold. To confirm this idea, Zon and Rapoport (1968) carried out extensive calculations. Their results, accurate to order $(Z\alpha)^2$, show that the form factor for radiative K capture varies continuously in this region, and thus, there is no such anomaly in the predicted spectrum at this level of accuracy.

Influence of uncaptured atomic electrons. In all of the foregoing calculations, only the electron which undergoes radiative capture is considered, and the presence of all other atomic electrons has been ignored. We now consider how, and to what extent, the one-electron results are modified when the presence of the remaining atomic electrons is taken into account.

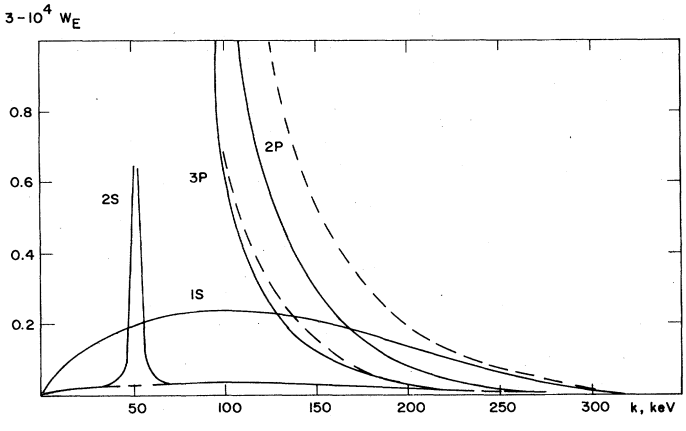

FIG. 35. IB spectra for radiative capture from various atomic shells of ^{165}Er. The solid curves represent the fully relativistic results of Zon (1971), while the dashed curves are deduced from the results of Glauber and Martin (1956). [After Zon (1971)].

Screening corrections. Screening by the remaining electrons affects the amplitude for radiative capture both by altering the initial configuration of the electron to be captured and by altering the probability amplitude for an electron to reach the nucleus after the virtual emission of a photon. To analyze these effects most simply, Martin and Glauber (1958) employed an independent-particle model in which the stationary states of the individual electrons are determined as the self-consistent-field solutions for the full many-body atomic Hamiltonian. In this approximation, no further account of the remaining electrons needs to be taken when the radiative transition probability for a single electron is calculated.

By far the more important effect of screening is the modification of the wavefunction that describes the initial electronic state. This modification is quite similar to that which occurs in ordinary electron capture, except that the effective size of the region from which capture can occur is somewhat larger. In ordinary electron capture, this region is determined by the nuclear radius, while in radiative electron capture it is determined by the range of the Green's function. For photon energies of greatest practical interest, above the binding energy of the initial electron and below the threshold for positron production, the range of the Green's function is of the order of the electron's Compton wavelength. While it is much larger than the nuclear radius, this range is still very small on an atomic scale. Thus it is argued by Martin and Glauber (1958) that a simple and seemingly reasonable procedure for taking into account screening effects on the initial state of an electron undergoing radiative capture is to multiply the unscreened results for the radiative capture

probability amplitude by the ratio of the screened to unscreened initial-state wavefunctions, evaluated in the neighborhood of the origin.

The second effect of screening, the alteration in the structure of the Green's function, is expected to be quite small; this can be understood qualitatively from the following considerations (Martin and Glauber, 1958). Over the relatively small region defined by the range of the Green's function, the electron field is well approximated by the nuclear Coulomb field. Indeed, if the electronic charge cloud associated with the remaining atomic electrons did not penetrate this region at all, its external presence would simply result in a shift in the zero of energy and thus produce no physical effects. For all but the lowest-energy photons, the range of the Green's function is so small that penetration of the electronic charge cloud into the region defined by this range is not expected to be appreciable, and therefore no significant modification in the Green's function is expected. It should be emphasized, however, that this reasoning is not valid for photon energies near the binding energy, where the range of the Green's function becomes quite large and a more elaborate treatment of screening is required.

To establish in quantitative terms the accuracy of the simple approximation scheme of Martin and Glauber (1958), these authors carried out more extensive calculations in which the screened Coulomb potential was approximated by a Hulthen potential. The results of these calculations indicate that the above conclusions are quite well-founded. In particular, Martin and Glauber (1958) calculated the screening corrections for the $2p$ state of Fe to lowest order in the Hulthen parameter. The results were compared with unscreened results multiplied by the ratio of the screened to unscreened probability densities at the origin. At a photon energy equal to the K-shell binding energy in Fe, the difference between these two results was found to be ~20% (i.e., of order $Z\alpha$), while at a photon energy three times as large the difference is only ~2%. Thus it appears that, except at very low photon energies (in the immediate neighborhood of the K-shell binding energy), screening effects can be taken into account satisfactorily by simply multiplying the unscreened rate for radiative capture from the state α by the screening factor

$$S_\alpha = |\Phi_\alpha^{sc}(R_N)|^2 / |\Phi_\alpha(R_N)|^2, \tag{4.46}$$

where R_N is the nuclear radius.

From results of Brysk and Rose (1958) and available Hartree calculations, Martin and Glauber (1958) have constructed a graph of S_α vs Z for initial states of interest (see Fig. 36). It appears that the intensities of the IB spectra for radiative capture from the L shell are considerably reduced by screening effects and those for radiative capture from higher shells become insignificant.

If the intensities of the various IB spectra are normalized to a single K-capture event, or to a single electron-capture event, then only the ratios S_α/S_{1s} appear in the final formulae. To evaluate these ratios for the most important case, the L shell, results of Sec. II.B.2 can be used when a high degree of accuracy is desired.[23] The ratios are

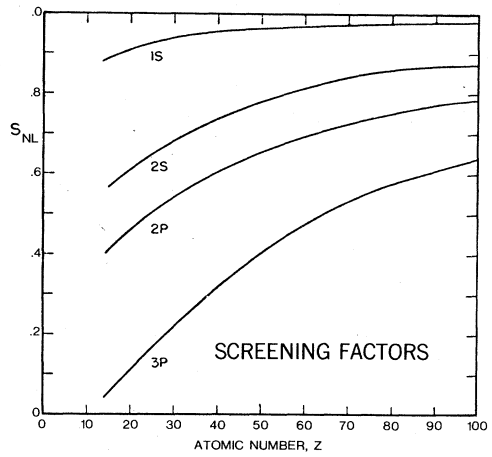

FIG. 36. Screening factors $s_{\alpha\alpha}$ according to Martin and Glauber (1958).

$$\frac{S_{2s}}{S_{1s}} = \left| \frac{G_K}{G_{L_1}} \frac{g_{L_1}}{g_K} \right|^2 \tag{4.47a}$$

and

$$\frac{S_{2p}}{S_{1s}} = \left| \frac{G_K}{F_{L_2}} \frac{f_{L_2}}{g_K} \right|^2 . \tag{4.47b}$$

Here, G_K, G_{L_1}, and F_{L_2} are the large components of the unscreened Dirac wavefunction for the $1s$, $2s$, and $2p$ states, respectively, evaluated at the nuclear radius of a hydrogenic atom. The large components are denoted by g_K, g_{L_1}, and f_{L_2}, respectively, when the effects of screening are included.

Plots of G_K, G_{L_1}, and F_{L_2} for a point nucleus and corrections for finite nuclear size are given by Brysk and Rose (1958) (finite-nuclear-size corrections to the L-shell screening ratios are always <1%).[24] As discussed in Sec. II.B.2 the ratios $(g_{L_1}/g_K)^2$ and $(f_{L_2}/g_{L_1})^2$ have been calculated by several authors; the most reliable results being those displayed in Table IX. These ratios were computed with a relativistic Hartree–Fock self-consistent potential with allowance for finite nuclear size.

The procedure described above is but one possible way in which screening effects can be treated. Alternatively, Zon (1971) has included screening effects by employing relativistic initial-state Coulomb wavefunctions with effective charges. These effective charges, as suggested by work on internal conversion, were taken to be $Z_{\text{eff}} = Z - \sigma$, with $\sigma_K = 0.3$, $\sigma_L = 3.5$, and $\sigma_M = 5$. Zon (1971) has

[23] As pointed out in Sec. II.B.2, the $(g_{L_1}/g_K)^2$ ratios given in Brysk and Rose (1958) deviate systematically from all other reported calculations on screened electron wavefunctions. However, these deviations, and the resulting uncertainties in Fig. 36, appear to be never greater than about 5–6%. The errors, of order $Z\alpha$, associated with the results of Glauber and Martin (1956) for the $2s, 2p, 3p$ spectra are always much larger (except for the special case of ^{4}Be). Thus the results displayed in Fig. 36 are more than adequate for present purposes and, as a convenience, will be used to determine all screening corrections in Sec. IV.B unless otherwise noted.

[24] An excellent summary of these results is given by Schopper (1966).

carried out several numerical calculations but does not compare his results with those obtained by the simpler procedure of Martin and Glauber (1958).

Exchange and overlap corrections. All results described so far, including screening corrections, are based on independent-particle approximations and take no account of exchange and overlap effects which result from the many-particle nature of the atom (see also Sec. II.E). Corrections for such effects have been applied to the Martin-Glauber theory by Persson and Koonin (1972), using a procedure analogous to that applied by Bahcall (1962) to L/K electron-capture ratios. The calculations of Persson and Koonin (1972) deal specifically with the electron-capturing nucleus ^{7}Be, but are easily generalized.

It is found that, for electron-capture decays of ^{7}Be to the 477-keV state of ^{7}Li, the predominant effect of exchange and overlap corrections is to increase the ratio of $2s$-state radiative capture to $1s$-state radiative capture w_{2s}/w_{1s} by a factor of 2.9. The ratio of the $1s$-state radiative capture rate to the total $(K+L)$ nonradiative capture rate $w_{1s}/(w_K+w_L)$ is decreased by 7%. However, the net effect on the ratio $(w_{1s}+w_{2s})/(w_K+w_L)$ is found to be negligibly small (<1%). Changes in the shape of the IB spectrum at energies above 50 keV are found to be negligible.

Calculations of overlap and exchange effects in radiative electron capture of ^{51}Cr and ^{54}Mn are reported by Koonin and Persson (1972), who find that w_{2s}/w_{1s} is increased by 15% over the Martin–Glauber predictions. This increase is canceled, however, by a similar increase in the corresponding ratio for nonradiative capture, so that the correction to the ratio $(w_{1s}+w_{2s})/(w_K+w_L)$ is again found to be insignificant (<0.5%).

3. IB correlation effects in allowed transitions

With the discovery of parity nonconservation in weak interactions, interest in radiative electron capture shifted to studies of those correlation effects whose existence requires a parity-violating interaction. Calculations on such phenomena were reported by Cutkosky (1957), Koh *et al.* (1957, 1962), Berestetskii (1958), Martin and Glauber (1958), Gandel'man (1959), Bloom and Uretsky (1960), and Timashev and Kaminskii (1960).

Cutkosky (1957) first showed that a two-component neutrino theory predicts that IB radiation will be circularly polarized. Terms of order $Z\alpha$ were neglected in Cutkosky's calculations, but a determination of the polarization of the IB associated with K capture, valid to all orders in $Z\alpha$, was reported shortly thereafter by Martin and Glauber (1958). Only the polarization of the $1s$-state contribution to the IB spectrum is considered in these papers, yet it is evident from the results of Sec. IV.A.2 that at low photon energies the contributions from L- and M-shell radiative capture must also be taken into account. For allowed transitions, this is easily accomplished using the theory of Glauber and Martin (1958). More elaborate calculations, based on a generalization of the Martin–Glauber theory, are reported by Zon (1971), who lists numerical results for ^{37}Ar.

The parity-nonconserving character of the weak interaction is also responsible for the existence of an anisotropy in the angular distribution of the IB radiation emitted from oriented nuclei, as may be inferred from the work of Cutkosky (1957). This makes IB angular-distribution studies of interest as a potential source of information on nuclear spin changes and the relative magnitudes of the electron-capture nuclear matrix elements. The angular distribution of the IB emitted from oriented nuclei during K capture was first calculated by Timashev and Kaminskii (1960) and by Koh *et al.* (1962), assuming a nonrelativistic description of the electronic motion and neglecting all Coulomb effects of the intermediate states of the electron. The results of these calculations are quite simple, but they have proved inadequate to explain the experimental data at low photon energies, where both intermediate-state Coulomb effects and the contributions from L- and M-shell radiative capture become important. More exact and extensive calculations, based on the work of Glauber and Martin, have been reported by Intemann (1971) and by Zon (1971).

While the existence of the IB correlation effects described above depends on the parity-nonconserving property of the weak interaction, a variety of other correlation phenomena exist which could arise even if parity were conserved. (From the point of view of testing weak-interaction theory, these phenomena are of little interest, but they can provide information on nuclear structure.) In particular, Koh *et al.* (1957, 1962) have studied the correlations between the direction of nuclear spin, the momentum of the IB photon, and the momentum of a subsequent nuclear γ ray, and have reported detailed results on the correlation between the directions of the IB photon and the nuclear γ ray. These calculations were, however, carried out for allowed and first-forbidden transitions and neglect Coulomb effects on the intermediate electron states; thus they are limited to high photon energies. More extensive calculations of this correlation function, based on a generalization of the work of Martin and Glauber (1958), have been reported by Zon (1971). This latter work includes a determination of the correlation between the directions of the IB photon and a subsequently emitted atomic x ray.

a. IB circular polarization

The polarization $P_\alpha(k)$ of the internal bremsstrahlung accompanying electron capture from the state α is defined as the difference in the intensities of the right- and left-circularly polarized radiation, divided by their sum:

$$P_\alpha(k)=\frac{dw_\alpha^{+1}-dw_\alpha^{-1}}{dw_\alpha^{+1}+dw_\alpha^{-1}}\,. \tag{4.48}$$

For $1s$-state radiative capture, the required expressions for the intensity of the polarized radiation are obtained from Eq. (4.34) by squaring and summing over all final states of the unobserved neutrino and over the spin states of the initial electron. The result for randomly oriented nuclei is

$$dw_{1s}^{s}(k)\propto[A_{1s}(k)+sB_{1s}(k)]^2,\quad (s=\pm1)\,.$$

The polarization of the IB accompanying $1s$-state capture is found to be

$$P_{1s}(k)=\frac{(A_{1s}+B_{1s})^2-(A_{1s}-B_{1s})^2}{(A_{1s}+B_{1s})^2+(A_{1s}-B_{1s})^2}=A_{1s}B_{1s}/R_{1s}. \qquad (4.49)$$

At low photon energies, the $1s$-state radiation is almost completely unpolarized since $B_{1s}(k)\to 0$ as $k\to 0$. At high energies, we have $A_{1s}=B_{1s}=1$, neglecting terms of order $Z\alpha$, and due to cancellation, $P_{1s}(k)=+1$ neglecting terms of order $(Z\alpha)^2$. More precisely, the high-energy form of $P_{1s}(k)$ is

$$P_{1s}(k)=1-(Z\alpha)^2\left\{\frac{\mu}{k}+2\left(1-\frac{1}{k}\right)\tan^{-1}\left(\frac{k}{\mu}\right)\right\}^2\Big/2k^2, \qquad (4.50)$$

which follows from Eq. (4.40).

The polarization of the $2s$-state radiation can be analyzed similarly, starting with Eq. (4.20). The final result has the same structure as Eq. (4.49) except that, in the approximation which underlies Eq. (4.20), $A_{2s}(k)=1$. Thus we have

$$P_{2s}(k)=B_{2s}/R_{2s}. \qquad (4.51)$$

While it is expected in the high-energy limit that $P_{2s}(k)=1-\mathcal{O}(Z\alpha)^2$, the results which follow from Eq. (4.20) are not sufficiently accurate to allow the determination of the coefficient of the $(Z\alpha)^2$ term. The low-energy limit of $P_{2s}(k)$ is easily obtained, however, by using the fact that $B_{2s}(0)=-\frac{3}{2}$. From this result it follows that $P_{2s}(0)=-\frac{12}{13}$.

To illustrate the above results, the functions A_{1s}, B_{1s}, B_{2s} and the resulting polarization functions have been evaluated for two nuclei of interest, viz. ^{37}Ar and ^{119}Sb (Figs. 37 and 38).

It is evident from Eqs. (4.29) and (4.30) that, when terms of order $Z\alpha$ are neglected, p-state radiation should be completely unpolarized. At low photon energies, where the p-state spectra dominate, one therefore expects an even greater reduction of the IB polarization than predicted by the function $P_{1s}(k)$. The overall polarization of the total IB radiation accompanying electron capture is

$$P(k)=\sum_{n=1}^{2}s_{ns}P_{ns}(k)dw_{ns}\Big/\sum_{\alpha}s_{\alpha}dw_{\alpha}, \qquad (4.52)$$

where the sum on α extends over $1s$, $2s$, $2p$, and $3p$ states.

b. Angular distribution of IB from oriented nuclei

When the initial nuclei are aligned, it is convenient to represent each by its polarization vector $P_M=\langle J_iM|\mathbf{J}|J_iM\rangle/J_i$, where $\mathbf{J}$ is the angular-momentum operator, and J_i, M are the angular-momentum eigenvalues which label the initial nuclear state. In this case, squaring Eq. (4.34) and summing over all final states of the neutrino, the spin states of the initial electron, and the final magnetic substates of the nucleus leads to the following result for $1s$-state radiative capture:

$$dw_{1s}^{s}(k)\propto(A_{1s}+sB_{1s})^2[1+sa_kP_M\cos\theta]. \qquad (4.53)$$

Here, θ is the angle between the vectors P_M and $\mathbf{k}$. The factor a_k vanishes for a pure Fermi transition, while for a pure Gamow–Teller transition we have

$$a_k=\begin{cases}-J_i/(J_i+1) & \text{if } J_f=J_i+1\\ 1/(J_i+1) & \text{if } J_f=J_i\\ 1 & \text{if } J_f=J_i-1,\end{cases} \qquad (4.54)$$

where J_f is the angular-momentum quantum number of the final nuclear state. For transitions in which both allowed electron-capture matrix elements are operative, a_k is given by

$$a_k=\left[\frac{\lambda^2|R|^2}{(J_i+1)}+\frac{\lambda J_i(R+R^*)}{[J_i(J_i+1)]^{1/2}}\right](1+\lambda^2|R|^2)^{-1} \qquad (4.55)$$

with

$$R=\langle f\|\sigma\|i\rangle/\langle f\|1\|i\rangle.$$

If the circular polarization s of the IB is measured, then the angular-distribution function has the simple form

$$W_{1s}(\theta,s)=1+sa_kP_M\cos\theta, \qquad (4.56)$$

whence the shape of the angular distribution is seen to be independent of the energy of the IB photon.

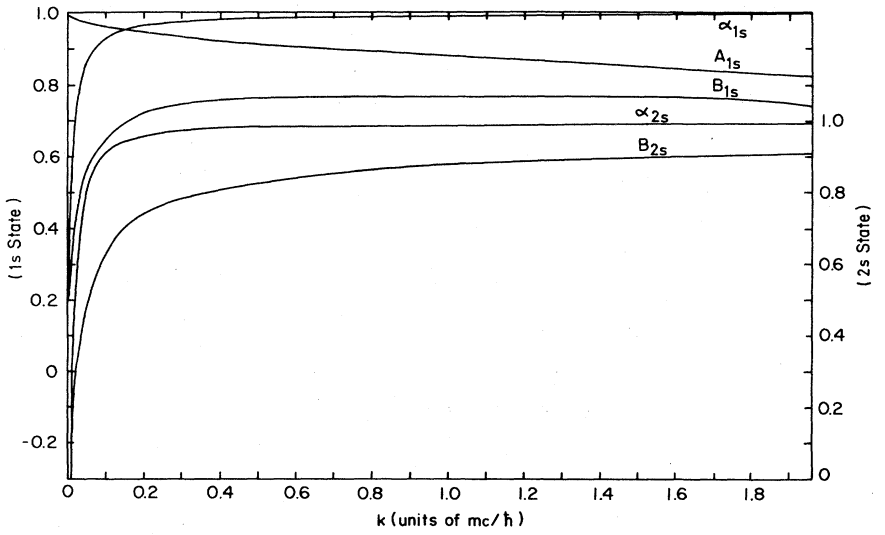

FIG. 37. Polarization and asymmetry functions, $P_{1s}(k)=\alpha_{1s}(k)$ and $P_{2s}(k)=\alpha_{2s}(k)$, and related functions for $Z=18$. The $1s$-state curves are deduced from the exact results of Martin and Glauber (1958) and Intemann (1971), the $2s$-state curves, from the results of Glauber and Martin (1956).

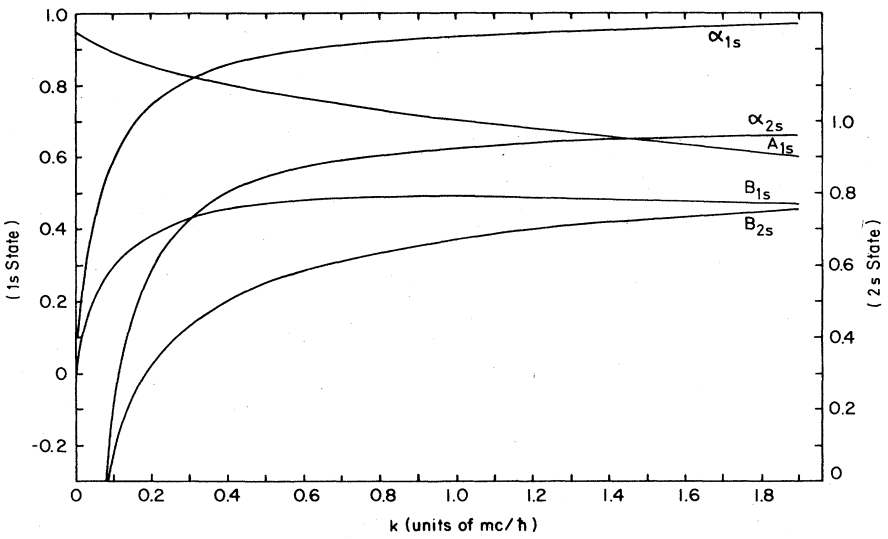

FIG. 38. Polarization and asymmetry functions, $P_{1s}(k) = \alpha_{1s}(k)$ and $P_{2s}(k) = \alpha_{2s}(k)$, and related functions for $Z = 51$. The $1s$-state curves are deduced from the exact results of Martin and Glauber (1958) and Intemann (1971), the $2s$-state curves, from the results of Glauber and Martin (1956).

If the photon polarization is not measured, Eq. (4.53) must be summed over $s = \pm 1$. This leads to an angular-distribution function of the form

$$W_{1s}(\theta) = 1 + \alpha_{1s}(k) a_k P_M \cos\theta \,. \tag{4.57}$$

The function $\alpha_{1s}(k)$ is defined by

$$\alpha_{1s}(k) = A_{1s} B_{1s} / R_{1s} \tag{4.58}$$

and is seen to be identical with the polarization function $P_{1s}(k)$ discussed earlier. Indeed, this one function is sufficient to account for the IB energy dependence of all $1s$-state capture correlations considered here.

The angular distribution of the IB radiation accompanying $2s$-state capture can be determined in a similar manner, starting with Eq. (4.20). It is found that the distribution function $W_{2s}(\theta, s)$ is identical with $W_{1s}(\theta, s)$. The function $W_{2s}(\theta)$ has the same general form as that for $1s$-state capture, viz.,

$$W_{2s}(\theta) = 1 + \alpha_{2s}(k) a_k P_M \cos\theta \,, \tag{4.59}$$

but $\alpha_{2s}(k)$ is defined as

$$\alpha_{2s}(k) = B_{2s} / R_{2s} \,, \tag{4.60}$$

describing the dependence of the angular-distribution function on the energy of the IB photon. Again we have $\alpha_{2s}(k) = P_{2s}(k)$.

With regard to p-state radiation, it has already been noted that the structure of Eq. (4.29) implies an isotropic distribution, i.e., $\alpha_{np}(k) = 0$. This result is expected to be valid only to a relative accuracy of order $Z\alpha$. Indeed, Zon (1971) reports that exact computer calculations for α_{np} show α_{2p} and α_{3p} to be small negative quantities.

The over-all angular-distribution function is given by

$$W(\theta) = \sum_\alpha s_\alpha dw_\alpha W_\alpha(\theta) \Big/ \sum_\alpha s_\alpha dw_\alpha$$

$$= 1 + A(k) a_k P_M \cos\theta \,, \tag{4.61}$$

with the over-all asymmetry function $A(k)$ defined by

$$A(k) = \sum_\beta s_\beta dw_\beta \alpha_\beta \Big/ \sum_\beta s_\beta dw_\beta \,. \tag{4.62}$$

In view of the equality of the asymmetry function and the polarization function for both s and p states, it follows that the over-all asymmetry function $A(k)$ is identical with the over-all polarization function $P(k)$ [Eq. (4.52)].

c. Correlation of IB and subsequent nuclear γ rays

The simplest type of decay scheme for which the directional correlation between an IB photon and a subsequent nuclear γ ray can be studied is one in which the radiative capture transition leads to an excited nuclear state $|N_f^*\rangle$ from which there is a single γ-ray mode for deexcitation, leading to the final nuclear state $|N_f\rangle$. To determine the correlation between the directions of emission of the IB and γ-ray photons, a knowledge of the radiative capture matrix element must be combined with results from the theory of nuclear angular correlations (Frauenfelder and Steffen, 1966). The required calculation is straightforward but employs much mathematical machinery from the theory of angular momentum (Edmonds, 1960) and will not be described here. Such calculations were first reported by Gandel'man (1959) for allowed transitions, and by Koh *et al.* (1962) for allowed and first-forbidden transitions. Although Coulomb effects on the intermediate electron states are neglected in these calculations, Zon (1971) has reported results of much more extensive calculations based on a generalization of the Martin–Glauber theory to radiative capture from arbitrary shells and for any order of forbiddenness of the electron-capture transition. Only for the case of allowed radiative K capture, however, has Zon's theory been worked out in complete detail, and we shall restrict our discussion to this particular case.

For allowed K-capture transitions, the radiative capture matrix element of Zon (1971) reduces to that of Martin and Glauber (1958). For this particular case, Zon's final results can be summarized as follows. For an IB quantum of circular polarization s and a nuclear γ quantum of circular polarization t, the directional correlation function is of the form

$$W_\gamma(\theta, s, t) \propto (A_{1s} + sB_{1s})^2$$

$$+ (t/\sqrt{3}) A_1 (LL' J_f J_f) b_k S (A_{1s} + sB_{1s})^2 \cos\theta \,, \tag{4.63}$$

where the quantum numbers J_f and J_{ff} refer to the angular momentum of the nuclear states $|N_f^*\rangle$ and $|N_f\rangle$, respectively, and θ is the angle between the directions of the two photons. The factor b_k vanishes for a pure Fermi transition, while for a pure Gamow–Teller transition it is

$$b_k = \begin{cases} [(J_f+1)/J_f]^{1/2} & \text{if } J_f = J_i + 1 \\ 1/[J_f(J_f+1)]^{1/2} & \text{if } J_f = J_i \\ -[J_f/(J_f+1)]^{1/2} & \text{if } J_f = J_i - 1 . \end{cases} \tag{4.64}$$

For transitions in which both electron-capture matrix elements are operative, we have

$$b_k = \left[\frac{\lambda^2|R|^2}{[J_f(J_f+1)]^{1/2}} + \lambda(R+R^*)\right](1+\lambda^2|R|^2)^{-1}. \tag{4.65}$$

The coefficient A_1, familiar from the theory of angular correlations, is defined by

$$A_1(LL'J_{ff}J_f) = [F_1(LLJ_{ff}J_f) + 2\delta F_1(LL'J_{ff}J_f) + \delta^2 F_1(L'L'J_{ff}J_f)](1+\delta^2)^{-1}, \tag{4.66}$$

where the angular-momentum and parity quantum numbers $L\pi$ and $L'\pi'$ characterize the multipolarities of the γ transition, and the ratio of the corresponding reduced matrix elements is $\delta = \langle J_{ff} \| L'\pi' \| J_f\rangle / \langle J_{ff} \| L\pi \| J_f\rangle$. For pure multipole radiation, we have $L' = L$ and $\pi' = \pi$. The F coefficients are defined by

$$F_1(LL'J_{ff}J_f) = (-1)^{J_{ff}+J_f-1}[(2L+1)(2L'+1)(2J_f+1)3]^{1/2} \times \begin{pmatrix} L & L' & 1 \\ 1 & -1 & 0 \end{pmatrix} \begin{Bmatrix} L & L' & 1 \\ J_f & J_f & J_{ff} \end{Bmatrix}, \tag{4.67}$$

where the standard designations ( ) and { } indicate Wigner $3j$ and $6j$ symbols.

It is immediately apparent from the form of Eq. (4.63) that the circular polarization of the γ-ray photon must be measured if one is to observe any correlation between the directions of the two photons. If the circular polarization of the IB photon is also measured, then the directional correlation function is

$$W_\gamma(\theta, s, t) = 1 + (ts/\sqrt{3})A_1(LL'J_{ff}J_f)b_k \cos\theta, \tag{4.68}$$

independent of the IB-photon energy. If the polarization of the IB photon is not measured, Eq. (4.63) must be summed over $s = \pm 1$. In this case, the directional correlation function is given by

$$W_\gamma(\theta, t) = 1 + (t/\sqrt{3})A_1(LL'J_{ff}J_f)b_k\alpha_{1s}(k)\cos\theta, \tag{4.69}$$

and shows a dependence on the energy of the IB photon characterized by the asymmetry function $\alpha_{1s}(k)$ previously discussed.

The above results are exact, but in the derivation of the IB-γ directional-correlation functions it is assumed that no forces act on the nucleus while it is in the intermediate state $|N_f^*\rangle$. Generally, this assumption is not well satisfied, because the hole in the atomic shell produces strong magnetic and inhomogeneous electric fields at the nucleus, leading to a perturbation of the directional correlations.

d. Correlations of IB and succeeding atomic x rays

The determination of the directional correlation function for an IB photon and a succeeding x-ray quantum requires a calculation which is essentially analogous to that of IB-photon–γ-ray directional correlations. Zon (1971) has carried out such a calculation and reported final formulas for the case of radiative K capture. For allowed transitions, these results can be summarized as follows.

For an IB quantum of circular polarization s and an atomic x-ray quantum of circular polarization t, the directional-correlation function is of the form

$$W_x(\theta, s, t) \propto (2J+1)(A_{1s} + sB_{1s})^2 + (-1)^{J+1/2}(ts/3)(A_{1s} + sB_{1s})^2 \cos\theta, \tag{4.70}$$

where θ is the angle between the directions of the two photons, and $J = \frac{1}{2}, \frac{3}{2}$ is the angular momentum of the atomic electron which fills the hole in the K shell.

Further results are parallel to those for the nuclear γ-ray case. For example, it is evident from Eq. (4.70) that, in order to observe a directional correlation between the two photons, the circular polarization of the x-ray photon must be measured. If the circular polarization of the IB photon is also measured, we have

$$W_x(\theta, s, t) = 1 + \frac{(-1)^{J+1/2}}{(2J+1)}\frac{ts}{3}\cos\theta, \tag{4.71}$$

and the directional correlation shows no dependence on the energy of the IB photon. If the polarization of the IB photon is not measured, we have

$$W_x(\theta, t) = 1 + \frac{(-1)^{J+1/2}}{(2J+1)}\frac{t}{3}\alpha_{1s}(k)\cos\theta, \tag{4.72}$$

and the correlation function again displays a dependence on the energy of the IB photon characterized by the asymmetry function $\alpha_{1s}(k)$.

4. IB spectra and correlation effects in forbidden transitions

Early attempts to formulate a theory of IB for forbidden transitions were made by Cutkosky (1954), Turovtsev and Shapiro (1954), Yukawa (1956), and Koh *et al.* (1957, 1962). Turovtsev and Shapiro calculated the radiative K-capture spectrum for first-forbidden transitions, assuming vector and tensor couplings, while Cutkosky derived the matrix element for radiative K capture for arbitrary coupling, neglecting terms strictly of order $Z\alpha$ or smaller and terms contributing only to third- or higher-order transitions. Cutkosky's principal result was a theorem, often referred to as the "Cutkosky rule," which relates the spectra and angular correlations of the K-capture IB to the spectra and angular correlations of positrons. Basically, these calculations are extensions of the work of Morrison and Schiff (1940) to forbidden transitions. Yukawa (1956) made an attempt to include relativistic and Coulomb effects in the calculation of allowed and first-forbidden K-capture IB spectra. The formulas he obtained proved to be so complicated that this work has never led to useful results. Koh *et al.* (1957, 1962) first reported correlation studies for first-forbidden transitions;

Coulomb effects were neglected in these calculations.

The modern theory of radiative electron capture in forbidden transitions is due to Zon and Rapoport (1968), who developed a generalization of the theory of Martin and Glauber (1958) to transitions of arbitrary order of forbiddenness. They also derived general formulas for the IB energy spectra. For K capture, detailed results were obtained. Zon (1971) developed this theory further for radiative capture from an arbitrary atomic shell, derived general formulas for various correlation and polarization effects, and obtained detailed results for the case of K capture.

The theory of Zon and Rapoport (1968) starts from Eqs. (4.9) and (4.10) for the radiative capture matrix element and transition rate. In order to evaluate the matrix element (4.9) exactly, including relativistic and Coulomb effects to all orders in $Z\alpha$, Zon and Rapoport first decompose and simplify it by introducing the irreducible tensor operators and the second-order Dirac–Coulomb Green's function of Martin and Glauber. This decomposition makes the angular-momentum dependence of the transition amplitude explicit. Integration over the angular coordinates is then completed through extensive use of the methods of the theory of angular momentum.

In evaluating the transition amplitude, Zon and Rapoport introduce the Konopinski–Uhlenbeck approximation,

$$\int_0^{R_N} dr\, r^{\lambda_L} \cdots \approx R_N^{\lambda_L - L} \int_0^{R_N} dr\, r^L ,$$

where $\lambda_L = (L^2 - a^2)^{1/2}$, and the ξ approximation which is based on the assumption $(Q_{\mathrm{EC}} - 1)R_N \ll Z\alpha$, a condition that is always well-satisfied when competing positron emission is not energetically possible. Under only these approximations, Zon and Rapoport obtain a general expression for the transition rate for radiative electron capture from an arbitrary shell. The form of the result reveals that for radiative electron capture in the ξ approximation, just as in β decay, nonunique forbidden spectra have the same shape as the unique spectra of the next-lower order of forbiddenness.

Only for K capture do Zon and Rapoport carry their calculations to completion. For capture from higher shells, the theory is developed further by Zon (1971), but the resulting expressions prove to be too complicated to permit exact analytic evaluation or even the development of expressions that are correct to first order in $Z\alpha$. Indeed, the only detailed results which have so far been reported are those contained in the table of Zon (1973) for the L- and M-shell IB spectra associated with the first-forbidden unique transition in ^{41}Ca; these results were derived through completely numerical procedures.

Zon and Rapoport's transition rate for radiative K capture can be summarized as follows. Assuming the polarization of the IB radiation is not observed, the transition rate can be written

$$dw_{1s} = \frac{8\alpha}{\pi} \left| \langle \Phi_{1s} \rangle_\Omega \right|^2 k (q_{1s} - k)^2 F_{1s}(k)\, dk. \tag{4.73}$$

The form factor $F_{1s}(k)$ is defined in terms of two correction factors, $R_{1s}^{(1)}(k)$ and $R_{1s}^{(2)}(k)$, and the appropriate combination of nuclear matrix elements $R_{Nj_\nu}^{\Lambda}$:

$$F_{1s}(k) = \sum_{\Lambda N j_\nu} (2\mu R_N)^{2(\lambda_N - \lambda_1) - 2(N-1)} \left[\frac{2^{N-1}(N-1)!}{(2j_\nu)!!\,(2N-1)!} \right]^2 \times \left| R_{Nj_\nu}^{\Lambda} \right|^2 R_{1s}^{(N)} (q_{1s} - k)^{2j_\nu - 1} k^{2N-2}. \tag{4.74}$$

Here, R_N is the nuclear radius, and λ_N equals $(N^2 - a^2)^{1/2}$. The quantities $R_{Nj_\nu}^{\Lambda}$, for all contributing values of Λ, N, and j_ν, have been tabulated by Zon and Rapoport for up to third-forbidden transitions (Table XXV). The correction factors $R_{1s}^{(N)}$ are defined in terms of the more fundamental quantities $A_{1s}^{N,M}$ and $B_{1s}^{N,M}$, which are generalizations of the functions A_{1s} and B_{1s} of Martin and Glauber (1958):

$$R_{1s}^{(N)} = \frac{1}{4N} \left[(N-1)\left(\left| A_{1s}^{N,N-1} \right|^2 + \left| B_{1s}^{N,N-1} \right|^2 \right) + (N+1)\left(\left| A_{1s}^{N,N} \right|^2 + \left| B_{1s}^{N,N} \right|^2 \right) \right]. \tag{4.75}$$

To specify the transition rate, formulae for A and B are required. Zon and Rapoport (1968) have developed exact general expressions for these functions, but these formulae contain a large number of integrals involving Whittaker functions, none of which can be evaluated exactly analytically.

For moderately light nuclei, it may be sufficient to expand the above-mentioned integrals in powers of $Z\alpha$ and thereby evaluate A and B to first order in $Z\alpha$. Such calculations are reported by Zon and Rapoport (1968) with the result

$$A_{1s}^{N,M}(B_{1s}^{N,M}) = 1 - Z\alpha \sum_{n=0} \left[a_n \left(\frac{\mu}{k} \right) + b_n \tan^{-1}\left(\frac{k}{\mu} \right) \right] \left(\frac{1}{k} \right)^n . \tag{4.76}$$

The coefficients a_n and b_n are listed in Table XXVI. At the present time, Eq. (4.76) is the only formula available for the determination of A and B. Unfortunately, even for light elements these formulae are not valid for low k. The nature of the expansion underlying Eq. (4.76) is such that these results are expected to break down for $k \lesssim Z\alpha$. For the special case $k \to 0$, however, A and B can be evaluated exactly to all order in $Z\alpha$. The $k \to 0$ results, listed in the last column of Table XXVI, are valuable for estimating the low-energy behavior of A and B and to test numerical procedures for the exact evaluation of A and B for arbitrary k.

In examining the predicted IB spectra for K capture in further detail, we restrict our discussion to first-forbidden transitions.

a. Nonunique first-forbidden transitions

In the ξ approximation, the K-capture IB spectrum of a nonunique first-forbidden transition is predicted to have the allowed shape. Indeed, when the above results are evaluated for this case and normalized by the corresponding nonradiative K-capture rate, exactly the same result is obtained as for the allowed case

$$\frac{dw_{1s}}{w_K} = \frac{\alpha}{\pi} \frac{k (q_{1s} - k)^2}{q_{1s}^2} R_{1s}^{(1)}\, dk, \tag{4.77}$$

where $R_{1s}^{(1)}$ is easily identified as the function R_{1s} of Martin and Glauber (1958), defined by Eq. (4.37) and displayed in Fig. 32.

TABLE XXV. Nuclear matrix elements $R^{\Lambda}_{N j_\nu}$ [Eq. (4.74)], after Zon and Rapoport (1968).

Type of transition	Λ	N	j_ν	$R^{\Lambda}_{N j_\nu}$	$\lvert\Delta J\rvert$	$\Delta\pi$
Allowed	0	1	1/2	$C_v \int T_{000}$	0	No
	1	1	1/2	$-C_A \int T_{101}\gamma_5$	0.1 except $0\to 0$	
1st-forbidden nonunique	0	1	1/2	$C_A \int T_{000}\gamma_5 - \frac{Z\alpha}{1+\lambda_1} C_A \int T_{011}\gamma_5$	0	Yes
	1	1	1/2	$-C_v \int T_{101} - \frac{1}{\sqrt{3}} \frac{Z\alpha}{1+\lambda_1}\left(C_v \int T_{110} + \sqrt{2}\, C_A \int T_{111}\gamma_5\right)$	0.1 except $0\to 0$	
1st-forbidden unique	2	2	1/2	$(-1)^N i C_A \int r T_{211}\gamma_5$	2	
	2	1	3/2			
2nd-forbidden nonunique	2	2	1/2	$(-1)^{N_i}\left[C_v \int r T_{211} + \frac{1}{\sqrt{5}} \frac{Z\alpha}{N+\lambda_N} \times\left(\sqrt{2}\, C_v \int r T_{220} + \sqrt{3}\, C_A \int r T_{221}\gamma_5\right)\right]$	2	No
	2	1	3/2			
2nd-forbidden unique	3	3	1/2	$(-1)^{N+1}\left[1 + \frac{1}{2}(\sqrt{6/5} - 1)(1 - (-1)^{N+2j_\nu})\right] C_A \int r^2 T_{321}\gamma_5$	3	
	3	2	3/2			
	3	1	5/2			
3rd-forbidden nonunique	3	3	1/2	$(-1)^{N+1}\left[1 + \frac{1}{2}(\sqrt{6/5} - 1)(1 - (-1)^{N+2j_\nu})\right]$	3	Yes
	3	2	3/2			
	3	1	5/2	$\times\left[C_v \int r^2 T_{321} + \frac{1}{\sqrt{7}} \frac{Z\alpha}{N+\lambda_N}\left(\sqrt{3}\, C_v \int r^2 T_{330} + 2 C_A \int r^2 T_{331}\gamma_5\right)\right]$		

TABLE XXVI. Coefficients a_n and b_n [Eq. (4.76)], after Zon and Rapoport (1968), including corrections by Zon (1971).

	a_0	a_1	a_2	a_3	b_0	b_1	b_2	b_3	b_4	$k\to 0$
A^{11}_{1s}	1				2	−2				$\frac{1}{2}(1+\lambda_1)\left[1 - \frac{1}{3}\left(\frac{Z\alpha}{1+\lambda_1}\right)^2\right]$
B^{11}_{1s}	1	1			2		−2			0
A^{21}_{1s}	7/2	−9/4			2	−5	9/2			$-\frac{6}{1+\lambda_1} \frac{2+\lambda_2}{\Gamma(1+2\lambda_2)} \Gamma(\lambda_2-\lambda_1) \times \Gamma(\lambda_2+\lambda_1+1)\,\Gamma(\lambda_1+2-\lambda_2)$
B^{21}_{1s}	7/4	−19/4	4		2	−7	29/2	−8		$\Theta(1/k)$
A^{22}_{1s}	7/4	−5/4			2	−3	5/2			0
B^{22}_{1s}	7/4	3/4	−3		2	−1	−7/2	6		0
A^{32}_{1s}	13/6	−35/6	5		2	−8	15	−10		$-\frac{4}{1+\lambda_1} \frac{3+\lambda_3}{\Gamma(1+2\lambda_3)} \Gamma(\lambda_3-\lambda_1) \times \Gamma(\lambda_3+\lambda_1+2)\,\Gamma(\lambda_1+3-\lambda_2)$
B^{32}_{1s}	13/6	−22/33	1/2	−9	2	−10	31	−37	18	$\Theta(1/k)$
A^{33}_{1s}	13/6	−17/6	2		2	−4	7	−4		0
B^{33}_{1s}	13/6	−1/3	−6	15/2	2	−2	−3	17	−15	0

b. Unique first-forbidden transitions

In unique forbidden transitions, only one nuclear matrix element contributes and the ξ approximation becomes irrelevant. For unique first-forbidden electron capture, the radiative transition rate normalized by the corresponding nonradiative K-capture rate is

$$\frac{dw_{1s}}{w_K} = \frac{\alpha}{\pi}\frac{k\,(q_{1s}-k)^2}{q_{1s}^2} \times\left[R_{1s}^{(1)}\left(1-\frac{k}{q_{1s}}\right)^2+(2\mu R_N)^{2(\lambda_2-\lambda_1)-2}R_{1s}^{(2)}\left(\frac{k}{q_{1s}}\right)^2\right]dk. \tag{4.78}$$

The factor in the brackets replaces the function $R_{1s}^{(1)}$ which appears in the allowed result.

While the factor $R_{1s}^{(1)}$ has been evaluated exactly numerically and in several analytic approximations, this has not been done for $R_{1s}^{(2)}$. The only available basis for the evaluation of $R_{1s}^{(2)}$ is Eq. (4.76), from which $R_{1s}^{(2)}$ can be calculated to first order in $Z\alpha$, with results only valid for $k \gtrsim Z\alpha$. For $k \to 0$, it follows from Table XXVI that $R_{1s}^{(2)} \propto 1/k^2$. Thus it may be expected that $R_{1s}^{(2)}$ will contribute substantially to the determination of the IB spectrum at all photon energies. Little is therefore gained by evaluating $R_{1s}^{(1)}$ to any greater accuracy than $R_{1s}^{(2)}$. To illustrate the behavior of the correction factors, we have evaluated the functions $R_{1s}^{(1)}$ and $R_{1s}^{(2)}$ to first order in $Z\alpha$, using Eqs. (4.75) and (4.76), for two atomic numbers (Fig. 39).

It is of interest to consider the limit $Z \to 0$, corresponding to the neglect of Coulomb effects on the intermediate electron states and the momentum of the initial electron. In this limit, $\lambda_N = N, R_{1s}^{(1)} = R_{1s}^{(2)} = 1$, and Eq. (4.78) is simplified to

$$\left(\frac{dw_{1s}}{w_K}\right)_{CF} = \frac{\alpha}{\pi}\frac{k(q_{1s}-k)^2}{q_{1s}^2}\left[\left(1-\frac{k}{q_{1s}}\right)^2+\left(\frac{k}{q_{1s}}\right)^2\right]dk. \tag{4.79}$$

This result can also be obtained by extending the calculations of Morrison and Schiff (1940) to unique first-forbidden transitions. Equation (4.79) is interesting because of its simplicity but is not expected to be very accurate, although it does describe the general shape of the IB spectrum. The expression is useful for estimating the integrated intensity over any given portion of the spectrum, providing an upper bound.

In order to assess the importance of Coulomb effects in unique first-forbidden transitions and to illustrate the difference between allowed and forbidden shapes, we have plotted several different predictions for the K-capture IB spectrum of ^{41}Ca in Fig. 40.

The two Morrison-and-Schiff curves, labeled MS-A and MS-F, illustrate the basic differences in spectral shape between allowed and first-forbidden unique transitions. The behavior of the Zon-Rapoport (ZR) result at $k > Z\alpha$ suggests that, for unique first-forbidden transitions, the main effect resulting from the inclusion of Coulomb effects is an overall reduction in the intensity of the IB spectrum, similar to that found in the allowed case.

B. Experiments

Experimental studies of the radiative capture process are valuable for providing information on electron-capture decay, analogous to the information on β decay derived from the study of β spectra. The energy spectrum and the intensity of internal-bremsstrahlung (IB) photons provide a measure of the total energy release and the change of spin and parity in the decay. Experiments on the circular polarization and on various angular correlations provide basic information on weak interaction and nuclear structure. Furthermore, bremsstrahlung experiments may yield supplementary data for the characterization of nuclear decay schemes and for the determination of capture ratios from various subshells.

Precise experimental investigations of radiative electron capture do, however, require rather complicated techniques for experiment and analysis, due to the very low intensity ($\sim 10^{-4}$ photons per capture event) and the continuous nature of the IB spectra. The interpretation of experimental results is made difficult by the fact that electrons captured from different atomic subshells contribute to the emitted radiation.

Much effort has been devoted to IB experiments during the last thirty years. Critical reviews were compiled by Zylicz (1968) and Kádár (1972), and to a lesser extent

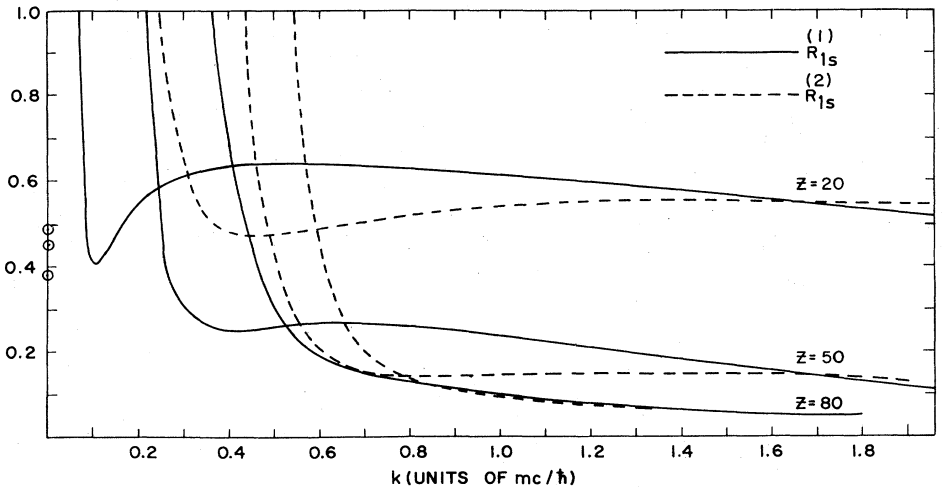

FIG. 39. Relativistic correction factors $R_{1s}^{(1)}(k)$ and $R_{1s}^{(2)}(k)$, according to Zon and Rapoport (1968), for several atomic numbers. The function $R_{1s}^{(1)}$ is the same as R_{1s} of Martin and Glauber (1958); it has been evaluated using the high-k approximation [Eqs. (4.40) or (4.76)], $R_{1s}^{(2)}$ has also been evaluated in the high-k approximation [Eq. (4.76)]. The three points shown on the ordinate represent the results of an exact evaluation of $R_{1s}^{(1)}(0)$, using Eq. (4.41) or Table XXVI, for $Z = 20, 50, 80$ (in descending order).

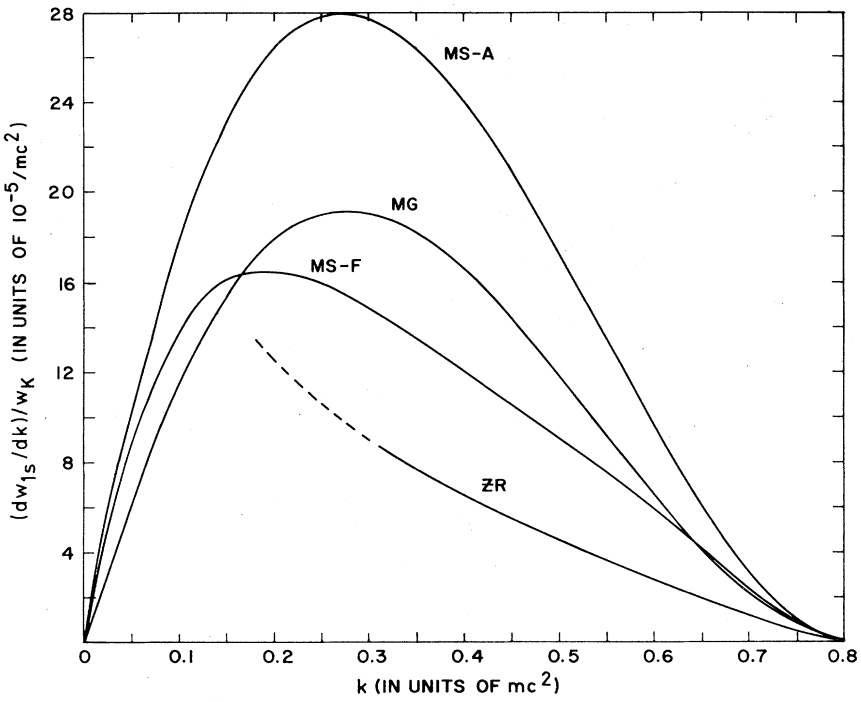

FIG. 40. Comparison of theoretical results for the K-capture IB spectrum for ^{41}Ca. The theories of Morrison and Schiff (1941) and Martin and Glauber (1958) for an allowed transition are represented by the curves MS-A and MG, respectively. For a unique first-forbidden transition, the corresponding curves are those labeled MS-F and ZR, deduced from Eq. (4.79) and the results of Zon and Rapoport (1968), evaluated to first order in $Z\alpha$.

by Bouchez and Depommier (1965), Petterson (1965), Schopper (1966), and Berényi (1968). Considerable progress has been achieved since, especially in the development of experimental techniques.

The low probability of radiative capture makes its observation sensitive to interference from other electromagnetic radiation. Expecially nuclear γ rays, annihilation radiation, and x rays emitted in the course of radioactive decay can considerably limit the energy range of an IB measurement and distort the measured IB pulse-height spectrum through pileup and summing effects. The measurement of coincidences between such primary radiation and the rare IB photons requires sophisticated techniques. In decays with competing β^+ or β^- branches or with highly converted γ transitions, corrections may be required for other types of electromagnetic radiation, comparable in intensity with IB: (i) internal bremsstrahlung accompanying β^+ or β^- decays, (ii) external bremsstrahlung emitted during absorption of β particles or conversion electrons in the source or surrounding materials, and (iii) continuously distributed annihilation radiation from positron annihilation in flight. In view of the large number of possible interfering effects, it is not surprising that IB measurements performed up to now have been restricted to electron-capture transitions in simple decay schemes. In most of the many nuclei decaying by electron capture, radiative capture has not yet been investigated.

It is also evident that IB experiments are very sensitive to small amounts of γ-ray emitting impurities in the sources. Experimental results therefore are only reliable if the source material is carefully checked and purified if necessary to remove spurious contaminates. Impurity checks of the required sensitivity were hardly possible before the advent of high-resolution Ge(Li) spectrometers, whence older experimental results must be regarded with reservations.

On reviewing the experimental literature, it appears that most measurements of IB spectra have been performed only to derive electron-capture transition energies from the IB end-point energies. This procedure was initiated by the early theory of Morrison and Schiff (1940) and Jauch's proposition to linearize IB spectra in a way that resembles the construction of Kurie plots for β spectra (Jauch, 1951; Bell *et al.*, 1952). For this purpose, most IB spectra were measured without normalization to the electron-capture rate. These shape measurements qualitatively confirmed the spectral shapes predicted by theory for s- and p-type radiation; in the case of forbidden decays, they yielded an estimate of the relative abundance of detour transitions. Measurements of spectral shapes alone, however, are not adequate for a detailed test of modern IB theory (Martin and Glauber, 1958; Intemann, 1971): as shown in Sec. IV.A, relativistic and Coulomb effects, screening, exchange and overlap influence the absolute IB yield, while affecting spectral shapes only slightly. Absolute IB measurements are, however, scarce. Some early results exist, of poor accuracy, pertaining to ground-state transitions; a few results on decays that include γ transitions were obtained recently.

In Sec. IV.B.1–IV.B.2, we have compiled the available experimental material and classified the techniques employed in the measurement of *normalized IB spectra* associated with different decay schemes. We do, however, frequently refer to incomplete studies and list all experiments known to us, to provide a guide for accurate future investigations.

1. Experiments on total IB spectra

An IB spectrum that is not measured in coincidence with x rays or Auger electrons constitutes the *total* spectrum dw_{IB}, which is a superposition of partial spectra dw_{nl} due to electron capture from different atomic states nl. This spectrum is mainly determined by s radiation for energies above $\sim Z\alpha$ (in units of mc^2) and by p radiation at lower energies; contributions from the innermost 1s and 2p shells dominate.

Experimental techniques applicable to the determination of total spectra can be divided broadly into two categories: single-spectrum methods and coincidence methods. In single-spectrum methods, IB spectra are measured relative to other emitted radiation that can be normalized to the ordinary capture rate. Measurements in coincidence with γ rays or conversion electrons permit separation of the IB spectra associated with individual electron-capture branches in a given decay.

In Table XXVII, we list published experiments on total IB spectra and indicate what methods and spectrometers were used and what quantities were deduced. A somewhat more detailed description of experimental methods follows.

a. Spectrometry of IB and of x rays and Auger electrons

Total IB spectra can most advantageously be observed in pure ground-state transitions and in decays that feed only low-energy transitions. Table XXVII shows that numerous total IB measurements have been performed on such simple decays, viz., on ^{37}Ar, ^{41}Ca, ^{49}V, ^{55}Fe, ^{71}Ge, ^{119}Sb, ^{125}I, ^{131}Cs, ^{145}Sm, ^{159}Dy, ^{165}Er, ^{181}W, and ^{193}Pt. NaI(Tl) and Ge(Li) spectrometers have been used. In cases in which the electron-capture transition energy is high compared with the K x-ray or γ-ray energy, a large fraction of the IB spectrum can be measured. Counting problems produced by the much higher x-ray or γ-ray rates can be avoided by placing suitable absorbers between source and spectrometer. For example, Fig. 41 shows IB pulse-height spectra of ^{131}Ca recorded with a NaI(Tl) spectrometer, a variety of Cu absorbers having been interposed (Saraf, 1954a). The procedure fails for transition energies not far above the K x-ray energy; in such cases, pileup from the K x-ray pulses strongly affects the IB spectrum. Methods for pileup reduction and correction are described below.

In most cases listed in Table XXVII, only IB spectral shapes were measured, and the accuracy is generally poor. Precise shape determinations with different types of NaI(Tl) spectrometers have been performed on ^{55}Fe (Berényi *et al.*, 1965b), and on the forbidden spectra from ^{36}Cl (Berényi *et al.*, 1965a, b; Smirnov and Batkin, 1973) and ^{59}Ni (Schmorak, 1963). Only recently were Ge(Li) spectrometers used, resulting in accurate shape measurements on ^{41}Ca (Mysl̆ek *et al.*, 1973) and ^{59}Ni (Berényi *et al.*, 1976) and on the IB spectrum from higher shells only in ^{193}Pr (Hopke and Naumann, 1969).

To obtain normalized IB spectra, the ordinary K-capture rate w_K must be determined from separate measurements of the K x-ray or K Auger-electron emission rates. Normalized IB spectra have been determined in only a few cases: for ^{37}Ar (Saraf, 1956), ^{55}Fe (Michalowicz, 1953; Saraf, 1956), ^{71}Ge (Bisi *et al.*, 1955a), ^{119}Sb (Olsen *et al.*, 1957), ^{131}Cs (Michalowicz, 1956), ^{145}Sm (Sujkowski *et al.*, 1968), ^{159}Dy (Sujkowski *et al.*, 1965), and ^{165}Er (Zylicz *et al.*, 1963; Sujkowski *et al.*, 1965). All these workers used NaI(Tl) crystals to detect the K x rays, with the exception of Saraf (1956), who applied a low-geometry proportional counter for the K x rays in ^{55}Fe and used internal gas counting to determine the K Auger-electron rate from ^{37}Ar. In the cases of ^{145}Sm and ^{159}Dy, the K x rays could not be resolved from low-energy γ rays, and decay-scheme corrections were applied. The accuracy of these early normalized IB spectra is generally poor (rarely better than 50%); considerable improvements would be possible today (see Sec. III). New measurements of total IB spectra would be of great value, especially for pure ground-state transitions which are listed in Table XXVIII.

b. IB and γ-ray spectrometry

For decays that involve emission of energetic γ rays, the measurement of total IB spectra is much more complicated. On the other hand, the γ rays make it possible to normalize the IB spectra, independently of fluorescence yields. If no IB–γ coincidences are measured, the available energy range is generally limited to energies above the highest γ energy. These measurements depend strongly on the details of the decay scheme, such as γ and electron-capture energies and branching ratios, and internal-conversion coefficients.

To date, IB and γ spectroscopy has only been applied to relatively simple decays, such as that of ^{7}Be (Mutterer, 1973b), ^{51}Cr (Bisi *et al.*, 1955b; Cohen and Ofer, 1955; Van der Kooi and Van der Bold, 1956; Ofer and Wiener, 1957; Murty and Jnanananda, 1967; Ribordy and Huber, 1970; and Mutterer, 1973a), and ^{113}Sn (Phillips and Hopkins, 1960). The isotopes ^{7}Be and ^{51}Cr have favorable decay schemes for this type of measurement. Both nuclides decay by two electron-capture branches, $\sim 90\%$ to the ground state and $\sim 10\%$ to an excited state with an energy of $\sim Q_{EC}/2$. Thus a large fraction of the IB spectrum associated with the ground-state branch can be measured without interference from the second electron-capture branch. A single γ spectrometer can be used to determine dw_{IB} relative to the γ emission rate. In order to normalize dw_{IB} to the ground-state electron-capture rate, the γ branching ratio $P_\gamma = N_\gamma/N_0$ is found precisely from measurements of the disintegration rate N_0 through 4π (x-ray, Auger)–γ coincidence counting, and of the γ rate N_γ by integral γ counting (Mutterer, 1971; De Roost and Lagoutine, 1973).

Above the γ-ray energy, the IB spectrum must be corrected for γ-ray pileup. In early measurements on ^{51}Cr and ^{113}Sn, NaI(Tl) spectrometers were used. With these, poor resolution and long pulse rise times cause the pileup spectra to be smeared out (Waibel, 1969, 1970) and it is not clear whether the measured IB spectra are free of pileup distortions. These measurements were considerably refined by Ribordy and Huber (1970) and Mutterer (1973a,b) who used Ge(Li) spectrometers with electronic pileup-rejection systems. Such systems prevent pileup of pulses spaced by ≥ 100 ns and can reduce total pileup by an order of magnitude. Fur-

TABLE XXVII. Experiments on total IB spectra.

Z	Elements	A	Final state (keV)	$J_i^\pi - J_f^\pi$	E_{EC} [a] (keV)	Deduced quantities E_{EC} (keV) [b]	Others [c]	Spectrometer	Method [d]	References
4	Be	7	0	$\frac{3}{2}^- - \frac{3}{2}^-$	861.75 ±0.09	851 ±12	I_{IB}, R_{eff}	Ge(Li)	IB/γ	Mutterer (1973b, c)
			477.6	$\frac{3}{2}^- - \frac{1}{2}^-$	384.1 ±0.1	395 ±25	I_{IB}	NaI	IB–γ-coinc.	Lancman (1971b)
						388 ±8	I_{IB}	NaI	IB–γ-coinc.	Persson (1972)
17	Cl	36	0	$2^+ - 0^+$	1144.1 ±1.7	1170 ±40		NaI		Dougan (1962)
						1162 ±45		NaI		Berényi (1962, 63b)
						1178 ±15		NaI		Lipnik (1964)
						1158 ±18		NaI		Berényi (1965a, b)
						1141 ±8	R_{eff}, DT	NaI		Smirnov (1973)
18	A	37	0	$\frac{3}{2}^+ - \frac{3}{2}^+$	814.1 ±0.6	818 ±15		NaI		Anderson (1952, 53)
						818 ±20		NaI		Emmerich (1954)
								NaI		Lindqvist (1955)
							I_{IB}	NaI	IB/K-Auger	Saraf (1956)
20	Ca	41	0	$\frac{7}{2}^- - \frac{3}{2}^+$	421.2 ±0.5		I_{IB}, R_{eff}	Ge(Li)	IB/N_0	Mysłek (1973)
23	V	49	0	$\frac{7}{2}^- - \frac{7}{2}^-$	601.2 ±1.0	621 ±10		NaI		Hayward (1956)
24	Cr	51	0	$\frac{7}{2}^- - \frac{7}{2}^-$	751.4 ±0.9	756 ±5		NaI		Bisi (1955b)
						786 ±50	P_γ from I_{IB}	NaI	IB/γ	Cohen (1955)
						752 ±22		NaI		Van der Kooi (1956)
						730 ±20	P_γ from I_{IB}	NaI	IB/γ	Ofer (1957)
						794 ±60	P_γ from I_{IB}	NaI	IB/γ	Murty (1967)
						748 ±14	P_γ from I_{IB}	Ge(Li)	IB/γ	Ribordy (1970)
						760 ±15	I_{IB}, R_{eff}	Ge(Li)	IB/γ	Mutterer (1973a, c)
			320.1	$\frac{7}{2}^- - \frac{5}{2}^-$	431.1 ±1.0	429 ±16	I_{IB}	NaI	IB–γ-coinc.	Koonin (1972)
25	Mn	54	835.3	$3^+ - 2^+$	540.1 ±3.6	512 ±25	I_{IB}	NaI	IB–γ-coinc.	Lancman (1969)
						639 ±100	I_{IB}	NaI	IB–γ-coinc.	Kádár (1970)
						518 ±8	I_{IB}	NaI	IB–γ-coinc.	Koonin (1972)
26	Fe	55	0	$\frac{3}{2}^- - \frac{5}{2}^-$	231.7 ±0.7	~150		GM-count.		Bradt (1946)
						212 ±10		NaI		Maeder (1951)
						212 ±20		NaI		Bell (1952)
						222 ±10	I_{IB}	NaI	IB/Kx	Michalovicz (1953)
						227		NaI		Madansky (1954)
						232 ±10		NaI		Emmerich (1954)
							I_{IB}	NaI	IB/Kx	Saraf (1956)
						227 ±10	I_{IB}	NaI	IB/Kx	Biavati (1959, 62)
						224 ±4	R_{eff}	NaI		Berényi (1965b)
						248 ±20		NaI		Raj (1969)
27	Co	57	136.3	$\frac{7}{2}^- - \frac{5}{2}^-$	700.4 ±0.7	434 ±30		NaI	IB–γ-coinc.	Jung (1956)
						674 ±30	I_{IB}	NaI	IB–γ-coinc.	Lancman (1971a)
28	Ni	59	0	$\frac{3}{2}^- - \frac{7}{2}^-$	1073.1 ±1.1	1073 ±30		NaI		Emmerich (1954)
							I_{IB}	NaI	IB/Kx	Saraf (1956)
								NaI		Hayashi (1960)
							DT	NaI		Schmorak (1963)
						1075.1 ±1.3	DT	NaI		Berényi (1976)

TABLE XXVII. *(Continued)*

Z	Elements	A	Final state (keV)	$J_i^\pi - J_f^\pi$	E [a] (keV)	Deduced quantities E (keV) [b]	Others [c]	Spectrometer	Method [d]	References
32	Ge	71	0	$\frac{1}{2}^- - \frac{3}{2}^-$	235.1 ±1.7	236 ±12		NaI		Saraf (1953)
							I_{IB}	NaI	IB/Kx	Saraf (1954b)
						237 ±5		NaI		Langevin (1954d)
						231 ±3	I_{IB}	NaI	IB/Kx	Bisi (1955a)
46	Pd	103	39.7	$\frac{5}{2}^+ - \frac{7}{2}^+$	513 ±27	517^{+27}_{-12}		NaI		Rietjens (1954)
50	Sn	113	391.0	$\frac{1}{2}^+ - \frac{1}{2}^-$	634 ±14	930 ±300		NaI		Phillips (1960)
			646.5	$\frac{1}{2}^+ - \frac{3}{2}^-$	378 ±14	108 ±5		NaI	IB–γ-coinc.	Bosch (1967)
51	Sb	119	23.8	$\frac{5}{2}^+ - \frac{3}{2}^+$	555 ±20	555 ±20	I_{IB}	NaI	IB/Kx	Olsen (1957)
53	I	125	35.5	$\frac{5}{2}^+ - \frac{3}{2}^+$	112.5 ±1.0	141.5 ±2.0		Ge(Li)		Gopinathan (1968)
55	Cs	131	0	$\frac{5}{2}^+ - \frac{3}{2}^+$	355 ±6	356 ±10	I_{IB}	NaI	IB/Kx	Saraf (1954a)
						356 ±10		NaI		Hoppes (1956)
							I_{IB}	NaI	IB/Kx	Michalowicz (1956)
							I_{IB}	NaI	IB/Kx	Biavati (1959, 62)
62	Sm	145	61.2	$\frac{7}{2}^- - \frac{7}{2}^+$	577 ±7	584 ±15		NaI		Brosi (1959)
						547 ±10	I_{IB} [e]	NaI	IB/($Kx+\gamma$), IB–e^--coinc.	Sujkowski (1968)
66	Dy	159	0	$\frac{3}{2}^- - \frac{3}{2}^+$	365.4 ±1.0	370 ±10		NaI		Ryde (1963b)
						370 ±9		NaI		Wotczek (1963)
							I_{IB} [f]	NaI	IB/($Kx+\gamma$)	Sujkowski (1965)
68	Er	165	0	$\frac{5}{2}^- - \frac{7}{2}^-$	371 ±4	370 ±10		NaI	IB/Kx	Ryde (1963a)
						372 ±8	I_{IB}	NaI	IB/Kx	Zylicz (1963)
							I_{IB}	NaI	IB/Kx	Sujkowski (1965)
74	W	181	0	$\frac{9}{2}^+ - \frac{7}{2}^+$	187 ±10	190 ±16		Ge(Li)		Rao (1966)
78	Pt	193	0	$\frac{1}{2}^- - \frac{3}{2}^+$	61.2 ±3.0	60.8 ±3.0		Ge(Li)		Hopke (1969)

[a] Calculated using Q_{EC} values from Wapstra and Gove (1971).
[b] Partly recalculated from measured 1s-IB endpoint energies, using electron binding energies from Bearden and Burr (1967).
[c] Symbols are used for the bremsstrahlung intensity (I_{IB}), the effective shape function (R_{eff}), information on the influence of detour transitions (DT), and the γ-branching ratio (P_γ). Information on the different spectral shapes are not indicated.
[d] Indicated only if normalized IB spectra have been determined.
[e] Includes bremsstrahlung of the 8%-EC branch to the ground state of ^{145}Pm.
[f] Includes bremsstrahlung of the 26%-EC branch to the 58.2 keV excited state in ^{159}Tb.

thermore, the residual pileup spectra show sharp sum peaks that can be distinguished from the smooth IB spectra (Fig. 42). A complete separation of the IB spectrum from the residual pileup spectrum cannot, however, be achieved in a single measurement, even with a weak ^{51}Cr source (Ribordy and Huber, 1970); an extrapolation from measurements with sources of different strengths is required. The extrapolation procedure used by Mutterer (1973a) is illustrated in Fig. 43. This technique has yielded normalized IB spectra of ^{7}Be and ^{51}Cr (Fig. 44) of good accuracy.

The spectrometry of IB in the presence of γ rays could be further improved by using large Ge(Li) detectors and suitable absorbers, in order to optimize the ratio of IB to γ-ray counting rates, and by using low-background arrangements. The reduction of background, either by applying optimal shielding or by using anticoincidence devices (Persson and Koonin, 1972), allows the use of weak sources and reduces the pileup correction accordingly. It would also be interesting to apply Ge(Li) anti-Compton spectrometers operated with pileup rejectors, because here pileup is confined to the region of the coincidence sum peaks. It can be expected that with improved techniques the accuracy with which total IB spectra of ^{51}Cr and ^{7}Be are now measured can also be attained in cases of decay schemes with higher P_γ, larger ratios of γ-ray energy to Q_{EC}, or with several γ branches. Spectrometry of the ground-state bremsstrahlung offers the possibility of determining ground-state branching ratios that in complex decays can otherwise only be obtained (often with very poor accuracy) from total γ- and x-ray intensities.

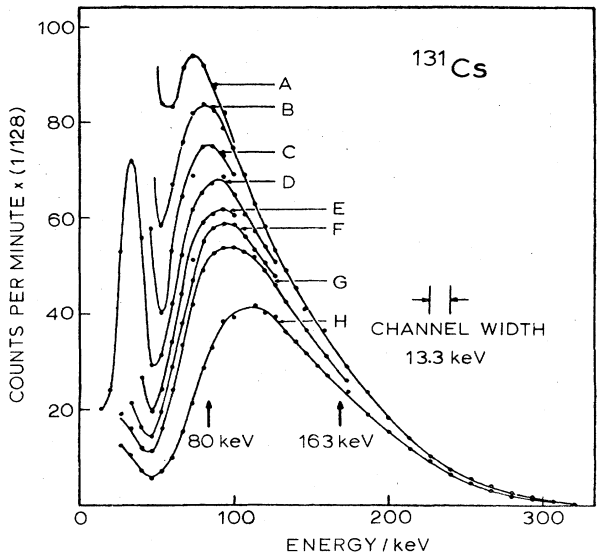

FIG. 41. IB pulse-height spectra of ^{131}Cs, measured with a 3.5×3.5-cm NaI(Tl) spectrometer. Copper absorbers were placed between source and detector, ranging from 710 mg/cm^2 (*A*) to 2200 mg/cm^2 (*H*). [From Saraf (1954a)].

c. *IB spectrometry in coincidence with γ rays*

Spectrometry of internal bremsstrahlung in coincidence with γ rays or conversion electrons permits one to separate the IB spectra accompanying decay to different excited states. Spectra can be measured over their entire energy range, above the K x-ray region, for electron-capture transitions that feed states which decay by prompt γ-ray emission to the ground state or to a lower-lying metastable state of the daughter nucleus. Normalization is easily accomplished by dividing a coincidence IB spectrum by the singles γ counting rate.

IB-γ coincidence experiments have been performed on electron-capture transitions to excited states in the decays of ^{7}Be (Lancman and Lebowitz, 1971a; Persson and Koonin, 1972), ^{51}Cr (Koonin and Persson, 1972), ^{54}Mn (Lancman and Lebowitz, 1969; Kádár *et al*, 1970; Koonin and Persson, 1972), ^{57}Co (Lancman and Lebowitz, 1971b), and ^{113}Sn (Bosch *et al.*, 1967). The main difficulty in IB–γ coincidence spectrometry arises from the large difference in intensity ($\sim 10^{-4}$) between IB and γ radiation, because the γ-ray spectra usually cover the same energy range as the weak IB spectra. Very short coincidence resolving times and high-efficiency detectors are therefore necessary to attain good true-to-chance coincidence ratios within reasonable counting times. Furthermore, scattering between the IB and γ detectors must be avoided to prevent false prompt coincidences and counting losses produced by sum effects in both channels. To meet these conditions, NaI(Tl) scintillators have been used as IB and γ detectors, arranged in close face-to-face geometry. Scattering has been reduced with suitable absorbers (Lancman and Lebowitz, 1969, 1971a,b), sometimes combined with lead collimators (Persson and Koonin, 1972; Koonin and Persson, 1972) (Fig. 45). Kádár *et al.* (1970) employed a 90° crystal arrangement of lower geometry with lead collimators. Timing was accomplished by Bosch *et al.* (1967), Lancman and Lebowitz (1969, 1971a,b), and Kádár *et al.* (1970) with conventional fast-slow coincidence circuits of 20–35 nsec resolving time.

TABLE XXVIII. Electron-capturing nuclides that decay by pure ground-state-to-ground-state transitions.

Z	Elements	A	$T_{1/2}$	Q_{EC} [a] (keV)	$J_i^\pi - J_f^\pi$	Degree of forbiddeness
18	A	37	35*d*	814.1 ± 0.6	$\frac{3}{2}^+ - \frac{3}{2}^+$	Allowed
23	V	49	330*d*	601.2 ± 1.0	$\frac{7}{2}^- - \frac{7}{2}^-$	
26	Fe	55	2.6*y*	231.7 ± 0.7	$\frac{3}{2}^- - \frac{5}{2}^-$	
32	Ge	71	11.4*d*	235.1 ± 1.7	$\frac{1}{2}^- - \frac{3}{2}^-$	
55	Cs	131	9.7*d*	355 ± 6	$\frac{5}{2}^+ - \frac{3}{2}^+$	
67	Ho	163	>10^3*y*	9.0 ± 1.5	$\frac{7}{2}^- - \frac{5}{2}^-$	
68	Er	163	75 min	1208 ± 6	$\frac{5}{2}^- - \frac{7}{2}^-$	
68	Er	165	10.3*h*	371 ± 4	$\frac{5}{2}^- - \frac{7}{2}^-$	
65	Tb	157	150*y*	64 ± 5	$\frac{3}{2}^+ - \frac{3}{2}^-$	First nonunique
78	Pt	193	620*y*	61.2 ± 3.0	$\frac{1}{2}^- - \frac{3}{2}^+$	
20	Ca	41	8×10^4*y*	421.2 ± 0.5	$\frac{7}{2}^- - \frac{3}{2}^+$	First unique
36	Kr	81	2.1×10^5*y*	290 ± 100	$\frac{7}{2}^+ - \frac{3}{2}^-$	
25	Mn	53	2×10^6*y*	597.3 ± 1.2	$\frac{7}{2}^- - \frac{3}{2}^-$	Second nonunique
28	Ni	59	8×10^4*y*	1073.1 ± 1.1	$\frac{3}{2}^- - \frac{7}{2}^-$	
43	Tc	97	2.6×10^6*y*	346 ± 9	$\frac{9}{2}^+ - \frac{5}{2}^+$	
57	La	137	6×10^4*y*	~500	$\frac{7}{2}^+ - \frac{3}{2}^+$	
52	Te	123	1.2×10^{13}*y*	57.2 ± 2.4	$\frac{1}{2}^+ - \frac{7}{2}^+$	Second unique

[a] From Wapstra and Gove (1971).

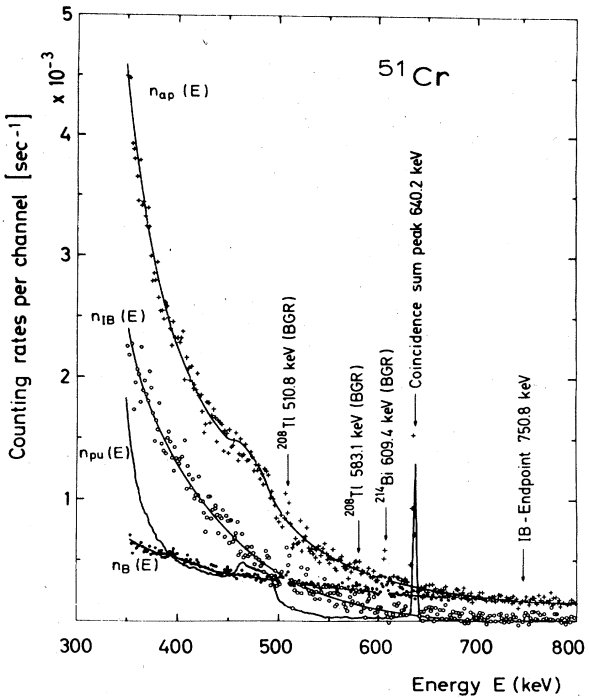

FIG. 42. Pulse-height spectrum of ^{51}Cr, as recorded with a 1.2-cm^3 Ge(Li) detector with a pileup rejector. The measured spectrum (N_{ap}) is shown in the energy range above the 320.1-keV γ-ray peak, with its individual components: internal bremsstrahlung (N_{IB}), residual pileup (N_{pu}), and background (N_B). [From Mutterer (1973a)].

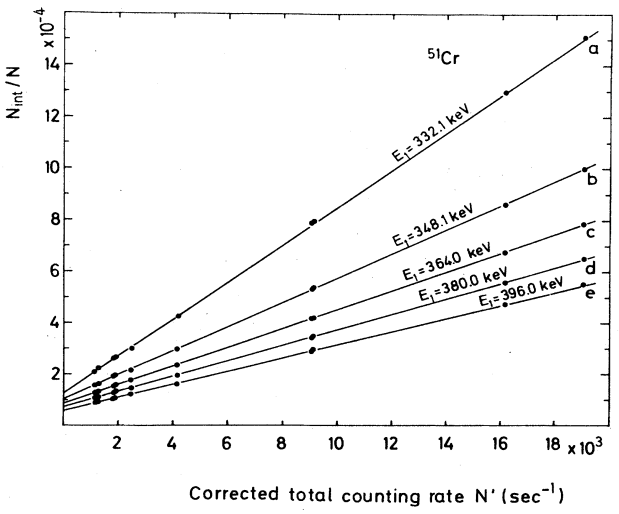

FIG. 43. Extrapolation plot for pileup correction of ^{51}Cr spectra, recorded from sources of different strengths with a Ge(Li) spectrometer. Ratios of integral counting rates (N_{int}) for different energy ranges $E > E_l$ above the 320.1-keV γ line and total counting rates (N) are plotted against corrected total counting rates (N'). The intercepts at $N' = 0$ give ratios of IB to γ counting rates above different energy thresholds E_l. [From Mutterer (1973a)].

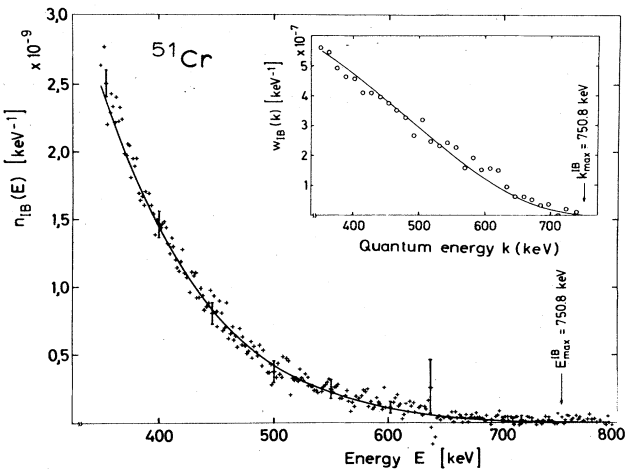

FIG. 44. IB pulse-height spectrum (n_{IB}) of ^{51}Cr, deduced from a set of spectra that were recorded with a Ge(Li) spectrometer and corrected for pileup applying the extrapolation method. The corresponding energy spectrum (w_{IB}) is shown in the inset. Solid lines represent theoretical spectra of Martin and Glauber (1958). [From Mutterer (1973a)].

Even so, random coincidences between γ events in both detectors made the main contribution to the measured coincidence spectra. Bremsstrahlung spectra were found by subtracting singles γ spectra, recorded with the IB detector, from the measured coincidence spectra; both sets of spectra had been normalized to equal photopeak areas (Fig. 46).

A considerable improvement in technique was achieved by Persson and Koonin (1972) by using a fast time-to-pulse-height converter and applying two-parameter analysis: the IB pulse-height spectrum and the energy-dependent delay between IB and γ pulses were recorded simultaneously. A block diagram of the electronic circuit is shown in Fig. 47. This technique has led to effective coincidence resolving times of ~ 4 nsec over the entire IB-spectrum range. Persson and Koonin (1972) have furthermore reduced the background rate by surrounding both crystals with a plastic-scintillator anti-coincidence shield, allowing the use of weak sources. With this technique, random coincidences could be reduced to a much lower level, and accurate IB spectra could be measured for ^{7}Be, ^{51}Cr, and ^{54}Mn. The result for ^{7}Be is shown in Fig. 48.

It would undoubtedly be of interest to apply this IB–γ coincidence technique to additional cases. Large Ge(Li) detectors or plastic scintillators might be used. In cases that involve low-energy γ transitions, measurements might be performed in coincidence with conversion electrons; this has been done only with ^{145}Sm (Sujkowski *et al.*, 1965).

d. Spectrometry of IB and of positrons or annihilation radiation

For high-energy transitions in which electron capture competes with positron emission, total IB spectra can be measured relative to the β^+ decay rate or to the anni-

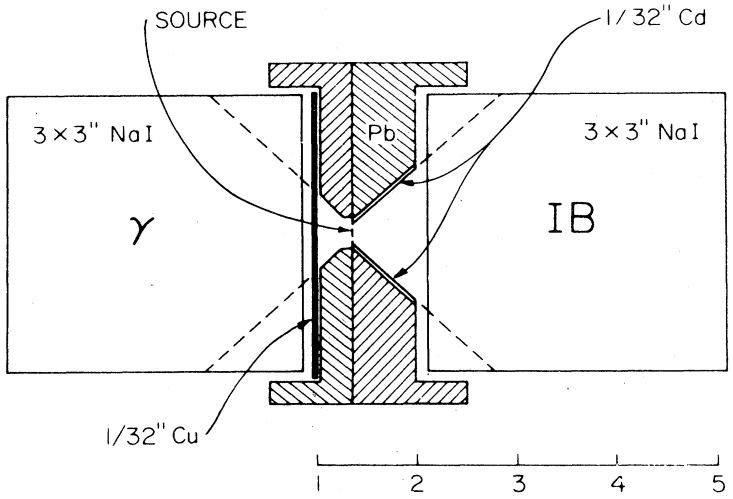

FIG. 45. Arrangement of two 3×3-in. NaI(Tl) detectors, used for IB spectrometry in coincidence with γ rays. [From Person and Koonin (1972)].

hilation radiation (γ_A) produced by the positrons in suitable source encapsulations. Methods for measuring EC/β^+ ratios, with which the IB spectra can be normalized, are discussed in Sec. III.D. Interference of annihilation radiation with the IB spectrum can be reduced by measured γ_A–γ_A anticoincidences with a detector placed opposite the IB detector. Alternatively, very thin sources and backings can be used and the β^+ particles can be magnetically bent away from the IB detector. This technique has been applied by Berényi and Varga (1969) to measure internal bremsstrahlung from β^- emission with minimal contribution from external bremsstrahlung. In isotopes that decay by electron capture and β^+ emission, the positrons give rise to such other continuously distributed radiation as internal and external bremsstrahlung and photons from positron annihilation in flight (Kantele and Valkonen, 1973). The electron-capture bremsstrahlung spectra will be affected by these conditions at energies below the β^+ end point and in the neighborhood of 511 keV.

The only reported IB measurements on a nuclide decaying by electron capture and β^+ emission are on ^{36}Cl, which has a very weak (0.001%) β^+ branch and decays 98.1% of the time by β^- emission. The bremsstrahlung accompanying the 1.9% electron-capture branch has been studied by Dougan *et al.* (1962), Berényi (1962, 1963b, 1965a) Lipnik *et al.* (1964), Berényi *et al.* (1965b), and Smirnov and Batkin (1973) with various types of NaI(Tl) spectrometers. The latter two experiments yielded very accurate results on the IB spectrum shape at energies above the β^- end point at 712 keV. No attempt was made, however, to normalize the spectra to the electron-capture rate.

Bremsstrahlung studies on isotopes that decay by electron capture and β^+ emission do not contribute decay-scheme information that could be derived more readily from β^+ spectrometry. Measurements of normalized IB spectra at high energies would, however, be extremely useful to check the treatment of relativistic and Coulomb

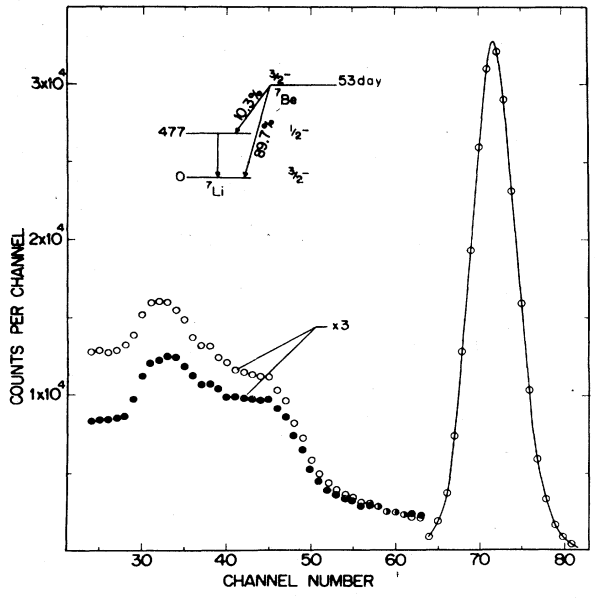

FIG. 46. Pulse-height spectra of ^{7}Be photons gated by γ rays, as obtained with two 3×3-in. NaI(Tl) spectrometers in close face-to-face geometry. The coincidence spectrum (open circles) is compared with the random coincidence spectrum (filled circles). The difference between the two spectra represents the pulse-height spectrum of internal bremsstrahlung that accompanies the electron-capture transition to the excited state in ^{7}Li. [From Lancman and Lebowitz (1971b)].

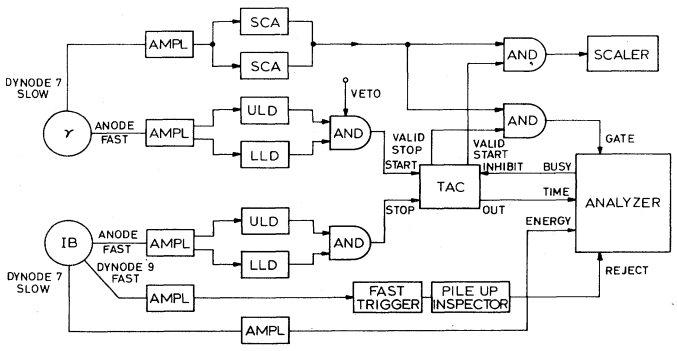

FIG. 47. Electronic circuit of IB spectrometry in coincidence with γ rays, for a device with two NaI(Tl) detectors (Fig. 45). [From Persson and Koonin (1972)].

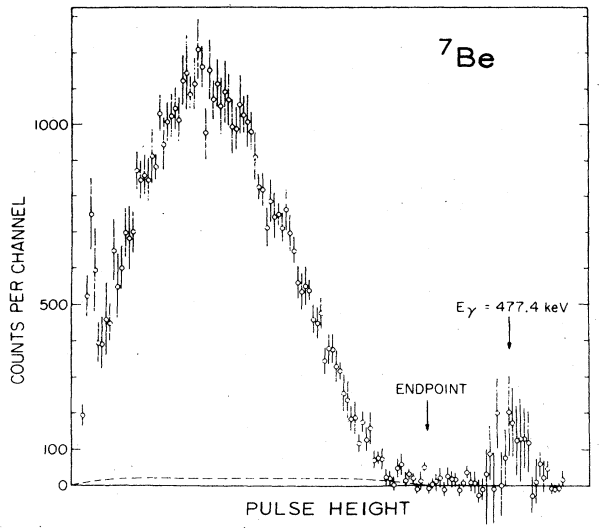

FIG. 48. IB pulse-height spectrum of ^{7}Be measured in coincidence with the 477-keV γ rays. The Be γ-ray peak at 477 keV remained after correction for random coincidences. The corresponding Compton distribution is shown as a dashed line. [From Persson and Koonin (1972)].

effects in the theory, which predicts that these effects reduce the IB yield with increasing energy (Fig. 32).

2. Experiments on partial IB spectra

Supplementary to the experiments described in Sec. IV.B.1, considerable effort has been expended to measure partial IB spectra associated with electron capture from specific shells, mainly the 1*s* IB spectrum associated with *K* capture. Such spectra can be observed by IB spectrometry in coincidence with x rays or Auger electrons. Higher-shell spectra can be determined by subtracting accurately measured 1*s* IB spectra from total IB spectra.

a. The 1s IB spectrum

Spectrometry of internal bremsstrahlung in coincidence with *K* x rays or *K* Auger electrons singles out the 1*s* IB spectrum dw_{1s}. The spectrum can be normalized to the corresponding *K*-capture rate by dividing the coincidence IB spectrum by the singles *K* x-ray (*K* Auger-electron) counting rate.

Only IB–*K*-x-ray coincidence experiments have been reported (Table XXIX). Most of these experiments have

TABLE XXIX. 1*s* IB spectra measured in coincidence with *K* x-rays.

			Final state		E_{EC} [a]	Deduced quantities			
Z	Elements	A	(keV)	$J_i^\pi - J_f^\pi$	(keV)	E_{EC}(keV) [b]	Others [c]	Spectrometer	References
25	Mn	54	835.0	$3^+ - 2^+$	540.1 ± 3.6	528 ± 20		NaI	Jung (1956)
26	Fe	55	0	$\frac{3}{2}^- - \frac{5}{2}^-$	231.7 ± 0.7		I_{IB}^{1s}	NaI	Biavati (1959, 62)
38	Sr	85	514.0	$\frac{9}{2}^+ - \frac{9}{2}^+$	550 ± 7	493 ± 30		NaI	McDonnell (1969)
48	Cd	109	87.7	$\frac{3}{2}^+ - \frac{7}{2}^+$	94 ± 3	94 ± 3		Ge(Li)	Gopinathan (1968)
50	Sn	113	646.5	$\frac{1}{2}^+ - \frac{3}{2}^-$	378 ± 14	100 ± 10		NaI	Jung (1956)
53	I	125	35.5	$\frac{5}{2}^+ - \frac{3}{2}^+$	112.5 ± 1.0	141.5 ± 2		Ge(Li)	Gopinathan (1968)
55	Cs	131	0	$\frac{5}{2}^+ - \frac{3}{2}^+$	355 ± 6		I_{IB}^{1s}	NaI	Michalowicz (1956)
							I_{IB}^{1s}	NaI	Biavati (1959, 62)
62	Sm	145	61.2	$\frac{7}{2}^- - \frac{7}{2}^+$	577 ± 7		I_{IB}^{1s} [d]	NaI	Sujkowski (1968)
68	Er	165	0	$\frac{5}{2}^- - \frac{7}{2}^-$	371 ± 4	370 ± 8		NaI	Zylicz (1963)
						384 ± 20		NaI	Sujkowski (1965)
74	W	181	0	$\frac{9}{2}^+ - \frac{7}{2}^+$	187 ± 10	184 ± 12		Ge(Li)	Rao (1966a)
80	Hg	197	77.3	$\frac{1}{2}^- - \frac{1}{2}^+$	338 ± 20	686 ± 40	I_{IB}^{1s}	NaI	Jasinski (1965)
81	Tl	204	0	$2^- - 0^+$	345 ± 4	335		NaI	Der Mateosian (1952)
						376 ± 20		NaI	Jung (1956)
						393 ± 10		NaI	Biavati (1959, 62)
								NaI	Goudsmit (1966)
						385 ± 20	I_{IB}^{1s}	NaI	Lancman (1973)

[a] Calculated using Q_{EC} values from Wapstra and Gove (1971).
[b] Partly recalculated from measured 1*s*-IB endpoint energies, using *K*-electron binding energies from Bearden and Burr (1967).
[c] I_{IB}^{1s} = 1*s*-IB intensity.
[d] Includes bremsstrahlung of the 8%-EC branch to the ground state of ^{145}Pm.

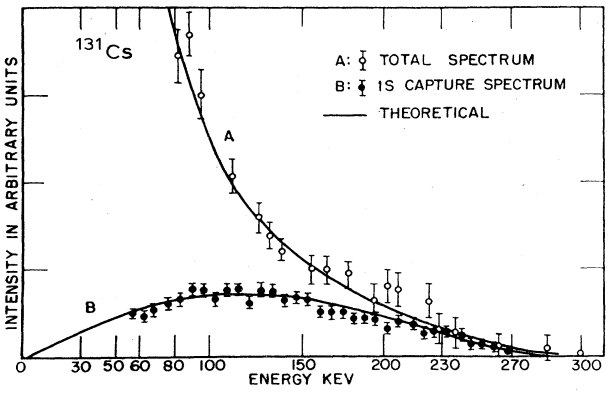

FIG. 49. Total IB spectrum of ^{131}Cs, measured with a $1\times1\frac{1}{2}$-in. NaI(Tl) crystal with a 0.0005-in. thick aluminum window. The 1*s* IB spectrum gated by ^{131}Xe *K* x rays that were recorded with a 1.5×0.080-in. NaI(Tl) crystal, is also shown. [From Biavati *et al.* (1962)].

yielded only spectral shapes. Normalized spectra have been determined only for some simple decays, viz., for ^{55}Fe (Biavati *et al.*, 1962), ^{131}Cs (Michalowicz, 1956; Biavati *et al.*, 1962) (Fig. 49), ^{145}Sm (Sujkowski *et al.*, 1968), and ^{165}Er (Zylicz *et al.*, 1963; Sujkowski *et al.*, 1965). NaI(Tl) detectors were used in these experiments for both the IB and *K* x-ray photons; interference of *K* x rays in the IB spectrometer was avoided with absorbers. For all isotopes but ^{145}Sm and ^{165}Er, only poor accuracy was achieved in these early experiments.

Measurements of bremsstrahlung in coincidence with *K* x rays can also be performed in the presence of higher-energy γ rays, with the restriction that prompt γ rays limit the observable 1*s* radiation to energies above the γ energy. Spectra accompanying electron-capture decays that feed a state deexcited by prompt γ rays of energies in excess of the electron-capture transition energy cannot be obtained by IB–*K*-x-ray coincidences with any degree of accuracy. One IB result on such a cascade in ^{54}Mn, reported by Jung and Pool (1956), should be disregarded. Delayed γ rays, such as arise if electron capture feeds isomeric states, have no direct influence but may contribute considerably to the random-coincidence rate below the γ energy. This was the case in the older coincidence experiments on ^{85}Sr by McDonnell and Ramaswamy (1969), ^{109}Cd by Gopinathan and Rubinson (1968), and ^{113}Sn by Jung and Pool (1956). Modern coincidence techniques, as used by Persson and Koonin (1972) in IB-γ spectrometry, would permit measurements of entire 1*s* IB spectra. Some results on 1*s* spectra have been reported for electron-capture transitions to isomeric states with mean lives of the order of the coincidence resolving time, viz., on ^{125}I (Gopinathan and Rubinson, 1968), ^{145}Sm (Sujkowski *et al.*, 1968), and ^{197}Hg (Jasinski *et al.*, 1965). In such cases, only the spectrum above the γ-ray energy is usually observable, and normalization is complicated.

In all measurements of coincidences between bremsstrahlung and *K* x rays on radioisotopes that emit prompt or delayed γ rays, a correction must be applied for the γ contribution in the *K* x-ray channel. This correction is determined through a second measurement with a discriminator window setting above the *K* x-ray line. Corrections for *K* x rays from internal conversion must also be considered.

Bremsstrahlung from 1*s* capture can be measured in coincidence with *K* x rays even in cases where β^+ or β^- decay competes with electron capture because the only *K* vacancies created in β decay are the few produced by *K*-shell internal ionization or shakeup (Sec. V). Thallium-204 has often been investigated; this isotope decays by 97.9% β^- emission and 2.1% electron capture. Lanchman and Bond (1973) have pointed out that double internal bremsstrahlung associated with the β^- branch may have to be considered.

Most measurements of 1*s* IB spectra could be considerably improved today. Careful new measurements on pure ground-state decays and electron-capture decays to isomeric states would be especially useful.

b. Higher-shell spectra

The possibilities for measuring the bremsstrahlung that accompanies electron capture from higher shells are more limited. Radiation from *ns* capture, $n>1$, has very similar shape to 1*s* radiation and constitutes only ~10% of the total bremsstrahlung in the energy range above $\sim Z\alpha$. The radiation accompanying capture of *p* electrons dominates only at low energies, $k<Z\alpha$; for low Z, this is difficult to separate from the characteristic x-ray lines.

The IB spectra associated with capture from higher shells are quite easily observed in the few low-energy transitions in which *K* capture is energetically forbidden, e.g., ^{193}Pt and ^{163}Ho. An accurate IB shape measurement on ^{193}Pt was performed by Hopke and Naumann (1969) with a Ge(Li) spectrometer (Fig. 50). In more energetic transitions, however, such spectra are very difficult to measure with good accuracy.

The *2s IB spectrum*, associated with radiative capture of L_1 electrons, can only be singled out in coincidence with *L* x rays if it is possible to gate on the $L\beta_3$ and $L\beta_4$ lines. Other *L* x rays can also arise from $L_{2,3}$ capture or follow $K\alpha$ x-ray emission after *K* capture. The method is thus restricted to high-Z atoms for which the *L* x-ray components can be resolved and the *K* fluorescence yield is large. For other nuclides, the 2*s* spectrum (including *s* spectra from higher shells) can only be obtained indirectly by comparing accurately mea-

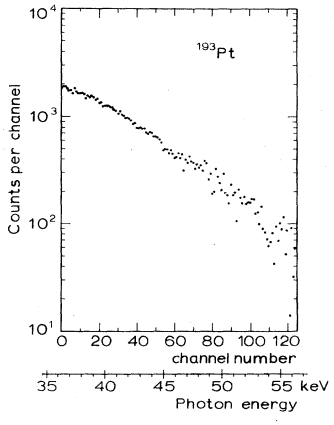

FIG. 50. Pure higher-shell IB spectrum of ^{193}Pt, measured with a 7-cm^3 coaxial Ge(Li) detector. [From Hopke and Naumann (1969), and private communication].

sured 1*s* and total IB spectra. No experimental results on separated 2*s* IB spectra have been reported.

The *2p IB spectrum* associated with radiative capture of electrons from the L_2 subshell (plus the small amount captured from the L_3 subshell) can be singled out by coincidence IB spectrometry in cases in which K capture is forbidden, such as ^{193}Pt. Here, an IB measurement in coincidence with those L x rays that fill L_2 and L_3 vacancies (all but $L\beta_3$ and $L\beta_4$) can be performed. The total p radiation, however, that differs strongly in spectral shape from s radiation, can be determined by subtracting from the total IB spectrum measured at energies below $Z\alpha$ the s IB spectrum that is measured at higher energies and extrapolated to the p IB region. Alternatively, one can subtract the 1*s* IB spectrum measured by IB–K-x-ray coincidences and corrected for the ~ 10% contribution from higher s states (Biavati *et al.*, 1962).

Measurements of total IB spectra at low energies, where p IB dominates, have been performed on several nuclides, viz., on ^{55}Fe by Biavati *et al.* (1962), ^{131}Cs by Michalowicz (1956), Hoppes and Haywards (1966), and Biavati *et al.* (1962) (Fig. 49), ^{145}Sm by Sujkowski *et al.* (1968), and ^{159}Dy and ^{165}Er by Sujkowski *et al.* (1965). Relative intensities of p radiation and s radiation were determined for ^{145}Sm, ^{159}Dy, and ^{165}Er. In all these experiments, NaI(Tl) detectors were used. With scintillation detectors, however, distortions of the IB spectrum due to pileup contributions from K x rays and K–L x-ray sum effects are difficult to control in the vicinity of the K x-ray energy. For the measurement of p radiation, Ge(Li) spectrometers should be used, preferably with pileup rejectors, and corrections for residual pileup should be considered. Platinum-193 would be a good case for study.

The measurement of the relative intensity of IB from s and p capture represents an independent method to determine the capture ratios; this may supplement corresponding x-ray and Auger-electron experiments.

3. Analysis of IB pulse-height spectra

In this section, we consider methods for deriving IB energy spectra $dw_{IB}(k)$ or $dw_{nl}(k)$ from measured pulse-height distributions. For continuous spectra, spectrometer calibration is more complicated and analysis more laborious than for line spectra. The calibration procedure must include determination of total detector response over the entire range of energy k and pulse height E that is covered by the continuous spectrum. The pulse-height spectrum $dn(E)$ and the corresponding photon energy spectrum $dw(k)$ are, in general, related as follows:

$$dn(E)=\int_0^{k_{max}} R(E,k)\,dw(k). \tag{4.80}$$

The response function $R(E,k)dE$ defines the probability that a photon emitted with energy k produces a pulse of height between E and $E+dE$ when detected. The accuracy to which a measured spectrum $dn(E)$ can be compared with a predicted IB spectrum $dw_{IB}(k)$ depends both on the accuracy of R and the method used to solve Eq. (4.80).

In analogy to extensive work on β spectra, various methods for making response corrections on continuous γ spectra have been worked out that are applicable to measurements with NaI(Tl) and Ge(Li) spectrometers. In the present paper, we can only make a few remarks on essential features. Electron-capture bremsstrahlung spectra have been subjected successively to procedures designed to correct for resolution, Compton distribution, total efficiency, iodine K x-ray escape, etc. (Lidén and Starfelt, 1954; Lindqvist and Wu, 1955; Persson and Koonin, 1972). As an example, Fig. 51 shows the various corrections applied by Lindqvist and Wu (1955) to the IB spectrum of ^{37}Ar. These procedures depend very much on the peculiarities of the detector arrangement and can differ considerably in accuracy. We discuss, instead, more generally applicable methods based on the application of complete response functions.

a. Determination of response functions for NaI(Tl) and Ge(Li) spectrometers

The response function R [Eq. (4.80)], which varies strongly with the type of spectrometer and the measured energy range (see, e.g., Heath, 1963), can in principle be calculated in terms of the different fundamental absorption processes in the detector. Monte Carlo calculations have been performed, e.g., by Beattie and Byrne (1972) for scintillators and by Meixner (1974) for Ge(Li) spectrometers. These calculations have reached a high level of accuracy; their application, however, is limited by the fact that the true dimensions of the detec-

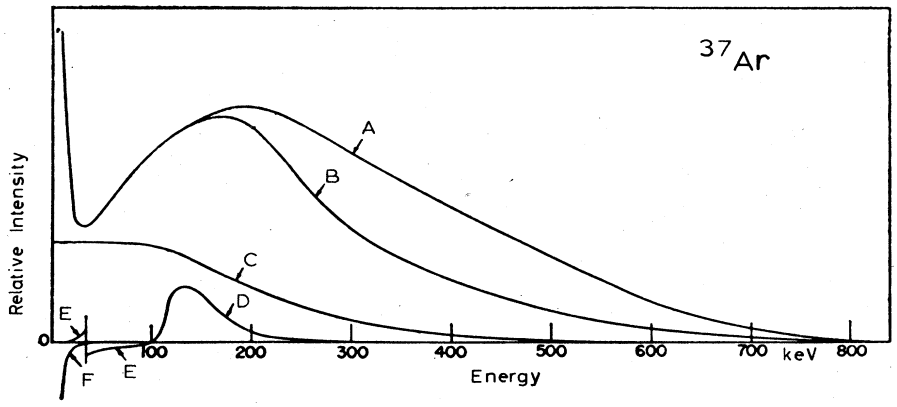

FIG. 51. Corrections applied to the predicted ^{37}Ar IB spectrum to convert it into a pulse-height spectrum as would be measured with a 1×1-in. NaI(Tl) spectrometer: (A) theoretical curve corrected for γ efficiency, and distribution curves for (B) photo electrons, (C) Compton electrons, (D) backscattered photons, (E) escaped photons, and (F) absorbed photons. [From Lindqvist and Wu (1955)].

tor's sensitive volume and the thickness of dead zones and encapsulations are often not accurately known. In fact, calculations deviate from measured response functions, especially at low energies.

All pertinent effects are correctly taken into account if the response function is determined empirically by interpolation, starting from pulse-height spectra produced by monoenergetic γ rays of known energies and intensities.

For *NaI(Tl) spectrometers*, numerous peak-fitting procedures have been developed (e.g., Prescott, 1963); these allow one to derive the energy dependence of the fitting parameters. For the interpolation of Compton distributions, Chester *et al.* (1963) have fitted parametrized analytical curves to measured spectra and determined the sets of parameters as functions of the energy k. Wapstra and Oberski (1963) and others have interpolated between calibration spectra that were transformed so as to bring all Compton edges to a common value of the transformed pulse height. Under special conditions, e.g., with large crystals in close geometry yielding a small Compton-to-peak ratio, it may suffice to approximate the Compton distributions by simple rectangular or trapezoidal shapes. The possibility of such simplification has been demonstrated by Persson and Koonin (1972) for IB spectra measured with a 3×3-in. NaI(Tl) crystal (Fig. 45).

With *Ge(Li) spectrometers*, the correct determination of peak areas is important, whereas the peak shapes can be approximated because the continuous spectra vary little over an energy interval corresponding to a peak width. On the other hand, correct fitting of the Compton distribution is of the utmost importance, especially for small detectors, because the Compton-to-peak ratio is large. Methods for interpolating Compton distributions by fitting parametrized curves (Ribordy and Huber, 1970) and by interpolating transformed calibration spectra (Mutterer, 1973a,c) were reported. Both procedures have yielded accurate Ge(Li)-response functions (Fig. 52).

b. Correction methods

With a known response function, a measured IB pulse-height spectrum dn_{IB} can be compared in either of two ways with a theoretical spectrum dw_{IB}: (i) the theoretical spectrum can be converted according to Eq. (4.80) into a "predicted" pulse-height spectrum that is compared with the measured spectrum (folding method), or the measured pulse-height spectrum can be converted into an experimental energy spectrum by solving Eq. (4.80) (unfolding method).

The *folding method* has been applied most often in the evaluation of IB results, e.g., for ^{7}Be by Lancman and Lebowitz (1971b) and Mutterer (1973b,c), ^{37}Ar by Anderson and Wheeler (1953), Lindqvist and Wu (1955), and Saraf (1956), ^{49}V by Hayward and Hoppes (1956), ^{51}Cr by Mutterer (1973a,c), ^{54}Mn by Lancman and Lebowitz (1969), ^{55}Fe by Maeder and Preiswerk (1951), Michalowicz (1953), and Biavati *et al.* (1962), ^{57}Co by Lancman and Lebowitz (1971a), ^{113}Sn by Phillips and Hopkins (1962), ^{165}Er by Ryde *et al.* (1963a), and ^{204}Tl by Lancman and Bond (1973). The folding method is simplest but has the great disadvantage that no direct experimental energy spectrum dw_{IB} is obtained. It is thus less valuable for a detailed comparison of IB experiments with theory. Furthermore, the important method for determining the transition energy E_{EC} by constructing a Jauch plot of dw_{IB} (Sec. IV.B.4) cannot be applied. Instead, a variational procedure has often been used to determine E_{EC}: dn_{IB} is calculated from IB theory and the known detector response as a function of the end-point energy q, and q is varied to give the best fit to the measured spectrum (Fig. 53). To obtain experimental results for the IB yield as well as E_{EC}, both a constant factor and q have often been varied in fitting calculated to experimental IB pulse-height spectra (e.g., Lancman and Lebowitz, 1969, 1971a,b). Experimental results on the IB yield obtained by this method evidently imply theoretical assumptions on the spectral shape.

The *unfolding method* is consequently to be preferred.

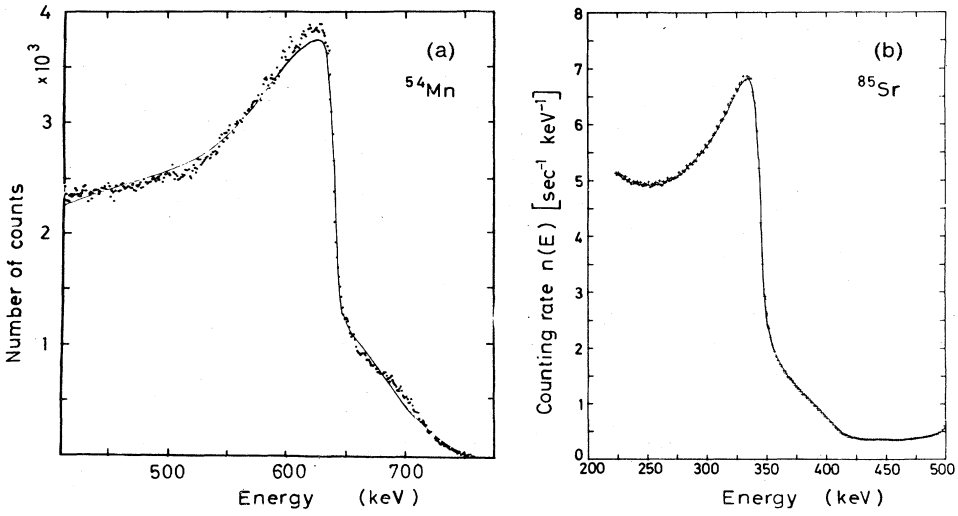

FIG. 52. Compton distributions of ^{54}Mn (a) and ^{85}Sr (b) recorded with small Ge(Li) spectrometers. Measured spectra are compared with those calculated from constructed response matrices. [(a) from Ribordy and Huber (1970), courtesy of Birkhäuser Publishing Co.; (b) from Mutterer (1973c), unpublished].

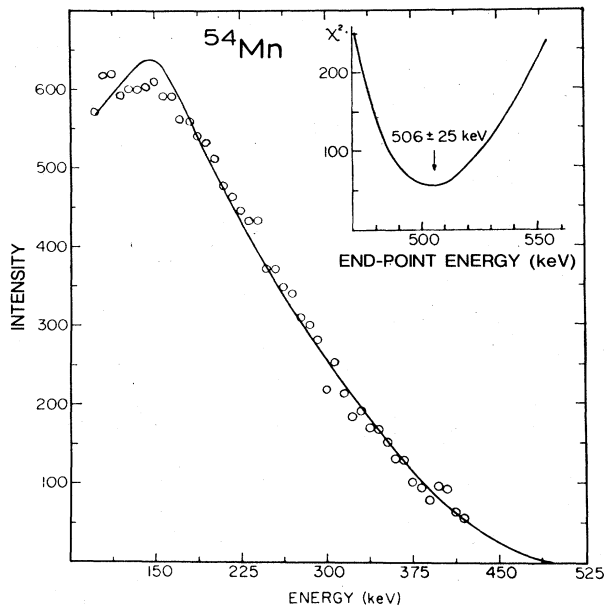

FIG. 53. IB pulse-height spectrum of ^{54}Mn, measured with a 3×3-in. NaI(Tl) spectrometer, in coincidence with the 835-keV γ rays from ^{54}Cr. The solid line is the best fit (corresponding to the minimum value of χ^2) of the curves obtained by folding the theoretical IB spectrum with the response matrix. The end-point energy is used as fitting parameter. [From Lancman and Lebowitz (1969)].

Various procedures have been reported in the literature. The solution of Eq. (4.80) by matrix inversion usually has to be limited to small matrices. This difficulty can be overcome by iterative methods, such as the correction-factor method of Scofield (1963) and the Gauss-Seidel method (e.g., Zurmühl, 1965). Both of these methods, which also have often been used for unfolding measured β spectra, normally lead to quite rapid convergence if the diagonal elements ($E=k$) in the response function dominate. Ribordy and Huber (1970) have compared different iterative methods for unfolding the IB spectrum of ^{51}Cr and find comparable results. The Gauss-Seidel method was applied to the ^{7}Be and ^{51}Cr IB spectra by Mutterer (1973a,b,c), who found rapid convergence of the iteration, provided that the response function was renormalized to unit peak areas. These unfolding techniques performed with the aid of modern computers have yielded accurate response corrections for bremsstrahlung spectra. It should be noted, however, that some problems remain concerning the propagation of statistical experimental errors (Weise, 1968).

4. Determination of electron-capture transition energies from measured IB spectra

The determination of IB end-point energies is of particular interest because it provides a direct method for measuring electron-capture transition energies E_{EC} and the corresponding isobaric atomic mass differences Q_{EC}. The end point of an IB spectrum is equal to the energy q of the neutrino emitted during ordinary (nonradiative) electron capture and, consequently, the transition energy is obtained by adding to the end-point energy the atomic binding energy (in the daughter atom) of the shell from which capture has occurred (Rubinson, 1971).

Transition energies have been determined in most IB experiments. In Tables XXVII and XXIX, E_{EC} results are listed which were obtained from measurements of total and 1s IB spectra. Tables XXVII and XXIX also contain E_{EC} values deduced from the atomic-mass compilation of Wapstra and Gove (1971). With few exceptions (^{113}Sn, ^{125}I, ^{197}Hg, and ^{204}Tl), the IB data are in fair agreement with the atomic-mass differences. It should, however, be noted that the two sets of data are not independent. Wapstra and Gove (1971) have considered part of the listed IB data in assigning the isobaric mass differences, supplementing data from nuclear reaction thresholds and electron-capture ratios. Especially in the medium and high-Z region (e.g., ^{103}Pd, ^{109}Cd, ^{119}Sb, ^{131}Cs, ^{145}Sm, and ^{181}W), the listed E_{EC} values from IB experiments appear, with slight changes, also in the atomic mass tables.

Because of the great importance of accurate mass differences, some comments on the determination of IB end-point energies are in order. Many electron-capture transition energies listed in Tables XXVII and XXIX originate from early experiments and are of low accuracy. These measurements could be much improved with modern techniques. The overall accuracy of E_{EC}, however, depends also upon the theoretical model which is used to extract the IB end-point energy q from a measured IB spectrum. This dependence on theory is most obvious in E_{EC} determinations based on the fitting of calculated spectra to measured ones, with q_{1s} as the fitting parameter (Sec. IV.B.3). That different theoretical assumptions in this procedure can yield quite different values of q_{1s} was demonstrated by Lancman and Bond (1973) in the case of the first-forbidden unique electron-capture decay of ^{204}Tl: fitting procedures with different allowed IB shapes yielded E_{EC} values that differ by 25 keV. Shape functions from theories for forbidden transitions were, however, not considered. Berényi *et al.* (1976) studied the variation of E_{EC} of ^{59}Ni, obtained from an accurately measured ^{59}Ni IB spectrum, by fitting spectra calculated from different theoretical approaches to forbidden radiative capture; they found differences of a few keV.

Most experimental transition-energy determinations from (unfolded) IB spectra dw_{IB} (or dw_{1s}) have been made by linearizing the spectra in a way that resembles the construction of Kurie plots for β spectra. The procedure for constructing such a *Jauch plot* (Jauch, 1951; Bell *et al.*, 1952) is based on the elementary shape of the 1s IB spectrum [Eq. (4.17)] as predicted by the early Coulomb-free theory of Morrison and Schiff (1940). A linear plot is obtained by converting a measured spectrum dw_{1s} into *Jauch coordinates* by plotting $(dw_{1s}/k)^{1/2}$ vs k. Because of the predicted proportionality

$$(dw_{1s}/k)^{1/2} \propto k - q_{1s}, \tag{4.81}$$

the intercept with the k axis occurs at q_{1s}. The accuracy of this procedure evidently depends on how closely the investigated spectrum is approximated by the Morrison–Schiff theory. For a strictly correct linearization, various corrections to the spectrum must be considered which appear in the modern theory for allowed decays

(Sec. IV.A.2) and for forbidden decays (Sec. IV.A.4).

The 1*s* IB spectrum from allowed and first-forbidden nonunique decays can be linearized more strictly on the basis of the relation

$$\left[\frac{dw_{1s}}{kR_{1s}(k)}\right]^{1/2} \propto k - q_{1s}. \tag{4.82}$$

The 1*s* IB shape function $R_{1s}(k)$ corrects for relativistic and Coulomb effects; it can be calculated exactly from Eq. (4.44). This shape function is displayed in Fig. 32 for various atomic numbers. The influence of R_{1s} on the determination of q_{1s} has been studied by Zylicz *et al.* (1963) in the case of the ^{165}Er IB spectrum (Fig. 54). It was found that a Jauch plot according to the relation (4.82) yields an end-point energy that differs by 3 keV from that obtained with a simple plot based on the proportionality (4.81). In this analysis, however, an approximate result for the relativistic shape factor R_{1s} was used, as derived by Martin and Glauber (1958). For ^{165}Er ($Z = 68$) and in the measured energy range, 150 keV $\leq k \leq$ 300 keV, the approximate function deviates considerably from the exact function R_{1s} (Fig. 33), so that a greater effect of R_{1s} on q_{1s} is expected. Larger differences are also expected in the case of IB spectra that cover wider energy intervals and are not measured as close to the end point.

In order to determine 1*s* IB end-point energies from measured total IB spectra dw_{IB}, a correction must be applied for the higher-shell components which have end points q_{nl} larger than q_{1s}. In the energy range $k < q_{1s}$, this correction can be written

$$dw_{IB} = dw_{1s}\left[1 + \left(\sum_{nl} dw_{nl}\right) \Big/ dw_{1s}\right]; \tag{4.83}$$

this leads to an additional energy-dependent correction

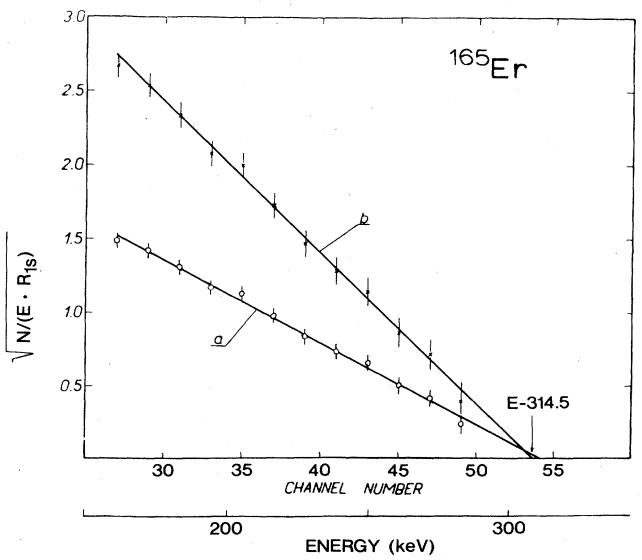

FIG. 54. The 1*s* IB spectrum of ^{165}Er, as measured with an $1\frac{1}{2}\times 1$-in. NaI(Tl) spectrometer, in coincidence with Ho K x rays. Jauch plots are shown according to Eq. (4.81) (curve a) and Eq. (4.82) (curve b). [From Zylicz *et al.* (1963), courtesy of North-Holland Publishing Co.].

$f(k)$ in the Jauch coordinate:

$$[dw_{IB}/kR_{1s}(k)f(k)]^{1/2} \propto k - q_{1s}. \tag{4.84}$$

The k dependence of $f(k)$ is complicated because it generally contains the higher-shell shape functions R_{ns} and Q^2_{np} (Tables XXIII and XXIV) as well as corrections for the different end-point energies q_{nl}. In most practical cases, however, only higher-shell s radiation is important at higher energies. The correction for the dominant 2*s* radiation is adequately taken into account by

$$f(k) = 1 + \frac{P_L}{P_K}\frac{R_{2s}(k)}{R_{1s}(k)}\left(1 + \frac{k_{Kx}}{q_{1s} - k}\right)^2. \tag{4.85}$$

Here, P_L/P_K is the L/K electron-capture ratio, and the K x-ray energy k_{Kx} has been written for the difference $q_{2s} - q_{1s}$. The term containing k_{Kx} constitutes an important correction for experimental data that are close to q_{1s}, within a few times k_{Kx}. Because this term implicitly also contains q_{1s}, the correction (4.85) can only be calculated iteratively.

Equation (4.84) has been used by Mutterer (1973a,b) in determining the IB end-point energies of ^{7}Be and ^{51}Cr, with R_{ns} functions calculated from Martin and Glauber's theory, setting $R_{1s} = R_{2s} = 1$.

In total IB spectra that accompany low-energy transitions between high-Z nuclei, p radiation dominates; a correction function $f(k)$ can be calculated from theory, using shape functions Q^2_{np} and the corresponding subshell capture ratios. Because p-type spectra deviate considerably from the Morrison–Schiff spectrum, it is expected that a simple Jauch plot according to Eq. (4.81) may yield quite incorrect results. Consequently, the result for E_{EC} of ^{193}Pt derived by Hopke and Naumann (1969) from both the L- and M-capture bremsstrahlung (Fig. 50) by using Eq. (4.81) should be regarded with reservations.

It is clear that reliable theoretical calculations are necessary for obtaining accurate E_{EC} values from measured IB spectra. A strong argument for the performance of accurate new IB experiments is implied. Measurements on those decays for which accurate E_{EC} values are available from independent experiments are most valuable for testing IB theories.

5. Experimental results and comparison with theory: Allowed and first-forbidden nonunique transitions

Most experiments described so far deal with allowed electron-capture decays. They are to be compared with the theory of Martin and Glauber (1958) which, in the ξ approximation, is expected to apply also for first-forbidden nonunique decays.

In most experiments, only spectral shapes have been determined. The results, of varying accuracy, generally agree with theory. This agreement is found both for total IB spectra (experiments listed in Table XXVII) with dominating s- and p-type radiation and for 1*s* IB spectra singled out by IB–K-x-ray coincidences (Table XXIX). The situation is illustrated in Figs. 44, 55, and 56 for the s IB spectra of ^{51}Cr, ^{49}V, and ^{55}Fe, which cover different energy ranges. Figure 49 contains a comparison with theory of the 1*s* IB spectrum of ^{131}Cs and of the total IB spectrum which in this case covers an energy

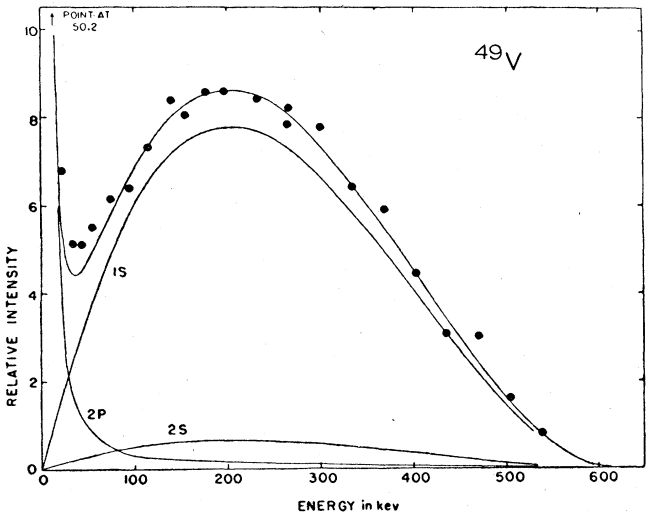

FIG. 55. IB spectrum of ^{49}V, measured with a well-type NaI(Tl) spectrometer. The full line represents the theoretical spectrum of Glauber and Martin (1956). The experimental points are normalized at 200 keV. [From Hayward and Hoppes (1956)].

range below αZ, so that p radiation dominates. Measured s IB spectra (including 1s IB spectra), however, are generally not sufficiently accurate to reveal the weak energy dependence of the predicted IB shape factors (mainly R_{1s}). The measured IB shapes can therefore not be used to distinguish between the theory of Martin and Glauber and the pioneering work of Møller (1937a) and Morrison and Schiff (1940). It is seen from Fig. 32 that R_{1s} depends on the energy k quite differently for different atomic numbers and in different energy regions. The most precise measurement of an allowed IB shape was performed by Berényi *et al.* (1965b) on ^{55}Fe. In Fig. 56, their result is displayed in terms of the effective shape factor $R_{\rm eff}$, defined by

$$R_{\rm eff}(k) \propto dw_{\rm IB}(k)/[k(q_{1s}-k)^2]. \tag{4.86}$$

The function $R_{\rm eff}$ is equal to R_{1s}, multiplied by the correction function $f(k)$ for higher-shell contributions [Eq. (4.85)]. The accuracy of the experiment of Berényi *et al.* (1965b) is comparable with the accuracy attainable in determinations of β shape factors. The constancy of $R_{\rm eff}$ within 1%, found in this measurement, can also be

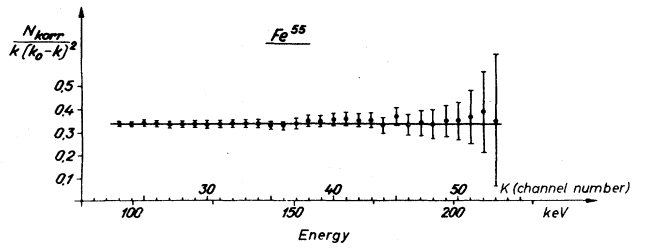

FIG. 56. Total IB spectrum of ^{55}Fe, measured by Berényi *et al.* (1965) with a 10.2×15.2-cm NaI(Tl) spectrometer. Data points represent the effective shape factor $R_{\rm eff}$, obtained by dividing the corrected spectrum ($N_{\rm Korr}$) by the Morrison–Schiff term $k(k_0-k)^2$. [From Varga (1970), courtesy of Hungarian Academy of Science].

compared in this special case with the Martin-Glauber theory. It is seen from Fig. 32 that, for $Z = 26$, the theoretical 1s shape factor has a flat maximum between 100 and 218 keV, the range covered by the ^{55}Fe experiment. To reveal the dependence of R_{1s} on k, accurate shape measurements below ~100 keV and on transitions of high energy (e.g., ^{37}Ar and ^{49}V) shoud be performed.

Only in a few experiments has the IB intensity been measured in addition to the shape. Some of the data on normalized IB spectra have been compiled and compared with theory by Bouchez and Depommier (1965), Kádár *et al.* (1970), Lancman and Lebowitz (1971a), Vanderleeden *et al.* (1971), Kádár (1971), Koonin and Persson (1972), and Mutterer (1973c). Conclusions from these summaries were partly inconsistent, depending on whether or not theoretical values were recalculated and which values for the transition energies $E_{\rm EC}$ were inserted. Here we therefore compare experimental results with consistently calculated theoretical values.

The selected experimental data on normalized IB spectra from allowed and first-forbidden nonunique decays are compiled in Table XXX. These data represent integral values $I_{\rm IB}(k_1,k_2)$ of normalized spectra $dw_{\rm IB}$, measured between energy limits k_1 and k_2. The upper limits k_2 are always equal to or slightly below the end-point energies q. We did not consider data for which k_1 and k_2 were not specified, as in measurements on ^{51}Cr by Cohen and Ofer (1955), Ofer and Wiener (1957), Murty and Jnanananda (1957), and Ribordy and Huber (1970). In these experiments, the γ branching ratio in ^{51}Cr was determined by comparing IB and γ intensities. We also have omitted results on ^{51}Cr reported by Vanderleeden *et al.* (1971) and Kuphal *et al.* (1973), which were deduced from measurements of circularly polarized bremsstrahlung, because the measured energy range could not be inferred clearly. It is to be noted that experimental $I_{\rm IB}$ values obtained from measured IB pulse-height spectra through the folding method (Sec. IV.B.3) also do not exactly represent the IB intensity within stated limits, but rather constitute ratios of counting rates between corresponding limits E_1 and E_2. These values are included in the comparison, but are specially identified in Table XXX. In this table, we distinguish between values for 1s IB intensities I_{1s} and intensities of total IB spectra, measured relative to the ordinary K or total electron-capture rates.

The experimental values listed in Table XXX are compared with predictions according to different approaches to the theory of allowed radiative capture. Predictions for 1s IB intensities (which dominate as well in most of the listed total spectra) have been calculated from the Coulomb-free theory of Morrison and Schiff (MS) (1940) and from the theory of Martin and Glauber (MG) (1958). Results are listed from both the (analytical) low-energy approximation of Eq. (4.38) (MG) and the (numerically calculated) exact solution [Eq. (4.44)] as derived by Intemann (Int) (1971). The higher-shell contributions were consistently calculated from the approximate relativistic Martin–Glauber theory (Glauber and Martin, 1956) with screening corrections of Fig. 36. We consistently used transition energies $E_{\rm EC}$ derived from the atomic mass compilation of Wapstra and Gove (1971) and, for electron-capture decays to exited states, from γ energies

TABLE XXX. Measured IB intensities for allowed and first nonunique forbidden transitions, compared with theoretical values.

Z	Elements	A	Final state (keV)	$J_i^\pi - J_f^\pi$	E_{EC}[1] (keV)	Energy range (keV)	Intensity ratio	Expt. value ($\times 10^{-5}$)	Theoretical values ($\times 10^{-5}$) MS	MG	Int	References[2]
						A. Allowed transitions $\Delta J = 0, 1;\ \pi_i \pi_f = +1$						
4	Be	7	0	$\frac{3}{2}^- - \frac{3}{2}^-$	861.75 ± 0.09	523.7–k_{max}	I_{IB}/W_{EC}	9.0 ± 0.6	9.35	8.56	8.57	Mutterer (1973b)[a]
			477.6	$\frac{3}{2}^- - \frac{1}{2}^-$	384.1 ± 0.1	50 –360	I_{IB}/W_{EC}	10.3 ± 0.6	9.95	9.19	9.20	Persson (1972)[b]
						100 –360	I_{IB}/W_{EC}	8.6 ± 0.6	7.82	7.25	7.26	Persson (1972)[b]
						120 –360	I_{IB}/W_{EC}	7.7 ± 0.5	6.83	6.39	6.35	Persson (1972)[b]
						120 –360	I_{IB}/W_{EC}	4.9 ± 1.0[3,4]	6.83	6.39	6.35	Lancman (1971b)[c]
18	A	37	0	$\frac{3}{2}^+ - \frac{3}{2}^+$	814.1 ± 0.6	35 –k_{max}	I_{IB}/W_K	52 ± 13[5]	52.1	36.9	37.6	Saraf (1956)[d]
24	Cr	51	0	$\frac{7}{2}^- - \frac{7}{2}^-$	751.6 ± 0.9	348.1–k_{max}	I_{IB}/W_{EC}	9.56 ± 0.60	14.6	9.13	9.43	Mutterer (1973a)[e]
			320.1	$\frac{7}{2}^- - \frac{5}{2}^-$	431.1 ± 1.0	130 –425	I_{IB}/W_{EC}	7.2 ± 0.4	8.34	5.41	5.58	Koonin (1972)[f]
25	Mn	54	835.3	$3^+ - 2^+$	540.1 ± 3.6	100 –420	I_{IB}/W_{EC}	5.8 ± 1.3[3,4]	16.5	10.5	10.8	Lancman (1969)[g]
						82 –k_{max}	I_{IB}/W_{EC}	17.2 ± 3.0[3,4]	18.1	11.5	11.9	Kádár (1970)[h]
						82 –515	I_{IB}/W_{EC}	15.4 ± 0.8	18.1	11.5	11.9	Koonin (1972)[i]
26	Fe	55	0	$\frac{3}{2}^- - \frac{5}{2}^-$	231.7 ± 0.7	50 –k_{max}	I_{IB}/W_K	4.0 ± 1.0[4]	3.42	2.20	2.28	Michalowicz (1953)[j]
						100 –k_{max}	I_{IB}/W_K	1.4 ± 0.4[5]	1.68	1.07	1.11	Saraf (1956)[k]
						0 –k_{max}	I_{IB}^{1s}/W_K	1.5 ± 0.8	3.76	2.15	2.26	Biavati (1959, 62)[l]
27	Co	57	136.3	$\frac{7}{2}^- - \frac{5}{2}^-$	700.4 ± 0.7	180 –465	I_{IB}/W_{EC}	8.8 ± 1.8[3,4]	21.0	12.8	13.3	Lancman (1971a)[m]
32	Ge	71	0	$\frac{1}{2}^- - \frac{3}{2}^-$	235.1 ± 1.7	70 –k_{max}	I_{IB}/W_K	2.3 ± 0.5	2.82	1.70	1.79	Bisi (1955a)[n]
51	Sb	119	23.8	$\frac{5}{2}^+ - \frac{3}{2}^+$	555 ± 20	0 –k_{max}	I_{IB}^{s}/W_K	10.6 ± 1.2[6]	22.0	8.46	10.2	Olsen (1957)[o]
55	Cs	131	0	$\frac{5}{2}^+ - \frac{3}{2}^+$	355 ± 6	0 –k_{max}	I_{IB}^{1s}/W_K	1.4 ± 1.0	7.61	2.25	3.14	Biavati (1959, 62)[p]
68	Er	165	0	$\frac{5}{2}^- - \frac{7}{2}^-$	371 ± 4	93 –306	I_{IB}^{1s}/W_K	1.63 ± 0.16	4.87	1.05	1.67	Sujkowski (1965)[r]
						182 –306	I_{IB}^{1s}/W_K	0.53 ± 0.06	1.52	0.34	0.50	Sujkowski (1965)[r]
						185 –300	I_{IB}/W_K	0.9 ± 0.2	2.39	1.28	1.43	Zylicz (1963)
						185 –300	I_{IB}/W_K	0.89 ± 0.12	2.39	1.28	1.43	Sujkowski (1965)
						B. First nonunique forbidden transitions $\Delta J = 0, 1;\ \pi_i \pi_f = -1$						
62	Sm	145	61.2	$\frac{7}{2}^- - \frac{7}{2}^+$	577 ± 7	120 –239	I_{IB}/W_K	6.7 ± 0.7[7]	11.9	5.87	6.73	Sujkowski (1968)
						120 –412	I_{IB}/W_K	10.1 ± 1.0[7]	20.7	9.18	10.6	Sujkowski (1968)
						169 –412	I_{IB}/W_K	7.3 ± 1.2[7]	15.1	6.08	7.14	Sujkowski (1968)
						129 –412	I_{IB}^{1s}/W_K	4.6 ± 0.8	14.9	3.90	5.28	Sujkowski (1968)[q]
						169 –412	I_{IB}^{1s}/W_K	3.6 ± 0.5	12.2	2.19	4.25	Sujkowski (1968)[q]
66	Dy	159	0	$\frac{3}{2}^- - \frac{3}{2}^+$	365.4 ± 1.0	185 –300	I_{IB}/W_K	1.0 ± 0.3[8]	2.24	1.18	1.32	Sujkowski (1965)
80	Hg	197	77.3	$\frac{1}{2}^- - \frac{1}{2}^+$	686 ± 40	350 –550	I_{IB}^{1s}/W_K	1.6 ± 0.3	5.49	0.83	1.26	Jasinski (1965)[s]

[1]Calculated using Q_{EC} values from Wapstra and Gove (1971), except for ^{197}Hg where E_{EC} as derived from the measured endpoint is given.
[2]Labeled with corresponding letters in Figs. 57–59.
[3]Recalculated from quoted I_{IB}/W_K values with the P_K values used in the original papers.
[4]Derived by using the folding method (Sec. IV.B.3.b).
[5]Recalculated from stated experimental to theoretical yield by using 1s IB shape factors from the approximate relativistic theory of Glauber and Martin (1956).
[6]Extrapolated from the spectrum as measured for energies higher than 180 keV.
[7]Includes bremsstrahlung of 8% EC branch to the ground state of ^{145}Pm.
[8]Includes bremsstrahlung of the 26% EC branch to the 58.2 keV excited state in ^{159}Tb.

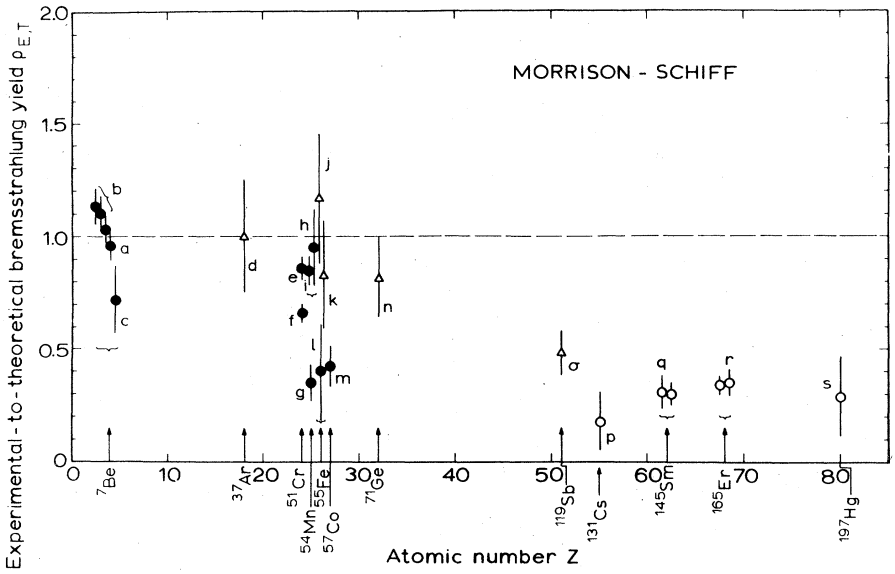

FIG. 57. Ratios $\rho_{E,T}$ of experimental to theoretical bremsstrahlung yields, calculated with theoretical IB intensities according to Morrison and Schiff (1940). Values are given for 1s IB intensities per K capture (open circles); total IB intensities in which s contributions predominate, relative to K-capture rates (triangles); and total IB intensities relative to total electron-capture rates (filled circles). References for experimental data are given in Table XXX.

as evaluated by Meixner (1971). Energies q_{nl} were calculated from atomic binding energies (Bearden and Burr, 1967). The only exception is ^{197}Hg, where the E_{EC} value of 338 ± 20 keV derived from the mass table (which originates from a $P_K\omega_K$ measurement by DeWit and Wapstra, 1965) falls completely outside of the range of the measured IB spectrum. Uncertainties in the calculated intensities which are due to the stated errors in the energy E_{EC} were estimated from the Coulomb-free theory by differentiating Eq. (4.16) with respect to q_{1s}. These uncertainties were found to be generally below 1%, except for ^{71}Ge, ^{131}Cs, ^{145}Sm and ^{165}Er, where they lie between 2% and 7%, and for ^{197}Hg, where it is 40%.

In Figs. 57 to 59, ratios $\rho_{E,T}$ of experimental and theoretical bremsstrahlung intensities are plotted as a function of atomic number. We have included only data which pertain predominantly to s radiation. The indicated error bars correspond to the sum of experimental and theoretical errors.

In Table XXXI, unweighted average values $\langle \rho_{E,T} \rangle$ of independent measurements are listed.

The summary of experimental and theoretical IB intensities proves the advantage of the theory of Martin and Glauber over the Coulomb-free approach. The measured data, although widely scattered, clearly reveal the predicted reduction of the IB intensity, increasing with Z, that is caused by relativistic and Coulomb effects. While this lowering of the intensity is most obvious in the heavier nuclides with $51 \leq Z \leq 80$, it can also be noted, on the average, in the data on lighter nuclides with $18 \leq Z \leq 32$.

The ratios $\rho_{E,T}$ between measured data and theoretical intensity according to either MG or Int deviate from unity by up to 50%; the deviations in most cases are larger than the error bars. The available data do not allow one to distinguish between the approximate solution of MG and the exact solution of Int. The average values $\langle \rho_{E,T} \rangle$ in Table XXXI provide no evidence that

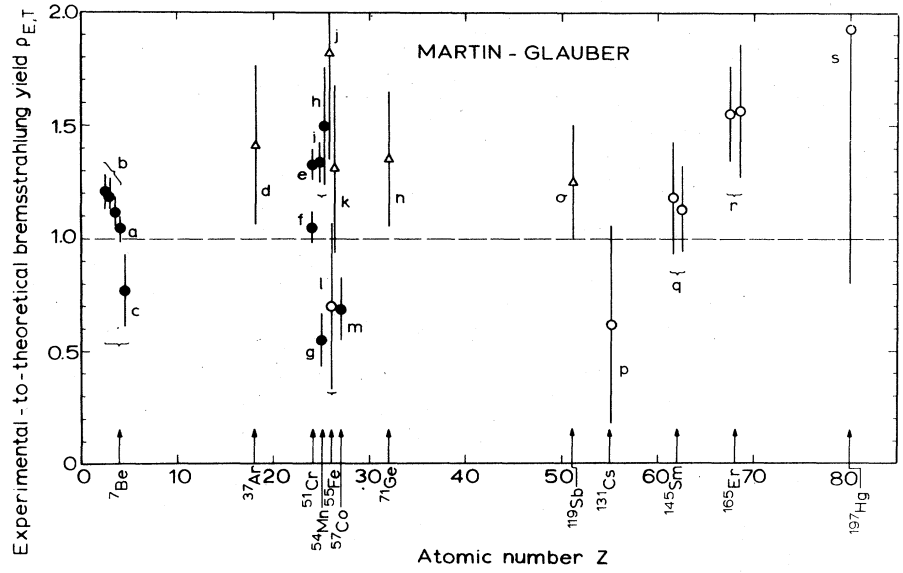

FIG. 58. Ratios of experimental to theoretical bremsstrahlung yields, calculated with theoretical IB intensities from the theory of Martin and Glauber (1958), with $R_{1s}(Z,k)$ from Eqs. (4.37) and (4.38). For notation and references see caption of Fig. 57.

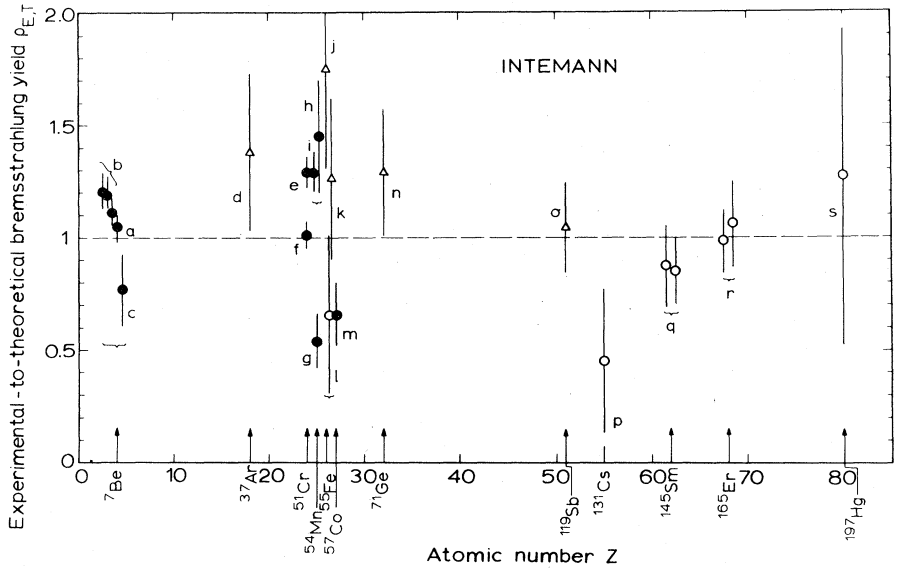

FIG. 59. Ratios of experimental to theoretical bremsstrahlung yields, calculated with theoretical IB intensities according to Intemann (1971) for $R_{1s}(Z,k)$ [Eq. (4.44)]. For notation and references see Fig. 57.

experiments deviate systematically from the Martin–Glauber theory, either at low Z or in general, contrary to indications in previous surveys by Lancman and Lebowitz (1971a) and Vanderleeden *et al.* (1971). On the other hand, the inconsistency between experimental results makes it difficult to assign a limit within which the present theory correctly seems to describe the intensity of bremsstrahlung.

Inspection of the experimental data shows that there is a special discrepancy between some of the most recent results obtained by different groups of authors, with quoted probable errors of 6% to 20%. The IB–γ coincidence experiments of Lancman and Lebowitz (1969, 1971a,b) on ^{7}Be, ^{54}Mn, and ^{57}Co yielded intensities that fall 20% to 50% below theoretical predictions, whereas similar experiments, performed with improved techniques by Persson and Koonin (1972) and Koonin and Persson (1972) on ^{7}Be, ^{51}Cr, and ^{54}Mn led to results that exceed theoretical intensities by up to 30%. The spectrometry of IB and γ rays in ^{7}Be and ^{51}Cr by Mutterer (1973a,b) yielded IB intensities which are in agreement with theory to within $\leq 8\%$. This inconsistency suggests that unknown sources of systematic errors of $\leq 10\%$ remain in the experimental techniques and in the procedures applied for the response correction.

Double IB. Experimental evidence for the simultaneous emission of two IB photons during electron capture, or double internal bremsstrahlung, has been reported by Ljubičič *et al.* (1974). Coincidences between two IB photons from ^{37}Ar were measured at an angle of 90° to each other. In the energy range from 210 to 810 keV, the ratio of double IB to single IB was found to be $(4.8 \pm 0.4) \times 10^{-5}$, which is comparable to the IB/EC rate, as might be expected. The only presently available theoretical results on double IB are those of Menhardt (1957), which unfortunately are not applicable to the experimental situation realized by Ljubičič *et al.* (1974).

TABLE XXXI. Average experimental-to-theoretical IB yield $\langle \rho_{E,T} \rangle$ for various regions of the atomic number Z.

Region of Z	$4 \leq Z \leq 80$	$Z = 4$	$18 \leq Z \leq 32$	$51 \leq Z \leq 80$
Number of independent measurements	19	3	11	5
Theory of:	$\langle \rho_{E,T} \rangle$			
Morrison and Schiff	0.66	0.91	0.76	0.32
Martin and Glauber	1.19	0.98	1.19	1.31
Intemann	1.06	0.98	1.10	0.92

6. Experimental results and comparison with theory: IB spectra from higher-forbidden decays

Experimental information on IB spectra that accompany higher-forbidden transitions is limited to a few cases of ground-state transitions by electron-capture alone (^{41}Ca and ^{59}Ni) or with competing β^- branches (^{36}Cl and ^{204}Tl). Some of these decays have been measured extensively (Tables XXVII and XXIX).

Bremsstrahlung from *first-forbidden unique transitions* has been studied with ^{41}Ca and ^{204}Tl. The total IB spectrum from ^{41}Ca was measured with a Ge(Li) spectrometer by Mysl̆ek *et al.* (1973). The observed shape (Fig. 60) is not in accord with the theory of Zon and Rapoport (1968) and Zon (1971). The shape agrees with theory only at low energies, $k < 250$ keV; at higher energies the spectrum has nearly allowed shape. Mysl̆ek *et al.* have also derived a crude value for the IB intensity by estimating the K capture rate from the weight of the source. A value of 3.9×10^{-4} IB photons between 90 and 421.5 keV per electron-capture event was found, much in excess of theoretical predictions. For forbidden transitions, theory in the Coulomb-free approach of Eq. (4.79) leads to an upper limit of 5.7×10^{-5} IB photons per decay. The low-Z expansion of Zon and Rapoport (1968) results in a value of 3.3×10^{-5} photons and more detailed calculations of Zon (1973) have yielded 4.9×10^{-5} photons per electron-capture transition.

On ^{204}Tl, several IB–K-x-ray coincidence experiments have been performed to measure the 1s IB spectrum that accompanies the 2.1% electron-capture branch to

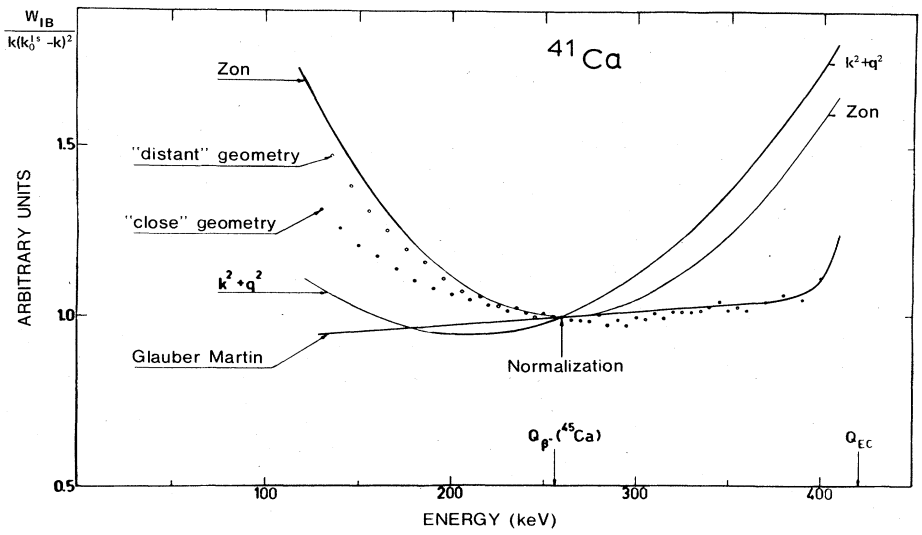

FIG. 60. IB spectrum of ^{41}Ca, measured with a Ge(Li) spectrometer in two different geometries. The spectra (w_{IB}) divided by the Morrison–Schiff spectrum $k(k_0^{1s} - k)^2$ are compared with predicted IB shape factors. [From Mysłek *et al.* (1973), courtesy of North-Holland Publishing Co.].

the ground state of ^{204}Hg. Severe doubts exist regarding the reliability of early experiments by Der Mateosian and Smith (1952), Jung and Pool (1956), and Biavati *et al.* (1962), because no corrections for the bremsstrahlung from the 97.9% β^- branch to ^{204}Pb were applied. It was first pointed out by Goudsmit *et al.* (1966) and established by a recent experiment of Lancman and Bond (1973) that scattering effects due to the β^- bremsstrahlung and double-IB emission can cause a continuous spectrum that closely resembles the IB spectrum expected from the weak electron-capture branch. The shape of the IB spectrum measured by Lancman and Bond, taking account of corrections for these effects, agrees well with the theory for allowed transitions. Such agreement is expected because only a small energy range is involved. The intensity per K capture was found to be 2.8×10^{-6} IB photons above 103 keV. This result is to be compared with an upper limit of 1.08×10^{-5}, from Eq. (4.79). More accurate theoretical results are not available. Zon (1973) has reported only values for the shape factors, and the $Z\alpha$ expansion of Zon and Rapoport (1968) is not applicable for ^{204}Tl, because the entire IB spectrum lies in the region of the K binding energy.

Bremsstrahlung spectra from *second-forbidden nonunique transitions* were studied with ^{36}Cl and ^{59}Ni by several groups. It has been well established that the total IB spectrum of ^{36}Cl closely follows an allowed shape at energies above 600 keV. This observation agrees with the calculation of Zon (1971), which predicts a noticeable deviation from allowed shape only at lower energies. The result of the most recent IB measurement on ^{36}Cl by Smirnov and Batkin (1973) is shown in Fig. 61. An attempt was made to look for possible contributions from detour transitions; a clear indication could, however, not be established.

In the case of ^{59}Ni, a distinct deviation of the IB spectrum from allowed shape was observed already in an early measurement by Saraf (1956); the IB intensity above 100 keV was reported to be 1.4 ± 0.4 times the theoretical value calculated from the early theory of Cutkowsky (1954). The shape of the ^{59}Ni IB spectrum was very carefully measured by Schmorak (1963), who used 3×3-in. and 5×5-in. NaI(Tl) detectors. An apparent deviation from the calculated shape, observed near the end point, was attributed to destructive interference with detour transitions, as predicted by Rose *et al.* (1962). Schmorak (1963) estimated the amount of

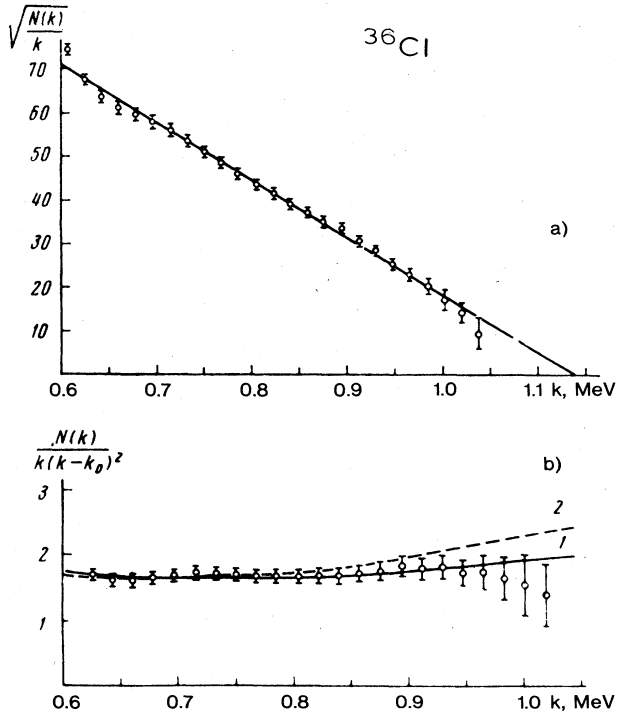

FIG. 61. Total IB spectrum accompanying the second-forbidden nonunique electron-capture decay of ^{36}Cl, measured with a 10×10-cm NaI(Tl) spectrometer. The spectrum is shown in Jauch coordinates (a) and in form of the effective shape function $\mathcal{R}_{eff}$ (b). The latter is compared with theoretical shape functions, calculated with (1) and without (2) including detour transitions. [From Smirnov and Batkin (1973), courtesy of Nauka Press].

detour transitions as between 6×10^{-3} and 5×10^{-4} of the total IB intensity. A careful Ge(Li) measurement of the ^{59}Ni IB spectrum was recently performed by Berényi *et al.* (1976), who report that the measured shape agrees well with calculations of Zon (1971) and shows no evidence for detour transitions.

In most experiments performed hitherto, only spectral shapes have been determined, albeit often with high precision. Without question, accurate measurements of *normalized* spectra would be of great value to improve our present knowledge of radiative capture in forbidden electron-capture transitions. Pertinent electron-capture nuclides are listed in Table XXVIII.

7. Experiments on IB correlation effects

Experiments on the various IB correlation effects that are discussed in Secs. IV.A.3–IV.A.4 are scarce. They are confined to allowed decays and to measurements of circular polarization and to some work on the angular distribution of IB photons emitted from oriented nuclei.

a. Circular polarization of internal bremsstrahlung

Experiments on the circular polarization of the IB accompanying electron capture are listed in Table XXXII. Polarimeters employed in these measurements are based on the effect of spin-dependent Compton scattering from electrons in magnetized iron. Usually, forward-scattering magnets have been used, but in the most recent experiment by Kuphal *et al.* (1974), a specially designed radial-transmission magnet was employed.

The polarization P, defined by Eq. (4.48), is proportional to the relative change $\Delta N/N$ of the measured intensity when the magnetic field in the scattering magnet is reversed

$$P \propto \Delta N/N = 2(N_+ - N_-)/(N_+ + N_- - 2N_0). \qquad (4.87)$$

Here, N_+ (N_-) is the counting rate with the electron spins in iron parallel (antiparallel) to the incident-photon momentum. The counting rate N_0 is due to background, including γ impurities in the source. If nuclides are measured which emit also nuclear γ rays, the denominator in Eq. (4.87) is represented by the counting rate of the unpolarized γ rays. The measured effect is then extremely low.

The polarization of IB in pure ground-state transitions was studied in early measurements on ^{37}Ar by Hartwig and Schopper (1958) and Mann *et al.* (1959), ^{55}Fe by Parfenova (1960), and ^{71}Ge by Bernardini *et al.* (1958). Only recently, IB polarization has also been measured in the presence of a background of much more intense γ rays. In such experiments on ^{51}Cr, Vanderleeden *et al.* (1971) used a Ge(Li) detector, whereas Kuphal *et al.* (1974) used a ring of 8 NaI(Tl) scintillators. In both experiments, very strong ^{51}Cr sources of up to 500 Ci were employed, and current integration was applied instead of counting techniques. The statistical errors could be kept below 10^{-6}. Clearly, the polarimeter efficiency must be accurately know to derive the absolute polarization from the measured rate $\Delta N/N$. This efficiency has generally been calculated from basic assumptions. Kuphal *et al.* (1974) have tested their calculation by measuring polarized (internal and external) bremsstrahlung from several β^--decaying nuclides.

Measurements summarized in Table XXXII confirm within errors that s-type bremsstrahlung is nearly 100% right-circularly polarized, due to the parity-nonconserving character of the weak interaction. The measured polarization of IB from ^{37}Ar (Hartwig and Schopper, 1958) is displayed in Fig. 62. Figure 63 shows $\Delta N/N$ values measured for ^{51}Cr, compared with calculations from theory. The incomplete polarization observed in ^{37}Ar at low energies and the low result for ^{71}Ge found by Germanoli *et al.* (1958) can qualitatively be explained by Coulomb effects and the influence of unpolarized p-type bremsstrahlung. Both effects, which enter in the overall polarization function $P(k)$ according to Eq. (4.52), reduce the polarization at low energies. A noticeable reduction of P is not expected, however, in the high-energy bremsstrahlung from ^{51}Cr; the low value of 0.67 ± 0.07 found by Vanderleeden *et al.* (1971) can probably be attributed to an erroneous calculation of the polarimeter efficiency, in view of the work of Kuphal *et al.* (1974).

b. Angular distribution of IB emitted from oriented nuclei

Anisotropy of IB emitted from oriented nuclei has been observed only once. Brewer and Shirley (1968) studied the forward-backward asymmetry of IB from oriented ^{119}Sb. Carrier-free ^{119}Sb had been implanted in an iron lattice, cooled to ~0.02 °K, and magnetized in a field of 2.3 kOe. The IB radiation was measured with two 3×3-in. NaI(Tl) detectors placed at 0° and 180° relative to the direction of the magnetic field. Figure 64 shows the measured asymmetry $W(\pi)/W(0)$ as a function of the sample temperature T that defines the degree of source

TABLE XXXII. Circular Polarization of IB in allowed electron-capture transitions.

Z	Elements	A	Final state (keV)	E_{EC} [a] (keV)	Energy range (keV)	Degree of Polarization	Polarimeter type [b]	References
18	A	37	0	814.1±0.6	200–k_{max}	1.03±0.04	f.s.m.	Hartwig (1958)
						0.97±0.15 [c]	f.s.m.	Mann (1958)
24	Cr	51	0 (90.2%)	751.4±0.9		0.67±0.07 [c]	f.s.m.	Vanderleeden (1971)
			320.1 (9.8%)	431.3±1.0		1.2 ±0.1	r.t.m.	Kuphal (1974)
26	Fe	55	0	231.7±0.7	85–220	0.98±0.1	f.s.m.	Parfenova (1960)
32	Ge	71	0	235.1±1.7	70–120	~0.4	f.s.m.	Bernardini (1958)

[a] From Wapstra and Gove (1971).
[b] f.s.m. = forward-scattering magnet. r.t.m. = radial transmission magnet.
[c] Polarization of IB from both EC branches.

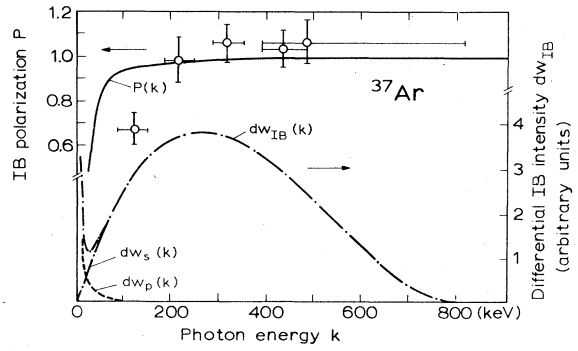

FIG. 62. Circular polarization (P) of the IB from ^{37}Ar as a function of energy, measured with a forward-scattering Compton polarimeter provided with a NaI(Tl) detector. (Hartwig and Schopper, 1958). The solid line is the theoretical curve, calculated from Eq. (4.52) with the polarization functions α_{1s} and α_{2s} of Fig. 37. The IB spectrum of ^{37}Ar is also shown.

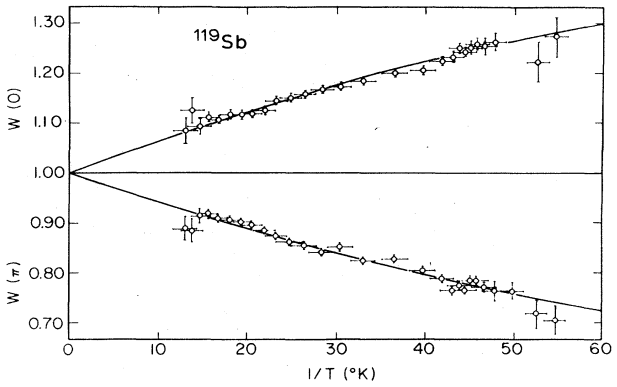

FIG. 64. Forward-backward asymmetry $W(\pi)/W(0)$ in the emission of IB photons from polarized ^{119}Sb nuclei, as a function of sample temperature. [From Brewer and Shirley (1968)].

polarization. The measurement of this ratio for different energy intervals has revealed an unexpected energy dependence of the asymmetry.

The experimental results of Brewer and Shirley have been compared with theory by Intemann (1971) in terms of the over-all asymmetry function $A(k)$ of Eq. (4.62). It was found that the measured decrease of $A(k)$ at low energies can be well explained (Fig. 65). This decrease is consistent with the observed decrease of the over-all polarization, described above. Other nuclei that might be suitable for measuring IB angular correlations have been listed by Koh *et al.* (1962).

A preliminary measurement of the angular correlation between bremsstrahlung and nuclear γ rays in the decay of ^{84}Rb has been performed by Chasan and Chandra (1967). The result was reported to be in approximate agreement with calculations of Koh *et al.* (1962). The experimental error, however, is ~50% and details of the measurement have not been fully reported, so that a detailed comparison with theory is not feasible.

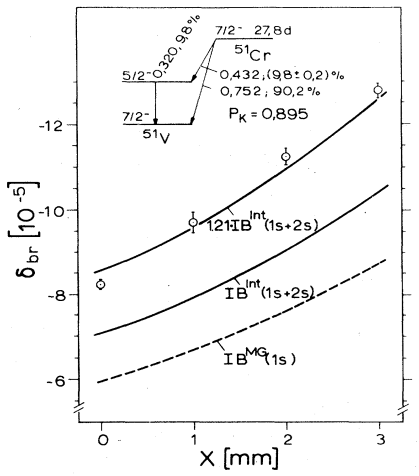

FIG. 63. Relative change $\delta(x)$ in the Compton absorption of ^{51}Cr photons in iron that is magnetized parallel and antiparallel, respectively, to the photon momentum. The Compton polarimeter has a special radial-transmission magnet. Photons are recorded with NaI(Tl) detectors applying current integration techniques. Values of $\delta(x)$ for different Pb absorbers of thickness x between source and magnet are shown. Solid lines are calculated from IB theory. [From Kuphal *et al.* (1974)].

8. Concluding remarks

The study of second-order effects, such as internal bremsstrahlung, is of particular interest in electron-capture decay because experimental information on the primary process is very limited because of the extremely low interaction probability of the emitted neutrino. The main features of the low-intensity radiative-capture process are generally understood today. There is still a great need, however, for experimental work to test the details of the theory. Open questions remain concerning the influence of screening and exchange and overlap effects (Persson and Koonin, 1972) on the shape and intensity of IB spectra. Experimental information is still very scarce on forbidden decays, where nuclear matrix elements play an important role.

Precise measurements of *normalized IB spectra* are very much needed. The same holds for measurements of partial spectra that accompany the capture of electrons from specific atomic subshells. Experimental techniques have been developed to high accuracy in recent years. This applies especially to the determination

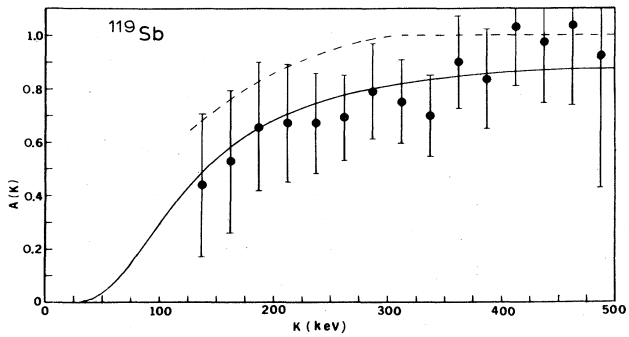

FIG. 65. Over-all asymmetry coefficient $A(k)$ of IB emission from oriented ^{119}Sb nuclei, measured by Brewer and Shirley (1968). Data points are compared with theoretical predictions, calculated with the asymmetry functions α_{1s} and α_{2s} of Fig. 38 (full curve), and with $\alpha_{1s}=\alpha_{2s}=1$ (dashed curve). [From Intemann (1971)].

of electron-capture rates, to coincidence experiments with bremsstrahlung, and to calibration procedures for γ spectrometers which yield complete response functions. It can be expected that it will be possible to measure normalized IB spectra in the near future with an over-all accuracy of a few percent, at least in some favorable decays such as pure ground-state transitions. As pointed out before, precise experiments are also very valuable for providing accurate isobaric atomic-mass differences, supplementary data on subshell capture ratios, and spectroscopic information on branching ratios. In this context, refined computations of higher-shell IB spectra, based on the present theory, would be of interest.

The variety of IB correlation effects, discussed in Sec. IV.A.3–IV.A.4, opens another wide field for future experimental work, from which valuable information on the weak interaction and nuclear structure can be expected. Bremsstrahlung measurements may also help to solve some specific problems of radionuclide metrology (Spernol *et al.*, 1973; Mutterer, 1973c), such as the (relative and absolute) determination of disintegration rates of pure electron-capture nuclides.

V. ATOMIC TRANSITIONS ACCOMPANYING NUCLEAR ELECTRON CAPTURE

A. Introduction

In first approximation, the probability of allowed capture of a K electron by the nucleus is

$$\lambda_K \propto G^2 q^2 \xi \left|\psi^{(K,Z)}(0)\right|^2, \tag{5.1}$$

where G is the β-decay coupling constant, q is the energy of the emitted neutrino, ξ the appropriate combination of nuclear matrix elements, and $\psi^{(K,Z)}(0)$ is the $1s$-electron wavefunction, evaluated at the origin (Sec. II). The only electron wavefunction contained in this formulation is that of the electron which is destroyed. Two significant aspects of the problem are neglected in Eq. (5.1): (1) the indistinguishability of electrons, and (2) the nuclear charge change by one unit, which entails that parent and daughter atomic wavefunctions are eigenfunctions of different Hamiltonians.

The importance of treating β decay and nuclear electron capture as transformations of the whole atom, and hence, of including atomic variables in the description of initial and final states, was first emphasized by Benoist-Gueutal (1950, 1953a,b), pursued by Odiot and Daudel (1956), and comprehensively formulated by Bahcall (1962a, 1963a,b). In fact, an infinite number of final atomic states, including continuum states, contribute to any given electron-capture probability. The effect on transition rates is discussed in Sec. II. In the present section, we consider observable atomic effects that result during nuclear decay by electron capture. Atomic rearrangements that take place *after* the decay process are not included in this discussion, even though x rays emitted in the course of such rearrangements have led to the discovery of the process (Alvarez, 1937, 1938a,b) and constitute the most readily detectable signals indicating that capture has taken place. Details of the rearrangement process have been surveyed by Rao *et al.* (1972) and Bambynek *et al.* (1972). Here, we consider atomic transitions that take place *in the course* of the electron-capture decay process, due to imperfect overlap between parent and daughter atomic wave functions. This effect is variously denoted as electron shakeup and shakeoff, autoionization, or internal ionization.

B. Internal ionization: Nonrelativistic theory

Nuclear electron capture is accompanied by the emission of low-intensity, continuous photon and electron spectra. The *internal-bremsstrahlung* photon spectrum emitted during radiative electron capture was first calculated by Møller (1937a) and by Morrison and Schiff (1940); this subject is discussed in Sec. IV. The process of *internal ionization* was first treated by Primakoff and Porter (1953), who calculated the probability of K-electron ejection during K capture and derived an expression for the ejected-electron spectrum, in analogy with work by Migdal (1941) and Feinberg (1941) on orbital-electron ejection accompanying β-particle emission.

The weak interaction which is responsible for nuclear electron capture is of very short range. On the atomic time scale, the transformation of the parent nucleus with Z protons into the daughter nucleus with atomic number Z' can be assumed to be instantaneous. One can gain an intuitive feeling for the mechanism that causes internal ionization by considering the nucleus plus the orbital vacancy created by the capture simply as the source of a suddenly changing Coulomb potential. A $1s$ electron, for example, with the wavefunction $\psi^{(K,Z)}$ in the parent atom does not have time to adjust its wavefunction adiabatically to the change in potential; the sudden approximation of time-dependent perturbation theory applies. The amplitude of the probability that the electron retains its original quantum numbers is then proportional to the overlap of its original wavefunction with the $1s$ wavefunction in the daughter ion with one inner vacancy[25]:

$$P_{\text{remain}} \propto \left| \int \psi^{(K,Z')*}(\mathbf{r}) \psi^{(K,Z)}(\mathbf{r})\, d\tau \right|^2. \tag{5.2}$$

Similarly, the overlap of $\psi^{(K,Z)}$ with excited- and continuum-state wavefunctions in the potential of the daughter ion provides an indication of the probability amplitudes of excitation or ejection of the K electron. The Pauli principle excludes excitation into occupied orbitals, and conservation of angular momentum allows only $l=0$ final states for s-electron shakeup or shakeoff.

It is a gross oversimplification, however, to consider the nucleus-plus-vacancy as a mere source of an abruptly changing electrostatic potential, and the internal excitation and ionization probabilities as determined by wavefunction overlap alone. In particular, energy conservation and the demands of quantum statistics are not included unless the process is treated as a transformation of the whole atom, and nuclear and lepton variables (including those characterizing the pertinent atomic

[25]The vacancy created by nuclear electron capture tends to counteract the effect of the decrease in nuclear charge from Ze to $(Z-1)e$. For this reason, the overlap integral of Eq. (5.2) is smaller than its analogs in $\beta^{\pm}$ decay.

electrons) are incorporated in the description of the initial and final states of the system. Especially, the available energy is shared statistically between ejected electron and neutrino, and the transition probability is weighted by the density of available final states. The energy-conserving delta function must be included in the expression for the transition probability.

Quantitatively, the transition probability can be expressed in the sudden perturbation approximation through "Fermi's Golden Rule No. 2." The general applicability of this approach to the present problem has been examined by Bahcall (1963a). The transition rate for K-electron ejection during K capture is

$$dw = 2\pi \int \tfrac{1}{2}\sum |M|^2 \delta(W_0 + 1 - |E'_K| - W - q)\, d\mathbf{q}\, d\mathbf{p}, \quad (5.3)$$

where $\mathbf{p}$ and W are the momentum and total relativistic energy of the ejected electron, $\mathbf{q}$ is the neutrino momentum, and q its energy, $1 - |E'_K|$ is the total energy of a K electron in the daughter atom (with binding energy E'_K), and $W_0 + 1$ is the energy difference between the parent atom and the neutral daughter atom (Sec. I.A). The matrix element M is discussed below. The units used throughout this discussion are such that $\hbar = m = c = 1$, and hence, $e^2 = \alpha \cong 1/137$. The summation sign in Eq. (5.3) indicates summing over spin states of ejected electron and neutrino, and over spin states of the two initial K electrons. One must also sum over final nuclear spin states and average over initial nuclear spin states. Because $\sum |M|^2$ is independent of $\mathbf{q}$, the integration over all possible neutrino momenta can be carried out at this stage.[26] The result, after performing the spin summations, is

$$dw = 16\pi^3 (W_0 + 1 - |E'_K| - W)^2 p^2 dp \sum |M|^2 \quad (5.4)$$

(Intemann, 1972).

In a representation in which the interaction Hamiltonian consists of the β interaction H_β alone, the matrix element for K-electron ejection during K capture can be written

$$M = (1 - P_{12}) \int \psi^{(\infty, Z')*}(\mathbf{r}) \psi^*_\nu(0) \psi^*_{N'} |H_\beta| \psi_N \psi^{(K,Z)}_{1,2}(0, \mathbf{r}) d\mathbf{r}. \quad (5.5)$$

Here, $\psi_{N'}$ and ψ_N are the final and initial nuclear wavefunctions, respectively, and ψ_ν is the neutrino wavefunction. The wavefunctions of the leptons that participate in the β interaction have been replaced by their values at the origin. It is assumed that all but the two K electrons retain their original quantum numbers, and that their initial and final wavefunctions overlap perfectly. The exchange operator P_{12} exchanges the two K electrons.

The main difficulty in explicitly writing out the matrix element (5.5) resides in expressing the initial-state two-electron wavefunction $\psi^{(K,Z)}_{1,2}$ including correlation effects between the two electrons. Primakoff and Porter (1953), in their classic calculation, used an approximate wavefunction of the form

$$\psi^{(K,Z)}_{1,2}(r_1, r_2) = N \psi^{(K,Z)}_1(r_1) \psi^{(K,Z)}_2(r_2) e^{\alpha r_1 r_{12}} e^{\alpha r_2 (r_1 + r_2)}, \quad (5.6)$$

where ψ_1 and ψ_2 are hydrogenic 1s wavefunctions, and N is chosen to assure normalization. The factor $e^{\alpha r_1 r_{12}}$ takes account of the effect of the electron–electron Coulomb interaction on their spatial correlation, and the factor $e^{\alpha r_2 (r_1 + r_2)}$ accounts for screening of the nucleus, effectively replacing Z by $Z - \gamma_2$ in ψ_1 and ψ_2. The parameters γ_1 and γ_2 were chosen so that ψ_{12} is a good approximation to the Hylleraas variational wavefunction for a two-electron atom. With a Coulomb wavefunction $\psi^{(\infty, Z')}$ to describe the ejected electron and a plane wave to describe the neutrino, the matrix element (5.5), and hence, the transition rate (5.3) were computed. Dividing by the transition rate w_K for ordinary allowed K capture, Primakoff and Porter derived an expression for the probability, per K-capture event, for ejection of the other K electron with a momentum in the range dp. This result can be written

$$dw_{\text{ejec}} = \frac{dw}{w_K} = \frac{16\alpha^2 \zeta^4 p \exp[-(4\zeta/p)\tan^{-1}(p/\zeta)]}{(\zeta^2 + p^2)^4 (1 - e^{-2\pi\zeta/p})} \times \left[1 - \frac{p^2/2 + |E'_K|}{W_0 + 1}\right]^2 dp. \quad (5.7)$$

Again, W_0 and the K-electron binding energy E'_K are in units of mc^2, the ejected-electron momentum p is in multiples of mc, and ζ stands for αZ. We have neglected $\gamma_1 + \gamma_2 \cong 0.5$ and unity compared with Z in the final result, and have set $\beta = p$, i.e., $W \approx 1$ for the ejected electrons, whose kinetic energy is generally very much smaller than mc^2. As before, $1 + W_0 = \Delta W_{\text{nucl}} - \Delta(\Sigma E_x) + 1$ is the mass difference between parent and daughter neutral *atoms*: ΔW_{nucl} is the nuclear energy release, and $\Delta(\Sigma E_x)$ is the change in the total electronic binding energy between parent and daughter atoms—a positive quantity in electron capture (Sec. I.B).

A very different method for constructing the initial two-electron wavefunction was devised by Intemann and Pollock (1967), who calculated it from perturbation theory. They treated the electron–electron interaction as a perturbation on the nuclear Coulomb interaction, including it in the perturbed part of the Hamiltonian, rather than in the unperturbed part as Primakoff and Porter had done. In essence, they performed a perturbation expansion on the exact two-electron wavefunction, with the perturbation taken to be the electron–electron interaction. With this approach, the problem of K-shell internal ionization during K capture is one in third-order perturbation theory, involving a sum over intermediate electron states. Intemann and Pollock found it possible to represent this sum in closed form by drawing upon the analogy between internal ionization and internal-bremsstrahlung emission. In fact, the electron-ejection process can be looked upon as a radiative capture process in which the emitted photon is virtual, and is absorbed by the electron that is ejected. Exploiting this aspect of the problem, Intemann and Pollock were able to take advantage of a crucial observation made by Glauber and Martin (1956; Martin and Glauber, 1958)

[26] The upper limit of the neutrino energy is only approximately $W_0 + 1 - |E'_K| - W$ as implied by the energy-conserving delta function in Eq. (5.3). The neutrino energy is reduced by the binding energy of the second K electron in the daughter atom that already contains one K hole, and increased by the additional relaxation energy of the electron cloud.

in their development of the theory of radiative capture, viz., that the sum over intermediate electron states which appears in the calculation is the Green's function for the Dirac equation with a nuclear Coulomb potential and can be represented in closed form. This approach made a more exact analysis of the internal-ionization process possible. The result for the differential transition rate per K-capture event is

$$dw_{\text{ejec}} = \frac{64\alpha^2\zeta^4 p \exp\{-(4\zeta/p)\tan^{-1}[p/(2\zeta+\mu)]\}}{(\mu+\zeta)^4[(2\zeta+\mu)^2+p^2]^2(1-e^{-2\pi\zeta/p})} \times[(1-p^2)/2(W_0+1)]^2 I^2\, dp. \tag{5.8}$$

Here, we have $\mu=[2(1-\epsilon)]^{1/2}$, where ϵ is the intermediate-state energy (in units of mc^2) of the electron undergoing capture: $\epsilon=\epsilon_1+\epsilon_2-W$, where ϵ_1 and ϵ_2 are the energies of the initial K electrons, and W is the energy of the ejected electron. In the Intemann–Pollock treatment, the relation $\epsilon=1-\zeta^2-p^2/2$ holds, because $\epsilon_1=\epsilon_2=1-\zeta^2/2$ and $W=1+p^2/2$.

The integral I is

$$I = 1+\eta\int_0^1 x^{-\eta-1}[1-(1-x)^4 f(x)]\,dx, \tag{5.9}$$

where

$$f(x)=\frac{\exp\{-(2\zeta/p)\tan^{-1}[(2\zeta+\mu)/p]\}\exp\{(2\zeta/p)\tan^{-1}[(2\zeta/p)+\mu(1+x)/p(1-x)]\}}{(1+\lambda x)^2(1+\sigma x)(1+\sigma^* x)} \tag{5.10}$$

and the remaining symbols are defined as $\eta=\zeta/\mu$, $\sigma=(\mu-2\zeta-ip)/(\mu+2\zeta+ip)$, $\lambda=(\mu-\zeta)/(\mu+\zeta)$. Fortunately, a rapidly converging Maclaurin series exists for I

$$I=\eta\sum_{n=0}^{\infty}\frac{f^{(n)}(0)}{n!}\left[-\frac{1}{(n-\eta)}+\frac{4}{(n+1-\eta)}-\frac{6}{(n+2-\eta)}+\frac{4}{(n+3-\eta)}-\frac{1}{(n+4-\eta)}\right]. \tag{5.11}$$

Intemann and Pollock find that, for $Z=26$, an error only of order ζ^2 results from breaking the series off after the first three terms.

The energy spectrum of electrons ejected from ^{55}Fe, predicted by this more exact theoretical approach, does not appear to differ materially from that of Eq. (5.7) when placed on a semilogarithmic plot (Intemann and Pollock, 1967). Some writers have consequently assumed that the results of the two theories are truly identical. This is not the case. In fact, the momentum spectra from the two approaches differ appreciably on a linear plot; they have approximately the same shape, but the Intemann–Pollock spectrum has somewhat lower intensity. Hence it yields significantly smaller values for the total ejection rate than the Primakoff–Porter theory (Intemann, private communication). That the difference is not greater appears to indicate that Primakoff and Porter's variational wavefunction takes unexpectedly accurate account of screening and correlations in the initial two-electron state. Improving the accuracy of the continuum wavefunction to take screening in the final state into consideration is only expected to affect the results of Eqs. (5.7) and (5.8) by $\lesssim 5\%$ for $Z=26$.

The neglect of relativistic effects inherently limits the accuracy of the results to a relative error of order αZ, even at the lowest ejection energies. The nonrelativistic calculations were pushed to this limit in a refinement, due to Intemann (1972), of the Intemann–Pollock approach, which involves the use of a more elaborate Coulomb Green function. This modification has the effect of considerably reducing the calculated K ejection probabilities w_{ejec}, particularly at high Z, as compared with the Intemann–Pollock results (Intemann, 1974). The reduction in the predicted intensity of the ejected-electron spectrum can be understood in the following terms (Intemann, 1975). In all calculations based on the Intemann–Pollock approach (including the one discussed in Sec. V.C), retardation effects are neglected and the interaction between the two electrons is taken to be an instantaneous Coulomb interaction, so that the exchange of only longitudinal and scalar virtual photons can be considered. In the approximation used by Intemann and Pollock (1967), only s-wave intermediate states make a contribution to the transition amplitude, and thus, only scalar photon exchange is taken into account. In his later paper, Intemann (1972) employed the more accurate Green's function used by Glauber and Martin (1956). In this more refined calculation, p-wave intermediate states also contribute to the amplitude, and thus, longitudinal photon exchange is also being taken into account. The relative importance of longitudinal photon exchange is indicated by the extent to which the intensity of the electron spectrum is reduced (Fig. 66).

C. Relativistic calculations of electron ejection

Both of the basic approaches described in Sec. V.B have been extended to include relativistic effects. Intemann (1969) modified the work of Intemann and Pollock

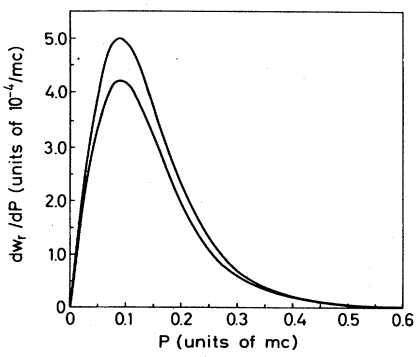

FIG. 66. Theoretical momentum spectrum of K electrons ejected during K capture of ^{55}Fe. The upper curve is calculated according to Intemann and Pollock (1967), taking into account only the exchange of scalar virtual photons during transitions between spherically symmetric states. The lower curve, calculated by Intemann (1972), results if p-wave intermediate states and the exchange of longitudinal virtual photons are taken into account. (After Intemann, 1972).

(1967), using the solutions of the symmetric Hamiltonian of Biedenharn and Swamy (1964). This is a relativistic Hamiltonian with symmetry so that the radial parts of the spinor components of its solutions are formally nonrelativistic. The solutions form a complete canonical basis, and their close correspondence to the nonrelativistic problem leads to substantial computational simplifications. The Biedenharn Hamiltonian differs from the exact Dirac-Coulomb Hamiltonian by a precisely known fine-structure term; the eigenfunctions differ from the exact Dirac–Coulomb eigenfunctions by terms of order $(\alpha Z)^2$.

Except for the use of semirelativistic Coulomb eigenfunctions in the overlap integral and an appropriately modified expression for the density of final states available to the ejected electron, the calculation of Intemann (1969) follows the lines of his earlier work, i.e., the interaction between the two K electrons is treated as a perturbation along with the weak interaction, leading to an exact calculation of the electron ejection probability without the need of introducing adjustable parameters such as screening constants or effective nuclear charges. Even though relativistic effects partly cancel the reduction in w_{ejec} that arises when longitudinal photon exchange is included, the ejected-electron spectrum calculated semirelativistically in Intemann (1969) is considerably less intense than that derived from the Primakoff–Porter (1953) approach (Fig. 67).

An independent relativistic calculation of autoionization in electron-capture decay was performed by Law and Campbell (1973b), in terms of second-quantization formalism and in analogy with extensive work by the same authors on internal ionization accompanying β decay (Campbell *et al.*, 1971; Campbell and Law, 1972; Law and Campbell, 1972a, 1972b, 1973a). It was, however, shown by Intemann (1974) that the model of Law and Campbell (1973b) is actually identical with that of Intemann and Pollock (1967) and Intemann (1969), and that the large difference in the results can be traced to the fact that Law and Campbell cut off the eigenfunction expansion for the Coulomb Green function too soon. Law and Campbell approximated the infinite series by a few terms because it appeared to converge rapidly; Intemann (1974), drawing upon an analogous calculation by Paquette (1962), pointed out that the sum over discrete eigenstates in the Green function expansion does indeed converge rapidly, but that continuum states make a large contribution that cannot be neglected.

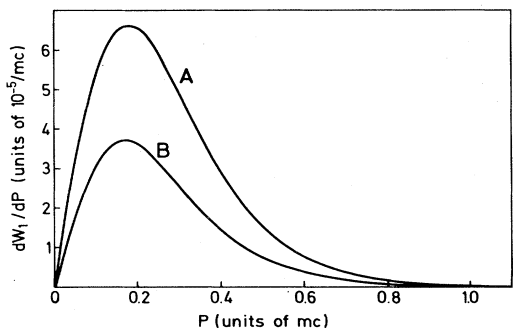

FIG. 67. Calculated momentum spectrum of K electrons ejected during K-capture decay of ^{131}Cs. Curve A is according to the nonrelativistic theory of Primakoff and Porter (1953); curve B represents the semirelativistic calculation of Intemann (1969). (From Intemann, 1969).

The (historically older) alternative to the Intemann approach for the calculation of internal ionization is the "overlap" *ansatz*, used in the pioneering work of Primakoff and Porter (1953). As indicated in Sec. V.B, in this method one attempts to take account of all screening and correlation effects in the initial two-electron wavefunction by an adjustable parameter, viz., the effective nuclear charge. The calculations are simplified considerably, but it is difficult to make a choice of the key parameter, and some arbitrariness is bound to remain. Moreover, the near-orthogonality of the wavefunctions makes the overlap integral very sensitive to the exact form of the wavefunctions and to the values chosen for the effective charges. Thus the accuracy of the results cannot be established *a priori*, as in the Intemann approach; on the other hand, the overlap method does not rely on the condition $Z \gg 1$, and hence may be superior for very light elements.

The most recent and complete calculation based on the "overlap" method is due to Mukoyama *et al.* (1973). In their formulation, Mukoyama *et al.* draw upon the work of Stephas (1969), who had employed an atomic matrix element calculated from analytic hydrogenic relativistic wavefunctions for the purpose of studying internal ionization accompanying β decay (Stephas and Crasemann, 1967, 1971; Crasemann and Stephas, 1969). However, in their evaluation of the wavefunction overlap integral, Stephas and Crasemann (1967) made an approximation that causes their expression to diverge at low electron momenta, where most electrons are ejected; thus the result cannot meaningfully be integrated to compute total electron-ejection probabilities (Isozumi and Shimizu, 1971; Kitahara *et al.*, 1972; Nagy *et al.*, 1972). Mord (1972, 1973) and, independently, Mukoyama *et al.* (1973) have calculated the atomic matrix element by alternative techniques and derived a result that is exact, within the limitations stated above; it agrees in the nonrelativistic limit with the formulae of Primakoff and Porter (1953) and Stephas and Crasemann (1971).

The screening constants σ that determine the effective nuclear charge $Z_{\text{eff}} = Z - \sigma$, to take account of electron–electron interaction, are determined by Mukoyama *et al.* (1973) in the following manner. In the parent atom, they take

$$\sigma = Z(1 - \bar{r}_Z/\bar{r}_{\text{SCF}}), \tag{5.12}$$

where $\bar{r}_Z$ is the mean value of r determined from the relativistic hydrogenic wavefunctions, and $\bar{r}_{\text{SCF}}$ is $\bar{r}$ from relativistic self-consistent field wavefunctions, as computed by Carlson *et al.* (1970). For the continuum electron, Mukoyama *et al.* use the same screening constant as for the bound electron to be ejected. They take account of the fact that a vacancy resulting from electron capture is present in the daughter atom by reducing σ from Eq. (5.12) by the ratio of the appropriate Slater screening constant for an atom that is ionized in an inner shell to that for a neutral atom (Slater, 1930).

The total K-electron ejection probabilities per K capture, calculated by Mukoyama *et al.* (1973), agree with those of Intemann (1969, 1974) as well as could be ex-

TABLE XXXIII. Electron ejection probabilities per K capture (in multiples of 10^{-5}).

Isotope	Primakoff–Porter [a]	MIKS [b]	Intemann [c]	K- or L-electron ejection [d]
$^{37}_{18}$Ar	27.7	14.2	21.12	57
$^{55}_{26}$Fe	11.2	8.81	8.26	6.4
$^{71}_{32}$Ge	6.68	4.56	4.72	3.3
$^{131}_{55}$Cs	1.62	0.709	0.92	2.6
$^{165}_{68}$Er	0.767	0.304	0.39	2.9

[a] Primakoff and Porter (1953), evaluated by Mukoyama *et al.* (1973).
[b] Mukoyama *et al.* (1973).
[c] Intemann (1969), as evaluated by Intemann (1974).
[d] K-electron ejection accompanying L capture and L-electron ejection accompanying K capture, after Mukoyama and Shimizu (1974).

pected, given the uncertainties in the choice of screening parameters (Table XXXIII).

Excitation to a bound state ("shakeup") of the second K electron, while the first one is captured, has also been computed by Mukoyama *et al.* (1973). Such calculations are important for comparison with experiments in which double K x-ray emission is measured. The main difficulty here is to make adequate provision for omitting occupied final states to which shakeup is forbidden by the Pauli principle. Mukoyama *et al.* (1973) find that the probability for double K-vacancy production (including excitation), like the K electron-ejection probability, is reduced when relativistic effects are included, compared with the nonrelativistic results of Primakoff and Porter (1953) (Table XXXIV).

D. Electron ejection from higher shells

It was first emphasized by Wolfsberg (1954) that a spectrum of electrons ejected during nuclear electron capture, measured in coincidence with a single K x ray, contains contributions from L electrons shaken off during K capture and from K electrons ejected during L capture. Wolfsberg evaluated these effects in terms of the Primakoff–Porter formalism. Internal ionization of this type, resulting in K and L_1 vacancies, has also been discussed by Law and Campbell (1973a,b). The energy distribution of K electrons ejected during nuclear electron capture from higher shells was considered by Ryde *et al.* (1963).

The subject has been extensively treated in terms of the wavefunction overlap approach by Mukoyama and Shimizu (1974). Starting with the formalism of Stephas (1969), but using the relativistic hydrogenic atomic matrix element of Mukoyama *et al.* (1973), these workers have computed the probability per K capture for L_i-shell electron ejection with total energy W

$$P_{Ki}(W)dW=\frac{n_i}{2\pi^2}\,|M_{Ki}|^2\,\frac{S(W_K-W)}{S(W_0)}\,\frac{(W_K-W)^2}{W_0^2}\,pW\,dW. \tag{5.13}$$

Here, W_0 is the transition energy for K capture, W_K is the maximum total energy of the ejected electron, and n_i is the number of electrons in the L_i shell. S is the shape factor, and the wavefunction overlap integral is

$$M_{Ki}=\langle\psi(Z-1,W)\,|\,\psi(Z,L_i)\rangle. \tag{5.14}$$

Similarly, Mukoyama and Shimizu have computed the K-shell internal ionization probability per L_i capture, expressed as a ratio to the K-capture probability

$$P_{iK}(W)dW=\frac{n_i}{2\pi^2}\,\frac{\epsilon_i}{\epsilon_K}\,|M_{iK}|^2\,\frac{S(W_K-W)}{S(W_0')}\,\frac{(W_K-W)^2}{W_0'^2}\,pW\,dW, \tag{5.15}$$

where ϵ_i/ϵ_K is the L_i-to-K capture ratio, and W_0' is the mass difference between initial and final nuclei, minus the L_i binding energy, plus one (in units of mc^2). The atomic matrix element is

$$M_{iK}=\langle\psi(Z-1,W)\,|\,\psi(Z,K)\rangle. \tag{5.16}$$

The authors construct a properly antisymmetrized expression for the total probability for the direct and exchange processes (5.13) and (5.15) and evaluate the result for cases of practical interest (Table XXXIII). It is predicted that the L-shell internal-ionization prob-

TABLE XXXIV. Double K-vacancy production probability (due to internal ionization and excitation), per K-capture event (in multiples of 10^{-5}).

Isotope	Theory: Primakoff–Porter [a]	Theory: MIKS [b]	Experiments [c]	
$^{37}_{18}$Ar	38.6	23.0	37 ±9	Kiser and Johnston (1959)
			44 ±8	Miskel and Perlman (1954)
$^{55}_{26}$Fe	18.5	15.8	38 ±17	Charpak (1953)
$^{71}_{32}$Ge	12.2	8.85	24	Briand *et al.* (1971)
			13 ±8	Oertzen (1964)
			13.3 ±1.4	Langevin (1957, 1958)
$^{131}_{55}$Cs	4.13	1.79	1.33 ±0.33	Nagy *et al.* (1972)
			2.0 ±1.3	Smith (1964)
			5.0 ±1.0	Daniel *et al.* (1960)
			2.5 ±0.2	Lark and Perlman (1960)
$^{165}_{68}$Er	2.70	1.09	0.67 ±0.39	Nagy *et al.* (1972)
			1.5 ±0.4	Ryde *et al.* (1963)

[a] Primakoff and Porter (1953), as evaluated by Mukoyama *et al.* (1973).
[b] Mukoyama *et al.* (1973).
[c] K-x-ray–K-x-ray coincidence experiments, except for K x-ray satellite measurements on ^{71}Ge by Oertzen (1964) and Briand *et al.* (1971).

ability accompanying K capture is of almost the same order of magnitude as the K ejection probability during L capture. The probability that the atom undergoing electron capture and internal ionization is left with holes in the K and L shells increases with Z, relative to the double K-hole production probability. The L-shell ionization probability decreases more slowly with Z than the K-electron ejection probability, per K capture.

Calculated spectra of electrons ejected during K and L capture of ^{55}Fe are shown in Fig. 67. It is predicted that electrons ejected from the L_1 shell contribute substantially over the entire spectrum.

Comparable calculations of L-shell internal ionization accompanying L capture have been carried out by Mukoyama *et al.* (1974).

In this context, it should be noted that only allowed transitions have so far been treated by the Intemann–Pollock approach. By contrast, because of its simplicity, the overlap-integral approach has led to results for arbitrary beta transitions. The simplifying feature of this approach is the assumption that the initial state of the two electrons involved in the process is describable in terms of an independent-particle model, i.e., the two-electron wavefunction can be written as an uncorrelated product of one-electron wavefunctions. It is this assumption which permits the factorization of the matrix element. For forbidden transitions, however, with the entrance of higher beta moments, it is to be expected that the amplitude for internal ionization will be more sensitive to the details of the structure of the initial electronic configuration, and therefore the overlap-integral approach will be less reliable. On the other hand, relativistic effects, which are of particular importance for forbidden transitions, are much more easily included in this approach than in the Intemann–Pollock approach.

Furthermore, in connection with all wavefunction overlap calculations, on which the most extensive predictions of internal-ionization probabilities are based, it must be kept in mind that near-orthogonality makes the atomic matrix element exceedingly sensitive to the accuracy of the wavefunctions. This point is discussed in detail in Sec. II.E. It is likely that quantitative results derived from hydrogenic wavefunctions may lack in accuracy, particularly in the case of outer shells.

E. Measurements of internal ionization

Excellent critical reviews of experimental work on internal ionization and excitation accompanying electron capture have been compiled by Law and Campbell (1973), Mukoyama *et al.* (1973), Freedman (1974), and Walen and Briançon (1975); somewhat earlier results have been discussed by Stephas (1969).

Experiments on shakeup and shakeoff during electron capture are made difficult *a priori* by the fact that the probability of these processes is much lower, perhaps by an order of magnitude, than in β decay: the effect of the sudden increase in nuclear charge upon the Coulomb field seen by the atomic electrons is, to a considerable extent, compensated by the reduction in screening that ensues when one K electron is captured. Consequently, the experimental information on the subject is quite limited; it is confined to the five isotopes with simple ground-state-to-ground-state decays listed in Tables XXXIII and XXXIV, and to some recent work on ^{7}Be (Mutterer, 1970).

Relatively least difficult are measurements of the probability of double K-vacancy production through the detection of coincidences between two K x rays (or K Auger electrons, or both). Two decades ago, Charpak (1953) used two 2π proportional counters for such measurements on ^{55}Fe. Langevin (1957, 1958) measured the K Auger-electron sum peak in a single proportional counter with a gaseous internal ^{71}Ge source. Miskel and Perlman (1954) and Kiser and Johnston (1959) measured K Auger electrons and K shakeoff electrons from ^{37}Ar in a proportional counter.

Upon the advent of NaI(Tl) scintillation detectors, these were employed in several measurements (Daniel *et al.* 1960; Lark and Perlman, 1960; Ryde *et al.*, 1963; Smith, 1964). A further advance in the technique was made possible when solid state detectors were developed with which K x rays from elements with adjoining atomic numbers can be resolved, so that one can discriminate sensitively against impurities. Nagy *et al.* (1972) used a Si(Li) semiconductor detector in coincidence with a scintillation counter in double K-vacancy production measurements on ^{131}Cs and ^{165}Er.

The creation of double K holes can also be determined by detecting radiative transitions to the empty K shell. Such transitions produce $K\alpha$ x-ray "hypersatellites" that are shifted up in energy with respect to the diagram line. A hypersatellite measurement was first used by Oertzen (1964), who employed a bent-crystal diffraction spectrometer to determine the double K-vacancy production rate in ^{71}Ge; the result agrees extremely well with that of Langevin (1957, 1958). Briand *et al.* (1971) measured the $K\alpha$ hypersatellite from ^{71}Ge decay in coincidence with the ensuing $K\alpha_{3,4}$ satellite.

Results of all these measurements of double K-vacancy production probability during nuclear K capture are included in Table XXXIV.

Total electron ejection probabilities are much more difficult to determine. Spectrum measurements necessarily have a low-energy threshold, determined by detector noise, electron scattering, and window transmission problems. Because most electrons are ejected with very low energies (Fig. 68), total ejection probabilities can only be inferred from measured spectra, that extend over a limited range, by fitting the data to some theoretical spectral shape. The admixture of L electrons ejected during K capture, and of K electrons ejected during L capture, introduces additional uncertainties that are difficult to account for, unless the electron counts are gated by double K x-ray events. The results depend so heavily on the theoretical model in terms of which the data are interpreted and often contain such large probable errors that they have not been included in Table XXXIII. Pertinent information can be found in the original literature and in the papers by Stephas (1969), Mukoyama *et al.* (1973), Freedman (1974), and Walen and Briançon (1975).

While ejected-electron spectrum measurements have not, in the past, led to unequivocal and precise determinations of the total electron ejection probability, they

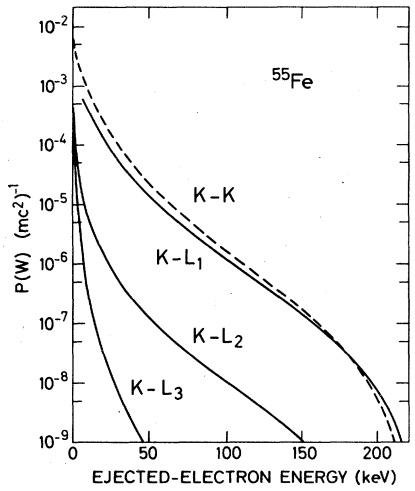

FIG. 68. Calculated energy spectra of electrons ejected in the decay of ^{55}Fe. The dashed curve labeled "K–K" represents K electrons ejected during K capture; the curves "K–L_i" indicate L_i electrons ejected during K capture plus the exchange effect, viz., K electrons ejected during L_i capture. All rates are given per K-capture event. After Mukoyama and Shimizu (1974).

are nevertheless of value for testing theoretically predicted spectrum shapes. The ^{7}Be electron spectrum has been measured by Mutterer (1970), and that of ^{37}Ar, by Miskel and Perlman (1954), with proportional counters. Pengra and Crasemann (1963) gated on Mn K x rays, detected with a scintillation counter, to measure the ^{55}Fe electron spectrum with a proportional counter, at low energies, and with an early solid state detector, at higher energies. Modern measurements of the ^{55}Fe electron spectrum have been performed by Nagy (1971) with two plastic scintillators in coincidence, and by Kitahara and Shimizu (1975), who performed a triple-coincidence (x-x-β^-) experiment with proportional counters. The ^{71}Ge spectrum was determined by Langevin (1958) with a proportional counter. Daniel *et al.* (1960) used a magnetic spectrometer to study the spectrum from ^{131}Cs; this spectrum was measured more recently by Sujkowski *et al.* (1973) with a Si(Li) detector placed at the focus of a zero-dispersion homogeneous magnetic-field spectrometer. A magnetic β-ray spectrometer was used by Ryde *et al.* (1963) on ^{165}Er.

The measured spectra appear to agree, within errors, with the general shape that all theories predict; this shape is largely determined by the statistical factor. Without question, precise absolute measurements of ejected-electron spectra, preferably in coincidence with two K x rays, would be of great value as a guide for more refined computations of the atomic matrix element.

F. Correlation of x rays and γ rays following electron capture

If aligned nuclei undergo electron capture, the atomic inner-shell vacancies created thereby can be polarized, and subsequently emitted x rays can be circularly polarized (for an illustrative example, see Emery, 1975). Dolginov (1956–1957, 1958a,b) has described these circular polarization effects and pointed out that even in the decay of unaligned atoms a correlation can exist between the circular polarization of x rays and of γ rays emitted following the nuclear decay.

An anisotropic directional correlation of the type

$$W(\theta)=1+A_2P_2(\cos\theta) \tag{5.17}$$

can exist between x rays and γ rays emitted after nuclear electron capture if the intermediate atomic state is characterized by a vacancy with $j>\frac{1}{2}$. The theory has been developed by Dolginov (1958b). (An early discussion of the problem is given by Tolhoek *et al.*, 1955). Somewhat simplified expressions based on Dolginov's theory are given by Rupnik and Crasemann (1972), who also worked out the directional-correlation function for x rays emitted in transitions to the L_3 level and γ rays, following second-forbidden nonunique electron-capture transitions.[27]

The experimental detection of anisotropic x–γ correlations is hampered by the condition that the intermediate atomic vacancy must have $j>\frac{1}{2}$, whence only L_3 capture is of interest.[28] The L_3/L_1 capture ratio in allowed transitions is always small ($<10^{-7}$); one must choose a radioisotope that decays through a second- or higher-forbidden electron-capture transition to a short-lived excited state of the daughter. The only readily available isotope that fulfills these requirements is ^{207}Bi, but its decay scheme is cluttered with other transitions. Efforts to detect anisotropy in the x–γ directional correlation from ^{207}Bi decay have been unsuccessful (Rupnik and Crasemann, 1972; Cambiaggio *et al.*, 1975), although the results are not inconsistent with theoretical predictions.

ACKNOWLEDGMENTS

We are indebted to many colleagues for helpful discussions and for making their results available to us in advance of publication. In particular, we wish to thank H. Appel of the Universität and Kernforschungszentrum Karlsruhe, W. Bühring of the Universität Heidelberg, M. S. Freedman of the Argonne National Laboratory, and B. E. Persson of the Technische Hochschule Darmstadt for reading and criticizing parts of early drafts of this paper. J. B. Mann of the Los Alamos Scientific Laboratory, University of California, kindly supplied us with unpublished wavefunctions, and B. Fricke of the Gesamthochschule Kassel generously made his Hartree–Fock–Slater computer codes available. One of us (M.L.F.) is indebted to the University of Glasgow for a research fellowship.

---

[27]The directional correlation function for x rays from L_3-shell internal conversion of an $M4$ γ transition and a cascade γ ray in ^{207}Bi, given by Rupnik and Crasemann (1972) [their Eqs. (36) and (37)] is in error: contrary to these authors' assumption, the radial integrals cannot be factored out of the correlation expression (J. S. Geiger, private communication, 1974). New calculations are being carried out by Geiger and Ferguson (1974) and Carvalho *et al.* (1975).

[28]While nuclear electron capture as a rule occurs predominantly from s states, it is interesting to note that ~97% of the primary vacancies produced in the decay of ^{202}Pb and ^{205}Pb are in the L_3 shell (Emery, 1975; Bambynek *et al.*, 1974).

APPENDIX 1. EXPRESSIONS FOR $M_K(k_x,k_\nu)$ AND $m_K(k_x,k_\nu)$

Only the dominant terms of the quantities $M_K(k_x,k_\nu)$ and $m_K(k_x,k_\nu)$ are given in Eqs. (2.106). The complete formulae for $k_\nu^{(1)}$ and $k_\nu^{(2)}$ follow (Behrens and Bühring, 1971, modified for electron capture).

1. $k_\nu = k_\nu^{(1)} = K - k_x + 1$

$$
\begin{aligned}
M_K(k_x,k_\nu) = {} & \left(\frac{K!}{(2K+1)!!}\,\frac{1}{(2k_x-1)!!\,(2k_\nu-1)!!\,(k_x-1)!\,(k_\nu-1)!}\right)^{1/2}(p_xR)^{k_x-1}(q_xR)^{k_\nu-1} \\
& \times\sum_{\lambda=0}^{\infty}\sum_{\mu=0}^{\infty}\frac{(2k_x-1)!!}{(2\mu)!!\,(2\mu+2k_x-1)!!}\,\frac{(2k_\nu-1)!!}{(2\lambda)!!\,(2\lambda+2k_\nu-1)!!}(q_xR)^{2\lambda}\sum_{\sigma=0}^{\mu}(-1)^{\lambda+\sigma}\binom{\mu}{\sigma}\sum_{\rho=0}^{2\sigma+1}(m_eR)^{2\mu-2\sigma}(W_xR)^{2\sigma-\rho}(\alpha Z)^{\rho} \\
& \times\Bigg\{-\left(\frac{2K+1}{K}\right)^{1/2}\Bigg[\binom{2\sigma}{\rho}F^{\mu+\lambda}_{KK-11}(k_x,2\mu,2\sigma,\rho)-\frac{1}{2K+1}\,\frac{1}{2\lambda+2k_\nu+1}\,\frac{1}{2\mu+2k_x+1}\,q_xRW_xR\binom{2\sigma+1}{\rho}F^{\mu+\lambda+1}_{KK-11}(k_x,2\mu+1,2\sigma+1,\rho)\Bigg] \\
& \quad+\Bigg[\frac{1}{2\mu+2k_x+1}W_xR\binom{2\sigma+1}{\rho}F^{\mu+\lambda}_{KK0}(k_x,2\mu+1,2\sigma+1,\rho)-\frac{1}{2\lambda+2k_\nu+1}q_xR\binom{2\sigma}{\rho}F^{\mu+\lambda}_{KK0}(k_x,2\mu,2\sigma,\rho)\Bigg] \\
& \quad-\left(\frac{K+1}{K}\right)^{1/2}\Bigg[\frac{1}{2\mu+2k_x+1}W_xR\binom{2\sigma+1}{\rho}F^{\mu+\lambda}_{KK1}(k_x,2\mu+1,2\sigma+1,\rho)+\frac{1}{2\lambda+2k_\nu+1}q_xR\binom{2\sigma}{\rho}F^{\mu+\lambda}_{KK1}(k_x,2\mu,2\sigma,\rho)\Bigg] \\
& \quad-\left(\frac{K+1}{2K+1}\right)^{1/2}\frac{2}{2\lambda+2k_\nu+1}\,\frac{1}{2\mu+2k_x+1}\,q_xRW_xR\binom{2\sigma+1}{\rho}F^{\mu+\lambda}_{KK+11}(k_x,2\mu+1,2\sigma+1,\rho)\Bigg\},
\end{aligned}
\tag{A1}
$$

$$
\begin{aligned}
m_K(k_x,k_\nu) = {} & \left(\frac{K!}{(2K+1)!!}\,\frac{1}{(2k_x-1)!!\,(2k_\nu-1)!!\,(k_x-1)!\,(k_\nu-1)!}\right)^{1/2}(p_xR)^{k_x-1}(q_xR)^{k_\nu-1} \\
& \times\sum_{\lambda=0}^{\infty}\sum_{\mu=0}^{\infty}\frac{(2k_x-1)!!}{(2\mu)!!\,(2\mu+2k_x-1)!!}\,\frac{(2k_\nu-1)!!}{(2\lambda)!!\,(2\lambda+2k_\nu-1)!!}(q_xR)^{2\lambda}\sum_{\sigma=0}^{\mu}(-1)^{\lambda+\sigma}\binom{\mu}{\sigma}\sum_{\rho=0}^{2\sigma}(m_eR)^{2\mu-2\sigma}(W_xR)^{2\sigma-\rho}(\alpha Z)^{\rho} \\
& \times\Bigg\{-\left(\frac{2K+1}{K}\right)^{1/2}\Bigg[m_eR(W_xR)^{-1}\Delta\binom{2\sigma-1}{\rho}F^{\mu+\lambda}_{KK-11}(k_x,2\mu,2\sigma-1,\rho) \\
& \qquad-\frac{1}{2K+1}\,\frac{1}{2\lambda+2k_\nu+1}\,\frac{1}{2\mu+2k_x+1}qRm_eR\binom{2\sigma}{\rho}F^{\mu+\lambda+1}_{KK-11}(k_x,2\mu+1,2\sigma,\rho)\Bigg] \\
& \quad+\Bigg[\frac{1}{2\mu+2k_x+1}m_eR\binom{2\sigma}{\rho}F^{\mu+\lambda}_{KK0}(k_x,2\mu+1,2\sigma,\rho)-\frac{1}{2\lambda+2k_\nu+1}q_xRm_eR(W_xR)^{-1}\Delta\binom{2\sigma-1}{\rho}F^{\mu+\lambda}_{KK0}(k_x,2\mu,2\sigma-1,\rho)\Bigg] \\
& \quad-\left(\frac{K+1}{K}\right)^{1/2}\Bigg[\frac{1}{2\mu+2k_x+1}m_eR\binom{2\sigma}{\rho}F^{\mu+\lambda}_{KK1}(k_x,2\mu+1,2\sigma,\rho) \\
& \qquad+\frac{1}{2\lambda+2k_\nu+1}q_xRm_eR(W_xR)^{-1}\Delta\binom{2\sigma-1}{\rho}F^{\mu+\lambda}_{KK1}(k_x,2\mu,2\sigma-1,\rho)\Bigg] \\
& \quad-\left(\frac{K+1}{2K+1}\right)^{1/2}\frac{2}{2\lambda+2k_\nu+1}\,\frac{1}{2\mu+2k_x+1}qRm_eR\binom{2\sigma}{\rho}F^{\mu+\lambda}_{KK+11}(k_x,2\mu+1,2\sigma,\rho)\Bigg\}.
\end{aligned}
\tag{A2}
$$

2. $k_\nu = k_\nu^{(2)} = K - k_x + 2$

$$
\begin{aligned}
M_K(k_x,k_\nu) = {} & -\left(\frac{K!}{(2K+1)!!}\,\frac{1}{(2k_x-1)!!\,(2k_\nu-1)!!\,(k_x-1)!\,(k_\nu-1)!}\right)^{1/2}(p_xR)^{k_x-1}(q_xR)^{k_\nu-1}\left(\frac{K+1}{(2k_x-1)(2k_\nu-1)}\right)^{1/2} \\
& \times\sum_{\lambda=0}^{\infty}\sum_{\mu=0}^{\infty}\frac{(2k_x-1)!!}{(2\mu)!!\,(2\mu+2k_x-1)!!}\,\frac{(2k_\nu-1)!!}{(2\lambda)!!\,(2\lambda+2k_\nu-1)!!}(q_xR)^{2\lambda}\sum_{\sigma=0}^{\mu}(-1)^{\lambda+\sigma}\binom{\mu}{\sigma}\sum_{\rho=0}^{2\sigma+1}(m_eR)^{2\mu-2\sigma}(W_xR)^{2\sigma-\rho}(\alpha Z)^{\rho} \\
& \times\Bigg\{\Bigg[\binom{2\sigma}{\rho}F^{\mu+\lambda}_{KK0}(k_x,2\mu,2\sigma,\rho)+\frac{1}{2\lambda+2k_\nu+1}\,\frac{1}{2\mu+2k_x+1}q_xRW_xR\binom{2\sigma+1}{\rho}F^{\mu+\lambda+1}_{KK0}(k_x,2\mu+1,2\sigma+1,\rho)\Bigg] \\
& \quad+\frac{k_x-k_\nu}{K+1}\left(\frac{K+1}{K}\right)^{1/2}\Bigg[\binom{2\sigma}{\rho}F^{\mu+\lambda}_{KK1}(k_x,2\mu,2\sigma,\rho)-\frac{1}{2\lambda+2k_\nu+1}\,\frac{1}{2\mu+2k_x+1}q_xRW_xR\binom{2\sigma+1}{\rho}F^{\mu+\lambda+1}_{KK1}(k_x,2\mu+1,2\sigma+1,\rho)\Bigg] \\
& \quad+\left(\frac{1}{K(2K+1)}\right)^{1/2}\Bigg[2(k_\nu-1)\,\frac{1}{2\mu+2k_x+1}WR\binom{2\sigma+1}{\rho}F^{\mu+\lambda+1}_{KK-11}(k_x,2\mu+1,2\sigma+1,\rho) \\
& \qquad-\frac{2(k_x-1)}{2\lambda+2k_\nu+1}q_xR\binom{2\sigma}{\rho}F^{\mu+\lambda+1}_{KK-11}(k_x,2\mu,2\sigma,\rho)\Bigg] \\
& \quad+\left(\frac{1}{(K+1)(2K+1)}\right)^{1/2}\Bigg[(2k_x-1)\,\frac{1}{2\mu+2k_x+1}W_xR\binom{2\sigma+1}{\rho}F^{\mu+\lambda}_{KK+11}(k_x,2\mu+1,2\sigma+1,\rho) \\
& \qquad-\frac{2k_\nu-1}{2\lambda+2k_\nu+1}q_xR\binom{2\sigma}{\rho}F^{\mu+\lambda}_{KK+11}(k_x,2\mu,2\sigma,\rho)\Bigg]\Bigg\},
\end{aligned}
\tag{A3}
$$

$$m_K(k_x,k_\nu)=\left(\frac{K!}{(2K+1)!!}\frac{1}{(2k_x-1)!!(2k_\nu-1)!!(k_x-1)!(k_\nu-1)!}\right)^{1/2}(p_xR)^{k_x-1}(q_xR)^{k_\nu-1}\left(\frac{K+1}{(2k_x-1)(2k_\nu-1)}\right)^{1/2}$$
$$\times\sum_{\lambda=0}^{\infty}\sum_{\mu=0}^{\infty}\frac{(2k_x-1)!!}{(2\mu)!!(2\mu+2k_x-1)!!}\frac{(2k_\nu-1)!!}{(2\lambda)!!(2\lambda+2k_\nu-1)!!}(q_xR)^{2\lambda}\sum_{\sigma=0}^{\mu}(-1)^{\lambda+\sigma}\binom{\mu}{\sigma}\sum_{\rho=0}^{2\sigma}(m_eR)^{2\mu-2\sigma}(W_xR)^{2\sigma-\rho}(\alpha Z)^\rho$$
$$\times\left\{\left[m_eR(W_xR)^{-1}\Delta\binom{2\sigma-1}{\rho}F^{\mu+\lambda}_{KK0}(k_e,2\mu,2\sigma-1,\rho)+\frac{1}{2\lambda+2k_\nu+1}\frac{1}{2\mu+2k_x+1}q_xRm_eR\binom{2\sigma}{\rho}F^{\mu+\lambda+1}_{KK0}(k_x,2\mu+1,2\sigma,\rho)\right]\right.$$
$$+\frac{k_x-k_\nu}{K+1}\left(\frac{K+1}{K}\right)^{1/2}\left[m_eR(W_xR)^{-1}\Delta\binom{2\sigma-1}{\rho}F^{\mu+\lambda}_{KK1}(k_x,2\mu,2\sigma-1,\rho)\right.$$
$$\left.-\frac{1}{2\lambda+2k_\nu+1}\frac{1}{2\mu+2k_x+1}q_xRm_eR\binom{2\sigma}{\rho}F^{\mu+\lambda+1}_{KK1}(k_x,2\mu+1,2\sigma,\rho)\right]$$
$$+\left(\frac{1}{K(2K+1)}\right)^{1/2}\left[2(k_\nu-1)\frac{1}{2\mu+2k_x+1}m_eR\binom{2\sigma}{\rho}F^{\mu+\lambda+1}_{KK-11}(k_x,2\mu+1,2\sigma,\rho)\right.$$
$$\left.-\frac{2(k_x-1)}{2\lambda+2k_\nu+1}q_xRm_eR(W_xR)^{-1}\Delta\binom{2\sigma-1}{\rho}F^{\mu+\lambda+1}_{KK-11}(k_x,2\mu,2\sigma-1,\rho)\right]$$
$$+\left(\frac{1}{(K+1)(2K+1)}\right)^{1/2}\left[(2k_x-1)\frac{1}{2\mu+2k_x+1}m_eR\binom{2\sigma}{\rho}F^{\mu+\lambda}_{KK+11}(k_x,2\mu+1,2\sigma,\rho)\right.$$
$$\left.\left.-\frac{2k_\nu-1}{2\lambda+2k_\nu+1}q_xRm_eR(W_xR)^{-1}\Delta\binom{2\sigma-1}{\rho}F^{\mu+\lambda}_{KK+11}(k_x,2\mu,2\sigma-1,\rho)\right]\right\}. \tag{A4}$$

In these expressions, we have

$$\Delta=\begin{cases}0 \text{ if } \mu=0\\ 0 \text{ if } \sigma=0\\ 0 \text{ if } \rho=0\\ 1 \text{ otherwise.}\end{cases}$$

For nth-forbidden unique transitions, Eqs. (A1)–(A4) apply, with $K=n+1$, ${}^AF_{(n+1)n1}$, ${}^AF_{(n+1)(n+1)0}$, ${}^VF_{(n+1)(n+1)1}$, ${}^AF_{(n+1)(n+2)1}$. For nth forbidden nonunique transitions, Eqs. (A1)–(A4) apply with $K=n$, ${}^VF_{n(n-1)1}$, ${}^VF_{nn0}$, ${}^AF_{nn1}$, ${}^VF_{n(n+1)1}$. If $n=1$, there is a further contribution from Eqs. (A1)–(A4) with $K=0$, ${}^AF_{000}$, ${}^AF_{011}$. Allowed transitions involve Eqs. (A1) and (A4) with $K=0$, ${}^VF_{000}$, ${}^VF_{011}$ and Eqs. (A1) and (A2) with $K=1$, ${}^AF_{101}$, ${}^AF_{110}$, ${}^AF_{121}$. The magnitude of the various terms in Eqs. (A1) through (A4) is determined, first, by powers of the factors (p_xR), (q_xR), (W_xR), (m_eR), and (αZ), and second, by the difference of one order of magnitude between the relativistic and nonrelativistic form-factor coefficients. Thus, the dominant terms of Eqs. (A1)–(A4) are a subset of the terms with $\lambda=0$, $\mu=0$ [Eqs. (2.104)–(2.106)]. The correction terms of the next order are:

(i) terms with $\mu=0,\lambda=0$ which were not included in Eqs. (2.104)–(2.106);

(ii) terms with $\mu=0,\lambda=1$ and $\mu=1,\lambda=0$ corresponding to the terms with $\mu=0,\lambda=0$ of Eqs. (2.104)–(2.106).

All terms, however, with powers of m_eR and W_xR can usually be omitted since m_eR and W_xR are generally much smaller than αZ. It should be noted that for electron capture the correction terms are important only in cases where cancellations occur among the dominant terms.

APPENDIX 2. EXPANSION COEFFICIENTS $I(k,m,n,\rho;r)$ UP TO ORDER $m=3$

The expansion coefficients $I(k,m,n,\rho;r)$ of the electron radial wavefunctions, up to order $m=3$, are as follows (Behrens and Bühring, 1971):

$$I(k,1,1,1;r)=(2k+1)r^{-2k-1}\int_0^r x^{2k}U(x)\,dx,$$

$$I(k,2,2,2;r)=2(2k+1)r^{-2}\int_0^r U(y)y^{-2k}\int_0^y x^{2k}U(x)\,dx\,dy,$$

$$I(k,2,2,1;r)=-\frac{2k+1}{2k-1}r^{-2k-1}\int_0^r x^{2k}U(x)\,dx+\frac{4k}{2k-1}r^{-2}\int_0^r xU(x)\,dx,$$

$$I(k,2,1,1;r)=+\frac{2(2k+1)}{2k-1}r^{-2k-1}\int_0^r x^{2k}U(x)\,dx-\frac{4}{2k-1}r^{-2}\int_0^r xU(x)\,dx,$$

$$I(k,3,3,3;r)=2(2k+1)(2k+3)r^{-2k-3}\int_0^r z^{2k}U(z)\times\int_0^z U(y)y^{-2k}\int_0^y x^{2k}U(x)\,dx\,dy\,dz,$$

$$I(k,3,3,2;r)=\frac{2}{3}(2k+3)r^{-2}\int_0^r U(y)y^{-2k}\int_0^y x^{2k}U(x)\,dx\,dy+\frac{8k(2k+3)}{3(2k-1)}r^{-2k-3}\int_0^r y^{2k}U(y)\int_0^y xU(x)\,dx\,dy-\frac{8k(2k+3)}{3(2k-1)}r^{-2k-3}\int_0^r yU(y)\int_0^y x^{2k}U(x)\,dx\,dy,$$

$$I(k,3,2,2;r)=2(2k+3)r^{-2}\int_0^r U(y)y^{-2k}\int_0^y x^{2k}U(x)\,dx\,dy-\frac{4(2k+3)}{2k-1}r^{-2k-3}\int_0^r y^{2k}U(y)\int_0^y xU(x)\,dx\,dy+\frac{4(2k+3)}{2k-1}r^{-2k-3}\int_0^r yU(y)\int_0^y x^{2k}U(x)\,dx\,dy,$$

$$I(k,3,3,1;r)=\frac{4k(2k+3)}{3(2k+1)}r^{-2k-3}\int_0^r x^{2k+2}U(x)\,dx-\frac{(2k+1)(2k+3)}{3(2k-1)}r^{-2k-1}\int_0^r x^{2k}U(x)\,dx+\frac{8k(2k+3)}{3(2k+1)(2k-1)}r^{-2}\int_0^r xU(x)\,dx,$$

$$I(k,3,2,1;r)=\frac{2(2k+3)}{2k+1}r^{-2}\int_0^r xU(x)\,dx - \frac{2(2k+3)}{2k+1}r^{-2k-3}\int_0^r x^{2k+2}U(x)\,dx,$$

$$I(k,3,1,1;r)=\frac{4(k+1)(2k+3)}{2k+1}r^{-2k-3}\int_0^r x^{2k+2}U(x)\,dx - \frac{(2k+1)(2k+3)}{2k-1}r^{-2k-1}\int_0^r x^{2k}U(x)\,dx + \frac{4(2k+3)}{(2k+1)(2k-1)}r^{-2}\int_0^r xU(x)\,dx. \quad \text{(B1)}$$

The function $U(x)$ in these expressions is defined by

$$V(x)=-(\alpha Z/R)U(x), \quad \text{(B2)}$$

where $V(x)$ is the potential of the nuclear and atomic charge distributions.

REFERENCES

Abdurazakov, A. A., G. Beyer, K. Ya. Gromov, E. Herrmann, T. A. Islamov, M. Jachim, F. Molnar, G. Musiol, H.-U. Siebert, H. Strusny, H. Tyrroff, and S. A. Usmanova, 1974, Joint Institute for Nuclear Research, Dubna Report JINR–E6–8008 (unpublished).

Abers, E. S. and B. W. Lee, 1973, Phys. Rep. **9C**, 1.

Adam, I., K. S. Toth, and R. A. Meyer, 1967a, Phys. Rev. **159**, 985.

Adam, N., K. Wilsky, Zh. Zhelev, M. Jorgensen, M. Krivopostov, V. Kuznetsov, O. B. Nielsen, and M. Finger, 1967b, Izv. Akad. Nauk. SSSR Ser. Fiz. **31**, 122 [Bull. Acad. Sci. USSR, Phys. Ser. **31**, 114].

Adamovicz, B., Z. Moroz, Z. Preibisz, and A. Zglinski, 1968, Acta Phys. Pol. **34**, 529.

Albrecht, G. and J. W. Hammer, 1975, Z. Phys. A **273**, 405.

Alburger, D. E., 1972, Phys. Rev. C **6**, 1167.

Alburger, D. E. and D. H. Wilkinson, 1970, Phys. Lett. B **32**, 190.

Aleksandrov, V. S., V. S. Buttsev, T. Vylov, K. Y. Gromov, and V. G. Kalinnikov, 1972, Joint Institute for Nuclear Research, Dubna, Report JINR–P6–6794 (unpublished).

Allen, R. A., W. E. Burcham, K. F. Chackett, G. L. Munday, and P. Reasbeck, 1955, Proc. Phys. Soc. Lond. A **68**, 681.

Alvarez, L. W., 1937, Phys. Rev. **52**, 134.

Alvarez, L. W., 1938a, Phys. Rev. **53**, 606.

Alvarez, L. W., 1938b, Phys. Rev. **54**, 486.

Anderson, C. E., G. W. Wheeler, and W. W. Watson, 1952, Phys. Rev. **87**, 668.

Anderson, C. E., G. W. Wheeler, and W. W. Watson, 1953, Phys. Rev. **90**, 606.

Andersson, G., G. Rudstam, and G. Sörensen, 1965, Ark. Fys. **28**, 37.

Arbman, E. and N. Svartholm, 1955, Ark. Fys. **10**, 1.

Armstrong, L. and C. W. Kim, 1972, Phys. Rev. C **6**, 1924.

Asai, J. and H. Ogata, 1974, Nucl. Phys. A **233**, 55.

Aston, G. H., 1927, Proc. Camb. Philos. Soc. **22**, 935.

Auble, R. L., 1971a, Nucl. Data Sheets B **5**, 568.

Auble, R. L., 1971b, Nucl. Data Sheets B **5**, 588.

Avignon, P., 1953, J. Phys. Radium **14**, 637.

Avignon, P., 1956, Ann. Phys. (Paris) **1**, 10.

Avignon, P., A. Michalowicz, and R. Bouchez, 1955, J. Phys. Radium **14**, 404.

Avotina, M. P., E. P. Grigor'ev, Zh. T. Zhelev, A. V. Zolotavin, and V. O. Sergeev, 1965a, Dubna Report 2272 (unpublished), quoted by Berényi, 1967.

Avotina, M. P., E. P. Grigor'ev, A. V. Zolotavin, N. A. Lebedev, and V. O. Sergeev, 1965b, Dubna Report 2271 (unpublished), quoted by Berényi, 1967.

Avotina, M. P., E. P. Grigor'ev, A. V. Zolotavin, V. O. Sergeev, V. E. Ter-Nersesyants, J. Vrzal, N. A. Lebedev, J. Liptak, and Ya. Urbanets, 1966, Izv. Akad. Nauk. SSSR Ser. Fiz. **30**, 1292 [Bull. Acad. Sci. USSR, Phys. Ser. **30**, 1350].

Ažman, A., A. Moljk, and J. Pahor, 1968, Z. Phys. **208**, 234.

Bagus, P. S., 1964, Argonne National Laboratory Rept. No. ANL–6959 (unpublished).

Bagus, P. S., 1965, Phys. Rev. **139**, A619.

Bahcall, J. N., 1962a, Phys. Rev. Lett. **9**, 500.

Bahcall, J. N., 1962b, Phys. Rev. **128**, 1297.

Bahcall, J. N., 1963a, Phys. Rev. **129**, 2683.

Bahcall, J. N., 1963b, Phys. Rev. **131**, 1756.

Bahcall, J. N., 1963c, Phys. Rev. **132**, 362.

Bahcall, J. N., 1965a, Nucl. Phys. **71**, 267.

Bahcall, J. N., 1965b, in *Proceedings of the International Conference on the Role of Atomic Electrons in Nuclear Transformations* (Nuclear Energy Information Center, Warsaw), p. 336.

Bahcall, J. N., 1972, Comments Nucl. Part. Phys. **5**, 59.

Bakhru, H. and I. L. Preiss, 1967, Phys. Rev. **154**, 1091.

Bambynek, W., 1967a, Z. Phys. **206**, 66.

Bambynek, W., 1967b, *Standardization of Radionuclides* (International Atomic Energy Agency, Vienna), p. 373.

Bambynek, W., B. Crasemann, R. W. Fink, H.-U. Freund, Hans Mark, C. D. Swift, R. E. Price, and P. Venugopala Rao, 1972, Rev. Mod. Phys. **44**, 716, and Erratum, 1974, **46**, 853.

Bambynek, W., E. De Roost, and E. Funck, 1968, in Berényi (1968b), p. 253.

Bambynek, W., O. Lerch, and A. Spernol, 1966, Nucl. Instrum. Methods **39**, 104.

Bambynek, W. and D. Reher, 1968a, Z. Phys. **214**, 374.

Bambynek, W. and D. Reher, 1970, Z. Phys. **238**, 49.

Bambynek, W. and D. Reher, 1973, Z. Phys. **264**, 253.

Band, I. M., L. N. Zyryanova, and Tsin Chen-Zhui, 1956, Izv. Akad. Nauk. SSSR Ser. Fiz. **20**, 1387 [Bull. Acad. Sci. USSR, Phys. Ser. **20**, 1269].

Band, I. M., L. M. Zyryanova, and Yu. P. Suslov, 1958, Izv. Akad. Nauk. SSSR Ser. Fiz. **22**, 952 [Bull. Acad. Sci. USSR, Phys. Ser. **22**, 943].

Baskova, K. A., S. S. Vasil'ev, No Seng Ch'ang, and L. Ya. Shavtvalov, 1961, Zh. Eksp. Teor. Fiz. **41**, 1484 [Sov. Phys. JETP **14**, 1060 (1962)].

Baskova, K. A., S. S. Vasil'ev, M. A. Khamo-Leila, and L. Ya. Shavtvalov, 1964, Zh. Eksp. Teor. Fiz. **47**, 1162 [Sov. Phys. JETP **20**, 781 (1965)].

Bayer, G., V. S. Butsev, K. Ya. Gromov, V. G. Kalinnikov, K. O. Mortensen, G. L. Nilssen, and N. A. Tikhonov, 1972, Izv. Akad. Nauk. SSSR Ser. Fiz. **36**, 782 [Bull. Acad. Sci. USSR, Phys. Ser. **36**, 705].

Bayer, G., V. S. Butsev, Ts. Vylov, V. G. Kalinnikov, and I. Penev, 1974, [Program and Abstracts of 24. Conference on Nuclear Spectroscopy and Nuclear Structure, Kharkov, 29 January–1 February, INIS–mf–1850], p. 91.

Bearden, J. A. and A. F. Burr, 1967, Rev. Mod. Phys. **39**, 125.

Beattie, R. J. D. and J. Byrne, 1971, Nucl. Phys. A **161**, 650.

Beattie, R. J. D. and J. Byrne, 1972, Nucl. Instrum. Methods **104**, 163.

Beery, D. B., W. H. Kelly, and W. C. McHarris, 1968, Phys. Rev. **171**, 1283.

Beg, M. A., B. J. Bernstein, and A. Sirlin, 1972, Phys. Rev. D **6**, 2597.

Beg, M. A. and A. Sirlin, 1974, Annu. Rev. Nucl. Sci. **24**, 379.

Behrens, H. and W. Bühring, 1968, Nucl. Phys. A **106**, 433.

Behrens, H. and W. Bühring, 1970, Nucl. Phys. A **150**, 481.

Behrens, H. and W. Bühring, 1971, Nucl. Phys. A **162**, 111.

Behrens, H. and W. Bühring, 1972, Nucl. Phys. A **179**, 297.

Behrens, H. and W. Bühring, 1974, Nucl. Phys. A **232**, 230.

Behrens, H. and J. Jänecke, 1969, Landolt-Börnstein, *Num-*

erical Data and Functional Relationships in Science and Technology, Numerical Tables for β-Decay and Electron Capture (Springer-Verlag, Berlin), New Series, Group I, Vol. 4.
Bell, P. R., J. M. Jauch, and J. M. Cassidy, 1952, Science **15**, 12.
Belyanin, Yu. I., E. I. Biryukov, and N. S. Shimanskaya, 1966, Izv. Akad. Nauk. SSSR Ser. Fiz. **30**, 1130 [Bull. Acad. Sci. USSR, Phys. Ser. **30**, 1182].
Benoist-Gueutal, P., 1950, C. R. Acad. Sci. (Paris) **230**, 624.
Benoist-Gueutal, P., 1953a, Thèses (Masson, Paris, unpublished).
Benoist-Gueutal, P., 1953b, Ann. Phys. (Paris) **8**, 593.
Berényi, D., 1962, Phys. Lett. **2**, 332.
Berényi, D., 1963a, Nucl. Phys. **48**, 121.
Berényi, D., 1963b, Acta Phys. Hung. **16**, 101.
Berényi, D., 1965a, in *Role of Atomic Electrons in Nuclear Transformations* (Nuclear Energy Information Center, Warsaw, Poland), p. 609.
Berényi, D., 1967, Acta Phys. Hung. **22**, 25.
Berényi, D., 1968a, Rev. Mod. Phys. **40**, 390.
Berényi, D., ed. 1968b, *Proceedings of the Conference on the Electron Capture and Higher Order Processes in Nuclear Decays* (Eötvös Lóránd Physical Society, Budapest).
Berényi, D., 1970, Magy. Fiz. Foly. **18**, 23.
Berényi, D., Gs. Ujhelyi, and J. Fehér, 1965b, Phys. Lett. **18**, 293.
Berényi, D. and L. Kazai, 1965c, Nucl. Phys. **61**, 657.
Berényi, D. and D. Varga, 1969, Nucl. Phys. A **138**, 685.
Berényi, D., A. Szalay, D. Varga, F. Molenar, and J. Uchrin, 1970, Acta Phys. Hung. **28**, 431.
Berényi, D., G. Hock, A. Ménes, G. Szekely, Cs. Ujhelyi, and B. A. Zon, 1976, Nucl. Phys. A **256**, 205.
Berestetskii, V. B., 1958, Nuovo Cimento **10**, 385.
Bergström, I., 1951, Phys. Rev. **82**, 112.
Bergström, I., 1952, Ark. Phys. **5**, 191.
Bernardini, M., P. Brovetto, S. Debenedetti, and S. Ferroni, 1958, Nuovo Cimento **7**, 419.
Bernstein, J., 1974, Rev. Mod. Phys. **46**, 7.
Berthier, J. and P. Lipnik, 1966, Nucl. Phys. **78**, 448.
Bertmann, U., F. Krahn, and E. Huster, 1972, Z. Phys. **251**, 382.
Bertolini, G., A. Bisi, E. Lazzarini, and L. Zappa, 1954, Nuovo Cimento **11**, 539.
Bertrand, F. E., 1974, Nucl. Data Sheets **11**, 473.
Bertsch, G. F. and A. Mekjian, 1972, Annu. Rev. Nucl. Sci. **22**, 25.
Bethe, H. A. and R. F. Bacher, 1936, Rev. Mod. Phys. **8**, 82.
Bhalla, C. P., 1964, National Bureau of Standards Monograph NBS–81.
Bhalla, C. P. and M. E. Rose, 1960, Oak Ridge National Laboratory Report ORNL–2954.
Bhalla, C. P. and M. E. Rose, 1961, Oak Ridge National Laboratory Report ORNL–3207.
Bhalla, C. P. and M. E. Rose, 1962, Phys. Rev. **128**, 774.
Bhat, M. R. and M. L. Pool, 1962, Phys. Rev. **127**, 1704.
Bhatki, K. S., R. K. Gupta, S. Jha, and B. K. Madan, 1957, Nuovo Cimento **6**, 1461.
Bhattacherjee, S. K. and S. Raman, 1956, Nucl. Phys. **1**, 486.
Biavati, M. H., 1959, Thesis, Columbia University, N. Y., U. S. Atomic Energy Commission Rep. CU–190 (unpublished).
Biavati, M. H., S. J. Nassiff, and C. S. Wu, 1962, Phys. Rev. **125**, 1364.
Biedenharn, L. C. and N. V. V. J. Swamy, 1964, Phys. Rev. **133**, B1353.
Biryukov, E. I. and N. S. Shimanskaya, 1962, Izv. Akad. Nauk. SSSR Ser. Fiz. **26**, 215 [Bull. Acad. Sci. USSR, Phys. Ser. **26**, 215].
Biryukov, E. I. and N. S. Shimanskaya, 1963a, Izv. Akad. Nauk. SSSR Ser. Fiz. **27**, 1402 [Bull. Acad. Sci. USSR, Phys. Ser. 27, 1377].
Biryukov, E. I. and N. S. Shimanskaya, 1970, Yad. Fiz. **11**, 246 (Sov. J. Nucl. Phys. **11**, 138).
Biryukov, E. I., O. I. Grigor'ev, B. S. Kuznetsov, and N. S. Shimanskaya, 1960, Izv. Akad. Nauk. SSSR Ser. Fiz. **24**, 1135 [Bull. Acad. Sci. USSR, Phys. Ser. **24**, 1138].
Biryukov, E. I., V. T. Novikov, and N. S. Shimanskaya, 1963b, Izv. Akad. Nauk. SSSR Ser. Fiz. **27**, 1406 [Bull. Acad. Sci. USSR, Phys. Ser. **27**, 1383].
Biryukov, E. I., V. T. Novikov, and N. S. Shimanskaya, 1965, Izv. Akad. Nauk. SSSR Ser. Fiz. **29**, 151 [Bull. Acad. Sci. USSR, Phys. Ser. **29**, 148].
Biryukov, E. I., E. G. Zaletskii, and N. S. Shimanskaya, 1966, Izv. Akad. Nauk. SSSR Ser. Fiz. **30**, 504 [Bull. Acad. Sci. USSR, Phys. Ser. **30**, 514].
Bisi, A., E. Germagnoli, L. Zappa, and E. Zimmer, 1955a, Nuovo Cimento **2**, 290.
Bisi, A., E. Germagnoli, and L. Zappa, 1955b, Nuovo Cimento **2**, 1052.
Bisi, A., E. Germagnoli, and L. Zappa, 1956b, Nucl. Phys. **1**, 593.
Bisi, A., E. Germagnoli, and L. Zappa, 1957, Nuovo Cimento **6**, 299.
Bisi, A., E. Germagnoli, and L. Zappa, 1959, Nuovo Cimento **11**, 843.
Bisi, A., S. Terrani, and L. Zappa, 1955c, Nuovo Cimento **1**, 651.
Bisi, A. and L. Zappa, 1954, Nuovo Cimento **12**, 539.
Bisi, A., L. Zappa, and E. Germagnoli, 1956a, Nuovo Cimento **4**, 764.
Bisi, A., L. Zappa, and E. Zimmer, 1956c, Nuovo Cimento **4**, 307.
Bjorken, J. D. and S. D. Drell, 1965, *Relativistic Quantum Fields* (McGraw-Hill, New York).
Blin-Stoyle, R. J., 1969, Phys. Lett. B **29**, 12.
Blin-Stoyle, R. J., 1973, *Fundamental Interactions and the Nucleus* (North-Holland, Amsterdam).
Blin-Stoyle, R. J., J. A. Evans, and A. M. Knau, 1971, Phys. Lett. B **36**, 202.
Blin-Stoyle, R. J. and S. C. K. Nair, 1966, Adv. Phys. **15**, 493.
Bloch, F., 1936, Phys. Rev. **50**, 272.
Blok, L., T. J. de Boer, and J. Blok, 1959, Physica **25**, 333.
Blok, L., W. Goedbloed, E. Mastenbroek, and J. Blok, 1962, Physica **28**, 993.
Blomquist, J., 1971, Phys. Lett. B **35**, 375.
Bloom, S. D. and J. L. Uretsky, 1960, Nuovo Cimento **17**, 304.
Blue, J. W. and E. Bleuler, 1955, Phys. Rev. **100**, 1324.
Bock, R., 1955, private communication to K. Way, R. W. King, C. L. McGinnis, and R. van Lieshout, 1955, *Nuclear Level Schemes*, United States Atomic Energy Commission Report TID–5300 (unpublished).
Bohr, A. and B. R. Mottelson, 1969, Nuclear Structure (Benjamin, New York, Amsterdam).
Bolotin, H. H., 1964, Phys. Rev. **136**, 1566B.
Bolotin, H. H., A. C. Li, and A. Schwarzschild, 1961, Phys. Rev. **124**, 213.
Bonacalza, E. C. O., P. Thieberger, and I. Bergström, 1962, Ark. Fys. **22**, 111.
Bosch, H. E., M. A. Fariolli, N. Martin, and M. C. Simon, 1969, Nucl. Instrum Methods **73**, 323.
Bosch, H. E., M. C. Simon, E. Szichman, L. Gatto, and S. M. Abecasis, 1967, Phys. Rev. **159**, 1029.
Bottino, A. and G. Ciochetti, 1973, Phys. Lett. B **43**, 170.
Bouchez, R., 1952, Physica **18**, 1171.
Bouchez, R., S. R. de Groot, R. Nataf, and H. A. Tolhoek, 1950, J. Phys. Radium **11**, 105.
Bouchez, R. and P. Depommier, 1960, Rep. Prog. Phys. **23**, 395.
Bouchez, R. and P. Depommier, 1965, in *Role of Atomic Electrons in Nuclear Transformations* (Nuclear Energy Information Center, Warsaw, Poland), p. 30.

Bouchez, R. and G. Kayas, 1949, J. Phys. Radium **10**, 110.
Bouchiat, M. A. and C. Bouchiat, 1974, J. Phys. (Paris) **35**, 899.
Bouchiat, M. A. and C. Bouchiat, 1975, J. Phys. (Paris) **36**, 493.
Brabec, V., B. Kracík, and M. Vobecký, 1960, Czech. J. Phys. **10**, 855.
Bradt, H., P. C. Gugelot, O. Huber, H. Medicus, P. Preiswerk, and P. Scherrer, 1945, Helv. Phys. Acta **18**, 351.
Bradt, H., P. C. Gugelot, O. Huber, H. Medicus, P. Preiswerk, P. Scherrer, and R. Steffen, 1946, Helv. Phys. Acta **19**, 222.
Bramson, S., 1930, Z. Phys. **66**, 721.
Bresesti, M., F. Cappellani, and A. M. Del Turco, 1964, Nucl. Phys. **58**, 491.
Brewer, H. R., D. S. Harmer, and D. H. Hay, 1961, Phys. Rev. Lett. **7**, 319, Georgia Institute of Technology Report GIT–ES–B 151-1 (unpublished).
Brewer, W. D. and D. A. Shirley, 1968, Phys. Rev. Lett. **20**, 885.
Briand, J. P., P. Chevallier, M. Tavernier, and J. P. Rozet, 1971, Phys. Rev. Lett. **27**, 777.
Brosi, A. R., B. H. Ketelle, H. C. Thomas, and R. J. Kerr, 1959, Phys. Rev. **113**, 239.
Brown, L. S., 1964, Phys. Rev. **135**, 314B.
Browne, C. I., J. O. Rasmussen, J. P. Surls, and D. R. Martin, 1952, Phys. Rev. **85**, 146.
Brysk, H., 1952, Phys. Rev. **86**, 996.
Brysk, H. and M. E. Rose, 1955, Oak Ridge National Laboratory Report ORNL–1830 (unpublished).
Brysk, H. and M. E. Rose, 1958, Rev. Mod. Phys. **30**, 1169.
Bühring, W., 1963a, Nucl. Phys. **40**, 472.
Bühring, W., 1963b, Nucl. Phys. **49**, 190.
Bühring, W., 1965, Nucl. Phys. **61**, 110.
Bühring, W., 1967, Kernforschungszentrum Karlsruhe Report KFK 559.
Bühring, W. and L. Schülke, 1965, Nucl. Phys. **65**, 369.
Burke, V. M. and I. P. Grant, 1967, Proc. Phys. Soc. (London) **90**, 297.
Cambiaggio, M. C., J. Davidson, V. Silbergleit, and M. Behar, 1975, Phys. Rev. C **12**, 699.
Campbell, J. L. and K. W. D. Ledingham, 1966, Brit. J. Appl. Phys. **17**, 786.
Campbell, J. L., W. Leiper, K. W. D. Ledingham, and R. W. P. Drever, 1967, Nucl. Phys. A **96**, 279.
Campbell, J. L., L. A. McNelles, and J. Law, 1971, Can. J. Phys. **49**, 3142.
Campbell, J. L. and J. Law, 1972, Can. J. Phys. **50**, 2451.
Campbell, J. L. and L. A. McNelles, 1972, Nucl. Instrum. Methods **98**, 433.
Campbell, M., K. W. D. Ledingham, A. D. Baillie, M. L. Fitzpatrick, J. Y. Gourlay, and J. G. Lynch, 1975, Nucl. Phys. A **249**, 349.
Campion, P. J., 1959, Int. J. Appl. Radiat. Iso. **4**, 232.
Campion, P. J., 1968, Int. J. Appl. Radiat. Iso. **19**, 219.
Campion, P. J., 1973, Nucl. Instrum. Methods **112**, 75.
Carey, W. E., R. P. Sullivan, M. R. Bhat, and M. L. Pool, 1958, Bull. Am. Phys. Soc., Sec. II, **3**, 63.
Carlson, T. A., C. C. Lu, T. C. Tucker, C. W. Nestor, and F. B. Malik, 1970, Oak Ridge National Laboratory Report ORNL–4614 (unpublished).
Carvalho, M. J., A. Barroso, and F. B. Gil, 1975, private communication.
Casson, H., L. S. Goodman, and V. E. Krohn, 1953, Phys. Rev. **92**, 1517.
Charpak, G., 1953, C. R. Acad. Sci. B **237**, 243.
Charpak, G., 1955, J. Phys. Radium **16**, 62.
Chasan, B. and R. Chandra, 1967, Bull. Am. Phys. Soc. **12**, 74.
Chen, M. H., B. Crasemann, P. Venugopala Rao, J. M. Palms, and R. E. Wood, 1971, Phys. Rev. A **4**, 846.
Chester, R. O., R. W. Peelle, and F. C. Maienschein, 1963, in O'Kelley (1963), p. 201.
Chew, W. M., J. C. McGeorge, and R. W. Fink, 1973, in *Proceedings of the International Conference on Inner Shell Ionization Phenomena and Future Applications*, edited by R. W. Fink, S. T. Manson, J. M. Palms, and P. Venugopala Rao (U. S. Atomic Energy Commission, Report No. CONF–720404 unpublished), p. 197.
Chew, W. M., A. C. Xenoulis, R. W. Fink, and J. J. Pinajian, 1974a, Nucl. Phys. A **218**, 372.
Chew, W. M., A. C. Xenoulis, R. W. Fink, F. J. Schima, and W. B. Mann, 1974b, Nucl. Phys. A **229**, 79.
Chilosi, G., S. Monaro, and R. A. Ricci, 1962, Nuovo Cimento **26**, 440.
Christmas, P., 1964, Nucl. Phys. **55**, 577.
Christmas, P., 1965, Nucl. Phys. **61**, 352.
Chu, Y. Y., 1971, Phys. Rev. C **4**, 642.
Cohen, S. G. and S. Ofer, 1955, Phys. Rev. **100**, 856.
Cook, C. S. and L. M. Langer, 1948, Phys. Rev. **74**, 1241.
Cook, C. S. and F. M. Tomnovec, 1956, Phys. Rev. **104**, 1407.
Cook, W. B. and M. W. Johns, 1969, Can. J. Phys. **47**, 1899.
Cooper, J. A., J. M. Hollander, M. I. Kalkstein, and J. O. Rasmussen, 1965, Nucl. Phys. **72**, 113.
Crane, H. R., 1948, Rev. Mod. Phys. **20**, 278.
Crasemann, B., 1973, Nucl. Instrum. Methods **112**, 33.
Crasemann, B. and P. Stephas, 1969, Nucl. Phys. A **134**, 641.
Creager, C. B., C. W. Kocher, and A. C. G. Mitchell, 1959/60, Nucl. Phys. **14**, 578.
Cretzu, T., K. Hohmuth, and J. Schintlmeister, 1965, Nucl. Phys. **70**, 129.
Cretzu, T., K. Hohmuth, and G. Winter, 1964, Nucl. Phys. **56**, 415.
Cutkosky, R. E., 1954, Phys. Rev. **95**, 1222.
Cutkosky, R. E., 1957, Phys. Rev. **107**, 330.
Damgaard, J. and A. Winther, 1965, Phys. Lett. **23**, 345.
Danby, G. T., J. S. Foster, and A. L. Thomson, 1958, Can. J. Phys. **36**, 1487.
Daniel, H., 1968, Rev. Mod. Phys. **40**, 659.
Daniel, H., 1969, Z. Phys. **223**, 150.
Daniel, H., G. Schupp, and E. N. Jensen, 1960, Phys. Rev. **117**, 823.
Dasmahapatra, B., 1972, Radiochem. Radioanal. Lett. **12**, 185.
Dasmahapatra, B., 1975a, Phys. Rev. C **12**, 702.
Dasmahapatra, B., 1975b, Pramana. **4**, 218.
Das Mahapatra, B. K. and P. Mukherjee, 1974, J. Phys. A **7**, 388.
Davis, R., D. S. Harmer, and K. C. Hoffman, 1968, Phys. Rev. Lett. **20**, 1205.
de Beer, A., H. P. Blok, and J. Blok, 1964, Physica **30**, 1938.
Delabaye, M. and P. Lipnik, 1966, Nucl. Phys. **86**, 668.
Delorme, J. and M. Rho, 1971, Nucl. Phys. B **34**, 317.
Depommier, P., 1968, in Berényi (1968b), p. 202.
Der Mateosian, E., 1953, Phys. Rev. **92**, 938.
Der Mateosian, E. and A. Smith, 1952, Phys. Rev. **88**, 1186.
de Raedt, J., 1968, in *Proceedings Beta Spectroscopy and Nuclear Structure* (Natuurkundig Laboratorium, Rijksuniversiteit, Groningen), p. 78.
De Roost, E. and F. Lagoutine, 1973, in Grinberg *et al.* (1973), Atomic Energy Review **11**, 515.
Desclaux, J. P., 1973, Atomic and Nuclear Data **12**, 311.
de Shalit, A. and I. Talmi, 1963, *Nuclear Shell Theory* (Academic, New York and London).
de Wit, S. A. and A. H. Wapstra, 1965, Nucl. Phys. **73**, 49.
Dicus, D. A. and R. E. Norton, 1970, Phys. Rev. D **1**, 1360.
Dillman, L. T., 1968, J. Nucl. Med. **10**, Suppl. 2.
Dillman, L. T., 1970, J. Nucl. Med. **11**, Suppl. 4.
Dillman, L. T., J. J. Kraushaar, and J. D. McCullen, 1963, Nucl. Phys. **42**, 383.

Dobrilović, L., V. Voljin, D. Bek-Uzarov, K. Buraei, and A. Milojević, 1972, *V Kongres na matematicharite, fizicharite i astronomite na Jugoslavia* (Zbornik na trudorite, Tom. II, Fizika, Skopje), p. 151.
Dolginov, A. Z., 1956/1957, Nucl. Phys. **2**, 723.
Dolginov, A. Z., 1958a, Nucl. Phys. **6**, 460.
Dolginov, A. Z., 1958b, Zh. Eksp. Teor. Fiz. **34**, 931 [Sov. Phys. JETP **34**, 644].
Donnelly, T. W. and J. D. Walecka, 1972, Phys. Lett. B **41**, 275.
Donnelly, T. W. and J. D. Walecka, 1973, Phys. Lett. B **44**, 330.
Dougan, P. W., 1961, Ph.D. Thesis, University of Glasgow (unpublished).
Dougan, P. W., K. W. D. Ledingham, and R. W. P. Drever, 1962a, Phil. Mag. **7**, 475.
Dougan, P. W., K. W. D. Ledingham, and R. W. P. Drever, 1962b, Phil. Mag. **7**, 1223.
Drever, R. W. P., 1959, private communication to R. W. Fink, quoted in Robinson and Fink, 1960.
Drever, R. W. P. and A. Moljk, 1957a, Phil. Mag. **2**, 427.
Drever, R. W. P., A. Moljk, and S. C. Curran, 1957b, Nucl. Instrum. Methods **1**, 41.
Drever, R. W. P., A. Moljk, and J. Scobie, 1956, Phil. Mag. **1**, 942.
Durand, III, L., 1964, Phys. Rev. **135**, 310B.
Durosinmi-Etti, I. O., D. R. Brundrit, and S. K. Sen, 1966, in *Internal Conversion Processes*, edited by J. H. Hamilton (Academic, New York), p. 201.
Dzhelepov, B. S. and L. N. Zyryanova, 1956, *Influence of Atomic Electric Fields on Beta Decay* (Akad. Nauka, Moscow).
Dzhelepov, B. S., L. N. Zyryanova, and Yu. P. Suslov, 1972, *Beta Processes, Functions for the Analysis of Beta-Spectra and Electron Capture* (Nauka, Leningrad).
Edmonds, A. R., 1960, *Angular Momentum in Quantum Mechanics* (Princeton University, Princeton).
Eichler, J., 1963, Z. Phys. **171**, 463.
Ellis, Y. A., 1973, Nucl. Data Sheets **9**, 353.
Eman, B., B. Gubertina, and D. Tadić, 1973, Phys. Rev. C **8**, 1301.
Emery, G. T., 1972, Annu. Rev. Nucl. Sci. **22**, 165.
Emery, G. T., 1975, in *Atomic Inner Shell Processes*, edited by B. Crasemann (Academic, New York), Vol. 1, p. 201.
Emery, G. T., W. R. Kane, M. McKeown, M. L. Perlman, and G. Scharff-Goldhaber, 1963, Phys. Rev. **129**, 2597.
Emmerich, W. S., S. E. Singer, and J. D. Kurbatov, 1954, Phys. Rev. **94**, 113.
Ericson, M., A. Figureau, and C. Thévenet, 1973, Phys. Lett. B **45**, 19.
Evans, J. L., J. R. Cooper, D. M. Moore, and W. L. Alford, 1972, Phys. Rev. C **6**, 1372.
Faessler, A., E. Huster, O. Krafft, and F. Krahn, 1970, Z. Phys. **238**, 352.
Fasoli, U., C. Manduchi, and G. Zannoni, 1962, Nuovo Cimento **23**, 1126.
Fermi, E., 1934, Z. Phys. **88**, 161, translated in *The Development of Weak Interaction Theory*, edited by P. K. Kabir (Gordon and Breach, New York, 1963).
Feinberg, E. L., 1941, J. Phys. USSR **4**, 423.
Feynman, R. P., 1949, Phys. Rev. **76**, 749.
Fierz, M., 1937, Z. Physik **104**, 553.
Fink, R. W., 1965, in *Role of Atomic Electrons in Nuclear Transformations* (Nuclear Energy Information Center, Warsaw, Poland), p. 365.
Fink, R. W., 1968a, in Berényi (1968b), p. 23.
Fink, R. W., 1968b, Nucl. Phys. A **110**, 379.
Fink, R. W., 1969, Phys. Rev. **180**, 1220.
Fink, R. W., G. Andersson, and J. Kantele, 1961, Ark. Fys. **19**, 323.
Fink, R. W. and K. W. D. Ledingham, 1966, Bull. Am. Phys. Soc. **11**, 352.
Firestone, R. B., R. A. Warner, and W. C. McHarris, and W. H. Kelly, 1974, Phys. Rev. Lett. **33**, 30.
Firestone, R. B., R. A. Warner, W. C. McHarris, and W. H. Kelly, 1975a, Phys. Rev. Lett. **35**, 401.
Firestone, R. B., R. A. Warner, W. C. McHarris, and W. H. Kelly, 1975b, Phys. Rev. Lett. **35**, 713.
Fitzpatrick, M. L., 1973, Ph.D. Thesis, University of Glasgow (unpublished).
Fitzpatrick, M. L., K. W. D. Ledingham, M. Campbell, A. D. Baillie, J. Y. Gourlay, and J. G. Lynch, 1976, to be published.
Ford, G. W. and C. F. Martin, 1969, Nucl. Phys. A **134**, 457.
Ford, J. W., A. V. Ramaya, and J. J. Pinajian, 1970, Nucl. Phys. A **146**, 397.
Frauenfelder, G. and R. M. Steffen, 1966, in *Alpha-, Beta-, and Gamma-Ray Spectroscopy*, edited by K. Siegbahn (North-Holland, Amsterdam).
Freedman, M. S., 1974, Annu. Rev. Nucl. Sci. **24**, 209.
Freedman, M. S., F. Wagner, Jr., F. T. Porter, and H. H. Bolotin, 1966, Phys. Rev. **146**, 791.
Frevert, L., R. Schöneberg, and A. Flammersfeld, 1965, Z. Phys. **182**, 439.
Fricke, B., W. Greiner, and J. T. Waber, 1971, Theoret. Chim. Acta **21**, 235.
Friedlander, G. and J. M. Miller, 1951a, Phys. Rev. **84**, 588.
Friedlander, G. and W. C. Orr, 1951b, Phys. Rev. **84**, 484.
Friedlander, G., M. L. Perlman, D. Alburger, and A. W. Sunyar, 1950, Phys. Rev. **80**, 30.
Friedlander, G. and L. Yaffe, 1962, Can. J. Phys. **40**, 1249.
Froese-Fischer, C., 1965, Phys. Rev. **137**, 1644A.
Froese-Fischer, C., 1969, Comput. Phys. Commun. **1**, 151.
Froese-Fischer, C., 1972a, Comput. Phys. Commun. **4**, 107.
Froese-Fischer, C., 1972b, Atomic Data **4**, 301.
Fujita, J. I., 1962, Phys. Rev. **126**, 202.
Fujioka, M., K. Hisatake, and K. Takahashi, 1964, Nucl. Phys. **60**, 294.
Fujiwara, I., S. Iwata, T. Nishi, S. Goda, M. Tabushi, and T. Shigematsu, 1964, Nucl. Phys. **50**, 346.
Funk, Jr., E. G., J. W. Mihelich, and C. F. Schwerdtfeger, 1962, Nucl. Phys. **39**, 147.
Funke, L., H. Graber, K. H. Kaun, H. Sodan, and L. Werner, 1965, Nucl. Phys. **70**, 347.
Gallagher, C. J., H. L. Nielsen, and O. B. Nielsen, 1961, Phys. Rev. **122**, 1590.
Gandel'man, G. M., 1959, Zh. Eksp. Teor. Fiz. **36**, 585 [Sov. Phys. JETP **36**, 406 (1959)].
Geiger, J. S. and A. J. Ferguson, 1974 (private communication).
Genz, H., 1968, in Berényi (1968b), p. 81.
Genz, H., 1971b, Ph.D. Thesis, Emory University, Atlanta (unpublished).
Genz, H., 1973a, in *Proceedings of the International Conference on Inner-Shell Ionization Phenomena*, edited by R. W. Fink, S. T. Manson, J. M. Palms, and P. Venugopala Rao, U. S. Atomic Energy Comission Report No. CONF-720404 (unpublished), p. 1965.
Genz, H., 1973b, Nucl. Instrum. Methods **112**, 83.
Genz, H., D. S. Harmer, and R. W. Fink, 1968, Nucl. Instrum. Methods **60**, 195.
Genz, H., J. P. Renier, and R. W. Fink, 1972, in *Radioactivity in Nuclear Spectroscopy*, edited by J. H. Hamilton and J. C. Manthuruthil (Gordon and Breach, New York), p. 1335.
Genz, H., J. P. Renier, J. G. Pengra, and R. W. Fink, 1971a, Phys. Rev. C **3**, 172.
Genz, H., R. E. Wood, J. M. Palms, and P. Venugopala Rao, 1973c, Z. Phys. **260**, 47.
Gindler, J. E., J. R. Huizenga, and D. W. Engelkemeir, 1958, Phys. Rev. **109**, 1263.
Girgis, R. K. and R. van Lieshout, 1959a, Physica, **25**, 133.
Girgis, R. K., R. A. Ricci, R. van Lieshout, and J. Konijn, 1959b, Nucl. Phys. **13**, 473.
Glauber, R. J. and P. C. Martin, 1955a, J. Phys. Radium **16**,

573.
Glauber, R. J., P. C. Martin, T. Lindqvist, and C. S. Wu, 1955b, Phys. Rev. **101**, 905.
Glauber, R. J. and P. C. Martin, 1956, Phys. Rev. **104**, 158.
Glaubman, M. J., 1955, Phys. Rev. **98**, 645.
Gleason, G. I., 1959, Phys. Rev. **113**, 287.
Gnatovich, I., V. Svols'ka, Y. Svols'ki, Y. Rjikovska, M. Fisher, and I. Yursik, 1974, [Program and abstracts of 24. Conference on nuclear spectroscopy and nuclear structure Khar'kov, 29 January–1 February, INIS–mf–1850], p. 136.
Goedbloed, W., 1968, in Berényi (1968b), p. 92.
Goedbloed, W., 1970, Ph.D. Thesis, Vrije Universiteit, Amsterdam (unpublished).
Goedbloed, W., S. C. Goverse, A. Brinkman, and J. Blok, 1970c, Nucl. Phys. A **159**, 409.
Goedbloed, W., S. C. Goverse, C. P. Gerner, A. Brinkman, and J. Blok, 1970a, Nucl. Instrum. Methods **88**, 197.
Goedbloed, W., S. C. Goverse, C. P. Gerner, A. Brinkman, and J. Blok, 1970b, Nucl. Phys. A **159**, 417.
Goedbloed, W., E. Mastenbroek, A. Kemper, and J. Blok, 1964, Physica **30**, 2041.
Gold, R. and E. F. Bennett, 1966, Phys. Rev. **147**, 201.
Goldhaber, M., E. der Mateosian, G. Scharff-Goldhaber, A. W. Sunyar, M. Deutsch, and N. S. Wall, 1951, Phys. Rev. **83**, 661L.
Goldhaber, M., L. Grodzins, and A. W. Sunyar, 1958, Phys. Rev. **109**, 1015.
Gombás, P., 1956, in *Handb. Phys.*, **36**, 109.
Gombás, P., 1967, *Pseudopotentiale* (Springer-Verlag, Wien, New York).
Good, W. M. and W. C. Peacock, 1946, Phys. Rev. **69**, 680.
Good, W. M., D. Peaslee, and M. Deutsch, 1946, Phys. Rev. **69**, 313.
Goodier, I. W., M. J. Woods, and A. Williams, 1971, in *Chemical Nuclear Data*, edited by M. L. Hurrel (The British Nuclear Energy Society, London), p. 175.
Gopinathan, K. P. and W. Rubinson, 1968, Bull. Am. Phys. Soc. **13**, 1452.
Gopych, P. M., I. I. Gromova, A. F. Novgorodov, Kh.-G. Urtlepp, and A. Yasinski, 1974, [Program and abstracts of 24. Conference on nuclear spectroscopy and nuclear structure, Kharkov 29 January–1 February, INIS–mf–1850], p. 85.
Goudsmit, P. F. A., J. F. W. Jansen, B. J. Mijnheer, and A. H. Wapstra, 1966, Physica **32**, 2161.
Gove, N. B. and M. J. Martin, 1971, Nucl. Data A **10**, 205.
Goverse, S. C. and J. Blok, 1974c, Phys. Lett. A **50**, 135.
Goverse, S. C., J. van Pelt, J. van den Berg, J. C. Klein, and J. Blok, 1973, Nucl. Phys. A **201**, 326.
Goverse, S. C., J. C. Klein, J. Kuijper, and J. Blok, 1974a, Nucl. Phys. A **227**, 506.
Goverse, S. C., J. Kuijper, and J. Blok, 1974b, Z. Phys. **269**, 111.
Grant, I. P., 1970, Adv. Phys. **19**, 747.
Grator, I., M. le Pape, J. Olkowsky, and G. Ranc, 1959, Nucl. Phys. **13**, 303.
Greenland, P. T., 1975, J. Phys. G **1**, 1.
Greenwood, R. C. and E. Brannen, 1960, Phys. Rev. **120**, 1411.
Greenwood, R. C. and E. Brannen, 1961, Phys. Rev. **122**, 1849.
Grigor'ev, E. P., B. S. Dzhelepov, A. V. Zolotavin, and V. Ia. Mishin, V. P. Prikhodtseva, Iu. V. Khol'nov, and G. E. Shchukin, 1958a, Izv. Akad. Nauk. SSSR Ser. Fiz. **22**, 831 [Bull. Acad. Sci. USSR, Phys. Ser. **22**, 825].
Grigor'ev, O. I., B. S. Kuznetsov, N. S. Shimanskaia, and I. A. Iutlandov, 1958b, Izv. Akad. Nauk. SSSR Ser. Fiz. **22**, 850, [Bull. Acad. Sci. USSR, Phys. Ser. **22**, 845].
Grinberg, B., J. P. Brethon, F. Lagoutine, Y. Le Gallic, J. Legrand, A. H. Wapstra, and H. M. Weiss, W. Bambynek, E. De Roost, H. H. Hansen, and A. Spernol, At. Energy Rev. 1973, **11**, 516.
Grissom, J. T., D. R. Koehler, and W. I. Alford, 1966, Phys. Rev. **142**, 725.
Grodzins, L. and H. Motz, 1956, Phys. Rev. **102**, 761.
Gromov, K. Ya., Zh. T. Zhelev, V. Zvolska, and V. G. Kalinnikov, 1965, Yad. Fiz. **2**, 783 [Sov. J. Nucl. Phys. **2**, 559].
Grotheer, H. H., J. W. Hammer, and K.-W. Hoffmann, 1969, Z. Phys. **225**, 293.
Gupta, R. K., 1958a, Proc. Phys. Soc. Lond. **71**, 330.
Gupta, R. K., 1960, Ark. Fys. **17**, 337.
Gupta, R. K. and S. Jha, 1956, Nuovo Cimento **4**, 88.
Gupta, R. K. and S. Jha, 1957, Nuovo Cimento **5**, 1524.
Gupta, R. K., S. Jha, M. C. Joshi, and B. K. Madan, 1958b, Nuovo Cimento **8**, 48.
Hagedoorn, H. L., 1958, Ph.D. Thesis, Technische Hogeschool, Delft (unpublished).
Hagedoorn, H. L. and J. Konijn, 1957, Physica **23**, 1069.
Hamers, H. C., A. Marseille, and T. J. de Boer, 1957, Physica **23**, 1056.
Hamilton, J. H., K. E. G. Löbner, A. R. Sattler, and R. van Lieshout, 1964, Physica **30**, 1802.
Hammer, J. W., 1968, Z. Phys. **216**, 355.
Hansen, H. H. and D. Mouchel, 1975, Z. Phys. **274**, 335.
Hanson, R. J., P. G. Hansen, H. L. Nielsen, and G. Sørensen, 1968, Nucl. Phys. A **115**, 641.
Harmer, D. S. and M. L. Perlman, 1959, Phys. Rev. **114**, 1133.
Harris, J. R., G. M. Rothberg, and N. Benczer-Koller, 1965, Phys. Rev. **138**, 554B.
Hartree, D. R., 1957, *The Calculation of Atomic Structures* (Wiley, New York).
Hartwig, G. and H. Schopper, 1958, Z. Phys. **152**, 314.
Hayashi, T. and J. R. Comerford, Jr., 1968, U. S. Atomic Energy Commission Report TID–6080 (unpublished).
Hayward, R. W., 1950, Phys. Rev. **79**, 541.
Hayward, R. W. and D. D. Hoppes, 1956, Phys. Rev. **104**, 183.
Heath, R. L., 1963, in O'Kelley (1963), p. 93.
Heintze, J., 1954, Z. Naturforsch. A **9**, 469.
Henry, E. A., 1974, Nucl. Data Sheets **11**, 529.
Herman, F. and S. Skillman, 1963, *Atomic Structure Calculations* (Prentice-Hall, Englewood Cliffs).
Heuer, W., 1966, Z. Phys. **194**, 224.
Heuer, W. and E. Huster, 1964, Z. Naturforsch. A **19**, 517.
Hinrichsen, P. F., 1968, Nucl. Phys. A **118**, 538.
Hoff, R. W., 1953, University of California, Radiation Laboratory Report UCRL–2325 (unpublished).
Hoff, R. W., J. L. Olsen, and L. G. Mann, 1956, Phys. Rev. **102**, 805.
Hoffman, E. J. and D. G. Sarantites, 1969, Phys. Rev. **177**, 1640.
Hoffmann, D. C., and B. J. Dropesky, 1958, Phys. Rev. **109**, 1282.
Hohmuth, K., G. Müller, and J. Schintlmeister, 1964, Nucl. Phys. **52**, 590.
Holstein, B. R., 1974, Rev. Mod. Phys. **46**, 789.
Holstein, B. R. and S. B. Treiman, 1971, Phys. Rev. C **3**, 1921.
Hopke, P. K. and R. A. Naumann, 1969, Phys. Rev. **4**, 185.
Hoppes, D. D. and R. W. Hayward, 1956, Phys. Rev. **104**, 368.
Horen, D. J., W. E. Meyerhof, J. J. Kraushaar, D. O. Wells, E. Brun, and J. E. Neighbor, 1959, Phys. Rev. **113**, 875.
Horowitz, J., 1952, J. Phys. Radium **13**, 429.
Huber, O., R. Rüetschi, and P. Scherrer, 1949, Helv. Phys. Acta **22**, 375.
Huffaker, J. N. and E. Greuling, 1963, Phys. Rev. **132**, 738.
Huffaker, J. N. and C. E. Laird, 1967, Nucl. Phys. A **92**, 584.
Huizenga, J. R. and C. M. Stevens, 1954, Phys. Rev. **96**, 548.
Intemann, R. L. and F. Pollock, 1967, Phys. Rev. **157**, 41.

Intemann, R. L., 1969, Phys. Rev. **178**, 1543, corrected in Phys. Rev. **188**, 1963.
Intemann, R. L., 1971, Phys. Rev. C **3**, 1.
Intemann, R. L., 1972, Phys. Rev. C **6**, 211.
Intemann, R. L., 1974, Nucl. Phys. A **219**, 20.
Isozumi, Y. and S. Shimizu, 1971, Phys. Rev. C **4**, 522.
Jacobsen, J. C., 1937, Nature **139**, 879.
Jaffe, H., 1954, University of California, Radiation Laboratory Report, UCRL–2537 (unpublished).
Jasinski, A. and C. J. Herrlander, 1968, Ark. Fys. **37**, 585.
Jasinski, A., J. Kownacki, H. Lancman, J. Ludziejewski, S. Chojnacki, and I. Yutlandov, 1963, Nucl. Phys. **41**, 303.
Jasinski, A., J. Kownacki, H. Lancman, and J. Ludziejewski, 1965, *Role of Atomic Electrons in Nuclear Transformations* [Nuclear Energy Information Center, Warsaw, Poland], p. 625.
Jastram, P. S., W. L. Skeel, and M. K. Ramaswamy, 1961, Bull. Am. Phys. Soc. **6**, 38.
Jastrzebski, J. and P. Kilcher, 1961, J. Phys. Radium **22**, 525.
Jauch, J. M., 1951, Oak Ridge National Laboratory Report, ORNL–1102 (unpublished).
Jaus, W., 1972, Phys. Lett. **40**, 616.
Jaus, W. and G. Rasche, 1970, Nucl. Phys. A **143**, 202.
Jha, S. and H. G. Devare, 1959, Nuovo Cimento **14**, 509.
Jha, S., R. K. Gupta, H. G. Devare, and G. C. Pramila, 1961, Nuovo Cimento **20**, 1067.
Johansson, S., Y. Cauchois, and K. Siegbahn, 1951, Phys. Rev. **82**, 275.
Johns, M. W., S. V. Nablo, and W. J. King, 1957, Can. J. Phys. **35**, 1159.
Jopson, R. C., Hans Mark, C. D. Swift, and J. H. Zenger, 1961, Phys. Rev. **124**, 157.
Joshi, B. R., 1961, Proc. Phys. Soc. Lond. **77**, 1205.
Joshi, B. R. and G. M. Lewis, 1960, Proc. Phys. Soc. Lond. **76**, 349.
Joshi, B. R. and G. M. Lewis, 1961, Proc. Phys. Soc. Lond. **78**, 1056.
Joshi, B. R., G. M. Lewis, and K. M. Smith, 1963, Nucl. Instrum. Methods **24**, 77.
Juliano, J. O., C. W. Kocher, T. D. Nainan, and A. C. G. Mitchell, 1959, Phys. Rev. **113**, 602.
Jung, R. G. and M. L. Pool, 1956, Bull. Am. Phys. Soc. **1**, 172.
Kabasakal, Y. and M. K. Ramaswamy, 1969, Nuovo Cimento B **61**, 220.
Kádár, I., 1971, Atomki Közl. **13**, 29.
Kádár, I., 1972, Fiz. Szemle **22**, 10.
Kádár, I., D. Berényi, and B. Myslek, 1970, Nucl. Phys. A **153**, 383.
Källen, G., 1967, Nucl. Phys. B **1**, 225.
Kalkstein, M. I., 1957, private communication, quoted by Thomas *et al.* (1957).
Kantele, J. and M. Valkonen, 1973, Nucl. Instrum. Methods **112**, 501.
Karraker, D. G. and D. H. Templeton, 1950, Phys. Rev. **80**, 646.
Karttunen, E., H.-U. Freund, and R. W. Fink, 1969, Nucl. Phys. A **131**, 343.
Katcoff, S., 1958, Phys. Rev. **111**, 575.
Katcoff, S. and H. Abrash, 1956, Phys. Rev. **103**, 966.
Ketelle, B. H., A. R. Brosi, and J. R. van Hise, 1971, Phys. Rev. C **4**, 1431.
Ketelle, B. H., H. Thomas, and A. R. Brosi, 1956, Phys. Rev. **103**, 190.
Kim, C. W., 1971, Phys. Lett. B **34**, 383.
Kim, C. W., 1974, Riv. Nuovo Cimento **4**, 189.
Kim, C. W. and T. Fulton, 1971, Phys. Rev. C **4**, 390.
Kim, C. W. and H. Primakoff, 1969, Phys. Rev. **180**, 1502.
Kirkwood, D. H. W., B. Pontecorvo, and G. C. Hanna, 1948, Phys. Rev. **74**, 497.
Kiselev, B. G. and V. R. Burmistrov, 1969, Yad. Fiz. **10**, 1105 [Sov. J. Nucl. Phys. **10**, 629].
Kiser, R. W. and W. H. Johnston, 1959, J. Am. Chem. Soc. **81**, 1810.
Kitahara, T., Y. Isozumi, and S. Shimizu, 1972, Phys. Rev. C **5**, 1810.
Kitahara, T. and S. Shimizu, 1975, Phys. Rev. C **11**, 920.
Klein, H. and H. Leutz, 1966, Nucl. Phys. **79**, 27.
Knipp, J. K. and G. E. Uhlenbeck, 1936, Physica **3**, 425.
Koerts, L., P. Macklin, B. Farrelly, R. van Lieshout, and C. S. Wu, 1955, Phys. Rev. **98**, 1230.
Koh, Y., 1965, in *Role of Atomic Electrons in Nuclear Transformations*, (Nuclear Energy Information Center, Warsaw), p. 637.
Koh, Y., O. Miyatake, and Y. Watanabe, 1957, Prog. Theor. Phys. **18**, 663.
Koh, Y., O. Miyatake, and Y. Watanabe, 1962, Nucl. Phys. **32**, 246.
Kohn, W. and L. J. Sham, 1965, Phys. Rev. A **140**, 1133.
Koički, S. D., A. M. Mijatović, and J. M. Simić, 1958, Bull. Boris Kidric Inst. Nucl. Sci. **8**, 1.
Konijn, J., B. van Nooijen, P. Mostert, and P. M. Endt, 1956, Physica **22**, 887.
Konijn, J., H. L. Hagedoorn, H. van Krugten, and J. Slobben, 1958a, Physica **24**, 931.
Konijn, J., H. L. Hagedoorn, and B. van Nooijen, 1958b, Physica **24**, 129.
Konijn, J., B. van Nooijen, and H. L. Hagedoorn, 1958c, Physica **24**, 377.
Konijn, J., B. van Nooijen, H. L. Hagedoorn, and A. H. Wapstra, 1958/59, Nucl. Phys. **9**, 296.
Konijn, J., B. van Nooijen, and A. H. Wapstra, 1960, Nucl. Phys. **16**, 683.
Konijn, J., E. W. A. Lingeman, and S. A. de Wit, 1967a, Nucl. Phys. A **90**, 558.
Konijn, J., W. H. G. Lewin, B. van Nooijen, H. F. van Beek, S. A. de Wit, and E. W. A. Lingeman, 1967b, Nucl. Phys. A **102**, 129.
Konopinski, E. J., 1966, *The Theory of Beta Radioactivity* (Clarendon, Oxford).
Konstantinov, A. A. and V. V. Perepelkin, 1961, Izv. Akad. Nauk. SSSR Ser. Fiz. **25**, 106 [Bull. Acad. Sci. USSR, Phys. Ser. **25**, 103].
Koonin, S. E. and B. I. Persson, 1972, Phys. Rev. C **6**, 1713.
Krafft, O., 1970, Z. Phys. **238**, 78.
Krahn, F., 1972, Z. Phys. **251**, 375.
Kramer, P., E. C. Bos, A. de Beer, and J. Blok, 1962a, Physica **28**, 569.
Kramer, P., A. de Beer, and J. Blok, 1962b, Physica, **28**, 587.
Kramer, P., H. C. Hamers, and G. Meijer, 1956, Physica **22**, 208.
Kreger, W. E., 1954, Phys. Rev. **96**, 1554.
Kroger, L. A. and C. W. Reich, 1973, Nucl. Data Sheets **10**, 447.
Kropf, A. and H. Paul, 1974, Z. Phys. **267**, 129.
Krutov, V. A. and L. N. Savashkin, 1973, J. Phys. A **6**, 93.
Krutov, V. A., V. N. Fomenko, and L. N. Savashkin, 1974, J. Phys. A **7**, 372.
Kubodera, K., J. Delorme, and M. Rho, 1973, Nucl. Phys. B **66**, 253.
Kuhlmann, E. and K. E. G. Löbner, 1969, Z. Phys. **222**, 144.
Kuphal, E., P. Dewes, and E. Kankeleit, 1974, Nucl. Phys. A **234**, 308.
Kyles, J., J. C. McGeorge, F. Shaikh, and J. Byrne, 1970, Nucl. Phys. A **150**, 143.
Lancman, H. and A. Bond, 1973, Phys. Rev. C **7**, 2600.
Lancman, H. and J. M. Lebowitz, 1969, Phys. Rev. **188**, 1683.
Lancman, H. and J. M. Lebowitz, 1971a, Phys. Rev. C **3**, 188.
Lancman, H. and J. M. Lebowitz, 1971b, Phys. Rev. C **3**, 465.
Langer, L. M. and R. D. Moffat, 1950, Phys. Rev. **80**, 651.

Langevin, M., 1954b, C. R. Acad. Sci. (Paris) **239**, 1625.
Langevin, M., 1954d, C. R. Acad. Sci. (Paris) **238**, 2518.
Langevin, M., 1955a, J. Phys. Radium, **16**, 516.
Langevin, M., 1955b, C. R. Acad. Sci. (Paris) **240**, 289.
Langevin, M., 1956, Ann. Phys. (Paris) **1**, 57.
Langevin, M., 1957, C. R. Acad. Sci. (Paris) **245**, 664.
Langevin, M., 1958, J. Phys. Radium **19**, 34.
Langevin, M. and N. Marty, 1954c, J. Phys. Radium **15**, 127.
Langevin, M. and P. Radvanyi, 1954a, C. R. Acad. Sci. (Paris) **238**, 77.
Langevin, M. and P. Radvanyi, 1955c, C. R. Acad. Sci. (Paris) **241**, 33.
Langhoff, H., P. Kilian, and A. Flammersfeld, 1961, Z. Phys. **165**, 393.
Langhoff, H., L. Frevert, W. Schött, and A. Flammersfeld, 1966, Nucl. Phys. **79**, 145.
Lark, N. L. and M. L. Perlman, 1960, Phys. Rev. **120**, 536.
Lassila, K. E., 1963, Phys. Rev. **131**, 807.
Latter, R., 1955, Phys. Rev. **99**, 510.
Laverne, A. and G. Do. Dang, 1971, Nucl. Phys. A **177**, 665.
Law, J. and J. L. Campbell, 1972a, Nucl. Phys. A **185**, 529.
Law, J. and J. L. Campbell, 1972b, Nucl. Phys. A **187**, 525.
Law, J. and J. L. Campbell, 1973a, in *Proceedings of the International Conference on Inner-Shell Ionization Phenomena*, edited by R. W. Fink, S. T. Manson, J. M. Palms, and P. Venugopala Rao (U. S. Atomic Energy Commission Report No. CONF–720404 unpublished), p. 2110.
Law, J. and J. L. Campbell, 1973b, Nucl. Phys. A **199**, 481.
Lederer, C. M., J. M. Hollander, and I. Perlman, 1967, *Table of Isotopes*, (Wiley, New York).
Ledingham, K. W. D., J. A. Payne, and R. W. P. Drever, 1965, *Role of Atomic Electrons in Nuclear Transformations*, (Nuclear Information Center, Warsaw), p. 359.
Ledingham, K. W. D., J. Y. Gourlay, J. L. Campbell, M. L. Fitzpatrick, J. G. Lynch, and J. McDonald, 1971, Nucl. Phys. A **170**, 663.
Lee, T. D., 1973, Phys. Rep. **9C**, 143.
Leiper, W. and R. W. P. Drever, 1972, Phys. Rev. C **6**, 1132.
Leiper, W. and O. P. Jolly, 1971, Can. J. Phys. **49**, 582.
Leistner, M. and K. Friedrich, 1965, Atomkernenergie **10**, 311.
Leutz, H., 1960, Z. Phys. **159**, 462.
Leutz, H., K. Schneckenberger, and H. Wenninger, 1965, Nucl. Phys. **63**, 263.
Leutz, H., G. Schulz, and H. Wenninger, 1966, Nucl. Phys. **75**, 81.
Leutz, H. and H. Wenninger, 1967, Nucl. Phys. A **99**, 55.
Leutz, H. and K. Ziegler, 1962, Z. Phys. **166**, 582.
Leutz, H. and K. Ziegler, 1964, Nucl. Phys. **50**, 648.
Levi, C. and L. Papineau, 1954, C. R. Acad. Sci. (Paris) **238**, 2313.
Levi, C. and L. Papineau, 1957, C. R. Acad. Sci. (Paris) **244**, 1358.
Levi, C., L. Papineau, C. Latapie-Redon, and N. Saunier, 1959, C. R. Acad. Sci. (Paris) **249**, 410.
Lewin, W. H. G., J. Bezemer, and C. W. E. van Eijk, 1965a, Nucl. Phys. **62**, 337.
Lewin, W. H. G., J. Lettinga, B. van Nooijen, and A. H. Wapstra, 1965b, Nucl. Phys. **65**, 337.
Liberman, D., J. T. Waber, and Don T. Cromer, 1965, Phys. Rev. **137**, 27A.
Lidén, K. and N. Starfelt, 1954, Ark. Fys. **7**, 427.
Lindgren, I. and A. Rosen, 1974, Case Studies in Atomic Physics **4**, 93.
Lindgren, I. and K. Schwarz, 1971, Phys. Rev. A **5**, 542.
Lindner, M. and I. Perlman, 1948, Phys. Rev. **73**, 1202.
Lindqvist, T. and C. S. Wu, 1955, Phys. Rev. **100**, 145.
Lipnik, P., G. Pralong, and J. W. Sunier, 1964, Nucl. Phys. **59**, 504.
Lipnik, P. and J. W. Sunier, 1966, Phys. Rev. **145**, 746.
Lipkin, H. J., 1970, Phys. Lett. B **34**, 202.
Lipkin, H. J., 1971, Phys. Rev. Lett. **27**, 432.
Ljubičič, A., R. T. Jones, and B. A. Logan, 1974, Nucl. Phys. A **236**, 158.
Lock, J. A., L. L. Foldy, and F. R. Buskirk, 1974, Nucl. Phys. A **220**, 103.
Longmire, C. L., 1949, Phys. Rev. **75**, 15.
Lourens, W., B. O. ten Brink, and A. H. Wapstra, 1970, Nucl. Phys. A **152**, 463.
Lu, C. C., T. A. Carlson, F. B. Malik, T. C. Tucker, and C. W. Nestor, Jr., 1971, Atomic Data **3**, 1.
Lu, D. C. and G. Schlupp, 1962, Bull. Am. Phys. Soc. **7**, 353.
MacMahon, T. D. and A. P. Baerg, 1970, Bull. Am. Phys. Soc., Ser. II, **15**, 755; 1970, Physics in Canada, **26**, no. 4; Can. J. Phys. **54**, 1433.
Madansky, L. and R. Rasetti, 1954, Phys. Rev. **94**, 407.
Maeder, D. and P. Preiswerk, 1951, Phys. Rev. **84**, 595.
Magnusson, L. B., A. M. Friedman, D. Engelkemeir, P. R. Fields, and F. Wagner, Jr., 1956, Phys. Rev. **102**, 1097.
Major, J. K., 1952, Phys. Rev. **86**, 631.
Malli, G., 1966, Can. J. Phys. **44**, 3121 and 3131.
Manduchi, C., G. Nardelli, M. T. Russo-Manduchi, and G. Zannoni, 1964a, Nuovo Cimento **31**, 1380.
Manduchi, C., G. C. Nardelli, M. T. Russo-Manduchi, and G. Zannoni, 1964b, Nuovo Cimento **33**, 49.
Manduchi, C. and G. Zannoni, 1961, Nuovo Cimento **22**, 462.
Manduchi, C. and G. Zannoni, 1962a, Nucl. Phys. **36**, 497.
Manduchi, C. and G. Zannoni, 1962b, Nuovo Cimento **24**, 181.
Manduchi, G. and G. Zannoni, 1963, Nuovo Cimento **27**, 251.
Mann, J. B., 1967, *Atomic Structure Calculations*, Los Alamos Scientific Laboratory Report No. LA–3690 (unpublished).
Mann, J. B., 1968, *Atomic Structure Calculations*, Los Alamos Scientific Laboratory Report No. Los Alamos Scientific Laboratory Report No. LA–3691 (unpublished).
Mann, J. B. and J. T. Waber, 1973, for $57 \leq Z \leq 70$ Atomic Data **5**, 201, for the other Z private communication.
Mann, L. G., J. A. Miskel, and S. D. Bloom, 1958, Phys. Rev. Lett. **1**, 82.
Marelius, A., P. Sparrman, and S.-E. Hägglund, 1967, Nucl. Phys. A **95**, 632.
Marquez, L. and I. Perlman, 1950, Phys. Rev. **78**, 189.
Marshak, R. E., 1942, Phys. Rev. **61**, 431.
Marshak, R. E., Riazuddin, and C. P. Ryan, 1969, *Theory of Weak Interactions in Particle Physics* (Wiley, New York).
Martin, M. J. and P. H. Blichert-Toft, 1970, Nucl. Data A **8**, 1.
Martin, P. C. and R. J. Glauber, 1958, Phys. Rev. **109**, 1307.
Marty, N., H. Langevin, and P. Hubert, 1953, J. Phys. Radium **14**, 663.
Matese, J. J. and R. Johnson, 1966, Phys. Rev. **150**, 846.
Matuszek, Jr., J. M. and T. T. Sugihara, 1963, Nucl. Phys. **42**, 582.
Mayers, D. F., 1972, *Relativistic Self-Consistent Fields* in *New Directions in Atomic Physics*, edited by F. U. Condon and O. Sinanoglu (Yale University Press, New Haven and London), Vol. 1.
McCann, M. F., G. M. Lewis, and K. M. Smith, 1967, Nucl. Phys. A **98**, 577.
McCann, M. F. and K. M. Smith, 1968, Nucl. Phys. A **121**, 233.
McCann, M. F. and K. M. Smith, 1969, J. Phys. A **2**, 392.
McCown, D. A., L. L. Woodward, and M. L. Pool, 1948a, Phys. Rev. **74**, 1311.
McCown, D. A., L. L. Woodward, and M. L. Pool, 1948b, Phys. Rev. **74**, 1315.
McDonnell, M. and M. K. Ramaswamy, 1968, Phys. Rev. **168**, 1393.
McDonnell, M. and M. K. Ramaswamy, 1969, Nucl. Phys. A **127**, 531.
McGinnis, C. L., 1951, Phys. Rev. **81**, 734.
McGinnis, C. L., 1955, Phys. Rev. **97**, 93.
Medicus, H., P. Preiswerk, and P. Scherrer, 1950, Helv. Phys. Acta **23**, 299.
Menhardt, W., 1957, Acta Phys. Austriaca **11**, 101.

Meixner, C. H., 1971, KfA Jülich Report, JÜL–811–Rx (unpublished).
Meixner, C. H., 1974, Nucl. Instrum. Methods **119**, 521.
Merz, E. R. and A. A. Caretto, Jr., 1961, Phys. Rev. **122**, 1558.
Michalowicz, A., 1953, J. Phys. Radium **14**, 214.
Michalowicz, A., 1956, C. R. Acad. Sci. (Paris) **242**, 108.
Migdal, A., 1941, J. Phys. USSR **4**, 449.
Millar, C. H., T. A. Eastwood, and J. C. Roy, 1959, Can. J. Phys. **37**, 1126.
Miller, L. D., 1972, Phys. Rev. Lett. **28**, 1281.
Miller, L. D. and A. E. S. Green, 1972, Phys. Rev. C **5**, 241.
Miller, M. M. and R. G. Wilkinson, 1951, Phys. Rev. **83**, 1050.
Miskel, J. A. and M. L. Perlman, 1954, Phys. Rev. **94**, 1683.
Mitchell, A. C. G., J. O. Juliano, C. B. Creager, and C. W. Kocher, 1959, Phys. Rev. **113**, 628.
Møller, C., 1937a, Phys. Z. Sowjetunion **11**, 9.
Møller, C., 1937b, Phys. Rev. **51**, 84.
Moler, R. B. and R. W. Fink, 1963, Phys. Rev. **131**, 821.
Moler, R. B. and R. W. Fink, 1965, Phys. Rev. **139**, 282B.
Monaro, S., G. B. Vingiani, and R. van Lieshout, 1961, Physica **27**, 985.
Monaro, S., G. B. Vingiani, R. A. Ricci, and R. van Lieshout, 1962, Physica **28**, 63.
Mord, A. J., 1972, Nucl. Phys. A **192**, 305.
Mord, A. J., 1973, in *Proceedings of the International Conference on Inner-Shell Ionization Phenomena*, edited by R. W. Fink, S. T. Manson, J. M. Palms, and P. Venugopala Rao (U. S. Atomic Energy Commission Report No. CONF–720404, unpublished), p. 2079.
Morita, M., 1973, *Beta Decay and Muon Capture* (W. A. Benjamin, Reading).
Morrison, P. and L. I. Schiff, 1940, Phys. Rev. **58**, 24.
Moussa, A. and A. Juillard, 1956, C. R. Acad. Sci. (Paris) **243**, 1515.
Muir, Jr., A. H., and F. Boehm, 1961, Phys. Rev. **122**, 1564.
Mukerji, A., T. M. Carlton, and G. D. Cole, 1965, Bull. Am. Phys. Soc. **10**, 93.
Mukerji, A. and L. Chin, 1973, in *Proceedings of the International Conference on Inner Shell Ionization Phenomena and Future Applications*, edited by R. W. Fink, S. T. Manson, J. M. Palms, P. Venugopala Rao (U. S. Atomic Energy Commission, Report No. CONF–720404, unpublished), p. 164.
Mukerji, A. and J. B. McGouch, Jr., 1967a, Nucl. Phys. A **94**, 95.
Mukerji, A., J. B. McGouch, Jr., and G. D. Cole, 1967b, Nucl. Phys. A **100**, 81.
Mukoyama, T., Y. Isozumi, T. Kitahara, and S. Shimizu, 1973, Phys. Rev. C **8**, 1308.
Mukoyama, T., T. Kitahara, and S. Shimizu, 1974, Phys. Rev. C **9**, 2307.
Mukoyama, T. and S. Shimizu, 1974, Phys. Rev. C **9**, 2300.
Murty, K. N. and S. Jnanananda, 1967, Indian J. Pure Appl. Phys. **5**, 557.
Mutterer, M., 1971, *Neutron Standards and Flux Normalization*, edited by A. B. Smith, AEC Symp. Ser. 23 (U. S. Atomic Energy Commission Rep. CONF–701002, unpublished), p. 452.
Mutterer, M., 1973a, Phys. Rev. C **8**, 1370.
Mutterer, M., 1973b, Phys. Rev. C **8**, 2089.
Mutterer, M., 1973c, Ph.D. Thesis, Technische Universität München, Germany (unpublished).
Muziol', G., 1966, Dubna Report 6–2920 (unpublished), quoted by Berényi, 1968a.
Myslek, B., B. Pietrzyk, Z. Sujkowski, and J. Szczepankowski, 1971, Acta Phys. Pol. B **2**, 441.
Myslek, B., Z. Sujkowski, and J. Zylicz, 1973, Nucl. Phys. A **215**, 79.
Nagy, J., 1971, Atomki Közl. **13**, 101.
Nagy, H. J., G. Schupp, and R. R. Hurst, 1972, Phys. Rev. C **6**, 607.
Narang, V. and H. Houtermans, 1968, in Berényi, (1968b), p. 97.
National Bureau of Standards, 1952, Applied Mathematics Series, No. 13: *Tables for the Analysis of Beta Spectra*.
Naumann, R. A. and P. K. Hopke, 1967, Phys. Rev. **160**, 1035.
Naumann, R. A., F. L. Reynolds, and I. Perlman, 1950, Phys. Rev. **77**, 398.
Nestor, C. W., T. C. Tucker, T. A. Carlson, L. D. Roberts, F. B. Malik, and C. Froese, 1966, Oak Ridge National Laboratory Report, ORNL–4027 (unpublished).
Nicaise, W. F. and A. W. Waltner, 1975, Nucl. Instrum. Meth. **131**, 477.
Nielsen, H. L., K. Wilsky, J. Zylicz, and G. Sørensen, 1967, Nucl. Phys. A **93**, 385.
Norris, A. E., G. Friedlander, and E. M. Franz, 1966, Nucl. Phys. **86**, 102.
Odiot, S. and R. Daudel, 1956, J. Phys. Radium **17**, 60.
Ofer, S. and R. Wiener, 1957, Phys. Rev. **107**, 1639.
Ohta, K. and M. Wakamatsu, 1974, Nucl. Phys. A **234**, 445.
Oldenburg, O., 1938, Phys. Rev. **53**, 35.
Olsen, J. L., L. G. Mann, and M. Lindner, 1957, Phys. Rev. **106**, 985.
O'Kelley, G. D., 1963, *Applications of Computers to Nuclear and Radiochemistry*, U. S. Atomic Energy Commission Report, NAS–NS 3107 (unpublished).
Orth, D. A. and G. D. O'Kelley, 1951, Phys. Rev. **82**, 758.
Paquette, G., 1962, Can. J. Phys. **40**, 1765.
Parfenova, V. P., 1960, Zh. Eksp. Teor. Fiz. **38**, 56 [Sov. Phys.–JETP **11**, 42].
Paul, H., 1966, Nucl. Data A **2**, 281.
Penev, I., K. Zuber, Ya. Zuber, A. Lyatushinsk, and A. Potemka, 1974, [Program and abstracts of 24. Conference on nuclear spectroscopy and nuclear structure, Kharkov 29 January–1 February, INIS–mf–1850], p. 93.
Pengra, J. G. and B. Crasemann, 1963, Phys. Rev. **131**, 2642.
Pengra, J. G., H. Genz, J. P. Renier, and R. W. Fink, 1972, Phys. Rev. C **5**, 2007.
Pengra, J. G., 1976, in Abstracts of Contributed Papers, Second International Conference on Inner Shell Ionization Phenomena, University Freiburg, p. 194.
Perkins, J. F. and S. K. Haynes, 1953, Phys. Rev. **92**, 687.
Perlman, M. L. and J. P. Welker, 1954, Phys. Rev. **95**, 133.
Perlman, M. L., W. Bernstein, and R. B. Schwartz, 1953, Phys. Rev. **92**, 1236.
Perlman, M. L., J. P. Welker, and M. Wolfsberg, 1958, Phys. Rev. **110**, 381.
Perrin, N. N., 1960, Ann. Phys. (Paris) **5**, 71.
Persson, B. I. and S. E. Koonin, 1972, Phys. Rev. C **5**, 1443.
Persson, L., H. Ryde, and K. Oelsner-Ryde, 1963, Nucl. Phys. **44**, 653.
Persson, L. and Z. Sujkowski, 1961, Ark. Fys. **19**, 309.
Petel, M. and H. Houtermans, 1967, in *Standardization of Radionuclides* (International Atomic Energy Agency, Vienna), p. 301 and private communication to W. Bambynek.
Petterson, B. G., 1965, in K. Siegbahn (1965), p. 1569.
Phillips, W. E. and J. E. Hopkins, 1960, Phys. Rev. **119**, 1315.
Plassmann, E. and F. R. Scott, 1951, Phys. Rev. **84**, 156.
Plch, J., J. Zderadička, and I. Bučina, 1971, Radioisotopy **12**, 131.
Plch, J. and J. Zderadička, 1974a, Czech. J. Phys. B **24**, 1311.
Plch, J., J. Zderadička, and L. Kokta, 1974b, Int. J. Appl. Radiat. Iso. **25**, 433.
Plch, J., J. Zderadička, and O. Dragoun, 1975, Int. J. Appl. Radiat. Isot. **26**, 579.
Polak, H. L., W. Schoo, B. L. Schram, R. K. Girgis, and R. van Lieshout, 1958, Nucl. Phys. **5**, 271.
Pontecorvo, B., D. H. W. Kirkwood, and G. C. Hanna, 1949,

Phys. Rev. **75**, 982.
Prescott, J. R., 1954, Proc. Phys. Soc. Lond. A **67**, 254.
Prescott, J. R., 1963, Nucl. Instrum. Methods **22**, 256.
Primakoff, H. and F. T. Porter, 1953, Phys. Rev. **89**, 930.
Pruet, C. H. and R. G. Wilkinson, 1954, Phys. Rev. **96**, 1340.
Radvanyi, P., 1952a, C. R. Acad. Sci. (Paris) **235**, 428.
Radvanyi, P., 1952b, C. R. Acad. Sci. (Paris) **235**, 289.
Radvanyi, P., 1955a, J. Phys. Radium **16**, 509.
Radvanyi, P., 1955b, Ann. Phys. (Paris) **10**, 584.
Raeside, D. E., M. A. Ludington, J. J. Reidy, and M. L. Wiedenbeck, 1969, Nucl. Phys. A **130**, 677.
Raj, K. and M. K. Ramaswamy, 1969, Am. J. Phys. **37**, 70.
Raman, S., H. J. Kim, T. A. Walkiewicz, and M. J. Martin, 1973, Phys. Lett. B **44**, 225.
Ramaswamy, M. K., 1959a, Indian J. Phys. **33**, 285.
Ramaswamy, M. K., 1959b, Nucl. Phys. **10**, 205.
Ramaswamy, M. K., 1961, Indian J. Phys. **35**, 610.
Ramaswamy, M. K., W. L. Skeel, and P. S. Jastram, 1960, Nucl. Phys. **19**, 299.
Rao, P. Venugopala and B. Crasemann, 1965, Phys. Rev. **137**, 64B.
Rao, P. Venugopala and B. Crasemann, 1966a, Phys. Rev. **142**, 768.
Rao, P. Venugopala, M. H. Chen, and B. Crasemann, 1972, Phys. Rev. A **5**, 997.
Rao, P. Venugopala, D. K. McDaniels, and B. Crasemann, 1966b, Nucl. Phys. **81**, 296.
Rasmussen, J. O., 1957, private communication to D. Strominger, J. M. Hollander, and G. T. Seaborg, 1958, Rev. Mod. Phys. **30**, 585.
Ravn, H. L. and P. Bøgeholt, 1971, Phys. Rev. C **4**, 601.
Rehfuss, D. E. and B. Crasemann, 1959, Phys. Rev. **114**, 1609.
Reitz, J. R., 1950, Phys. Rev. **77**, 10.
Renier, J. P., H. Genz, K. W. D. Ledingham, and R. W. Fink, 1968, Phys. Rev. **166**, 935.
Reynolds, J. R., 1950, Phys. Rev. **79**, 789.
Ribordy, C. and O. Huber, 1970, Helv. Phys. Acta **43**, 345.
Ricci, R. A., R. K. Girgis, and R. van Lieshout, 1960, Nucl. Phys. **21**, 177.
Rietjens, L. H. Th., H. J. Van den Bold, and P. M. Endt, 1954, Physica **20**, 107.
Rightmire, R. A., J. R. Simanton, and T. P. Kohman, 1959, Phys. Rev. **113**, 1069.
Ristinen, R. A., A. A. Bartlett, and J. J. Kraushaar, 1963, Nucl. Phys. **45**, 321.
Rivier, J. and R. Moret, 1971, C. R. Acad. Sci. (Paris) B **272**, 1022.
Robinson, B. L., 1963, private communication quoted by Klein and Leutz, 1966.
Robinson, B. L. and R. W. Fink, 1955, Rev. Mod. Phys. **27**, 424.
Robinson, B. L. and R. W. Fink, 1960, Rev. Mod. Phys. **32**, 117.
Robinson, B. L., N. R. Johnson, and E. Eichler, 1962, Phys. Rev. **128**, 252.
Roetti, C. and E. Clementi, 1974, J. Chem. Phys. **60**, 3342, and references quoted therein.
Roos, M., 1974, Nucl. Phys. B **77**, 420.
Roothaan, C. C. J., 1960, Rev. Mod. Phys. **32**, 179.
Roothaan, C. C. J. and P. S. Bagus, 1963, *Methods in Computational Physics* (Academic, New York), Vol. 2.
Rose, M. E., 1961, *Relativistic Electron Theory* (Wiley, New York).
Rose, M. E. and R. K. Osborn, 1954, Phys. Rev. **93**, 1315, and 1326.
Rose, M. E., R. Perrin, and L. L. Foldy, 1962, Phys. Rev. **128**, 1776.
Rose, M. E. and C. L. Perry, 1953, Phys. Rev. **90**, 479.
Rosén, A. and I. Lindgren, 1968, Phys. Rev. **176**, 114.
Rubinson, W., 1971, Nucl. Phys. A **169**, 629.
Rubinson, W. and K. P. Gopinathan, 1968, Phys. Rev. **170**, 969.
Rupnik, T., 1972, Phys. Rev. C **6**, 1433.
Rupnik, T. and B. Crasemann, 1972, Phys. Rev. C **6**, 1780. See erratum in Phys. Rev. C **13**, 890 (1976).
Ryde, H., L. Persson, and K. Oelsner-Ryde, 1962a, Ark. Fys. **23**, 171.
Ryde, H., L. Persson, and K. Oelsner-Ryde, 1962b, Ark. Fys. **23**, 195.
Ryde, H., L. Persson, and K. Oelsner-Ryde, 1963, Nucl. Phys. **47**, 614.
Sakai, M., J. L. Dick, W. S. Anderson, and J. D. Kurbatrov, 1954, Phys. Rev. **95**, 101.
Salam, A., 1968, in *Nobel Symposium*, edited by N. Svartholm. (18th Meeting of Nobel Laureates, Lindau, Germany.)
Salem, S. I., S. L. Panossian, and R. A. Krause, 1974, Atomic Data and Nucl. Data Tables **14**, 91.
Santos Ocampo, A. G., 1961, Ph.D. Thesis, Purdue University, TID Report 13490 (unpublished).
Santos Ocampo, A. G. and D. C. Conway, 1960, Phys. Rev. **120**, 2196.
Santos Ocampo, A. G. and D. C. Conway, 1962, Phys. Rev. **128**, 258.
Saraf, B., 1954a, Phys. Rev. **94**, 642.
Saraf, B., 1954b, Phys. Rev. **95**, 97.
Saraf, B., 1956, Phys. Rev. **102**, 466.
Saraf, B., J. Varma, and C. F. Mandeville, 1953, Phys. Rev. **91**, 1216.
Schima, F., E. G. Funk, Jr., and J. W. Mihelich, 1963, Phys. Rev. **132**, 2650.
Schmidt-Ott, W.-D., 1970a, Z. Phys. **232**, 298.
Schmidt-Ott, W.-D., 1970b, Z. Phys. **236**, 445.
Schmidt-Ott, W.-D. and R. W. Fink, 1972, Z. Phys. **249**, 286.
Schmidt-Ott, W.-D., W. Weirauch, F. Smend, H. Langhoff, and D. Gföller, 1968, Z. Phys. **217**, 282.
Schmorak, M., 1963, Phys. Rev. **129**, 1668.
Schopper, H. F., 1966, *Weak Interactions and Nuclear Beta Decay* (North-Holland, Amsterdam).
Schopper, H. F., 1968, in Berényi 1968b, p. 488.
Schucan, T. H., 1965, Nucl. Phys. **61**, 417.
Schülke, L., 1964, Z. Phys. **179**, 331.
Schulz, G., 1967a, Nucl. Phys. A **101**, 177.
Schulz, G., 1967b, Nucl. Instrum Methods **53**, 320.
Schulz, G., 1967c, Z. Phys. **203**, 289.
Schulz, G. and K. Ziegler, 1967d, Nucl. Phys. A **104**, 692.
Scobie, J., 1957a, Nucl. Phys. **3**, 465.
Scobie, J. and E. Gabathuler, 1958, Proc. Phys. Soc. Lond. **72**, 437.
Scobie, J. and G. M. Lewis, 1957b, Phil. Mag. **2**, 1089.
Scobie, J., R. B. Moler, and R. W. Fink, 1959, Phys. Rev. **116**, 657.
Scofield, J. E., 1974, Atomic Data and Nucl. Data Tables **14**, 121.
Scofield, J. E., 1975, in *Atomic Inner-Shell Processes*, edited by B. Crasemann, (Academic, New York, San Francisco, London), Vol. I, p. 265.
Scofield, N. E., 1963, in O'Kelley (1963), p. 108.
Scott, F. R., 1951, Phys. Rev. **84**, 659.
Sehr, R., 1954, Z. Phys. **137**, 523.
Shalitin, D., 1965, Phys. Rev. **140**, 1857A.
Shalitin, D., 1967, Phys. Rev. **155**, 20.
Sherr, R. and R. H. Miller, 1954, Phys. Rev. **93**, 1076.
Shore, F. J., W. L. Bendel, H. N. Brown, and R. A. Becker, 1953, Phys. Rev. **91**, 1203.
Siegbahn, K., 1965, *Alpha-, Beta-, and Gamma-Ray Spectroscopy* (North-Holland, Amsterdam).
Singh, B. and H. W. Taylor, 1970, Nucl. Phys. A **147**, 12.
Sirlin, A., 1967, Phys. Rev. **164**, 1767.
Sirlin, A., 1974, Nucl. Phys. B **71**, 29.
Slater, J. C., 1930, Phys. Rev. **36**, 57.
Slater, J. C., 1960, *Quantum Theory of Atomic Structures*

(McGraw-Hill, New York), Vol. 1 and 2.
Smirnov, Yu. G., and I. S. Batkin, 1973, Yad. Fiz. **18**, 239 [Sov. J. Nucl. Phys. **18**, 122].
Smith, K. M., 1964, Ph.D. Thesis, University of Glasgow (unpublished).
Smith, K. M. and B. R. Joshi, 1963, Proc. Phys. Soc. Lond. **82**, 918.
Smith, K. M. and G. M. Lewis, 1966, Nucl. Phys. **89**, 561.
Snyder, J. W. and M. L. Pool, 1965, Phys. Rev. **138**, 770B.
Sparrman, P., T. Sundström, and A. Marelius, 1966, Nucl. Phys. **81**, 548.
Spernol, A., 1967, *Standardization of Radionuclides* (International Atomic Energy Agency, Vienna), p. 277.
Spernol, A., E. De Roost, and M. Mutterer, 1973, Nucl. Instrum. Methods **112**, 169.
Stanford, Jr., A. L., C. H. Braden, and L. D. Wyly, 1960, Bull. Am. Phys. Soc. **5**, 449.
Stech, B. and L. Schülke, 1964, Z. Phys. **179**, 314.
Stephas, P., 1969, Phys. Rev. **186**, 1013.
Stephas, P. and B. Crasemann, 1967, Phys. Rev. **164**, 1509.
Stephas, P. and B. Crasemann, 1971, Phys. Rev. C **3**, 2495.
Sterk, M. J., A. H. Wapstra, and R. F. W. Kropveld, 1953, Physica **19**, 135.
Steyn, J. and A. S. M. De Jesus, 1966, South African CSIR Special Report FIS 15 (unpublished).
Stover, B. J., 1951, Phys. Rev. **81**, 8.
Strubbe, H. J. and D. K. Callebaut, 1970, Nucl. Phys. A **143**, 537.
Sujkowski, Z., J. Jastrzebski, A. Zglínski, and J. Zylicz, 1965, in *Role of Atomic Electrons in Nuclear Transformations* (Nuclear Energy Information Center, Warsaw, Poland), p. 614.
Sujkowski, Z., B. Mysłek, J. Lukasiak, and B. Kotlinska-Filipek, 1973, in *Proceedings of the International Conference on Inner-Shell Ionization Phenomena*, edited by R. W. Fink, S. T. Manson, J. M. Palms, and P. Venugopala Rao (U. S. Atomic Energy Commission Report No. CONF–720404 unpublished), p. 2005.
Sujkowski, Z., B. Mysłek, A. Zglínski, and B. Adamowicz, 1968, in Berényi (1968b), p. 163.
Suslov, Yu. P., 1966, Izv. Akad. Nauk. SSSR Ser. Fiz. **30**, 1248 [Bull. Acad. Sci. USSR, Phys. Ser. **30**, 1305].
Suslov, Yu. P., 1967, Izv. Akad. Nauk. SSSR Ser. Fiz. **31**, 688 [Bull. Acad. Sci. USSR, Phys. Ser. **31**, 684].
Suslov, Yu. P., 1968a, Izv. Akad. Nauk. SSSR Ser. Fiz. **32**, 213 [Bull. Acad. Sci. USSR, Phys. Ser. **32**, 192].
Suslov, Yu. P., 1968b, in Berényi (1968b), p. 51.
Suslov, Yu. P., 1969, Izv. Akad. Nauk. SSSR Ser. Fiz. **33**, 78 [Bull. Acad. Sci. USSR, Phys. Ser. **33**, 74].
Suslov, Yu. P., 1970a, Izv. Akad. Nauk. SSSR Ser. Fiz. **34**, 97 [Bull. Acad. Sci. USSR, Phys. Ser. **34**, 91].
Suslov, Yu. P., 1970b, Izv. Akad. Nauk. SSSR Ser. Fiz. **34**, 2223 [Bull. Acad. Sci. USSR, Phys. Ser. **34**, 1983].
Suzuki, Sh. and Y. Yokoo, 1975, Nucl. Phys. B **94**, 431.
Szybisz, L., 1975, Z. Phys. A **273**, 277.
Takekoshi, E., Z. Matsumoto, M. Ishi, K. Sugiyama, S. Hayashibe, H. Sekiguchi, and H. Natsume, 1964, J. Phys. Soc. Jpn. **19**, 587.
Talmi, I., 1953, Phys. Rev. **91**, 122.
Taylor, H. W., G. N. Whyte, and R. McPherson, 1963, Nucl. Phys. **41**, 221.
Taylor, J. G. V. and J. S. Merritt, 1965, in *Role of Atomic Electrons in Nuclear Transformations* (Nuclear Energy Information Center, Warsaw, Poland), p. 465.
Thomas, H. C., C. F. Griffin, W. E. Phillips, and E. C. Davis, Jr., 1963, Nucl. Phys. **44**, 268.
Thomas, L. H., 1954, J. Chem. Phys. **22**, 1758.
Thomas, T. D., R. Vandenbosch, R. A. Glass, and G. T. Seaborg, 1957, Phys. Rev. **106**, 1228.
Thulin, S., 1955, Ark. Fys. **9**, 137.
Thulin, S., J. Moreau, and H. Atterling, 1954a, Ark. Fys. **8**, 219.
Thulin, S., J. Moreau, and H. Atterling, 1954b, Ark. Fys. **8**, 229.
Thun, J. E., S. Törnkvist, K. B. Nielsen, H. Snellman, F. Falk, and A. Mocoroa, 1966, Nucl. Phys. **88**, 289.
Timashev, S. F. and V. A. Kaminskii, 1960, Zh. Eksp. Teor. Fiz. **38**, 284 [Sov. Phys.–JETP **11**, 206].
Törnkvist, S. and S. Ström, 1968, Ark. Fys. **38**, 261.
Tolea, F., K. R. Baker, W. D. Schmidt-Ott, and R. W. Fink, 1974, Z. Phys. **268**, 289.
Tolhoek, H. A., C. D. Hartogh, and S. R. de Groot, 1955, J. Phys. Radium **16**, 615.
Totzek, D. and K.-H. Hoffmann, 1967, Z. Phys. **205**, 137.
Towner, I. S., 1973, Nucl. Phys. A **216**, 589.
Tribble, R. E. and G. T. Garvey, 1974, Phys. Rev. Lett. **32**, 314.
Trimble, V. and F. Reines, 1973, Rev. Mod. Phys. **45**, 1.
Tucker, T. C., L. D. Roberts, C. W. Nestor, Jr., T. A. Carlson, and F. B. Malik, 1969, Phys. Rev. **178**, 998.
Turchinetz, W. and R. W. Pringle; 1956, Phys. Rev. **103**, 1000.
Turovtsev, V. V. and I. S. Shapiro, 1954, Dokl. Akad. Nauk. SSSR **95**, 777.
Unik, J. P. and J. O. Rasmussen, 1959, Phys. Rev. **115**, 1687.
van der Kooi, J. B. and H. J. van den Bold, 1956, Physica **22**, 681.
Vanderleeden, J. C., F. Boehm, and E. D. Lipson, 1971, Phys. Rev. C **4**, 2218.
Van Hise, J. R., B. H. Ketelle, and A. R. Brosi, 1967, Phys. Rev. **153**, 1287.
van Nooijen, B., J. Konijn, A. Heyligers, J. F. van der Brugge, and A. H. Wapstra, 1957, Physica **23**, 753.
van Nooijen, B., H. van Krugten, W. J. Wiesehahn, and A. H. Wapstra, 1962, Nucl. Phys. **31**, 406.
Van Patter, D. M. and S. M. Shafroth, 1964, Nucl. Phys. **50**, 113.
Vaninbroukx, R., and A. Spernol, 1965, Int. J. Appl. Radiat. Isot. **16**, 289.
Vaninbroukx, R. and G. Grosse, 1966, Int. J. Appl. Radiat. Isot. **17**, 41.
Varga, D., 1970, Atomki Közl. **12**, 165.
Vartanov, N. A., 1963, Zh. Eksp. Teor. Fiz. **45**, 1875 [Sov. Phys.–JETP **18**, 1286 (1964)].
Vatai, E., 1966, Acta Phys. Hung. **20**, 217.
Vatai, E., 1968b, in Berényi (1968b), p. 71.
Vatai, E., 1968d, in Berényi (1968b), p. 112.
Vatai, E., 1970a, Nucl. Phys. A **156**, 541.
Vatai, E., 1970b, Acta Phys. Hung. **28**, 103.
Vatai, E., 1971, Phys. Lett. B **34**, 395.
Vatai, E., 1972b, Atomki Közl. **14**, 233.
Vatai, E., 1973a, Nucl. Phys. A **212**, 413.
Vatai, E., 1973b, Atomki Közl. **15**, 225.
Vatai, E., 1973c, in *Proceedings of the International Conference on Inner-Shell Ionization Phenomena*, edited by R. W. Fink, S. T. Manson, J. M. Palms, and P. Venugopala Rao, U. S. Atomic Energy Commission Report No. CONF–720404 (unpublished)., p. 1957.
Vatai, E., 1974, Atomki Közl. Suppl. 16/2, 91.
Vatai, E. and K. Hohmuth, 1968a, in Berényi (1968b), p. 88.
Vatai, E., D. Varga, and J. Uchrin, 1968c, Nucl. Phys. A **116**, 637.
Vatai, E., A. C. Xenoulis, K. R. Baker, F. Tolea, and R. W. Fink, 1974, Nucl. Phys. A **219**, 595.
Vitnam, V. D., D. S. Dzhelepov, A. A. Pavlov, S. V. Semenov, and S. A. Shestopalova, 1960, Izv. Akad. Nauk. SSSR Ser. Fiz. **24**, 934 [Bull. Acad. Sci. USSR, Phys. Ser. **24**, 931].
von Oertzen, W., 1964, Z. Phys. **182**, 130.
Wahlgren, M. A. and W. W. Meinke, 1960, Phys. Rev. **118**, 181.
Waibel, E., 1969, Nucl. Instrum. Methods **74**, 69.
Waibel, E., 1970, Nucl. Instrum. Methods **86**, 29.

Walen, R. J. and C. Briançon, 1975, in *Atomic Inner-Shell Processes*, edited by B. Crasemann (Academic, New York), Vol. 1, p. 233.
Wapstra, A. H. and N. B. Gove, 1971, Nucl. Data Tables A **9**, 267.
Wapstra, A. H., J. F. W. Jansen, P. F. A. Goudsmit, and J. Oberski, 1962, Nucl. Phys. **31**, 575.
Wapstra, A. H., D. Maeder, G. J. Nijgh, and L. T. M. Ornstein, 1954, Physica **20**, 169.
Wapstra, A. H., G. J. Nijgh, and R. van Lieshout, 1959, *Nuclear Spectroscopy Tables* (North-Holland, Amsterdam).
Wapstra, A. H. and J. Oberski, 1963, in O'Kelley (1963), p. 137.
Wapstra, A. H. and W. van der Eijk, 1957, Nucl. Phys. **4**, 325.
Watase, Y., J. Itoh, and E. Takeda, 1940, Proc. Phys.-Math. Soc. Jpn. **22**, 90.
Watson, R. E., 1960, Phys. Rev. **118**, 1036.
Watson, R. E. and A. J. Freeman, 1961a, Phys. Rev. **123**, 521.
Watson, R. E. and A. J. Freeman, 1961b, Phys. Rev. **124**, 1117.
Weidenmüller, H. A., 1961, Rev. Mod. Phys. **33**, 574.
Weinberg, S., 1958, Phys. Rev. **112**, 1375.
Weinberg, S., 1967, Phys. Rev. Lett. **19**, 1964.
Weinberg, S., 1974, Rev. Mod. Phys. **46**, 255.
Weise, K., 1968, Nucl. Instrum. Methods **65**, 189, and private communication.
Welker, J. P. and M. L. Perlman, 1955, Phys. Rev. **100**, 74.
West, Jr., H. I., L. G. Mann, and R. J. Nagle, 1961, Phys. Rev. **124**, 527.
Wilkinson, D. H., 1970a, Phys. Lett. B **31**, 447.
Wilkinson, D. H., 1970b, Nucl. Phys. A **143**, 365.
Wilkinson, D. H., 1970c, Nucl. Instrum. Methods **82**, 122.
Wilkinson, D. H., 1970d, Nucl. Phys. A **150**, 478.
Wilkinson, D. H., 1970e, Nucl. Phys. A **158**, 476.
Wilkinson, D. H., 1971, Phys. Rev. Lett. **27**, 1018.
Wilkinson, D. H., 1971/72, Proc. R. Soc. Edinb. A **70**, 307.
Wilkinson, D. H., 1972a, Nucl. Phys. A **179**, 289.
Wilkinson, D. H., 1972b, Nucl. Instrum. Methods **105**, 505.
Wilkinson, D. H., 1973a, Phys. Rev. C **7**, 930.
Wilkinson, D. H., 1973b, Nucl. Phys. A **209**, 470.
Wilkinson, D. H., 1973c, Nucl. Phys. A **205**, 363.
Wilkinson, D. H., 1974a, Nucl. Phys. A **225**, 365.
Wilkinson, D. H., 1974b, Phys. Lett. B **48**, 169.
Wilkinson, D. H., 1975, Nature **257**, 189.
Wilkinson, D. H. and D. E. Alburger, 1971, Phys. Rev. Lett. **18**, 1127.
Wilkinson, D. H. and B. E. F. Macefield, 1970, Nucl. Phys. A **158**, 110.
Wilkinson, D. H. and B. E. F. Macefield, 1974, Nucl. Phys. A **232**, 58.
Wilkinson, G. and H. G. Hicks, 1949, Phys. Rev. **75**, 1370, 1687.
Williams, A., 1964, Nucl. Phys. **52**, 324.
Williams, A., 1968, Nucl. Phys. A **117**, 238.
Williams, A., 1970, Nucl. Phys. A **153**, 665.
Williams, E. J. and E. Pickup, 1938, Nature **141**, 199.
Wilson, R. G., 1969, Phys. Rev. **178**, 1949.
Wilson, R. G. and M. L. Pool, 1960, Phys. Rev. **119**, 262.
Wilson, R. G., A. A. Bartlett, J. J. Kraushaar, J. D. McCullen, and R. A. Ristinen, 1962, Phys. Rev. **125**, 1655.
Winter, G., 1968, Nucl. Phys. A **113**, 617.
Winter, G., K. Hohmuth, and J. Schintlmeister, 1964, Exp. Tech. Phys. **12**, 141.
Winter, G., K. Hohmuth, R. Ross, H. Kästner, and J. Schintlmeister, 1965a, Ann. Phys. (Leipz.) **16**, 207.
Winter, G., K. Hohmuth, R. Ross, H. Kästner, and J. Schintlmeister, 1967, Z. Phys. Chem. **234**, 305.
Winter, G., K. Hohmuth, and J. Schintlmeister, 1965b, Nucl. Phys. **73**, 91.
Winter, R. G., 1957, Am. J. Phys. **25**, 79.
Wolfenstein, L. and E. M. Henley, 1971, Phys. Lett. B **36**, 28.
Wolfsberg, M., 1954, Phys. Rev. **96**, 1712.
Wolczek, O., Tat-To Nguyen, and I. Yutlandov, 1963, Institute for Nuclear Research, Warsaw, Report INR–430/1 (unpublished).
Woodward, L. L., D. A. McCown, and M. L. Pool, 1948a, Phys. Rev. **74**, 761.
Woodward, L. L., D. A. McCown, and M. L. Pool, 1948b, Phys. Rev. **74**, 870.
Wu, C. S. and S. A. Moszkowski, 1966, *Beta Decay* (Wiley, New York).
Yonei, K., 1966, J. Phys. Soc. Jpn. **21**, 142.
Yonei, K., 1967, J. Phys. Soc. Jpn. **22**, 1127.
Yuasa, T., 1952, Physica **18**, 1267.
Yukawa, J., 1956, Prog. Theor. Phys. **15**, 561.
Yukawa, H. and S. Sakata, 1935, Proc. Phys.-Math. Soc. Jpn. **17**, 467.
Yukawa, H. and S. Sakata, 1936, Proc. Phys.-Math. Soc. Jpn. **18**, 128.
Yukawa, H. and S. Sakata, 1937, Phys. Rev. **51**, 677.
Zhelev, Zh. and G. Muziol', 1967, Yad. Fiz. **4**, 1 [Sov. J. Nucl. Phys. **4**, 1].
Zoller, W. H., W. B. Walters, and C. D. Coryell, 1969, Phys. Rev. **185**, 1537.
Zon, B. A., 1971, Yad. Fiz. **13**, 963 [Sov. J. Nucl. Phys. **13**, 554].
Zon, B. A., 1973, Izv. Akad. Nauk. SSSR Ser. Fiz. **37**, 1978 [Bull. Acad. Sci. USSR, Phys. Ser. **37**, 153].
Zon, B. A. and L. P. Rapoport, 1968, Yad. Fiz. **7**, 528 [Sov. J. Nucl. Phys. **7**, 330].
Zurmühl, R., 1965, *Praktische Mathematik für Ingenieure und Physiker* (Springer Verlag, Berlin, Heidelberg and New York), p. 157.
Zumwalt, L. R., 1947, Plutonium Project Report, Mon N–432, 54 (unpublished).
Zweifel, P. F., 1954, Phys. Rev. **96**, 1572.
Zweifel, P. F., 1957, Phys. Rev. **107**, 329.
Zweifel, P. F., 1958, in *Proceedings of the Rehovoth Conference on Nuclear Structure*, edited by H. L. Lipkin (North-Holland, Amsterdam), p. 300.
Zylicz, J., 1968, in D. Berényi (1968b), p. 123.
Zylicz, J., Z. Sujkowski, J. Jastrzebski, and O. Wołczek, 1963, Nucl. Phys. **42**, 330.
Zyryanova, L. N. and Yu. P. Suslov, 1968, in Berényi (1968b), p. 45.
Zyryanova, L. N. and Yu. P. Suslov, 1969, Izv. Akad. Nauk. SSSR Ser. Fiz. **33**, 1693 [Bull. Acad. Sci. USSR, Phys. Ser. **33**, 1553].
Zyryanova, L. N. and Yu. P. Suslov, 1970, Izv. Akad. Nauk. SSSR Ser. Fiz. **34**, 101 [Bull. Akad. Sci. USSR, Phys. Ser. **34**, 95].